CORAL LIES

Unveiling Technological Exchange and Trade in the Early Iron Age

Giulia Berruto

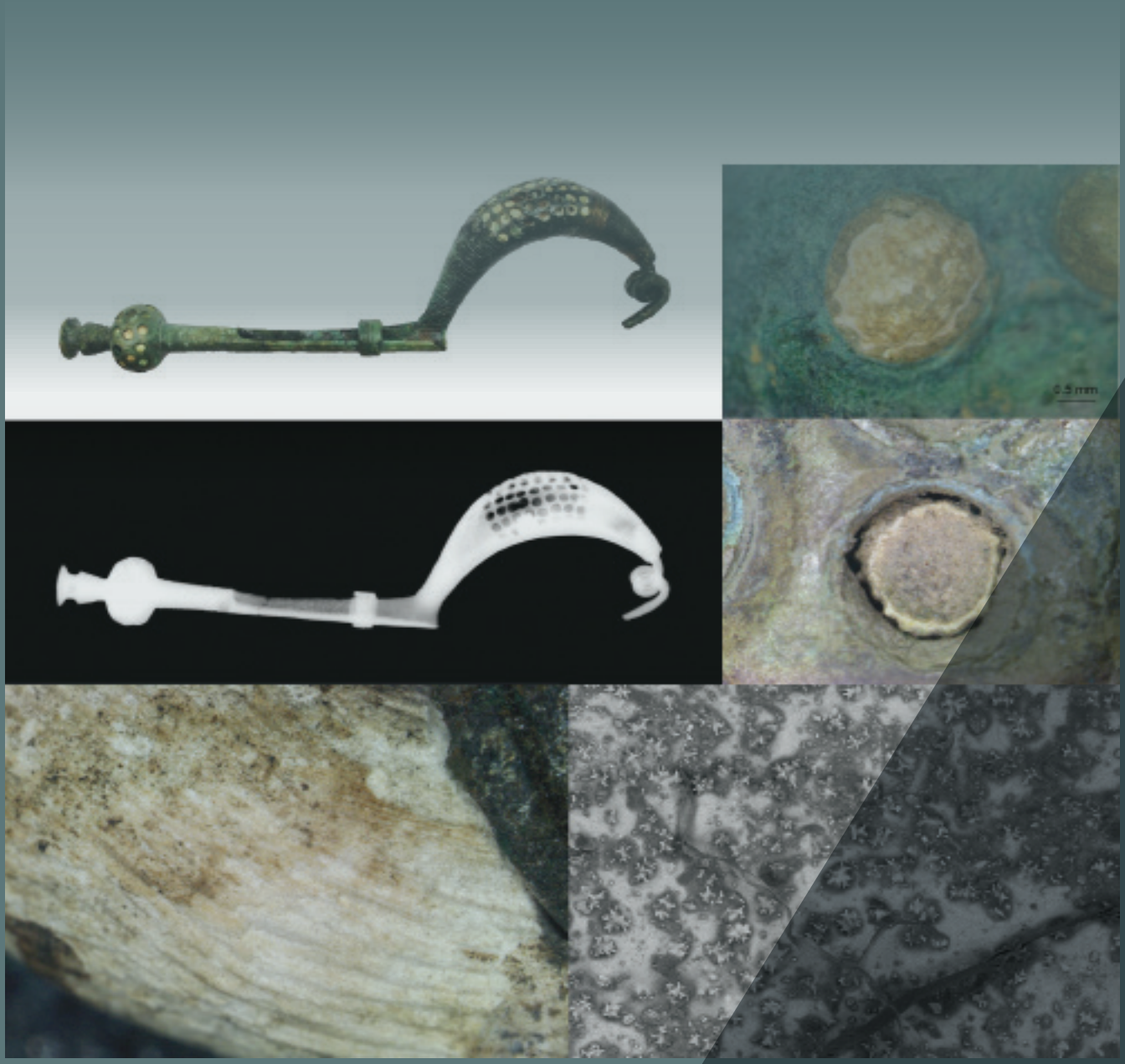

CVS
Cisalpine Studies

Milano University Press

Coral Lies

Unveiling Technological Exchange and Trade in the Early Iron Age

Giulia Berruto

Milano University Press

Coral Lies. Unveiling Technological Exchange and Trade in the Early Iron Age / Giulia Berruto. Milano: Milano University Press, 2026. (Cisalpine studies; 4)

ISBN 979-12-5510-403-2 (Print)
ISBN 979-12-5510-404-9 (PDF)
ISBN 979-12-5510-405-6 (EPUB)
DOI 10.54103/cisalpinestudies.261

Works published under Cisalpine Studies are subject to the Editorial Board's review and approval, ensuring full compliance with peer review standards, ethical guidelines, and anti-plagiarism protocols.

The present work is released under Creative Commons Attribution 4.0 - CC-BY-SA, accessible at: https://creativecommons.org/licenses/by/4.0/deed.it

This and other volumes of Milano University Press are available in open access at: https://libri.unimi.it/index.php/milanoup

The Author(s), 2026
Milano University Press, per la presente edizione

Published by:
Milano University Press
Via Festa del Perdono 7 – 20122 Milano
Sito web: https://milanoup.unimi.it
e-mail: redazione.milanoup@unimi.it

The print edition of this volume can be ordered from bookstores, and is distributed by Ledizioni (www.ledizioni.it)

All photographs of archaeological finds are reproduced with the kind permission of the Italian Ministry of Culture, unless otherwise indicated.

Index

Preface 9

Editor's note 11

1. Introduction 13
Overview 13
Abbreviations 15

2. Corals. Biology and History 17
Introduction 17
2.1. Skeletal mineralisation in corals 18
2.2. Mediterranean red coral 19
2.3. White corals in the Mediterranean Sea 22
2.4. The study of corals: origins and advancements 23
2.4.1. Coral: myth and magic 23
2.4.2. Coral in scientific research: mineral, plant or animal? 25

3. Ornamental Use of Coral from the Neolithic to the 19th century 27
3.1. Neolithic (5th – 4th millennium BCE) 27
3.2. Copper Age - Bronze Age (3rd - 2nd millennium BCE) 29
3.3. Iron Age (9th - 2nd century BCE) 30
3.3.1 Coral for ancient Greeks 30
3.3.2 Coral in Egypt 30
3.3.3 Coral in the Phoenician-Punic domain 31
3.3.4 Coral among the Italic populations 32
3.3.5 Coral in Iron Age Europe 34
3.3.6 Supply areas in pre-Roman times 36
3.4. Roman period 40
3.5. Middle Ages (476-1492) 41
3.6. Modern Age (1492-1789) 42
3.7. Contemporary Age (1789-1904) 43

4. Coral in Northern Italy in the Iron Age 45
Introduction 46
4.1 The archaeological background. Northern Italy in the Iron Age 48
4.1.1 Golasecca 48
4.1.2 Liguria 50
4.1.3. Este and northeastern Italy 52
4.1.4. Etruria Padana 54
4.1.5 The Late Iron Age 56
4.2 The use of coral in the Golasecca culture 57
4.2.1 Longone al Segrino type pendant 58
4.2.2 Coral composite bow fibula 59
4.2.3 Leech fibulae 61

4.2.4 Leech fibulae with circular insets 61
4.2.5 Leech fibulae with linear decoration 72
4.2.6 Cross-panel leech fibulae 73
4.2.7 Leech fibulae with transversal grooves 74
4.2.8 Late Hallstattian fibulae 76
Ornithomorphic fibulae 76
Fußzierfibeln 79
4.2.9 Navicella fibulae 80
4.2.10 Bucket Pendants 81
4.2.11 Grooming tools 85
4.3 The use of coral in Liguria Interna and coastal Liguria 86
4.4 The use of coral in Este culture and north-eastern Italy 87
4.4.1 Beads and pendants 87
4.4.2 Dragon-shaped fibulae with daisies 88
4.5 The use of coral in Etruria Padana 90
4.6 The use of coral in the Late Iron Age 91
4.6.1 Ancient La Tène fibulae, furrowed bow and coral applications 92
4.6.2 Massive bow fibulae with wide central application and disc-shaped appendix 93
4.7 Discussion. Coral in Iron Age northern Italy 96

5. Archaeometry and Corals 99
5.1. The archaeological question 100
5.2. Previous studies 101
5.3. The provenance problem 103
5.3.1. Isotopic analysis 103
5.3.2. Trace elements analysis 104
5.3.3. Others possible approaches 105

6. Materials and Methods 107
6.1. Analytical record 107
6.1.1. Archaeological record 107
6.1.2. Modern samples 113
6.2. Analytical protocol 113
6.2.1. Analytical approaches 113
6.2.2. Involved techniques 114
6.2.2.1. Optical microscopy 114
6.2.2.2. Raman spectroscopy 115
6.2.2.3. Infrared spectroscopy 118
6.2.2.4. Micro-X-Ray diffraction analysis 119
6.2.2.5. Chemical analysis: μ-XRF and SEM-EDS 120
6.2.2.6. Radiographic analyses 122

7. Archaeometric Analyses: Results 123
7.1. Whitish decorative materials 124
7.1.1. Modern samples 124
7.1.1.1. Optical stereomicroscope 124
7.1.1.2. μ-Raman analysis 124

7.1.1.3. FT-IR analysis 128
7.1.1.4. μ-XRD analysis 128
7.1.1.5. SEM-EDS analysis 131
7.1.2. Archaeological finds 135
7.1.2.1. Optical microscopy 135
7.1.2.2. Raman analysis 138
7.1.2.3. FT-IR analysis 146
7.1.2.4. μ-XRD analysis 151
7.1.2.5. SEM-EDS analysis 158
7.1.3 Combustion experiments 164
7.1.3.1. μ-Raman analyses 164
7.1.3.2. FT-IR analyses 166
7.1.3.3. SEM-EDS analyses 166
7.1.4 Considerations 168
7.2 Metal surface 179
7.2.1. Optical microscopy 179
7.2.2. μ-Raman analysis 182
7.2.3. μ-XRD analysis 182
7.2.4. SEM-EDS analysis 188
7.2.5. Considerations 193

8. Experimental archaeology contribution 195
Introduction 195
8.1. Technological study 195
8.2. Radiographic examination 201
8.3. Experimental archaeology tests 203
8.3.1. Placement and bonding of coral insets 203
8.3.2. Bronze casting 206
8.4 Considerations 211

9. Conclusions 219
9.1 Project overview 219
9.2 Archaeotypological study: archaeological trends 220
9.3 Archaeometric analysis: protocol and results 221
9.4 Critical issues: LMC problem 222
9.5 Critical issues: coral provenance 223
9.6 Archaeometallurgical insights 223
9.7 Archaeo-technology 224
9.8 Future perspectives 224
Acknowledgments 226

Topographical index 227

References 233

Appendix 1 – Supplementary Figures 257

Appendix 2 – Tables 275

Preface

Eliano Diana [(*)], Roberto Giustetto [(**)], Marica Venturino [(***)]

[(*)] Università degli Studi di Torino, Dipartimento di Chimica; [(**)] Università degli Studi di Torino, Dipartimento di Scienze della Terra; [(***)] former Soprintendenza archeologia, belle arti e paesaggio per le province di Alessandria, Asti e Cuneo

This volume represents the highest point of a long-time collaboration existing between the (former) '*Soprintendenza per i Beni Archeologici del Piemonte*' (Superintendence for the Archaeological Heritage of Piedmont) and the University of Turin – Departments of Earth Sciences and Chemistry, which started in 2008 to study whitish decorative encrustations on proto-historic pottery in the Piedmont region (Northwestern Italy). In the years that followed, this initiative was extended – by also dragging in several international institutions – to the study of particular encrustations and/or insets made of presumed coral (*Corallium rubrum*) on bronze fibulae of the Iron Age – a subject hardly considered in the literature existing so far.

In this context, the project "*Tecnologia e scambi nella prima età del Ferro tra Europa e Mediterraneo: studio archeometrico delle decorazioni campite su ornamenti metallici*" (Technologies and Trades in the early Iron Age between Europe and the Mediterranean Sea: Archaeometric Studies of inset decorations on metal ornaments), developed between 2020 and 2023 at the University of Turin by the Author – Giulia Berruto, PhD – within the "Technology Driven Sciences: Technologies for Cultural Heritage (*Tech4Culture*) PhD projects, certainly represents a key issue.

This sophisticated investigation, in fact, not only covered a very large sample-set of artefacts (mainly fibulae, pendants and beads), collected from various Iron Age sites of Northern Italy, but also followed an innovative and comprehensive approach, which includes both archaeological and scientific methods. The true benefit is represented by that fact that all these competences were directed and summoned by a single person – namely, the Author – whose expertise covered both fields. This dual and parallel investigation allowed intertwining the obtained outcomes from both a historical-artistic (literature studies, production and trades of these artefacts between prehistory and the beginning of the last century, census of specimens and related chrono-typological background) and archaeometric (non – or micro-destructive analyses, characterization and provenance of the constituent materials, conservation issues) point of view, elaborating them in the competent geographical context and pursuing straightforward results, hardly achievable in a different way.

Red coral from the Mediterranean Sea (some raw branches of which, with known contextualization and provenance, were also studied for comparison purposes) was widely used in Italy, starting from the earlier attestations during Neolithic (V-IV millennium BC) until the Iron Age (VIII-V century BC), to decorate ornaments and clothing (especially for women). The survey was focused in the latter period, which undoubtedly represents the best-attested age in which coral was widely used and diffused in Northern Italy, by sketching and outlining as a premise the relationships existing between the main involved cultural areas (i.e., Golasecca, Ligurian, Este and Northeastern Italy, Etruria padana). This goal was achieved at first through a detailed and meticulous census activity, involving both local and national institutions, an activity that brought to a thorough contextualization and chrono-typological revision of the artefacts and provided updated photographic reports of the finds and the decorations to be analyzed. The resulting catalogue is wide and exhaustive and comprehends any possible problematic related to these objects finding and raw materials circulation.

The scientific magnitude of this survey stands out for both its high methodological standard and the originality of the archaeometric framework. The core of the research, in particular, lies

in the development of a rigorous analytical protocol, specifically calibrated for highly delicate archaeological artefacts such as those studied here, aimed at reliably identifying the light-coloured inlay materials, traditionally attributed to Mediterranean red coral.

This protocol consisted of a multi-technique, non-destructive (or only micro-destructive, whenever required and allowed) approach, based on the synergistic integration of vibrational spectroscopies (μ-Raman and FT-IR), micro X-ray diffraction (μ-XRD) optical microscopy and scanning electron microscopy with energy-dispersive spectrometry (SEM-EDS). This combined methodology allowed discriminating different Ca-carbonate polymorphs (calcite and aragonite), detecting possible diagenetic transformations, characterizing diagnostic microstructures/textures and identifying the accessory components or binding media. By systematically applying this procedure on a wide corpus of artefacts, integrated by the analysis of modern reference samples and controlled experimental tests, the robustness and reproducibility of the obtained results was ensured.

This study showed that the macroscopic attribution and characterization of materials may be misleading, highlighting the necessity of analytical checks aptly supported by objective mineralogical and chemical-structural data. The dissertation is characterized by methodological consistency, analytical precision, and a high level of expertise in instrumental techniques. The Author's work represents thus a solid and innovative contribution to the establishment of archaeometric standards, applicable to the study of organogenic and composite materials in the archaeological context.

As an alternative approach, these artefacts were also studied from a strictly technological point of view – i.e., facing the difficulties encountered by the prehistoric artisans deputed to their production. To do this, experimental archaeologists were involved, with whom the Author tested the feasibility and the pros-and-cons of the manufacturing and decorating techniques possibly available at the time. Even for this aspect, the archaeometric approach proved to be fundamental, since a preliminary radiographic and tomographic survey on the ancient artefacts represented the key to unveil fundamental details about their production techniques.

Editor’s note

Lorenzo Zamboni

I am particularly pleased to welcome Giulia Berruto’s volume to the *Cisalpine Studies* series, for two main reasons. First, this is the first book in the series to be published in English, thus addressing – we hope – a broader international readership. Second, Giulia’s work represents a remarkable example of a line of research that remains underrepresented not only in the Italian scholarly tradition but also within academic curricula, especially for late protohistoric and classical contexts: namely, archaeological science.
By this I mean a rigorous scientific approach applied to archaeological assemblages, conducted not only by external specialists in physics or chemistry, but also by scholars trained within the humanities who have also acquired laboratory expertise and methodological competence in archaeometric analysis. This integration of disciplinary perspectives embodied in the present volume demonstrates how productive such a trajectory can be. The results presented here are, in my view, exemplary, and point toward what may become, if not the only, certainly a central professional path for future generations of archaeologists.

A few final words on the title. *Coral Lies* cryptically echoes poetry and music – from Edward Elgar’s *Where Corals Lie* (1899) to The Beatles’ “Octopus’s Garden” (1969): “We would shout and swim about the coral that lies beneath the waves.” At the same time, the title plays on the elusive and ambiguous nature of this precious and alluring material, especially in archaeological contexts. As this book makes clear, coral was highly sought after, and likely highly valued, in antiquity. Yet artisans could sometimes deceive, and buyers may have accepted compromises. In this tension between authenticity and imitation – and in the scientific protocols that enable us to understand it – lies one of the most fascinating aspects of the story this volume unfolds.

1. Introduction

Abstract

Nel nord Italia a partire dalla prima età del Ferro il corallo rosso del Mediterraneo è utilizzato per decorare oggetti di ornamento in bronzo, quali fibule e pendenti. In particolare, le fibule a sanguisuga con intarsi bianchi o rosati sono tra i reperti più comuni tra la metà del VI e la metà del V sec. a.C.
Il materiale decorativo, tradizionalmente identificato come *Corallium rubrum* sbiancato, potrebbe in realtà essere costituito da altre sostanze, tra cui osso, avorio, smalto, rocce carbonatiche o talco. Le analisi scientifiche condotte finora sono state di limitata portata e spesso condotte con metodologie incomplete. Gli intarsi, spesso inferiori ai 2 mm, richiedono indagini archeometriche specifiche per una corretta identificazione. Studi recenti hanno evidenziato l'uso di pigmenti sintetici (come il 'bianco d'ossa') nella decorazione di intarsi su ceramiche dell'età del Ferro, o sostanze artificiali usate in restauri storici di ornamenti metallici, come il biossido di titanio.
Questo studio vuole proporre un approccio innovativo che unisce archeologia tradizionale, archeometria e analisi tecnologiche, superando i limiti del metodo crono-tipologico. Un progetto condotto fin dal 2014 presso l'Università di Torino ha consentiro di sviluppare un protocollo multi-analitico, non distruttivo o micro-invasivo, basato su tecniche come μ-Raman, FT-IR, μ-XRD e SEM-EDS. Il protocollo è stato applicato allo studio di 372 reperti, oltre a campioni di corallo moderno, nell'ambito del progetto di dottorato della scrivente che culmina in questa pubblicazione.
Lo studio ha inoltre incluso un approccio archeo-tecnologico, con sperimentazioni pratiche di produzione e decorazione, rivelando informazioni preziose sulla tecnologia dell'epoca, i materiali utilizzati e i legami culturali tra le società antiche dell'Europa settentrionale e meridionale.

Overview

In northern Italy, in the Early Iron Age, particularly from the 7th century BCE, Mediterranean red coral is widely used in the production of bronze ornamental and dress accessories, such as pendants and fibulae. It appears in a range of forms, from the simplest use of raw coral branches to more complex applications as inlays in technologically sophisticated decorations. Both the decorative insets and the coral branches generally display a whitish or whitish-to-pink hue, rather than the characteristic red colour.
Leech fibulae with insets (Fig. 1) are the most widespread artefacts. Quite common from the mid-6th to the mid-5th century BCE (Schindler, de Marinis 2000), these objects are characterised by a leech-shaped bow, generally containing a terracotta core, and a long foot ending in a small globe with a vase or truncated cone-shaped terminal. Their decoration is defined by the presence of small circular perforations filled with a whitish-to-pink material, arranged in multiple rows on the bow (the number of which increases as the type evolves over time) and, in later phases, also on the small globe.

Figure 1. Archeomuseo 2.0, Arona, Motto Lagone, Mercurago, tomb 1: leech fibula with circular insets, first half 5th century BCE (ph. Berruto; metric reference 1 cm).

Archaeological literature has traditionally identified this light-coloured material with *Corallium rubrum*, assumed to have been whitened by the effects of time. However, scientific analyses addressing this issue are scarce and have generally been conducted using outdated methods (de Marinis 2000; Mangani 2016; Perrin 2000;

Schvoerer *et al.* 2000). In the case of raw coral, macroscopic and microscopic observation of the surface typically allows for a general characterisation, but in the case of small circular intarsia, even of very limited size (Ø ≈ 2 mm for leech fibulae), a more in-depth archaeometric investigation is required. Moreover, whitish or grey inlays can be made of different materials, such as bone, ivory, pressed carbonate powder, enamel, carbonate rocks, kaolin or talc.

Red or reddish inlays may also consist of materials such as enamel, amber, carnelian, minium (Bente *et al.* 2015a) or dyed white stony corals. In addition, a replacement of coral by ZnO (zincite) and TiO_2 (anatase) was identified in an Iron Age fibula from central Germany (Hänichen), probably inserted during a restoration around 1900 (K. Bente, personal communication). Therefore, artefacts macroscopically and archaeologically identified as coral must be systematically verified using a combination of advanced archaeometric methods.

Previous studies on Early Iron Age ceramic decorations from the Golasecca area, filled with whitish material, have demonstrated the use of a synthetic pigment obtained through the calcination of bones (the so-called "Bone White"), revealing the presence of biogenic hydroxyapatite. This contrasts, for example, with ceramics from earlier periods (Neolithic and Bronze Age), in which a different white agent – talc – was used (Berruto *et al.* 2014; Giustetto *et al.* 2012; 2013).

Enamel should also be considered among the possible materials used to replace coral, as attested in Late Iron Age La Tène artefacts from the transalpine area. The use of red enamel, probably an imitation of coral, is well documented among the transalpine populations already before the 4th century BCE. Two techniques are documented: glass coatings fused onto metal substrates, and the application of decorative moulded glass fragments to artefacts, often secured with rivets (Early La Tène period torcs and brooches: Zlámalová Cílová *et al.* 2024). Red enamel, however, does not whiten over time; therefore, it is unlikely to have been used in the decoration of Early Iron Age Cisalpine artefacts.

Therefore, this study proposes a shift in perspective for the investigation of these archaeological materials, which are often studied primarily through traditional typological and chronological approaches. Such an approach does not allow for a comprehensive understanding of the technological development of ancient societies, the specific production techniques of different artefacts, and, consequently, the system of cultural interactions in which these societies were embedded. In contrast, an archaeometric and multi-analytical approach is innovative and, by complementing traditional methods, can provide a more accurate analysis and a deeper understanding of the relationships between ancient societies in central and southern Europe.

The archaeological record considered includes bronze ornaments from northern Italy with presumed coral decorations, primarily dating to the Iron Age (mainly the Early Iron Age), with a particular focus on leech fibulae with insets. For the sake of completeness and comparison, other artefacts of similar chronology with presumed coral elements have also been examined.

Based on the results of some preliminary investigations, conducted since 2014 by the University of Turin in collaboration with the former Soprintendenza per i Beni Archeologici del Piemonte (Berruto *et al.* 2018; Cicolani, Berruto 2017) and on an extensive bibliographic research, a multi-analytical, non-destructive (or only micro-destructive) protocol has been developed to identify the presence of Mediterranean red coral. It involves the synergic combination of vibrational spectroscopies (μ-Raman and FT-IR), micro-X-ray-diffraction (μ-XRD) and scanning electron microscopy with microprobe (SEM-EDS). These techniques were selected based on the primary archaeological questions, namely the identification of the whitish raw material and the possible presence of binders. The choice was also determined by the nature of the samples, i.e., archaeological artefacts whose integrity must be preserved. Analyses were therefore conducted using entirely non-destructive methods, or, when artefacts could not be moved to laboratories, minimally invasive micro-destructive techniques involving the extraction of micro-samples invisible to the naked eye.

As part of this project, 372 archaeological artefacts were examined using both traditional archaeological and archaeometric, as well as technological approaches (Berruto 2025). Compared to the literature survey conducted during the early stages, only a portion of these artefacts could be studied in depth, due to bureaucratic obstacles and/or delays.

These archaeological finds come from a wide

geographical area and are held in different institutions (e.g., local and national museums, Soprintendenze Archeologia Belle Arti Paesaggio – SABAP), each subject to different protection regulations. Nevertheless, the analysed record is exhaustive with respect to the total number of finds, particularly regarding the main types. The same protocol was also applied to a set of modern coral samples for comparative purposes.
The research also included an experimental technological study, occasionally supported by radiography to investigate aspects of the production processes. This approach involved experimental tests focused on the manufacture and decoration of newly crafted artefacts, providing valuable insights into the production technology of these objects and the use of coral. These results are largely consistent with the data obtained from the archaeometric analyses. This broad-ranging approach, combining archaeological, archaeometric, and technological perspectives, enabled a comprehensive overview of these artefacts. It provided information about the raw material used in the whitish decorations, the binders, the composition of the metal alloy and the technological processes.

Abbreviations

The abbreviations used in this volume, particularly in the lists of findings for the various types, are explained in detail below:

A-MANM	Ancona - Museo Archeologico Nazionale delle Marche
A-MAA	Arona - Museo Archeologico del Comune di Arona
A-MAN	Altino - Museo Archeologico Nazionale
B-CG	Bellinzona - Castelgrande
B-MC	Belluno - Museo Civico
B-MA	Bergamo - Museo Archeologico
B-MVF	Berlin - Museum für Vor- und Frühgeschichte
B-IB	Borromeo Isola Bella
Bra	Bra - Museo civicio di Palazzo Traversa
Bre	Brescia - Museo di Storia Naturale
BSV	Bagnolo San Vito - Antiquarium
C-ADGH	Chur - Archäologischer Dienst Graubünden Haldenstein SLM
C-CPD	Corbetta - Collezione Pisani Dossi
C-MC	Como - Museo Civico Giovio
C-RM	Chur - Rätisches Museum
CT-GSAC	Castelletto Ticino - Sede GSAC
E-MNA	Este - Museo Nazionale Atestino
G-MA	Gavardo - Museo Archeologico
G-MPSA	Gorizia - Museo Provinciale di Storia ed Arte
G-MPSA	Gorizia - Museo Provinciale di Storia ed Arte
G-MAP	Genova - Museo Archeologico Pegli
G-SABAP	Genova - Soprintendenza Archeologia Belle Arti Paesaggio
I-TLF	Innsbruck - Tiroler Landesmuseum Ferdinandeum
L-M	Lugano - Museo
L-MCA	Locarno - Museo Civico Archeologico
M-M	Marzabotto - Museo
MAM	Mel - Museo Archeologico di Mel
M-MCA	Milano - Museo Civico Archeologico Castello Sforzesco
M-MC	Merano - Museo Civico
M-MN	Mantova - Museo Nazionale
M-PS	Munchen - Prahistorische Staatssamml
M-MSNA	Montebelluna - Museo di Storia Naturale ed Archeologia
MRT	Musei Reali - Museo di Antichità di Torino

M-SABAP	Milano - Soprintendenza Archeologia Belle Arti Paesaggio
MUCIV	Roma - Museo delle Civiltà, Museo Pigorini
N-MC	Novara - Museo Civico
NA	Numana - Antiquarium
O-MCF	Oleggio - Civico Museo Fanchini
P-MC	Padova - Musei civici
P-SABAP	Padova - Soprintendenza Archeologia Belle Arti Paesaggio
P-UNIPD	Padova – Università
PV-MC	Pavia - Musei Civici
P-MAVT	Pianello V.T. - Museo Archeologico della Valle Tidone
P-M	Pilsen - Museum
RE-MGC	Reggio Emilia - Museo Gaetano Chierici di Paletnologia
SC-CMA	Sesto Calende - Civico Museo Archeologico
S-H	Singen - Hegaumuseum
S-VM	Slaný - Vlastivědné muzeum
SC-MC	Sesto Calende - Museo Civico
S-CS	Stenico - Castello di Stenico
S-MA	Sulmona - Museo Archeologico
SGL-MAN	Paris - Saint-Germain-en-Laye - Musée d'Archeologie Nationale
SL-CV	Somma Lombardo - Castello Visconti
T-CB	Trento - Castello del Buonconsiglio
T-MC	Treviso - Museo Civico
T-MCSA	Trieste - Museo Civico di Storia ed Arte
UNIPD	Padua - University
V-MC	Varese - Museo Civico Villa Mirabello
V-MCSN	Verona - Museo Civico di Storia Naturale
V-MCA	Verucchio - Museo Civico Archeologico di Verucchio
V-MSN	Wien - Naturhistorisches Museum
MANL	Vigevano - Museo Archeologico Nazionale della Lomellina
WL	Stuttgart - Württembergisches Landesmuseum
Z-LM	Zurich - Landes Museum

Country abbreviation:

A	Austria
I	Italia
F	France
G	Germany
Sl	Slovenia
Sw	Switzerland
Li	Liechtenstein
Po	Poland

Region abbreviation:

A	Valle d'Aosta
ER	Emilia-Romagna
FVG	Friuli-Venezia Giulia
LI	Liguria
LO	Lombardy
M	Marche
P	Piedmont
T	Trentino-Alto Adige
TO	Toscana
U	Umbria
V	Veneto

Considered abbreviation:

A	Analysed
N	Not searched
L	Looked
M	Missing, impossible to found

2. Corals. Biology and History

Abstract

Fin dall'antichità, il corallo ha suscitato fascino e mistero per la sua origine incerta, essendo ritenuto ora minerale, ora vegetale o animale. Autori come Teofrasto, Dioscoride e Plinio ne descrivono l'aspetto e le proprietà, anche collegandolo a miti come quello di Medusa. Ritenuto in possesso di poteri magici e terapeutici, veniva usato come amuleto e medicinale. Solo nel XVIII secolo si dimostra scientificamente la sua natura animale, grazie a studiosi come Marsigli e Peyssonel. Lamarck lo classifica come *Corallium rubrum* nel 1816. Nel XIX secolo Lacaze-Duthiers fonda la scienza moderna sui coralli preziosi, con la pubblicazione di un volume dedicato a questo materiale. Le ricerche si interrompono nella prima metà del XX secolo a causa delle guerre mondiali e riprendono in seguito, anche grazie a nuove tecniche subacquee.
I coralli sono un ampio gruppo di organismi, gli cnidari, principalmente marini, alcuni dei quali con scheletri minerali (cornei, fosfatici o carbonatici) secreti dal cenosarca.
Gli Ottocoralli, come le gorgonie e il corallo rosso (*Corallium rubrum*), hanno piccoli polipi a otto tentacoli connessi dal 'coenenchima'. Il corallo rosso mediterraneo è l'unico dotato di scheletro rigido, di colore rosso intenso. Vive in ambienti poco illuminati tra pochi e 400 metri di profondità e cresce lentamente. Il suo scheletro è usato in gioielleria ed è composto da calcite magnesiaca e pigmenti organici, la cui alterazione può sbiancare il materiale.
Nel Mediterraneo esistono anche coralli bianchi di acque profonde (Cold-Water Corals), relitti post-glaciali, oggi spesso in stato di degrado. La loro pesca non era compatibile con le tecniche antiche (ad esempio l'apnea), ma frammenti morti potevano essere raccolti e utilizzati. Fonti storiche e ritrovamenti archeologici (tra i quali Tas Silg a Malta) attestano il possibile uso di questi coralli.

Introduction

The term "coral" refers to a large group of marine organisms, the cnidarians, some of which possess mineralised skeletons. Belonging to the *phylum* Coelenterates, they are almost exclusively marine, except for a few freshwater species (i.e., the *Hydrozoa*). Coelenterates have a sack-shaped body with a cavity, the *coelenteron*, from which the *phylum* derives its name. Their reproductive cycle alternates between fixed and mobile forms, polyps and jellyfish. The fixed forms may produce skeletons composed of corneous or phosphate substance, aragonite or calcite. In the *Hydrozoa* and *Anthozoa*, the sessile, skeleton-producing form predominates, leaving abundant fossil traces, whereas in the *Scyphozoa*, fossil evidence is sporadic (D'Arpa, Di Patti 2006).
Corals include both solitary and colonial species. In colonial forms, the skeleton is secreted by the *coenosarc*, a soft tissue that occupies the spaces between individuals. The corals involved in reef construction belong to the *Anthozoans* and possess skeletons composed of either chitin or calcium carbonate. They are divided into classes, including the *Octocorals* and the *Zoantharians*. The latter encompasses *Tetracorals* and *Hexacorals*, among which the most significant are the *Coelenterates* (D'Arpa, Di Patti 2006).
Hexacorals (*Scleractinia*) first appeared in the Mesozoic, particularly in the Middle Triassic (250 million years ago), and continue to exist today. The last coral reefs in the Mediterranean date to the Middle Miocene (20 million years ago). They grow with the formation of six septa or multiples thereof. They may be solitary, consisting of a single polyp, as in sea anemones and cerianthids, or colonial, formed by multiple interconnected polyps, as in sea daisies and black corals. Madrepores can be either solitary or colonial, depending on the species. They secrete a robust and complex Ca-carbonate skeleton of variable morphology. In colonial forms, the growth rate of the calcareous skeleton is very slow. Hexacorals are among the main reef-builders, partly due to their symbiotic relationship

with the unicellular algae *Zooxanthellae*. At present, there are virtually no reef builders in the Mediterranean Sea, except for *Cladocora coespitosa*, which still builds relatively large bushes, and *Astroides calycularis*, an encrusting madrepore from the southern Mediterranean that produces rounded pillows (D'Arpa, Di Patti 2006; Trainito, Baldacconi 2016). However, relict colonies of scleractinian corals have recently been documented in the Mediterranean basin, including *Desmophyllium diantus*, *Madrepora oculata*, *Desmophyllum Pertusum*, *Dendrophyllia ramea* (D'Arpa, Di Patti 2006; Freiwald *et al.* 2009; Taviani *et al.* 2005).

Octocorals (or Alcyonarians) have very small eight-tentacled polyps, always associated in colonies. The tissue connecting the polyps within the same colony is called *coenenchyme*. Among Octocorals, the *Gorgoniaria* include the Gorgonians and *C. rubrum*, as well as the *Tubipora musica*. These organisms do not always possess a rigid skeleton; some species secrete small calcareous elements known as *sclerites*. Gorgonians also produce a proteinaceous skeleton composed of gorgonin, which is rigid yet flexible and may be partially calcified or not, allowing colonies to reach large sizes. The Mediterranean red coral is the only gorgonian that produces a calcite skeleton, hard and branched (D'Arpa, Di Patti 2006; Harmelin 2000; Taviani 1997; Trainito, Baldacconi 2016).

2.1. Skeletal mineralisation in corals

Most mineralised corals belong to the hexacorals, which have a calcareous skeleton based on aragonite – the least stable phase of Ca-carbonate (Fig. 2). In contrast, the Mediterranean red coral, *C. rubrum*, is an octocoral with a calcite-based calcareous skeleton and a bright red colour (Taviani 1997). The mineralised skeleton of corals can consist of calcite and/or aragonite, two polymorphs of Ca-carbonate ($CaCO_3$) that sometimes contain small amounts of Mg^{2+} in the crystal lattice (Hasegawa *et al.* 2012, p. 1; Rahman *et al.* 2011). Carbonate ions (CO_3^{2-}) are the building blocks of these minerals, but the precipitation of a given polymorph depends on several factors. Although some crystallisation mechanisms have been described, a complete understanding of the carbonate precipitation in corals remains limited (Amos *et al.* 2010; Belcher *et al.* 1996; D'Souza *et al.* 1999; Stephenson *et al.* 2008). In the marine environment, at different depths, the concentration of CO_3^{2-} can decrease below thermodynamically favourable levels for the formation of Ca-carbonate minerals. The 'aragonite saturation horizon' (ASH) is defined as the depth at which the saturation state of aragonite (Ω_{Ar}) is < 1 and its dissolution is favoured. This depth has risen significantly over the past centuries (Chung *et al.* 2003; Feely *et al.* 2004; 2008; Sabine *et al.* 2002). In addition, carbonate

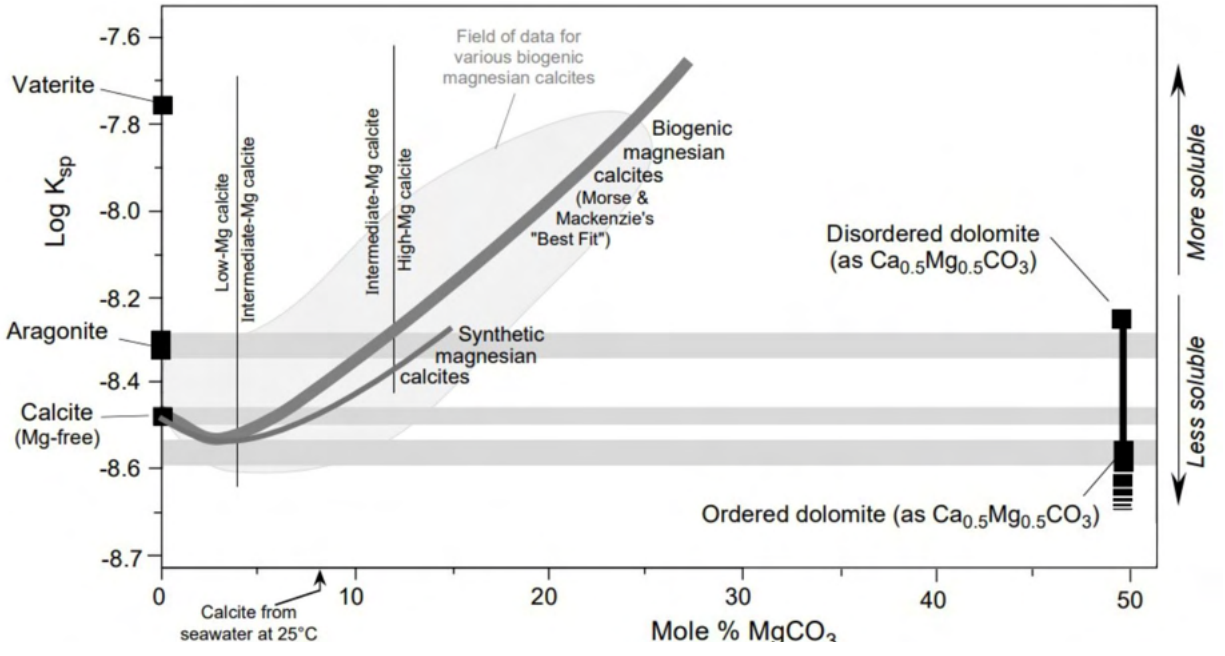

Figure 2. Solubility of common carbonate minerals (after Railsback 2006).

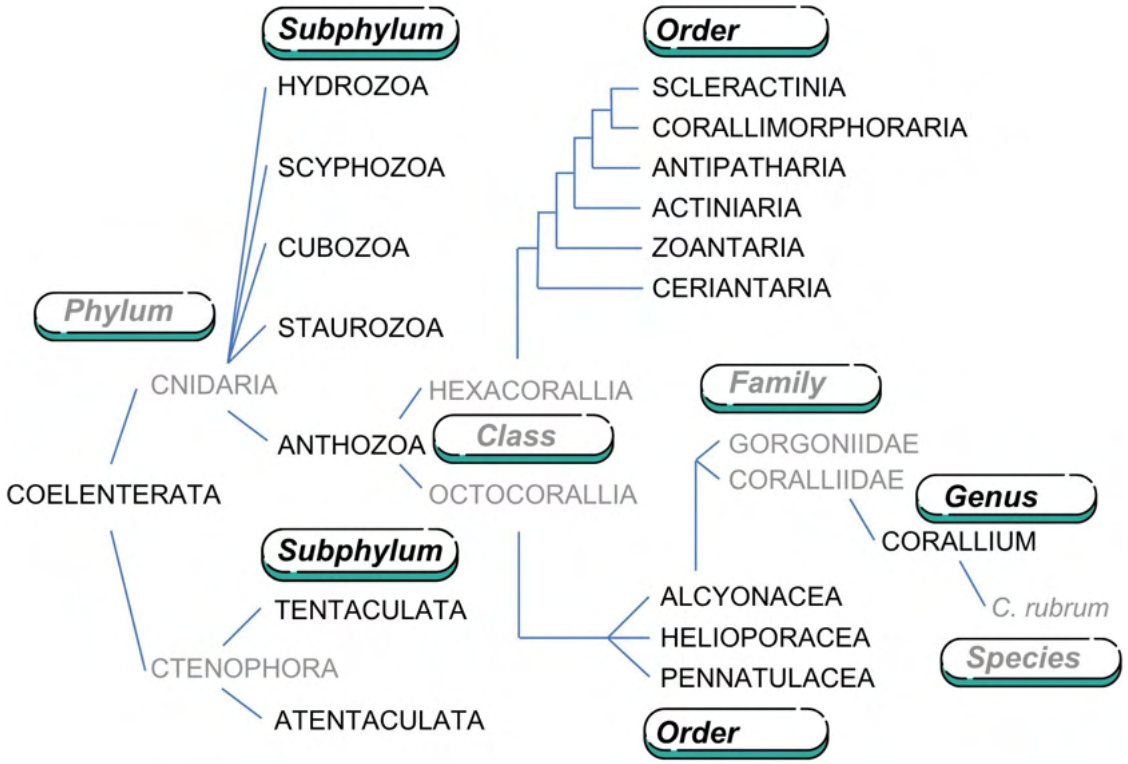

Figure 3. Phylogenetic family tree of *Corallium rubrum*, in relation to other corals (modified after D'Arpa, Di Patti 2006; Harmelin 2000; Quek, Huang 2022; Trainito, Baldacconi 2016; *WoRMS Editorial Board* 2024).

phases tend to become more soluble in colder environments and at higher pressures, making them even more vulnerable to dissolution in deep oceans (Mucci 1983; Acker *et al.* 1987). In the past, coral skeletal composition in the oceans alternated between calcite and aragonite dominance, depending on the concentrations of dissolved Mg^{2+} and Ca^{2+}, the ratio of which is influenced by variations in seafloor spreading rates at mid-ocean ridges. During crystallisation *in vivo*, Mg^{2+} inhibits calcite formation producing metastable, Mg containing calcite meta-crystals. Sometimes aragonite coexists, together with calcite (Davis *et al.* 2000). Historically, a period of 'aragonite seas' (Stanley, Hardie 1998) and two distinct periods of 'calcite seas' have been reported (Sandberg 1983).
Today, the Mg^{2+}/Ca^{2+} ratio is 5:1, thus favouring the formation of aragonite, which is more soluble than calcite. Many tropical and cold-water hard corals, pteropods and molluscs form needle-shaped skeletons consisting exclusively of this material. In contrast, soft corals only form calcite crystals without aragonite. Recent studies claim that the secretion of extracellular proteins may be the key factor in inducing calcite precipitation in soft corals, regardless of the chemical conditions of the surrounding seawater (Rahman *et al.* 2011).
The presence of coral in archaeological finds is generally referred to *C. rubrum*. However, other types of coral from relatively recent deposits may also have been used since antiquity (Taviani 1997). The possible use of fossil materials can be investigated through the analysis of Sr, B, O, and C isotopes (Bente *et al.* 2023).

2.2. Mediterranean red coral

The phylogenic position of the Mediterranean red coral is summarised in: Phylum *Cnidaria;* Subphylum *Anthozoa;* Class *Octocorallia;* Order *Alcyonacea;* Family *Corallidae;* Genus *Corallium;* Species *rubrum* (Fig. 3) (D'Arpa, Di Patti 2006; Harmelin 2000; Quek, Huang 2022; Trainito, Baldacconi 2016; *WoRMS Editorial Board* 2024). *C. rubrum* grows in poorly illuminated environments, such as caves and steep walls, and is difficult to supply (Cattaneo-Vietti, Cicogna 1994; D'Arpa, Di Patti 2006; Taviani 1997). The bathymetric range in which it can be encountered is vast, extending from a few metres below the surface in caves, to environments some

300 metres deep on rocky canyon walls. It has also recently been collected at a depth of 400 metres in the Sicilian channel (Cattaneo-Vietti, Cicogna 1994; Harmelin 2000).

Red coral is a colonial animal, meaning that each branch hosts numerous individual organisms, the polyps, each of which is independent in terms of nutrition and reproduction. Their body is composed of three layers: the outer epiderm, the inner gastroderm, which lines the intestinal cavity, and the mesoglea, the middle layer. The intestinal cavity has only one external opening, the mouth, surrounded by tentacles (Cattaneo-Vietti, Cicogna 1994; Harmelin 2000).

The polyps are joined by channels, the gastrodermal tubes, through which the products of metabolism and information circulate. They are included in a common mass, called the coenenchyme, consisting of a thick mass of mesoglea. The surface of the entire colony is covered by a layer of ectoderm that connects with the ectoderm of the polyps. The coenenchyme grows around a robust calcareous skeleton, called sclerasse. This grows in an arborescent manner, under the influence of multiple micro-environmental parameters, including hydrodynamics, trophic inputs, light intensity and sedimentation, to which it is particularly sensitive. *C. rubrum* therefore tends to grow mainly on vertical walls or rocky rooftops, with geocentric growth. Colonies are on average 10 or 15 cm high; their growth rate is quite slow: 2-8 mm per year. Colouration also varies depending on the area and depth of growth; very rare albino colonies are also attested (Cattaneo-Vietti, Cicogna 1994; Harmelin 2000). The skeleton of *C. rubrum* comprises a skeletal axis and various sclerites, dispersed in the mesoglea. The axis is formed by the sclerites; each is surrounded by a small epithelium, which produces calcite. The first outline of the axis appears after six months and grows by aggregation of the sclerites themselves in a concentric manner (Harmelin 2000, p. 285). The part of *C. rubrum* used in jewellery is the red-coloured skeleton, once the coenenchyme has been removed. Beneath this layer, the coral surface displays a characteristic canalicular morphology, oriented parallel to the axis of branch growth and reflecting the traces of the animal's gastrodermal canals (Fig. 4; Fürst *et al.* 2016).

The skeleton of *C. rubrum* is mainly composed of Ca-carbonate ($CaCO_3$) in the form calcite, with a varying content of Mg^{2+} in the crystal lattice and some trace elements. The Mg-content in high-magnesian calcite (HMC) varies between 8 and 15 mol% $MgCO_3$. The organic matrix of the axial skeleton consists of acidic proteins and sugars, together with a small amount of organic pigments, polyenes or carotenoids with different numbers of double C=C bonding. The skeleton has a bright red hue, due to organic pigments. The chemistry of these pigments is still debated: some authors report presence of carotenoids while others identify them as a mixture of partially/completely demethylated polyenes (Barnard, de Waal 2006; Bente *et al.* 2017; Bergamonti *et al.* 2011; 2013; Berruto *et al.* 2023a; Brambilla *et al.* 2012; Dauphin 2006; Fan 2018; Fernandes *et al.* 2015, p. 438; Fürst *et al.* 2016; Grillo *et al.* 1993; Hasegawa *et al.* 2012; Kaczorowska *et al.* 2003; Kiefert, Karampelas 2011; Kupka *et al.* 2009; Macchia *et al.* 2016; Maia *et al.* 2010; Rahman *et al.* 2011; Smith *et al.* 2007; Urmos *et al.* 1991; Vielzeuf *et al.* 2008; 2013).

When red coral undergoes alteration, its colour tends to fade gradually, possibly as a result of the encapsulation of organic pigments within the axial skeleton (Fürst *et al.* 2016). This whitening makes primary *C. rubrum* more difficult to identify, owing to the degradation of both organic pigments and carbonates. When exposed to burning, coral turns grey (Mangani 2016; Perrin 2000). In addition, coral is easily confused with other materials, such as ivory, bone, shell, limestone, or carnelian (chalcedony).

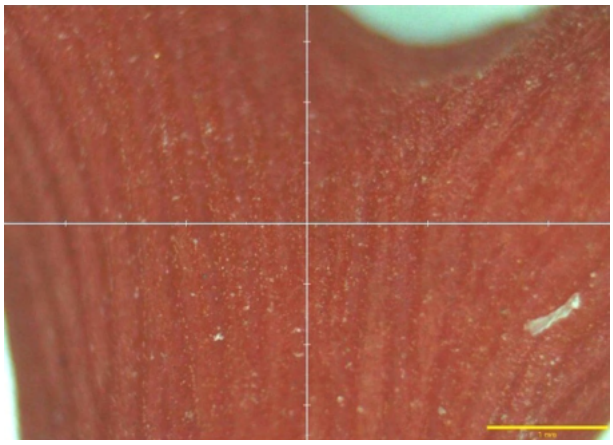

Figure 4. Detail of the canalicular surface of a sprig of *C. rubrum* under the optical microscope (ph. Berruto; metric reference 1 mm).

C. rubrum can be considered an Atlantic-Mediterranean species, mostly concentrated in the western and central Mediterranean. In the

Atlantic Ocean, it occurs on the rocky seabed off southern Portugal, in the area of Lagos, where it was exploited between the 15th and 18th centuries. It is also found along the Atlantic coasts of Morocco, where exploitation has been intensive in recent years. Its presence in the archipelagos of Madeira and the Canary Islands remains uncertain. Red coral has been recorded in the Strait of Gibraltar and the Alboran Sea (approximately 120 km southwest of Almería, Spain), an area of recent exploitation. In the Mediterranean, red coral occurs along the coasts of the Maghreb, with Tunisia and Algeria hosting large deposits. Its presence off the coast of Libya has never been reported (Cattaneo-Vietti, Cicogna 1994; Harmelin 2000).

In the Mediterranean Sea, it is found mainly in the western basin. In the northern part of this basin, coral can be found on almost all rocky coastlines. The most renowned corals are those of Catalonia, Sardinia, Corsica and the Hyères Islands (French Rivera). The Marseille region in particular reveals an abundant presence, even at shallow depths of less than 10 meters in caves. Coral is also well known in Liguria and on the coasts of the Tyrrhenian Sea, where the deposits are more superficial, at a depth of 30 or 40 metres, and heavily overexploited. In the eastern Mediterranean, by contrast, coral occurs only sporadically (Harmelin 2000).

In the Adriatic Sea, red coral occurs along the coasts of Croatia, Albania, and the Ionian Islands; along the Italian coast, it is found only as far south as Apulia, below the Gargano Peninsula. There are no records of exploitation of these deposits in antiquity. In Greece, red coral has been reported from very few localities (Cattaneo-Vietti, Cicogna 1994; Schmid-Sikimić 2000a) (Fig. 5a).

At the end of the 19th century, huge beds of sub-fossil coral with by a pinkish hue were discovered at a depth of 300 and 200 metres in Sciacca, in the Strait of Sicily, probably formed as a result of seismic movement linked to volcanic activity (Harmelin 2000). Due to the considerable depth of the outcrop, they cannot be considered potential sources of supply in antiquity. Mediterranean red coral is now a protected

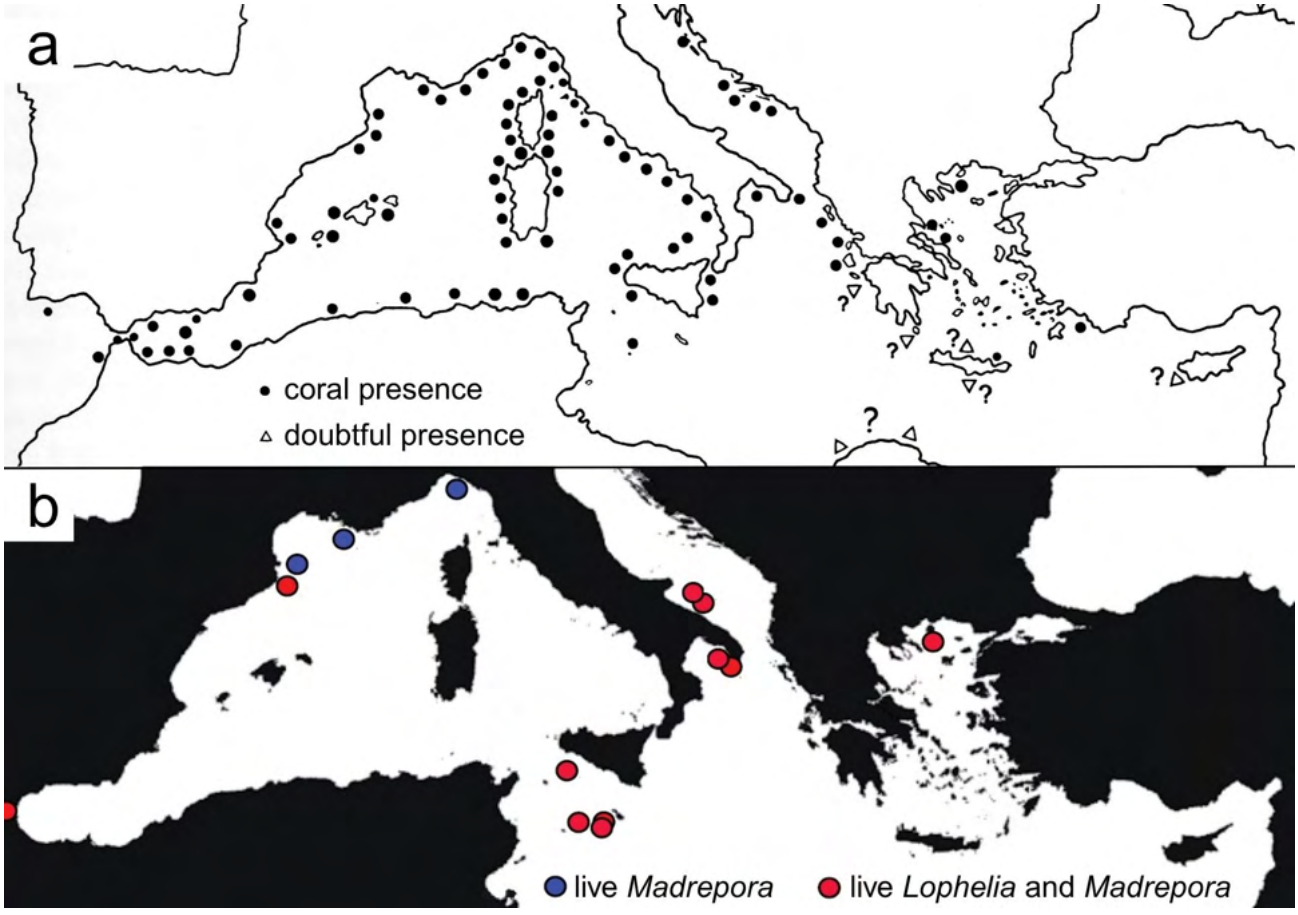

Figure 5. a) Geographical distribution of *C. rubrum* (modified after Harmelin 2000, p. 15, fig. 4); b) Distribution of living colonies of deep white corals (modified after Freiwald *et al.* 2009, fig. 1).

species. In antiquity, it was harvested using the *ingegno*, or "St Andrew's cross," from a boat – a method that caused considerable damage, as for every 10–20 kg brought on board, often more than twice that amount remained broken and ruined on the seabed. This technique allowed coral to be collected at depths of up to 200 meters (Cicogna 2000, p. 286). Today, coral is harvested by divers, who may also remove portions of the bedrock, but their methods are more selective and considerably less destructive (Filocamo 2000).

2.3. White corals in the Mediterranean Sea

In most oceans, at cold-water depths ranging from 200–300 to 3,000–4,000 metres, shoals of white corals (*Scleractinia*), commonly referred to as cold-water corals (CWC) or "madrepores," are widespread. They are also present in the Mediterranean Sea (Fig. 5b), at depths between 180 and 1100 m, with sporadic colonies generally in a state of decay, relicts from the Last Ice Age (30,000-12,000 years ago), along with, of course, many fossils. The Mediterranean's white corals are the result of the postglacial decline in benthic colonisation of the basin following the reflooding of the Atlantic through the Strait of Gibraltar, after approximately 5.3 million years ago (D'Arpa, Di Patti 2006; Freiwald *et al.* 2009; Taviani *et al.* 2005).

Reports on the presence of deep white corals generally rely on data obtained from scientific and fishing dredge and trawl hauls, although recent studies have increasingly employed remotely operated vehicles (ROVs). Cold-water corals (CWCs) in the Mediterranean can be found in two types of areas: provinces and connectivity sites. Provinces correspond to the path of the mid-Levantine water in the northwestern and central parts of the basin, while connectivity sites are smaller, less complex areas where these corals still persist (e.g., the Levante Ligure canyon). CWCs include solitary species, such as *Desmophyllium diantus* (or *Desmophyllium cristagalli*), and colonial species. For the colonial species in the Ligurian and Tyrrhenian Seas, *Madrepora oculata* reefs have been found at a depth of 450 metres, and *Desmophyllum pertusum* (or *Lophelia pertusa*) sprigs in the Sicilian Channel, also identified in the Gallic Gulf, on the coasts of Puglia and in Greece (Fig. 5b) (Angiolillo *et al.* 2023; D'Arpa, Di Patti 2006; Freiwald *et al.* 2009; Schembri *et al.* 2007; Taviani *et al.* 2005; Zibrowius, Taviani 2005).

The presence of CWCs has also been recently documented in the Levantine Mediterranean Sea. *Dendrophyllia ramea* occurs in this area and has also been reported along the south Mediterranean coasts on rocky slopes and cliffs, in the Ionian Sea on soft substrates, and in the Alboran Sea on shallow rocky bottoms (Angiolillo *et al.* 2022; Orejas *et al.* 2019; Salvati *et al.* 2004).

The presence of white coral in the Mediterranean Sea is of particular interest for the study of whitish coral decorations on the metal ornaments common in Early Iron Age northern Italy. This material may have been traded in a manner similar to *C. rubrum* and used in the production of these artefacts, producing a different colour effect in relation to the bronze.

However, the bathymetric distribution area of these corals is not compatible with free-diving fishing methods that were likely used in the Iron Age. Nevertheless, some evidence suggests that their use in antiquity cannot be entirely ruled out: dead fragments have been recovered in fishermen's nets in the Ligurian Sea, and historical sources from western Provence (13th – 16th centuries CE) document the trade of white coral alongside red coral, primarily for pharmaceutical purposes (Chazottes 2018). The Greek botanist Dioscorides, in the 1st century CE, mentions red coral as well as white, black, and purple varieties (Faget, Vielzeuf 2018). Archaeological evidence records the presence of *Dendrophyllia ramea* in Malta, at the sanctuary of Tas Silg, interpreted as a votive deposition dating to the 4th and 3rd centuries BCE and again during the late Republican and early Imperial Roman period (Quercia 2008).

As hexacorals, *Scleratinia* are characterised by a calcareous aragonite skeleton (Taviani 1997). In principle, the distinction between the aragonitic skeleton of these madrepores and the calcitic skeleton of *C. rubrum* can be achieved using various analytical techniques (e.g., X-ray diffraction, Raman spectroscopy, or infrared spectroscopy). However, aragonite may undergo post-mortem diagenetic transformation into secondary calcite within a few thousand years, either through dissolution and redeposition or by direct inversion (Budd 1988; Hall, Kennedy 1967). Under specific conditions, such as reducing environments, the preservation of aragonite

Figure 6. Coral fishing by free diving - Stradano, 16th century CE - engraving (modified after Tagliente 2006, p. 15).

is possible, as demonstrated by studies of certain Tertiary and Mesozoic fossils (Hall, Kennedy 1967). However, such conditions do not correspond to those of an archaeological context. Consequently, any *madrepores* used in the decoration of archaeological finds would likely no longer retain an aragonite-based skeleton, but instead be calcite-based, making differentiation from the *C. rubrum* skeleton more difficult. In the case of burnt materials, such as those associated with funerary practices (e.g., cremation), polyenes and Mg-containing calcites undergo decomposition depending on the temperature. The transformation of metastable aragonite to stable calcite through heating at high temperatures has been widely documented (Parker *et al.* 2010; Yoshioka, Kitano 1985).

2.4. The study of corals: origins and advancements

2.4.1. Coral: myth and magic

Coral has always been shrouded in mystery due to its nature and origin. In antiquity, its classification – whether mineral, animal, or plant – was widely debated, and discussions on this topic continued into the 18th century (Harmelin 2000). Ancient literary sources describe this material as being associated with blood and life, and they discuss its origins (Tagliente 2006).
In 300 BCE, Theophrastus (*De Lapidibus*, fr. 38 W) describes it as resembling a root growing in the sea. In the 1st century CE, Dioscorides (*De Materia Medica*, V, 121, 1-3) referred to it as a "sea bush" that hardens upon contact with air after being removed from the water (Leurini 2000; Weinberg 1994).
Pliny the Elder in the 1st century CE tells of its controversial origin: «coral turns into hard stone after being soft in the sea» (*Naturalis Historia*, XXXII, 11, 22). He also describes coral fishing, which was carried out using two iron arms joined by a central lead pin, to which nets were attached and dragged by boats: «if it is alive, it immediately petrifies and can be caught and torn away with nets or severed with a sharp iron instrument» (*Naturalis Historia*, Liber XXXII, 11, 22; Mastrocinque 2006; Tagliente 2006) (Fig. 6).

> forma est ei fruticis, colos viridis. bacae eius candidae sub aqua et molles, exemptae confestim durantur et rubescunt qua corna sativa specie atque magnitudine. aiunt tactu protinus lapidescere, si vivat; itaque occupari evellique retibus aut acri ferramento

> praecidi, qua de causa curalium vocitatum interpretantur. probatissimum quam maxime rubens et quam ramosissimum nec scabiosum aut lapideum aut rursus inane et concavum (Pliny the Elder, *Naturalis Historia*, XXXII, 11, 21).

The ancient belief that coral originated from the petrification of sea plants is linked to the myth of Medusa, a figure from Greek mythology who lived on an island at the edge of the world and was the daughter of the sea gods *Ketos* and *Phorkys*. Medusa had the power to turn anyone to stone with her gaze. Ovid mentions her in the *Metamorphoses* (IV liber, v. 740-752) and recounts how Perseus, after killing Medusa, paused on his way home to cleanse himself. He carried her severed head in a bag, placing it on reeds so that it would not be ruined. Upon contact with Medusa's blood, the reeds were transformed into coral. The sea nymphs, enamoured with this material, scattered the seeds of the reeds among the waves, thereby spreading it. Pliny also recounts this origin of coral, explaining that it is for this reason that it is called "Gorgia" or "Gorgonia" (Leurini 2006, pp. 85-86; Mastrocinque 2006; Tagliente 2006; Purpura 2005).

> Ipse manus hausta victrices abluit unda, anguiferumque caput dura ne laedat harena, mollit humum foliis natasque sub aequore virgas sternit et inponit Phorcynidos ora Medusae. virga recens bibulaque etiamnum viva medulla vim rapuit monstri tactuque induruit huius percepitque novum ramis et fronde rigorem. at pelagi nymphae factum mirabile temptant pluribus in virgis et idem contingere gaudent seminaque ex illis iterant iactata per undas: nunc quoque curalis eadem natura remansit, duritiam tacto capiant ut ab aere quodque vimen in aequore erat, fiat super aequora saxum (Ovidius, *Metamorphoses*, IV, 740-752*)*

Pliny (*Naturalis Historia*, XXXII, 24) reports that coral protected children, safeguarded those going to war, and warded off lightning and typhoons. Similarly, the *Orphic Lithika*, ancient magical-astrological treatises, attribute to coral a variety of protective properties: aiding sailors and merchants, shielding against storms and bad weather, guarding against ghosts, nightmares, spells, envy, traps, and snake venom, as well as influencing matters of love and passion. Medical treatises recognise its astringent and refreshing properties. According to Pliny (*Naturalis Historia*, XXXII, 24), it was used against colic if burnt and drunk with water, or with wine to promote sleep, against fever with water, or as an astringent and anti-inflammatory if used as eye drops. According to Dioscorides, coral is useful against diseases of the urinary tract. Coral was described as having numerous medicinal properties: anti-rheumatic, anti-arthritic, anti-colitic, and anti-dysenteric, as well as diuretic, and particularly useful in ophthalmology for the treatment of cataracts and eye spots. It was also considered beneficial in dentistry – as a whitener and for treating dental trauma – soothing for spleen ailments, effective against papillomas, capable of thinning the blood, and helpful in healing ulcers and scars, as well as promoting sleep. Coral was administered crushed or mixed with liquids such as water, wine, or pomegranate juice, and was also used as ash or in tablet form (Leurini 2000; Marastoni 2006; Tagliente 2006; Ugolini 2006a).

> surculi infantiae adalligati tutelam habere creduntur contraque torminum ac vesicae et calculorum mala in pulverem igni redacti potique cum aqua auxiliantur, simili modo ex vino poti aut, si febris sit, ex aqua somnum adferunt – ignibus diu repugnat –, sed eodem medicamine saepius poto tradunt lienem quoque absumi. sanguinem reicientibus excreantibusve medetur cinis eorum; miscetur oculorum medicamentis, spissat enim ac refrigerat, ulcu cava explet, cicatrices extenuat. (Pliny the Elder, *Naturalis Historia*, XXXII, 11, 24).

Regarding the Iron Age, it is not possible to state with certainty whether coral was attributed an apotropaic function. However, it is noteworthy that finds containing coral in Early Iron Age northern Italy, particularly associated with the Este and Golasecca cultures, are primarily linked to funerary contexts and female burials, according to published literature. The presence of amulets and rough coral branches has also been reported in child burials within these cultures, as well as in Etruria Padana (e.g.,Borgo Virgilio, Arginotto, tomb 5), the Hallstattian area (Spain, Emporion - Gerona: two infantile tombs, Ha D3) and in southern Italy (Foggia, Ordona: two infantile tombs) (de Marinis 2000, p. 172; Fürst 2014, pp. 54-55). This practice is

analogous to the use of coral described by Pliny the Elder in the 1st century CE.

2.4.2. Coral in scientific research: mineral, plant or animal?

Ancient authors were the first to describe coral and debate its mineral or vegetal nature. Theophrastus, a Greek philosopher of the 4th-3rd centuries BCE, was the first to discuss it, including it among stones in his *De Lapidibus*. Later, the Greek Dioscorides of Anazarbus mentions coral in *De Materia Medica*, a text composed around the 1st century CE, with the oldest known copy dating to the 4th century. He questioned its true nature, noting its hardness once removed from the water, yet comparing it to plants. Pliny the Elder, also writing in the 1st century CE, continued to express substantial uncertainty over whether coral was mineral or vegetal (Faget, Vielzeuf 2018; Weinberg 1994).

During the Renaissance, the translation and dissemination of important ancient texts, facilitated by the advent of printing, revived the theories of the Greek and Roman worlds. By the 17th century, scientific research had largely settled on the mineral nature of coral, with few exceptions, building on the studies of naturalists from the previous century. During this period, attempts were also made to explain coral formation, and the myth that coral resulted from the hardening of a soft material in water upon contact with air was debunked by Fabri de Peiresc in 1624 and Paolo Silvio Boccone in 1674. Boccone studied this material extensively and published in his *Recherces et observations naturelles* a theory about its formation, called «juxtaposition», which involves the agglomeration of a sea mineral salt, the «tartre corallin», around a central element, «matière glutineuse semblable de la cire fondue». Boccone's publication compiles a series of letters he wrote to various personalities between 1670 and 1673, along with a few replies. Among these, Jean Swammerdam reports for the first time having observed the sclerites of octocorals.

In the same period, the London Royal Society confirmed coral's classification as a mineral and explained its plant-like morphology as the result of progressive encrustation of a wooden structure by mineral deposits. In 1700, Tournefort addressed the Royal Academy of Sciences in Paris on marine plants, including coral among them, and was the first to describe the larva of *C. rubrum*, although he did not recognise it as such (Faget, Vielzeuf 2018; Weinberg 1994).

It was not until the 18th century that truly scientific research on coral began, with the rise of systematic experimental practice. Ferdinando Marsigli worked in Provence, collecting numerous samples of coral and other marine organisms. In December 1706, he became the first to demonstrate the living nature of Mediterranean red coral by placing a freshly harvested branch in a glass jar of water and observing the presence of white "flowers" supported by a calyx, from which eight rays radiate to form a star. Marsigli is credited with definitively excluding coral from the mineral kingdom and providing the first accurate description of its natural habitat (Faget, Vielzeuf 2018; Weinberg 1994).

In 1723, Jean-André Peyssonel repeated Marsigli's experiment and was the first to identify the animal nature of coral. He described Marsigli's "flowers" as "insects, similar to jellyfish or small octopuses," noting how they leave holes in the red skeleton when removed. Peyssonel's theory initially met with opposition but was ultimately accepted in 1742, when it was included in Réaumur's *Treatise on Insects*. At the same time, Diacinto Cestoni also recognised the animal nature of coral, although his observations went unnoticed. In 1742, Filippo Cavolini, working in the Gulf of Naples, was the first to describe how coral reproduction, observing the expulsion of larvae that settle near the mother colony. Later, in 1760, Jean-Étienne Guettard correctly classified coral as a colonial organism (Faget, Vielzeuf 2018; Weinberg 1994).

In 1758, red coral entered scientific nomenclature with the inclusion of *Madrepora rubra* in Carl Linnaeus's *Systema Naturae*. However, Linnaeus considered its polyps to be plants (*plantae vegetantes floribus animatis*) and did not classify them as animals until 1784, when he included them among the *Vermes*. The first to designate the Mediterranean red coral as *Corallium rubrum* was Jean-Baptiste de Lamarck in 1816 (Weinberg 1994).

In 1860, the French government commissioned Henry de Lacaze-Duthiers to investigate the methods, seasons, and conditions most favourable for red coral fishing, dispatching him on a mission to Algeria. This assignment was motivated by the need to establish a reliable scientific basis for regulating the exploitation of this resource.

In 1864, H. de Lacaze-Duthiers published his influential work *Histoire Naturelle du Corail*, which laid the foundations of modern scientific research on precious corals. In this study, he provided a detailed account of their geographical distribution, ecology, anatomy (recognizing the presence of a central axis and sclerites), reproduction, fishing practices, as well as the related industries and trade (Faget, Vielzeuf 2018; Weinberg 1994).

Research on red coral was interrupted in the early 20th century and resumed only after the Second World War, facilitated by the introduction of snorkelling and the use of submarines. In the 1980s and 1990s, research shifted toward conservation-oriented approaches, leading to a substantial increase in publications on this species in the following century (Faget, Vielzeuf 2018; Weinberg 1994).

3. Ornamental Use of Coral from the Neolithic to the 19th century

Abstract

L'uso del corallo è documentato in Europa a partire dal Neolitico (dal IV millennio a.C.). Oggetti ornamentali come perle e pendenti in corallo rosso mediterraneo sono stati rinvenuti in tombe e contesti abitativi. Nell'area egiziana e anatolica, si utilizzavano anche specie del Mar Rosso, spesso legate a culti religiosi. Dall'età del Rame all'età del Bronzo le attestazioni di corallo diventano più sporadiche.
Nel corso dell'età del Ferro (IX – II sec. a.C.), il corallo mediterraneo si diffuse in tutta l'area greca, egizia, fenicio-punica, italica e celtica. Nella Grecia arcaica era presente soprattutto in santuari legati a divinità femminili e marittime. In Egitto fu importato attraverso i commerci greci a partire dal VII sec. a.C. Nel mondo punico il suo uso è documentato nei centri del Mediterraneo occidentale. In Italia, seppur raro, si trova in tombe e luoghi di culto. In Europa continentale il corallo decorava fibule, elmi e ornamenti, simboli di status e potere.
In Italia settentrionale preromana il corallo era ampiamente utilizzato, ad esempio nell'ambito delle culture di Golasecca e veneta, ed è stata ipotizzata una sua provenienza dalla Campania tramite gli Etruschi, sebbene manchino prove dirette di pesca o lavorazione. Il corallo poteva anche arrivare dal Mar Adriatico, dalla Liguria o da Marsiglia, importante centro di pesca e commercio nel VI secolo a.C., mentre a partire dal IV secolo a.C. il commercio si spostò verso la Linguadoca e la Catalogna.
Nel periodo romano il corallo più pregiato proveniva dal Golfo del Leone, dalle isole Eolie, da Trapani e Napoli, mentre Plinio il Vecchio segnala coralli scadenti da Asia Minore e Mar Rosso. Altre aree di esportazione erano l'India, l'Egitto e la Cina. Tuttavia, i riscontri archeologici in queste zone sono scarsi. Nel Medioevo la pesca si sviluppò nel Maghreb, in Sicilia, in Provenza, in Corsica, in Liguria e in Catalogna. In età moderna la produzione si concentrò a Genova e soprattutto a Napoli.

3.1. Neolithic (5th – 4th millennium BCE)

The use of coral in European prehistory is relatively rare, primarily due to the difficulties associated with its procurement (Taviani 1997). Coral is attested from the Neolithic period onward. In particular, by the beginning of the 4th millennium BCE, the use of coral ornaments began to spread notably in the Western Alpine region and Central Europe (Fig. 7; see also de Marinis 1997).
In continental Europe, the earliest evidence consists of three coral beads from the tomb of a young male at the Pully Chamblandes necropolis (Pully, Vaud, Switzerland), dated 4100-3700 BCE (Borrello 2001, p. 192; de Marinis 1997). Between the end of the 5th and the beginning of the 4th millennium BCE, further finds of beads and pendants made of coral and seashells are documented. In Saint Léonard / Carrière (Valais, Switzerland), 10 tubular coral beads were found in an infant burial dated to the Middle Valaisan Neolithic (4320-4050 BCE) (Borrello *et al.* 2012, pp. 74-75). In Gavà (Barcelona, Spain), a burial dating from the end of the 5th to the beginning of the 4th millennium BCE (radiocarbon dating 5220 ± 100 BP) from the Square Mouthed Pottery (SMP) Culture yielded numerous variscite and coral beads: the 241 coral beads are all tubular, ranging in colour from pale pink to orange-red, with some altered specimens appearing whitish (Borrello *et al.* 2012, pp. 76-77). At Cal Rjolic (Olius, Spain), a Middle Neolithic burial from Catalonia has yielded a coral bead, previously identified as magnesite, associated with beads in other materials (Borrello *et al.* 2012, pp. 77-78). At La Serreta (Barcelona, Spain), five cylindrical coral beads have been documented in burials dated between the Ancient Cardial and the Final Veraza periods (Borrello *et al.* 2012, pp. 78-79). Red coral was found in unknown stratigraphic position at the Seuil des Chèvres cave in La Balme-les-Grottes (Auvergne-Rhône-Alpes, Savoy, France): small red coral bead (de Marinis

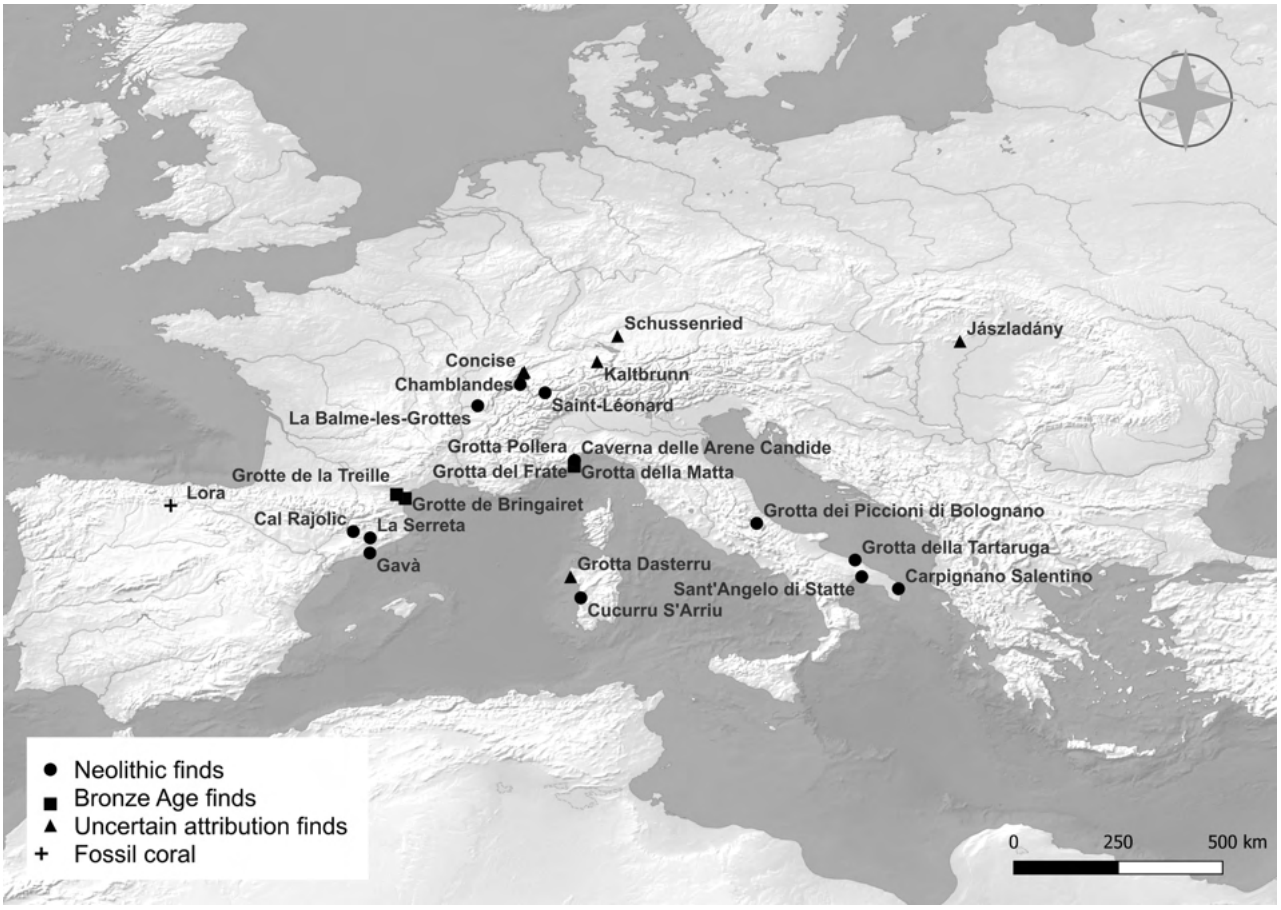

Figure 7. Distribution of coral between the Mediterranean and continental Europe from the Neolithic to the Bronze Age. Elaborated by the author in QGIS 3.40.8 (2025); base map: Natural Earth (Gray Earth raster "GRAY_LR_SR_OB_DR"), public domain.

1997; Borello 2001, pp. 191, 193; Borrello *et al.* 2012, p. 71).

For Neolithic coral ornaments in the Alpine area and Central Europe dating to the 4th millennium BCE, an origin from the west coast of Sardinia has been hypothesised, based on the large size of the Chamblandes beads. This provenance has been linked to the obsidian trade from Monte Arci (Morgongiori), which is well documented in Corsica, southern France and northern Italy in the Middle and Late Neolithic (de Marinis 1997).

At Lora (Burgos, Spain), a megalithic burial site dated to the 4th millennium BCE yielded coral identified as fossil, consistent with the nearby Upper Cretaceous formations at Paramo de Las Tuerces (Palencia, Spain) (Borrello *et al.* 2012, p. 71). This finding raises the question of whether fossil coral may have been used as a raw material wherever it was locally available.

In the north-western Mediterranean, in addition to the Spanish finds mentioned above, red coral is also attested in Italy. The oldest example is a partially worked and pierced sprig of Mediterranean red coral from the levels of the Impressed Ware Culture (5260–5040 BCE) at the Caverna delle Arene Candide. This specimen represents the earliest known occurrence of red coral in the western Mediterranean (Borrello 2001, p. 193; Borrello *et al.* 2012). A more recent example is a pendant from Grotta dei Piccioni di Bolognano, found in a level of the Ripoli Culture (4700–3800 BCE). It consists of a fragment of a coral branch, showing the beginning of a bifurcation and a perforation for suspension. Surface traces indicate that the raw material may have been transported by the sea (Borrello 2001, p. 193; Borrello *et al.* 2012; de Marinis 1997). At Sant'Angelo di Statte, near Taranto, a polished and carved branch of coral was found in association with Scaloria-style pottery (4500 BCE) in cave settlement levels (Borrello 2001, p. 193; Borrello *et al.* 2012). Finally, in Carpignano Salentino, burials within artificial cavities dated to the Final Neolithic (4560-3440 BCE) yielded a pendant consisting of a perforated coral branch,

with a partially polished surface (Borrello *et al.* 2012, pp. 72-73).
It is also worth mentioning coral finds discovered out of stratigraphic context, datable approximately from the Cardial to the Bronze Age, in Liguria (Grotta della Matta and Grotta del Frate), Sardinia (Cucurru S'Arriu), and Apulia (Grotta della Tartaruga – Lama Giotta). No specific studies or analyses have been carried out on these materials (Borrello 2001, p. 193; Borrello *et al.* 2012, p. 71).
In the eastern Mediterranean, the use of corals is documented in Egypt and Turkey, where several species from the Red Sea are also identified. In Turkey, coral has been reported among the cult offerings at Çatalhöyük (4th millennium BCE; Morel 2006; Meeks 2000, pp. 105-106).
In Egypt, 'madrepores' appear to have been preferred over *C. rubrum* (Meeks 2000). The literature reports the discovery of *Tubipora musica*, along with other *madrepores* common in the Red Sea, in burial contexts dating to the 5th – 4th millennium BCE. In contrast, the use of *C. rubrum* in Egypt is associated with the arrival of the Greeks near the Nile Delta in the 7th century BCE (*infra*) and appears to have been limited to this area (de Marinis 1997; Mastrocinque 2006; Meeks 2000, pp. 104-105; Morel 2006). However, these identifications are not supported by archaeometric analyses, and, in many cases, the materials are no longer traceable (Meeks 2000).
Archaeological documentation reports the discovery of red tubular coral branches, as well as white or yellow coral branches. However, *Dentalium*, a tubular shell found in the Red Sea, was likely occasionally mistaken for tubular coral (Meeks 2000).
Egyptian finds are sometimes associated to votive deposits dedicated the goddess Hathor, as well as with sanctuaries connected to the underworld, the journey to the afterlife, or watery realms (Meeks 2000, pp. 105-106). There is also mention of the use of black coral from the Red Sea, which the Egyptians called the "hair of Isis", a deity associated with the moon and navigation, often connected to Hathor (Mastrocinque 2006; Meeks 2000, pp. 109-110; Morel 2006).
Regarding this material, the scientific literature identifies two black corals whose distributions are compatible with the reported finds. The first is *Antipatharia*, a cnidarian with a black axis and iridescent surface spots, whose skeleton is not calcareous but composed of a chitin-like substance. It occurs in the Mediterranean Sea at considerable depths, typically over 100 metres. The second is the "gerardia" (*Savalia savaglia*), also called "false black coral", which settles on the axes of gorgonians and secretes a non-calcareous skeleton made of black chitin. This species is uncommon in the northern Mediterranean but frequent in the Sea of Marmara (Harmelin 2000, p. 285).

3.2. Copper Age - Bronze Age (3rd - 2nd millennium BCE)

In the central-western Mediterranean and continental Europe, the use of coral is not documented from the Copper Age until the end of the Bronze Age (de Marinis 1997). Between the Early and Middle Bronze Age this material is attested (Fig. 7) by some beads at the Grotte de Bringairet (Armissan, Aude, France) and by a single bead from the site of the Grotte de la Treille (Mailhac, Aude, France), generically attributed to the Bronze Age (Borrello 2001, p. 193; Rondi-Costanzo, Ugolini 2000, pp. 178-179).
The coral from the settlement of Schussenried (Baden-Württemberg, Germany; de Marinis 1997) has a doubtful chronological attribution, as do the two perforated coral discs from tomb 32 of the Jászladány necropolis (Jász-Nagykun-Szolnok, Hungary), attributed to the Bodrogkeresztúr Culture (de Marinis 1997), as well as reports of two coral-decorated bracelets at Kaltbrunn on Lake Constance (Switzerland; Borrello 2001, p. 193). White coral is reported from settlements of the Cortaillod culture in Concise (Neuchâtel, Switzerland: worked white coral) and Port Conthy (Neuchâtel, Switzerland: a white coral bead) (de Marinis 1997; Borello 2001, p. 191; Skeates 1993). In addition, a coral ornament with a suspension hole, reportedly found by G. B. Amerano in the Pollera Cave (Finale Ligure), lacks precise provenance and contextual data (Borrello 2001, p. 193; Borrello *et al.* 2012; de Marinis 1997).
Archaeological literature also reports the discovery of numerous coral beads attributed to the Ozieri culture at the Dasterru Cave (Punta Giglio, province of Sassari, Sardinia) (Borrello 2001, p. 193; Borrello *et al.* 2012; de Marinis 1997). Chemical and microscopical analyses carried out on one of them revealed a ceramic-based composition – possibly an imitation of coral (de Marinis 1997).

As far as the central and eastern Mediterranean are concerned, available data are scarce. Coral was probably known to Minoan populations, but there is no evidence that it was used. It appears to be depicted on Late Minoan IB pottery in the so-called "marine style," yet it has never been found in archaeological contexts as a raw material or used for ornamentation (DE MARINIS 1997; MOREL 2006). Evidence for the presence of coral in the Bronze Age is nonetheless attested at Mallia, Kos, Episcopi-Hierapetras, Perati, and Hagia Triada (BORRELLO 2001, p. 193).

3.3. Iron Age (9th - 2nd century BCE)

Between the late 8th and the 7th century BCE, the use of Mediterranean coral spread to Greece, Egypt, the Punic world, and peninsular Italy. From the end of the 6th century BCE onward, it also extended north of the Alps, reaching southern France, Austria, and Germany, within various regions associated with the Hallstatt and La Tène cultures (DE MARINIS 1997).

3.3.1 Coral for ancient Greeks

In the Ancient Greek world, coral is rare in archaeological contexts and generally dates to the Archaic period (7th - 6th century BCE) (Fig. 8; MOREL 2006; HERMARY 2000).
Coral is often associated with the feminine sphere. In the Greek world, his material is found along the coast, particularly in sanctuaries dedicated to female deities or in contexts connected with maritime trade. The absence of coral offerings in inland sanctuaries suggests that they were intended as gifts to deities associated with navigation (DE MARINIS 2000, p. 172; TAGLIENTE 2006, p. 13; MASTROCINQUE 2006; MOREL 2006).
The highest concentrations in the Archaic period are found in the region north-east of the Peloponnese and Corinth. These include sanctuaries dedicated to Hera at Perachora (17 coral artefacts, partly raw and partly worked) and at Argos (1 coral fragment), temples dedicated to Demeter and Kore at Corinth, and to Poseidon and Palemon near the Isthmus of Corinth. Also, finds in the Cyclades at Delos (sanctuary of Hera), at Samos in eastern Greece (sanctuary of Hera), at Ephesus (sanctuary of Artemis), at Rhodes (sanctuaries of Athena at Lindos and at Camiro), at Megara Hyblaea in Sicily, at Velia, at Paestum (sanctuary of Hera del Silari) belong to the Archaic period (MOREL 2006; HERMARY 2000). In the Greek temple of Gravisca, the harbour of the Etruscan city of Tarquinia, a sarcophagus containing the simulacrum of Adonis was buried, accompanied by a crater full of coral. The cult of Adonis was linked to Aphrodite; in fact, Adonis was a young man loved by the goddess who died of a wound inflicted by a wild boar. Coral represented all that is beautiful but sterile; a plant born from the sea, like the goddess, and therefore associated with her. Gravisca is also one of the most important coral supply areas in the north-western Mediterranean (TAGLIENTE 2006, pp. 13-14; MASTROCINQUE 2006; MOREL 2006; UGOLINI *et al.* 2000, p. 139; UGOLINI 2006b, p. 91).
Eight white coral fragments were recovered in Malta from the sanctuary of Tas Silg: one dated to the 4th - 3rd century BCE and the others from late Republican or early Imperial levels[1], mostly from discharges in secondary position. These finds have been interpreted as votive deposits, also based on their association with inscriptions to Hera (QUERCIA 2008; MASTROCINQUE 2006; MOREL 2000, p. 125; 2006, p. 69). The coral fragments (length ≈ 6-14 cm) were attributed to the species *Dendrophyllia ramea,* a white coral of the south-western Mediterranean living at depths between 100 and 300 meters (QUERCIA 2008, pp. 204-207).

3.3.2 Coral in Egypt

The Mediterranean Sea played a key role in Egypt's trade with the wider world since the new empire (7th century BCE). Among the various sites where *C. rubrum* was found are Memphis (coral beads, settlement, late 6th century BCE; coral necklaces, settlement, 5th - 4th century BCE), Défenneh (white coral branches, 6th century BCE), Nébéchen, Naucratis (red coral beads, settlement, 5th century BCE). The presence of *C. rubrum* in Egypt is particularly associated with settlements near the Nile Delta, coinciding with the arrival of the Greeks (7th century BCE). Other finds occur in different areas of the Nile Valley,

1 The sanctuary has been used since 2500 BCE. The megalithic temple was integrated into the phoenician sanctuary dedicated to Astarte from the 8th century BCE. In the same place later in Hellenistic and then Roman times, the cult of Hera and Juno is attested respectively, and then in the Byzantine age, around the 5th - 6th century CE, a readaptation and the formation of a church with baptistery.

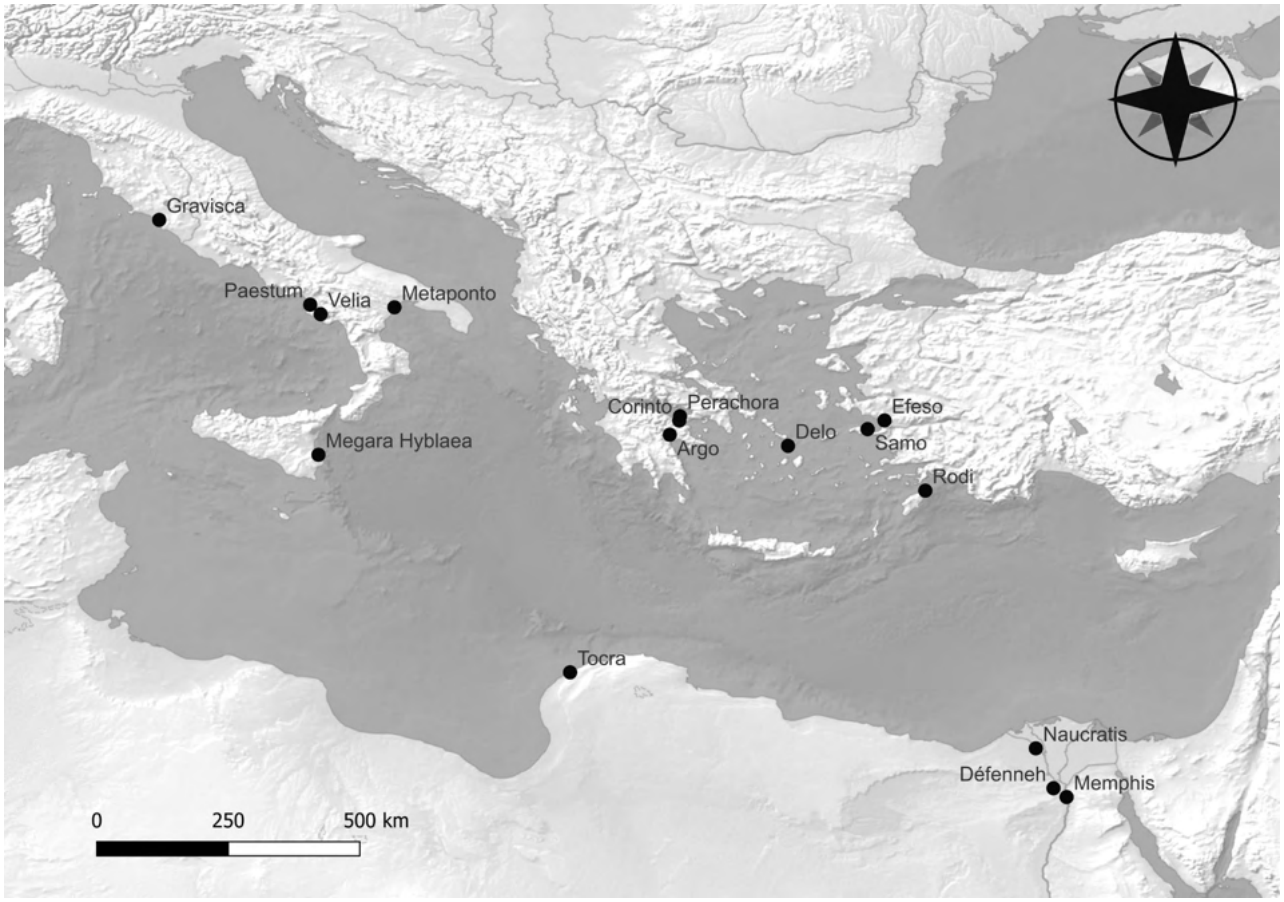

Figure 8. Location of coral evidence in the Greek world in Archaic period. Elaborated by the author in QGIS 3.40.8 (2025); base map: Natural Earth (Gray Earth raster "GRAY_LR_SR_OB_DR"), public domain.

extending as far south as Nubia, but these are much later in date (2nd - 4th century CE) and reflect Roman trade networks (Morel 2006).

3.3.3 Coral in the Phoenician-Punic domain

Coral was used in the Phoenician-Punic world from early periods, but the majority of documented finds date to the 7th century BCE and occur in both funerary and cultic contexts (Mastrocinque 2006). At present, the presence of coral in Phoenicia and in Cyprus (i.e. in the Syrian and Libyan littoral) is unknown, whereas it is well attested in the colonised territories of the western Mediterranean. Coral was widely available in Malta, western Sicily, western and southern Sardinia, the Balearic Islands, Andalusia, and the Algerian-Tunisian area (although the latter does not seem to have been exploited in these ancient phases: Morel 2000; 2006, pp. 68-69) (Fig. 9).

At Carthage, *C. rubrum* has been documented in both funerary and settlement contexts. Fifteen tombs, dated between the second half of the 7th and the first half of the 2nd century BCE, yielded raw coral sprigs, worked items, and a few branches of *Dendrophyllia ramea*. The coral from Carthage is generally of low quality, often displaying a "moth-eaten" appearance, likely due to collection from secondary deposits along the beach. Examples include nearly 30 small branches recovered from the metallurgical workshops of Byrsa, in layers datable between the 4th and mid-2nd century BCE, or those found (together with shells, obsidian, and carnelian) in a jeweller's workshop, also in Byrsa, attributed to the first half of the 2nd century BCE (Morel 2000; 2006, p. 68).

In general, coral is absent in Phoenician or Punic sites in Africa, with the exception of Hadrumentum (Sousse, Tunisia), where 60 coral cylinders were found in a 6th century BCE funerary context, primarily associated with child burials and possibly reflecting Libyan influences (Morel 2006, pp. 68-69). Outside Africa, coral is sporadically attested in burials in Andalusia

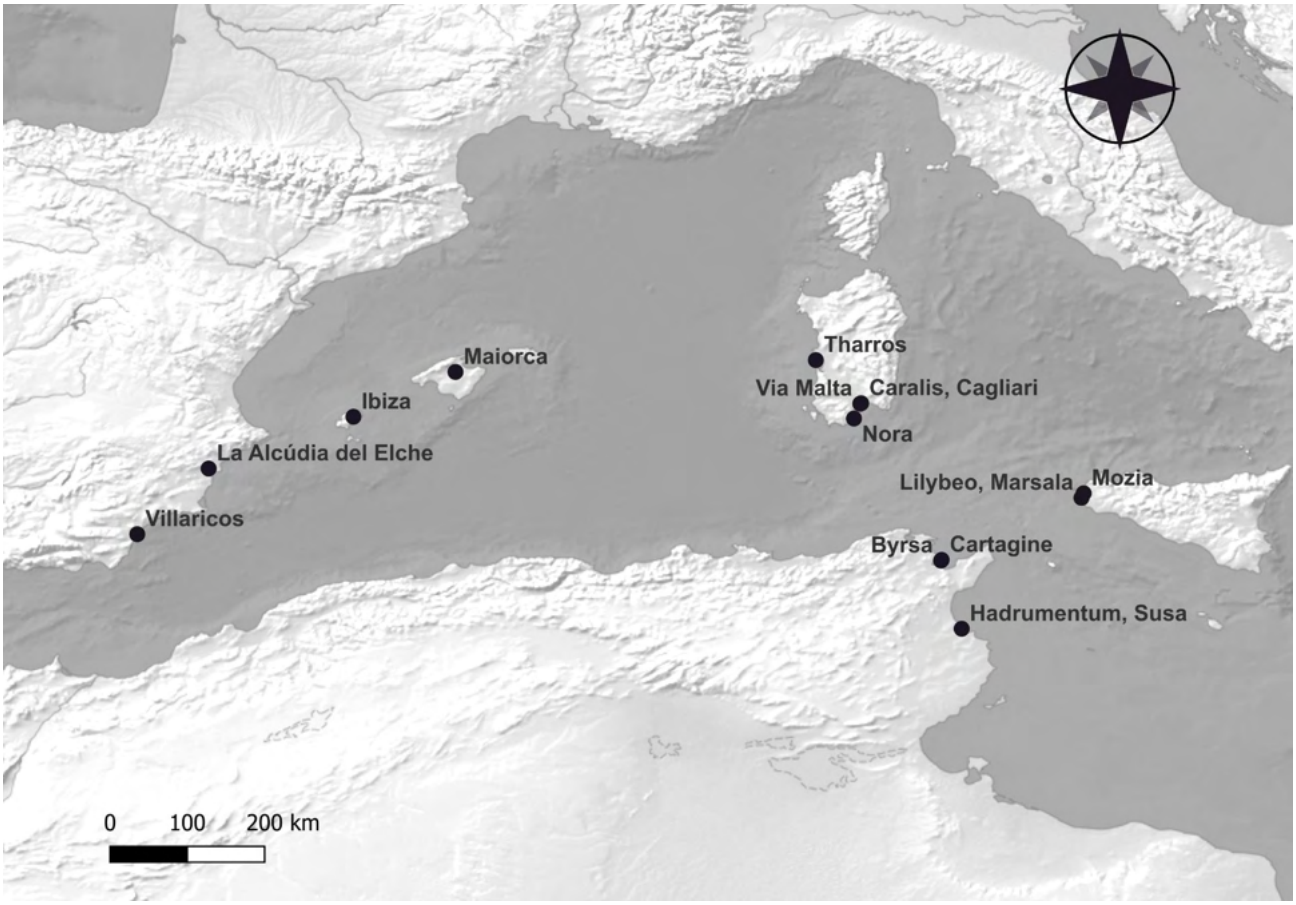

Figure 9. Location of coral evidence in the Phoenician-Punic world. Elaborated by the author in QGIS 3.40.8 (2025); base map: Natural Earth (Gray Earth raster "GRAY_LR_SR_OB_DR"), public domain.

(Spain) at Villaricos (unworked and worked), in Ibiza (Balearic Islands), in Sicily at Mozia and Lilybeo (Marsala), and in Sardinia at Nora, Caralis (Cagliari) and Tharros. In all these cases, it is generally unworked *C. rubrum* and to a lesser extent *Cladocora coespitosa* (found only in Cagliari). There are also finds in domestic contexts at Villaricos, Mozia, Nora and Tharros (Morel 2006, pp. 68-69). In Majorca (Balearic Islands), a sprig of polished red coral was found at a Phoenician-Punic shipwreck, dating to the second quarter of the 6th century BCE (Morel 2006, p. 69; Purpura 2005, p. 96). Raw coral findings, without any indication of the discovery context, are reported at La Alcudia del Elche in Spain, Mozia in Sicily, Cagliari, Nora and Tharros in Sardinia. Among the most important finds was the discovery of 3 kg of raw coral in the temple-theatre in Cagliari, in Via Malta, dedicated to the cults of Aphrodite-Astarte and Adonis, dating from the second half of the 3rd - 1st century BCE (Morel 2006).

3.3.4 Coral among the Italic populations

One of the earliest Iron Age evidences of coral use in Italy is a coral bead from a Villanovan tomb at Veio (tomb 15, Vaccareccia necropolis), dated to 770–720 BCE, now preserved in Rome at the Museo delle Civiltà (formerly Museo Nazionale Preistorico Etnografico Luigi Pigorini) (de Marinis 1997, p. 154; Ugolini *et al.* 2000, p. 139; Ugolini 2006b p. 91).

Coral is rarely found among Italic cultures, mainly in funerary contexts or cult areas (Fig. 11), such as the artefacts from Teano in Campania (Fondo Ruozzo sanctuary: coral and bronze pendant, 6th-4th century BCE) or the small branches from Capua (cult context, large coral branch), Pompei (votive deposit, calcined coral, late 3rd century BCE), Paestum (cultual context, two arborescent coral branches, 3rd century BCE) and in Apulia from Oria ('Thesmophorion', vase-shaped pendant, approximately 500 BCE) (Mastrocinque 2006; Ugolini *et al.* 2000, p. 142; Ugolini 2006b, p. 92).

In Basilicata (Fig. 11), during the 5th–4th century BCE, coral appears in funerary contexts, used to decorate iron fibulae with a bone dolphin-shaped bow (Fig. 10a), whose red eyes are made of presumed coral or carnelian (Tagliente 2006; Ugolini 2006b, p. 92; Ferrero, Rubat Borel 2017). These artefacts were found in the burials of contrada Tesoro, via Di Palma and contrada Madre Grazia (tomb VIII) in Taranto, dated to the 4th century BCE, and do not always retain the inset (Ugolini 2006b, p. 92; Bianco 2006, p. 127). There are parallels in Greek (Herakleia) or indigenous burials, such as at Metaponto (Pantanello necropolis, indigenous tomb, 5th century BCE: fibulae decorated with shells or coral and a rough coral branch), Lavello and Sant'Arcangelo in Basilicata (Tagliente 2006; Ugolini *et al.* 2000, p. 141). Two dolphin-shaped bone fibulae were found in Herakleia (Policoro, Basilicata) in female burial 50 in Via Avellino, dated to the end of the 4th century BCE. Another example of a dolphin-shaped fibula also comes from the Sanctuary of Demeter in Herakleia, whose body was made of ivory accompanied by a coral inlay in the eyes (Bianco 2006, p. 127).
Three analogous specimens from the Assi collection, with no indication of provenance, are preserved in the Musei Reali in Turin (Fig. 10a). For them, the raw material of the eyes was identified macroscopically as hard stone, but based on no archaeometric analysis (Ferrero, Rubat Borel 2017, pp. 5-6, fig. 13). Due to this, these artefacts were included in the current project, on specific request of the Musei Reali: two of them retain eye insets, identified as *C. rubrum* and probable *Spondylus gaederopus*, respectively.
Another dolphin-shaped fibula, presumably of Apulian origin, is preserved in the Museo Archeologico Nazionale in Florence. It is made of bovine bone and decorated with circular inlays of presumed ivory (Iozzo 2013, fig. 3) in the eyes and along the entire body, giving the artefact a spotted appearance, unique among the known specimens (Fig. 10b).
Lead imitations of coral sprigs were discovered on the acropolis of Herakleia (Bianco 2006, p. 127). Rough coral branches were found in Archaic tombs in Alife (Caserta) and in a tomb in Pontecagnano, adapted as pendants, dated to the first quarter of the 6th century BCE (Ugolini *et al.* 2000, p. 142; Ugolini 2006b, pp. 92-94).
Between the 4th and 2nd century BCE, coral was widespread throughout the indigenous world in the Italian peninsula. One of the most famous finds is the iron and bronze parade helmet found in Canosa and dated to the 4th century BCE, embossed and decorated with coral, of Celtic import and manufacture. The coral cabochons of this artefact are similar to those found in Montlaurès, in France (Ugolini 2006b, pp.

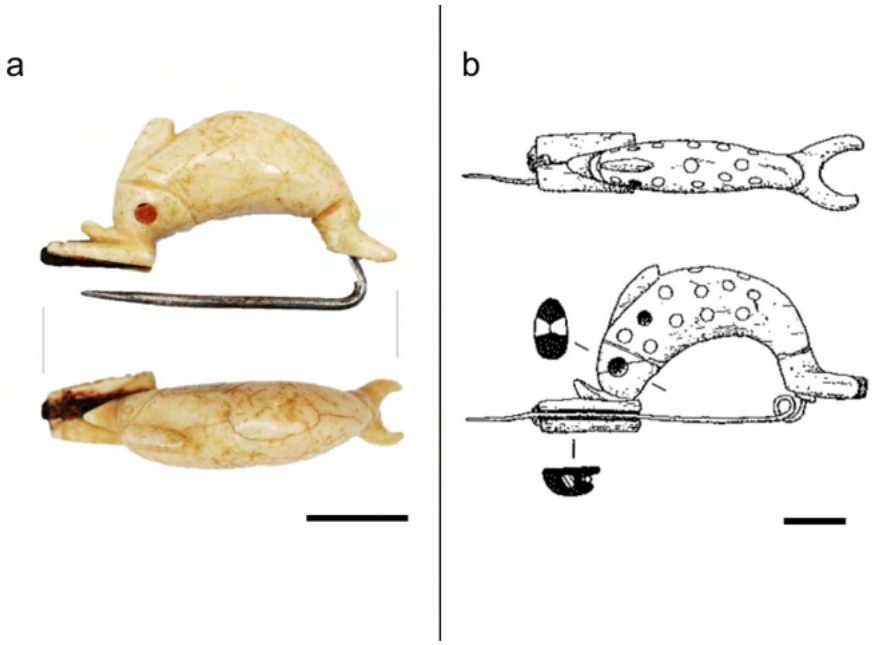

Figure 10. a) Dolphin-shaped fibula, Musei Reali inv. 23.M380-9.8 (Assi collection 15/18; ph. Berruto; metric reference 1 cm); b) Dolphin-shaped fibula, Museo Archeologico Nazionale di Firenze (metric reference 1 cm; modified after Iozzo 2013, fig. 3).

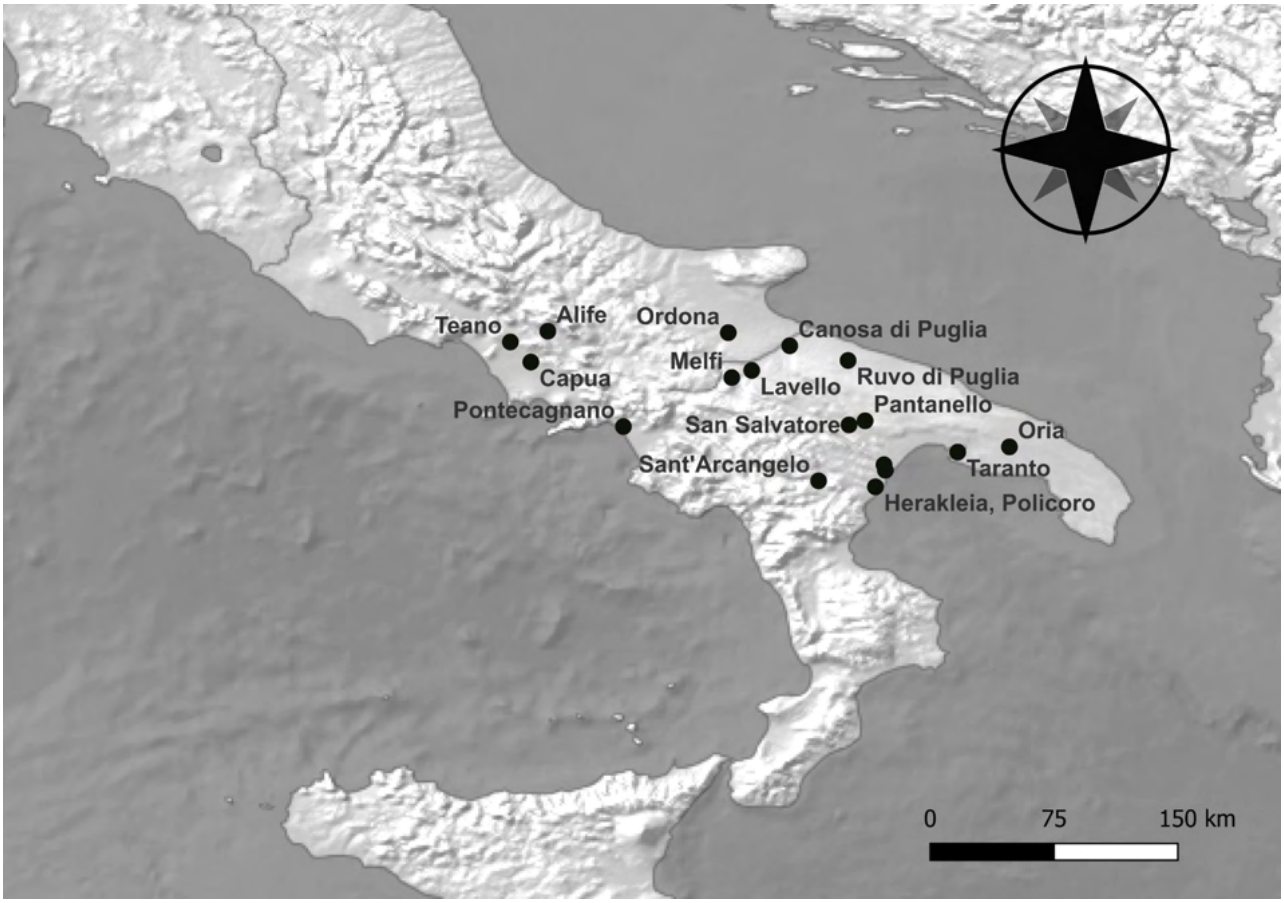

Figure 11. Location of coral evidence in southern Italy in the pre-Roman period. Elaborated by the author in QGIS 3.40.8 (2025); base map: Natural Earth (Gray Earth raster "GRAY_LR_SR_OB_DR"), public domain.

92-94). In burials, fibulae with coral decorations, referable to the 4th century BCE, are made of iron (Ordona, 5th century BCE; Paestum), bronze, silver (Teano and Paestum) or gold (Lavello tomb 955 and Melfi; Paestum and Alife) (Ugolini *et al.* 2000, p. 142; Ugolini 2006b, pp. 94-95). Iron fibulae with foots covered by perforated cylindrical white elements were found in grave goods from Metapontum or the 'chora Metapontina'[2]. These cylindrical elements have been variously attributed to shells or corals, though scientific investigations are not detailed (Bianco 2006, pp. 120-131). Coral beads come from child graves in Ordona (4th century BCE) and from a burial in Ruvo (6th - 3rd century BCE) (Ugolini *et al.* 2000, p. 142; Ugolini 2006b, p. 94).

3.3.5 Coral in Iron Age Europe

In the Early Iron Age, coral was widely used in Italy in the regions to the north of the Po River, namely by the Golasecca culture to the west and the Venetic-Atestine culture to the east (de Marinis 2000). Most discoveries come from funerary contexts, especially female burials, although some finds also appear in settlements, such as at Forcello di Bagnolo San Vito in Etruria Padana. Studies on Golasecca sites, as well as on other Iron Age cemeteries in Europe, indicate that coral amulets were predominantly placed in the graves of women and children, suggesting a close association with the female sphere and childbirth (de Marinis 2000, p. 172). In the Golasecca area, from the 4th century BCE onwards, these objects also appear in male burials, likely reflecting the influence of the La Tène culture (de Marinis 2000, p. 172).
In the Iron Age, the use of coral is particularly common among Celtic populations (Taviani 1997), probably due to trade networks with north-italic communities or italic and mediterranean regions (de Marinis 2000, p. 172),

2 Tombs 66, 83, 95, 350 from Pizzica Pantanello; tomb 11 from Agrobios Pantanello, tomb 45 from San Salvatore, tomb 2 From Bivio Franchi, tomb 125 from Casinello, tomb 358 from Destra Basento-SS106.

where this material was used for manufacturing beads, pinheads and composite beads, or used raw in necklaces (Fig. 12; DE MARINIS 1997, p. 157). Between the end of the 6th and 5th century BCE, this material is widespread in the Cisalpine, Golasecca (GIIB and GIIIA1 phases), Venetic-Atestine (Este III-medium) and transalpine Hallstattian (Hallstatt D 3) areas. Western Hallstattian fibulae, with ornithomorphic foot or *Fußzier* type, often show three or four transverse grooves on the bow filled with a white material, identified as bleached coral. Fibulae with a dovetailed foot or a long foot ending in a double small globe also display the same decoration (DE MARINIS 1997, p. 157).

The use of coral in the Early Iron Age is documented in Languedoc by two beads dated to the mid-7th century BCE, isolated finds from two burials, near the Pyrenees and in the lower Aude valley (UGOLINI 2006a, p. 80). This material is attested in central and eastern France, as well as in Switzerland, as a raw material and in the form of jewellery during the 6th century BC and especially between the end of the 6th and the first half of the 5th century BC in settlements and necropolises. It is much more common in the later phases in Provence and Languedoc, in relation to its use by Celtic craftsmen from La Tène A onwards (UGOLINI 2006a, pp. 86-87). In Catalonia and Provence between the 6th and 3rd century BCE, coral is relatively abundant. In the centers occupied by the Greeks (Marseille, Béziers, Emporion, Olbia, Arles, Agde), raw coral branches are predominantly found, whereas worked artefacts prevail in the indigenous settlements (UGOLINI 2006a, p. 86).

Celts in the late Iron Age used this raw material to decorate fibulae, torques, armillae, rings, belt plates, helmets, sword scabbards and bronze vessels (DE MARINIS 1997, p. 158; FÜRST 2014; UGOLINI 2006a, p. 79; ZLÁMALOVÁ CÍLOVÁ *et al.* 2024). They attributed great value to red coral, which was difficult to obtain and therefore quite expensive. Artefacts decorated with coral are, in fact, few in number and highly refined (UGOLINI 2006a, p. 79). They probably imported raw coral and processed it locally[3]. Raw coral was indeed found in the so-called princely residences of the Heuneburg (Hundersingen, Baden-Württemberg), Mont Lassois (Châtillon-sur-Seine, Côte-d'Or; BORRELLO 2001, p. 194; DE MARINIS 1997, p. 157; FÜRST 2014), Bourges-Port Sec (together with finished products; end of 6th-5th centuries BCE: AUGIER *et al.* 2012, p. 229; CICOLANI 2017) and Zvoleněves (3rd century BCE: ZLÁMALOVÁ CÍLOVÁ *et al.* 2024). It was also found in a hillfort, Bourguignon-lès-Morey 'Camp de César' (FÜRST 2014, p. 54), and frequently in Hallstattian settlements in the plains: Weingarten 'Krummäcker' (Germersheim district), Gerlingen 'Obere Gerteisen' (Ludwigsburg district), Geispolsheim 'Bruechel' (Lower Rhine department), Bragny-sur-Saône (Saône and Loire department) (FÜRST 2014, p. 54).

This exotic product was used ostentatiously and is also found in high-ranking tombs as part of the grave goods. A unique example is represented by the statuettes supporting the bronze bench discovered in the male tomb of Hochdorf (Eberdingen, Baden-Württemberg), which feature coral inlays reproducing jewellery on the depicted human figures. Dated to around 530 BCE, it was likely imported from northern Italy (VERGER 2006a).

Coral use is also documented in the female tomb of Vix in France, underlining the use of this material in princely tombs, i.e. of individuals with political, religious and warrior functions (PERRIN 2000, p. 196).

In the Late Iron Age, the use of coral moved northwards, especially in Champagne region in France (La Tène A and La Tène B periods) and in the south-western area of Germany from La Tène A period (FÜRST 2014). Among these cultures, strong attraction to coral has been related to the use of wine and the male deity associated with the symbolism of the tree of life and its magical powers since the 5th century BCE (KRUTA 1986; 1987; MOREL 2006, p. 77; PERRIN 2000, pp. 196-198).

From LT C (c. 300 BCE) the presence of coral-decorated artefacts is reduced (ZLÁMALOVÁ CÍLOVÁ *et al.* 2024). A representative example is that of the *Mitteldeutsche Korallenfibeln*, generally made of iron with bronze parts (rarely in other precious metals) and decorated with whitish beads in alleged coral. Three main types can be distinguished (LT C2 – LT D1): Brücken (e.g. Hänichen, Kleinkorbetha, Gräfenhainichen, Langenau, Leimbach fibulae), Andisleben and Körner. Scientific analyses revealed the use of materials other than coral in the manufacturing

3 As probably already occurred in earlier times; raw coral has also been found in Hallstattian contexts: e.g., Bourguignonès-lès-Morey, France, and Poříčany, Czech Republic (PERRIN 2000, p. 196; ZLÁMALOVÁ CÍLOVÁ *et al.* 2024).

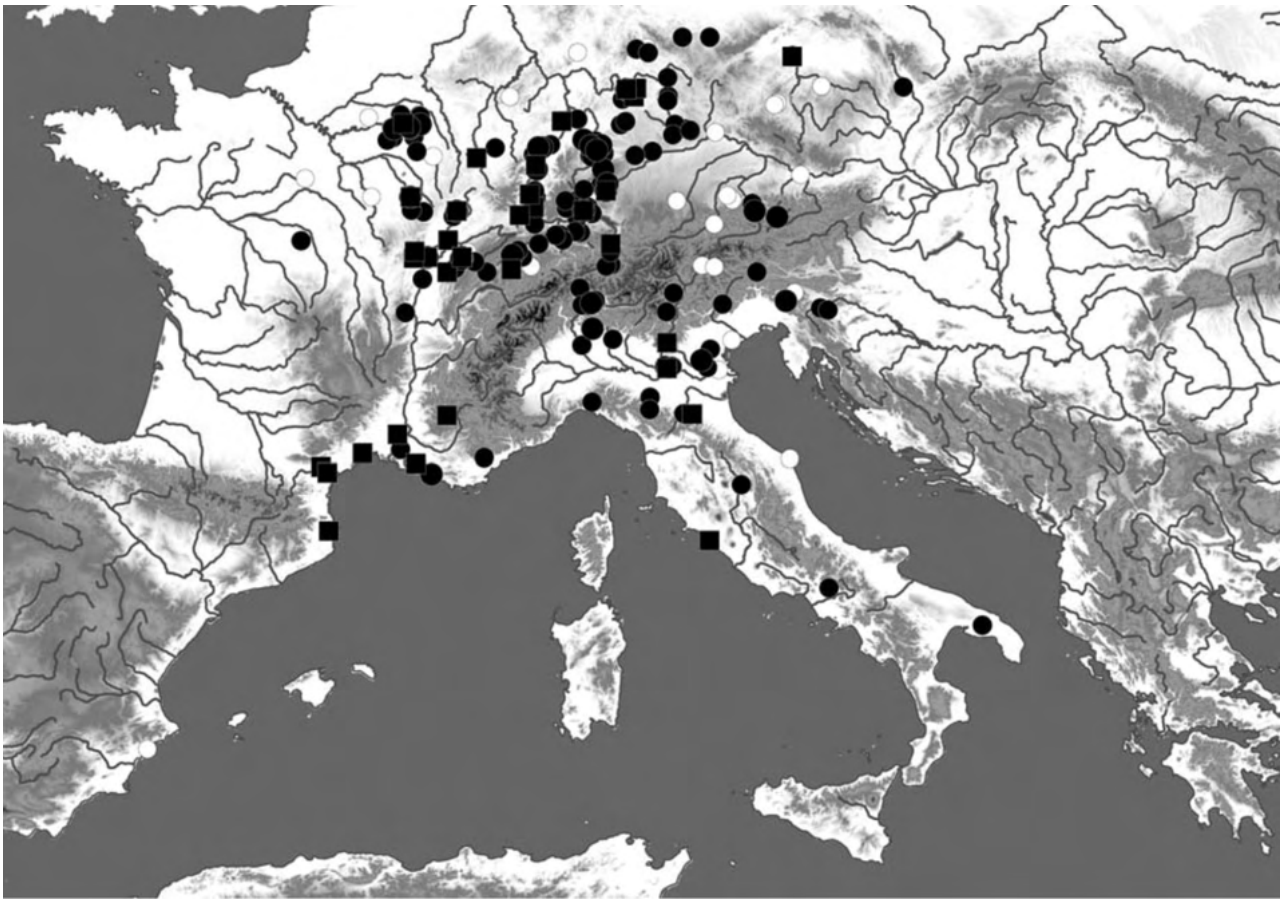

Figure 12. Distribution map of coral artefacts in Europe during the Hallstatt D2-D3 phases (c. 575-450 BCE); black circles = more than 5 coral artefacts; white circles: artefacts that have lost their insets; squares = settlements with corals (after Fürst 2014, fig. 2).

of these objects – such as white fossil coral limestone from the Baltic Sea region or the glaciers of northern Germany. Composite artefacts are also found, involving the use of red and white corals (e.g. fibula from tomb 227 in Dürrnberg/Hallein), coral and enamel (e.g. fibula from tomb 17 in the Nebringen necropolis, Böblingen district) (Bente *et al.* 2014; 2020; Rauchfuss 2016; Schrickel, Bente 2013; Schrickel *et al.* 2014).
In some regions, such as Champagne, coral continued to be used extensively for highly refined objects, including armaments and war chariots. In other areas, substitute materials, such as red glass and enamel, became increasingly widespread, particularly from the 4th century BCE onward (Perrin 2000, p. 198). It is unclear whether this change was due to the depletion of sources, shifts in trade networks, or simply a change in preference. However, the continued use of coral in later periods suggests that the first explanation can likely be ruled out (Zlámalová Cílová *et al.* 2024; Fürst 2014).

3.3.6 Supply areas in pre-Roman times

For the coral used in the Golasecca and Este cultures (see further in this volume), a provenance from Campania, mediated by the Etruscans, is traditionally assumed. This hypothesis is based on the spread of the raw material from around 700 BCE, coinciding with the arrival of the first imported objects from Etruria (de Marinis 2000, p. 164; Ugolini 2006b, p. 90). Numerous fragments of raw coral were found in the De Luca, Arnoaldi and Certosa cemeteries in Bologna, which are considered to support this hypothesis (Fig. 14; Tab. 1; de Marinis 1997, p. 157). However, there is almost no evidence regarding the extraction or use of coral in the Etruscan world (e.g., fishing or processing tools), despite the presence of coral banks within the areas influenced by these populations (Ugolini *et al.* 2000, p. 139; Ugolini 2006b, pp. 90-91).
The discovery of numerous raw coral fragments at Forcello di Bagnolo San Vito (near Mantua) apparently further supports this hypothesis (Figs. 13-14; Tab. 1; de Marinis 1997, p. 157). It

is allegedly an Etruscan settlement and a trading center along the route that led from the Adriatic ports to Mantua, Brescia and Como (De Marinis 1987) (see also Chapter 4, this volume). Molluscs of Adriatic origin were also found in the same site, confirming exchanges with these areas (Schmid-Sikimić 2000a, pp. 152-153; 2002, p. 129). A small branch of raw coral is also present in the infant burial (tomb 5, inv. 169394) in Borgo Virgilio-Arginotto (Mantua).

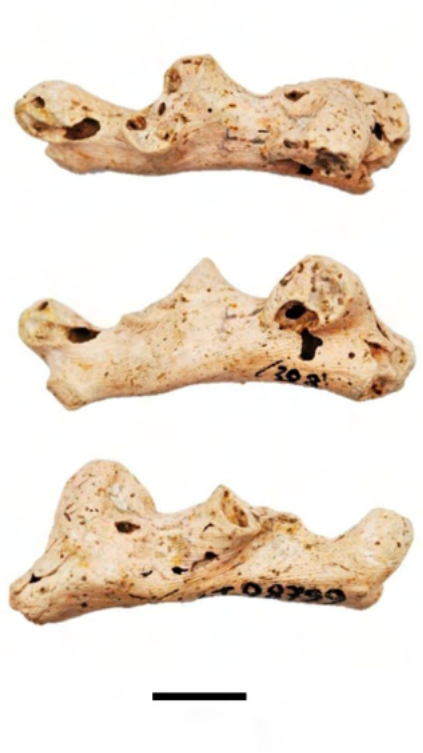

Figure 13. Forcello di Bagnolo San Vito, raw coral branch, inv. no. St. 98799 (ph. Berruto; metric reference 1 cm).

A provenance mediated by the Etruscans does not necessarily imply that the coral originated in Campania. The raw material could also have come from the Ligurian or Adriatic Seas, as well as from the coasts of Istria and Dalmatia, which were rich in coral beds and maintained early cultural and commercial contacts with the Italian shores (Ugolini 2006b, p. 90; Schmid-Sikimić 2000a; 2002, p. 129). The latter hypothesis would be supported by the frequent discovery of coral necklaces near Budapest in Hungary. However, these findings are more recent (La Tène B, 4th century BCE), suggesting a possible Adriatic origin of the coral, transported along the Sava Valley and reaching the Danube near Vukovar. If the Adriatic origin is correct, coral would likely have been readily available in the markets of Adria and/or Spina, where the Etruscans stocked up (Schmid-Sikimić 2000a). Trade along the Adriatic route is well attested by the presence of Apulian-Daunian pottery, starting from the 8th century BCE, towards Istria and the Dolenjsko group. Moreover, the distribution of Venetic, Apulian and Greek ceramics confirms the exchanges with these areas (Schmid-Sikimić 2000b; Nascimbene 2009, p. 7).

A fragment of raw coral is also reported in Genoa (San Silvestro, Oppidum del Colle di Castello), dating to the 5th century BCE (Figs. 14, 22; Tab. 1; Melli 2021, p. 75, fig. 48; Milanese 1987, pp. 155 (n. 243), 352, 380; Rondi-Costanzo, Ugolini 2000, p. 181; Ugolini 2006b, p. 91), which could be related to a possible local origin, since coral fishing on the Rapallo coast is documented in historical times.

The Greek colony of Marseille played a key role in the coral trade during the 6th century BCE. Large concentrations of raw coral have been found in settlement levels from this period (La Tourette and Butte Saint-Laurent), and further insights come from a shipwreck discovered in 1993 during excavations at the ancient port (Place Jules Verne) (Figs. 14-15; Tab. 1; Rondi-Costanzo, Ugolini, 2000, p. 177; Purpura 2005, pp. 97-98; Ugolini 2006a, pp. 80-81). The shipwreck – a small Greek boat dating from the second half of the 6th century BCE – is the oldest evidence of coral fishing. The boat's interior had been waterproofed with pitch, which preserved 12 small coral branches that had accidentally fallen during the initial processing of the raw material on board (Pomey 2000; Purpura 2005, pp. 97-98).

In the immediate surroundings of Marseille, worked coral is already present in the 7th century BCE at Mailhac. In the following century, engraved coral ('corail incisé') appears at Baou de Saint-Marcel (580-550 BCE), while both rough coral and a fibula decorated with coral are documented at Gros Ped and in a settlement at Saint-Blaise (6th century BCE) (Fig. 15; Rondi-Costanzo, Ugolini 2000, pp. 178-179).

In this period, the use of coral is also widespread in Burgundy, where is used to decorate fibulae (Ugolini 2006a, pp. 80-81), as well as in the Jura and Centre-Val de Loire (Bourges) regions (Augier *et al.* 2012, p. 229; Cicolani 2017) and in northern Italy. It is therefore plausible that the Etruscans played an active role in the coral trade, following an alternative route

(Ugolini 2006b, p. 91) that involved the upper Tyrrhenian Sea and, after the foundation of the Etruscan-Ligurian emporium at Genoa in the 6th century BCE, reached the Po Valley via the Scrivia Valley (Melli 2021).

For the trans-Alpine Celtic area in the Late Iron Age, it is generally assumed that coral was imported via *Massalia* and the Rhone and Saône valleys, providing access to central and eastern France as well as the Helvetian trans-Alpine region. However, a provenance from Etruria via the Alpine passes cannot be ruled out (de Marinis 1997, p. 157; Ugolini 2006a, pp. 80-81). Coral was not widely used in the coastal centers where it was harvested, suggesting that it may not have been considered particularly valuable by the fishing and collecting communities (Ugolini 2006a).

In the 5th century BCE, evidence in Marseille (Tunnel de la Major) and Provence (Saint-Blaise; Arles; Marduel; Grotte de La Lioure) is scarce, whereas abundant in western Languedoc, especially in the center of Béziers, a settlement with a strong Greek presence, active in the 5th and 4th century BCE (Fig. 15; Rondi-Costanzo, Ugolini 2000, pp. 179-180; Ugolini 2006a, pp. 81, 86). In Languedoc, raw coral is abundant in residential levels, while processed material originates from indigenous centers. However, coral is found only in coastal sites or along trade routes and is absent from the rest of the territory (Fig. 15). Marseille probably remained a coral-fishing center during these phases but lost its commercial function. The sandy coasts of Languedoc did not allow coral to grow, so it likely continued to come from Provence and the Pyrenean coasts, which were still rich in coral banks. From Béziers, coral was traded northwards to France via the Aquitaine route, which leads to the Gironde estuary and then the Loire basin, or along the right bank of the Rhône (Ugolini 2006a, pp. 81, 86). At Béziers, coral is found unworked and relatively dispersed within the settlement. Worked material (beads or pierced branches), on the other hand, comes from nearby sites (Montfo, Montlaurès, Mailhac, Cesseras,

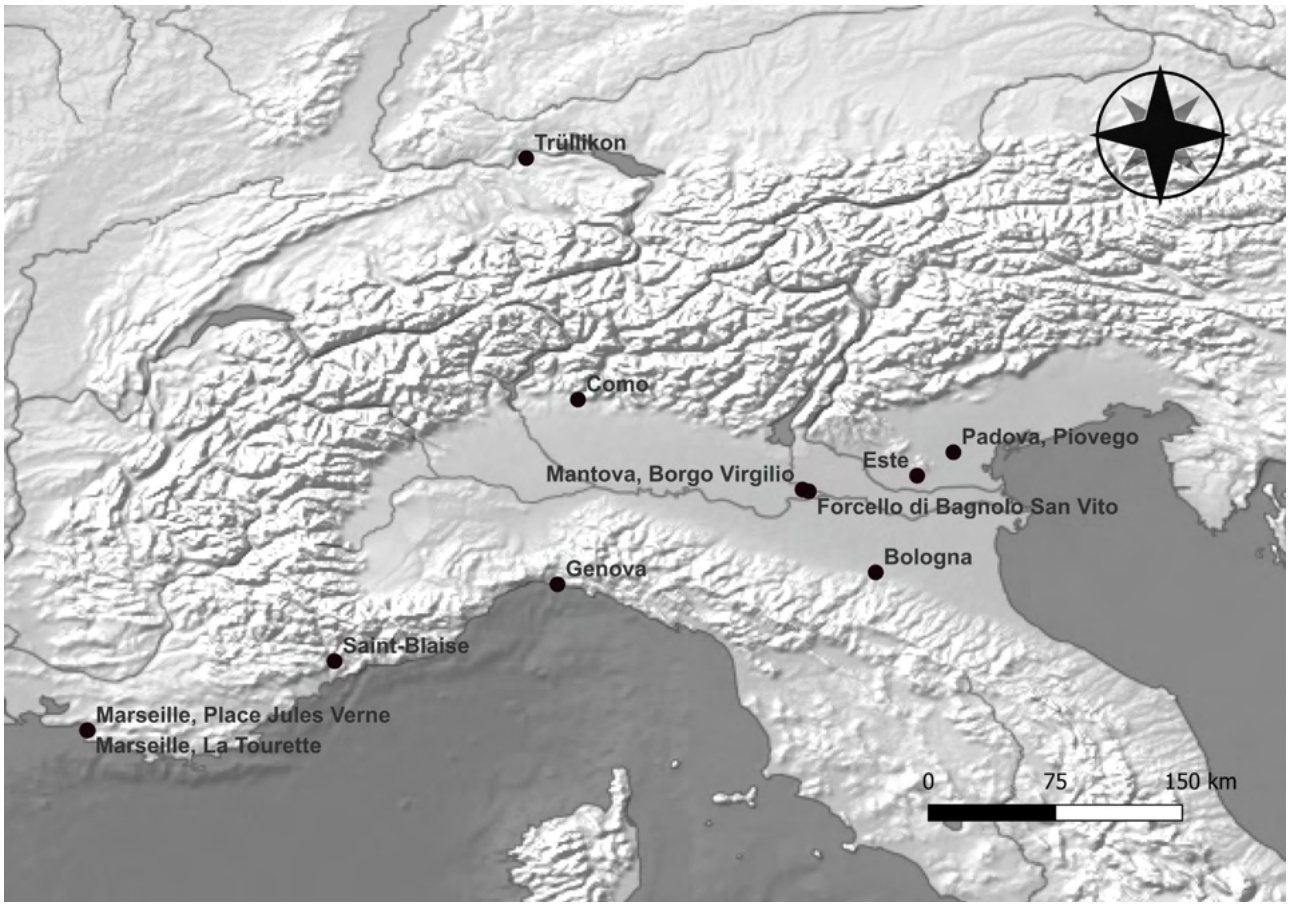

Figure 14. Distribution of raw coral branch discoveries north and south of the Alps between the 8th and 6th century BCE. Elaborated by the author in QGIS 3.40.8 (2025); base map: Natural Earth (Gray Earth raster "GRAY_LR_SR_OB_DR"), public domain.

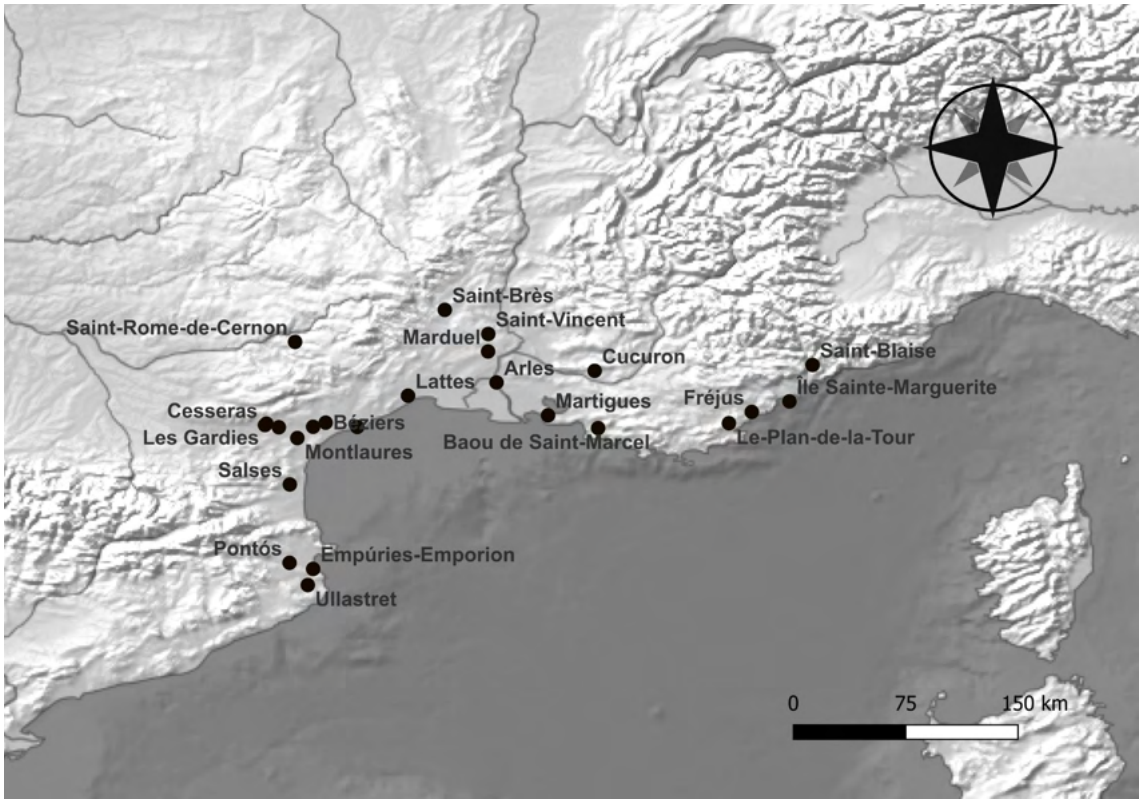

Figure 15. Coral discoveries in Iron Age archaeological contexts in Provence, Languedoc and Catalonia between the 7th and 3rd century BCE. Elaborated by the author in QGIS 3.40.8 (2025); base map: Natural Earth (Gray Earth raster "GRAY_LR_SR_OB_DR"), public domain.

Saint-Brès, Salses-Le Port, Les Gardies, Plan de la Tour, Saint Vincent – Gaujac; Rondi-Costanzo, Ugolini 2000, p. 180). Towards the end of the 5th century BCE (after 420-400 BCE), coral-decorated metal ornaments in Celtic style, especially fibulae, are common along the coast (Grotte de Sargen en Rouergue, Saint-Rome-de-Cernon; Fig. 15).

In Catalonia, at the Greek colony of Emporion, two raw coral branches were found in child burials, while raw or worked coral objects have been reported from Pontòs and Ullastret (Fig. 15; Rondi-Costanzo, Ugolini 2000, p. 180; Ugolini 2006a, pp. 81, 86).

Between the 4th and 3rd century BCE, evidence for the presence of coral becomes considerably scarcer in Provence and is completely absent in Marseille (Fig. 15). In Provence, fibulae with coral appear in Martigues, Saint-Pierre-Les-Martigues, on the Island of Sainte-Marguerite (Cannes) and raw coral on the Island of Sainte-Marguerite (Cannes), in Fréjus (Var) and Cucuron (Vaucluse). In Languedoc, coral is still present, being found only along the eastern coasts at Lattes and Le Marduel (Rondi-Costanzo, Ugolini 2000, p. 181), whereas it is abundant along the western coast.

In the 4th century BCE, Béziers still had abundant raw material, but this declined by 300 BCE. Ensérune, an indigenous settlement, was particularly rich in the 3rd century BCE, yielding both raw material and worked objects (beads, fibulae, zoomorphic heads, sword scabbards, embossed foils, decorated with coral and referable to Celtic models datable between the 5th and 3rd century BCE; Rondi-Costanzo, Ugolini 2000, pp. 181-183; Ugolini 2006a, pp. 81-84). Raw coral is also reported in Agde (Rondi-Costanzo, Ugolini 2000, p. 181) and worked coral in Montlaurès (Rondi-Costanzo, Ugolini 2000, p. 183). Between the 4th and 3rd century BCE, objects decorated with coral in La Tène style are found in indigenous settlements in Catalonia (Ullastret and Emporion), less frequently than in Gaul (Rondi-Costanzo, Ugolini 2000, p. 185; Ugolini 2006a, p. 86). In the second half of the 3rd

and 2nd century BCE, these finds decrease in general everywhere (Ugolini 2006a, p. 86). In the 4th century BCE, coral almost completely disappears in northern Italy, while in the south it is widely used between the 4th and 3rd century BCE in the indigenous world, particularly in Campania, Basilicata and Apulia. The origin of the raw material remains unknown, although a provenance from the nearby Campania coral banks has been hypothesised (Ugolini 2006b, p. 96).

3.4. Roman period

In Roman times, Pliny the Elder (*Naturalis Historia*, XXXII, 11, 21) reported that the darker-coloured coral came from the Persian Gulf and the Red Sea, while that from Eritre (Asia Minor) was soft and worthless (Fig. 16). Probably, this was not *C. rubrum* but another species, such as *Tubipora musica* which is also attested in Egypt in earlier periods (Meeks 2000). According to Pliny, the best coral came from the 'Gallic Gulf', near the 'Stoechadae' Islands ('îles d'Hyères' or 'îles d'Or', Var department, Provence) and the Sicilian Sea, near the Aeolian Islands and Trapani ('Drepana'), as well as from Naples and Gravisca. Among ancient authors, Dioscorides and Oribasius indicate its origin from Cape Pachino near Syracuse (Bresc 2000; Leurini 2006, p. 85; Mastrocinque 2006; Morel 2006, p. 71; Tagliente 2006). Not mentioned in these sources are the deposits in the Algerian-Tunisian area, which became important in later centuries, nor those in Catalonia or the Alboran Sea (Morel 2006, p. 72). Pliny the Elder describes the scarcity of this material, referring specifically to to deposits exploitable by free diving (Bresc 2000):

> Gignitur et in Rubro quidem mari, sed nigrius, item in Persico, vocatur lace, laudatissimum in Gallico sinu circa Stoechadas insulas et in Siculo circa Aeolias ac Drepana. Nascitur et apud Graviscas et ante Neapolim Campaniae maximeque rubens, sed molle et ideo vilissimum Erythris (*Naturalis Historia*, XXXII, 11, 21).

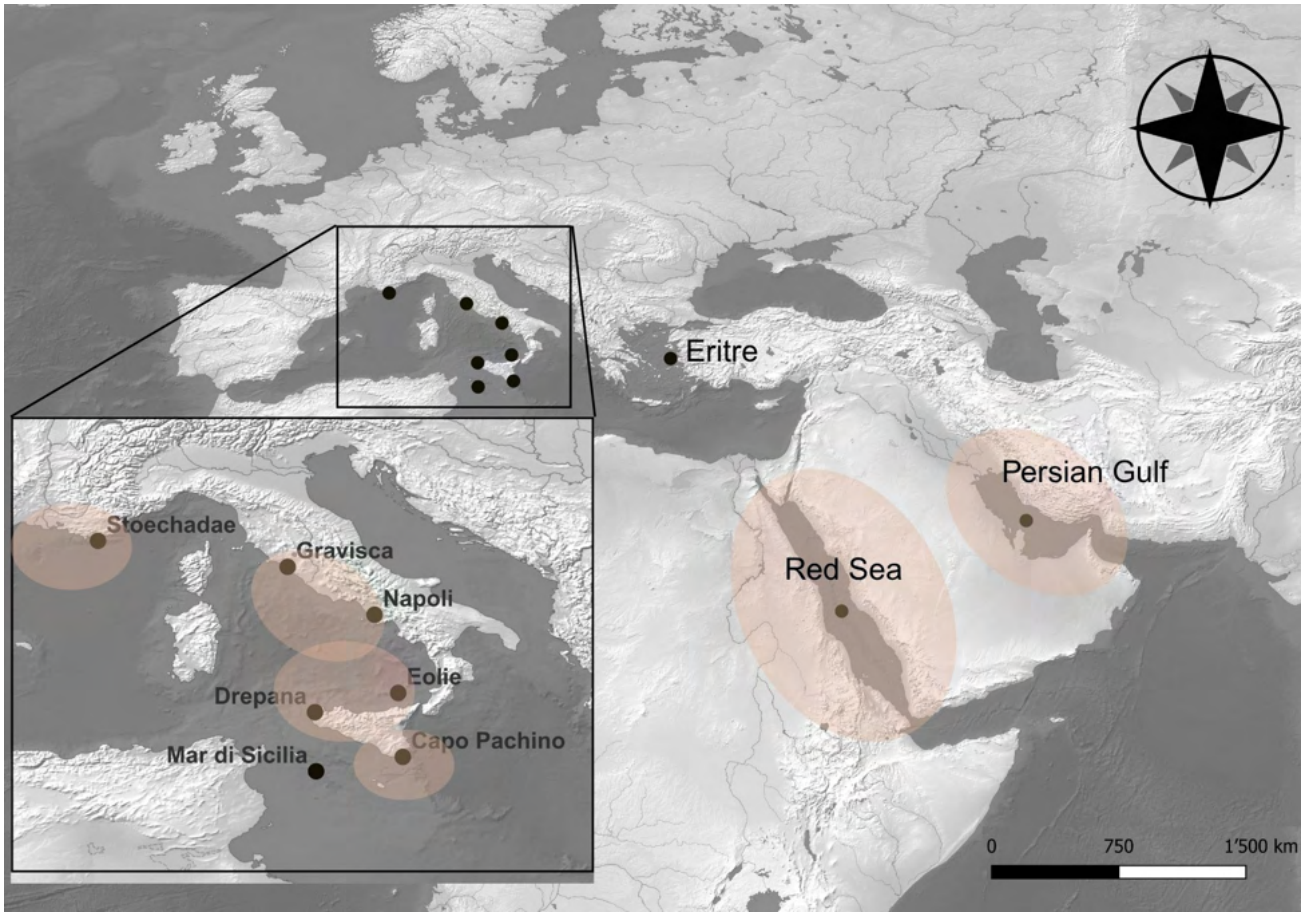

Figure 16. Coral supply areas in Roman times. Elaborated by the author in QGIS 3.40.8 (2025); base map: Natural Earth (Gray Earth raster "GRAY_LR_SR_OB_DR"), public domain.

In the Roman period, coral artefacts are few, generally amulets forming pendants associated with necklaces, necklace and figurine elements, gems, cameos and carvings. These artefacts generally relate to the 3rd and 4th century CE (Morel 2006, p. 72), whereas findings of raw coral are completely absent (Feugère 2000).
From the 1st century CE, most of the *C. rubrum* fished in the Mediterranean Sea was exported to India (Pliny, *Naturalis Historia*, XXXII, 21-23).

> Auctoritas bacarum eius non minus Indorum viris quoque pretiosa est quam feminis nostris unions gestamen amoliendis periculis arbitrantur. Ita et decore et religione gaudent. Prius quam hoc noresceret, Galli gladius, scuta, galeas adornabant eo. Nunc tanta paenuria est vendibili merce, ut prequam raro cernatur in suo orbe (*Naturalis Historia*, XXXII, 11, 23).

This information is also contained in the *Periplus Maris Erythraei* (1st century CE), maritime routes of the Red Sea, the Indian Ocean and the Persian Gulf (Morel 2006, p. 72), and in the *Descriptio Orbis* of Dionysius Periegetes (Leurini 2006, p. 86). Some authors (De Romanis 2000) identify four phases between the 2nd century BCE and the 1st century CE: 1) export of mediocre coral from the Persian Gulf; 2) export of better quality Mediterranean coral to the Nile delta (Meeks 2000), northern India, southern India and Sri Lanka; 3) the trade extends to Bactrian (Afghanistan) and 4) to China, as in Hellenistic times (Morel 2006, p. 72). However, archaeological records do not confirm such an abundance in India and Sri Lanka, where it is only reported in few locations (Morel 2006, pp. 73-75; Vidale 2001; Vidale *et al.* 2015). Amulets and coral jewellery of this phase are documented in Afghanistan and China (Tagliente 2006). In Egypt, findings of red coral are found in the Delta and surrounding areas; in Alexandria, 180 fragments of raw coral were found on the Broucherion Coast, identifying a probable production 'atelier'. In Nubia, jewellery dating from the 2nd to 4th century CE has been found (Meeks 2000, p. 104).

3.5. Middle Ages (476-1492)

In the Middle Ages, the areas of supply changed, according to Jewish geographers and traders in the 11th and 12th century CE (Fig. 17): the Maghreb coasts were exploited by local populations, particularly in the site of Marsa al-Kharaz, today's La Calle (Marsacarès-La Calle), where fishing is attested from the 10th century CE and two centuries later. Sicily, particularly the Trapani coast, still produces coral of excellent quality (Bresc 2000; Chazottes 2018; Piccinno 2006). Fishing areas were also located towards the Provençal rocky coast of Marseille in Saint-Raphael, near the Estérel, and the Ligurian Gulf (in particular from 1140 in Genoa, from 1154 in Portofino), in Corsica and on Catalan coast, also exploited from the 11th century, with an intensification in the 14th century CE (Bresc 2000). Coral fishing in Naples is attested between 1000 and 1200 CE, with Norman regulation (Sirago 2006).
In the 13th century, Provençals fished coral along the coasts of Provence, Sardinia, Corsica, Sicily, southern Italy and the Gulf of Naples (Bresc 2000; Chazottes 2018; Sirago 2006). Between the end of the 13th and the beginning of the 14th century, numerous fishing facilities were exploited in the Gulf of Naples and Capri (Bresc 2000). The port of Marseilles becomes very important (Chazottes 2018) and trades exist with the Levant or Egypt, Arab, Indian and Persian markets.
From the 12th century and particularly in the 14th century, Sardinia was exploited by the Provençals, in competition with the Pisans (in Cagliari) and the Ligurians (in Bonifacio). Between the end of the 14th and the beginning of the 15th century, the Catalans also began to fish in Sardinia, partly replacing the 'Marseillais' (Bresc 2000). Between the 14th and 15th century, small Jewish coral workshops opened in Trapani (Costanza 2006).
Archival documents in Provence mention the use of large amounts of red and white coral for pharmaceutical purposes between the end of the 14th and 15th century CE, in continuity with practices already documented in Roman times and later in the early modern period (Chazottes 2018, pp. 145-148).
Ligurians have been fishing in the Sardinian Sea since the beginning of the 14th century, when the Doria and Malaspina families settled on the west coast. In 1354, Venetians and Catalans succeeded in taking these fishing areas away from

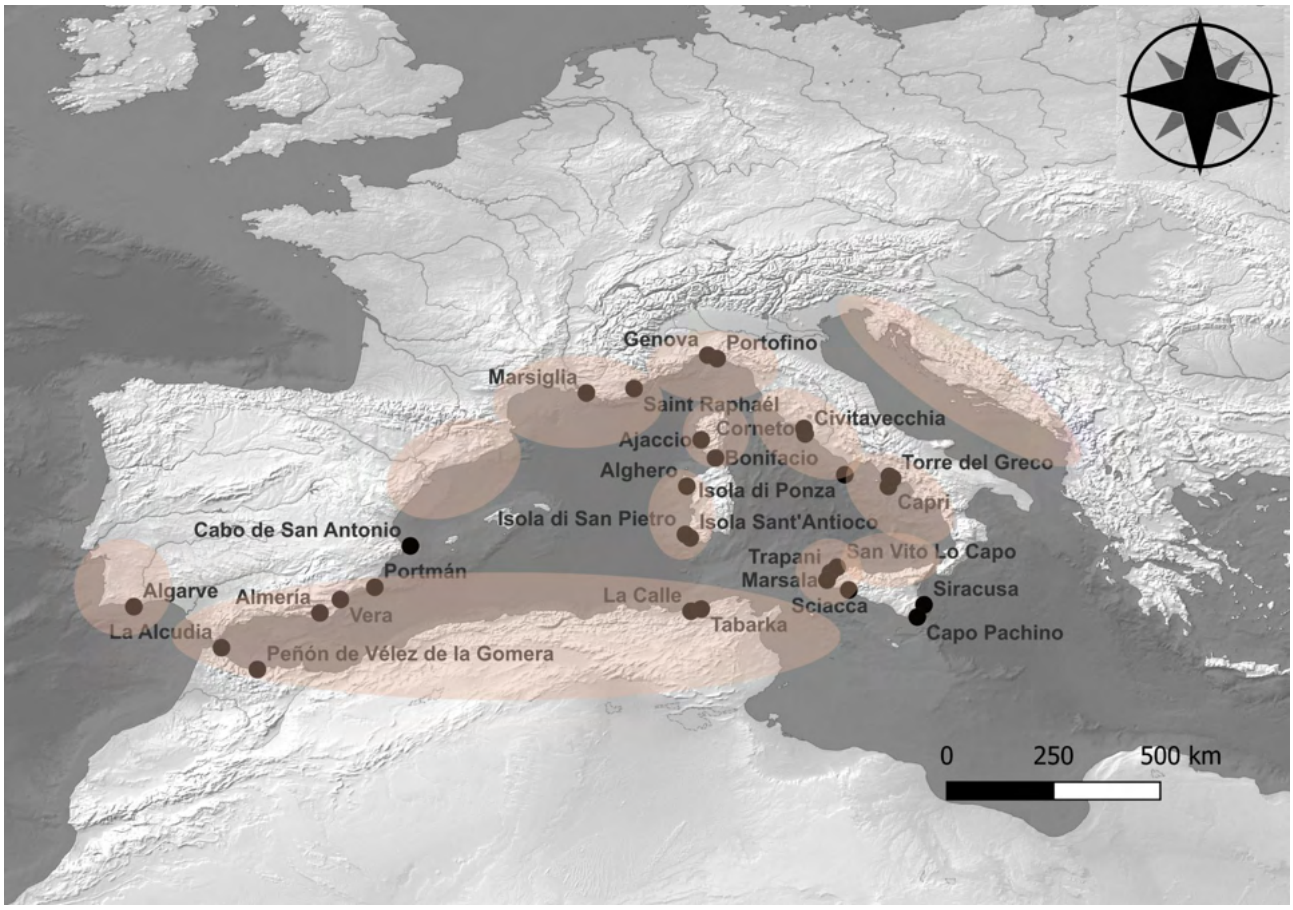

Figure 17. Coral supply areas in historical times. Elaborated by the author in QGIS 3.40.8 (2025); base map: Natural Earth (Gray Earth raster "GRAY_LR_SR_OB_DR"), public domain.

the Ligurian populations. The latter then moved to Corsica and along the African coast, where the Catalans and Provençals were already fishing (Piccinno 2006). In the 15th century, fishing restarted in Marsacarès-La Calle by the Catalans and from 1429 onwards also in Tabarka, where new deposits were discovered (Bresc 2000).
In 1469, Genoa had contracts with Alghero but later referred instead to the Spanish Crown (after 1528; Piccinno 2006).
After the sack of Marseilles, the loss of Naples and the exclusion of Marseilles from the deposits of Sardinia, the Provence coasts were exploited and explored anew. The Florentines and Venetians, with the Catalans, took advantage of the ambitions of René d'Anjou on the Aragonese throne to monopolize the Provençal coral. This was a time of exploration and search for new areas of supply. In 1418, new coral deposits were discovered in the sea of Trapani; searches were also made in Civitavecchia and Corneto, without much success. The Marseillais left the Mediterranean and in 1443 obtained an exclusive coral fishery in the Portuguese Algarve, the southernmost region of mainland Portugal, outside the Strait of Gibraltar; this was the first exploitation of Atlantic coral (Bresc 2000).

3.6. Modern Age (1492-1789)

In the 16th century, Ligurians and Provençals fished in Corsica and Sardinia. Manufacturing was concentrated in Genoa, in the Bisagno and Polcevera Valleys (Doneddu 2006; Piccinno 2006). In 1599, new coral banks were discovered near the islands of San Pietro and Sant'Antioco, where the Ligurians had exclusive exploitation (Piccinno 2006). Between the 15th and 16th century CE, other fishing sites are found in southern Italy (San Vito lo Capo in Sicily, Ponza, Marsala, Syracuse, Cape Pachino), along the coast of the Spanish Levant (Cabo de San Antonio, Portmàn, Vera, Almeria) and Mediterranean Morocco (La Alcudia and Penon de la Gomera) (Bresc 2000).
Between the 16th and 18th century CE, coral guilds were established in Trapani, while fishing activities also continued to be carried out

along the North African coasts. By the end of the 16th century, the coral banks in the Naples area had been largely depleted, prompting a shift in fishing towards Corsica and Sardinia, mainly by the *Livornesi* (Costanza 2006). Between the 16th and 17th century CE, coral processing developed in Naples (Sirago 2006).
In the 16th century, the Adriatic was also the focus of an important coral trade under the control of Venice (Schmid-Sikimić 2000a, p. 155; Ugolini 2006b, p. 91).
In the 17th century, coral fishing saw a Genoese hegemony, with boats leaving from Cervo, Santa Margherita Ligure and Laigueglia towards Ajaccio and Bonifacio; fishing by Sardinians and Corsicans was subordinate. Fishermen from Campania were also active in these areas, selling the raw coral to merchants from Livorno, who were responsible for its processing and marketing. In contrast, coral-related activities in the Trapani area experienced a decline (Doneddu 2006; Sirago 2006).
During the 18th century, the Genoese maintained their dominance, while the Corsicans began fishing and trading both corsican and sardinian coral. The corsican deposits went soon exhausted, but the exploitation of sardinian deposits continued until the end of the century (Doneddu 2006; Piccinno 2006). The people of Campania also continued to fish in these seas; however, unlike in the previous century, they sought to establish local processing and trading activities in order to increase profits, within the framework of the Bourbon attempts to regulate the coral trade (First Bourbon period: 1734–1806). Skilled workers from Trapani and Livorno were brought to Naples, where production activities were concentrated along the Sellaria road. In 1790, the *Regia Compagnia del Corallo* established a factory in Torre del Greco, but only four years later a volcanic eruption triggered a political and economic crisis that affected these initiatives (Sirago 2006). Later in the 18th century, fishing in Corsica and Sardinia became unprofitable due to the depletion of coral banks, and exploitation consequently shifted towards North Africa (Doneddu 2006).

3.7. Contemporary Age (1789-1904)

The profession of coral craftsman was characteristic of Naples throughout the 19th century. At the beginning of the 19th century (French period: 1806-1815), another factory was set up in Torre del Greco by a entrepreneur from Marseilles (1805), followed by the opening of numerous others. Coral fishing continued mainly in North Africa, despite the persistent risks of piracy. The second Bourbon period (1815–1860) was particularly turbulent: in 1816 a massacre of fishermen occurred in North Africa; in 1817 a plague outbreak affected the same areas; and in 1818 coral fishing was officially banned. As a result, the number of Neapolitan fishermen operating in other regions increased, alongside a revival of coral processing in Marseille around 1820 (Sirago 2006). In the second half of the 19th century, Torre del Greco was the most important center and the development of this trade culminated with the establishment of a school for corallers in 1878. At the same time, the Genoese were fishing in Provence (Gangemi 2006; Sirago 2006).
In 1875, following the discovery of abundant coral deposits in Sciacca, overproduction led to a collapse of the market. As a consequence, in 1887 a ban on fishing in the Sciacca area was imposed, prompting a return to the exploitation of older coral banks as well as renewed fishing activity in Lazio, near Civitavecchia. Between 1892 and 1904 there were signs of revitalisation of the sector; however, most coral banks were already largely depleted. In 1905, the import of Japanese coral began, marking a significant shift in supply. In 1932, the *Museo del Corallo* was founded in Torre del Greco (Gangemi, 2006; Sirago 2006).
The coral species exploited in more recent times have diverse origins and are generally deep-sea corals. The best-known examples are from the Far East, used in fashion jewellery, such as the red *C. japonicum* from Japan, *C. nobile* from the Philippines, and *C. secundum* from Hawaii, which is pink or otherwise pale in colour. These species, native to the Pacific Ocean, are much larger than Mediterranean red coral, whose branches generally do not exceed 30 cm in height or 1 kg in weight (Harmelin 2000).

4. Coral in Northern Italy in the Iron Age

Abstract

In Italia settentrionale durante la prima età del Ferro si riscontra un'ampia diffusione di manufatti variamente decorati con corallo. Questo materiale è frequentemente utilizzato in oggetti di ornamento e abbigliamento femminili, principalmente fibule e pendenti, soprattutto in contesti archeologici riconducibili all'area di Golasecca, a nord-ovest, e all'area paleoveneta-atestina, a nord-est. In queste aree, il corallo compare dall'VIII secolo a.C. e si diffonde ampiamente tra il VII e il V secolo a.C., con un'evoluzione tecnologica da forme più semplici (rami di corallo forati, perline) verso oggetti via via più complessi (fibule e pendenti).

Il tipo più diffuso è la fibula a sanguisuga con lunga staffa e arco con anima in cotto, decorata da piccoli inserti circolari. Esso è comune in due aree principali (cultura di Golasecca e di Este), ma attestato anche in zone limitrofe (la Liguria interna e costiera, l'Etruria padana, ecc.), probabilmente in relazione alle principali vie di transito e alla circolazione di persone, oggetti e modelli. In questo senso si può notare una certa variabilità territoriale. Nell'area paleoveneta si trovano le forme più antiche, caratterizzate da un minor numero di fori sull'arco, nonché dalla predominanza di una variante con motivi lineari tra i fori. Tali varianti sono ben rappresentate anche nell'area di Golasecca, dove però sono attestate anche forme più evolute, indicando questa come probabile zona di origine. Nella zona di confine tra le aree di Golasecca, ligure e padana (come Alessandrino, Astigiano e Piacentino), è stata identificata una variante forse legata a una produzione locale, caratterizzata da un arco pieno a sezione piatta, lunga staffa con estremità appiattita e talvolta un rigonfiamento, decorato solo sulla faccia superiore.

L'origine del corallo utilizzato non è certa, ma si ipotizza un ruolo di intermediazione da parte degli Etruschi, attivi in quei territori. Tuttavia, mancano prove dirette dell'uso o pesca del corallo in ambito etrusco. Combinando le aree di pesca indicate da Plinio il Vecchio per l'epoca romana, con le aree di influenza delle popolazioni etrusche, è possibile identificare come possibili zone di approvvigionamento: Gravisca, le 'Stoechades' e il Golfo gallico (Languedoc), e probabilmente anche le coste del Mar Ligure (Provenza e forse anche Liguria e Toscana).

Il corallo giunse nel mondo hallstattiano transalpino tramite le popolazioni dell'Italia settentrionale, dove fu utilizzato per la decorazione di fibule, in particolare delle fibule tardo-hallstattiane occidentali attestate anche in area cisalpina. Dai dati archeologici emerge una maggiore concentrazione di decorazioni in corallo nell'area cisalpina e soprattutto nel Nord-Est, come possibile indicazione di influenze locali e rielaborazione di modelli. Presso le culture Golasecca e di Este è attestata fibula a sanguisuga con decorazione a solchi trasversali sull'arco, intermedia tra i due tipi precedenti e probabilmente evolutasi localmente per la fusione di modelli cisalpini e transalpini. Il corallo diventa particolarmente apprezzato dalle popolazioni transalpine nei periodi La Tène A e B1, fino circa al 300 a.C., mentre in Italia settentrionale si registra un graduale declino a partire dal IV secolo a.C., fino alla sua scomparsa.

Introduction

The use of coral in northern Italy can be traced back to the early Iron Age, when various types of ornament were produced, each characteristic of the different cultures that crafted them (Fig. 18). The use of this material is well documented through a variety of artefacts, differing in form, distribution, and chronology. For each type, a description is provided, accompanied by one or more illustrations (at least of those examined in this study), distribution maps, and a table listing known occurrences.

The tables provide, for each artefact, the site of discovery, type of site and excavation details, country and region, inventory number, chronology, current location, relevant literature, and indications of optical and/or archaeometric analyses (for abbreviations, see the list at the beginning of this volume).

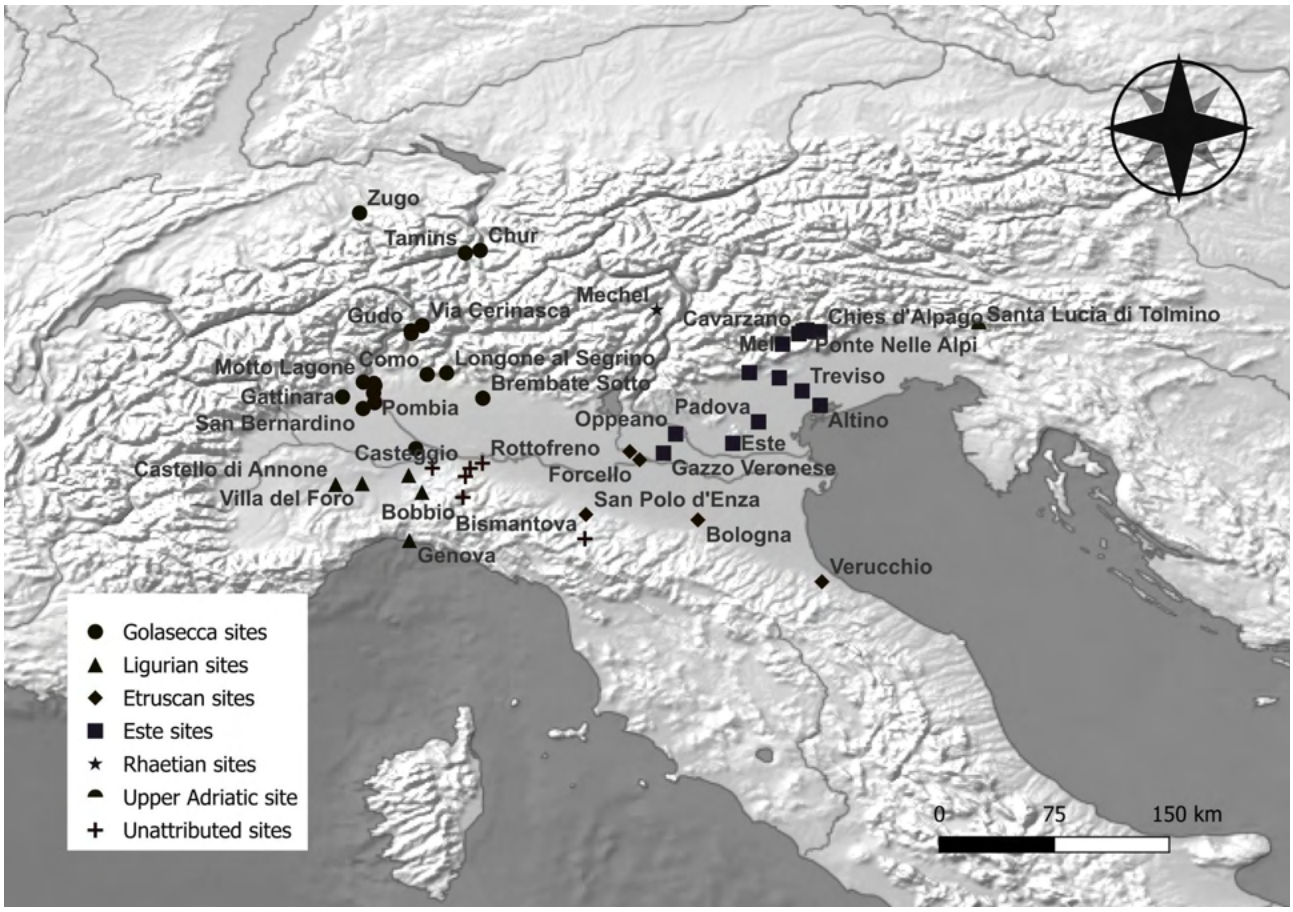

Figure 18. Evidence of the presence of supposed coral (raw coral and artefacts) in the Cisalpine area in the Early Iron Age. Elaborated by the author in QGIS 3.40.8 (2025); base map: Natural Earth (Gray Earth raster "GRAY_LR_SR_OB_DR"), public domain.

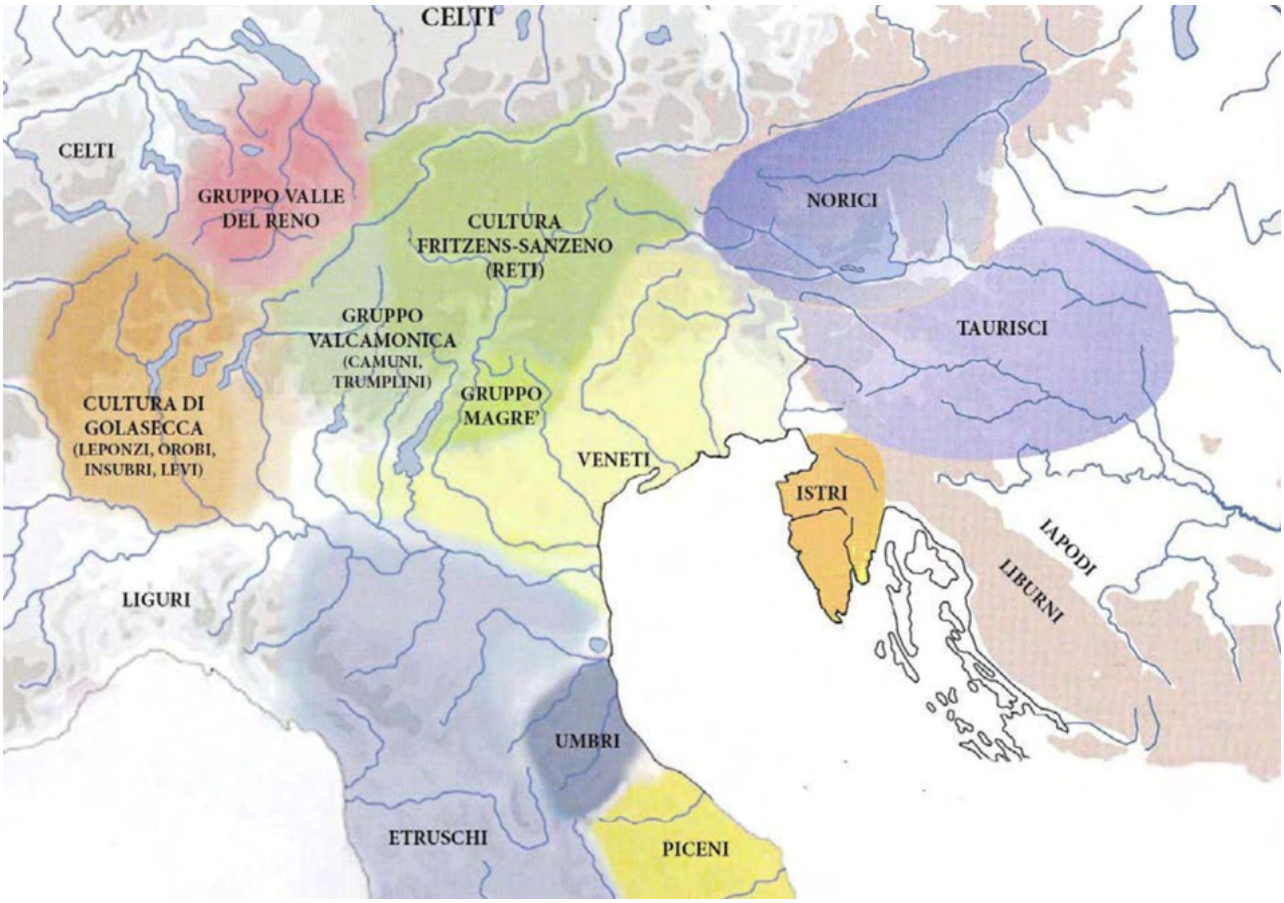

Figure 19. Populations and cultural groups in northern Italy in the Early Iron Age (after Marzatico 2019, fig. 4).

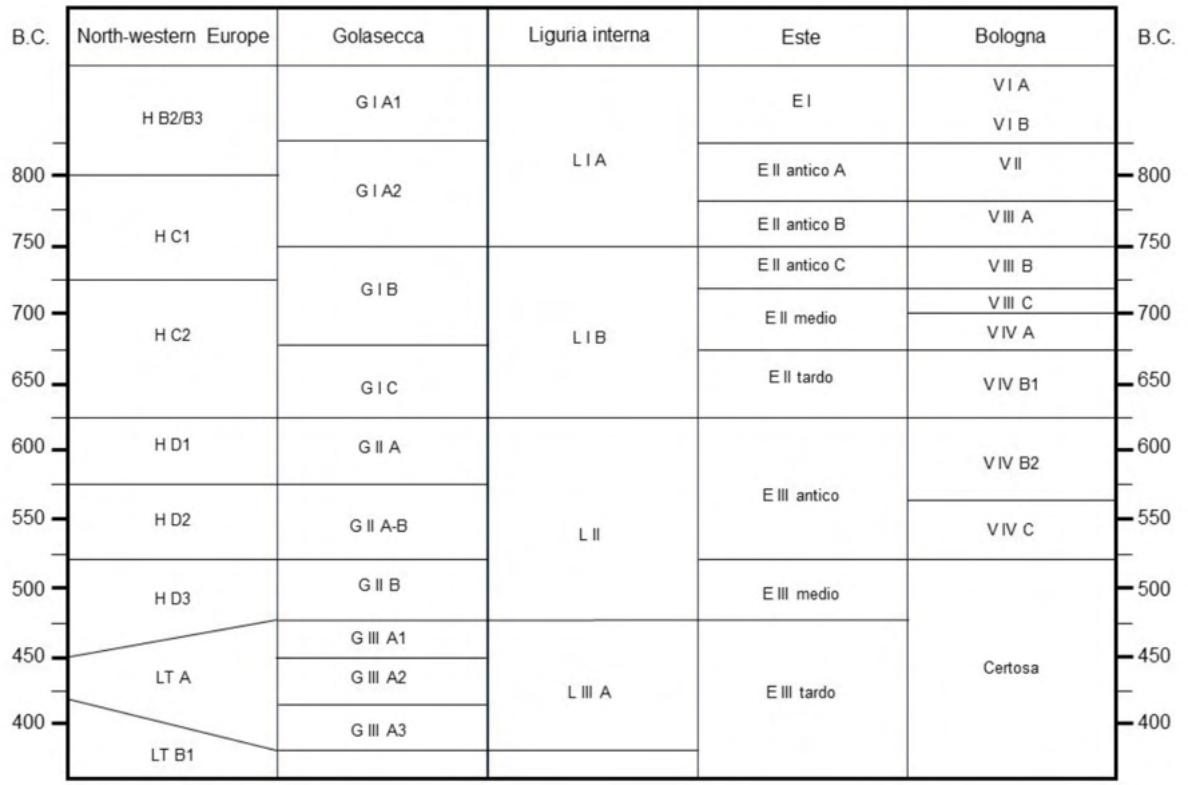

Figure 20. Chronological reference table: H = Hallstatt; LT = La Tène; G = Golasecca; L = Ligurian; E = Este; V = Villanovan (modified after Gambari 2019a; de Marinis, Gambari 2005).

4.1 The archaeological background. Northern Italy in the Iron Age

During the Early Iron Age, a transnational framework of cultural and commercial contacts and exchanges developed, centered on northern Italy. Within this framework, mutual influences emerged both across the Alps and between the regions bordering the Mediterranean. The Cisalpine population was internally diverse (Fig. 19) and traces its origins to earlier phases of the Late Bronze Age (Bietti Sestieri *et al.* 2015; 2019; de Marinis 1991a).

Among the Early Iron Age cultures, this study focuses on those involved in the trade and processing of Mediterranean red coral – namely the Golasecca culture, the 'Liguria Interna', the Venetic-Atestine Culture and the 'Etruria Padana'.

Northern Italy was an unavoidable transit area for trade, with continuous exchanges between the Hallstatt and Etruscan worlds, mediated bythe Golasecca populations. At the same time, the Venetic area flourished, and economic activity resumed in the upper Adriatic. Coral serves as an exemplary trade good, illustrating the cultural contacts, exchanges, and movements of people during this period.

4.1.1 Golasecca

The Golasecca area included western Lombardy, eastern Piedmont, Canton Ticino and the Mesolcina Valley (Fig. 21); it was bordered to the south by the Po River, to the west by the Sesia River and to the east by the Serio and Adda Rivers.

This territory is geomorphologically heterogeneous, including plains, rivers, lakes, moraines, valleys and Alpine passes. The Golasecca culture has been divided in different chronological phases, from the Final Bronze Age (proto-Golasecca) to the Late Iron Age (Cicolani 2017; de Marinis 2009a; de Marinis, Biaggio Simona 2000; Lorre, Cicolani 2009). In the Iron Age, the chronological articulation has three main *facies* in a chronological range from 900 BCE to 380 BCE. Each of these has been further divided (Fig. 20; Cicolani 2017; Peroni *et al.* 1975).

The origin of this culture can be traced back to the Final Bronze Age (12th and 11th century BCE), in the areas of 'Alto Verbano' (settlements) and Bellinzona and Sopraceneri-Alta Val Mesolcina. In the 10th century BCE, settlements also spread to the south of Monte Ceneri (on the Lombard and Piedmontese shores of Lake Maggiore), along the Ticino in the hilly areas of Castelletto Ticino-Sesto Calende-Golasecca, Somma Lombardo and Malpensa, Como, Bergamo and the Lecco area, with diffusion into Valsassina and upper lake area towards Valtellina and Graubünden began, along the Po River in the Pavia area (Fig. 21; Casini 2022; de Marinis, Biaggio Simona 2000; de Marinis, Casini 2020; Lorre, Cicolani 2009; Teržan, de Marinis 2018; Welc *et al.* 2020).

The territory of this culture occupies a particularly favourable trading position from south to north, situated on a direct route through the central Alps. During the 7th century BCE, two main urban sites existed, Castelletto Ticino-Sesto Calende-Golasecca, in the western part, and Como, in the eastern part (Cicolani, Gambari 2021; de Marinis 2009a; de Marinis 1991a). These two hubs, at the southern end of Lake Maggiore and Lake Como and in the gateway area of the Alpine regions, were strategically positioned and likely played a key role in supra-regional trade as transhipment and market centers. Their location along lakes and rivers provided both rapid and relatively safe transport of goods (Casini 2000a; Casini, Chaume 2014; Cicolani 2017; Cicolani, Huet 2019; Cicolani, Gambari 2021; Schmid-Sikimić 2002, p. 228).

The existence of trade networks connecting the Etruscan world to continental Europe, through the Golasecca area, influenced the development of the Golasecca culture itself and the western Hallstattian culture. In both the Golasecca area and the transalpine Celtic regions, valuable and prestigious artefacts, including items produced locally in Golasecca, testify to trade networks connecting Etruria with the Celts on one side and with the Greeks on the other (de Marinis 1991a).

At the end of the 6th century BCE, contextually with the decline of the urban center of Castelletto Ticino-Sesto Calende-Golasecca, the area of Milan gained importance with the foundation of *Mediolanum*, which experienced a great development between the 4th and 3rd century BCE (Casini 2022, p. 547).

Gropello Cairoli (Santo Spirito) is another relevant site, located at the southern border of the Golasecca Culture area, on a promontory north of the Po, on the route that connected Genoa

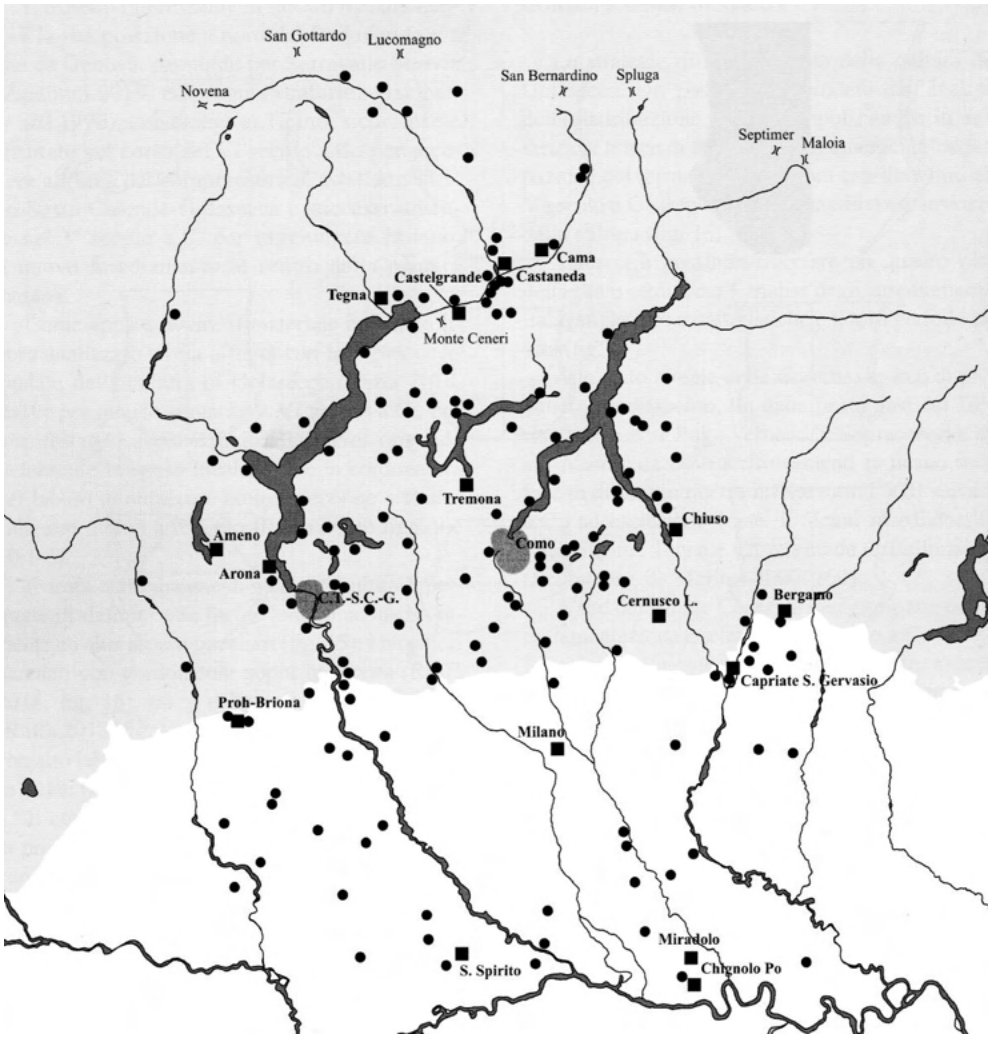

Figure 21. Golasecca area and main sites (after Casini 2022, fig. 16).

through the Scrivia Valley and Tortona to the Ticino in the 6th century BCE and then to Milan in the 5th century BCE (Casini 2022, pp. 552-553; Ruffa 2021).

Archaeological evidence for the Golasecca culture comes from both settlement and funerary contexts, known since the 19th century (Casini 2022, p. 532). The widespread funerary rite was cremation, at least until the 6th century BCE. The ashes of the deceased were put in the tomb inside an urn together with the grave goods. The tombs generally consisted of simple pits, sometimes lined with stone slabs or pebbles. The practice of inhumation is only found in the Swiss area north of Monte Ceneri, probably due to Central European influences (de Marinis 2019).

As far as funerary record is concerned, sumptuous tombs are present in the 7th century BCE, less documented from the 6th century BCE (GII). In this period, contacts with Etruscan populations become more evident and rich female tombs are attested. In a period of extensive trade, coral is one of the materials imported from the Mediterranean world (de Marinis 2009b).

In this later phase, the northern area of the Golasecca culture, including Monte Ceneri and the Mesolcina Valley (de Marinis 2009b), developed, although there is a gap in the documentation between the 10th and mid-7th century BCE (Casini 2022, p. 532).

During the GIIIA two different groups can be identified in the Golasecca culture area: the Lepontic/Alpine group in the Canton Ticino north of Monte Ceneri, the Mesolcina Valley in the Grisons, and the Ossola Valley in Piedmont, with evidence of the burial ritual of inhumation; on the other hand, in the area of Como, Canton Ticino south of Monte Ceneri, western Lombardy and 'Novarese' in Piedmont, the incineration ritual prevails, as in the previous phases (de Marinis 1981; 2019).

The economic development of the Swiss south-alpine valleys is also linked to supra-regional trade and transalpine traffic. The presence of Golasecca materials in these areas, as well as north of the Alps, was most likely due to their role as intermediaries in supra-regional exchange networks. The archaeological remains are mainly fibulae and jewellery, and thus allegedly correlated with the mobility of people and the creation of family ties between neighbouring populations, according to exogamous patrilocal strategies (Casini 2000b; 2011; Schmid-Sikimić 2002, pp. 235-236). The crossing of the Alps by the Etruscans or Greeks is otherwise not documented (Schmid-Sikimić 2002, pp. 217-219). Recent studies have suggested revising this interpretative approach, which is not supported by bioarchaeological data from Italy, and instead propose an interpretation based on the circulation and imitation of artefacts (Cicolani, Zamboni 2023).

To the North of the Alpine crest, in the Valais, Graubünden or Piedmont, copper-rich deposits must have played a role in the occupation of these areas and in the integration of the Golasecca Alpine group into a network of supra-regional economic relations (Schmid-Sikimić 2002, pp. 217-219). In support of this hypothesis, Schmid-Sikimić (2002) reports that the presence of high levels of arsenic, antimony, nickel and silver in some bronze artefacts from the Arbedo treasure trove may suggest that the raw material originated in the Alpine region.

One of the most important sites in southern Switzerland is Minusio, located at the northern end of Lake Maggiore, a point of transshipment from water to land along the road leading north. From this site, Arbedo could be reached by land proceeding towards Como, passing through Bellinzona and Giubiasco and passing the sites of the Sottoceneri (Cademario, Pazzallo, Porza, Pregassona; Schmid-Sikimić 2002, p. 228). Although no archaeological traces of a settlement have been found, but only large cemeteries and a metallurgical deposit (Schindler 1997; 1998a; 1998b; Verger 2006b), Arbedo gained fundamental importance. It is located at the confluence of two main valleys, the Ticino and the Moesa, exerting a control for accessing the important pass routes to the north, via the San Bernardino pass, with the contribution of transit tributes. In this network of exchanges, the Golasecca populations may also have been directly involved in transport, as well as intermediaries, as suggested by the discovery of Golasecca personal objects (in particular, fibulae) north of the Alps (Cicolani 2017; Güggisberg 2004; Schmid-Sikimić 2002, pp. 228-229). In the Swiss Plateau, as well as in south-western Germany, bronze artefacts of Golasecca origin or influence have been documented. The widespread use of coral there, probably for the local production of fibulae, is also likely linked to contacts with the Golasecca world (Cicolani 2017; Cicolani, Huet 2019; Schmid-Sikimić 2002, pp. 228-230).

4.1.2 Liguria

South of the Golasecca domain, the ancient Ligurian cultures are traditionally divided between 'Liguria interna' and coastal Liguria or 'Liguria propria'. The term 'Liguria interna' refers to the area now known as southern Piedmont, which was inhabited by Ligurian populations during the Iron Age. In the early Iron Age, the population of 'Liguria Interna' decreases, being concentrated in the highland settlements controlling the waterways, which consolidated in lower Piedmont in relation to Etruscan trade between the Early and Late Iron Age (Venturino 2024).

Contacts with the Etruscan productions are suggested between the 9th and 8th century BCE by imported artefacts, such as a crested Villanovan helmet found in Asti, in the Tanaro River. These areas were probably reached using the Po River and its tributaries. In addition, imitations of Etruscan figurative and technical influences can also be found. The Etruscan merchants may have been interested in establishing relations with the Ligurian population, opening new trade routes and acquiring raw materials including metals (Melli 2021, pp. 65-68; Gambari 2014; Aurino 2014, pp. 27-29; Venturino Gambari 2011a, pp. 21-25).

Late Villanovan materials found in coastal Liguria (mid-8th century BCE) suggest attempts by Greek and southern Etruscan groups to build a 'cabotage route' along the northern Tyrrhenian coast. In the 7th century BCE, coastal ports were founded in Liguria, including Genoa-Portofranco (Gambari 2022, pp. 627-628), and at the same time the Etruscans moved towards southern Gaul and Iberia. The Ligurian coasts were included in the area influenced by Pisa, which expanded its commercial range as far as the Gulf of Lion (Melli 2021, pp. 67-68).

In 600 BCE, Marseille was established in the centre of the Gulf of Lion. Between the 6th and 5th centuries BCE, a system of maritime ports and land trade routes to 'Liguria Interna' was established (Melli 2021, pp. 67-68; Gambari 2014, p. 34). New strategic settlements emerged in southern Piedmont, along the routes inland from the Po Valley, and in the Scrivia and Curone valleys (e.g., Serravalle Scrivia, Tortona and Guardamonte di Gremiasco) (Fig. 22; Gambari 2014).

The Serravalle Scrivia-Castello site yielded artifacts of the 6th century BCE (Zamboni 2021a), suggesting the existence of contacts between the Ligurian coast and the Golasecca and Po Valley area. The settlement of Collina di Castello in Tortona, inhabited from the second half of the 6th century BCE, shows contacts with the 'Liguria Interna' and the Golasecca areas. Guardamonte di Gremiasco, strategically located at the intersection of the Staffora and Curone valleys, shows a consistent phase of occupation between the 6th and 5th century BCE (Baratti 2014; Chiaramonte Trerè, Baratti 2016). Along the Scrivia route, the Ligurian area communicated also with the 'Pavese' and 'Lomellina' areas, at the southern limit of the Golasecca culture, where it connected to the Ticino way in the 6th century BCE and then to Milan in the 5th century BCE (Casini 2022, pp. 552-553; Ruffa 2021). Between the late 7th and 6th centuries BCE, a series of regularly spaced stopovers developed along the course of the Tanaro (Fig. 22): Montecastello, at the confluence of Bormida and Tanaro; Villa del Foro, at the confluence of Belbo and Tanaro; Castello di Annone and Variglie-Revigliasco; Alba and Pocapaglia. They show common archaeological features, except for Villa del Foro which shows a higher manufacturing specialization, producing 'bucchero' and other ceramics, bronzes and jewelry, as well as weaving and spinning tools (Venturino, Giaretti 2021).

Between the 7th and 6th century BCE, in the Cuneo area, a continuous occupation of sites already active in the Final Bronze Age occurs, such as Breolungi, Chiusa Pesio-Monte Cavanero, Castelvecchio di Peveragno, Valdieri (Faudino

Figure 22. Distribution of the sites mentioned in the different areas in relation to waterways (in light blue. Elaborated by the author in QGIS 3.40.8 (2025); base map: © CARTO, © OpenStreetMap contributors; hydrography data: Natural Earth (10m Rivers and Lake Centerlines, and Rivers Europe datasets, public domain).

et al. 2014; Gambari 2014, pp. 33-34; Melli 2021, pp. 72-73; Venturino Gambari 2001a, pp. 21-25; 2014, p. 61).
Genua is founded in the 6th century BCE, as suggested by archaeological finds at Collina del Castello (Gambari 2022, p. 631; Melli 2021, pp. 73-76). At the same time, a major Etruscan presence in the Po Valley is observed, repopulating *Felsina*/Bologna, Marzabotto and Adria and founding new centers, such as the Forcello di Bagnolo San Vito. 'Liguria Interna' benefited from this new territorial arrangement. Settlements located along the valleys of the Po's tributaries received materials from Tyrrhenian trade through contacts with Genoa, as evidenced by Golasecca (or imitation) materials found along the Polcevera and Scrivia valleys, which connected Genoa's port with southern Piedmont, as well as within the settlement and necropolis of Genoa (Gambari 2014, pp. 34-35; Melli 2017; 2021, pp. 73-76).
In the 5th century BCE 'Liguria Interna' witnessed a progressive abandonment of the commercial settlements that had flourished in the previous century. This depopulation can most likely be attributed, in addition to climatic deterioration, to economic factors related to a reorganization of Etruscan trade, which led to a reduced interest in these territories, with the notable exception of the Scrivia route to *Mediolanum* (Aurino 2014, p. 30; Gambari 2014, pp. 36-37; Melli 2021, pp. 76-77; Venturino Gambari 2014a, p. 61; Venturino 2024).

4.1.3. Este and northeastern Italy

In north-eastern Italy, the origin of the Iron Age population must be sought in the Bronze Age. The archaeological record reports the discoveries of Padua and Este – the two main centres in the Veneto region in the Early Iron Age (Bietti Sestieri 2015, p. 198; Chieco Bianchi 1988, pp. 8-13). From the beginning of the 8th century BCE, a gradual population increase is observed, along with the consolidation of new centers located in agriculturally favourable areas, close to river routes or the sea. A clearer territorial organization emerges, with differentiated land use. The course of the Adige River becomes a central axis supporting settlement, with most communities concentrated in the lower plain, where Este serves as the principal center. Smaller settlements arise to the west, in the Verona and Vicenza areas, following an itinerary that extends from Este through these zones toward Mantua, without a clearly defined boundary. A demographic increase is also evident in Padua, which develops an independent identity from Este, alongside the growth of the Montebelluna settlement toward the Piave valley (Chieco Bianchi 1988, pp. 14-15; Zamboni 2021b, p. 398).
The foundation of Este reflects a deliberate urban plan, with a clearly defined territorial organization. From the 8th century BCE, Este and other centers, such as those in the Verona area, entered the cultural sphere of the Villanovan world, while maintaining an autonomous identity, as indicated by funerary rituals and ceramic production, which also display Central European and Balkan influences. Metallurgical production in the 8th century BCE shows clear affinities with the Villanovan tradition, particularly in Bologna, and was likely carried out in independent workshops located in major centers, including Padua, Mel, Baldaria di Cologna Veneta, and Gazzo Veronese (Fig. 23). However, the flourishing production of situlae also shows the presence of central-eastern European influences, possibly linked to the arrival of itinerant craftsmen (Chieco Bianchi 1988, pp. 16-32).
Burials are predominantly single, occasionally double, and consist of simple pit graves with grave goods reflecting gender roles. Early burials are generally modest, but by the 8th century BCE they become increasingly elaborate, reflecting emerging social differentiation and the transition toward a more complex economy. There is also evidence of warrior burials with weapons (Chieco Bianchi 1988, pp. 31-34). During the 7th century BCE, cultural relations with the Etruscan areas are consolidated, with continuity in the privileged relationship with Bologna. Regarding funerary traditions, female tombs generally appear richer and more elaborate than male ones, distinguished by abundant grave goods, including metal ornaments crafted from various materials (Chieco Bianchi 1988, pp. 36-40).
From the 7th to the 5th century BCE, the different regions of the Adriatic Sea show several similarities in material culture. This phenomenon was defined by Renato Peroni as *Adriatic koiné* and affects certain sectors such as metalworkig involving highly specialised craft techniques (Peroni 1976). The distribution of these products is uneven. For some, diffusion by sea can be hypothesized; for others, a circum-Adriatic

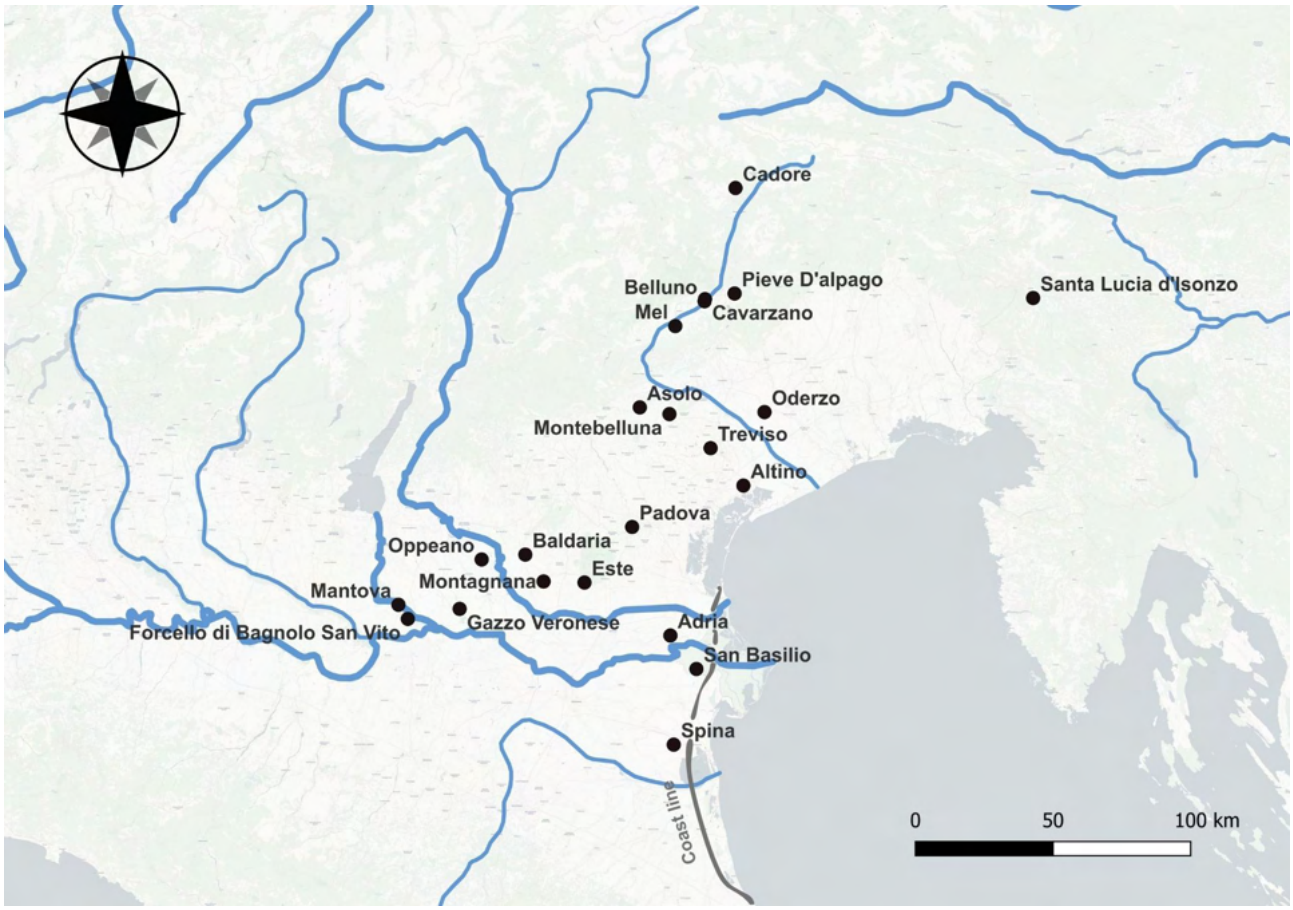

Figure 23. Distribution of the sites mentioned in relation to waterways (in light blue). Elaborated by the author in QGIS 3.40.8 (2025); base map: © CARTO, © OpenStreetMap contributors; hydrography data: Natural Earth (10m Rivers and Lake Centerlines, and Rivers Europe datasets, public domain).

route is apparent, encompassing the Veneto area, Slovenia, and the inland Balkans. In these cases, distribution likely occurred via continental routes or by coastal cabotage. For other materials, an Alpine component (referred to as the *Alpine koiné*) can be posited, spanning the territory of the Golasecca civilization, the Alpine and foothill regions, the Veneto area, Slovenia, and the Inner Balkans (Nascimbene 2009, pp. 7-13; Gangemi 2015, p. 25).

During the Iron Age, the Eastern Alps saw the development of distinct cultural groups, forming a heterogeneous and composite reality (Fig. 19). From the second half of the 6th to the 1st century BCE, the Fritzens-Sanzeno Culture appears in Trentino, South Tyrol and North Tyrol (Marzatico 2014). The ancient Venetians occupied the Veneto region, from the Pre-Alps of Verona to those of Belluno. The Friulian sector, by contrast, was characterised by a complex population that resists classification within a single cultural area, due to the marked dynamism of networks in the upper Adriatic and strong contacts with the Veneto populations. In the Upper Isonzo (Soča) region, specific archaeological facies are attested, defined by the necropolis of Santa Lucia di Tolmino (Most na Soči), excavated between the late 19th and early 20th century. The Slovenian territory was occupied by several groups showing varying degrees of Mediterranean influence, alongside Hallstattian cultural groups in the northern Alpine sector (Nascimbene 2009, pp. 13-18).

The population of Veneto is traditionally divided into several territorial areas. On the plains and in the Brenta and Piave valleys, Venetic populations developed cultural unitarity from the first centuries of the 1st millennium BCE. In contrast, in the Vicenza and Verona Pre-Alps, from the 6th century BCE an occupation developed with a dense network of hilltop villages in continuous cultural exchange (Ruta Serafini 1997, p. 543).

The Piave Valley, an eastern link to the north, is also part of this vast area. Located in the central southern sector of the Eastern Alps, it is a natural passage between the pre-alpine and alpine

zones, towards the passes of transalpine Europe. During the Iron Age, the material culture was relatively homogeneous, combining a Veneto matrix with influences from the surrounding areas, highlighting preferential contacts with the central-eastern perialpine regions, from Trentino to the Isontine valleys (Nascimbene 2009, pp. 18-23; Ruta Serafini 1997, p. 543; Gangemi 2015, p. 25). Archaeological sites in the Piave Valley, distributed at crucial points along the river, yielded material dating from the 7th to 5th century BCE (Fig. 23). At the opening of this valley into the plain, close to the course of the Brenta river, Montebelluna has craft structures specialised in the production of ceramics as early as the 9th-8th century BCE. In the Iron Age, this site developed characteristics similar to those of the dominant centers on the plain. Cemeteries have been known since the end of the 19th century, with cremation burials mainly from the 7th - 5th century BCE (Nascimbene 2009, pp. 18-23; Gangemi 2015). Several prestige objects come from the cemeteries of the Belluno territory, related especially to women's burials – a sign of development of these areas favoured by their position controlling the Alpine passes. The grave goods, dating from the late 7th to the 5th century BCE, indicate strong connections with the Alps, the plain, and the Adriatic. Notably, in contrast to the necropolises of the Venetic plain, there is an almost complete absence of ceramic vessels associated with funerary rituals. Conversely, the rich warrior panoply found in the tomb of Limade di Caverzano reflects influences from the central-eastern Alpine area, likely due to its position along the trade route of the 'lebetes' connecting the Hallstatt centers to Padua – a route also well attested in Montebelluna, Asolo, Mel, and Cadore (Fig. 23; Ruta Serafini 1997, p. 543).

The Adige valley represents the western commercial and cultural connection axis with the Alpine area in relation to the Veneto plain, through the territorial system of the highland sites of the Vicenza and Verona. Along this route, significant evidence of exchanges with the Rhaetian area is attested, which had a significant impact on various aspects of daily life, as shown primarily by settlement finds. Ornamental objects, however, appear to maintain a preferential connection with the Atestine area (Ruta Serafini 1997, p. 546).

In this network of relations between the Veneto plain and the transalpine world, the territories of present-day Friuli Venezia Giulia are also relevant, as various indicators point to a degree of 'osmosis' between these populations. From the late 8th century BCE, in the Carnic and Julian Alps, where a strong Venetic presence is attested, a series of foothill and valley centers developed, linked to the control of trade routes to the north, as well as contacts with the Hallstatt groups and the northern Balkans (Vitri 1997, pp. 566-567). The Friulian Alpine area maintained connections with Veneto and central Friuli until the 6th century BCE, and from then until the first half of the 4th century BCE with the Alpine and pre-alpine regions of Veneto, Trentino, and Slovenia (Vitri *et al.* 2014).

4.1.4. Etruria Padana

In the Final Bronze Age (11th –10th century BCE), the population in Emilia-Romagna was sparse, following the abandonment of the plain after the collapse of the Terramare culture in the 12th century BCE, with communities concentrating instead in western Veneto, particularly in the area around Frattesina (Bietti Sestieri *et al.* 2015; 2019; Zamboni 2021b). During this phase, traces of occupation are identifiable in Apenninic Emilia at certain strategic locations (Pianello Val Tidone, Bismantova, Montecastagneto and Monte Valestra).

In the Early Iron Age (9th–8th century BCE), the situation remained unchanged west of the Panaro River (Zamboni 2018, p. 35; 2022, pp. 79, 81), whereas in the eastern plain a shift towards new centers, such as Bologna and Verucchio, is observed (Fig. 24; Bietti Sestieri 2015, pp. 208, 212, 222; Zamboni 2021b, p. 393). The Emilian alluvial plain records signs of Etruscan influence, with *Felsina*/Bologna as the main center. The 7th century BCE is marked by a phase of cultural opening, influenced by wide-range contacts with the surrounding areas: Golasecca, Liguria, Veneto and the Adriatic region (Zamboni 2018, pp. 232-233). From the 6th century BCE, a 'urban revolution' took place with the foundation of trading hubs along the commercial routes, such as Adria, Spina, Forcello and Marzabotto (Fig. 24; Zamboni 2021b, p. 406; 2022, p. 81; Cicolani *et al.* 2024). Established during the third quarter of the 6th century BCE, the Etruscan settlement of Forcello, north of the Po, occupied a strategic position at the confluence of fluvial and terrestrial routes. The site has also yielded materials linked to the Golasecca and Hallstattian

cultures, attesting to interregional relationships and exchanges (Fig. 24; DE MARINIS *et al.* 2017, pp. 13, 36; SORDI 1986, p. 111).

In Emilia, *Felsina*/Bologna is the main center, a major crossroads in trade connection between the Mediterranean Sea, northern Italy, and central Europe. Its foundation is dated to the mid-8th century BCE and resulted from the planned unification of several villages established in the previous century. The creation of the new urban center was guided by a form of political union and involved the construction of public infrastructures (ORTALLI 2020; ORTALLI *et al.* 2024; VANZINI 2018; 2023). *Felsina*/Bologna differed from other important centres in northern and central Italy, as well as in the 'Etruria', in terms of environmental setting, poleogenesis and material culture (ORTALLI 2020).

In contrast, Verucchio, the other preeminent Villanovan site in eastern Romagna, shares several features with settlements in the Etruria region south of the Apennines. Emerging in the 9th century BCE, it developed into a hegemonic center controlling the coastal plain, maritime connections, and inland routes along the Marecchia valley. Between the 8th and mid-7th century BCE, the settlement expanded, becoming more complex and centralized. Funerary evidence indicates the emergence of a highly hierarchical society (RONDINI, ZAMBONI 2020). Verucchio underwent a complex process of internal development involving periods of both success and crisis, ultimately resulting in its abandonment in the 7th century BCE (ORTALLI 2020; RONDINI, ZAMBONI 2020).

Felsina/Bologna is the primary metallurgical production center of northern Italy, a role previously occupied by Frattesina. In the earliest phases, the metallic finds show a close relationship with the Veneto region and contemporary Tuscan complexes. Later, connections with the north persist, documented by presence of fibulae typically referable to northern Italy (Emilia, Veneto and Golasecca area; BIETTI SESTIERI 2015, pp. 216, 222).

In the region west of Bologna, a phase of slow

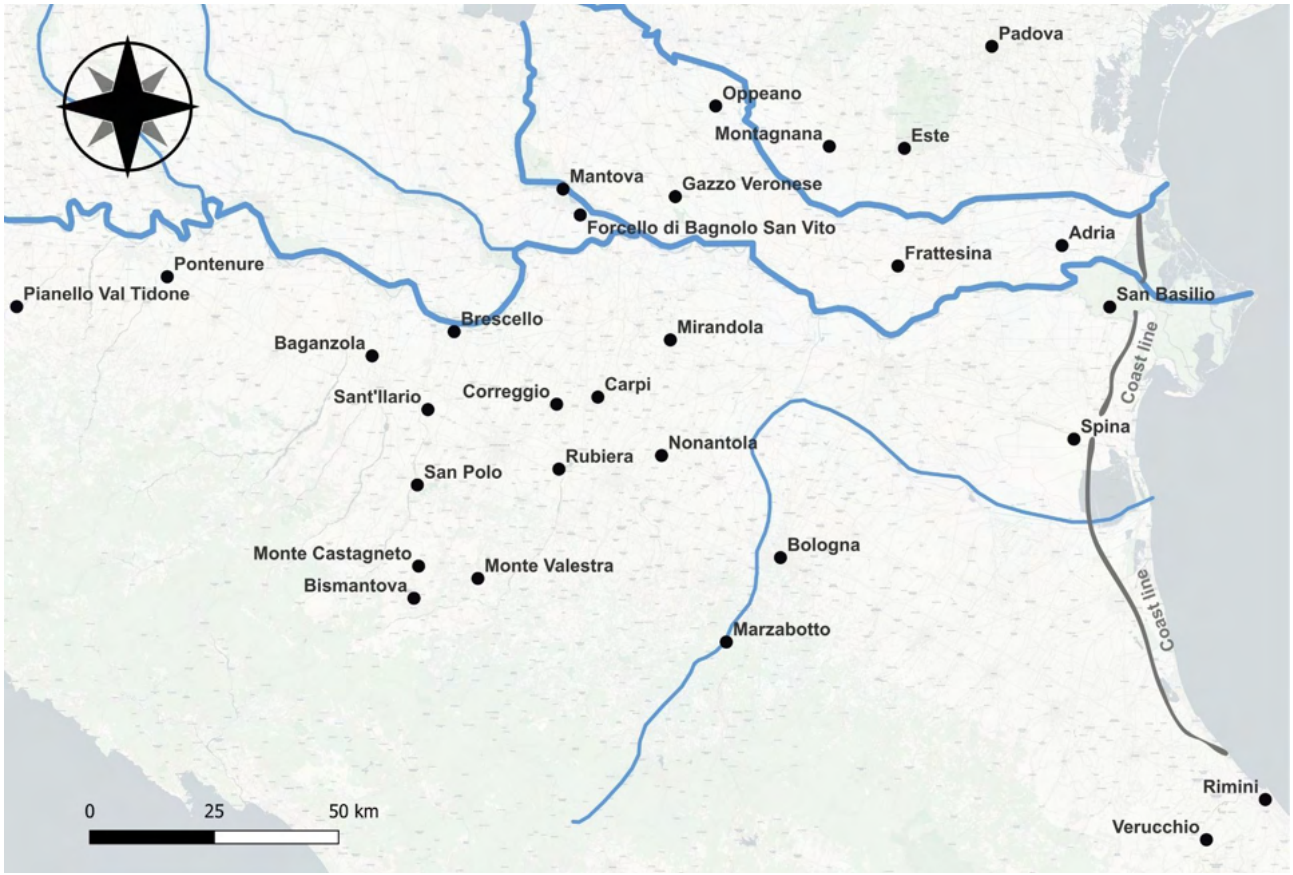

Figure 24. Distribution of the sites mentioned in relation to waterways (in light blue). Elaborated by the author in QGIS 3.40.8 (2025); base map: © CARTO, © OpenStreetMap contributors; hydrography data: Natural Earth (10m Rivers and Lake Centerlines, and Rivers Europe datasets, public domain).

repopulation started during the 8th century BCE, with the appearance newly established small sites. In the first half of the century, funerary evidence is reported between Bologna and the Samoggia, Panaro and Secchia valleys, with rank symbols in the burials. In the second half of the century, the evidence increased and population moved westwards towards the Secchia river, establishing contacts with the Golasecca and Veneto areas (Zamboni 2022, p. 80; 2018, pp. 36-37).
During the 7th century BCE, rural settlements began to appear in the areas west of Bologna ('Modenese' and 'Reggiano'). The population is scattered but strategically placed near trade routes. New successful settlements appear in the Modena area (Carpi, Nonantola) and between the Secchia and Enza riverbeads (Rubiera, Brescello and Servirola) (Fig. 24). The Parma and Piacenza areas seem to remain depopulated until the mid-6th century BCE. The material culture, and in particular the female funerary costume, shows a mixture of influences, combining local elements, as well as Golasecca, Venetian, Ligurian and eastern Hallstatt ornaments, in addition to Felsinian influence (Cicolani, Zamboni 2023, p. 262; Zamboni 2022, p. 77; 2018, pp. 37, 42, 45, 223).
Overall, a gap in the documentation is observed for the first half of the 6th century BCE, followed by a reverse trend in the second half of the century. This phase is likely connected to the activation of a settlement system centered on larger sites with a commercial vocation, which exercised control over smaller villages focused on agriculture (Zamboni 2018, pp. 45, 223). In western Emilia, it is difficult to correlate settlements and necropolises, due to the absence of ceramics in the latter and of metal ornaments in the former. The richest grave goods belong to women, whose dress elements show influences from the Golasecca and Veneto regions, while evidence of banqueting and drinking appears to be completely absent (Zamboni 2018, pp. 224-232).
In the second half of the 5th century BCE, a change becomes evident in Western Emilia, with the appearance of bronze and ceramic vessels related to the drinking of wine, including imported ones. During this phase inhumation becomes more common (Zamboni 2018, pp. 232).

4.1.5 The Late Iron Age

The Late Iron Age begins in the 4th century BCE and continues until the onset of the 'Romanization' process. The 4th century BCE marks the beginning of a period of territorial transformation. Archaeological evidence does not indicate any traumatic events, despite the general crisis affecting the period. In the 19th century, historical-cultural models relied on ancient authors to describe the peoples who settled in the Cisalpine region from the beginning of the 4th century BCE, particularly in central-western Transpadane Italy (Strabo, *Geografia*, V, 9), the Cispadane and the Middle Adriatic area (Polybius, *Storie*, II; 16-17; Livy, *Historiae*, XXX, 37,4; XXXIX, 55, 6; Strabo, *Geografia*, V, 4-12; Pliny, *Naturalis Historia*, III, 116) (Fig. 25; Vitali 1991, pp. 224-225; 2014, pp. 733-734, 740-741).
The 4th century BCE has traditionally been described as the period of the "Gallic invasions". However, recent studies have reinterpreted these events as military expeditions directed against the Etruscans expanding north-westwards (Gambari 2019b; 2022, p. 633), or, alternatively, as part of more complex mobility patterns (Zamboni 2025). During this period, some of the Cispadan Etruscan centers came to an end (e.g. Forcello di Bagnolo San Vito) (Gambari 2019b, pp. 58, 62).
According to some authors, despite the scarcity of archaeological evidence, such as the tumulus tomb of the Ospedale in Aosta and the Sant'Anna–Tre Camini monumental tomb in Como, the Celtic presence in these areas predates the 5th century BCE. It is interpreted as the result of a 'cumulative celticity', created through progressive transalpine influxes, attested as early as the 7th century BCE in western Piedmont north of the Po, with gradual reinforcement between the 6th and the early 5th century BCE (Gambari 2019b, pp. 57-59; 2022, p. 633; 2019b, pp. 61-62).
The Alpine area is characterized by easy circulation along large valleys, forming a complex network of both transverse and longitudinal routes. Within this context, patterns circulated widely, contributing to a degree of homogenization of 'Alpine styles', while still preserving local traits in different areas. During the Late Iron Age, Alpine ornamentation reflects a combination of Transalpine and Celtic influences, and, from the 4th century BCE onward, also influences from the Po Valley. These external elements were blended with local tastes, resulting

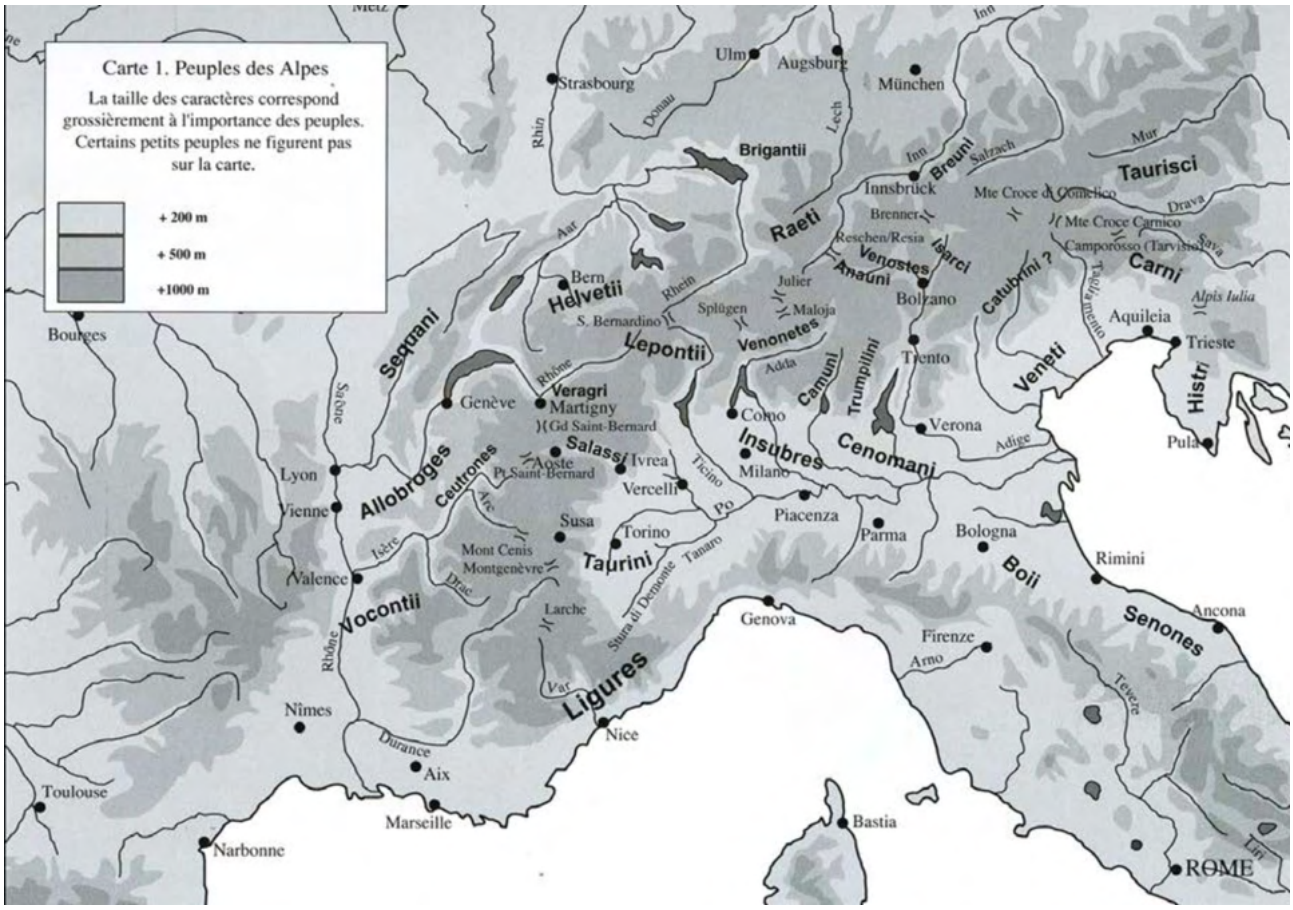

Figure 25. Localization of Cisalpine populations based on indications from written sources according to Tarpin *et al.* 2000 (after Marzatico 2019, fig. 2).

in large, visually striking ornaments featuring complex decorations, plastic motifs, and inlays in non-metallic materials (Adam 1997). Among the typical latenian materials, the presence of long swords (Vitali 2014, p. 744), pierced belt hooks (Frey 1991, p. 144) and especially fibulae (typologically comparable to transalpine ones and characterized by bilateral double/triple-wound spring, bow with regular semicircular curvature, and folded foot, sometimes touching or overtaking the top of the bow: Kruta 1978, p. 159; 1991, p. 195), suggests a significant cultural change.

4.2 The use of coral in the Golasecca culture

The use of red coral, an exotic good and prestige symbol imported from the Mediterranean, in the area of the Golasecca culture is documented from the 8th to the 5th century BCE (de Marinis 1997), contextually (around 700 BCE) to the first imported Etruscan objects. *C. rubrum* was traded over long distances, as well as being highly valued among the local populations. The transport of this raw material is particularly advantageous as a trade commodity, as there is an optimal ratio between the weight/volume of the goods and their value (Schmid-Sikimić 2002, pp. 227).

For what concerns the evolution in the use of coral over time, it is possible to identify an increasing skill in its workmanship, with the production of gradually more complex artefacts. During GIB and GIC (from the end of the 8th to the 7th century BCE), pendants of the Longone al Segrino type appear, consisting of a small branch of perforated coral tied to a bronze rod, wound in a spiral to form a 'T'-shaped pendant (de Marinis 2000). From GII (6th century BCE), coral is mainly used to decorate fibulae, in particular in composite bow fibulae, with an evolution towards more and more elaborate forms up to GIIIA1 (480-440 BCE), before disappearing in GIIIA2 (de Marinis 2000).

In the GIIA-B (late 6th century BCE), leech-shaped fibulae with long foot and bow with a

terracotta core (sometimes with a full-arch) appear, marked by circular insets filled with whitish material (presumed coral) on the bow and sometimes on the small globe at the foot-end. The earliest forms are characterised by two or three rows of inlays on the arch; this decoration evolves over time with an increase in the number of rows of inlays, until larger fibulae with a very high number of inlays on the arch and small globe(s) at the end of the foot are produced in the GIIIA1 (480-440 BCE; Casini 2000a; de Marinis 1981; 2000; von Eles Masi 1986, pp. 163-169). All the various forms of arch and foot decoration are well attested in this area, certifying an evolution of the type. It is worth noting the predominance in the Po-Apennine area (on the border between the Golasecca, Ligurian and Etruscan-Po Valley areas of influence) of a sub-variant, in which the foot has a flattened globe and a bulge, both generally decorated only on the upper part.

From the GII (6th century BCE), the decoration with circular inlays is also applied to richly decorated bronze grooming instruments and bronze bucket pendants, with a decoration consisting of five 'occhio di dado' motifs with a coral inset in a through-hole. Between the 6th and 5th century BCE, some leech fibulae show a variation in the decoration, consisting of inlays of presumed coral in longitudinal or transverse grooves to the main direction of bow development. This decoration is similar to late Western Hallstattian fibulae which were simultaneously present in northern Italy. Some of these types (e.g. leech fibulae, bucket pendants, grooming tools, late-Hallstattian fibulae) are also found outside the Golasecca area (Adam 1996; Barbieri 2019; Cicolani 2017; de Marinis 1981; 2000; Gambacurta, Serafini 2019; Mansfeld 1973; Nascimbene 1999; Roncoroni 2005).

4.2.1 Longone al Segrino type pendant

In the Golasecca IB (late 8th - early 7th century BCE) and mainly in the Golasecca IC (7th century BCE) tombs, coral is used in a simple manner, without any processing, in the so-called Longone al Segrino pendant. It is marked by presence of a rough sprig of coral attached with a simple or double loop to a twisted bronze

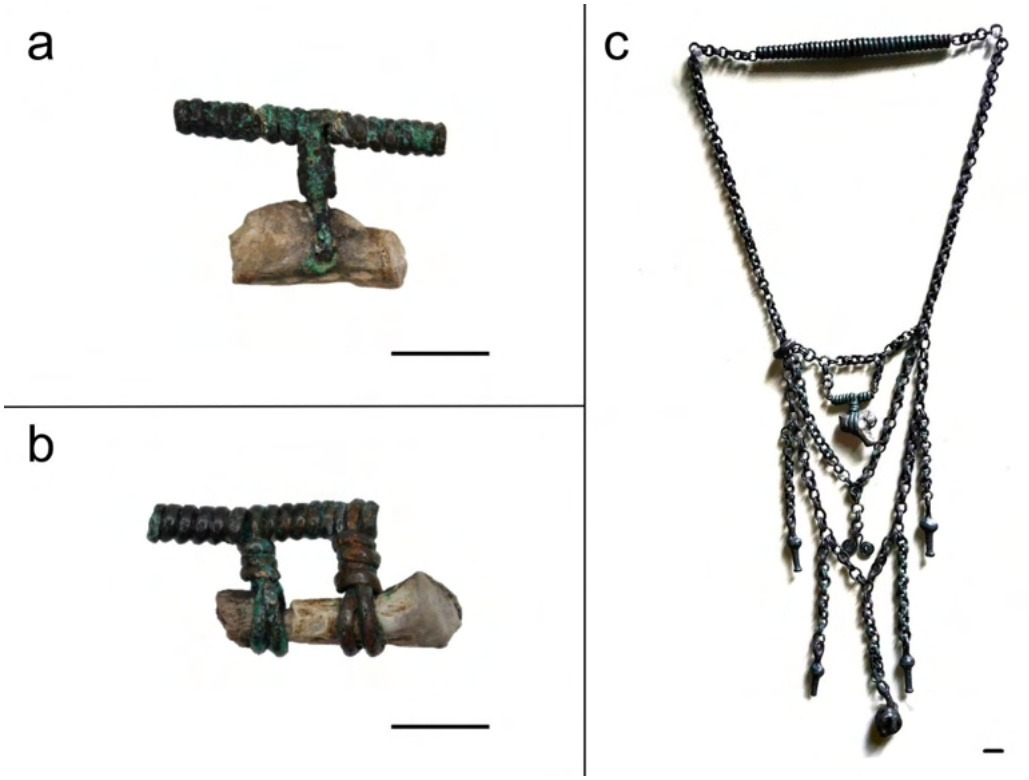

Figure 26. Longone al Segrino pendants, metric reference 1 cm: a) Como, Ca' Morta, IACP terrain, tomb. 302, inv. no. St33593 (ph. Berruto); b) Castelletto sopra Ticino, loc. Motto Falco; double Longone al Segrino type pendant, inv. no. CT179 (ph. Berruto); c) Golasecca; Longone al Segrino type pendant as parte of a necklace, inv. no. MV103 (ph. Diana).

rod, forming a T-shaped pendant (Fig. 26a; DE MARINIS 1997, pp. 156-157; 2000, pp. 159-162). In one case (tomb XX, Valtravaglia necropolis, Castelveccana), a pendant made of horn instead of coral is described (DE MARINIS 2000, p. 163). A particular find from Motto Falco (Castelletto sopra Ticino) required a double support with a bronze rod, probably due to the length of the coral branch (Fig. 26b).

This type of pendant could appear either in isolation or alongside similar examples. A clear instance of the former is the Longone al Segrino–type pendant from Golasecca (inv. no. MV103), preserved in the Villa Mirabello Civic Museums in Varese, still attached to the necklace of which it formed a part (Fig. 26c). Instead, multiple pendants in the same grave goods are reported (e.g., in tomb 302 from Ca' Morta, IACP terrain, Como; DE MARINIS 2000, p. 161, fig. 2)

The distribution of this pendant is limited to the territory of the Golasecca culture (Fig. 27; Tab. 2), with a higher frequency in the western area; there are examples in Castelletto Ticino, Sesto Calende, Golasecca, Como, Longone al Segrino and Castelveccana.

The Musei Reali/Museo di Antichità in Turin houses a singular artefact made of presumed coral and interpreted as a 19th century 'pastiche' – namely a necklace consisting of bronze spirals alternating with coral cylinders and coral pendants in the shape of bells, comprising 55 pieces of worked coral, the provenance of which is reported from Golasecca (DE MARINIS 2000, p. 163).

4.2.2 Coral composite bow fibula

In the Golasecca culture, from the end of the 7th century BCE, coral is used only to produce fibulae as a covering element for the bow. This fibula appears in the GIIA (late 7th - early 6th century BCE), GIIA-B (mid-6th century BCE) and GIIB (late 6th - early 5th century BCE). It is characterised by the presence of a bronze rod arch, on which coral (or amber) elements are inserted; these elements can also be inserted in the form of a bead in the foot. The is documented both in the Como area (more frequently) and in the western area of the Golasecca culture (Fig. 28).

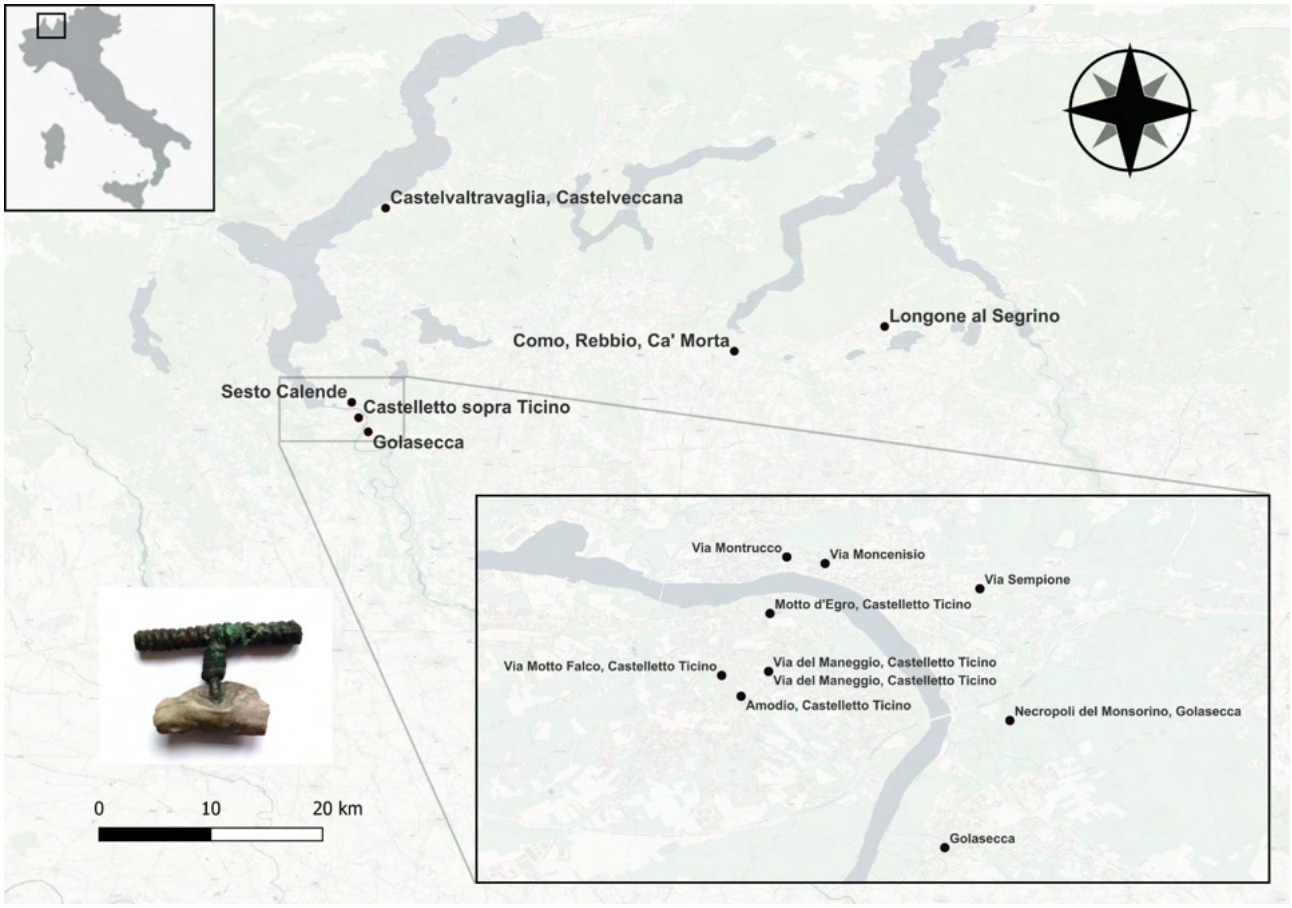

Figure 27. Distribution of the 'Longone al Segrino' type pendant. Elaborated by the author in QGIS 3.40.8 (2025); base map: © CARTO, © OpenStreetMap contributors; archaeological find: Como, inv. no. St.33593 (ph. BERRUTO).

Archaeological finds are hardly complete; generally, fragments of coral are found as a small branch, truncated obliquely and perpendicularly at both extremities, pierced by a longitudinal hole where the bronze rod forming the bow structure of the fibula is housed (de Marinis 1997, p. 157; 2000, pp. 165-166). In other cases, coral is not preserved and only the bronze rod remains, as in the case of tomb 4, known as 'del Tripode' (loc. Mulini Bellaria, Sesto Calende), where excavation data report presence of white marks in the deposition soil (de Marinis 2009c, p. 443, fig. 14.4). A number of variants (Ca' Morta type, Albate type, Golasecca type, Sesto Calende type and Lazzaretto type) were identified for this simpler type (referred to as type 1 in Tab. 3), based on the angle of the arch and the cross-section of the cladding elements (see Cicolani 2017, pp. 117-118; de Marinis 1992, p. 170, fig. 6).

The type evolved in later phases (GIIIA1, 480-440 BCE) towards a more elaborate shape (referred to as type 2 in Tab. 3), well documented at Ca' Morta in Como (tombs 116 and VIII-1926, tomb of the Chariot), in Cuggiono and Brembate Sotto-tomb 12 (de Marinis 1981, pp. 223-224; 2000, pp. 170-171). Now the coral segments covering the bow are shorter and more regular, each of them having one or two grooves for the insertion of a spiral-wound gold ribbon. As a result of the analyses carried out on coral in this study, it was also possible to identify, in two artefacts from Como (E5957-E5958, Respaù; Fig. 29), the presence of a silver thread.

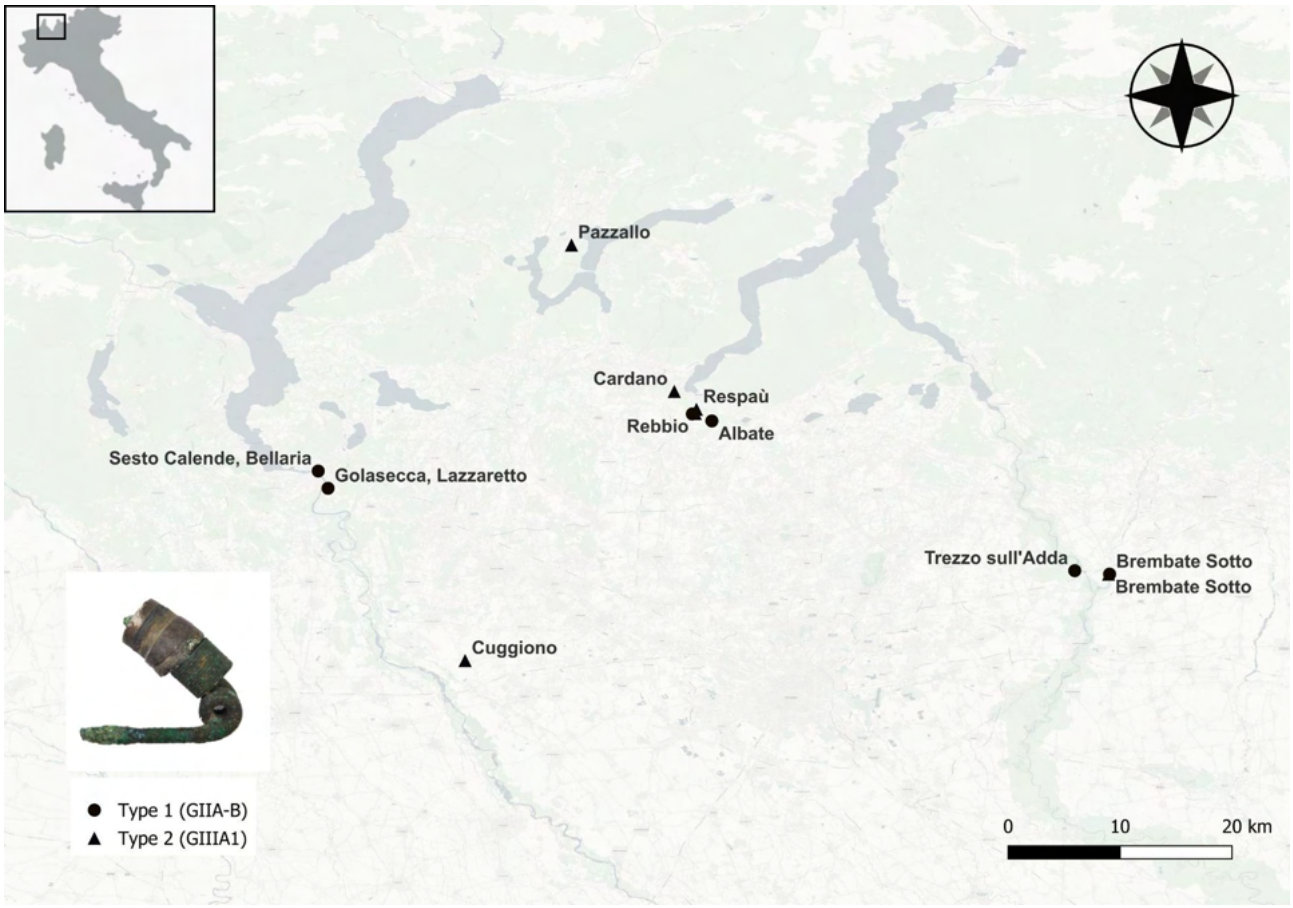

Figure 28. Distribution of the 'Coral composite bow fibula' type. Elaborated by the author in QGIS 3.40.8 (2025); base map: © CARTO, © OpenStreetMap contributors; archaeological find: Como, inv. no. 5957 (ph. Berruto).

Figure 29. Como, Respaù, composite bow fibula, type 2, inv. no. 5957 (ph. Berruto; metric reference 1 cm).

4.2.3 Leech fibulae

Leech fibulae ('fibula a sanguisuga') are widespread throughout northern Italy and transalpine area, with a chronological range from the middle of the 6th and the mid-5th century BCE. They exhibit considerable variability in morphology and decoration. The simplest and most common forms display only linear decoration along the bow, whereas the more elaborate examples are distinguished by insets. The size of the bow varies, and in some cases it contains a clay core. This type of fibula is typically associated with female burials (De Marinis 1981, p. 217; Peroni *et al.* 1975; von Eles Masi 1986, p. 144).

4.2.4 Leech fibulae with circular insets

Starting from the GIIA-B (late 6th century BCE), coral is used as an inset in the decoration of the bow, generally of medium size, with a terracotta core, a long foot with a small globe termination and a truncated vase-like appendix (Fig. 1). The decoration lies on the top of the bow, with rows of circular inlays between two bands of transversal lines, and sometimes also on the small globe (Tabs. 4-5; de Marinis 2000, pp. 169-171; von Eles Masi 1986, pp. 163-169; Schindler, de Marinis 2000, p. 167). Insets fill the holes (Ø ≈ 2 mm), usually arranged in parallel rows on the arch. When preserved, they are whitish, at times pinkish, traditionally identified in the literature as *C. rubrum* denatured over time – although scientific analyses are scarce and generally using unreliable methods. In some cases, dated to the late 6th and 5th century BCE, the bow has no terracotta core (in Tab. 5 in the column 'Preserved parts', indicated by an asterisk*) (de Marinis 2000; Perrin 2000; Schvoerer *et al.* 2000). This type of fibula is generally found in female or rarely mixed grave goods (probably bisome tombs) (Casini 2000a; 2000b; Cicolani, Zamboni 2022; de Marinis 1981, p. 217; 2000, p. 171) and is well dated, thanks to its discovery in various grave complexes. The earliest examples can be dated before the middle of the 6th century BCE, such as a burial from Sesto Calende; the later ones to the end of the 6th century BCE, including all Atestine artefacts (von Eles Masi 1986, p. 168).

The leech fibula with circular insets is common in the area of the Golasecca culture (Sesto Calende, Golasecca, Castelletto sopra Ticino, Como, Switzerland), but also in other regions such as Etruria Padana (Adria, Lago superiore di Mantova, Forcello di Bagnolo San Vito, San Polo d'Enza, Marzabotto, Verucchio), Liguria Interna (Brignano Frascata, Villa del Foro, Valbrevenna), the Pavese (Verretto) and Reggiano (Bismantova), the Venetic (Este, Padua, Oppeano, Gazzo Veronese, Castellazzo della Garolda, Montebelluna) and the Alpine in the Belluno region (Caverzano, Chies d'Alpago, Cugnan, Safforze), as well as in Santa Lucia di Tolmino (Most na Soči) and in Slovenian Hallstattian necropolises (Vače and Stična). Sporadically, it is found in the Rhaetian (Trentino, Mechel, Calferi di Stenico) and transalpine areas (Fig. 30; tab. 5; de Marinis 2000, p. 170).

It had a wide diffusion, evolving in the 5th century BCE towards increasingly complex forms, when the 'Palestro type' appeared in the western area, particularly in Canton Ticino. This type was larger and had more rows of inlays on the bow and on the foot, marked by one or more small globes (de Marinis 1981, p. 220, fig. 4). This type is particularly common in the GIIIA1 in the Golasecca necropolises (Como, Sesto Calende and Pombia) and Sopra Ceneri (Gudo, Cerinasca d'Arbedo, Gorduno, Dalpe, Minusio), in the Mesolcina Valley (Castaneda), as well as in the Po Valley (Palestro and Gropello Cairoli-Santo Spirito) (de Marinis 2000, p. 170), Venetic (Este) and Etruscan Po Valleys (Forcello di Bagnolo San Vito, Verucchio) and Belluno area (Caverzano, Safforze) (tab. 5).

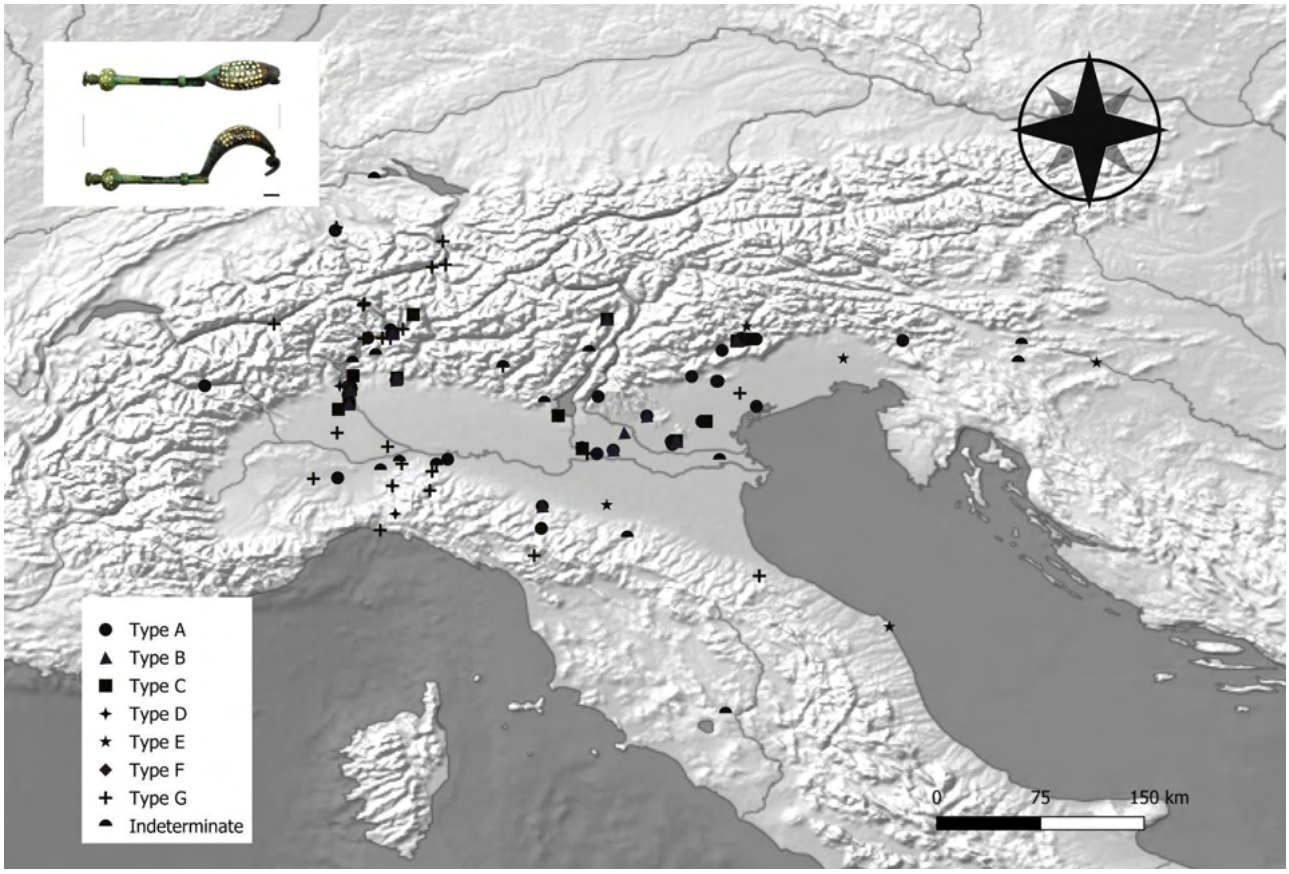

Figure 30. Type distribution of 'Leech fibula with circular inlays'. Elaborated by the author in QGIS 3.40.8 (2025); base map: Natural Earth (Gray Earth raster "GRAY_LR_SR_OB_DR"), public domain; archaeological find: Arona, Motto Lagone, tomb 1.

Based on the arrangement of the inlays on the arch, different sub-types (varieties) were described (von Eles Masi 1986, pp. 163-169), presented hereafter with some adaptations (Fig. 31):

- Variety A (in Tab. 5 column 'Bow type': A): coral insets arranged in three rows, between two bands of transverse lines, from which two main groups of small or large sizes are recognisable;
- Variety A-bis (in Tab. 5 column 'Bow type': A-bis): coral insets arranged in two rows, chronologically comparable to the previous one;
- Variety B (in Tab. 5 column 'Bow type': B): coral insets arranged in four rows, between two bands of transverse lines, each consisting of four or more elements;
- Variety C (in Tab. 5 column 'Bow type': C): coral insets arranged in five rows, between two bands of transverse lines;
- Variety D (in Tab. 5 column 'Bow type': D): very small, closely spaced insets arranged in many rows, sometimes in an unordered manner and occasionally also on the ventral face of the bow of the fibula, between two bands of transverse lines;
- Variety E (in Tab. 5 column 'Bow type': A-E or B-E): variant characterized in the central panel by the presence of lines arranged longitudinally to divide the rows of embedded elements (three or four rows), between two bands of transverse lines, chronologically framed between the late 6th and early 5th century BCE;
- Variety F (in Tab. 5 column 'Bow type': A-F, B-F, or C-F): a variant characterized by small ribs instead of bands of transverse lines on either side of the bow, present for types A, B, and C and chronologically framed between the second half of the 6th and the beginning of the 5th century BCE;
- Variety G (in Tab. 5 column 'Bow type': G), also called 'Palestro type' (de Marinis 1981, p. 220, fig. 4): large fibulae, completely covered by embedded elements in the central panel of the bow and on the terminal foot globet(s), chronologically framed in the 5th century BCE (480-440 BCE).

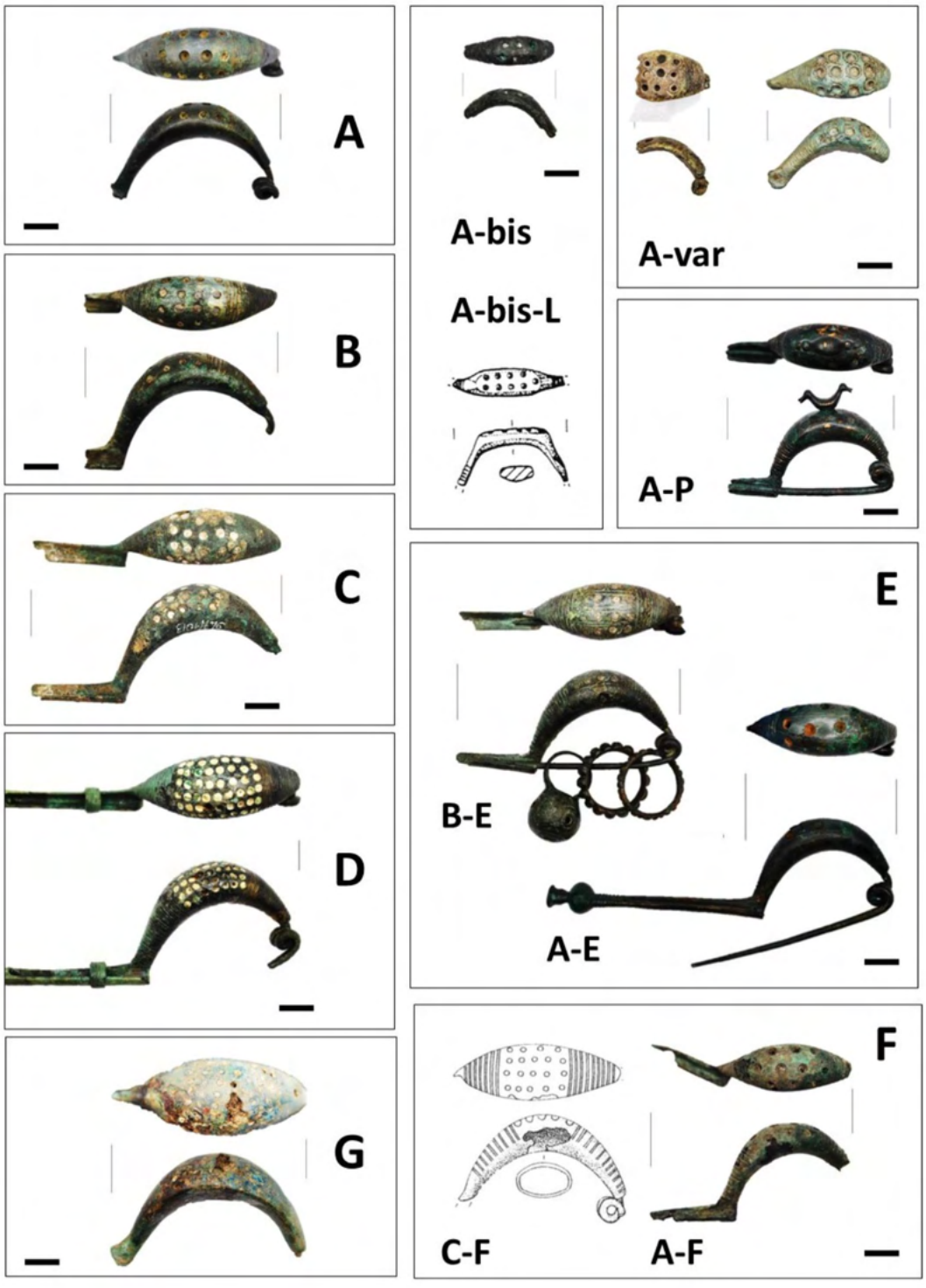

Figure 31. Classification of the different types of leech fibulae with coral insets on the base of the bow decoration (metric reference 1 cm); images modified after: A (ph.Berruto Castelletto Ticino, inv. no. St. 2140, Torino, Musei Reali); B (ph. Berruto Bellinzago Novarese, inv. no. 197 – Novara, Museo Civico); C (ph.Berruto Castelletto Ticino/ Vigevano, inv. no. 947, Novara, Museo Civico); D (ph. Berruto Motto Lagone tomb 1, Arona, Museo Civico); G (ph.Berruto Como, via Isonzo, inv. no. St. 57244, Como, Museo Civico); A-bis (ph. Berruto Como Ca' Morta, inv. no. St. 114084, Como, Museo Civico); A-bis-L (after Ruta Serafini 1997, fig. 5.5); A-var (ph. Berruto; sx: Villa del Foro, inv. no. St. 66132, Torino, Musei Reali; dx: Rottofreno, loc. Cascina Rondinino, inv. no. St. 259507, Museo Archeologico della Valle Tidone); B-E (ph. Berruto, Padova, Piovego, inv. no. IG 224255); A-E (ph. Berruto, Pieve d'Alpago, inv. no. IG 312349); C-F (after von Eles Masi 1986, n. 1585); A-F (ph. Berruto, Como Ca' Morta, inv. no. St. 879, Como, Museo Civico).

Some exceptions or variants to type A/A-bis have also been described, less diffused:

- The upper face of the bow may be flat with an oval cross-section, decorated with two lines of circular holes (in Tab. 5 'Bow type' column: A-bis-L), as in the case of the fibula from Este (PD; inv. no. 9628; von Eles Masi 1986, no. 1596) or that from Borso del Grappa (inv. no. 259929; Nascimbene 2009, p. 134, n. 3; Endrizzi, Marzatico 1997, p. 545, fig. 5,5).
- Decoration with small circular holes can be marked by a concentric pattern, with insets (in Tab. 5 column 'Bow type': A-var), on full-arch fibulae, as in the case of specimens from Este-Capodaglio (inv. no. 3145; Chieco Bianchi *et al.* 1976, pp. 19, 39, t. 13.10) and Rottofreno (inv. 259507), or with a wide, flattened full arch, as in the examples from Villa del Foro (inv. no. 66132; Faudino *et al.* 2014, p. 132, fig. 7.8), San Polo d'Enza (Damiani *et al.* 1992, pp. 129, 308, t. LXII.933) and Gazzo Veronese (Salzani 1976, pp. 422, 425, fig. 16.4).
- A bronze ornithomorphic double element may exist on the bow, inserted in the centre of the three-row circular inset decoration (in Tab. 5 column 'Bow type': A-P), as in three specimens from: Castelletto Ticino (inv. no. D2773; von Eles Masi 1986, t. 119.1459), Padova (inv. no. 60735; von Eles Masi 1986, p. 157, t. 119.1459A) and San Polo d'Enza (Damiani *et al.* 1992, pp. 128, 222, 307, fig. 10, t. LXI.931).

A sample from Mel (inv. no. 9271; Fig. 32) represents a 'unicum' (in Tab. 5 Bow type column: M); it is an intact miniature leech fibula (total length 2.9 cm) with a long foot with terminal swelling and decoration on the arch, consisting of a single hole for housing an inlay, between two bands of transverse ribs. It can be referred to the type of miniature leech fibulae, which however has no insets and often with a bow tending to a lozenge shape, unlike the specimen from Mel. These small fibulae are attested in 'Liguria Interna' (Villa del Foro, Castello di Annone and Cossano Belbo: Faudino *et al.* 2014, pp. 133-134, fig. 9), in Emilia-Romagna (Baganzola, Sant'Ilario d'Enza - Bettolino, *Felsina*/Bologna) and in the Venetic area (Faudino *et al.* 2014, p. 133; Damiani *et al.* 1992, t. LX, n. 900-902).

Figure 32. Mel, miniature leech fibula with inset, inv. no. 9271 (ph. Berruto; metric reference 1 cm).

The geographical distribution of the different variants (Tab. 4) shows that variant A is the most widespread in absolute terms (Fig. 34); variants B (Fig. 35) and C (Fig. 36) seem to be equally distributed and involve northern Italy and Canton Ticino; type D (Fig. 37) ia apparently most present in the Golasecca and Ligurian areas; type G is an evolution of the latter, but with a much more capillary diffusion (Fig. 40), again affecting northern Italy and Switzerland; type E (Fig. 38) seems most common in northeastern Italy and Slovenia, but has also attestation in the Golasecca area; type F is less significant in distribution (Fig. 39) and number of attestations.
A further classification can also be made based on the foot termination (Fig. 33), which can be:

- type P: pointed for the insertion of an amber 'vagus' (in Tab. 5 column 'Foot type': P);
- type R: dovetailed (in Tab. 5 column 'Foot type': R);
- type S: with globet end and spheroidal termination (in Tab. 5 column 'Foot type': S);
- type V: with globet end and vase termination (in Tab. 5 column 'Foot type': V);
- type Q: with foot bulge, decorated (in Tab. 5 column 'Foot type': QB) or not (in Tab. 5 column 'Foot type': QA), globet end and vase termination (in Tab. 5 column 'Foot type': Q);
- type GG: with double globet and vase termination (in Tab. 5 column 'Foot type': GG);
- type GGG: with triple globet and vase termination (in Tab. 5 column 'Foot type': GGG);
- type TA: enlarged foot with globet termination, similar to 'Late Alpine fibulae' (in Tab. 5 column 'Foot type': TA).

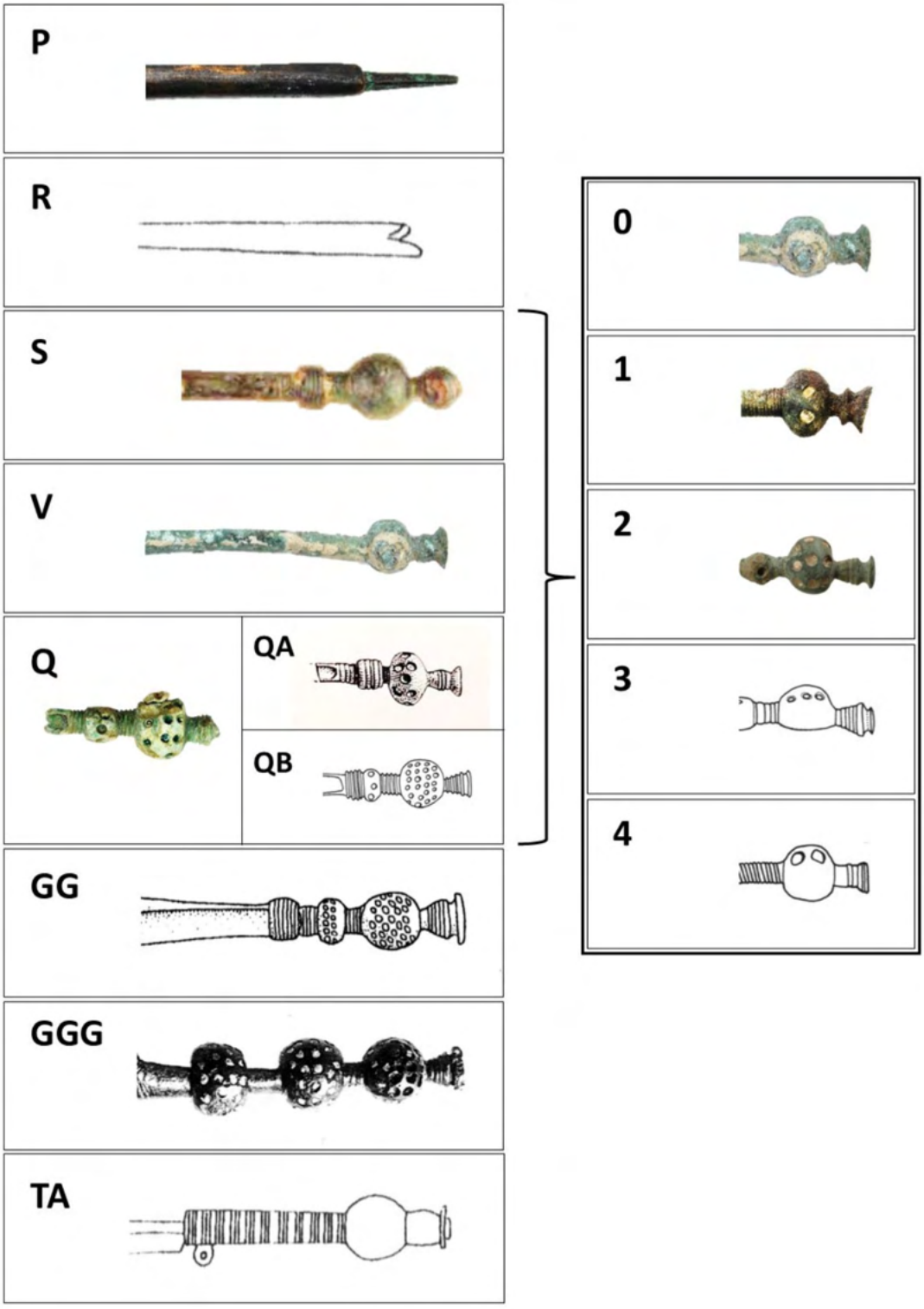

Figure 33. Classification of the different types of leech fibulae with coral insets on the base of the foot-ending; images modified after: P (ph. Berruto, Castelletto Ticino, inv. no. D2104); R (after von Eles Masi 1986, n. 1859); S (Museo Civico Giovio di Como, inv. no. E17022); V (ph. Berruto, Piovego, t. 108.3); Q (ph. Berruto, Pombia, inv. no. St. 83946); GG (after Ravaglia 2000, fig. 1, n. 2); GGG (after Rageth 1997, p. 244, fig. 15); TA (after von Eles Masi 1986, n. 1593); QA (after Schmid-Sikimić 2002, fig. 3.20.17); QB (after Damiani *et al.* 1992, t. LXII, n. 934); 0 (ph. Berruto Piovego, t. 108.3); 1 (after Berruto *et al.* 2023a, fig. 1, n. 1); 2 (after Berruto *et al.* 2023a, fig. 1, n. 3); 3 (after Damiani *et al.* 1992, t. LXII, n. 935); 4 (after Damiani *et al.* 1992, t. LXI, n. 930).

The terminal globet of the foot may or may not have (in Tab. 5, column 'Foot type': V0) decoration with circular insets; sometimes, only one inset is present in the vase-like termination (in Tab. 5, column 'Foot type' indicated by the presence of an asterisk*). Decoration, when present, may involve the entire surface of the globet, a single row (in Tab. 5 column 'Foot type': V1, S1, or GG1), several rows with rhomboidal or random distribution (in Tab. 5 column 'Foot type': V2, S2, Q2, GG2) or only the upper part of it (in Tab. 5 column 'Foot type': V3/Q3, if globet flattened on lower face, or V4/Q4, if globet is spheroidal).
Differences in the shape of the foot termination are more or less common. The following are uncommon: the late-alpine-like type (TA; Fig. 33), for which only one specimen is identified from Golasecca (inv. no. A0.9.4842; von Eles Masi 1986, no. 1593), and the swallowtail type (R; Fig. 33), such as the exemplar from Carceri d'Este (von Eles Masi 1986, p. 185, t. 144.1859). The pointed (P; Figs. 33, 41) and spheroidal-ended (S; Figs. 33, 42) types are slightly more common (note that the S type is attested exclusively in Switzerland and Como). The globet-ended and vase-terminated (V; Fig. 33) type is the most common of all (Fig. 43), both geographically and chronologically, with variation in the position of the inlays (late 6th to 5th century BCE). Finally, types with foot bulge (Q; Fig. 33), double or triple globet ending (GG and GGG; Fig. 33), are very common and chronologically more recent, generally associated with the G variant of the arch, 'Palestro type' (Fig. 40). However, a different geographic distribution should be highlighted, with the foot with double or triple globet ends (type GG or GGG) mainly found in the Swiss area of the Golasecca culture (Fig. 44), with three exceptions in the plains of Pavia (Palestro, Gropello Cairoli-Santo Spirito) and in the Apennines of Piacenza (Borgonovo Val Tidone), while the foot with bulge before the globet (type Q) – particularly the subvariant with flattened globet and bulge, both decorated only on the upper part (type QB3, blue in Fig. 45) – mostly occurs along the northern Apennines (Fig. 45).

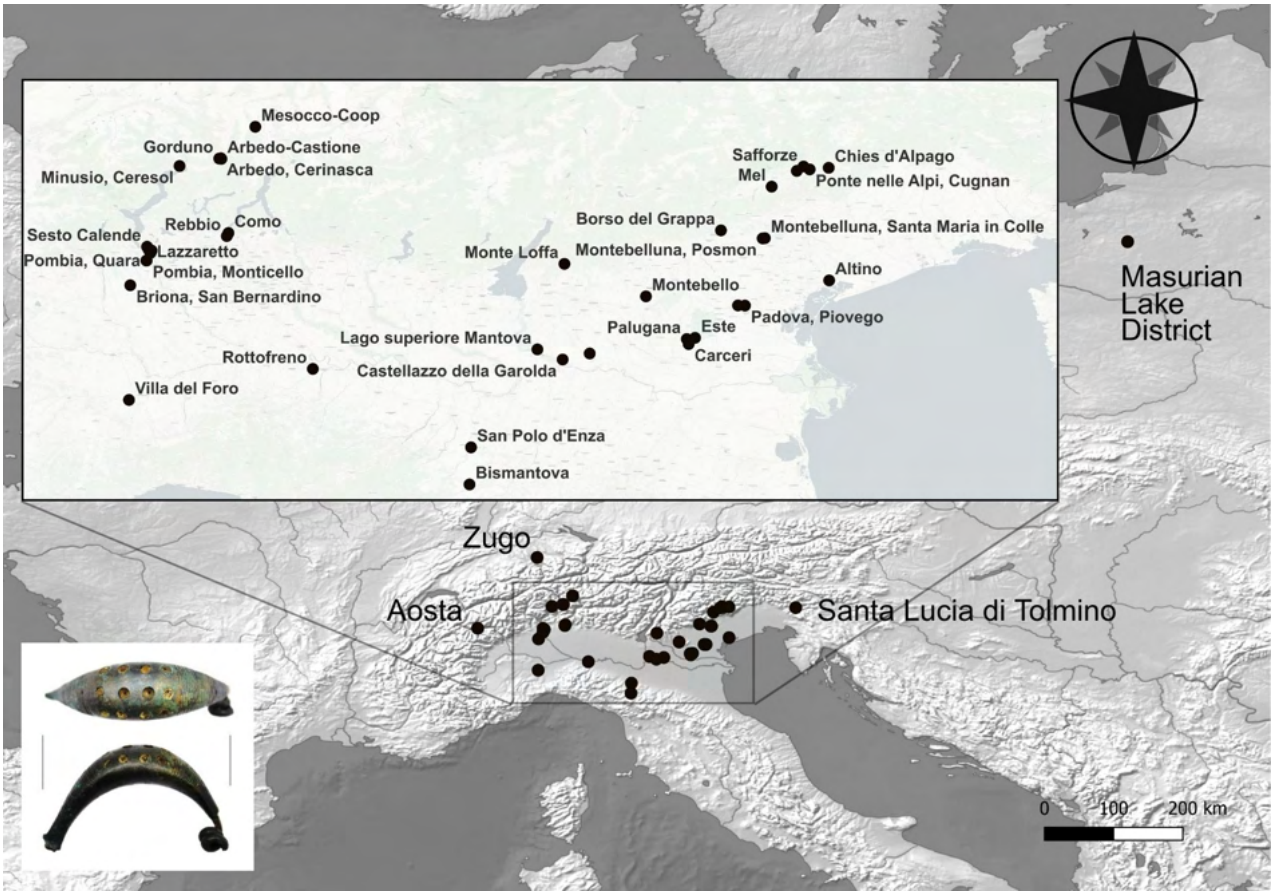

Figure 34. Type A (bow) distribution map. Elaborated by the author in QGIS 3.40.8 (2025); base map: Natural Earth (Gray Earth raster "GRAY_LR_SR_OB_DR"), public domain; archaeological find: Castelletto Ticino, inv. no. St. 2140 (ph. Berruto).

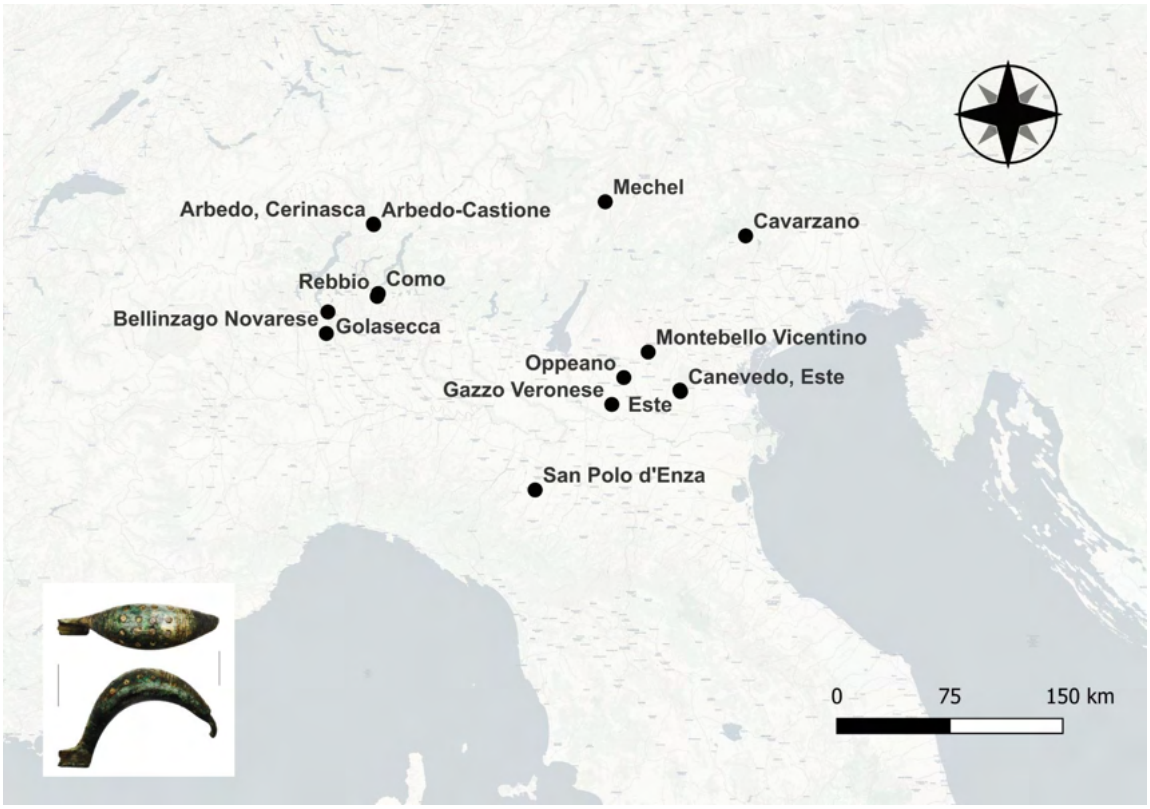

Figure 35. Type B (bow) distribution map. Elaborated by the author in QGIS 3.40.8 (2025); base map: © CARTO, © OpenStreetMap contributors; archaeological find: Bellinzago Novarese, inv. no. 197 (ph. Berruto).

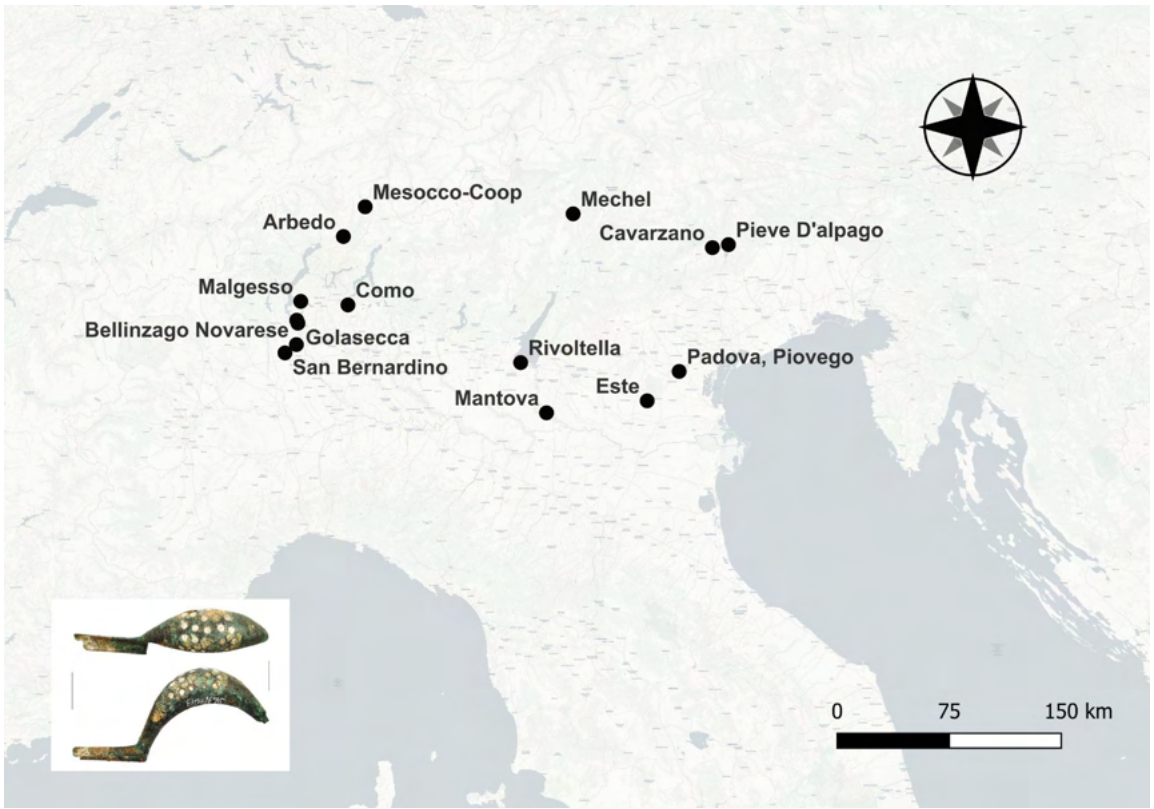

Figure 36. Type C (bow) distribution map. Elaborated by the author in QGIS 3.40.8 (2025); base map: © CARTO, © OpenStreetMap contributors; archaeaological find: Castelletto Ticino/Vigevano, inv. no. 947 (ph. Berruto).

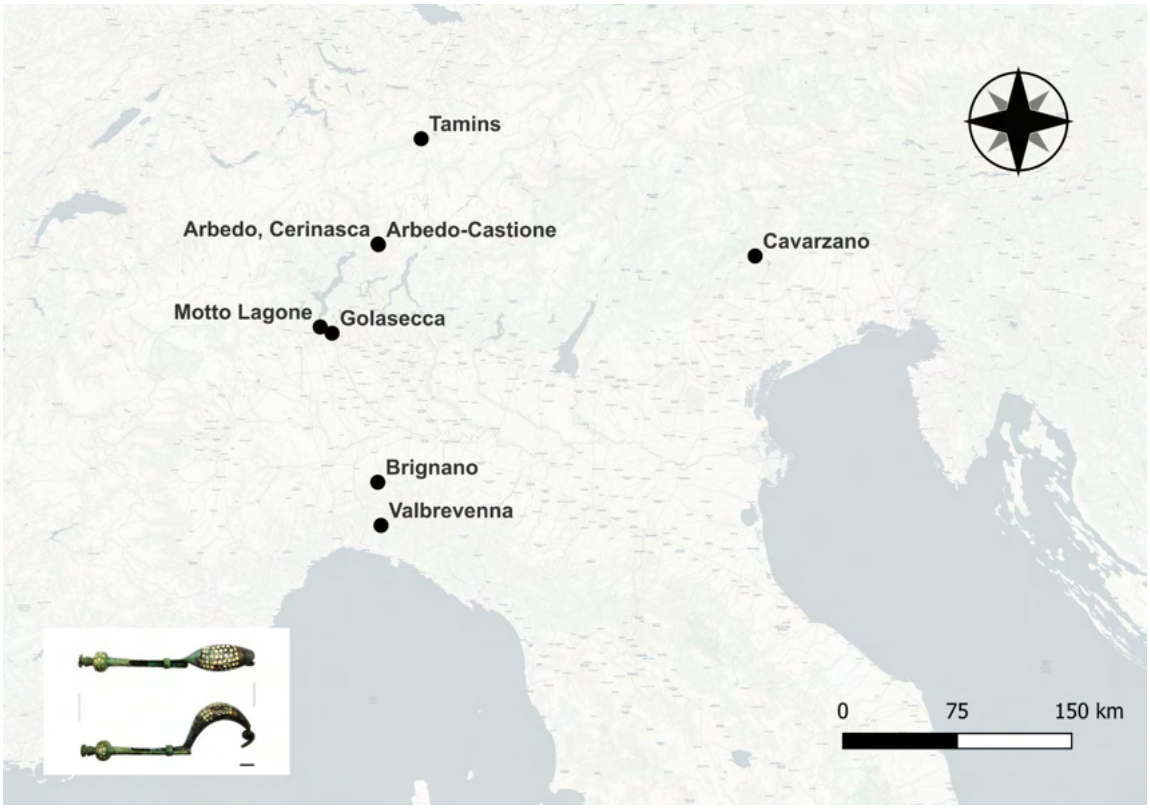

Figure 37. Type D (bow) distribution map. Elaborated by the author in QGIS 3.40.8 (2025); base map: © CARTO, © OpenStreetMap contributors; archaeological find: Arona, Motto Lagone, tomb 1 (ph. Berruto).

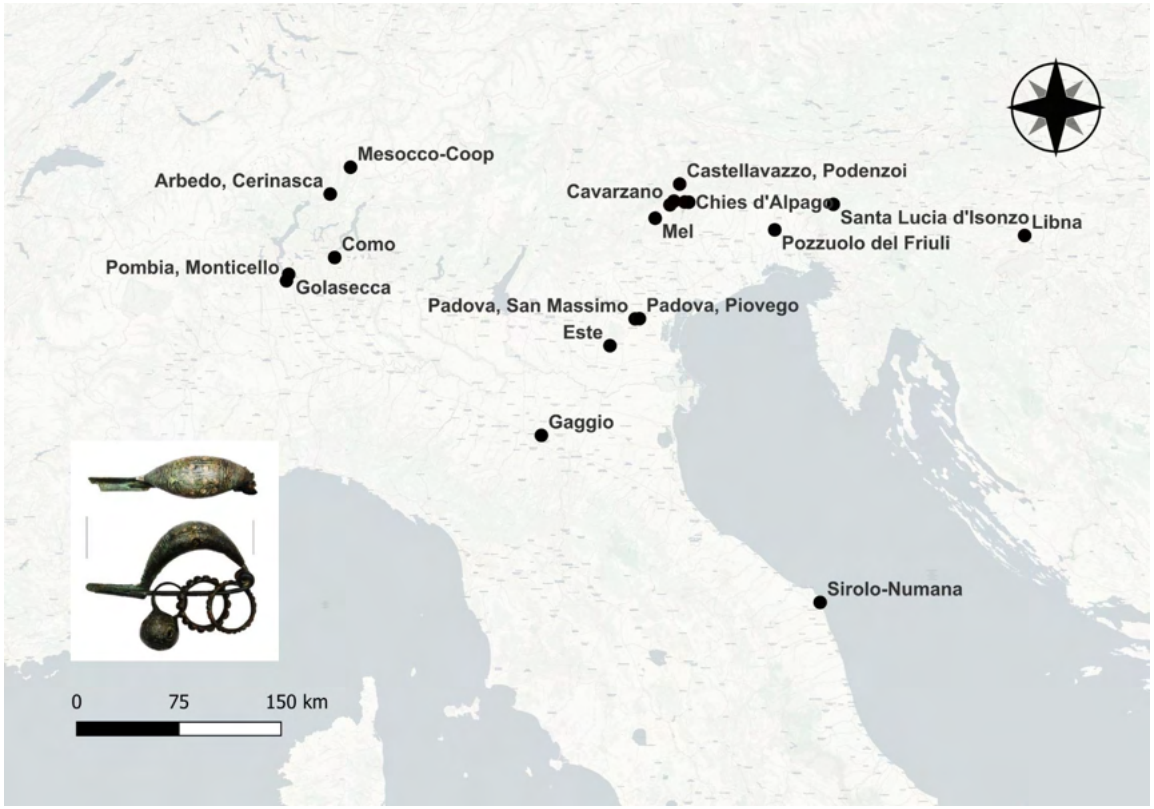

Figure 38. Type E (bow) distribution map. Elaborated by the author in QGIS 3.40.8 (2025); base map: © CARTO, © OpenStreetMap contributors; archaeological find: Pieve d'Alpago, inv. no. IG 312349 (ph. Berruto).

Figure 39. Type F (bow) distribution map. Elaborated by the author in QGIS 3.40.8 (2025); base map: © CARTO, © OpenStreetMap contributors; archaeological find: Como, inv. no. St. 879 (ph. Berruto).

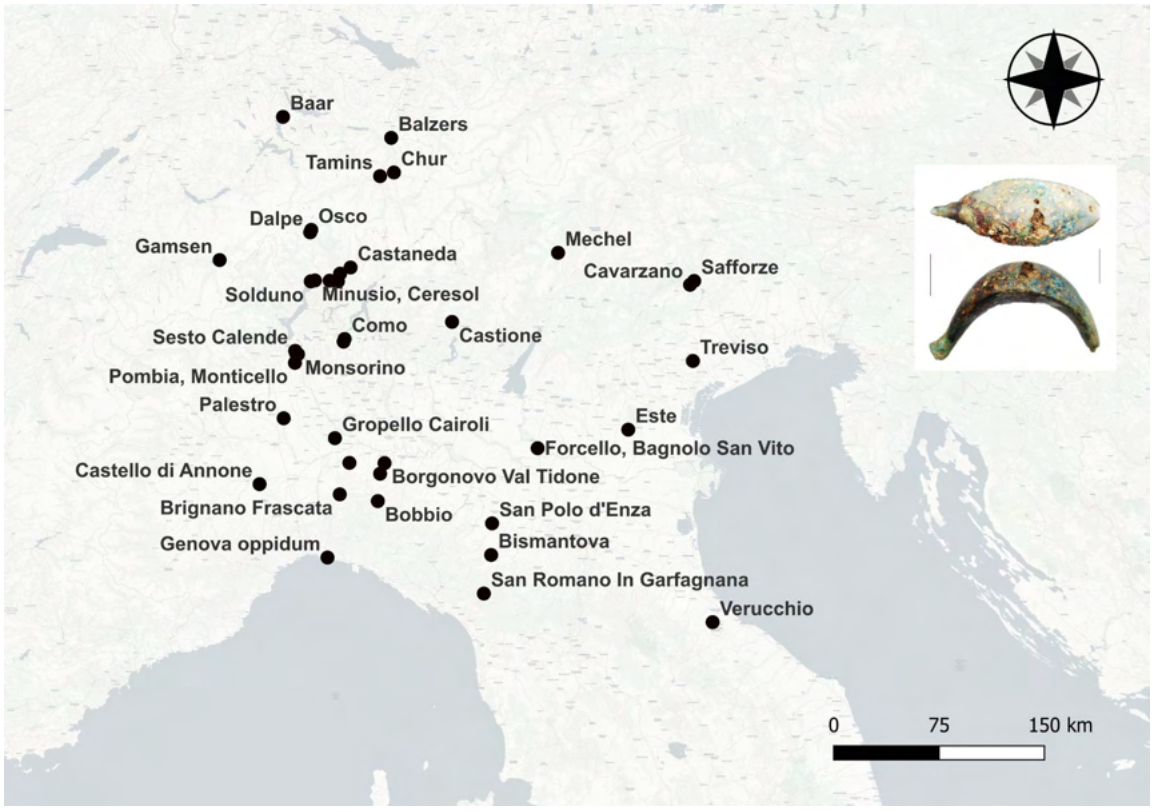

Figure 40. Type G (bow and foot: for the G variety ‘Palestro’, foot terminations with related characteristics, i.e., Q, GG, and GGG types, were also considered) distribution map. Elaborated by the author in QGIS 3.40.8 (2025); base map: © CARTO, © OpenStreetMap contributors; archaeological find: Como, inv. no. St. 57244 (ph. Berruto).

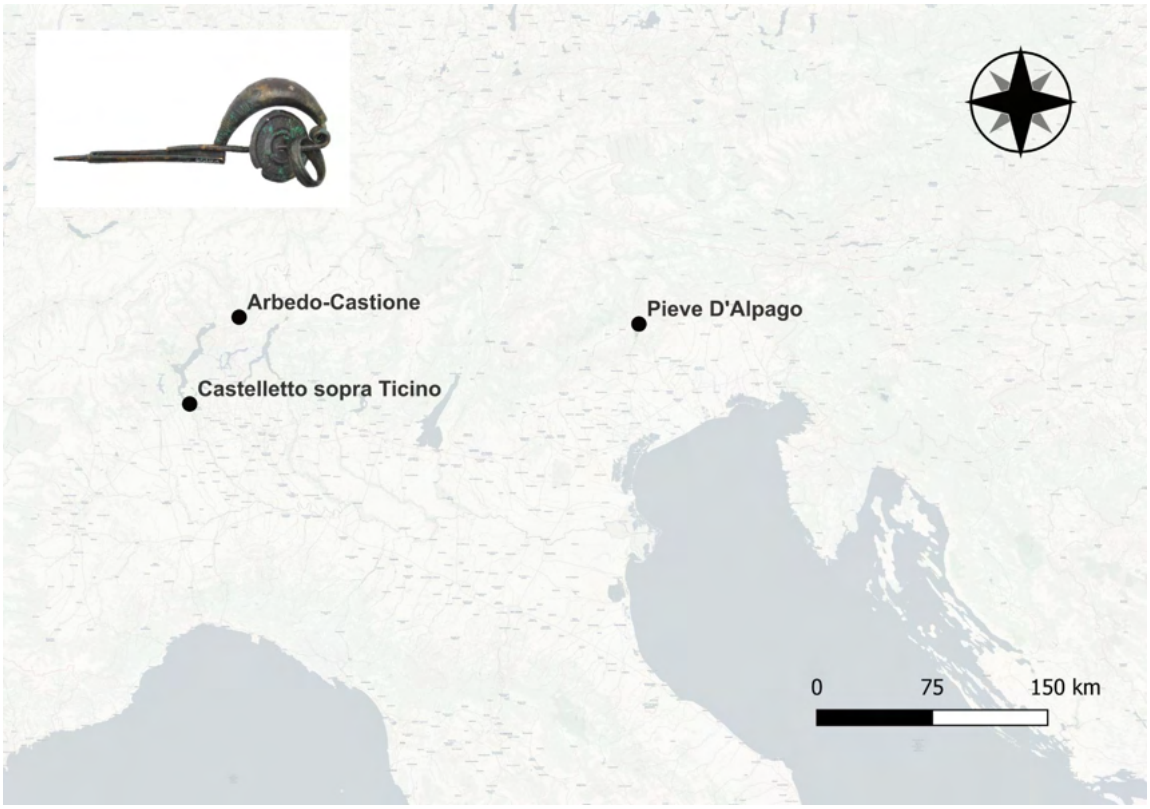

Figure 41. Type P (foot) distribution map. Elaborated by the author in QGIS 3.40.8 (2025); base map: © CARTO, © OpenStreetMap contributors; archaeological find: Castelletto Ticino, inv. no. D2104 (ph. Berruto).

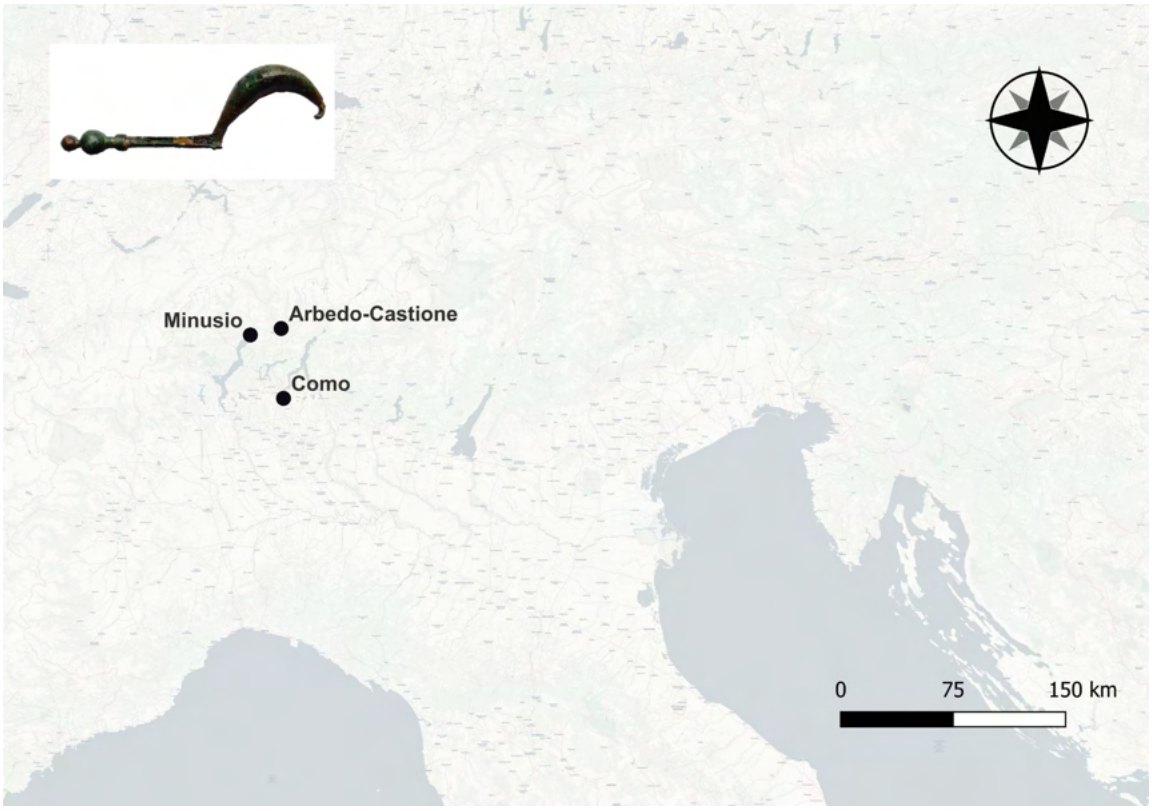

Figure 42. Type S (foot) distribution map. Elaborated by the author in QGIS 3.40.8 (2025); base map: © CARTO, © OpenStreetMap contributors; archaeological find: Como, inv. no. E17022 (ph. Berruto).

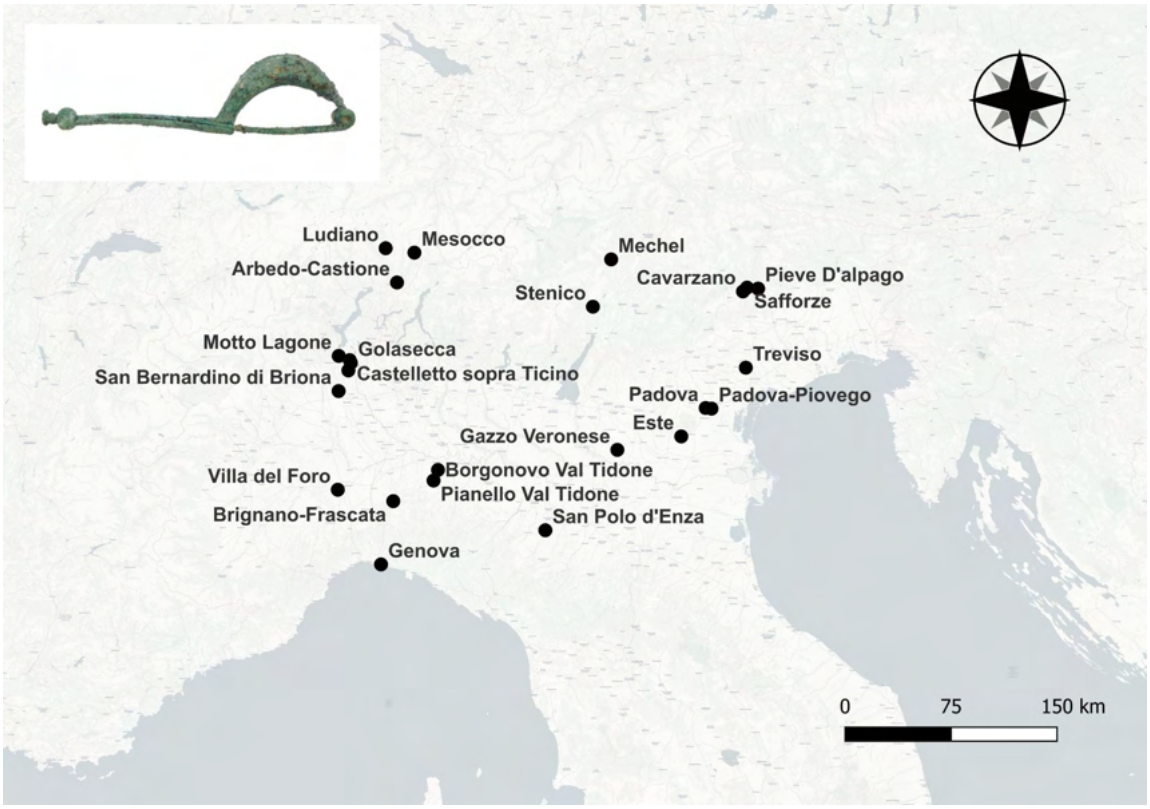

Figure 43. Type V (foot) distribution map. Elaborated by the author in QGIS 3.40.8 (2025); base map: © CARTO, © OpenStreetMap contributors; archaeological find: Piovego, t. 108.3 (ph. Berruto).

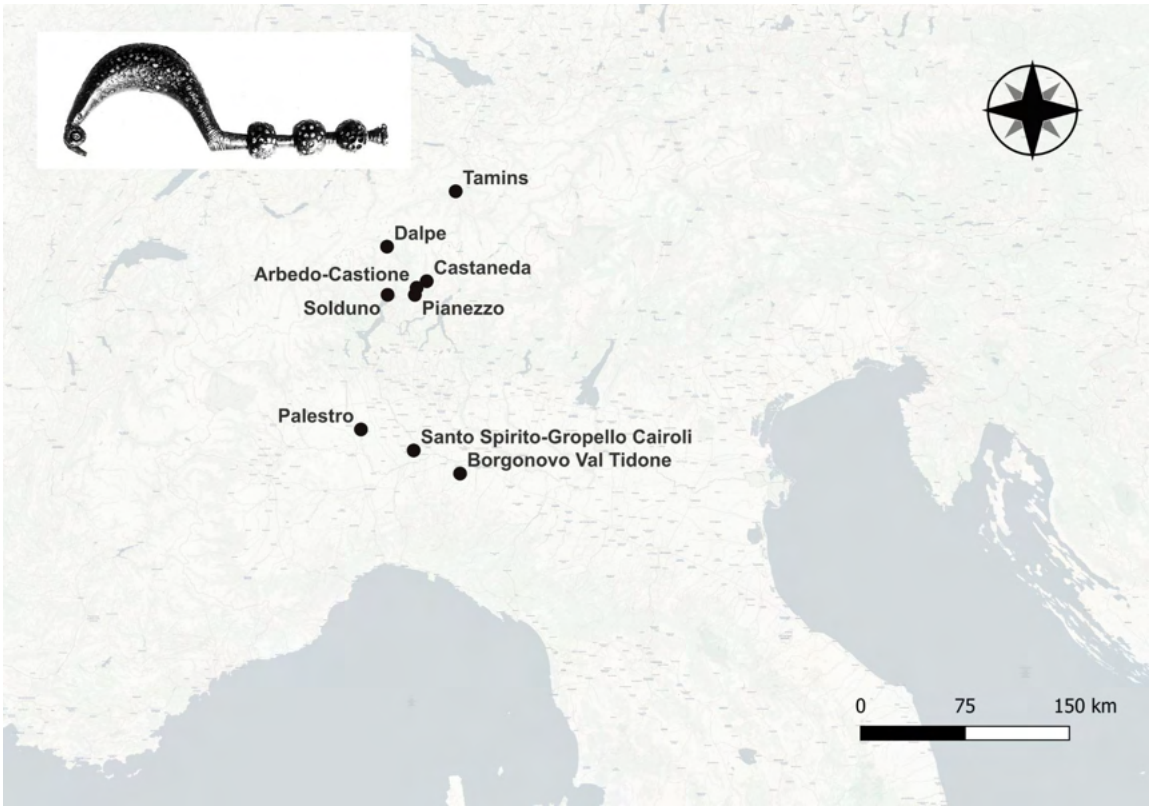

Figure 44. Type GG or GGG (foot) distribution map. Elaborated by the author in QGIS 3.40.8 (2025); base map: © CARTO, © OpenStreetMap contributors; archaeological find: after Rageth 1997, p. 244, fig. 15.

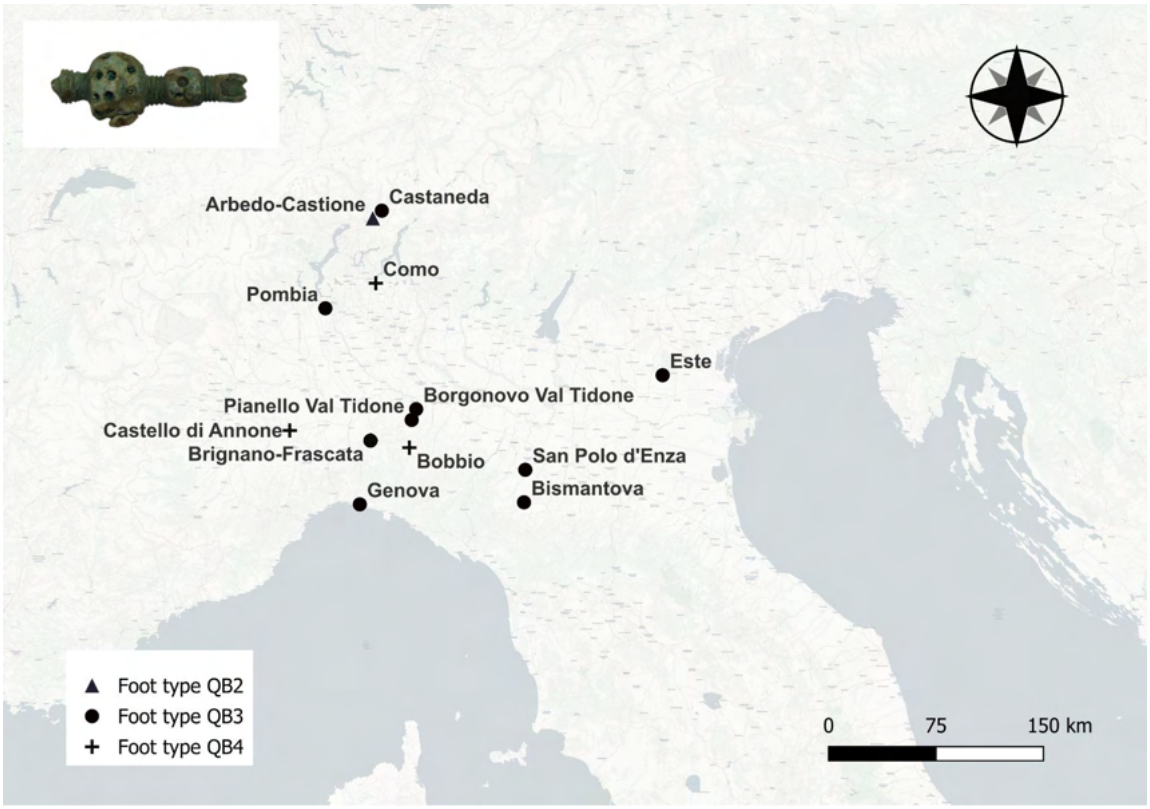

Figure 45. Type Q (foot) distribution map. Elaborated by the author in QGIS 3.40.8 (2025); base map: © CARTO, © OpenStreetMap contributors; archaeological find: Pombia, inv. no. St. 83946 (ph. Berruto).

4.2.5 Leech fibulae with linear decoration

Long-foot leech fibulae with vase termination, marked by simple linear decoration on the bow, are the most abundant; they date between the late 6th and early 5th century BCE and have a wide distribution throughout northern Italy and the transalpine area (Cicolani 2017, p. 107; de Marinis 1981, pp. 217-223; von Eles Masi 1986, pp. 169-177). For reasons of space, the full distribution and list of attestations are omitted due to their length.

They show great variability, especially in the size and morphology of the bow, which can be either full or with a terracotta core. Based on the arrangement of the decoration on the bow, several variants have been distinguished (von Eles Masi 1986, pp. 169-177):

- Variety A: presence of two groups of ribs on either side of the arch;
- Variety B: presence of groups of transverse lines on either side of the arch;
- Variety C: presence of broad transverse line bands on either side of the arch.

This type can also have a circular section at the beginning of the foot, decorated with ring lines, and a needle-stop ring. Again, there are other variants based on the termination of the foot, which is not always vase-shaped (double globe, triangular section, point terminating, dovetail terminating).

A particular variant is the leech fibula with swallow-tailed foot, in which the front end of the foot is elongated, ending in a double point. This type is documented mainly in northeastern Italy, especially in necropolis of the Atestina area, as well as in Most na Soči culture (e.g., cemetery of Santa Lucia in Tolmino), between the end of the 6th and the beginning of the 5th century BCE (von Eles Masi 1986, pp. 184-185).

While the filling of circular holes with alleged coral is widely documented, the possibility that the incised lines could also have been filled with decorative material had never been considered. Archaeometric analyses carried out in this project on a large number of samples from the site of Villa del Foro (inv. no. St. 66131; Fig. 46.a; Berruto *et al.* 2021; 2023) have proved for the first time that *C. rubrum* was indeed used to fill linear decorations too, possibly by using coral paste or some other kind of material. However, the obtained experimental outcomes show that the percentage of linear engravings

still retaining traces of such a filling is extremely small (e.g., 14% of the samples analysed in Berruto *et al.* 2021). The different conservation within the two types of decoration (circular holes and linear engravings) can probably be attributed to the reduced depth of these incisions with respect to the holes, together with an easier dispersion of the material in relation to the morphology of the support within which it was placed, which favoured a more or less durable adhesion over time and consequent preservation.
In this study, it was decided to extend the statistical record by also including some specimens with a different provenance – but without considering all the artefacts belonging to this type.

4.2.6 Cross-panel leech fibulae

Variants of the leech fibula include artefacts with cross-panel decoration on the bow. These are medium-sized fibulae, with a terracotta core and decoration on the arch with geometric motifs in various syntaxes. In only one case is the long foot preserved, with a terminal button and a double small globe (von Eles Masi 1986, pp. 161-162).
A variant, consisting of two fibulae found in the same tomb at the Ca' Morta in Como (inv. no. St. 864, St. 865; Figs. 46b, 46c; von Eles Masi 1986, no. 1502-1503), has a 'occhio di dado' decoration, i.e. composed of impressed circles. Traces of material within the engraved decoration were searched in this project, but the performed archaeometric analyses gave negative results.

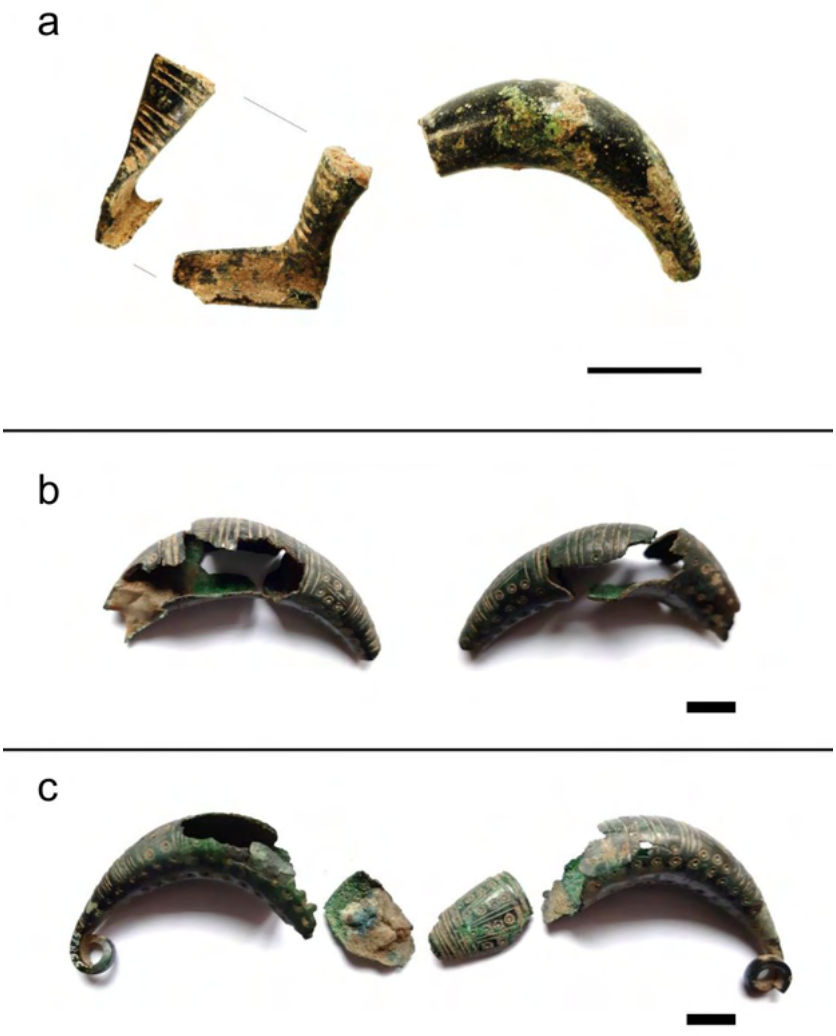

Figure 46. Leech fibulae (metric reference 1 cm): a) with linear decoration, Villa del Foro, inv. no. St. 66131, Musei Reali (e modified after ph. Sani); b) Como, Ca' Morta, with 'occhio di dado' decoration, inv. no. St. 864 (ph. Berruto); c) Como, Ca' Morta, with 'occhio di dado' decoration, inv. no. St. 865 (b) (ph. Berruto).

4.2.7 Leech fibulae with transversal grooves

A particular case is the leech fibula with grooved decoration (Fig. 47a). It is similar to the previous ones, but has a difference in the decoration of the bow, where transversal grooves are found between two bands of transversal lines. These grooves preserve, in some cases, a white filler of presumed coral. The bow usually has no terracotta core, and the foot is long with a globe-shaped end and a vase-like terminal appendix. The spring is one-sided. This type is not widely distributed: it is found almost exclusively in Italy (Adam 1996; Chieco Bianchi *et al.* 1976; Chierici 1999; Fogolari, Frey 1965; Frey 1969; Nascimbene 1999; Peroni *et al.* 1975; von Eles Masi 1986), with a few cases in Switzerland (Conradin 1978; Schmid-Sikimić 2002) and Slovenia (Marchesetti 1893), and can be dated between the end of the 6th and the first decades of the 5th century BCE (Fig. 48; Tab. 6).

It has some less common varieties, marked by different foot termination and/or bow decoration:

- type R: with a swallow-tailed end of the foot (Fig. 47a letter R; in Tab. 6, column 'type' = R); it is represented by only two specimens from the same Atestine tomb, dating from the late 6th to early 5th century BCE (Este-Pelà, tomb 14; von Eles Masi 1986, p. 186, t. 144.1861-1862);
- type C: with circular inlays (Fig. 47a letter C; in Tab. 6, column 'type' = C): characterised

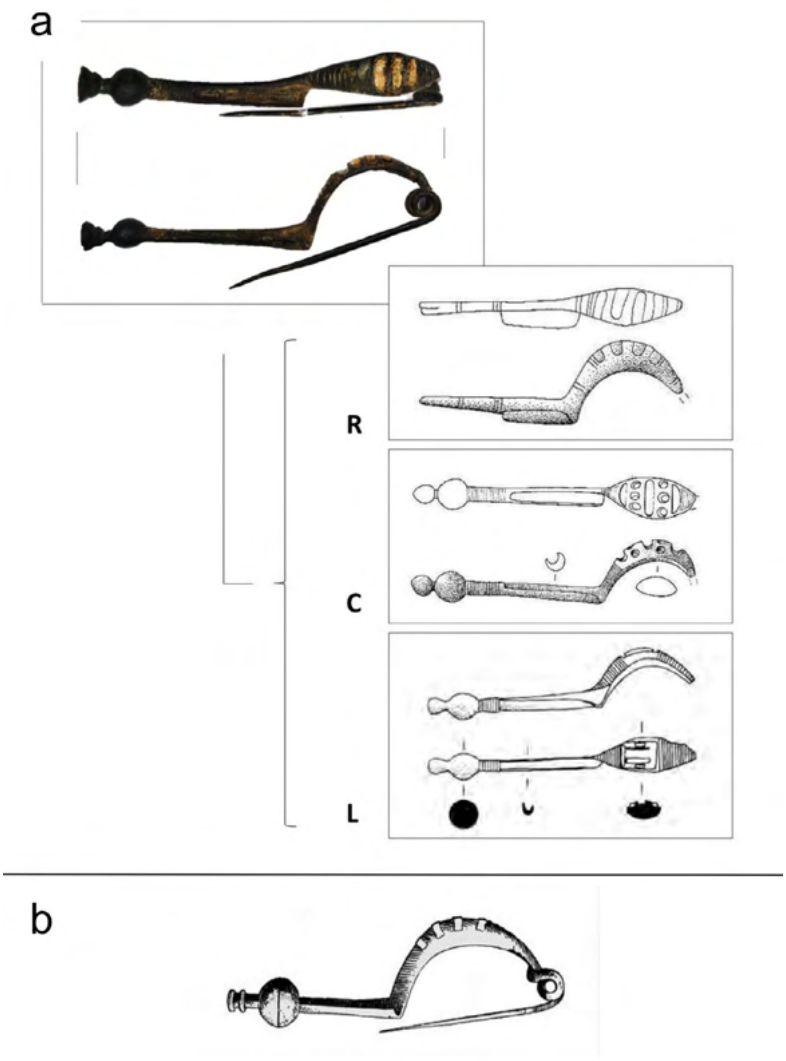

Figure 47. a) Classification of the different types of leech fibulae with grooves on the bow. Image modified after: top left, ph. Berruto, Bellunese, Belluno, Museo Civico; R von Eles Masi 1986, n. 1861; C von Eles Masi 1986, n. 1839; L Ruffa 1999, t. IV.7. b) Atypical exemplar with hybrid characteristics, Caverzano, loc. Masiera-Font (after Leicht 1871, fig. 13).

by a peculiar decoration on the bow, where several lines of circular insets are found at intervals with the grooves, and by a double small globe at the end of the foot; it is represented by few examples in the Venetic area and dated between the end of the 6th and the beginning of the 5th century BCE (Este, Costa-Martini, tomb 43 and Ospedaletto Euganeo, tomb Palugana; Chieco Bianchi *et al.* 1976, pp. 19, 39, t. 13.11; von Eles Masi 1986, p. 184, t. 143.1839);

- type L: with longitudinal grooves (Fig. 47a letter L; in Tab. 6, column 'type' = L): characterised by a peculiar decoration on the arch, where the grooves are longitudinal to the direction of the main bow length, and a double small globe at the end of the foot; it is represented by two specimens, one from the Golasecca area (Castelletto Ticino, loc. Cascina Riviera, Merlotitt; Ruffa 1999, p. 31, t. VI, no. 7) and the other from Venetic area (Carceri d'Este, tomb 48; von Eles Masi 1986, p. 184, t. 143.1840). For the Castelletto Ticino sample, pertinence to GIIIA1 (480-440 BCE) was proposed (Ruffa 1999, p. 31).

The decoration of this type of fibula closely resembles those of late western Hallstattian fibulae, and in particular the *Fußzierfibeln*, which often show similar decoration with a supposed coral coating.

The two types mainly differ in the thickness and width of the arch (more pronounced in the case of leech fibulae), as well as in the shape of the foot (leech fibulae have a long-straight foot, while *Fußzierfibel* fibulae are folded up, with various configurations) and the shape of the spring (generally unilateral for leech fibulae and bilateral for late-Hallstattian fibulae). In some fragmentary specimens, lacking foot and spring and with intermediate characteristics as far as the bow is concerned, it is difficult to distinguish the different types.

Some atypical artifacts exist, likely local productions, such as the small artefact from Caverzano, loc. Masiera-Font, with a long foot and a small globe-shaped end, a curvilinear arch decorated with transversal grooves and a bilateral spring (Fig. 47b; Nascimbene 1999, pp. 80-82, fig. 16, no. 164; Leicht 1871, fig. 13). Unfortunately, this sample could not be examined directly.

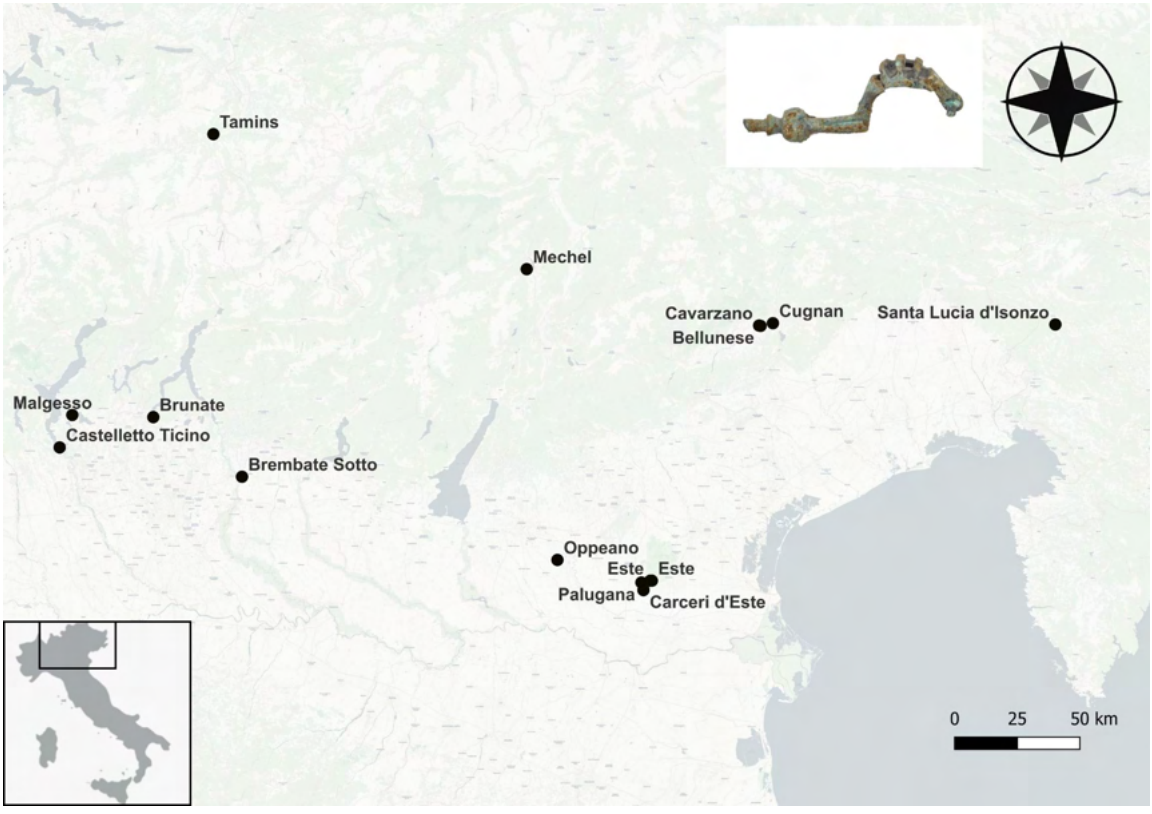

Figure 48. Distribution of the type 'Leech fibulae with grooves'. Elaborated by the author in QGIS 3.40.8 (2025); base map: © CARTO, © OpenStreetMap contributors; archaeological find: Castelletto Ticino, inv. no. 23.M380-9.3.

4.2.8 Late Hallstattian fibulae

This term identifies a large group of Celtic shape fibulae (Mansfeld 1973; Fig. 49), also attested occasionally in northern Italy from the late 6th and early 5th century BCE onwards (Frey 1969; 1971; Gambacurta, Ruta Serafini 2019, p. 19). In Italy, they indicate intervened contacts with north-Alpine populations.
Among the vaste Celtic production, the ornithomorphic and F2 Mansfeld type possibly present coral within the decorations. Some examples from the Italian territory are therefore also considered in the analytical record of this study. The two variants at times associated with presence of coral – i.e. the *Vogelkopffibeln*/*Entenkopffibeln* and the *Fußzierfibel* type F2 – are examined in detail.

Ornithomorphic fibulae

Fibulae with a duck-head foot termination – called *Entenkopffibeln* (type I.17; Nascimbene 2009, pp. 153-159; Frey 1969; 1971) or *Vogelkopffibeln* (de Marinis 1987; Frey 1969; 1971) – may retain parts of presumed coral. They are made of a bronze rod arch and foot with a U-shaped section, conformed to an ornithomorphic protome backwards with upward beak. The spring is bilateral, wound around a pin inserted into the pierced head of the bow. In general, the decoration consists of transverse grooves on the bow, with supposed coral inlays, and eye filled with the same material, sometimes found inside the beak or in a small transverse groove at the top of the duck's head (Adam 1996, p. 41).
Several classifications have been proposed for them. On a chronological basis, specimens with a curvilinear profile of the bow would be older (late 6th century BCE), while those with a rectangular profile would be more recent (5th century BCE; de Marinis 1987). On a geographical basis, an open beak with coral element would be found south of the Alps, while a closed beak would recur in the northern and eastern Alpine area.
In an attempt to unify these two classifications (Nascimbene 2009, pp. 152-155), two varieties are identified (in Tab. 7, column 'type' = A or B; Fig. 50) based on the shape of the bow, divided into subvariants based on their decoration:

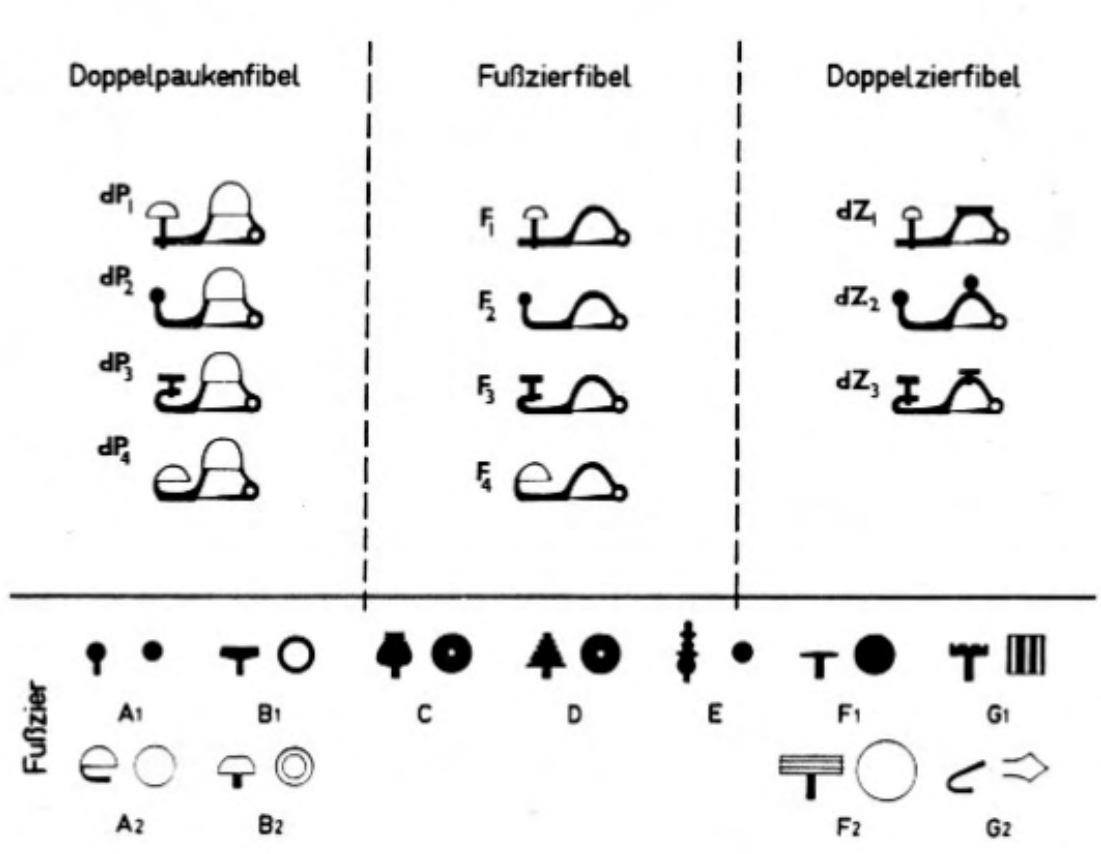

Figure 49. Mansfeld classification for late Hallstattian fibulae: groups DP, F e DZ (after Adam 1996, p. 36, fig. 1)

- Type A – round arch:
    - A1: transversal grooves decoration;
    - A2: longitudinal grooves decoration;
    - A3: bow without grooves, inorned or with ribs;
    - A4: decoration with transverse grooves alternated with circular insets, eye without inset
- Type B - rectangular profile arch, right-angled with flattening top, or attenuated angles and convex top:
    - B1: transversal grooves decoration;
    - B2: longitudinal groove decoration;
    - B3: linear decoration.

Even in this case there are specific variants, such as the one with the beak joined to the arch (in Tab. 7, column 'type' = J), attested in Italy at Mechel (Fig. 51) and at Padua-Piovego (Gallo 2023), and in France at Salins-les-bains (Champ de Chateau) and La Rivière-Drugeon (Adam 1996, pp. 34, 41, 43).

The type of late hallstattian ornithomorphic fibulae has a wide distribution between north-central Italy and central Europe (Tab. 7; Fig. 52). South of the Alps, these findings are concentrated along the course of the Adige River, in the Etruria Padana (Forcello di Bagnolo San Vito and Monte Bibele) and in the upper Adriatic involving the Venetic plain centers (Este and Padua), that of Altino and sporadically the middle course of the Piave River, the Trieste Karst and Slovenia (Santa Lucia di Tolmino – Most na Soči). In the transalpine area, these fibulae are common in France, east of the Saone and in the north, Germany, Austria and Bohemia. The variety

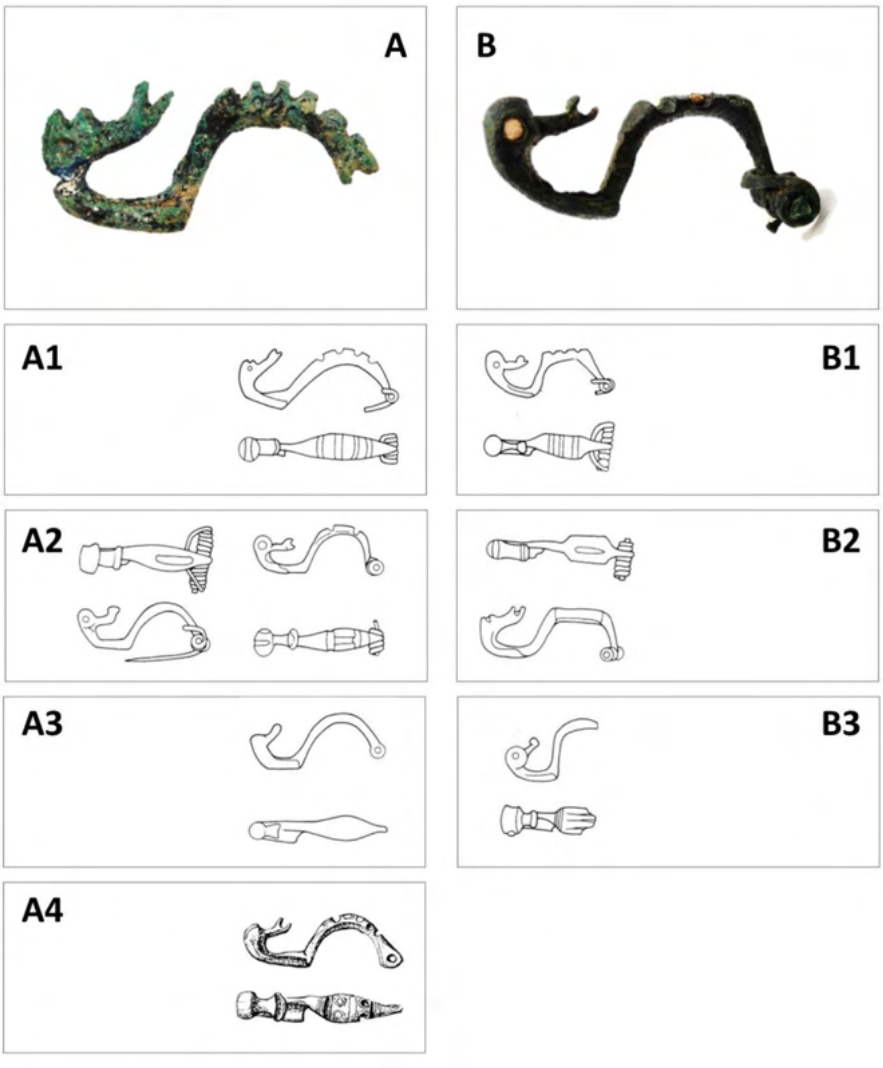

Figure 50. Classification of several type of Late Hallstattian ornithomorphic fibulae; image modified after: A (ph. Berruto, Piovego, inv. no. 95.11); B (ph. Berruto, Caverzano, loc. Masiera, inv. no. 284, Museo Civico Belluno); A1, A2, A3, B1, B2, B3 (after Adam 1996, p. 41, fig. 3); A4 (after Courtois 1968, fig. 2).

most represented is type A, while type B is documented in Veneto, in the Etruria Padana area and at Mark-Forst north of the Alps, from the last quarter of the 6th to the mid-5th century BCE. The type recurs in female burials, some of which prestigious (Nascimbene 2009, pp. 153-159).
Among the late Hallstattian fibulae, the ornithomorphic types are the most common south of the Alps, and a development in the Italian context, particularly in northeastern Italy, has been hypothesized for them. Since the Italian finds show more coral decoration, it has even been assumed that the presence of this material is a characteristic feature of south alpine 'officines' (Adam 1996, p. 42).

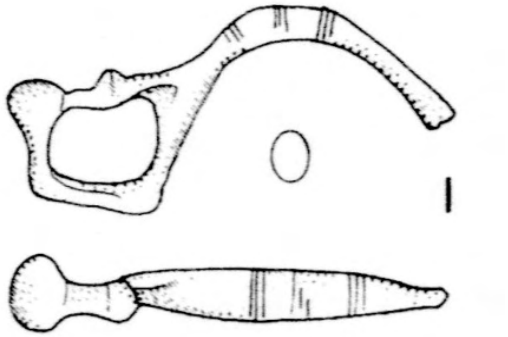

Figure 51. Ornithomorphic type, joint type, Mechel or Sanzeno (after Adam 1996, t. I.2).

Figure 52. Distribution of the Late-Hallastattian ornithomorphic fibula type. Elaborated by the author in QGIS 3.40.8 (2025); base map: © CARTO, © OpenStreetMap contributors; archaeological find: Forcello di Bagnolo San Vito, inv. no. St. 99211 (ph. Berruto).

Fußzierfibeln

F-group fibulae of Mansfeld typology, or *Fußzierfibeln*, are marked by a simple, more or less thick bow and a raised foot, wich morphology led to four major types (Mansfeld 1973; fig. 49).

The type F1 is marked by modest dimensions, a simple bow and a small mushroom-shaped element, attached to the end of the foot. They are widespread in Germany in Baden-Württemberg and north-eastern France, in Alsace and Champagne; some specimens have also been found in Dürrnberg (Austria) and northern Italy (Tab. 8; Fig. 53; Adam 1996, pp. 49-50; Frey 1971; Mansfeld 1973).

Fibulae of type F2 (Fig. 54; Tab. 9) are very common in the transalpine area in the Hallstatt D3 phase (indicatively 500-450 BCE), but in most cases they have a smooth bow (Chaume 2001, pp. 109-111; Mansfeld 1973).

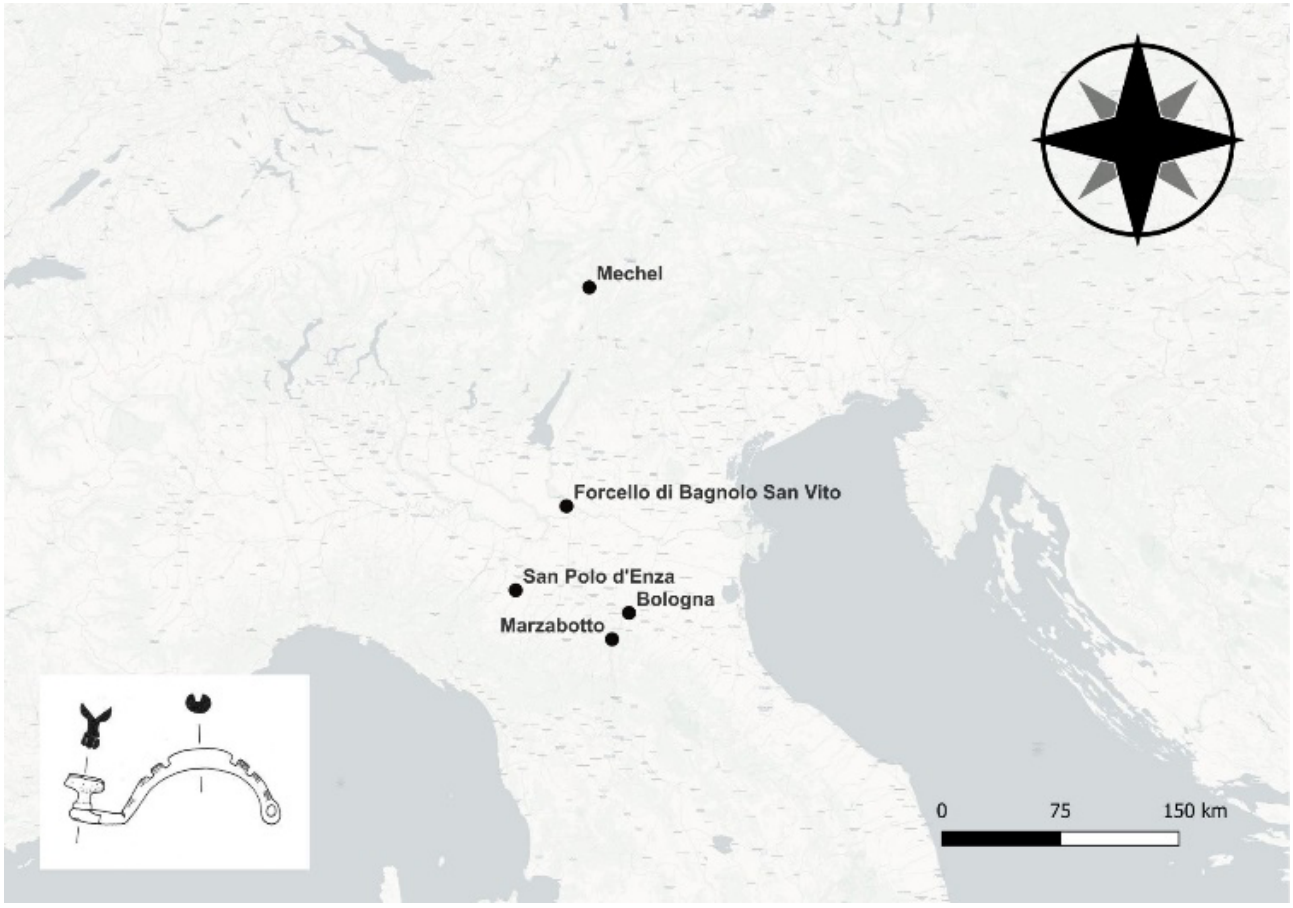

Figure 53. Distribution of the type *Fußzierfibel* F1 in Italy. Elaborated by the author in QGIS 3.40.8 (2025); base map: © CARTO, © OpenStreetMap contributors; archaeological find: after Damiani *et al.* 1992, t. LXIV.967.

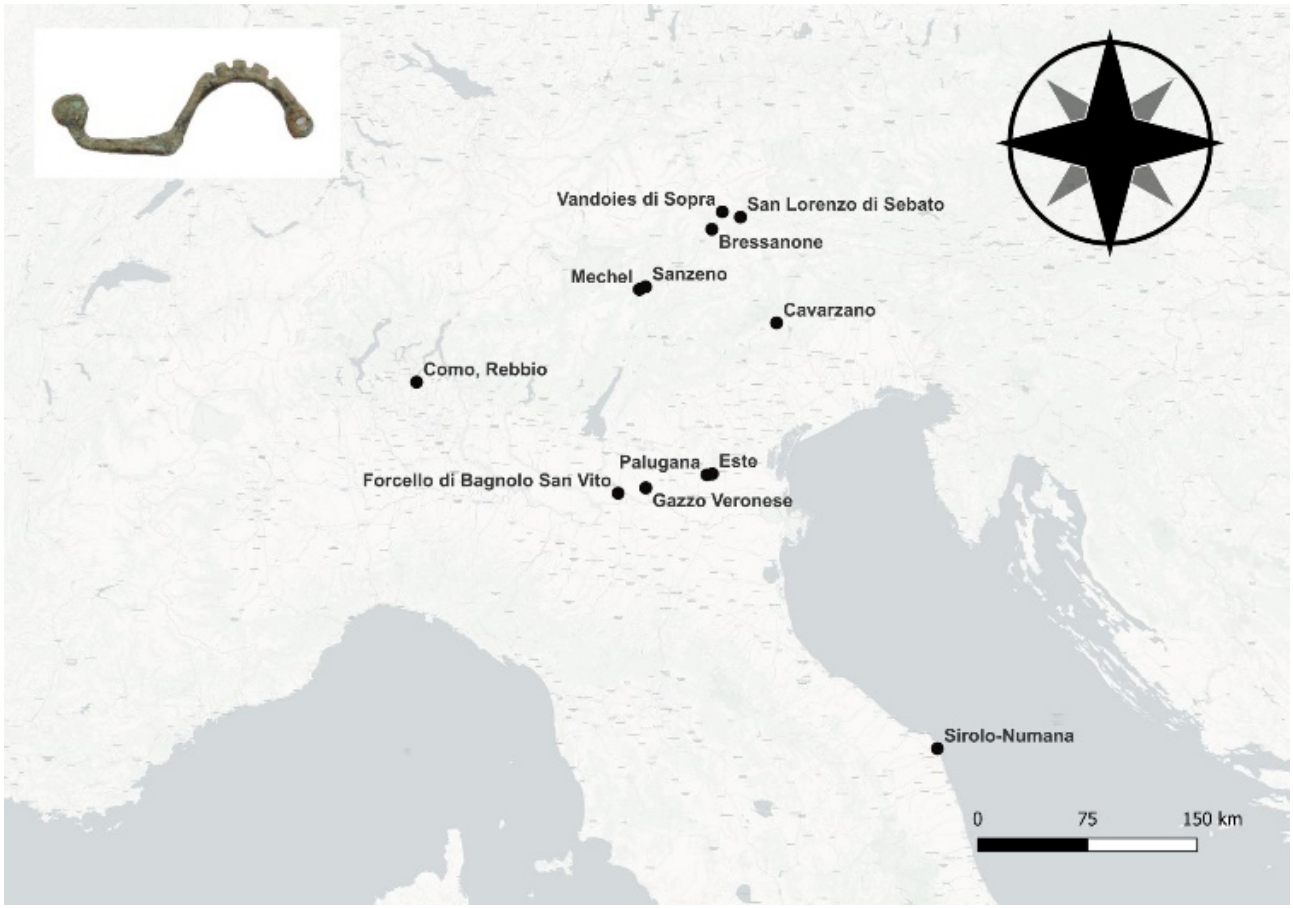

Figure 54. Distribution of type *Fußzierfibel* F2 in Italy. Elaborated by the author in QGIS 3.40.8 (2025); base map: © CARTO, © OpenStreetMap contributors; archaeological find: Forcello di Bagnolo San Vito, inv. no. St. 99209 (ph. Berruto).

4.2.9 Navicella fibulae

This term identifies a large group of fibulae characterised by a hollow bow, obtained by removal of the clay core through a ventral opening, which can vary in width and profile.
The earliest finds (mid-8th century BCE) come from north-eastern Italy and Bologna. In north-western Italy (Golasecca culture area), the type is documented from the end of the 7th century BCE, with variants with a lozenge arch, with or without lateral appendices, and with a simple arch, with several sub-varieties (Casini 2000a; de Marinis 1981; Faudino *et al.* 2014, pp. 129-131; Saronio 1970, t. VIII.11-12; von Eles Masi 1986, pp. 85-143). This type is characteristic of female grave goods from the GIC (675-625 BCE) onwards. In the western Alpine area, in the 6th century BCE, large navicella fibulae with a long foot and a spherical or modelled end, with a hollow bow decorated with bands of lines, associated or not to rows of small circles, are also documented. A list of attestations and a distribution map for the 'Navicella' and large 'Navicella' fibulae is not included here, referring to the classification proposed by von Eles (von Eles Masi 1986, pp. 85-143).
The possible presence of coral in the decorations of this type was assumed in this study mainly because of the evident whitish hue of the decorations of some finds from Parre (Civico Museo Archeologico di Bergamo) and considering the doubts about their authenticity raised by Raffaele de Marinis, due to the lack of specific analyses.
Linear geometric decorations on a few finds were therefore considered (Tab. 10), namely three from Parre (Museo Archeologico di Bergamo, inv. no. 48-49-119; Figs. 55a, 55b, 55c), one from Villa del Foro (Musei Reali di Torino, inv. no. St. 66120; Fig. 55.d) and circular decorations on a large 'Navicella' type fibula ('Val Varaita type'; Museo Civico Giovio Como, inv. no. E17738; Fig. 55e). The main purpose of the analyses was to identify the nature of the bright whitish material within these decorations. The survey identified no material related to ancient

Figure 55. Navicella fibula examples considered in the current work (ph. Berruto; metric reference 1 cm): a) Parre, inv. no. 119; b) Parre, inv. no. 48; c) Parre, inv. no. 49; d) Villa Del Foro, inv. no. St. 66120; Val Varaita, inv. no. E17738.

decorations, but only a modern restoration intervention for the three finds from Parre (i.e., the whitish decorations had been painted with White Indian Ink). For these reasons, the survey was not extended to the other specimens.

4.2.10 Bucket Pendants

In the Golasecca and Venetic areals, other copper alloy objects with coral inset decorations also appear, such as bucket pendants, grooming tools, and drop-shaped pendants at the end of chains in Trezzo-type pendants (de Marinis 1981, pp. 229-232; 2000, p. 170; Peroni *et al.* 1975, pp. 58-59).

Bucket pendants owe their name to their specific shape: they consist of a body and a semicircular suspension element for insertion into a support. They were cast in bronze with a matrix with a terracotta core, held by a suspension stick that often causes two opposing holes to appear on either side of the pendant. This technological reconstruction is confirmed by the discovery at Mondovì-Breolungi of a manufacturing waste (Venturino Gambari 2001a, pp. 24-25, fig. 17; Giaretti 2001, p. 159, fig. 131-2). Their function is that of an amulet or a simple ornament, due to their presence in female or infant burials (Barbieri 2019; de Marinis 1981, pp. 229-232; 2000, p. 170; Peroni *et al.* 1975).

This type has many variations and wide distribution in shape and profile, as well as decoration, and several classifications were attempted (de Marinis 1981, pp. 229-232; Casini 2000a; Tessmann 2007; Nagy 2012; Barbieri 2019). de Marinis (1981, pp. 229-232) divides them into three main groups, based on bottom shape: type 1) with rounded bottom; type 2) with conical bottom; type 3) with profiled termination, each divided in further subvariants, based on morphology. The rounded-bottomed bucket pendant (type 1), outside of Italy, is differently distributed depending on the variant (Casini 2000b; Cicolani 2017; Tessmann 2007).

Type 1A, with a rounded bottom, 8-shaped profile with a strong constriction at the handle junction, may have two types of decoration: i) with bands of horizontal lines, with a cross motif on the bottom, or ii) with a 'occhio di dado' motif. In northwestern Italy, it is typical of the GIIB phase (second half of the 6th century BCE) (Barbieri 2019; de Marinis 1981).

Type 1A pendants are found in northern Germany, Slovenia, and rarely in the French,

Swiss, and Austrian Alpine areas. Because of their pronounced presence in the Golasecca culture area, it has been hypothesized that this type may have spread northward from here to the other territories (Tessmann 2007, p. 669).
Type 1A pendants with 'occhio di dado' decoration are particularly interesting in this investigation (Fig. 57). They have five concentric circles (four on the sides and one on the bottom of the bucket) with a central through-hole for housing a small coral sprig. 28 specimens of this type were identified (Tab. 11; Fig. 59) in the Venetic areal (Padua, Piovego necropolis and vicolo San Massimo; Pieve d'Alpago, Pian della Gnela necropolis; Cavarzano; Gallo 2023; Barbieri 2019; Tessmann 2007; Gangemi *et al.* 2015; Nascimbene 1999), Golasecca areal (Bellinzago Novarese; Golasecca; San Bernardino di Briona; Barbieri 2019; de Marinis 1992), 'Etruria Padana' areal (Forcello di Bagnolo San Vito; Barbieri 2019; de Marinis 2007; de Marinis *et al.* 2017), Slovenia (Santa Lucia d'Isonzo; Barbieri 2019; Tessmann 2007; Marchesetti 1893) and Germany (Singen; Barbieri 2019; Maier 1957; 1958). The higher concentration, based on the available data, seems to be the Veneto region (17 finds; graph Fig. 56).
Type 1B, with a rounded bottom, has a semicircular profile and is typical, like the previous one, of the GIIB phase. It is found, in addition to Italy, in France and Switzerland. It may have double linear decoration in the upper part of the bucket, accompanied by multiple bordered circles on the lower face in a disordered disposition, presumably coated by coral (Casini 2000b; Casini, Chaume 2014; Faudino *et al.* 2014; Cicolani 2017, pp. 138-150; Barbieri 2019, p. 46).
Type 1B pendants with this decoration are attested at the Forcello di Bagnolo San Vito (inv. no. RR745; Barbieri 2019, fig. 10.3, 11.3; de Marinis 1991b, p. 243, fig. 3.3) and San Polo d'Enza (inv. no. S37/86; Barbieri 2019, p. 46; Damiani *et al.* 1992, pp. 167, 331, t. LXXXV.1324). Archaeometric analyses performed on the decorations of type 1B pendant from Forcello di Bagnolo San Vito (Fig. 58) did not confirm presence of coral.
Archaeometric analyses were also performed on a funnel pendant type 3D of de Marinis from Pianello Val Tidone (inv. no. St. 18711; unpublished; Fig. 60), with profiled and knob termination decorated with concentric circles motif (de Marinis 1981, pp. 229-232) but detected no decorating materials.

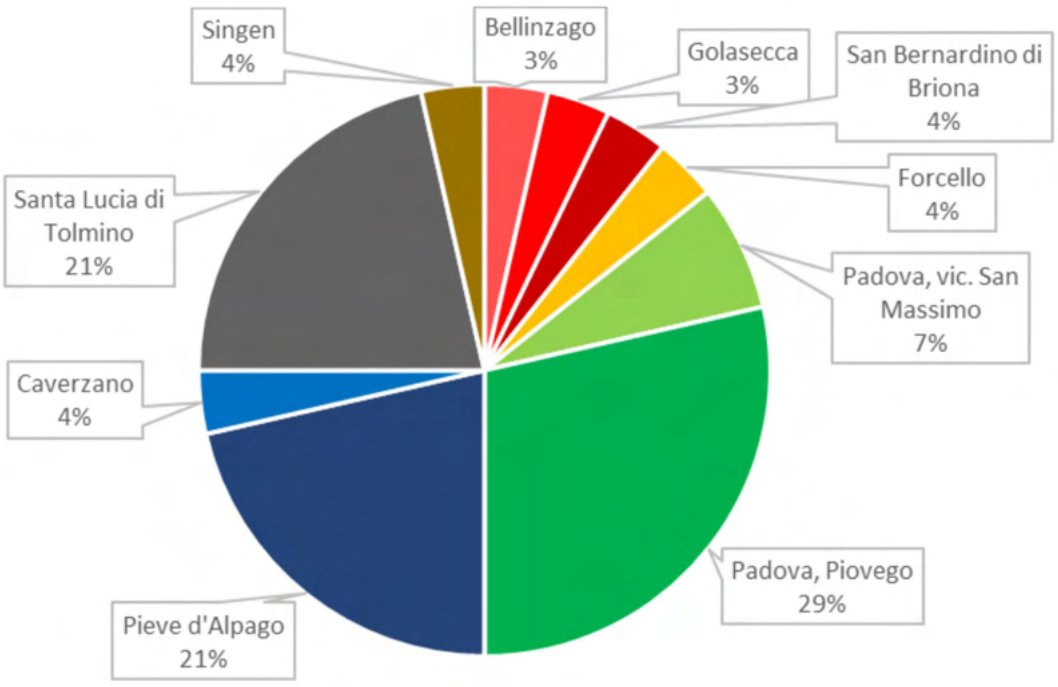

Figure 56. Graph regarding the number of 1A bucket pendants with 'occhio di dado' decoration at the different sites where they are being attested.

Figure 57. San Bernardino di Briona, Type 1A bucket pendant with ‘occhio di dado’ decoration, inv. no. 23.M380-9.7 (ph. Berruto; metric reference 1 cm).

Figure 58. Forcello di Bagnolo San Vito, Type 1B bucket pendant with circles decoration on the bottom, inv. no. RR745 (ph. Berruto; metric reference 1 cm).

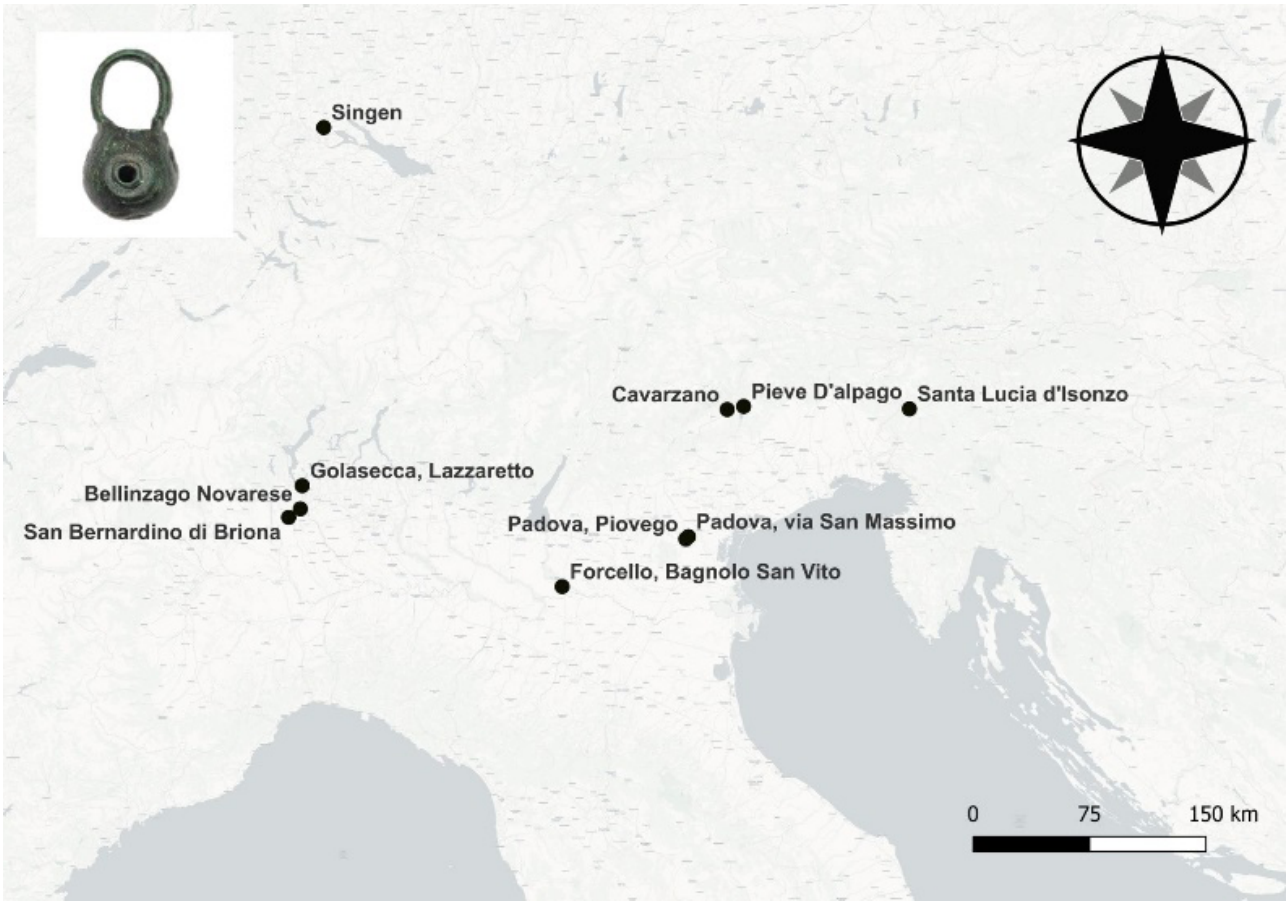

Figure 59. Distribution of type 1A bucket pendants with 'occhio di dado' decoration with coral insets. Elaborated by the author in QGIS 3.40.8 (2025); base map: © CARTO, © OpenStreetMap contributors; archaeological find: San Bernardino di Briona, inv. no. 23.M380-9.7 (ph. Berruto).

Figure 60. Pianello Val Tidone, Type 3D bucket pendant with 'occhio di dado' decoration, inv. no. 18711 (ph. Berruto; metric reference 1 cm).

4.2.11 Grooming tools

Grooming tools spread from the early 7th century BCE in the western Hallstattian and Golasecca areas (Figs. 61, 62; Tab. 12). Contextually, they are attested in Chiavari, Este, Oppeano, Bologna, Slovenia, and Etruria (Fig. 62; Tab. 12; Zamboni 2018, p. 187). In the Golasecca area, grooming sets date from GIC to GIIIA1 and are normally composed of six items (three in the case of iron sets): two *scalptoria* (clean-nails or clean-teeth) with dovetail termination, two *auriscalpium* spoon-shaped (ear-cleaner) and two tweezers (Peroni *et al.* 1975, pp. 220-221; Roncoroni 2005, pp. 46-47).

Sometimes, however, fewer elements may be present (such as in the case of Cuggiono, Cunardo, Sesto Calende-Gajaccio, Como Albate), or one element may have dual function (e.g., nail-cleaner and tweezer; Peroni *et al.* 1975, pp. 220-221). They are generally made of bronze, but iron (e.g., Castelveccana-Castel Valtravaglia; Peroni *et al.* 1975, pp. 220-221, fig. 61-2), gold and silver (e.g., Como-Rebbio) specimens are also documented. The oldest findings are in iron (7th century BCE), then from GII the most used material is bronze, while gold and silver appear from the 5th century BCE. They are functional as well as symbolic objects, associated either with male or female grave goods (Cicolani 2017, pp. 154-155; Roncoroni 2005, pp. 46-47).

Grooming tools generally consist of a metal rod with one or more bulges and a suspension hole; the rod ends in a spoon, tweezer (Fig. 61) or dovetail shape. The thickness of this rod varies according to use: it is thicker for body care and thinner when these objects begin to be worn as pendants suspended from fibulae, especially in female grave goods. Thinner artifacts are generally more decorated and may have coral encrustations or fine moldings; they can be dated to GIIB or GIIA1 (Casini 2000a, pp. 138-139; Cicolani 2017, pp. 154-155). Morphology and decoration can be simple or elaborate; the most common decoration is linear, which can be associated with holes for coral insertion (as in the case of Castelletto sopra Ticino; Golasecca; Gropello Cairoli; Padova-Piovego).

The attachment system also evolves in time towards more complex forms. In the early stages these objects are simply threaded into the pin of a fibula or inside a ring. From the GIIB-GIIIA1, a more complex suspension system, known as a 'hinge', is introduced, based on which five different types of suspension have been distinguished, produced in distinct cultural regions (Cicolani 2017, pp. 154-155).

Figure 61. Castelletto sopra Ticino, grooming tool (tweezer) with presumed coral decoration, inv. no. 1063 (Museo Civico Novara) (ph. Berruto, metric reference 1 cm).

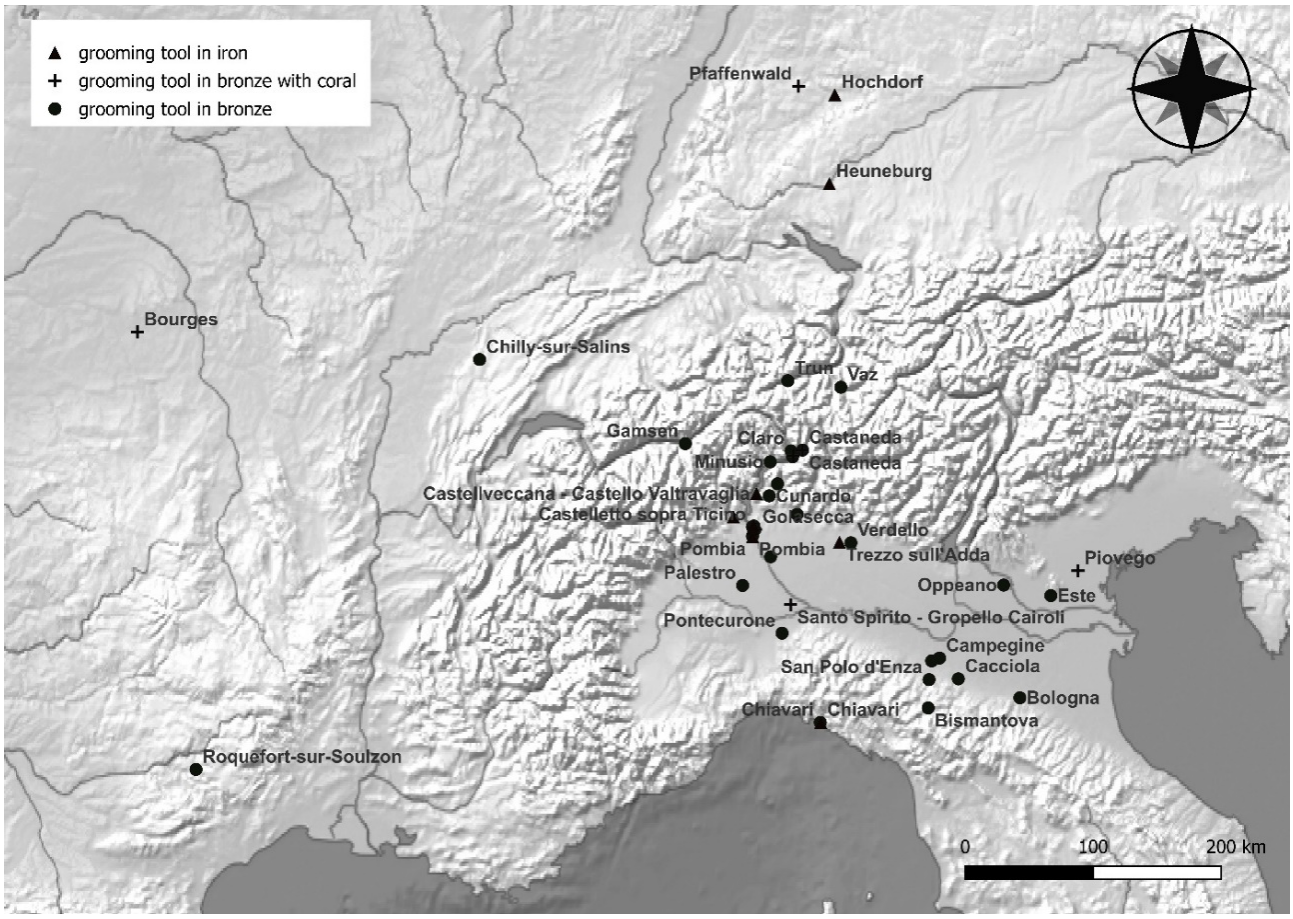

Figure 62. Distribution of grooming tools. Elaborated by the author in QGIS 3.40.8 (2025); base map: Natural Earth (Gray Earth raster "GRAY_LR_SR_OB_DR"), public domain.

4.3 The use of coral in Liguria Interna and coastal Liguria

The presence of coral during the Early Iron Age in southern Piedmont and Liguria was less pronounced than in the Golasecca cultural area and was likely connected to interactions with the Golasecca and Etruscan populations.

Leech fibulae with long foot and bow with terracotta core, decorated with circular inlays of presumed coral, are documented in southern Piedmont at Brignano Frascata (Berruto *et al.* in press), Villa del Foro, Pontecurone and Castello di Annone, with dates ranging from the 6th to 5th century BCE (Berruto *et al.* 2021, p. 552, fig. 337; 2023a, fig. 1; Cicolani 2021, p. 533, fig. 323; Cicolani *et al.* 2024; Faudino *et al.* 2014, p. 132, fig. 7). In Liguria, all evidence is confined to Genoa, 5th century BCE (three fibulae from Genoa Colle di Castello, and one fibula from Genoa-Valbrevenna; *Archeologia a Genova* 1977, p. 22, fig. 24; de Marinis, Spadea 2005, p. 323, V.2.19-21; Melli 2007, p. 50; von Eles Masi 1986, p. 167, t. 127.1574). A fragment of pinkish rough coral was also found in Genoa-San Silvestro (Colle di Castello), also dated to the 5th century BCE (Fig. 63; Melli 2021, p. 75, fig. 48; Milanese 1987, pp. 155 (n. 243), 352, 380; Rondi-Costanzo, Ugolini 2000, p. 181; Ugolini 2006b, p. 91).

Leech fibulae with insets from southern Piedmont are similar to Golasecca artefacts but exhibit distinctive features suggesting local production: a higher occurrence of the full-arch (without a terracotta core), flattened lenticular or biconvex bow morphology, and small size. In particular, the discovery of several bronze artifacts and their specific features would suggest the presence of a local production workshop at Villa del Foro (Cicolani 2021, pp. 533-534). The fibulae from Genoa and its surroundings do not seem to show the peculiarities identified for the artifacts from 'Liguria Interna', as far as can be deduced from literature (since it was not possible to study directly the artefacts), and they would seem to refer to the more evolved Golasecca type (i.e. 'Palestro type').

No further evidence of coral presence in these areas has been documented for the Iron Age.

This scarcity in coastal centers aligns with observations from the Catalan and Gaulish coasts between the 7th and 2nd centuries BCE, where a structured organization can be inferred, with harvesting occurring near the fishing areas and sale and/or processing taking place at inland centers (Ugolini 2006a, pp. 78-79).

Figure 63. Raw coral from Genova-San Silvestro (metric reference 1 cm; modified after Melli 2021, fig. 48).

4.4 The use of coral in Este culture and north-eastern Italy

In the Venetic area, the use of Mediterranean red coral is documented from the 8th century BCE, contemporaneous with its presence in the Golasecca culture and possibly facilitated by Etruscan intermediaries. Pearls and tubular elements are the oldest coral artefacts (e.g., 'Longone al Segrino-type' pendants are not documented in north-eastern Italy). Between the 7th and 6th century BCE, it is mainly used to produce beads and necklaces, together with other materials such as glass, amber, terracotta, copper and gold, from the Este II-late to Este III-late phases (approximately 7th - 5th century BCE; de Marinis 1997, p. 157; 2000, p. 172; Schmid-Sikimić 2002, pp. 219-221).
Leech fibulae with long foot, bow with a terracotta core, decorated with circular insets of presumed coral, spread in north-eastern Italy between the 6th and 5th century BCE, in the Este III-Middle period (525-475 BCE), as weel as in north-western Italy and Canton Ticino (de Marinis 2000, p. 172). However, a predominance of the 'older' types with fewer rows of inlays on the arch is observed in these areas, as well as a higher recurrence of the variant with longitudinal lines separating the circular inlays. The variant with a transversal or longitudinal grooves, filled with alleged coral, is also attested by few specimens in north-eastern Italy. Late western Hallstattian fibulae (*Entenkopffibeln* / *Vogelkopffibeln* – ornitomorphic type and *Fußzierfibel* type) decorated with coral inlays, bucket pendants with 'occhio di dado' decoration and bronze grooming tools, variously decorated with coral, are also documented (de Marinis 2000, p. 172). On the other hand, coral-composite bow fibulae, found in the Golasecca area, are completely absent (de Marinis 1997, p. 157; 2000, p. 172). A type occurring here but not in Golasecca area is the dragon fibulae (*Hornchenfibeln*) with lateral daisies and coral insets, well documented in the Slovenian area and across the Alpine arc (Nascimbene 2009, pp. 75-86). As already mentioned for Golasecca, some of these types are also widely distributed in other areas.

4.4.1 Beads and pendants

The earliest coral finds in the Venetic area are small raw corals, cut and pierced, from tombs 234 and 149 in Este, Casa di Ricovero, dated between the 8th century BCE and the beginning of the 7th century BCE (Fig. 65; Tab. 13). The presence of this raw material is therefore contemporaneous with its attestation in the Golasecca area, where pendants of the 'Longone al Segrino' type appear in these phases. In the Atestine area, in the 7th - 6th century BCE, coral was worked mainly in the form of beads (Figs. 64-65) and inserted into necklaces, together with other materials, such as glass, initially in a few units with a progressive increase in the following phases (Schmid-Sikimić 2002, pp. 219-221). From the 7th century BCE, coral is also found north of the Alps (Fig. 65; e.g., Heuneburg, Courtesoult, Kaltbrunn, Magdalenenberg). It occurs in the form of spherical beads from the 6th century BCE (e.g., Singen, Esslingen, Ditzingen-Schockingen, Nordhouse), also used as pinheads (e.g., Nordhouse, Kaltbrunn, Ditzingen-Schockingen) (Schmid-Sikimić 2002, pp. 219-221).

Figure 64. Pieve d'Alpago, Pian della Gnela, coral bead, I.G. 355534 (ph. Berruto; metric reference 1 cm).

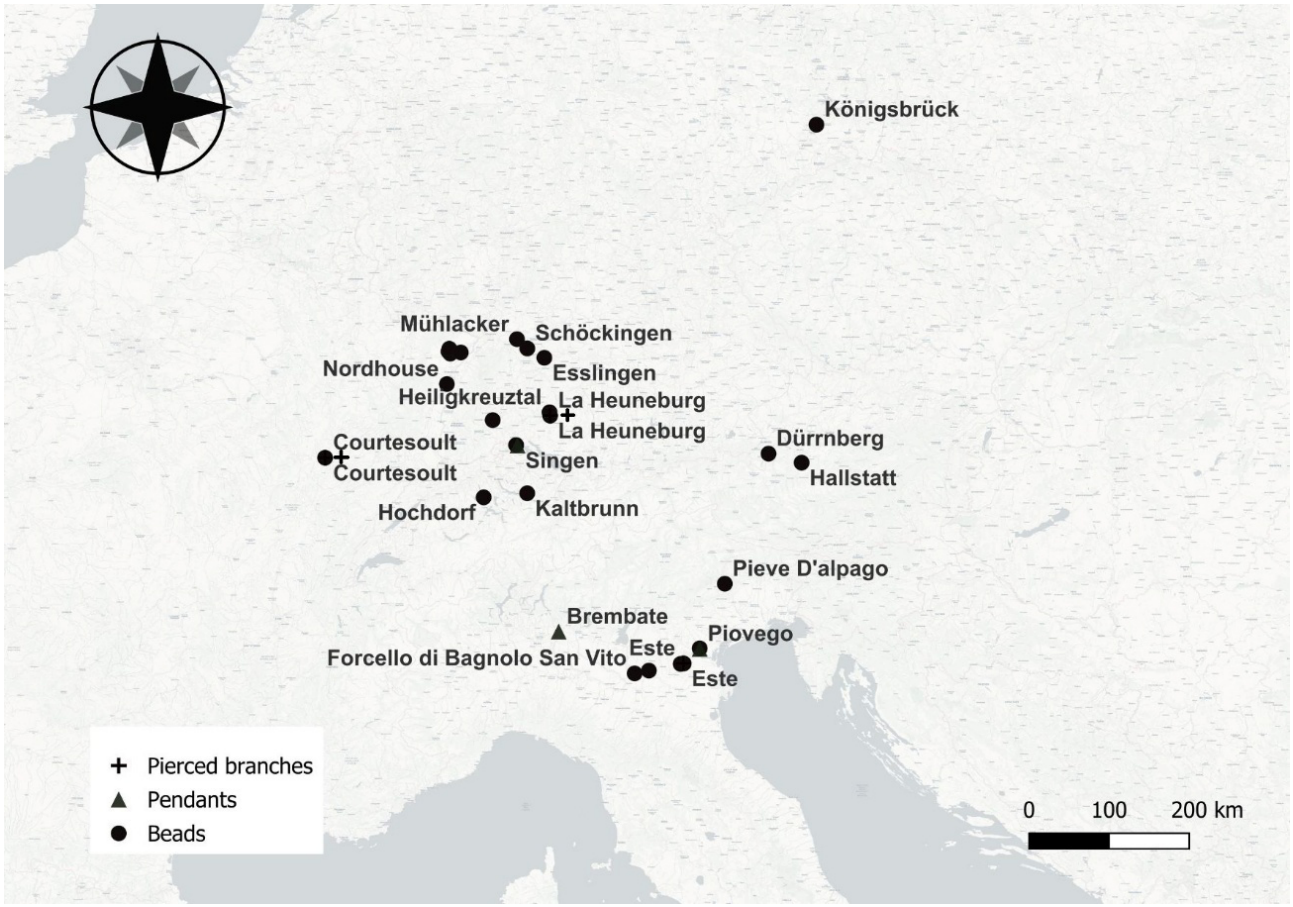

Figure 65. Distribution between the 7th and 6th century BCE of beads, pierced branches, and pendants. Elaborated by the author in QGIS 3.40.8 (2025); base map: © CARTO, © OpenStreetMap contributors.

4.4.2 Dragon-shaped fibulae with daisies

Dragon fibulae (*Hörnchenfibeln*), a type typically associated with male burials, are common across regions both south and north of the Alps. They are multicurvilinear bow fibulae, found in various types and variations and diffused throughout the Italian peninsula and Slovenian area from the late 8th to the late 6th century BCE (Mansfeld 1973, p. 9; Chieco Bianchi *et al.* 1976, tav 19; von Eles Masi 1986, p. 234; Cicolani 2017, pp. 87-98).

Specimens with presumed coral inlays include the variant with daisies and a three-lobed appendix (Chieco Bianchi *et al.* 1976; Nascimbene 2009, pp. 75-86, tipo I.2). The bronze rod bow is folded to form two elbows, as in the case of the serpentine bow fibulae. On the one next to the head of the bow a pair of daisies or discs with a three-globe appendix is attached. A fold-stopping disk is observed at the head of the bow. The foot is long with a J-shaped cross-section and a simple globet or vase termination.

Two varieties were identified: i) type A, which is larger in size and has linear decoration on the bow and foot, and ii) type B, which is smaller in size and undecorated. Variety A is further subdivided into two sub-varieties: type A1 also has elements embedded in the decoration, while type A2 has a conical expansion at the head of the arch (von Eles Masi 1986, pp. 241-242, nn. 2519-2524; Nascimbene 2009, pp. 75-86). A specimen with preserved whitish decoration from Ponte nelle Alpi-Casan (Fig. 66) was considered in this study.

More than 200 specimens of dragon fibulae with daisies have been found[1] in more than 30 archaeological sites pertinent to *Caput Adriae*, particularly in Most na Soči and Inland Slovenia, in Friuli and eastern Veneto, in the Belluno area, and in the Laguna area at Altino. Outside of the main area of distribution, sporadic occurrences appear in Veneto at Este, Rhaetian areal at Mechel and Rasun, Balkan territory at Donja Dolina, and transalpine area at Hallstatt, Gurina and Gracarca. More than half of the specimens come from male grave goods from the Santa

1 For the list of attestations, refer to Nascimbene 2009, pp. 78-85.

Lucia necropolis (Most na Soči). Among the different variants, variety B is predominant. The type is first attested in the second quarter of the 6th century BCE in Slovenia, where it becomes more frequent between the middle and the end of the same century and is still present in early 5th century BCE contexts. The Italian specimens come from grave goods dated to the second half of the 6th century BCE and from a 6th - 5th century BCE residential context (Fig. 67; Nascimbene 2009, pp. 75-86).

Figure 66. Ponte nelle Alpi, loc. Casan, Dragon-shaped fibula with daisies (ph. Berruto; metric reference 1 cm).

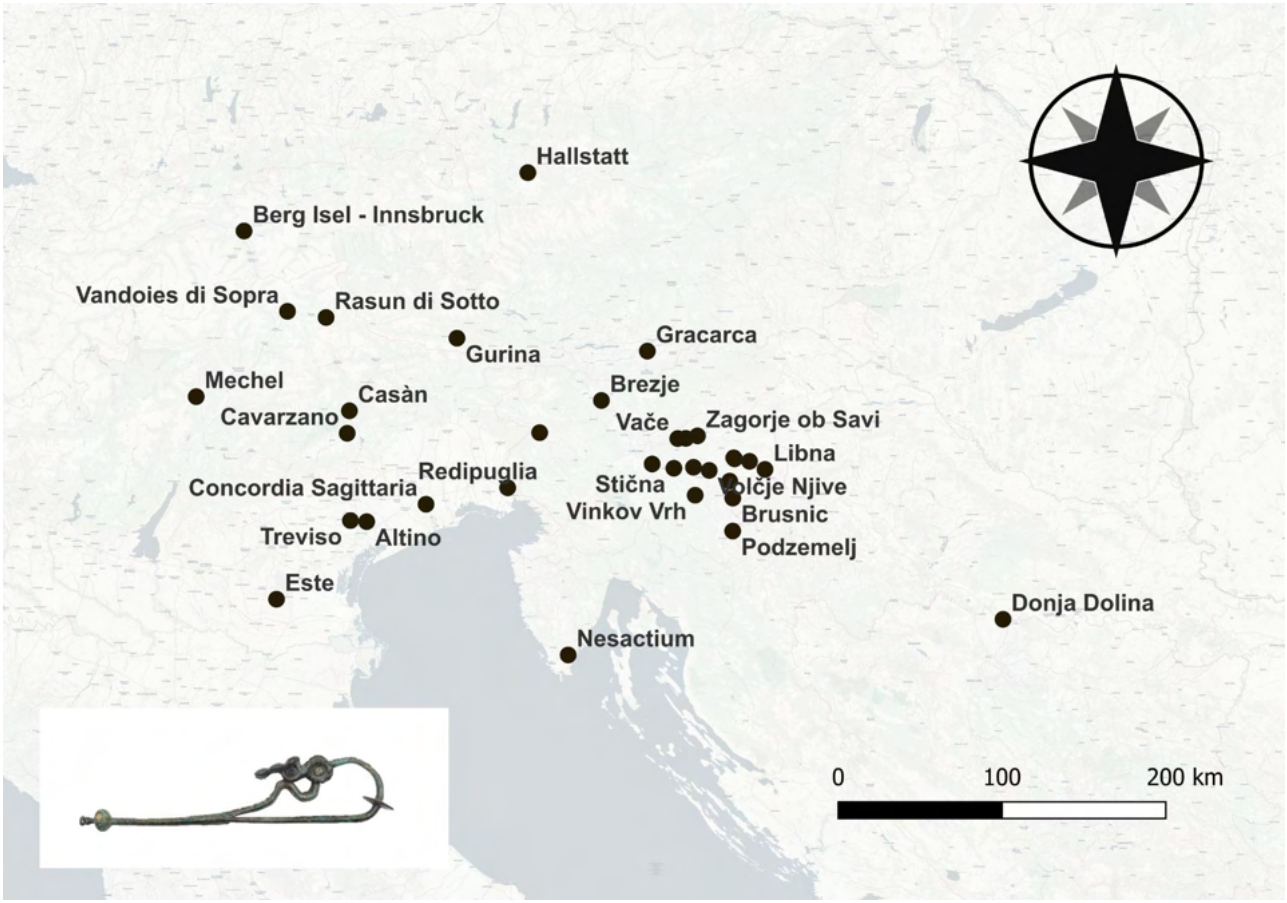

Figure 67. Distribution of the type 'Dragon-shaped fibulae with daisies and a three-lobed appendix'. Elaborated by the author in QGIS 3.40.8 (2025), after Nascimbene 2009; base map: © CARTO, © OpenStreetMap contributors; archaeological find: Ponte nelle Alpi, Casan (ph. Berruto).

4.5 The use of coral in Etruria Padana

Coral does not appear to have been widely distributed in eastern Etruria Padana, although it certainly circulated in these areas, likely in connection with trade. As discussed in the previous section, a supply via the Etruscans can be hypothesized for the Golasecca and Venetic populations in northern Italy, as well as for transalpine Hallstatt groups. Supporting this hypothesis are the numerous fragments of raw coral found at Forcello di Bagnolo San Vito, the small branch from Borgo Virgilio–Arginotto, and the pieces discovered in the De Luca, Arnoaldi, and Certosa necropolises in Bologna (de Marinis 1997, p. 157; Quirino 2011).

Regarding artefacts potentially made with coral, it is worth mentioning the discovery of long-foot leech fibulae with circular decoration. In the eastern area, one example was found at Marzabotto (de Marinis 2000, p. 170), another one at Gaggio (Giordani 2008, fig. 1) and two at Verucchio (Pozzo di Pian del Monte: Bentini *et al.* 2020, pp. 396-397, fig. 13; Casini 2000b, p. 88, n. 63; de Marinis 2000, p. 173, note 40; Morico 1987, pp. 270-273, fig. 176.9). Four fibulae are reported north of the Po in the Mantua area: at Mantua-piazza Santa Barbara (unpublished, inv. St. 169519; Fig. 68), Lago Superiore in Mantua (not found; de Marinis 2000, p. 170; Nascimbene 2009, p. 135, no. 23), Castellazzo della Garolda (not found; de Marinis 2000, p. 170; Tamassia 1979, pp. 520-521, t. LXXXII.b) and Forcello di Bagnolo San Vito (not found; de Marinis 2000, p. 173, note 40; Colonna 1979, t. LXXVII.b).

This type, however, is most frequently documented in the western Apennine sector of Emilia, bordering the Etruria Padana, Ligurian and Golasecca areas. In the Reggiano area, twelve artefacts are reported from San Polo-Campo Servirola (Damiani *et al.* 1992, pp. 128-129, 222, 226, 307-308) and four from Bismantova (Damiani *et al.* 1992, pp. 129, 308). In the Piacentino, one specimen (not found) from Bobbio should be mentioned (Casini 2000b, p. 88, n. 36; Catarsi, Dall'Aglio 1987, p. 407, fig. 2.8; Morelli 1888, p. 19, t. I, n. 2) and seven from the Tidone Valley (unpublished: Borgonovo, Pianello and Rottofreno). Some pieces found in the western Apennines show peculiarities already mentioned for artefacts from southern Piedmont, suggesting that they may sometimes be a local production or a variant: higher frequency of the full-arch without a terracotta core, flattened lenticular or biconvex arch morphology, flattened morphology of the terminal globe of the foot.

Figure 68. Mantua, Piazza Santa Barbara, leech fibula bow with coral insets, inv. no. St. 169519 (Museo Nazionale di Mantova, ph. Berruto, metric reference 1 cm).

Late-Hallstattian fibulae are well attested north of the Po, at Forcello di Bagnolo San Vito, among which some are characterized by presence of alleged coral: two *Fußzierfibeln* (de Marinis 1986b, fig. 146.6; 1987, p. 91-92, fig. 4.f; 1997, p. 157; 2007, p. 209, fig. 130.8; 2010, fig. 13.11; de Marinis *et al.* 2017, p. 33-34, fig. 6.11-14) and one ornithomorphic (de Marinis 1986b, p. 245, n. 334, fig. 146.2; 1987, pp. 91-92, 94, 95, ffig. 4.b, 5.11; 2007, p. 209, fig. 130.10; 2010, fig. 13.15; de Marinis *et al.* 2017, p. 35, fig. 7.1). Sporadic specimens are reported for the rest of Emilia: a *Fußzierfibel* from San Polo-Campo Servirola (Damiani *et al.* 1992, pp. 131-310, t. LXIV, n. 967; de Marinis 1987, p. 95, fig. 5.15; Frey 1971, p. 377, list 1, fig. 2.9) and one ornithomorphic from Montebibele-Monterenzio (de Marinis 1986b, p. 243; Kruta, Moucha 2018, p. 83, n. 34; Adam 1996, p. 43, n. 25). Among the artefacts with presumed coral decoration the discovery of a type 1A bucket pendant with 'occhio di dado' decoration should also be reported at the Forcello di Bagnolo San Vito (Barbieri 2019, pp. 45, 46, 50, 53, 56, fig. 10.1, 11.1; de Marinis 2007, p. 205, fig. 129.6; 2010 fig. 14.1; de Marinis *et al.* 2017, p. 32).

4.6 The use of coral in the Late Iron Age

The use of coral for decorating jewellery, weapons, and other valuable objects was widespread among the Celtic populations of the Late Iron Age (Fig. 69). Transalpine Celtic craftsmen use this material extensively from the La Tène A phase onwards (Fürst 2014; Ugolini 2006a, p. 87).
Beginning in the 4th century BCE, Celtic art experienced a renaissance characterized by a "vegetal" style, featuring racemes and palmettes arranged in sophisticated compositions. This development reflects the influence of transalpine Celtic populations on Italic communities. Such decoration is often associated with a particular type of fibula, distinguished by a discoidal foot designed to hold a coral cabochon. The use of raw coral is relatively common in the production of jewellery (e.g., fibulae, torques) and weapons (e.g., sword scabbards, helmets), compared with earlier phases in transalpine areas (Kruta 1991, pp. 198-199).
In northern Italy, the number of latenian artifacts dated to the 4th century BCE is generally scarce (Kruta 1991, p. 201). Few pieces of evidence attest to the use of coral in decorating fibulae, either as insets along longitudinal grooves on the bow or as a cabochon at the end of the foot.
In these phases, the use of coral presumably shifted southwards. From the La Tène phases onward, the overall quantity of artefacts decorated with coral increases in southern Italy with respect to the northern areas, where this raw material was widespread in the Early Iron Age. A similar trend is observed in the transalpine area, with an increase in coral finds in southern France – the assumed areas of provenance. This phenomenon has traditionally been linked to the so-called 'Celtic migrations', through which artefacts with worked coral may have circulated back southwards (Fürst 2014, pp. 55-56).
In this research, the examination of coral ornaments for this chronological period is limited to a partial survey of Piedmontese artefacts and does not aim to cover the entirety of the material from northern Italy.

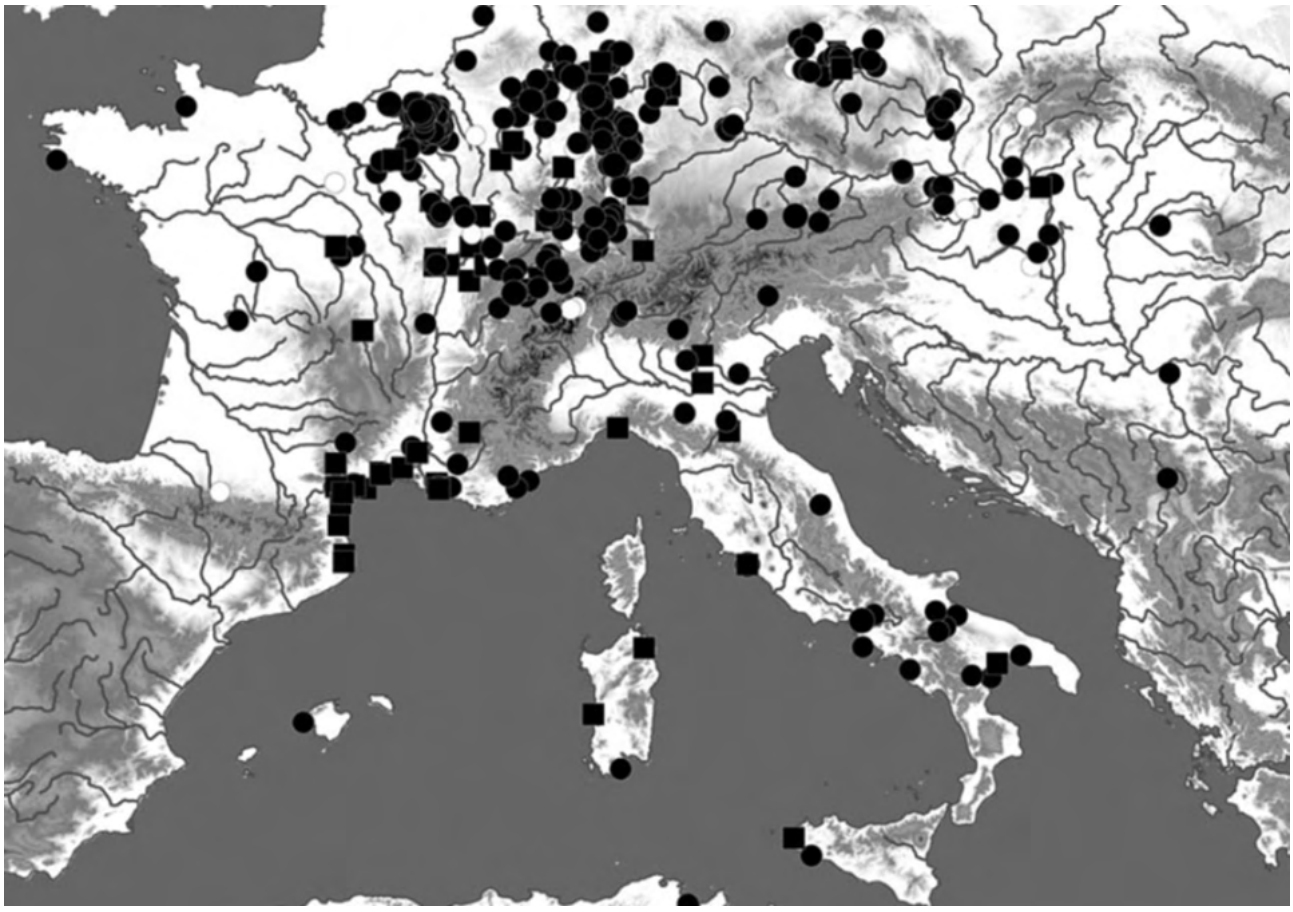

Figure 69. Distribution map of coral artifacts in the La Tène A-B period (450-275 BCE); black circles = more than 5 coral artifacts; white circles = artifacts that have lost coral insets; black squares = settlements with coral (after Fürst 2014, fig. 3).

4.6.1 Ancient La Tène fibulae, furrowed bow and coral applications

This group of fibulae is marked by a broad bow with a curved profile, which elongates and flattens to become angular. It sometimes has a thin central groove for the insertion of coral and various patterns of decoration, linear or in relief. This type has foot folded down to touch the top of the arch, sometimes passing over it, forming a cup, perhaps also decorated with coral, followed by a moulded spatula-shaped end, sometimes decorated with parallel or fan-shaped incisions. It generally has bilateral four- or six-turn springs of medium size (Adam 1996, pp. 118-120).

Its features are extremely variable and can be dated to the early to mid-early La Tène (5th century BCE), with a strong diffusion in the transalpine area, in Champagne, Switzerland, Austria, Bohemia and Bavaria. In northern Italy (Fig. 71), it is common in Emilia (Bologna, Arnoaldi necropolis; Kruta 1978, p. 158, fig. 6, n. 2-3; Marzabotto; Kruta-Poppi 1975, fig. 3.5; in 'Modenese'; Kruta-Poppi, 1977, p. 426, fig. 1), 'Vicentino' (Santorso, Montebello Vicentino, San Tomio di Malo; Ruta Serafini 1984, pp. 19-20, fig. 7) and Lombardy (Vho di Piadena), as well as in Trentino Alto Adige (Mechel and Campolino-Lothen) (Fig. 70; Adam 1996, pp. 118-120).

The use of coral in the decoration evolves in the Swiss plateau in the 'Münsingen' type, between LT B1 and LT B2 (4th century BCE).

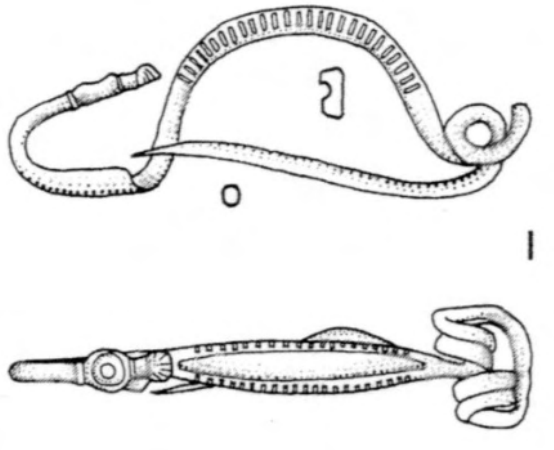

Figure 70. Fibula from Mechel (inv. no. 1470; after Adam 1996, p. 118. t. IV. 99).

Figure 71. Distribution of the 'Ancient La Tène furrowed bow fibula' type in northern Italy [elaborated by the author in QGIS 3.40.8 (2025); base map: © CARTO, © OpenStreetMap contributors].

4.6.2 Massive bow fibulae with wide central application and disc-shaped appendix

This group of fibulae is marked by a massive oval or hemispherical bow, decorated with a central groove for the insertion of coral, surrounded by variable decorative motifs; at the bottom of the groove a hole is visible, through which a hook passed, designed to hold the coral. This type has folded foot with discoidal appendix, varying in size and decoration, and generally bilateral six-turn spring (Adam 1996, p. 158).

It is documented in the southern Swiss valleys, particularly in the Canton Ticino (Fig. 72; Butti Ronchetti 2012, p. 18; Nagy 2012; Tori *et al.* 2010), as well as in 'Comasco' (Casini *et al.* 2001, fig. 19) and 'Bresciano' (Vitali 1991, p. 222), from the end of LT B2 (300-275 BCE), and also in Trentino Alto Adige, throughout LT B (4th century BCE), with a specific evolution within the cultural area (Adam 1996, pp. 162-163). Ticinese fibulae with applications developed in parallel with Trentine fibulae, based on Swiss and Ticinese models, from which both series derive. This is a typically Alpine production type, found up to LT C2 (200-150 BCE). The diffusion of this type indicates the development of new trade routes within the Alpine region, through the longitudinal valleys (Casini *et al.* 2001; de Marinis 1988a).

Adam (1996, pp. 158-161) identifies, for the Trentino area, several subtypes (Fig. 73):

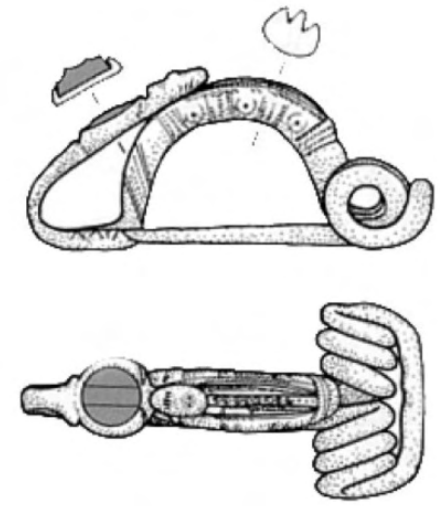

Figure 72. Fibula from tomb 21 Giubiasco (after Butti Ronchetti 2012, fig. 9a).

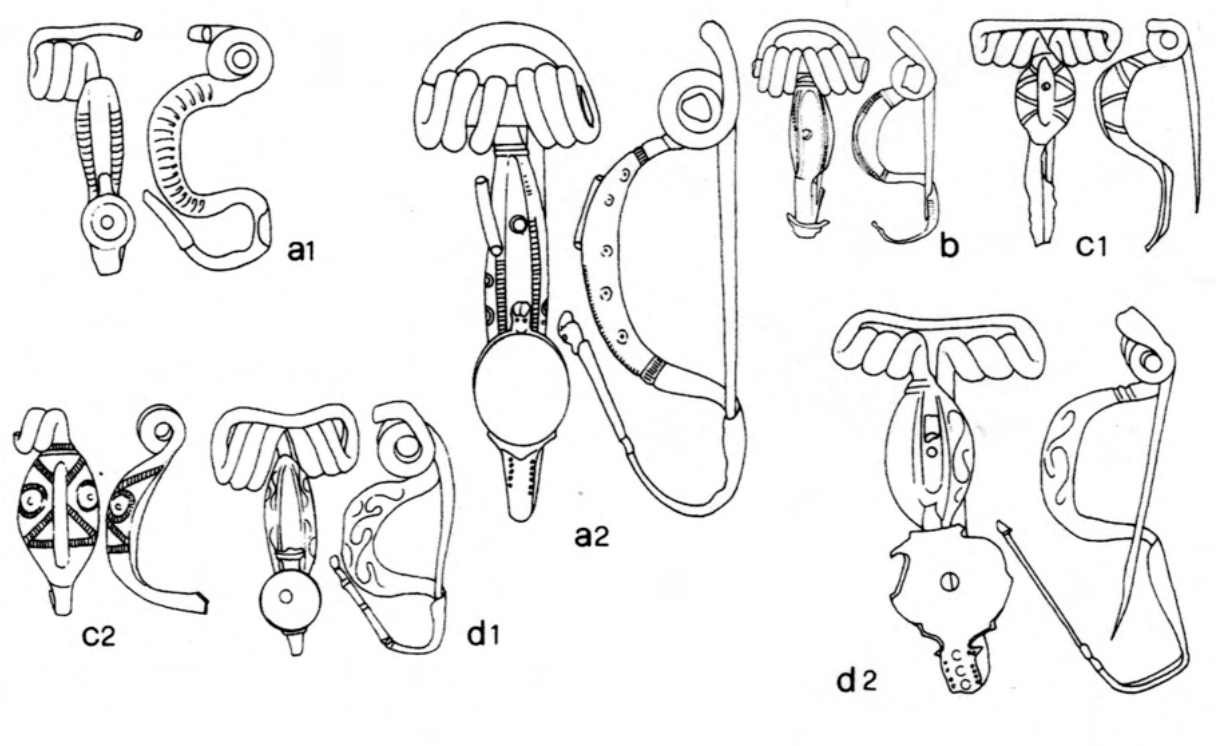

Figure 73. Massive bow fibulae with wide central application and disc-formed appendix: Trentino areal sub-types (after Adam 1996, p. 166).

a) Wide profile bow, slightly enlarged, marked by transverse groove (type a1) or curvilinear (type a2) decoration and human mask at the end of the terminal appendix of the foot; six-loop spring with circular cross section;
b) Bow with convex profile, marked by longitudinal and transverse rectilinear decoration; spring with six loops, circular section;
c) Mandolin bow, marked by oblique incised decoration and inverted V motifs (type c1), sometimes accompanied by 'occhio di dado' decoration (type c2); flattened section spring;
d) Massive arch, marked by 'meander' decoration; spring with flattened section.

Unfortunately, within this study it was not possible to examine Trentino fibulae with presumed coral applications; however, some typologically similar piedmontese specimens were instead considered.
As far as jewellery is concerned, there is continuity with previous phases in Piedmont during the Late Iron Age, while at the same time new types of transalpine origin are observed. Typical La Tène-style fibulae were found in the 'Novarese' area and in the Susa Valley (Gambari, Venturino Gambari 1997; Gambari 1998, p. 144). Among the latter, bronze fibulae datable to the Ancient La Tène (4th century BCE), discovered in the 19th century were retrieved during the construction of the Frejus tunnel (Gambari, Rubat Borel 2011, p. 63; Gambari 1998, pp. 143-144, fig. 125); more recent findings were found in a tomb at Villar Dora and two others at Chiomonte, dated to the 4th century BCE and excavated in the 1980s. Among the tombs of Chiomonte, loc. La Maddalena, in one case the burial of a high-ranking female individual can be identified, marked by presence of rich ornaments of mixed local-transalpine features (Gambari, Rubat Borel 2011, p. 65; Padovan, Thirault 2007, pp. 45-46). This burial yield two bronze folded foot fibulae with large disc appendix, containing presumed coral remains (inv. no. St. 74974-74975, Musei Reali; Fig. 74).
Archaeometric analyses performed on these two artifacts, however, ruled out the presence of *C. rubrum*. Conversely, quartz, possible illite and kaolinite were detected, suggesting that the residues could be referred to deposition soil or else a kaolinite-based decoration (Giustetto 2008; Giustetto *et al.* 2013). The use of adhesives to accommodate a coral cabochon or vitreous material is well documented for transalpine artifacts of similar chronology, contextually with the use of rivets (Zlámalová Cílová *et al.* 2024, pp. 59-60); however, presence of adhesive was not identified by the performed analyses (on only one archaeological find). Based on

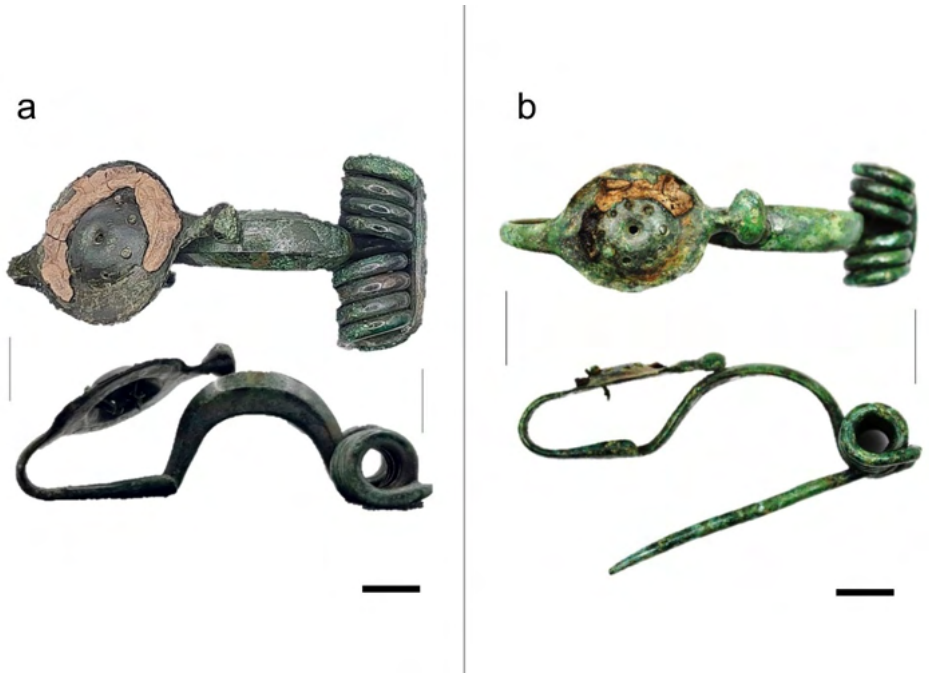

Figure 74. Chiomonte, loc. La Maddalena, female burial (4th century BCE): Latenian folded foot fibulae with disc-appendix containing presumed coral encrustations (ph. Berruto; metric reference 1 cm; inv. no. St. 74974, a - St. 74975, b, Musei Reali)

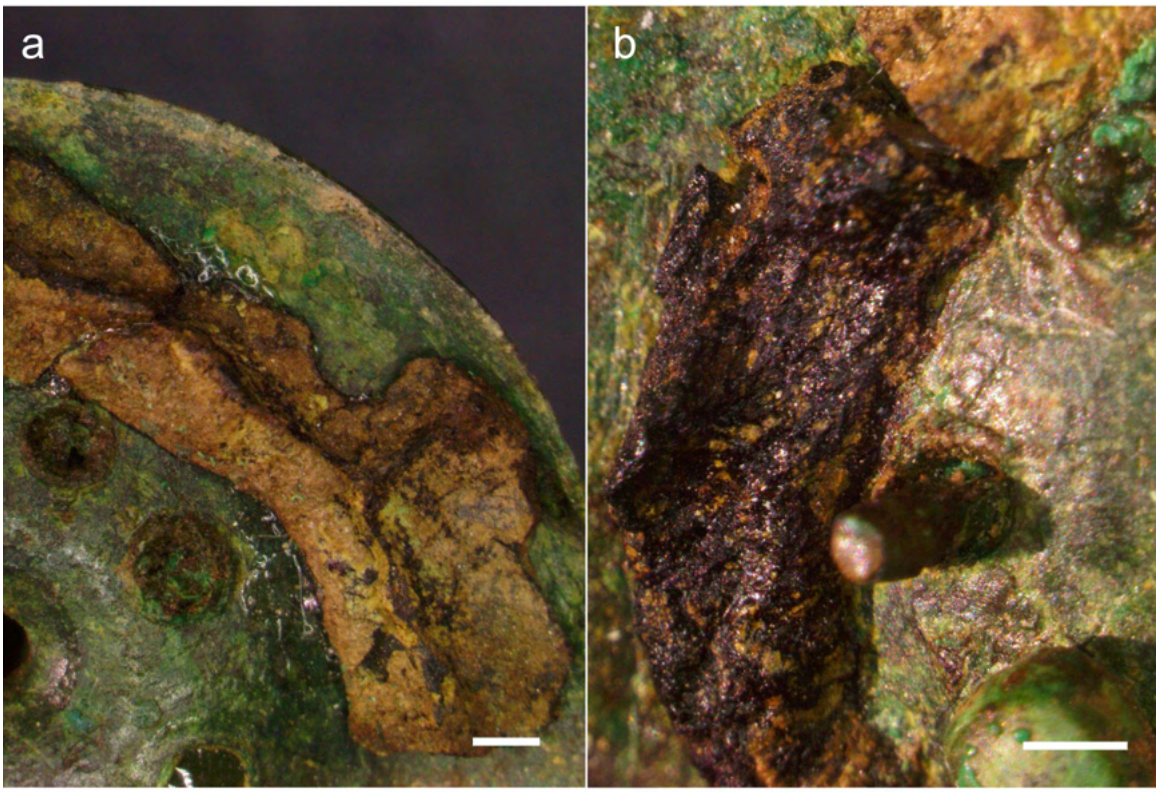

Figure 75. Chiomonte, loc. La Maddalena, female burial (4th century BCE): light microscope image of the material (ph. Berruto; metric reference 1 mm; inv. no. St. 74975, Musei Reali).

available data, a sharp material identification is thus not possible.

The anthropic traces visible on the residual material inside the disc-shaped appendix (Fig. 75a) could therefore be attributable to spatula marks of a 'decorative paste' – or viceversa imprint of a superimposed decorative material, which has been lost. The colour and appearance of the blackish material preserved on St. 74975 apparently supports the latter hypothesis, probably birch pitch (Fig. 75b) documented on similar artifacts in transalpine contexts (e.g., Münsingen brooches: Zlámalová Cílová *et al.* 2024). However, further analysis is needed to better understand the technological aspects of the artifacts.

Finds from the Novara area highlight the importance of the local celtic substrate, testifying to the presence of mixed cultural aspects and continuity of influxes from abroad (Gambari 1998, p. 144). At Galliate, some graves under tumulus were discovered, with cases of cremations, datable to LT B1 and LT B2. At Dormelletto a necropolis was found, with inhumation tombs datable to LT C1 (second half of the 3rd - early 2nd century BCE), with mixed elements of external influence and local elaboration (Gambari 1998, p. 144; Spagnolo Garzoli 2009). Among the typically Celtic ornaments, such as bronze ovoli ankle rings, free-foot bronze fibulae with human head button can be found, called *Kopffibeln*, also popular in Canton Ticino and sometimes characterized by the presence of coral elements (Deodato 2013, p. 20, fig. 5; Nagy 2012; Tori *et al.* 2010; Schmid-Sikimić 2002; Sormani 2013).

In this study, one of these fibulae was examined (Fig. 76), kept at the Archaeological Museum in Arona. Unfortunately, no trace of coral or other organic material was found (Fig. 77). It is dated to 250-175 BCE and marked by a massive arch, with a groove for coral insertion and geometric decoration, a folded foot with a disc-shaped appendix and a human head termination. The fibula can be referred to the 'A1 massive bow type' from Adam (Adam 1996, pp. 158-161).

Figure 76. Dormelletto, via San Rocco, tomba 43: Massive arched fibula with groove for coral insertion (ph. Diana; metric reference 1 cm; Arona, Museo Civico Archeologico).

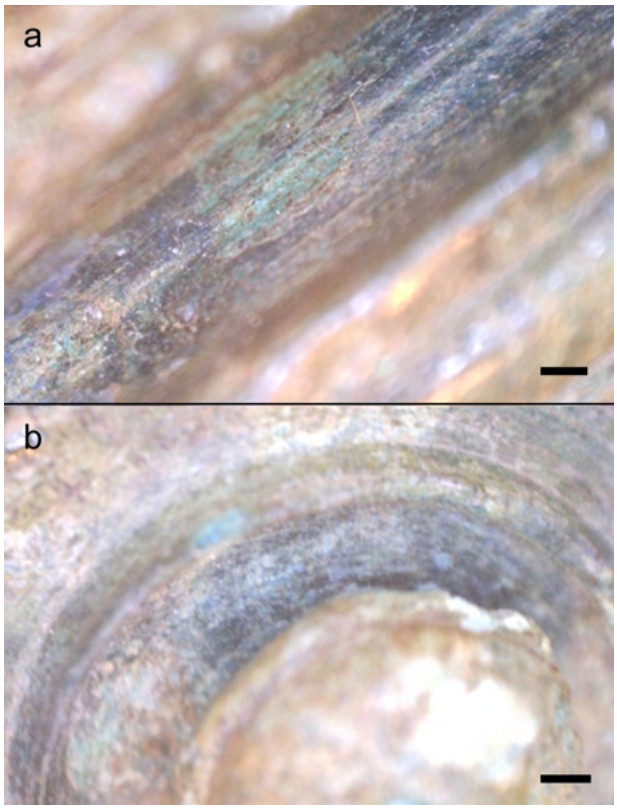

Figure 77. Dormelletto, via San Rocco, tomb 43. Digital microscope image of areas of possible coral insertion (ph. Berruto; metric reference 1 mm): a) groove along the arch; b) disc-like appendix.

4.7 Discussion. Coral in Iron Age northern Italy

In northern Italy during the Early Iron Age, artefacts decorated with coral were widely distributed. This material was frequently used to embellish women's ornaments and clothing accessories, particularly fibulae and pendants, especially in archaeological contexts associated with the Golasecca area in the northwest and the Venetic-Este area in the northeast.

In these areas, coral appears from the 8th century BCE and becomes widespread from the 7th to the 5th century BCE. It is possible to identify a technological evolution in the artefacts manufacture, from simpler forms (e.g., pendants with pierced coral branches, coral beads) towards increasingly complex objects (e.g., composite bow fibulae, 'Palestro-type' leech fibulae).

The most illustrative type is the leech fibulae with a long foot and bow with a terracotta core, variously decorated with small circular insets. It has several variants, identified based on decoration and morphology; it is common in two main areas (i.e., Golasecca and Este cultural areas), but also attested in neighbouring areas (e.g., 'Liguria Interna'; coastal Liguria; Etruria Padana), linking to the main transit routes and circulation of people and objects, but also of models.

Some territorial variability should be noted. In the Venetic area, the earliest forms are found, marked by fewer holes decorating the arch, as well as the predominance of a variant that shows linear motifs between the holes, forming squares on the bow. All these variants are well represented in the Golasecca area, highlighting this as the probable area of origin and evolution, with a predominance of the more evolved forms in the Ticino area of the Golasecca culture in the 5th century BCE. In the border area between the Golasecca, Ligurian, and Po Valley areas (e.g., Alessandrino, Astigiano, and Piacentino), the presence of a variant possibly linked to a local production was identified, marked by a full arch with flattened section, long foot with a flattened globet and sometimes a bulge, decorated only on the upper face.

The provenance of the coral remains unknown at the current state of research, but several hypotheses have been proposed, all of which involve the intermediation of Etruscan populations, whose trade networks were active in

these areas (de Marinis 2000, p. 164; Ugolini 2006b, p. 90). Unfortunately, no evidence is known regarding the fishing and use of coral in the Etruscan world (Ugolini *et al.* 2000, p. 139; Ugolini 2006b, pp. 90-91).

Pliny the Elder (*Naturalis Historia*, XXXII, 11, 21) mentions several supply areas active in the 1st century CE: to his knowledge, the best coral came from the *Stoechades* Islands (Îles d Hyères) in the Gulf of Lion and from the Aeolian Islands near the city of *Drepana* (Trapani), as well as from Gravisca and Naples: these were probably the supply areas exploitable with the techniques of the time. The actual fishing areas in the Early Iron Age, however, may not have corresponded to those active centuries later and mentioned by Pliny for the Roman Age. It is therefore possible to analyse the fishing grounds accessible to the Etruscans, who maintained contacts with the cultures of northern Italy during the Iron Age, by considering the areas of influence active at the time. Following this reasoning, the Aeolian Islands, under Punic control, and Naples, under Greek control, can be excluded. By contrast, the coast near Gravisca, the harbour of the Etruscan city of Tarquinia, may have represented potential supply areas. The *Stoechades* and the Gallic Gulf (Languedoc), and probably also the coasts of the Ligurian Sea (Provence and perhaps also Liguria and Tuscany), were areas of Etruscan influence from the 8th century BCE (Camporeale 2006). These regions may therefore have served as coral supply areas, with merchants possibly using waterways connected to the Po River or the lower Piedmont territories to ensure the distribution of coral to the Golasecca culture area.

Coral reached the transalpine Hallstattian world through the populations of northern Italy (de Marinis 1997, p. 157) where, in addition to the production of beads and brooches, it was used to decorate certain types of fibulae, the late Western Hallstattian fibulae, also attested in the Cisalpine area. From the archaeological record, it is possible to find a higher occurrence of coral decorations in the Cisalpine area and in north-eastern Italy in particular (Adam 1996, p. 47), a possible indication of local influences and reworking of models: ornithomorphic fibulae are mainly found in north-eastern Italy, with a few occurrences in Etruria Padana, and *Fußzierfibeln* are widespread and are also attested in the Golasecca area.

Both in the Golasecca and Este cultures an intermediate type is also attested, the leech fibula with grooved decoration on the bow – probably a local evolution, which originated from the fusion of Cisalpine coral leech models with the transalpine ones of the late Hallstattian fibulae. Coral became particularly popular among transalpine populations during the La Tène A and B1 periods, roughly until 300 BCE (Fürst 2014), whereas in northern Italy, its use gradually declined from the 4th century BCE until its eventual disappearance (de Marinis 2000, p. 172).

5. Archaeometry and Corals

Abstract

Il capitolo si concentra sull'analisi archeometrica di decorazioni in materiale biancastro, tradizionalmente identificato come corallo, applicate su ornamenti metallici della prima età del Ferro nell'Italia settentrionale. Se tradizionalmente lo studio di tali oggetti è stato affrontato prevalentementedal punto di vista formale e tipologico, negli ultimi anni si è manifestata una maggiore attenzione rivolta all'identificazione dei materiali decorativi, grazie all'applicazione di tecniche scientifiche multi-analitiche. Dovendo operare su manufatti di interesse archeologico, una delle difficoltà principali riguarda l'impossibilità di campionamento invasivo, rendendo necessaria l'applicazione di tecniche non distruttive o micro-distruttive. Il corallo rosso mediterraneo (*Corallium rubrum*) può essere identificato grazie alla presenza contestuale di calcite e pigmenti organici che donano il caratteristico colore rosso. Tuttavia, alterazioni post-deposizionali ne causano lo sbiancamento, complicando l'identificazione. Recenti studi hanno evidenziato microstrutture e composizioni chimiche caratteristiche, permettendone la distinzione da altri materiali biancastri.
La determinazione della provenienza del *Corallium rubrum* in contesto archeologico rappresenta una questione cruciale per comprendere reti di scambio e dinamiche socio-culturali antiche. Tuttavia, ad oggi, non esistono studi specifici dedicati a questo tema, se non in ambito paleo-ambientale. Le metodologie principali considerate sono l'analisi isotopica e quella degli elementi in traccia, entrambe complesse da applicare al corallo a causa di fattori come la diagenesi e la scarsa disponibilità di campioni comparativi.
L'analisi isotopica (Sr, C, O) può fornire indicazioni ambientali e geografiche, ma è ostacolata dall'alterazione post-deposizionale dei carbonati biogenici, che modifica la composizione originale. La distribuzione del *C. rubrum* si concentra inoltre nel bacino mediterraneo, rendendo difficile distinguere le singole aree di approvvigionamento antiche. L'analisi degli elementi in traccia, utile per identificare firme geochimiche locali, si scontra con problematiche analoghe, aggravate dall'impossibilità di confrontare i dati con campioni antichi, oggi esauriti o contaminati. Sono stati valutati anche approcci genetici e biomolecolari, che risultano inapplicabili a causa dell'esiguità del materiale organico conservato e della necessità di campioni di confronto con provenienza certa. In sintesi, nonostante la rilevanza della questione, al momento non esistono metodi pienamente efficaci per determinare con precisione la provenienza del corallo archeologico.

5.1. The archaeological question

Studies of metal artefacts have traditionally relied on standard archaeological approaches. Only recently have a few investigations focused on the archaeometric analysis of the materials used in the decorations of some metal artefacts. The research project presented here focuses on the study of metal ornaments – mainly fibulae – dating back to the Early Iron Age in northern Italy, which feature decorations or entire portions made of a whitish non-metallic material, traditionally identified in the literature as coral. However, similar materials were widely used in pre- and protohistory, and visual examination alone is insufficient to determine their precise nature. An innovative archaeometric and multi-analytical approach can provide a more accurate analysis of the technological development and the cultural interactions systems between ancient societies in northern and southern Europe.

This study adopts an interdisciplinary approach, examining these artefacts from an archaeometric perspective to identify their constituent materials and investigate their production technology

The traditional and typological archaeological study, presented in the previous chapter and based on the existing literature, also informed the selection of materials to be included in the analytical record. This combined approach provided new typological insights, thanks to the extensive area investigated and the large number of artefacts considered.

However, the archaeometric study is the main focus of this project. One major limitation is the nature of the artefacts – archaeological objects of great workmanship and value, for which sampling is generally not possible. The analytical protocol must therefore balance between this necessity and the actual efficiency of the analyses.

The main goal is the characterisation of the whitish material, traditionally identified with coral. An attempt was also made on pursuing information about the possible presence of organic binders, suitable for the adhesion of this

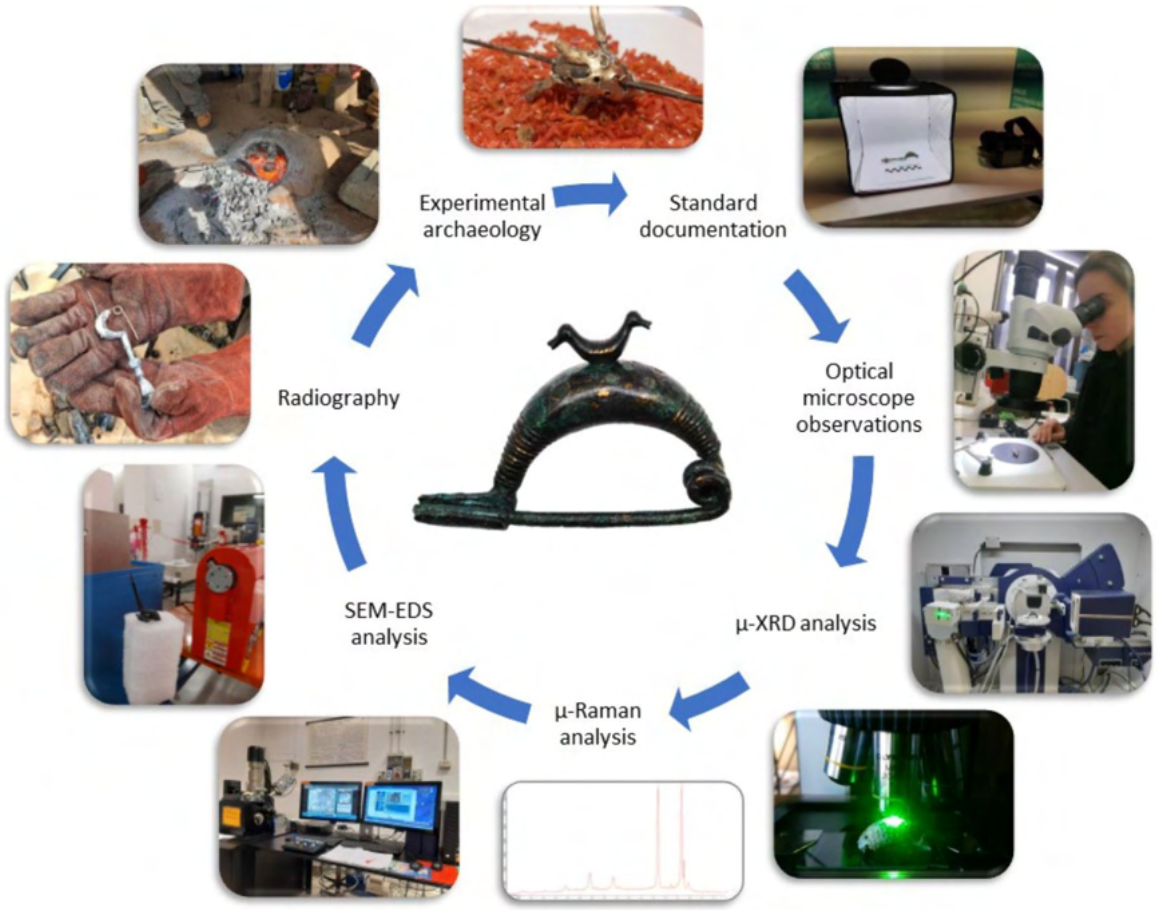

Figure 78. Schematic overview of the interdisciplinary approach applied in the study of the considered artefacts.

material to the metal support. Questions about the provenance of the whitish raw material were also raised. In the case of coral, determining the source of the material is fundamental for understanding the circulation networks and the contacts established between different populations.
Evidence of manufacturing traces on these archaeological finds was also investigated to identify details of the production technology. Further verifications were carried out through experimental archaeology (Fig. 78).

5.2. Previous studies

The occurrence of coral in archaeological contexts is generally underestimated, as this material is often not recognised. It tends to degrade in ancient artefacts, losing its original features and being macroscopically assimilable to other materials – such as bone, ivory or shell. Its alteration leads to the partial or total disappearance of the characteristic red hue, replaced by a whitish or pinkish colour, while in the event of combustion (as in cremation) it turns into grey (Perrin 2000; Mangani 2016)[1]. As far as colouration is concerned, it should be noted that coral varies in colour depending on its origin and depth of growth, ranging from the rare albino specimens to red, orange, pink, and chamois hues (Borrello 2001).
Improper methods were often used in the past for an archaeometric characterisation of coral, e.g., acid attack, resulting in effervescence through CO_2 release (Schvoerer *et al.* 2000; Viollier 1907). *Corallium rubrum* skeleton is in fact mainly composed of Ca-carbonate, and this reaction can discriminate coral from the red enamels used to imitate it – a common practice in the last stages of European protohistory (Perrin 2000; Schvoerer *et al.* 2000). However, this evidence is inadequate: carbonate can have different origins and, most of all, the material can be irreparably damaged (Viollier 1907).
Microscopic observation of the texture of the material is also a valid method[2]. The exoskeleton of *Corallium rubrum*, at the optical microscope, shows a typical radiate, woody structure, with lines parallel to the axis development (Borrello 2001; de Marinis 2000; Fürst *et al.* 2016; Perrin 2000; Schrickel *et al.* 2013; Schvoerer *et al.* 2000). Identification of unworked coral may thus be easy; when worked, on the other hand, it loses its shape and recognition is more difficult.
In 1996 (Schvoerer *et al.* 2000), a French team discussed an overview of methods to characterise or date ancient corals, such as X-ray diffraction (useful for the mineralogical characterisation), Raman (to recognise the dyes responsible for the red hue), X-ray fluorescence (XRF) and scanning electron microscopy with microprobe (SEM-EDS) (to determine chemistry). Other techniques include neutron activation gamma spectrometry [or analysis by neutron activation (AAN), to accurately determine major and trace elements], thermoluminescence (TL), the radiocarbon (^{14}C) or uranium-thorium (U-Th) method for dating. C isotopes are present in seawater, in which ^{238}U is soluble, where they participate to the construction of the aragonitic and calcitic carbonate skeleton of corals. Electron Spin Resonance (ESR) is also mentioned to measure the radiation dose received by coral sample after crystallisation (Schvoerer *et al.* 2000).
Regarding the types presented in this study – i.e., leech fibulae with inlays and pendants made of presumed coral – archaeometric investigations are scarce and often carried out with insufficient methodologies (Giumlia-Mair 1998; Mangani 2016; Schmid-Sikimić 2002; Viollier 1907)[3].

1 Coral is thermolabile and turns to yellow at 150°C, darkens at 200°C and then switch to grey, as is known from incineration burials (Borrello 2001).

2 There are numerous cases in the literature, such as the analyses carried out in 1885 by O. Tischler on a parure from Saalberg (Königsberg), those of M. Olshausen on a fibula with coral encrustations from Schwabsburg-Nierstein in Germany, those of M. Capellini in 1876 on a fibula from Bologna with coral decoration, the identification of coral by L. Campi in 1897, or Bleicher's analyses under an optical microscope of material from Haguenau forest in 1920 (de Marinis 2000; Perrin 2000). In 1969, following an investigation initiated by V. Moucha, staff at the Senckenberg Museum in Frankfurt am Main identified the shell of *Cypraecassis rufa*, a Mediterranean helmet snail, through microscopic analysis in the decoration of a shield from Tomb 1 of the Sulejovice necropolis in the Czech Republic. Moucha subsequently published the report (Schrickel *et al.* 2013).

3 In the Swiss Golasecca area, fibulae from Cerinasca d'Arbedo were investigated in 1907 by effervescence by D. Viollier, in 1996 by A. Meier (adopted methodologies not reported) and in the 2000s by C. N. Zwicky-Sobczyk with thin sections microscopical observation, leading to the identification of *C. rubrum*. In Slovenia some XRD analysis are reported for Santa Lucia – Most na Soči necropolis, with the identification of white fine-grained local limestone.

Among the Italian artefacts, two leech-like fibulae, a bucket pendant and a bead were recently studied from the Pian della Gnela necropolis in Pieve d'Alpago. XRPD and SEM-EDS were used, identifying a carbonate composition (calcite or Mg-calcite, seldom accompanied by dolomite) and excluding use of bone or ivory (Angelini, Molin 2015).

Giustetto *et al.* (2013) studied a leech fibula from the site of Castello di Annone, southern Piedmont, in a broader study focused on the characterisation of whitish materials on various supports (Berruto *et al.* 2014). In 2014, the decorations on 33 artefacts from the sites of Castelletto Ticino, Brignano Frascata and Villa del Foro, belonging to the Golasecca culture area and the 'Liguria Interna', were studied by FT-IR, Raman and XRPD, partly within an international project funded by the 'Agence nationale de la recherche' (CAECINA project; Cicolani, Berruto 2017). Analyses revealed presence of calcite and at times polyenes, typical of *Corallium rubrum*. A filler was also found in the engraved line decorations – a possibility never considered before. In almost all samples organic materials were found, perhaps related to processing techniques or previous surface treatments (Berruto *et al.* 2021; 2023a; 2023b).

Concerning the characterisation of coral on archaeological artefacts, recent studies are worth mentioning. As part of the Coral Trade Project (2014-2017), a Franco-German research team worked on the characterisation of presumed coral on trans-Alpine archaeological artefacts (Early to Late Iron Age) by using a non-destructive multi-analytical 'in situ' approach (p-optical digital, Raman and seldom XRF, XRD and SEM analyses) and comparing them to modern corals (Fürst *et al.* 2014; 2016). The characteristic micro-structure of coral (longitudinal crenulation on lateral observation and concentric wavy growth lines in cross-section; a 'coral foam' structure for big pieces from the base of a coral colony) were observed at the optical microscope. Raman spectroscopy allowed, recognizing both calcite and polyenes, an assumption of the effective nature of Mediterranean red coral. Distinction between different degree of crystallinity in calcite was performed basing on the peak shape in the Raman spectrum: both geogenic calcites (marble) and biogenic ones (shells from sea snails and mussels) have a higher degree of crystallinity than the high-Mg-calcite of *C. rubrum*. An unsolved problem involves discrimination between *Corallium rubrum* and *Spondylus gaederopus* – a Mediterranean shell whose red-coloured outer upper valva has a calcite and polyene composition. The two materials would be distinguishable only by measuring the Mg-content in calcite using elemental analysis techniques, as the upper *S. gaederopus* valva is composed of low-Mg-calcite (LMC). Another approach to assess Mg-content, based on evaluating the width of the carbonate bands by Raman, is not applicable to archaeological finds, due to the plausible substitution of magnesium over time (Fürst *et al.* 2016).

Loss of colour, a typical feature of *C. rubrum* on archaeological finds, was also investigated. Raman spectra on whitish parts of modern coral reveal absence of polyenes, while archaeological *C. rubrum* whitened by the action of time shows the constant presence of these pigments – even where the hue is not preserved. An encapsulation of the polyenes in the coral's axial skeleton process was assumed to explain discolouration, but the sure reason was not found. Some phenomena, e.g., the possible diagenesis of the high-magnesian calcite (HMC) into LMC (as demonstrated in aragonitic corals), are apparently involved (Bente *et al.* 2023; Budd 1988; Fürst *et al.* 2016; Hall, Kennedy 1967; McGregor, Gagan 2003).

In the same period, a German research group worked on the characterisation of coral on archaeological artefacts, investigating the beads used to decorate a specific type of fibula, the *Mitteldeutsche Korallenfibel*, widespread in the second Iron Age in central Germany. Also, later coral finds (1300 CE; late Middle Ages/Modern age), african ethnographic finds and modern corals and fossils were examined. μ-Raman (identification of polyenes), μ-XRD (identification of the Mg-amount), SEM and TEM (for internal micro-morphology), μ-XRF and La-ICP-MS (for the study of Sr, B, O and C isotopes, for dating and identification of coral formation water temperature, as well as formation in fresh or marine water; Bente *et al.* 2023) were used. Also, micro X-ray computer tomography (μ-XCT) was experimented for the first time. This technique is useful for non-destructive 3D imaging of the density and the inner structure of coral objects, such as inside relic structures and cavities, by comparison with modern coral samples (Bente *et al.* 2015a; 2015c; 2017; 2022; 2023; Keuper *et al.* 2015; Gerdes *et al.* 2015).

C. rubrum (polyenes and HMC with ~ 10-12

mol% $MgCO_3$) has consistently been identified in modern, medieval or ethnographic samples. Conversely, the analysis of protohistoric artefacts yields challenging results, identifying different materials. The fibulae from southern Germany and Austria are likely composed of *C. rubrum* (polyenes and calcite with ~ 8 mol% of $MgCO_3$, minimal Mg-content of leached coral), while the inlay material of those from central Germany consists of calcite or LMC. This suggests the possible use of fossil coral, or limestone, or white aragonitic corals (with secondary calcite recrystallisation), or glacial debris. The study of stable isotopes compositions provided further information, suggesting an origin from *C. rubrum* also for finds from central Germany as well, together with a contribution from secondary freshwater. Following laboratory experiments on modern corals, it has been hypothesised that central german grey coral artefacts were heat-treated at temperatures between 400 and 600°C, resulting in the loss of chromophores and magnesium content (Bente *et al.* 2014; 2017; 2020; 2022; 2023; Gerdes *et al.* 2015; Schrickel, Bente 2013; Schrickel *et al.* 2014).

This group considered several hypotheses for bleaching, from interment in post-depositional soil to the use of already bleached coral at the time of the artefact production. Possible bleaching conditions were simulated in laboratory on modern *C. rubrum* (accumulation on the seabed, anthropogenic bleaching while processing, post-depositional bleaching), in both acidic and basic environments, reducing and oxidising solutions and heating. Results were obtained at T » 200°C in oxidising solutions of potassium permanganate ($KMnO_4$), nitrate and ceric ammonium nitrate [NH_4NO_3; $Ce(NH_4)_2(NO_3)_6$] and sodium or ammonium sulphates [$(Na,NH_4)_2SO_4$][4].

In situ and ex situ high-temperature revealing data are shown in Bente *et al.* 2023. TEM and XRD data revealed that whitening is caused by the transition, within calcite mesocrystals, of oriented nanocrystals optically transparent to optically dispersive opaque nanocrystals, losing their orientation, without affecting the organic matrix and polyenes (Bente *et al.* 2015b; 2015c; 2016; 2023; Schrickel *et al.* 2013).

The provenance issue for bleached archaeological coral has also been discussed for Indo-Pakistani contexts in the same period, without direct archaeometrical investigations, hypothesising the use of Indo-Pacific corals, despite the different indications of historical sources (Vidale *et al.* 2015).

5.3. The provenance problem

The provenance determination for archaeological *C. rubrum* would be fundamental. In fact, the identification of possible supply areas in ancient times would provide very important information on trade, relations and influences in the ancient world.

Literature on this topic has been explored and no specific studies on coral exist, apart from paleoenvironmental studies (Chaabane *et al.* 2014; 2016). Two possible approaches are mentioned for carbonate materials of biogenic origin: isotopic and trace elemental analysis. Both techniques unfortunately proved to be difficult to apply to *C. rubrum*, but they should be tested in the future.

5.3.1. Isotopic analysis

Literature is mainly focused on aragonitic shells, through the study of Sr- C- and O-stable isotope compositions.

Strontium isotopes are used as indicator of climatic conditions and geographical origin. ^{87}Sr is radiogenic and originates by decay of ^{87}Rb. $^{87}Sr/^{86}Sr$ ratio is determined by age and composition of the rock substrate, reflecting the zone variation. Incorporated by tissue during meteorological processes, $^{87}Sr/^{86}Sr$ value is used to identify the living area of an organism. In marine organisms it reflects the isotopic composition

4 $KMnO_4$ transforms HMC in Mg-free compounds. $(Na,NH_4)_2SO_4$ leads to a surface bleaching by the formation of gypsum, thermonatrite, portlandite or aragonite. NH_4NO_3 whitens red skeletons without destroying neither the morphology nor the polyenes and the Mg-content. Also $Ce(NH_4)_2(NO_3)_6$ bleaches the surface, with loss of typical coral features and Mg-content reduction. Heat treatment (4 hours at 200°C) destroys polyenes and greys the coral, maintaining morphology and Mg-content. Heat treatment in air at different temperatures showed that at 190°C<T<220°C the polyenes become carotenoids and the colour of the coral changes to pink; at T>220°C the coral turns grey and the chromophores are lost; at 400°<T<625°C there is a loss of Mg-cation in the crystal lattice, due to lattice expansion; at T>625°C there is a transformation of HMC into secondary $CaCO_3$ (Bente *et al.* 2015b; 2015c; 2016; 2023; Schrickel *et al.* 2013).

of the aquatic environment. Absorption mechanisms depend directly on the mineralogy of the material, growth rate, diet, water salinity, temperature. In archaeomalacology, these analyses are aimed at studying climate, water temperature and paleo salinity, as well as determining provenance (Douka 2011). For ancient coral, they are used in dating, discriminating between fossil and recent marine coral (Bente *et al.* 2015a; 2015c; 2017; 2023; Gerdes *et al.* 2015).
Carbon occurs in nature with three isotopes (stable ^{12}C and ^{13}C and unstable ^{14}C), simultaneously incorporated during bio-mineralisation in equilibrium with the environment. It derives from dissolved inorganic carbon, assimilated during carbonate precipitation, and from CO_2 resulting from food metabolism. After the organism's death, ^{12}C and ^{13}C provide interesting paleoenvironmental and biological information. ^{14}C decays at a constant rate and its measurement returns a date of the death (Douka 2011; Sakalauskaite *et al.* 2019).
Oxygen has three stable isotopes in nature: ^{16}O, ^{17}O e ^{18}O. The $^{18}O/^{16}O$ ratio significantly varies on land in direct dependence on certain parameters such as latitude, longitude and altitude. In marine biogenic carbonate it is affected by water temperature and water isotope ratio, influenced by evaporation. This process causes an ^{18}O enrichment of water, preferentially extracting light water molecules. Conversely, the inflow of freshwater poor in ^{18}O (e.g. precipitation or river runoff) causes ^{18}O decrease. Oxygen isotopic variations in biogenic carbonate give seasonal and paleotemperature information and, consequently, provenance ones from supply areas with different isotopic compositions (Bajnóczi *et al.* 2013; Bente *et al.* 2023; Douka 2011; Leng, Lewis 2016; Pierre 1999).
The *C. rubrum* distribution is mainly related to the western Mediterranean basin, with some Atlantic exceptions in southern Portugal and Morocco (Cattaneo-Vietti, Cicogna 1994; Harmelin 2000; Liverino 1989; Vielzeuf *et al.* 2013). The precise provenance determination within the same basin is very problematic. Conversely, there are no problems in distinguishing between distinct basins, such as the Aegean and the Black Sea (Bajnóczi *et al.* 2013; Claassen, Sigmann 1993). In the Early Iron Age, it is plausible that the *C. rubrum* supply areas were limited to the Mediterranean Sea, and it is therefore difficult to apply a provenance study (e.g. to discriminate between supply in the Tyrrhenian or Adriatic Sea) based on stable isotope composition.
Another problem is the diagenesis: chemical, physical and biological factors can cause post-mortem changes in marine carbonates, such as the preferential leakage of certain elements, resulting in alterations of the original biochemical composition and incorporation of exogenous material (on the surface, or within the structure). HMC of *C. rubrum* and aragonite are metastable and generally reduced to stable LMC, with the variation of the isotopic composition, reflecting environmental conditions. The archaeometric approach is based on the absence of post-depositional processes. The effective presence and extent of diagenesis must be determined: this can be done quite easily by combining XRD and SEM-EDS to assess the structural and mineralogical integrity of the material, or by the use of cathodoluminescence. Any exogenous contaminants, tipically in the form of LMC or other substances such as Fe/Mn (oxy)hydroxides, phosphates, sulphates (gypsum), silicates/detritus, and/or copper corrosion products (in the case of bronze contact), must be identified, isolated and removed (Bajnóczi *et al.* 2013; Barbin 2013; Barbin, Schvoerer 1997; Douka 2011; England *et al.* 2006; Grellet-Tinner *et al.* 2010; Leng, Lewis 2016; Moreno-Azanza *et al.* 2016).

5.3.2. Trace elements analysis

The growth areas of different species have a different geochemical signature, given by the erosion of rocks and sediments, to which marine species are sensitive, as demonstrated for molluscs. Ions, the result of sediment erosion, pass through the water into the organism, which secretes its skeleton in $CaCO_3$ and organic matrix. Chemical elemental fingerprints are typical of the area of origin and its study provide consequently information about provenance (Bajnóczi *et al.* 2013; Claassen, Sigmann 1993).
Provenance studies on aquatic organisms (e.g., shells) are problematic, because these organisms are generally a continuous resource, i.e. wide hydrographic basins. In order to obtain indications of provenance, it is essential to have more difference between several possible supply regions considered, than within the same region. Such a phenomenon could occur in

different basins[5], or in the same basin along the coast, where the composition of seawater can vary considerably under the influence of local geology and hydrological inputs of freshwater (Claassen, Sigmann 1993; Eerkens *et al.* 2007; Macchia *et al.* 2016).
Determining the provenance of archaeological samples would require an exhaustive analysis of all potential historical collection sites for comparative purposes. In the case of *C. rubrum*, this assumption is not feasible, as the ancient supply sites, located at shallow depths, are now certainly depleted. Modern pollution represents an additional complication, as it can affect present-day reference samples, as demonstrated by previous studies on molluscs (Claassen, Sigmann 1993).
Diagenesis represents a further significant issue, as it can lead to changes in elemental composition influenced by soil pH, temperature, and humidity. Its effects are generally reduced in alkaline environments and enhanced in humid settings and at higher temperatures.
In order to evaluate its influence, soil samples of depositional ground should be examined, to verify whether any exchanges of elements with the soil could have occurred, that could prevent significant elemental assays (Claassen, Sigmann 1993; Eerkens *et al.* 2007). It should also be noted that the available literature refers mainly to molluscs and marine carbonates in general, without a specific focus on the biomineralogical and biogeochemical characteristics of *Corallium rubrum*, which should be considered in more depth.
In relation to the present study, an attempt to determine coral provenance through the study of chemical elemental fingerprints does not seem applicable. The considered artefacts mostly come from non-recent excavations, for which the specific context is sometimes unknown (i.e. it is impossible to have deposition soil samples for comparison), and generally from burial in association with metal artefacts, which may have caused the incorporation of their elements. Potential overprints are likely and should be demonstrated empirically on a case-by-case basis, spatially localised on the archaeological find (e.g., surface vs. core) and evaluated in relation to the specific analytical question. In fact, for carbonate biominerals, diagenetic and contaminative processes are strongly controlled by the depositional setting and micro-environment; they are common, but neither inevitable or uniform in terms of extent or spatial distribution.

5.3.3. Others possible approaches

Other potential approaches, such as genetic and biomolecular analyses, were also evaluated but proved impracticable for various reasons.
The existing scientific literature on the study of DNA on *C. rubrum* is mainly focused on living coral and therefore on the analysis of polyps. Some works has focused on the coral skeleton in modern artefacts, with the aim of identifying poaching activities in protected areas (Aurelle *et al.* 2011; Cartier *et al.* 2018; Costantini *et al.* 2016; Ledoux *et al.* 2010; 2013; 2016; Lendvay *et al.* 2020). This approach is very promising, but it requires a large amount of sample (2-38 mg) and the availability of comparison specimens with known provenance, impossible condition for ancient supply sites.
A biomolecular approach was also evaluated for the taxonomic identification of finds for which no typical features are recognisable by microscopic observation. This approach, derived from amino acid racemisation dating (AAR), requires the analysis of amino acids of the intracrystalline proteins present in any preserved organic fraction. It allows the taxonomic identification of organisms, with respect to the closest available taxa. Diagenesis must again be considered and the extent of its intervention assessed; however, it has been successfully applied to the study of molluscs in an archaeological context (sample of ~ 2 mg). Palaeoproteomics, using the peptide mass fingerprint (PMF), provides more precise taxonomic identification (e.g. successfully applied to shells) and is generally used in the study of the abundant collagen contained in bones and ivory, requiring minimal sampling. Unfortunately, shells and corals contain a much smaller organic fraction, trapped in carbonate nanocrystals, requiring significantly more invasive sampling (~ 20 mg: Demarchi *et al.* 2014; 2020; Sakalauskaite *et al.* 2019; 2020a; 2020b), impossible in the present case.

5 For modern coral, a study demonstrates the possibility of easily discriminating between Mediterranean and Pacific corals, which belong to distinct hydrographic basins, by analysing the difference in elemental composition (Macchia *et al.* 2016).

6. Materials and Methods

Abstract

Il sesto capitolo si concentra sull'analisi di reperti archeologici in presunto corallo, databili all'età del Ferro e provenienti dall'Italia settentrionale, con un'attenzione particolare alle fibule a sanguisuga con inserti circolari biancastri, tipiche delle culture di Este e Golasecca. Sono stati individuati 750 reperti con presunti inserti in corallo; tra questi, 372 sono stati analizzati 'in situ' con microscopio digitale portatile e 264 selezionati per approfondimenti archeometrici.
L'indagine ha comportato complesse interazioni con istituzioni italiane (Soprintendenze, musei nazionali e civici, università), che in gran parte hanno collaborato positivamente, permettendo anche l'analisi di materiali inediti. Il protocollo sviluppato, interamente non invasivo, ha dimostrato alta efficacia nel distinguere il *C. rubrum* da altri materiali simili, grazie all'impiego combinato di microscopia ottica, spettroscopia Raman e infrarossa (FT-IR), diffrazione a raggi X (XRD) e microscopia elettronica a scansione con spettrometria a dispersione di energia (SEM-EDS). Tre approcci analitici alternativi sono stati proposti, adattati ai vincoli conservativi: uno completamente non invasivo, uno micro-distruttivo (campionamento di circa 300 μm) e uno esclusivamente 'in situ'.
In particolare, Raman e SEM-EDS sono risultati fondamentali per identificare i pigmenti polienici e per determinare il contenuto in Mg della calcite, parametri discriminanti per confermare la presenza di corallo rosso. Radiografie e sperimentazioni tecnologiche hanno inoltre fornito ulteriori dati sui processi produttivi degli oggetti analizzati. Sono stati esaminati anche campioni moderni di corallo e potenziali leganti organici antichi (ambra, cera d'api, resine naturali), per confronto con i reperti antichi.

6.1. Analytical record

6.1.1. Archaeological record

The archaeological record considered in the present study includes all artefacts made of presumed coral, datable to the Iron Age and originating from northern Italy, with particular attention to leech fibulae featuring circular whitish insets. The focus on this type stems from the fact that the characterization of these inlays specifically requires an archaeometric approach: their small size and intricate manufacture prevent reliable identification through simple macroscopic observation, as is often possible with raw coral branches.
In a first step, a survey was conducted to identify the objects for analysis. Geographically, the entire territory of northern Italy was considered, in relation to the distribution area of leech fibulae with insets (Figs. 79, 81; see section 4.2.4). For practical reasons, the investigation was limited to artefacts preserved on Italian territory, thereby excluding all non-Italian finds (e.g., from Swiss territory).
A careful review of the literature (see Chapter 4) was carried out in order to identify the published finds, the related areas and periods of discovery and, wherever possible, their current location. In the consulted literature, findings of different types – but having a potential interest for the project, due to similarities in their constituent materials – were also considered and noted, such as:

- 'Longone al Segrino' type pendants (see 4.2.1);
- beads and pendants (see 4.4.1);
- coral composite bow fibulae (see 4.2.2);
- leech fibulae with incised line decoration (see 4.2.5) and transversal grooves (see 4.2.7);
- western late-hallstattian fibulae (see 4.2.8);
- dragon-shaped fibulae with lateral daisies (see 4.4.2);
- bucket pendants (see 4.2.10);
- grooming tools (see 4.2.11);
- La Tène fibulae (see 4.6.1);
- dolphin-shaped fibulae (see 3.3.4)[1];
- raw coral (see 3.3.6).

1 Three dolphin-shaped fibulae (*supra*, Fig. 10), held in the Musei Reali in Turin, characterised by a bone body with red eyes in presumed coral, were studied in close collaboration with A. Monticone (Department of Life Sciences and Systems Biology, University of Turin): the study of the presumed coral eyes is part of this project, while the bioarchaeological study of the bone material was carried out by my colleague.

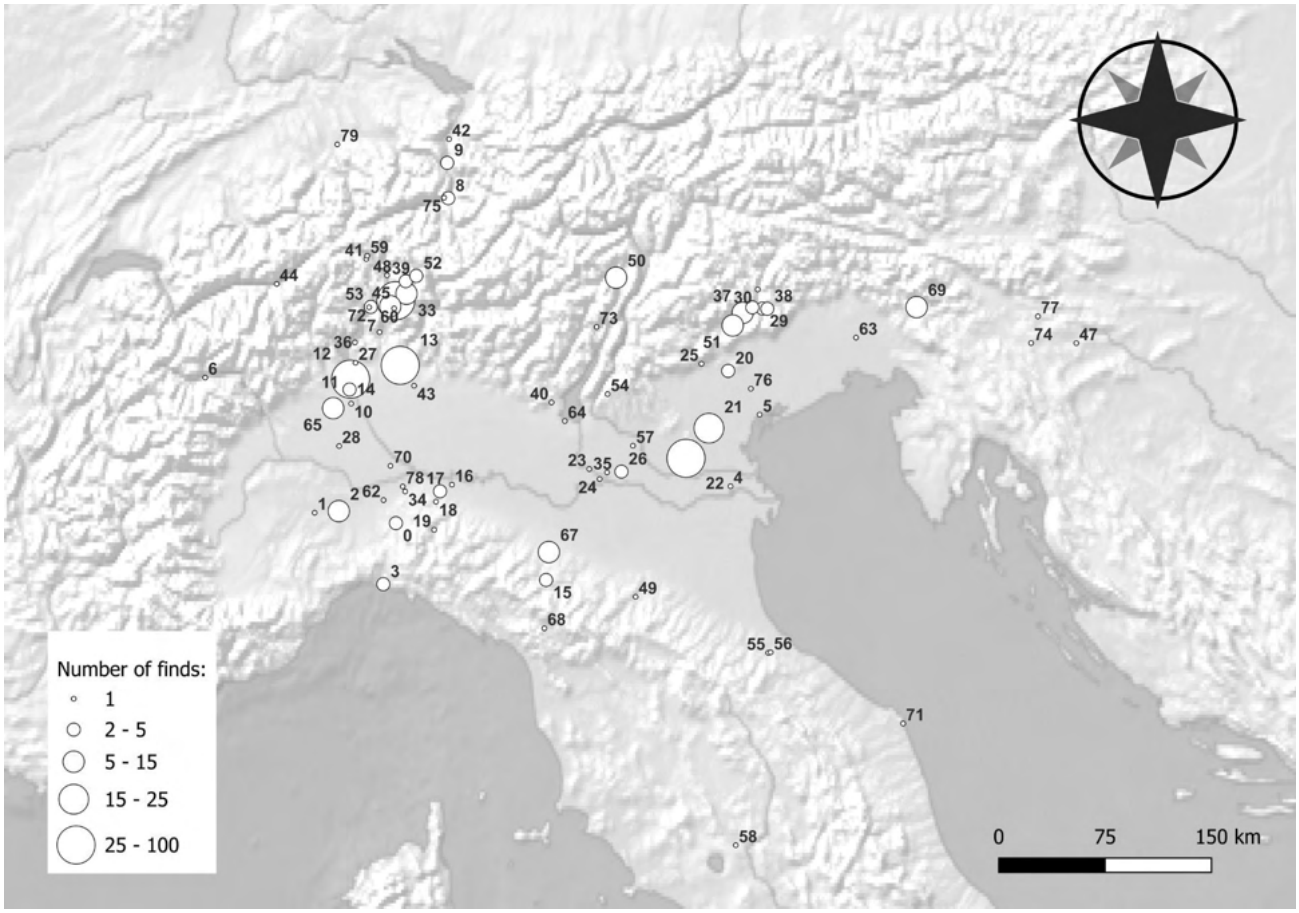

Figure 79. Distribution map of published leech fibulae with circular insets. Elaborated by the author in QGIS 3.40.8 (2025); base map: Natural Earth (Gray Earth raster "GRAY_LR_SR_OB_DR"), public domain: 0) Brignano Frascata; 1) Castello di Annone; 2) Villa del Foro; 3) Genova; 4) Adria; 5) Altino; 6) Aosta; 7) Arbedo; 8) Chur; 9) Balzers; 10) Bellinzago Novarese; 11) Motto Lagone; 12) Castelletto Ticino-Sesto Calende-Golasecca; 13) Como; 14) Pombia; 15) Bismantova; 16) Rottofreno; 17) Borgonovo V.T.; 18) Pianello V.T.; 19) Bobbio; 20) Montebelluna; 21) Padova; 22) Este; 23) Mantova; 24) Forcello di Bagnolo San Vito; 25) Borso del Grappa; 26) Gazzo Veronese; 27) Malgesso; 28) Palestro; 29) Pieve d'Alpago; 30) Ponte nelle Alpi; 31) Castellavazzo; 32) Cademario; 33) Castaneda; 34) Casteggio; 35) Roncoferraro; 36) Castello Valtravaglia; 37) Cavarzano; 38) Chies d'Alpago; 39) Claro alla Monda; 40) Gavardo; 41) Dalpe; 42) Eschen; 43) Gaggio; 44) Gamsen; 45) Gorduno; 46) Gudo; 47) Libna; 48) Ludiano; 49) Marzabotto; 50) Mechel; 51) Mel; 52) Mesocco; 53) Minusio; 54) Monte Loffa; 55) Montebello; 56) Verucchio; 57) Oppeano; 58) Orvieto; 59) Osco; 60) Pianezzo; 61) Masurian Lake District; 62) Pontecurone; 63) Pozzuolo del Friuli; 64) Rivoltella; 65) San Bernardino di Briona; 66) Safforze; 67) San Polo d'Enza; 68) San Romano in Garfagnana; 69) Santa Lucia di Tolmino; 70) Santo Spirito, Gropello Cairoli; 71) Sirolo-Numana; 72) Solduno; 73) Stenico; 74) Stična; 75) Tamins; 76) Treviso; 77) Vače; 78) Verretto; 79) Zugo-Baar.

The first survey leads to the identification of 750 published archaeological finds in Europe with presumed coral parts, having a similar chronology. Among these productions 534 archaeological finds are attested in Italy. The current location is known – on a bibliographic basis – for only 532 of these finds, of which 436 are in Italy. Of these, 372 could be examined 'in situ' with a portable digital microscope; from these, 264 were selected for archaeometric analysis, based on the actual preservation of presumed coral parts.

The capillary distribution of artefacts over northern Italy required interaction with numerous actors (i.e., Soprintendenze, National Museums, Civic Museums, small local archaeological groups, Universities). Although this considerably extended the bureaucratic procedures, it facilitated the development of an extensive network of productive contacts and valuable collaborations (Fig. 80)[2].

2 The response from the Authorities was generally positive and collaborative, even providing unpublished artefacts (Fig. 80a); However, in certain cases, bureaucratic obstacles prevented the inclusion of some areas in the study (Fig. 80b).

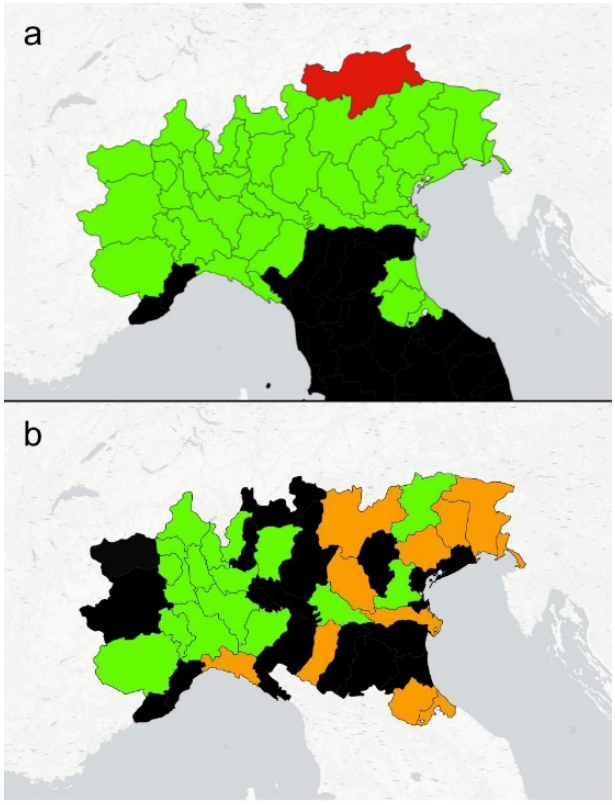

Figure 80. a) contact with the *Soprintendenze*, responses: positive in green, negative in red, absent in black; b) archaeological finds: in green examined, in orange unexamined, in grey not considered, in black absent. Elaborated by the author in QGIS 3.40.8 (2025); base map: © CARTO, © OpenStreetMap contributors; administrative boundaries: Natural Earth (10m Admin 1 – Provinces, public domain).

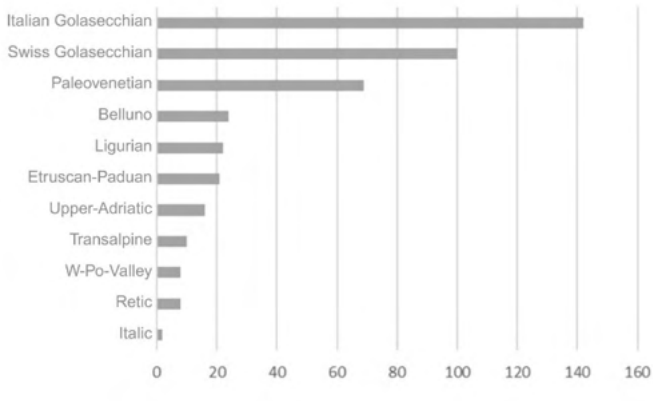

Figure 81. Leech fibulae with circular insets: distribution.

Out of a total of 422 published leech fibulae with circular insets (Figs. 79, 81), 220 were not considered (Fig. 82: letter N) for various reasons (e.g., location abroad, bureaucratic problems, unavailability), 133 were analysed (Fig. 82: letter A) and 31 were examined but discarded due to the lack of residues of the presumed coral decoration (Fig. 82: letter L). In some cases (37), no correspondence was found between literature information and availability of materials (Fig. 82: letter D).

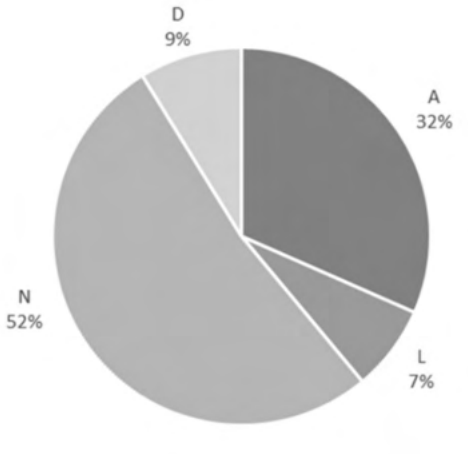

Figure 82. Leech fibulae with circular insets: A = analysed; L= looked; N = not searched; D = impossible to found.

For north-western Italy (Golasecca culture), an exhaustive sampling was performed: 103 (78 analysed and 25 viewed) out of 142 fibulae (Fig. 83). As far as north-eastern Italy is concerned (Venetic, Belluno and Rhaetian area: 101 finds), for bureaucratic problems only 41 artefacts were examined (34 analysed and 7 viewed; Fig. 83) from the Padua area and the Piave valley (Belluno, Montebelluna, Mel). From the Po Valley and Apennine area, 21 fibulae out of 51 could be analysed, mainly due to bureaucratic problems and delays (Fig. 83).
Furthermore, the statistical record was also extended to other types of similar items, either in the decorations or the material (Fig. 84). Including the aforementioned leech fibulae with circular insets, a total of 372 artefacts were examined 'in situ' with a portable digital microscope, 264 of which (71 %; Fig. 85) were selected for archaeometric analysis, on the basis of the actual preservation of presumed coral parts.

The findings were located in 22 different Institutions in northern Italy (Fig. 86, Tab. 14).

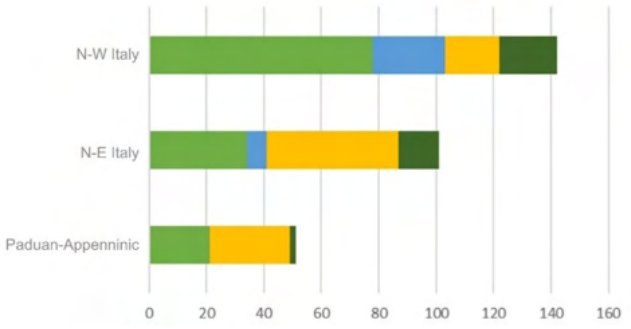

Figure 83. Leech fibulae with circular insets: percentage of artefacts analysed (A), viewed (L), not considered (N) and not found (D).

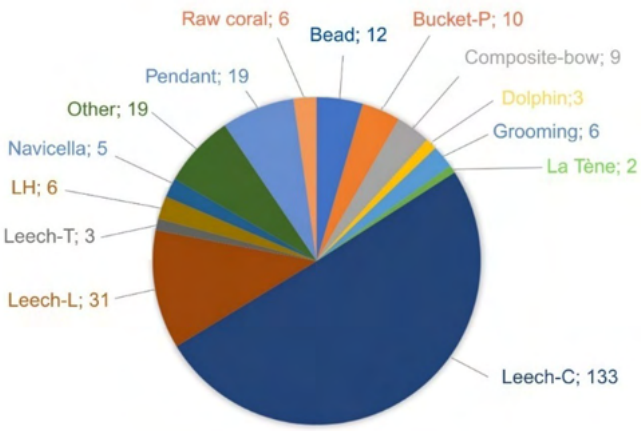

Figure 84. Graph of the quantity of archaeological finds analysed in relation to the different types considered [Leech-C = leech fibulae with circular decoration; Leech-L = leech fibulae with linear decoration; Leech-T = leech fibulae with transversal groove decoration; LH = late-hallstattian fibulae; Composite-bow = Composite bow fibulae; Navicella = Navicella fibulae; La Tène = La Tène fibulae; Dolphin = Dolphin-shaped fibulae; Grooming = grooming tools; Bucket-P = bucket pendants; Pendant = pendants and Longone al Segrino type pendants; Bead = beads; Raw coral = raw coral branches; Other =others types].

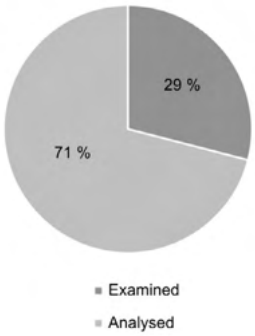

Figure 85. Graph of the percentage of archaeological finds analysed with archaeometric approach (71%) or only examined 'in situ' with digital microscope (29%).

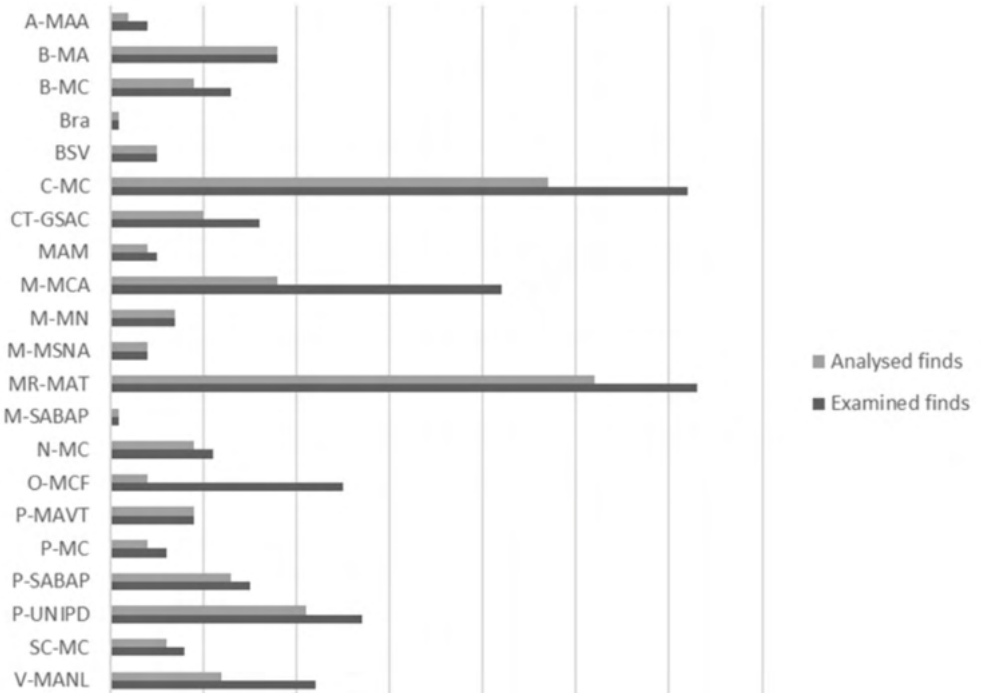

Figure 86. Graph of the percentage of archaeological artefacts examined 'in situ' with a digital microscope (Examined finds) and with an archaeometric approach (Analysed finds), in relation to the different locations (abbreviations: see pages 15-16).

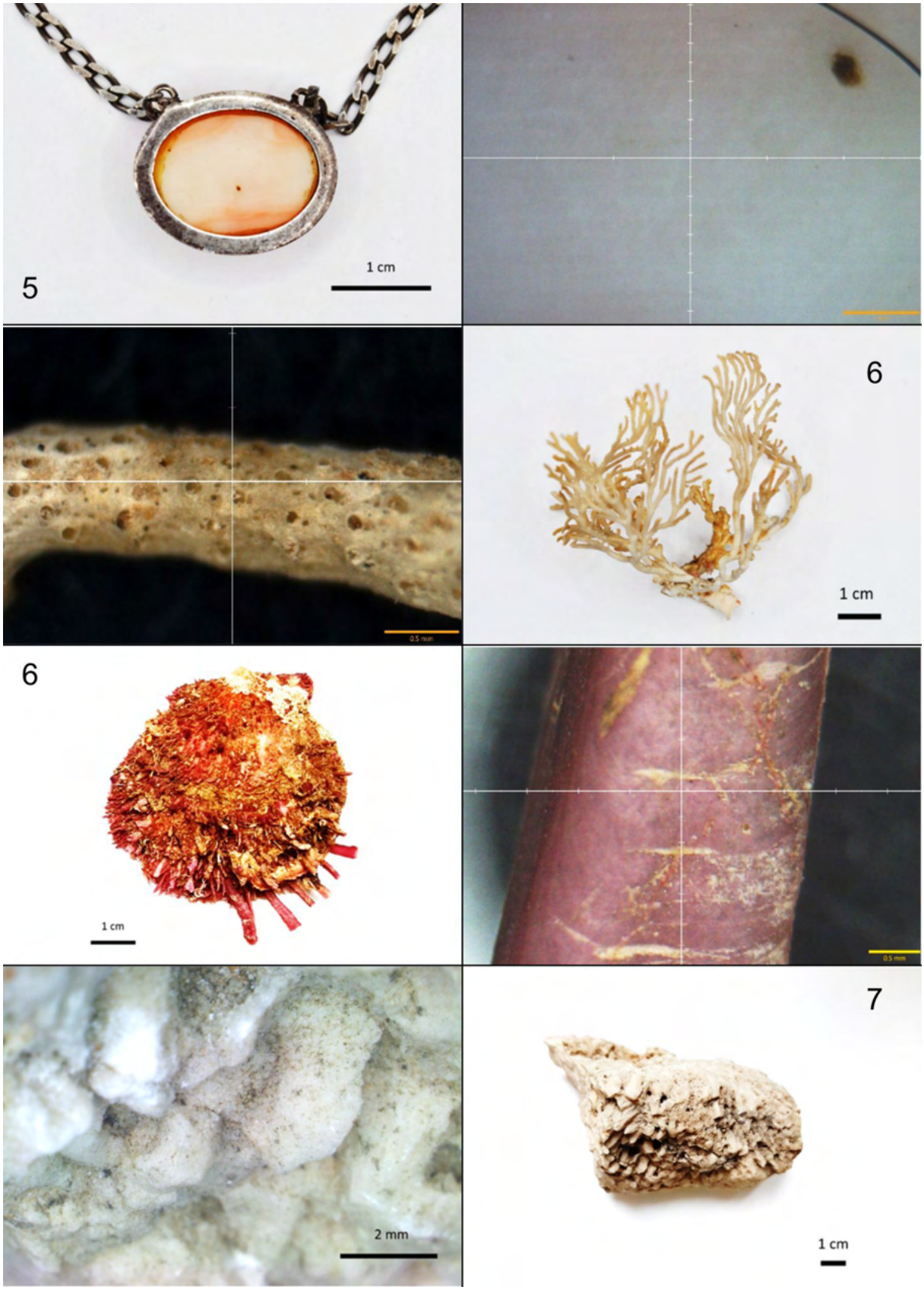

Figure 87. Modern samples of Mediterranean red coral (*Corallium rubrum*): (1) raw *C. rubrum* skeleton from the Ligurian sea (r_Cr_L); (2) surface-polished *C. rubrum* piece of unknown origin (w_Cr_u); (3) *C. rubrum* round bead from a from an early 20th century silver necklace (w_Cr_ub); (4) raw *C. rubrum* pierced branches from Sicily, collected on the beach and with whitish portions (r_Cr_Si)

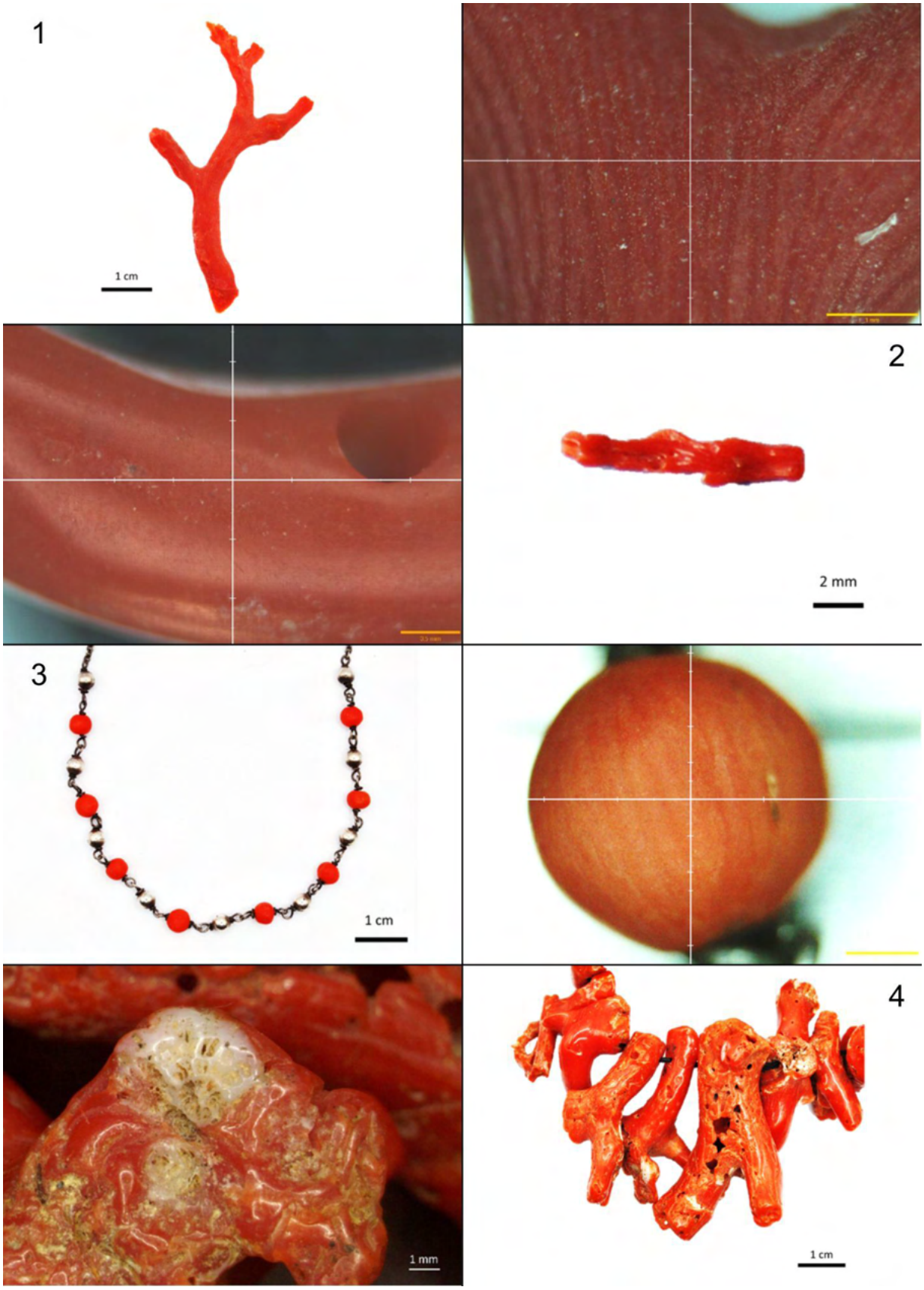

Figure 88. Modern samples of coral, Bivalvia and fossil coral: (5) pinkish-to-white, surface-polished coral from Sardinia (w_pCr_Sa); (6) white tin coral from Ligurian sea (r_c_L); (7) *Spondylus gaederopus* from Sardinia, collected at a depth of 5 m, on a rock, in the Cagliari Gulf (r_Sg_Sa); (8) Piedmontese fossil coral from the Asti area (r_fc_P).

6.1.2. Modern samples

For comparative purposes with the archaeological samples, some specimens of modern Mediterranean corals and a bivalve, belonging to private collections, were also investigated. These included samples of various colours and shapes, both worked and unworked. These specimens are shown in Figs. 87 and 88. Some samples were also submitted to heating treatments (see section 7.1.3), simulating exposure on funeral pyres, to check possible changes in colour, consistency, chemistry and permanence of polyenes.
After a survey on the possible antique organic binders consistent with the examined period (Chen *et al.* 2022; Courel *et al.* 2018; Rageot *et al.* 2019; Regert *et al.* 2019; Zlámalová Cílová *et al.* 2024), samples were collected and analysed using vibrational spectroscopies for comparison. These samples were partly purchased from the company Kremer Pigmente and partly kindly provided by the Center for Experimental Archaeology in Turin (CAST – Centro di Archeologia Sperimentale Torino):
- Amber (Kremer Pigmente, 60200);
- Beeswax (CAST);
- Bone glue cow (Kremer Pigmente, 63000);
- Birch bark tar (CAST);
- Casein (Kremer Pigmente, 63200);
- Colophony (Kremer Pigmente, 60300);
- Egg (CAST);
- Hide glue cow (Kremer Pigmente, 63021);
- Myrrh (Kremer Pigmente, 60260);
- Mastic from Chios (Kremer Pigmente, 60050);
- Olibane incense (Kremer Pigmente, 60270);
- Pine resin (CAST);
- Rabbit skin glue (Kremer Pigmente, 63025).

Two samples of Paraloid were also considered for comparison, to test possible presence of the consolidant on the archaeological artefacts:
- Paraloid B44;
- Paraloid B72.

6.2. Analytical protocol

A completely non-invasive multi-analytical archaeometric protocol has been developed to characterise the whitish material on the considered archaeological finds – tailored (basing of previous works in the scientific literature: Berruto *et al.* 2023a; Giustetto *et al.* 2013; see section 6.2) on the identification of *Corallium rubrum*. In addition to standard archaeological and photographic documentation, this protocol includes optical microscopy (OM), Raman and infrared spectroscopies, X-ray diffraction and scanning electron microscopy with Energy Dispersion Spectrometry (EDS). The same protocol was also applied to samples of archaeological coral, burnt or unburnt, and to samples of modern *C. rubrum* (burnt and unburnt), other corals, shells and fossil coral (Asti, Piedmont) for data comparison.
Complementary information about the alteration by-products of the ancient alloy were also obtained, offering interesting suggestions regarding its composition and technological choices. These data, improved by some radiographies and archaeo-technological experimentations, led to interesting conclusions about the production processes.

6.2.1. Analytical approaches

Taking into account the different protection requirements for the archaeological artefacts in relation to the analytical needs, three alternative analytical approaches were developed (Tab. 15) and proposed to the conservation Authorities for them to choose one, according to individual conservation requirements.
The first and second approaches proved to be the most fruitful, as the application of a multi-analytical protocol allows a clearer overview of the raw materials.
The first approach was preferred in most cases (Fig. 89), because of its complete non-invasiveness and completeness. It required moving the finds to the laboratories of the University of Turin, at the Department of Earth Science[3]. This protocol involves using 4 different methods (i.e. OM, μ-Raman, μ-XRD and SEM-EDS), allowing unequivocal identification of *C. rubrum* (when present and well preserved) and/or other materials (e.g., bone). More analytical spots are collected on the same object, enhancing the quality of the results.

3 All the equipment was located at the same department, requiring no further transfers and thus greatly facilitating the authorisation procedures. This is a very important factor in the management of archaeological finds.

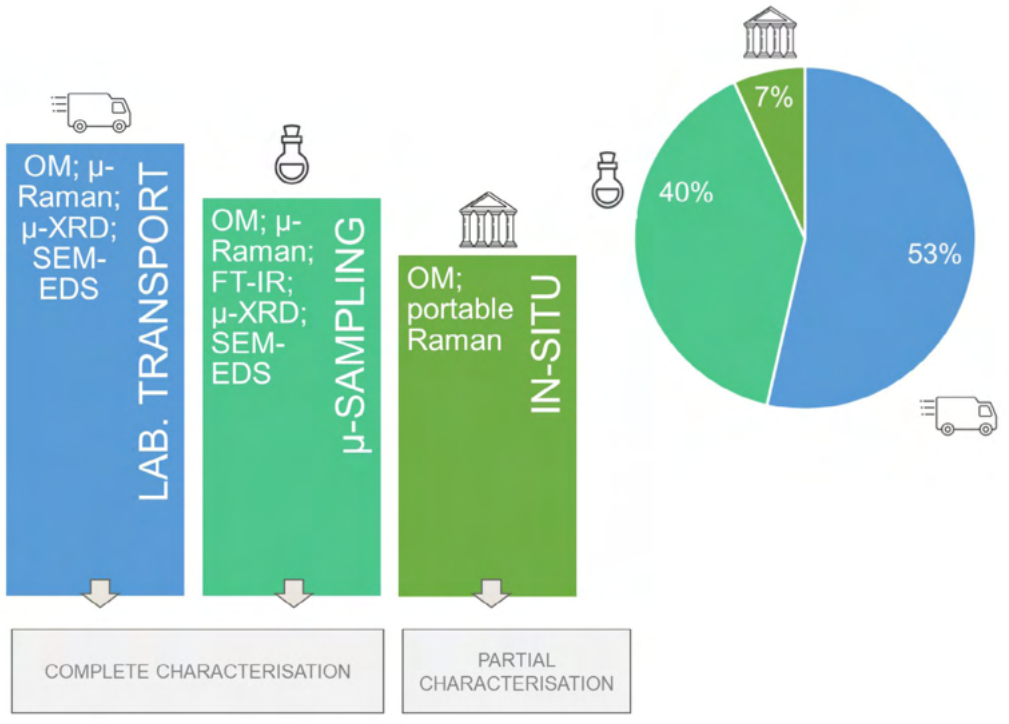

Figure 89. Different adopted approaches and percentage of choice (LAB. TRANSP. = direct analysis on the object by transporting to the laboratories; SAMPLE = μ-sampling and analysis; IN SITU = partial characterization by in-situ portable approach).

The second micro-destructive approach (extraction of μ-samples of ~ 300 μm with the help of a p-digital microscope for collection) was also frequently chosen – e.g., when conservation authorities preferred not to move artefacts from their locations, for reasons of protection or fruition (e.g. materials exposed to the public). Availability of samples allows for faster and more versatile analyses, also supplemented by diamond cell μ-FT-IR spectroscopy, to obtain further information on organic materials. However, a single site of analysis is considered, chosen at the time of sampling.

The third approach was proposed in those cases in which neither transport nor μ-sampling was possible. Unfortunately, it provides only partial information (p-optical digital and p-Raman spectroscopy)[4].

4 In the experimented case (Museo Civico Archeologico Castello Sforzesco in Milan) the analysis sessions were not very productive, partly due to the different characteristics and performance of the hand-held instrumentation compared to the bench-top one: high fluorescence, that hide diagnostic peaks. Furthermore, all examined finds came from 19th century excavations and had probably undergone several restorations over time, fact that probably influenced negatively analysis and require for the use of other techniques (i.e. XRD).

6.2.2. Involved techniques

The multi-analytical protocol was extensively tested during the project and proved to be very efficient. Among the involved techniques, two proved fundamental in the identification of *C. rubrum* – i.e. Raman spectroscopy and SEM-EDS. XRD is particularly useful when surface restoration products hinder other techniques. In the study of metal alteration by-products, μ-XRD and SEM-EDS analyses proved to be the most successful techniques.

6.2.2.1. Optical microscopy

Microscopic observation was carried out in two steps. In the first step, the archaeological artefacts were examined 'in situ' using a portable digital microscope, to verify presence of whitish material in the decorations and consequently an interest for archaeometric studies (Fig. 90a). Optical microscopy was also involved in a second step in the laboratory, by observing the archaeological artefacts in greater detail and extrapolating archaeological, archaeometric and technological information (Fig. 90b). A MAOZUA 5MP 20-300x optical digital microscope was used in the first instance and a OPTIKA SZO-4 stereomicroscope – equipped with a OPTIKA

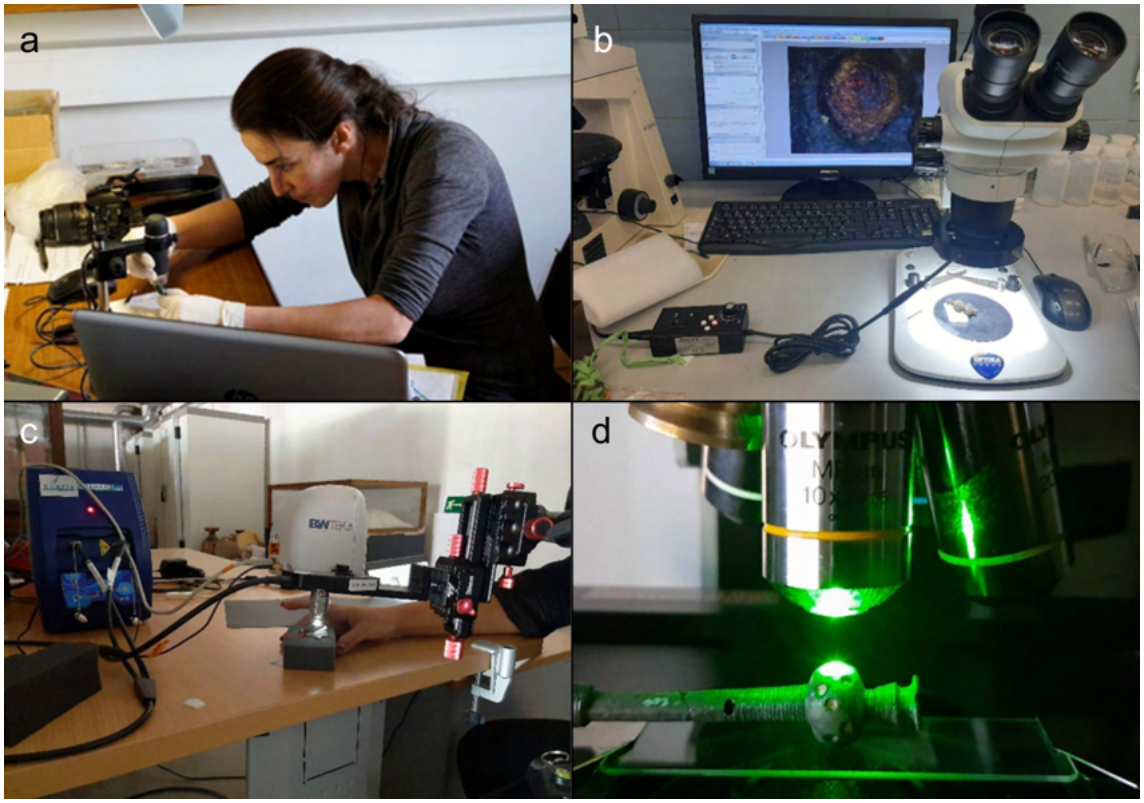

Figure 90. a) Observation of finds by p-digital microscope at the Musei Civici di Varese -Villa Mirabello; b) Observation of finds with OPTIKA SZO-4 microscope; c) Raman-analysis with portable instrumentation at the Musei Civici di Milano; d) μ-Raman-analysis at Centro Scansetti Laboratory.

C-B18+ camera – in the following one. For those artefacts for which no transfer was contemplated, the second step was carried out directly 'in situ' with the portable digital microscope.
μ-observation of the artifacts allows technological interpretation about their manufacture and decorations. It is also useful in raw material characterization, especially when typical structural features are visible (e.g., *C. rubrum* or bone). This is valid especially for not-worked coral branches, while in the decoration of the leech-shaped fibulae is more difficult. Characteristic structures of the red skeleton of *C. rubrum* are the longitudinal crenulations on the surfaces, visible both on the outer surface of the coral branches and in the cross-section, with the characteristic garland-like morphology, consisting in a wavy edge. *C. rubrum* also often shows presence of superficial speckling and pitting, as well as concentric structures in the cross-section, indicating the medullar region, corresponding to the growth rings of the organism. If the examined coral comes from the socket of a colony, a porous structure, so-called 'coral foam', is often visible (Debreuil *et al.* 2011; Fan 2018; Fürst *et al.* 2016; Perrin *et al.* 2015; Vielzeuf *et al.* 2008).

6.2.2.2. Raman spectroscopy

Raman is a vibrational spectroscopy, complementary to IR-spectrophotometry. When monochromatic radiation impacts on a given material, there can be elastic or inelastic interaction; the molecules of the material move to an unquantized virtual state, from which they decay with photon emission. If the interaction is elastic, these photons have the same energy as the incident ones (Rayleigh scattering); if it is inelastic, they have different energy (Raman effect), lower (Stokes lines) or higher (anti-Stokes lines). In the Raman spectrum, signals related to Rayleigh radiation, Stokes and anti-Stokes lines are present. Stokes lines give information about the functional groups of the material, providing the compounds identification (Kellnert 2003). This technique is non-destructive, does not require contact with the sample, and is suitable for gaseous, liquid and solid samples; the analysis is superficial. The applications for cultural heritage stuff are various; organic and inorganic substances can be characterised, including pigments, dyes and binders.
Portable Raman analysis were performed 'in situ', directly on the archaeological finds (Fig.

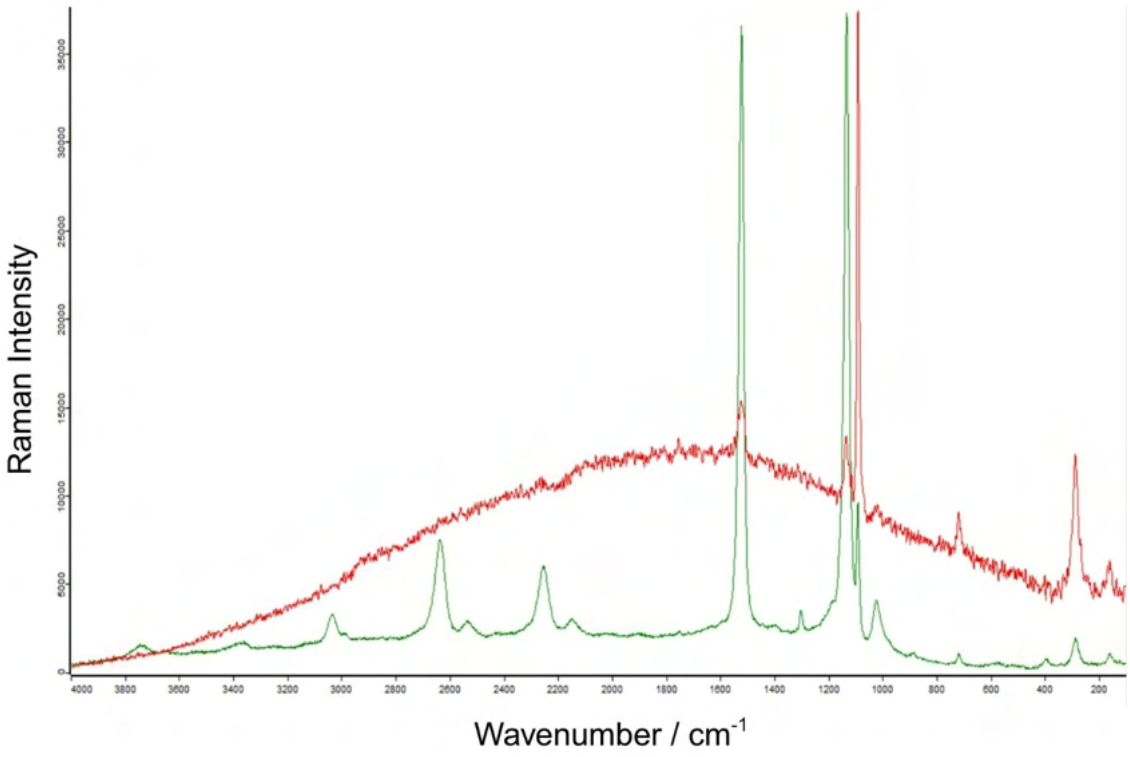

Figure 91. Raman spectra of the same modern coral sample (ball_800; *C. rubrum*) with green laser (532 nm) in green and with red laser (633 nm) in red: in the first case, the peaks relating to the presence of polyenes clearly predominate over those of calcite, while in the second case the calcite signals are preponderant.

90c), with a portable i-Raman Plus (BWTEK)[5], equipped with a green excitation laser (532 nm), a spectrometer (BWS465-532S) working in the range of 150 to 4200 cm^{-1}, with a resolution of 7.3 cm^{-1}, using a CCD sensor with a cooling system; to achieve better results the instrument was connected to the portable BAC151 compact Raman microscope, provided with several lenses able to focus the signal. Signal collection was carried out at room temperature and in the dark.

μ-Raman data were collected, directly on the archaeological finds, with a Horiba Jobin Yvon HR800 spectrometer[6], with polarized green laser (solid state Nd; wavelength 532 nm; power 250 mW; Fig. 90d) with edge filter, 600 grooves/mm gratings, an air-cooled CCD detector, equipped with an Olympus BX41 optical polarizing microscope. Analyses were carried out with 10X and 20X magnifications, different filters (between 0.3 and 2), in the spectral range 100-2000/4000 cm^{-1}. Pure silicon was used to calibrate the spectrometer. Signal collection was carried out at room temperature and in the dark. The Labspec 5 software was used for imaging and data collection and OPUS 6.0 software was used for elaboration and interpretation, by comparing the experimental signals with the RRUFF™ Project database (Lafuente *et al.* 2015). Raman spectroscopy is fundamental for identifying the organic pigments typical of *C. rubrum*, a mixture of partially or completely demethylated polyenes – the chemistry of which is still debated – which gradually denature over time (Barnard, de Waal 2006; Vielzeuf *et al.* 2008; 2013; Bergamonti *et al.* 2011; 2013; Rahman *et al.* 2011; Hasegawa *et al.* 2012; Brambilla *et al.* 2012; Fernandes *et al.* 2015; Fürst *et al.* 2016; Kaczorowska *et al.* 2003; Keuper *et al.* 2014; 2015; Kiefert, Karampelas 2011; Kupka *et al.* 2009; Macchia *et al.* 2016; Maia *et al.* 2010; Smith *et al.* 2007). This technique also allows detection of calcite or other carbonates, as well as other materials (i.e. other pigments or binders).

5 The execution of these analyses was possible thanks to a collaboration with Prof. S. Grassini and Dr. L. Es Sebar of the Polytechnic University of Turin.

6 The micro-Raman measures have been obtained with the equipment acquired by the Interdepartmental Center 'G. Scansetti' for Studies on Asbestos and Other Toxic Particulates with a grant from Compagnia di San Paolo, Torino, Italy.

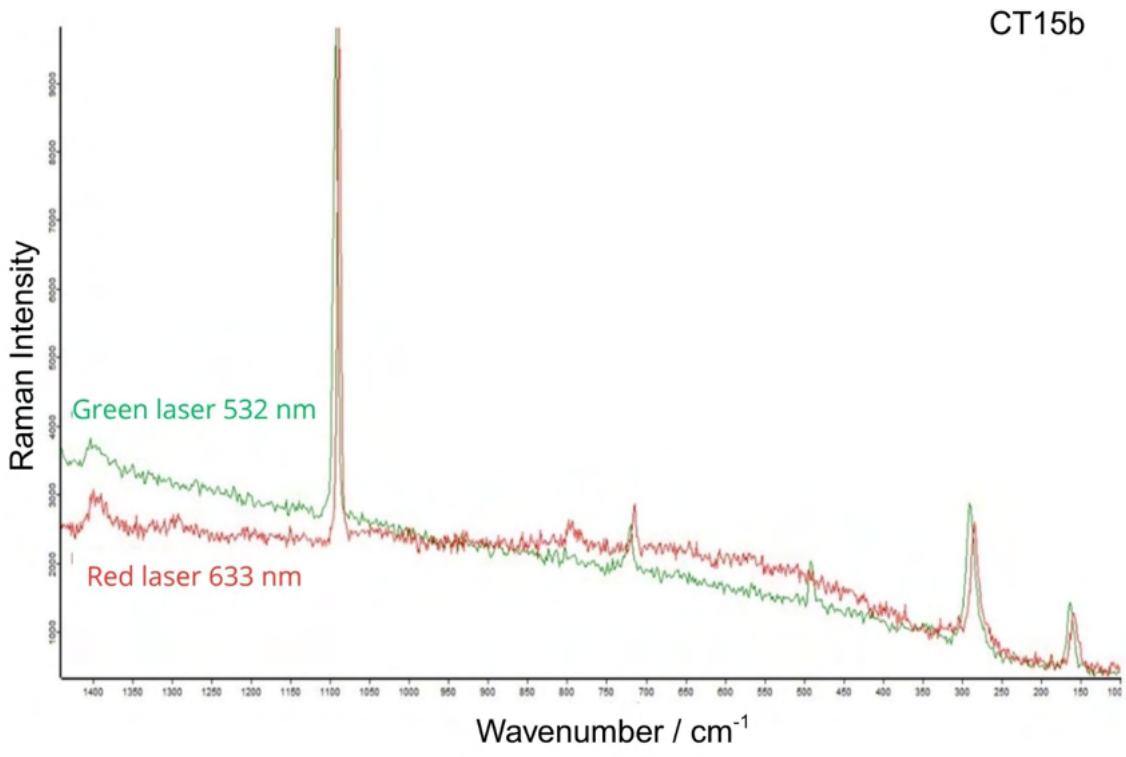

Figure 92. Raman spectra of the same sample (CT15b) with green laser (532 nm) in green and with red laser (633 nm) in red: small peak shift is evident using different lasers.

The green laser (wavelength 532 nm) is the most suitable for detecting polyenes, while the red one (785 nm) is for calcite (Fig. 91). At lower wavelength, these organic molecules have a strong resonance effect, which enhances their diffusion over the fluorescence emission and mineral signature. Conversely, higher wavelength better detect mineral phases, causing fluorescence reduction (Brambilla *et al.* 2012, p.1457 note 6; Fürst *et al.* 2016; Kiefert, Karampelas 2011; Kupka *et al.* 2009, p. 655). The green laser causes no physical degradation of the samples (Perrin, Smith 2007), in contrast to the red one, which generally causes surface μ-burning. By varying lasers, small shifts in the position of some peaks may occur (Fig. 92; Merlin, Delé Dubois 1986).

Figure 91 shows the Raman spectra obtained from the same *C. rubrum* sample by using the 532 and 785 nm lasers. The main peak of HMC occurs » 1089 cm^{-1}, related to the symmetric $(CO_3)^{2-}$ stretching mode (ν_1). Two signals appear in the lattice vibration region at 285 (L, librational mode) and 15 (T, translational mode) cm^{-1} (only one peak for aragonite at 208 cm^{-1}). The characteristic $(CO_3)^{2-}$ ν_4 in-plane bending appears at » 717 cm^{-1} (a double band for aragonite at » 702 and 706 cm^{-1}). The main peak shifts toward higher wavenumbers in the presence of high Mg-contents, as Raman spectra of carbonates are sensitive to the structural and chemical changes that occur when Mg^{2+} replaces Ca^{2+} in the crystal lattice. This substitution generates disorder, because of the smaller radius of the Mg^{2+} ion; the Mg-O bond becomes shorter and stronger than the Ca-O bond. The volume of the unit cell decreases as the Mg-concentration increases linearly, resulting in a change in the position of the Raman bands (Bischoff *et al.* 1985; Borromeo *et al.* 2017; Edwards *et al.* 2005; Fürst *et al.* 2016; Macchia *et al.* 2016; Urmos *et al.* 1991).

The spectral range between 1100 and 1400 cm^{-1} is the fingerprint region for organic pigments. In Fig. 91, the 1519 cm^{-1} band represents the strong ν_1 C=C stretching vibration mode of the polyenic chain and the 1131 cm^{-1} one the strong ν_2 C-C stretching mode. The ν_2 region (1100 and 1300 cm^{-1}) is sensitive to the chain configuration: differences in peak position indicate that the polyene chain structure varies, with a downshift when the number of methyl groups decreases. At » 1020 cm^{-1} we can see the low ν_3 CH=CH wagging mode and at 1300 cm^{-1} the low ν_4 CH_3 in-plane rocking motion of

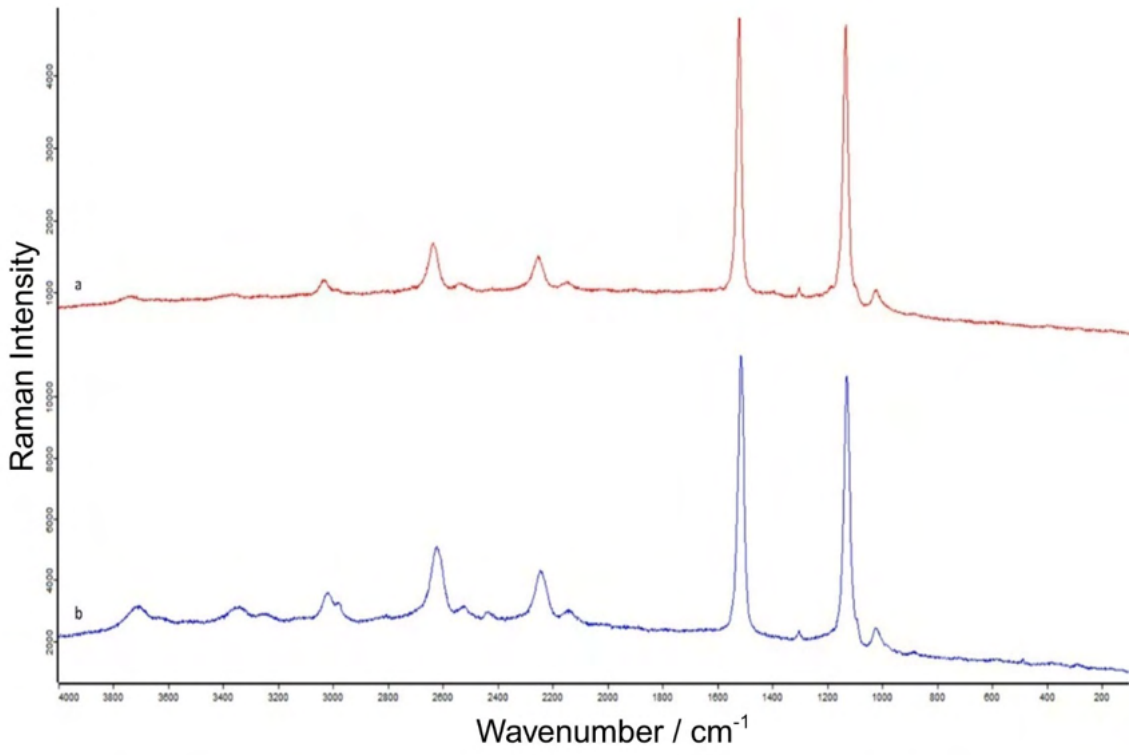

Figure 93. Raman spectra of *C. rubrum* in red and *S. gaederopus* in blue, acquired with green laser (532 nm).

methyl groups. In addition, a series of organic overtones and combinatorial bands are present in the range 1600-5000 cm^{-1} [at 2250 cm^{-1} ($2\nu_2$), 2635 cm^{-1} ($\nu_1 + \nu_2$), 3035 cm^{-1} ($2\nu_1$)], whose position is related to the number of C double-bonds in the polyene chain (Bergamonti *et al.* 2011; 2013; Brambilla *et al.* 2012; Kupka *et al.* 2009; Macchia *et al.* 2016; Merlin 1985). It is important to note that the ν_2 band shifts from demethylated (polyenes) to methylated (carotenoids) from ~ 1130 to 1160 cm^{-1}, as observed by Bente *et al.* 2023 during modern coral combustion experiments (at 190°C < T < 220°C).

However, detection of calcite and organic pigments by Raman does not mean certain identification of *C. rubrum*. Other organisms (i.e. *Spondylus gaederopus*), in fact, have the same Raman spectrum (Fig. 93; Fürst *et al.* 2014; 2016; Sakalauskaite *et al.* 2020). *S. gaederopus* has a large shell characterised by calcitic and aragonitic parts and was used since prehistory for ornamental purposes (Borrello, Micheli 2004; 2011; Micheli 2004; 2012; Sakalauskaite *et al.* 2020; Windler 2019). Other techniques are necessary to determine the Mg-content in calcite (Fürst *et al.* 2016; Vielzeuf *et al.* 2008; 2013).

6.2.2.3. Infrared spectroscopy

IR-spectrophotometry allows identifying molecules with respect to classes of compounds, recognising the presence of specific functional groups. Each functional group has several vibrational modes, involving specific energy consumption, which gives absorption in a specific region (Derrick *et al.* 1999; Kellnert 2003). This technique is useful to identify inorganic and organic compounds (e.g., the whitish raw material and possible organic binders used in the leech fibulae decoration).

Fourier transform infrared spectroscopy (FT-IR) was performed in transmission on a Bruker Vertex 70 spectrophotometer[7], coupled with a Bruker Hyperion 3000 IR microscope, equipped with an MCT detector (Infrared Associated Inc.) and an anvil cell (High Pressure 'Diamond Optics, Inc.'). For each spectrum, 32 or 64 scans were collected in the 4000-600 cm^{-1} range, with an average resolution of 4 cm^{-1}.

In the IR spectrum of *C. rubrum*, calcite signals predominate over those of organic pigments, which are generally hidden (Kupka *et al.* 2009). Calcite peaks appear at 1700/1804, 1450/1475,

7 Analyses were performed at Centro Conservazione e Restauro 'La Venaria Reale', Venaria Reale (TO).

881/913, 733/750 cm^{-1}, water at 3430/3450 cm^{-1}, aliphatic organic compounds at 2900/2914 (CH_2 symmetric stretching) and 2873/2887 (CH_3 symmetric stretching) cm^{-1} (Kaczorowska *et al.* 2003).

6.2.2.4. Micro-X-Ray diffraction analysis

X-ray diffraction (XRD) provides information about the crystalline structure. This technique generally requires grinding, but in 'µ-area mode' (µ-XRD) it can be applied directly to small poly-crystalline samples without any pre-treatment.
XRD allows discriminating different carbonates – such as aragonite, calcite and dolomite. Aragonite generally forms shells and madrepores while calcite forms the skeleton of *C. rubrum* and part of the upper valva of *S. gaederopus* (Schvoerer *et al.* 2000; Taviani 1997). Mg-free and Mg-poor calcite is more stable (Fig. 2) and can therefore originate from aragonite or HMC, through the combined effect of pressure, temperature and time (Schvoerer *et al.* 2000, p. 227). The angular position of the main reflection (104) of calcite gives information about presence of Mg in the crystal lattice: a shift towards higher values indicates higher Mg-contents (a HMC), after smaller lattice constants, due to the tinier ionic radius of Mg^{2+} (Bente *et al.* 2017). However, in µ-area mode, a peak-shift may also be influenced by different µ-orientations of the crystallites in the non-pulverised sample.
In this research, XRD analyses were mainly performed in µ-area mode. Some difficulties arose related to specimen morphology, which is not always flat: anomalous phenomena affected therefore the background, sometimes interfering with the peaks position. Nevertheless, in most cases analyses gave excellent qualitative results.
µ-XRD data were acquired on the artefacts 'as such' (i.e. with no preparation or preliminary sampling) using a SMARTLAB XE – Rigaku diffractometer, in µ-area mode (Fig. 94): Cu-kα radiation, optical device CBO (Cross Beam Optics; parallel beam), µ-area optical device CBO-f, 0.5 mm incident slit, detector HyPix-3000 (vertical). The analysis was carried out in the range of angular values from 3 to 70° 2θ, under the following conditions: Scan mode: 0D (continuous)/1D(scan)/2D (scan); Energy mode: standard; Slit: 2 mm; Step: 0,02°; Speed: 0,2-0,5°/min; average collection time 3h. Each point of analysis was annotated on the specimen image, and a microscopic image was acquired for each of these at varying magnification.
Also (3 cases), XRPD analysis were collected with:

- an automatic diffractometer 'MINIFLEX 600' - Rigaku in Bragg-Brentano geometry, with θ-θ setup, using monochromatized Cu-Kα radiation, in the angular range from 3 to 70° 2θ (step 0.02°), collection time 1 hour, on a flat sample holder, without any sample pre-treatment[8];
- an automated PW3050/60 PANalytical X'Pert-PRO diffractometer in Bragg-Brentano geometry, with θ-θ setup and an RTMS (Real Time Multiple Strip) detector using monochromatized Cu-Kα radiation, in the angular range from 3 to 70° 2θ (step 0.02°), collection time 1 hour, on a zero-background Si-monocrystal flat sample holder, by pre-crushing in an agate mortar[9].

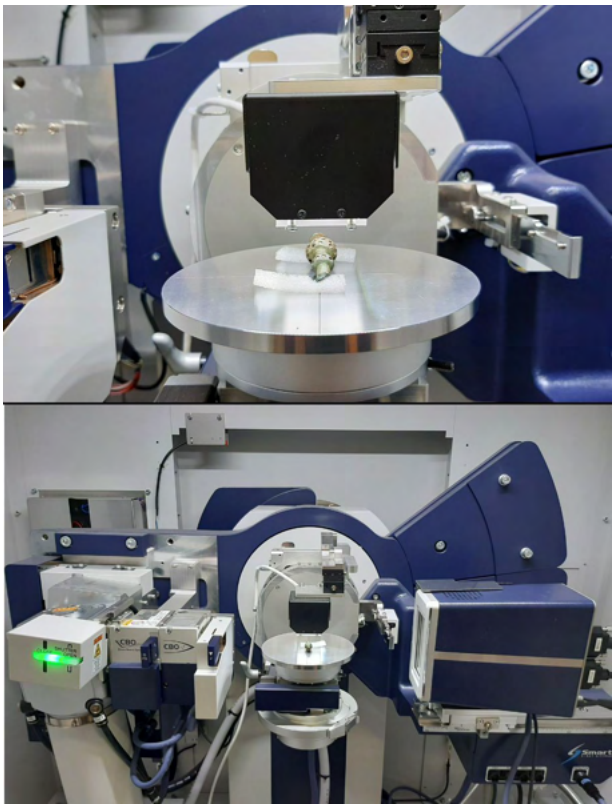

Figure 94. µ-XRD instrumentation during the analysis of some archaeological finds.

The results are displayed in the form of

8 Analysis of a leech fibula from Golasecca-loc. Galliasco (inv. no. 22.S288-1.205).
9 These data refer to previous analysis on samples BF1 (inv. no. C-FR-NE/1) and VF7 (inv. no. SP27), respectively from Brignano Frascata and Villa del Foro fibulae (Berruto *et al.* 2023).

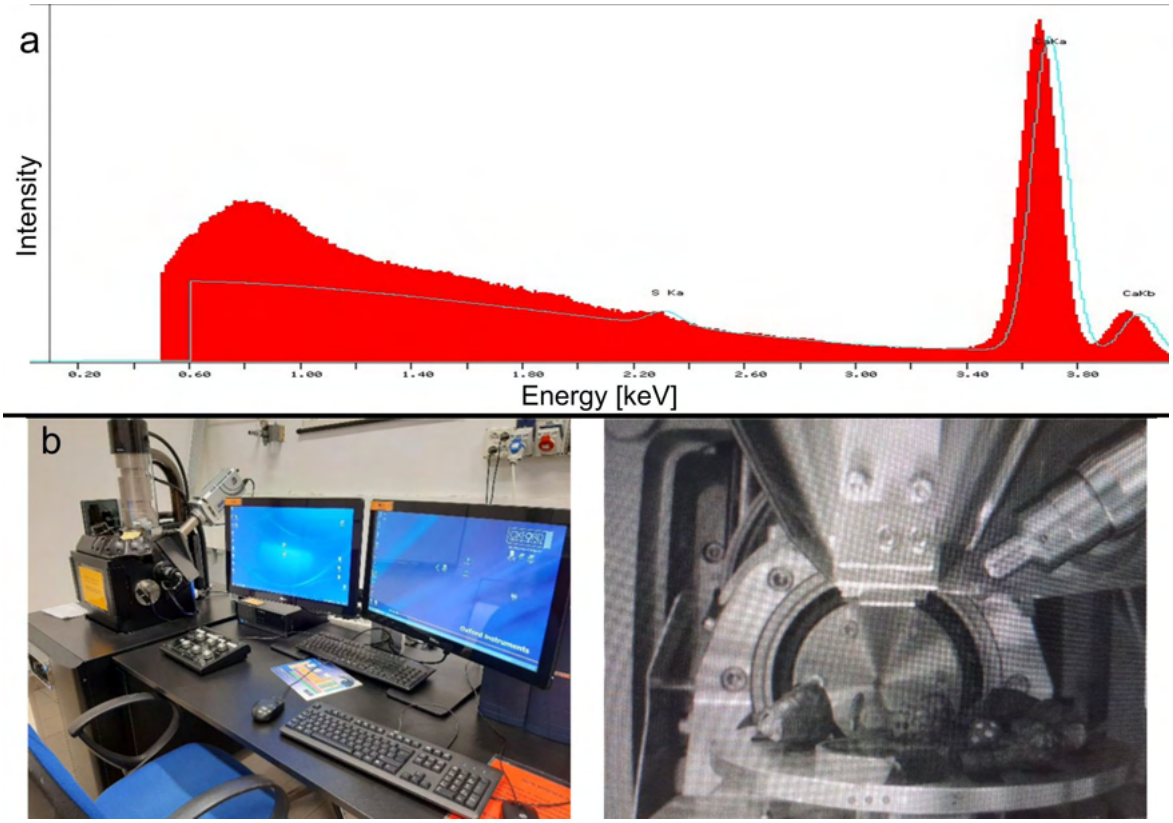

Figure 95. a) μ-XRF analysis on a modern *C. rubrum* sample: detail of the area corresponding to the emergence of the signals of the lighter elements, unfortunately not detectable; b) SEM-EDS non-invasive analysis on some archaeological finds from Gropello Cairoli, loc. Santo Spirito.

diffractograms, with angular 2θ values (x-axis) vs. intensity of the diffracted radiation (y-axis). For data interpretation, the software 'DIFFRAC PLUS, EVA Application 7.0.0.1' (2001) was used, by comparing the positions and intensities of diffraction peaks with suitable computer databases (JCPDS-ICCD; ICSD; PCPDFWIN).

6.2.2.5. Chemical analysis: μ-XRF and SEM-EDS

According to literature, a determination of the Mg-content in calcite is possible both by Raman (Borromeo *et al.* 2017; Fürst *et al.* 2016) and X-ray diffraction (Bente *et al.* 2017; 2022; Gerdes *et al.* 2015; Schrickel *et al.* 2014). However, to obtain more reliable data and cross-check the quantifications performed with other methods, elementary chemical analyses were also included in the protocol.

X-ray fluorescence spectrometry (XRF) was considered at first for this purpose (Macchia *et al.* 2016). This technique allows the quali-quantitative analysis for elements with an atomic number (Z) > 5 (bench-top instrumentation) or 10 (portable one), by measuring the energy generated by the fluorescence emission of electrons, shifted from their energy level due to the X-rays influence. Returning to their level, they generate characteristic radiation. Sensitivity depends on the investigated element (greater for elements with higher Z), as well as on the sample preparation and the instrument (Apollonia, Volpin 1999).

Portable instrumentation was excluded due to the size of the analytical spot and lower sensitivity. Tests were performed with X-ray micro-fluorescence instrumentation (μ-XRF)[10] on an archaeological sample and a modern *C. rubrum* one. The setup is made of a μ-XRF Eagle III-XPL spectrometer, equipped with an EDS Si (Li) detector and with an Edax Vision32 micro-analytical system. Unfortunately, this instrument was unable to identify elements with Z < 17 (Fig. 95a). SEM-EDS was therefore used to perform chemical analysis (Fig. 95a).

10 The micro-XRF measures have been obtained with the equipment acquired by the Interdepartmental Center 'G. Scansetti' for Studies on Asbestos and Other Toxic Particulates with a grant from Compagnia di San Paolo, Torino, Italy.

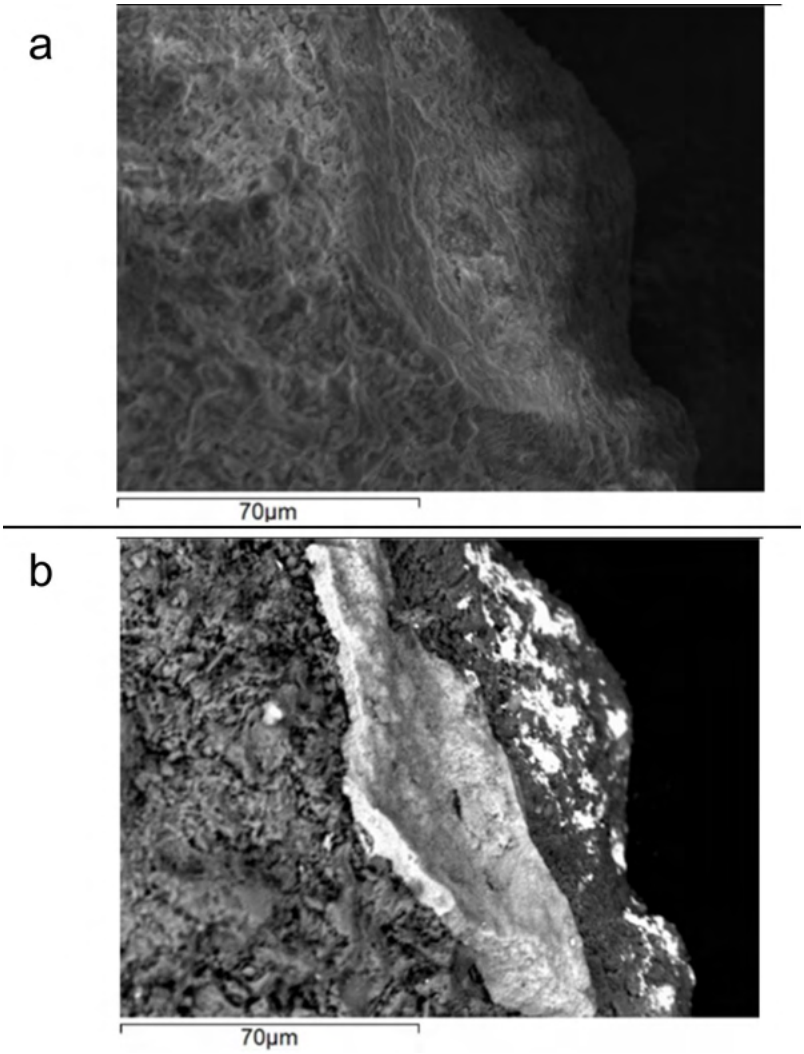

Figure 96. Archaeological decoration sample - copper and lead 'crust' on Ca/Mg-based material, high vacuum: a) image obtained with secondary electron detector (ESE); b) image obtained with backscattered electron detector (BSE).

Scanning electron microscope (SEM) on untreated specimens (i.e., neither Au nor C coating) allow observing at high magnifications the µ-morphology of the sample (Vielzeuf *et al.* 2008). Energy dispersion spectrometry (EDS) allows the collection of an elemental, albeit only semi-quantitative analysis.

A JEOL JSM IT300LV (High Vacuum - Low Vacuum 10/650 Pa - 0.3-30kV) was used, coupled with an EDS Oxford INCA Energy 200 equipped with an INCA X-act SDD 'thin window' detector, allowing chemical analysis of light elements down to Boron. Data were collected in low vacuum (35 Pa) on uncoated samples (neither C nor Au). Standardization was performed using pure Co. Working parameters: acceleration voltage 15 kV; working distance 10-13 mm; probe current 1 nA; spectra acquisition time 60-300 s (Fig. 95b). Specimens were fixed to an aluminium sample holder with double-sided carbon tape[11]. The Inca 200 Microanalysis Suite Software, version 4.08, was used for data collection and elaboration.

Images are generally recorded in the Backscattered Electron (BSE) mode, which is indicative of the elemental composition, depending on the atomic weight of the material[12]. Tests were also performed in high vacuum, with no sample preparation, but BSE-images (Fig. 96) become no more indicative of the composition of the material, due to the influence of charge differences.

SEM-EDS is very useful to identify the Ca^{2+}/Mg^{2+}

11 As a result of using an aluminium sample holder, the detection of this element can be distorted, especially in low vacuum (wider skirt: ~200-300 µm).

12 The penetration depth of the BSE into the material is approximately 3-4 µm: the presence of restorative/protective agents may therefore adversely affect the analysis.

ratio in *C. rubrum*, distinguishing between different biogenic calcites, and presence of trace elements that may provide further information about the material and its origin. Calcite composition in the *C. rubrum* skeleton ranges from 9 to 15 mol % $MgCO_3$, with an average 12±1.0 % value. The Mg-content in a single sample varies at mm, sub-mm scale and down to the mm. Chemical analyses of its skeleton show a predominance of Ca plus subordinate Mg. Other elements may also appear (Na, S, Sr, K, P, B, Ba, Fe, Li, Mn, Pb and U). Sulphur is a common element in marine and biogenic calcites, detected both in the inorganic and organic parts of *C. rubrum.* In contrast, phosphorus is predominantly in the organic matrix and is used as a marker of its presence in biominerals (Busenberg, Plummer 1985; Hasegawa *et al.* 2010; Hermans 2010; Floquet *et al.* 2015; Macchia *et al.* 2016; Perrin *et al.* 2017; Pingitore *et al.* 1995; Vielzeuf *et al.* 2008; 2013; Weinbauer *et al.* 2000).

Figure 97. Setup of radiographic analysis and detail of the artefact under investigation.

6.2.2.6. Radiographic analyses

The archaeo-technological study was implemented by radiographies of some archaeological finds[13]. A custom-tailored instrument for the study of artworks of different sizes and shapes was used. The used setup consists of an X-ray source, an X-ray detector and a rotating platform. The X-ray source is placed on a table to control the distance from the detector and the correct height of the focal point. The use of a mechanical X-Y scanning system to move the detector allows its alignment to the X-ray source (Fig. 97; Tansella *et al.* 2022; Vigorelli 2023).
The X-ray source consists of a Microfocus L8121-03 from Hamamatsu, with a tungsten anode, a 200 µm thick Be-window and equipped with an air-cooling system. Analytical conditions are: voltage 40-150 kV; current 10-500 µA; max. power 75W; focal spot size 5-50 µm; target material W; cone beam angle 43°; min. focus-object distance 17 mm. The X-ray detector used is a flat panel Shad-o-Box 6K HS from Teledyne Dalsa, consisting of a 2304 × 2940 pixel matrix, corresponding to an active area of 11.4 × 14.6 cm^2, with an individual pixel size of 49.5 µm, protected by a thin carbon fiber cover. Each pixel consists of a direct contact scintillator (Cs-iodide), a photodiode and a CMOS transistor. The rotating platform is the Newport URS150BPP model, installed on a triangular metal support for levelling during the alignment phase. An additional support is mounted on the platform to align the sample with the focal point of the X-ray source. The rotation speed of the sample and the angular step are adjusted with a software developed in LabVIEW to control the movements of the platform (Tansella *et al.* 2022; Vigorelli 2023).
Radiographic analyses at this stage focused exclusively on the technological study of the metal artefact (see section 8.2), without further investigation concerning the density of the coral. An approach involving high-resolution µ-X-ray computed tomography aimed at studying the internal structure of the coral parts, where not biased by the presence of metal, would be useful in confirming presence of *C. rubrum*, when dubious (Bente *et al.* 2015c; 2017).

13 This radiographical investigation were possible thanks to a collaboration with Physic Department of the University of Turin (A. Lo Giudice, A. Re, L. Vigorelli and F. Tansella).

7. Archaeometric Analyses: Results

Abstract

Lo studio archeometrico ha coinvolto 264 reperti archeologici. La scoperta più significativa è la ricorrenza di una fase carbonatica nei materiali decorativi della maggior parte dei reperti (163 casi), seppure declinata in differenti forme (calcite pura, calciti ad alto, medio o basso contenuto di Mg – HMC, MMC, LMC –, corallo rosso, ecc.). In particolare, il corallo rosso (*Corallium rubrum*) è identificato con certezza in 46 reperti (17 %), grazie alla compresenza di calcite alto magnesiaca (HMC o MMC) e pigmenti organici (polieni). L'identificazione di calcite basso o medio magnesiaca, in assenza dei polieni, può essere ricondotta all'impiego di altri materiali. Tuttavia, alterazioni post-deposizionali possono ridurre il contenuto di Mg, trasformando HMC in MMC o LMC, con perdita dei polieni; una riduzione nel contenuto di Mg può anche essere indotta da eventi termici (es. cremazione). Circa il 26 % dei reperti non mostra tracce di materiali decorativi, mentre piccole percentuali rivelano altri materiali, come 'inchiostro di China', vetro, apatite (osso), o gesso/anhidrite (verosimilmente riconducibile ad alterazione di materiale carbonatico). L'aragonite, meno comune, è stata rilevata in un solo oggetto, come anche l'impiego di *Spondylus gaederopus*.
La correlazione dei risultati in base alla tipologia, cronologia e provenienza geografica degli oggetti non ha identificato particolari tendenze. Per quanto riguarda le fibule a sanguisuga con inserti, tuttavia, il *C. rubrum* sembra essere più comune nei reperti più recenti (480–440 a.C.), mentre riscontriamo una maggiore diversificazione in quelli più antichi (560–480 a.C.), suggerendo una progressiva affermazione del corallo rosso.
L'identificazione della presenza di eventuali leganti organici è risultata problematica a causa della natura stessa di questi materiali, verosimilmente presenti solo in traccia, nonché della somiglianza spettrale con sostanze moderne usate nei restauri.
Le analisi condotte sulla superficie metallica degli oggetti suggeriscono una verosimile gestione intenzionale della composizione delle leghe in funzione delle esigenze tecniche di lavorazione. Questa prassi è coerente con quanto noto per l'età del Ferro nelle culture dell'Alto Adriatico, etrusca, fenicia, mesopotamica, della Magna Grecia e Hallstatt. Il tenore di stagno varia in base alla destinazione funzionale: è più elevato negli oggetti destinati alla sola fusione, dove aumenta fluidità e resistenza; è più basso nei manufatti soggetti a lavorazioni post-colata, poiché tenori superiori al 10% riducono la duttilità. Anche il piombo era probabilmente aggiunto nei materiali finiti dopo fusione, per migliorare la colabilità e la lavorabilità dell'oggetto, abbassando il punto di fusione e fungendo da lubrificante interno. Le fibule a sanguisuga con anima in cotto sembrano essere caratterizzate da elevati tenori di piombo, necessari per ottenere leghe altamente fluide, adatte a riempire stampi complessi e produrre decorazioni raffinate direttamente nel modello in cera. Inoltre, le analisi sembrano confermare la natura composita di tali manufatti, evidenziando differenze composizionali tra il corpo e l'ardiglione, coerenti con diverse esigenze funzionali e tecniche di produzione.
Lo studio sottolinea l'importanza di analisi multidisciplinari per ricostruire le tecniche in uso nell'antichità, l'origine e la trasformazione dei materiali decorativi nel tempo.

The characterisation of the whitish decorative materials is the main focus of the research (section 7.1), but significant results were also obtained from the analysis of the bronze alloy alteration by-products (section 7.2), performed in 141 cases out of 264 specimens (i.e. in case of direct approach).

7.1. Whitish decorative materials

The results are discussed on the basis of the analytical technique used. The same protocol has been applied to modern samples (section 7.1.1) and archaeological finds (section 7.1.2), as well as to samples resulting from combustion simulations on modern coral (section 7.1.3). In the concluding remarks (section 7.1.4), a final interpretation is provided relating it with the archaeological types, to check for trends.

7.1.1. Modern samples

The results reported in this paragraph refer to the analysis of 8 modern samples:

- 5 samples of *Corallium rubrum* with different origins and characteristics:
  - 1 sample of raw ligurian red *C. rubrum* collected under the sea (r_Cr_L),
  - 1 sample of worked red *C. rubrum* of unknown provenance (w_Cr_u),
  - 1 sample of worked (bead shape) red *C. rubrum* of unknown provenance (w_Cr_ub),
  - 1 sample of raw sicilian red *C. rubrum* collected on the beach (r_Cr_Si),
  - 1 sample of worked sardinian white-to-pinkish *C. rubrum* (w_pCr_Sa);
- 1 sample of raw ligurian white coral (r_c_L);
- 1 sample of raw sardinian *Spondilus gaederopus* (r_Sg_Sa);
- 1 sample of raw piedmontese fossil coral (r_fc_P).

These specimens are shown in Figs. 87 and 88 (see section 6.1.2).

7.1.1.1. Optical stereomicroscope

By comparing archaeological artefacts with modern specimens, we found that they shared the same typical µ-features of *C. rubrum*, such as longitudinal crenulation (Fig. 98a; Vielzeuf *et al.* 2008). In processed samples (i.e. samples 'w_Cr_u', 'w_Cr_ub' and 'w_pCr_Sa'), these µ-structures are hardly recognisable. Sample 'r_Sg_Sa' (*S. gaederopus*) reveals the presence of the characteristic squamae (Fig. 98b).

Specimen 'r_Cr_Si' (*C. rubrum* collected on the beach) is made of several small branches with a common origin. Longitudinal crenulations and bifurcations are well evident, as well as surface smoothing traces resulting from sea transport (Fig. 98c) and traces of bio attack by other organisms (Fig. 98d). These features are not so dissimilar from those recognisable on some archaeological finds[1], suggesting the latters might also have been collected on the beach[2].

Sample 'r_fc_P' (Figs. 98e, 98f) shows elongated µ-structures with Ø ≈ 2 mm, with a compact, granular surface, typical of secondary calcite resulting from recrystallisation.

7.1.1.2. µ-Raman analysis

Compared to the mineral calcite (Lafuente *et al.* 2015)[3], *C. rubrum* shows a slight peak shift attributable to its high-Mg-content (Bischoff *et al.* 1985; Borromeo *et al.* 2017; Edwards *et al.* 2005; Fürst *et al.* 2016; Macchia *et al.* 2016; Urmos *et al.* 1991). In the Raman spectra of modern of *C. rubrum*, bands of both calcite and polyenes are present, but the former are very weak if compared to the latter (e.g., sample 'w_Cr_ub': Fig. 99)[4].

In sample 'r_Cr_Si' (*C. rubrum*), different spectra are recorded in the red and white areas (Fig. 100): in the red ones, the bands of calcite and polyenes appear, whereas in the white ones the signal of aragonite is present[5]. Sample

1 e.g., inv. no. MV103 (Golasecca, Longone al Segrino type pendant, Fig. 26c), St. 78799 (Forcello di Bagnolo San Vito, coral branch, see Appendix 1, Fig. 217.d.h).

2 For further examples see Appendix 1, Figs. 224, 225a.

3 Mineral-derived calcite (RRUFF spectra id: R040070 and R050127) shows bands at 1086-1092 cm^{-1} (h), 282-284 cm^{-1} (m), 152-154 cm^{-1} (mw), 1750-1755 cm^{-1} (w), 1439-1443 cm^{-1} (w), 713-719 cm^{-1} (w) [peak intensity with 532 nm green laser: h=high; m=medium; w=weak; s=shoulder; v = very].

4 *C. rubrum* has contemporaneously both calcite [1089 cm^{-1} (m), 285 cm^{-1} (w), 1752 cm^{-1} (vw), 717 cm^{-1} (w), 157 cm^{-1} (vw)] and polyene signals [at 1519 cm^{-1} (h), 1131 cm^{-1} (h), 2253 cm^{-1} (m), 2636 cm^{-1} (m), 3034 cm^{-1} (w), 2984 cm^{-1} (s), 2533 cm^{-1} (w), 2147 cm^{-1} (w), 1021 cm^{-1} (mw), 1300 cm^{-1} (mw), 3375 cm^{-1} (vw), 3742 cm^{-1} (vw)].

5 The spectrum shows peaks at 1085 cm^{-1} (h), 703-707 cm^{-1} (w), 206 cm^{-1} (w) and 153 cm^{-1} (m). This latter peak in aragonite is not always present (e.g. RRUFF R040078) but is sometimes reported (e.g. RRUFF R060195).

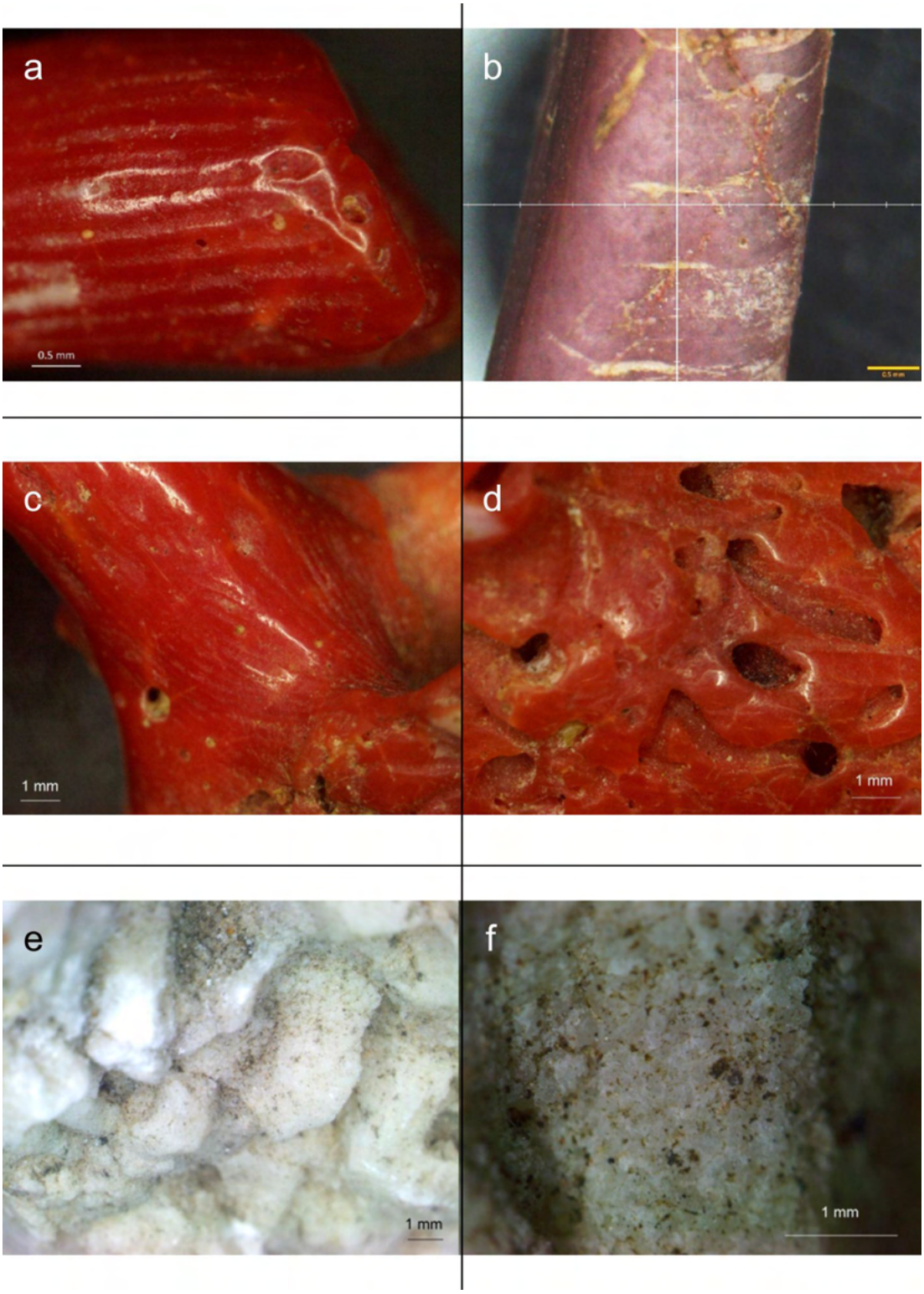

Figure 98. a) Crenulation (*C. rubrum*, 'r_Cr_Si'); b) Squamae (*S. gaederopus*, 'r_Sg_Sa'); c) Surface smoothing due to marine transport (*C. rubrum*, 'r_Cr_Si'); d) Traces of biogenic attack by other organisms (*C. rubrum*, 'r_Cr_Si'); e) Elongated μ-structures and a grainy, compact surface (fossil Piedmontese coral, 'r_fc_P'); f) Elongated μ-structures and a grainy, compact surface (fossil Piedmontese coral, 'r_fc_P').

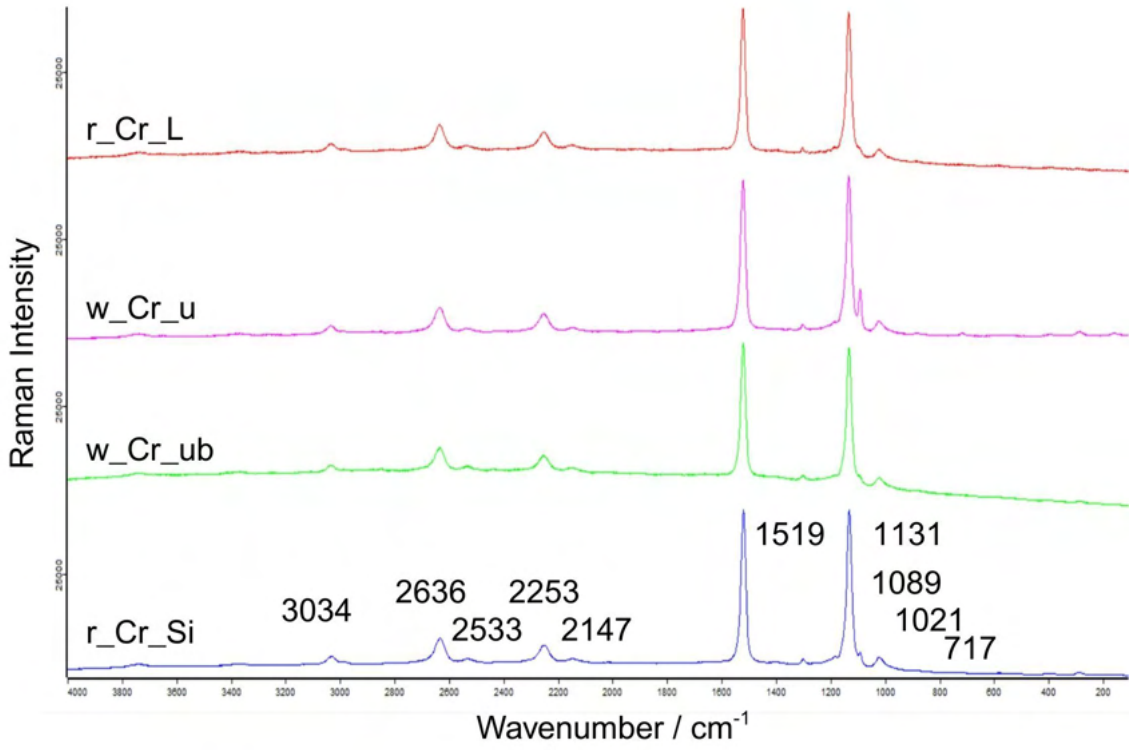

Figure 99. Comparison between Raman spectra of red *C. rubrum* (samples: 'r_Cr_L', 'w_Cr_u', 'w_Cr_ub', 'r_Cr_Si'); 532 nm green laser, extended range, 6 seconds for 6 cycles, 10x magnification, D0.6 filter.

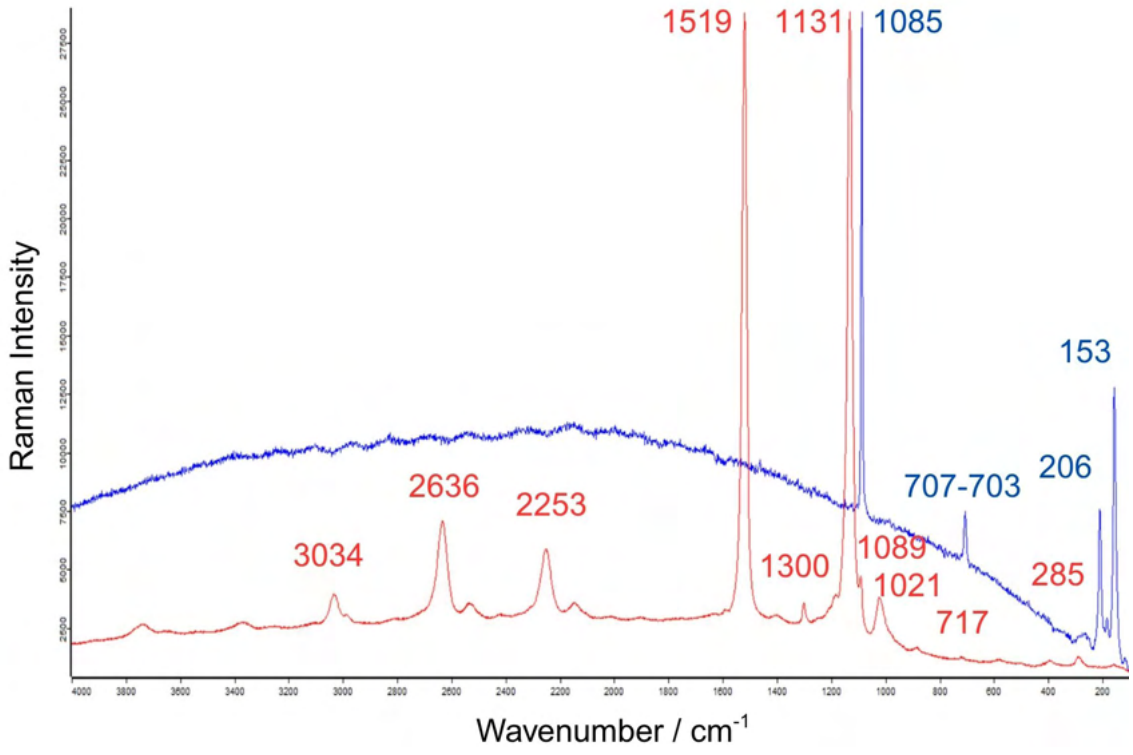

Figure 100. Comparison between Raman spectra collected on sample 'r_Cr_Si' in the red (red) and white (blue) portions, respectively composed of calcite with polyenes and aragonite; 532 nm green laser, extended range, 6 seconds for 6 cycles, 10x magnification, D0.6 filter.

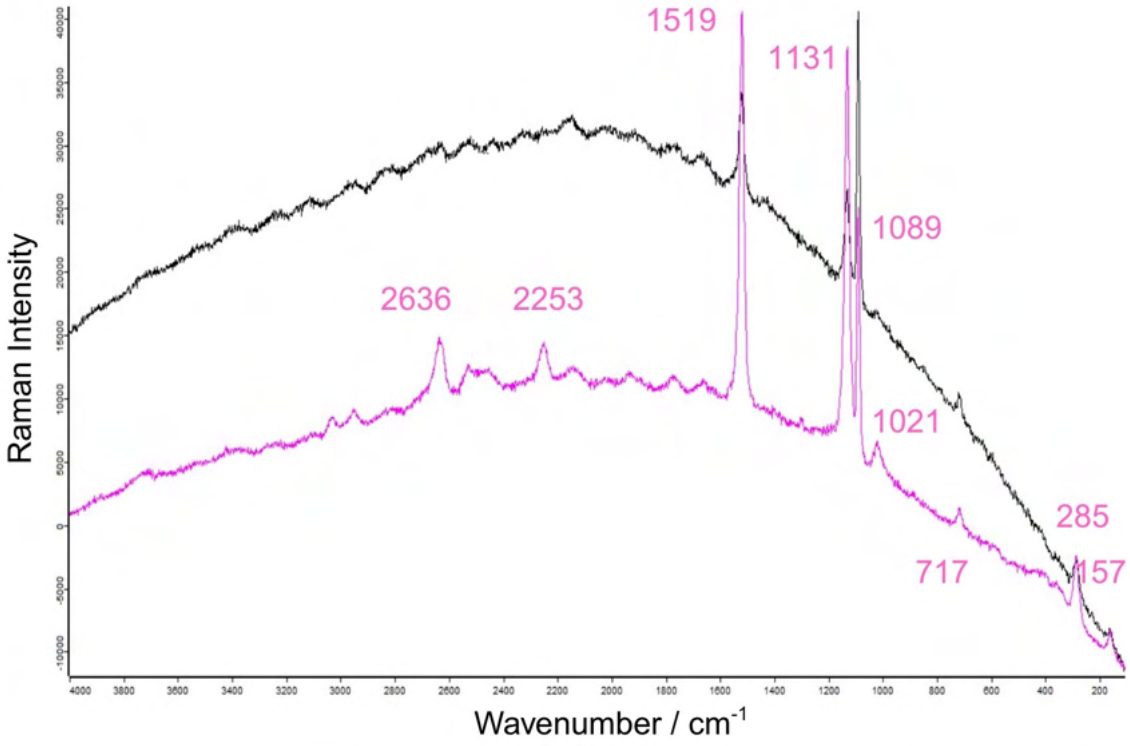

Figure 101. Comparison between Raman spectra of the Sardinian coral pendant (w_pCr_Sa) in the white portion (in black) and the pink portion (in fuchsia); 532 nm green laser, extended range, 6 seconds for 6 cycles, 10x magnification, D0.6 filter.

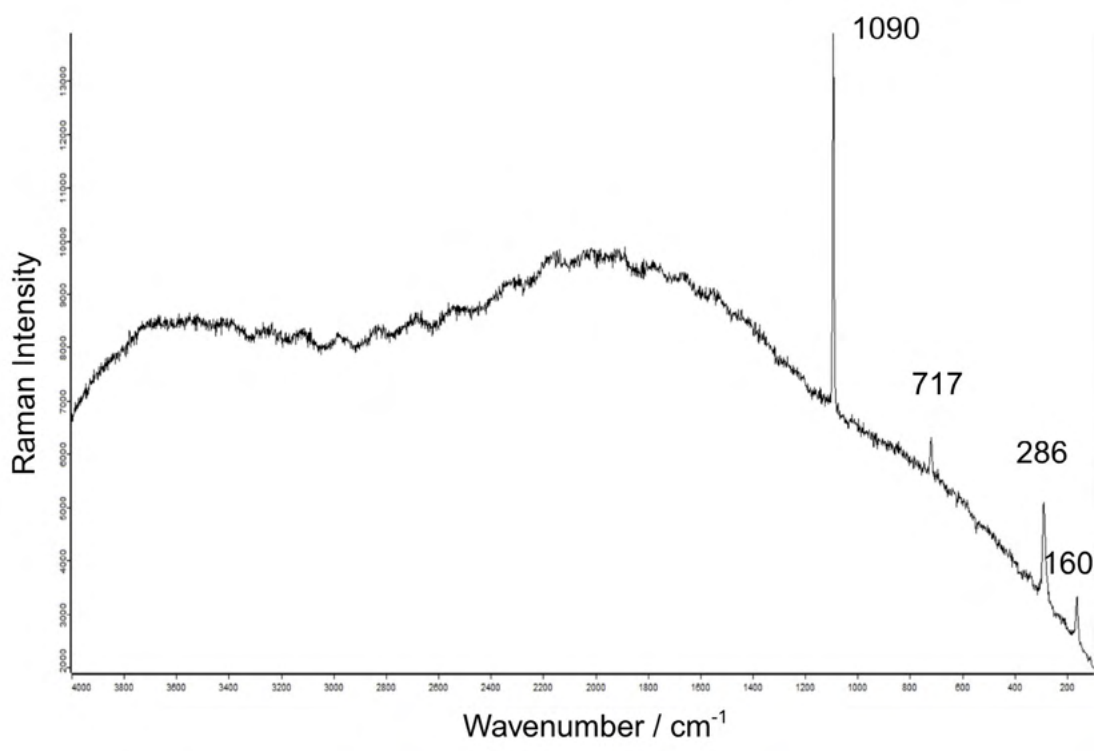

Figure 102. Raman spectrum of fossil coral from Piedmont (r_fc_P): calcite; green laser 532 nm, extended range, 6 seconds for 6 cycles, 10x magnification, D0.6 filter.

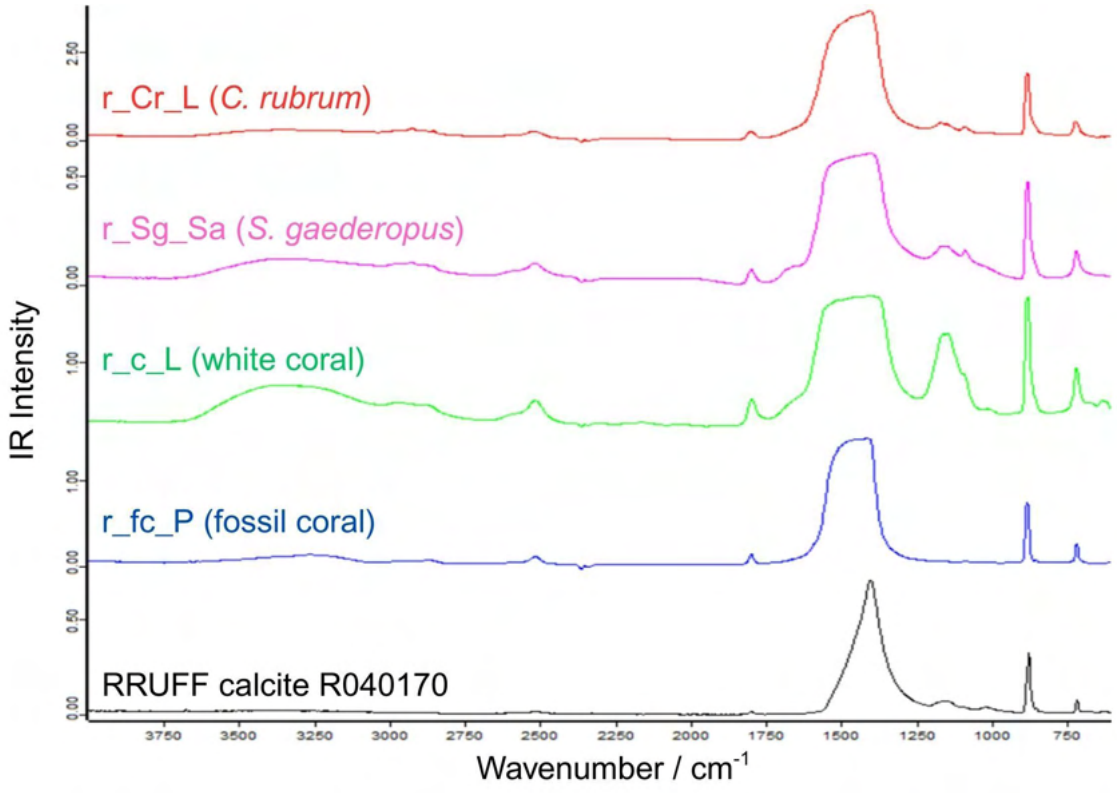
r_Cr_L (C. rubrum)
r_Sg_Sa (S. gaederopus)
r_c_L (white coral)
r_fc_P (fossil coral)
RRUFF calcite R040170
IR Intensity
3750 3500 3250 3000 2750 2500 2250 2000 1750 1500 1250 1000 750
Wavenumber / cm-1

Figure 103. FT-IR spectra of modern samples of *C. rubrum* (r_Cr_L), *S. gaederopus* ('r_Sg_Sa'; fuchsia), ligurian white coral ('r_c_L'; green), fossil piedmontese coral ('r_fc_P'; blue), RRUFF calcite R040170.

'w_pCr_Sa' (*C. rubrum*) reveals the typical calcite + polyenes bands in both the pink and white portions (Fig. 101), with polyenes signals being less pronounced in the latters. The spectrum of *S. gaederopus* (sample 'r_Sg_Sa'; Fig. 93) is similar to *C. rubrum* one[6]. Raman spectrum of the fossil coral (sample 'r_fc_P'; Fig. 102) reveals only the bands of calcite (1090, 717, 286, 160 cm^{-1}). Shift of the ν_1 peak suggests presence of Mg.

7.1.1.3. FT-IR analysis

Systematic presence of calcite is detected (main band at ≈ 1500-1400 cm^{-1}; others at 2516, 1795, 876 and 711 cm^{-1}: Fig. 103). In addition, some signals appear in the 3000-2800 cm^{-1} range (found also in archaeological samples: see section 7.1.2.3) – perhaps related to the organic fraction in the *C. rubrum* skeleton (Vielzeuf *et al.* 2008).

7.1.1.4. μ-XRD analysis

Calcite is identified in all samples, with a systematic shift in the positions of the reflections, possibly related to Ca^{2+}/Mg^{2+} substitution in the lattice but also to irregularities in the surface morphology. The magnitude of this shift is apparently higher for *Corallium rubrum* ('r_Cr_L'; Fig. 104), less marked for *S. gaederopus* ('r_Sg_Sa'; Fig. 106) and even lower for white Ligurian coral ('r_c_L'; Fig. 105) and the whitish-to-pink Sardinian coral ('w_pCr_Sa'). Whitish portions on sample 'r_Cr_Si' are identified as aragonite (Fig. 107). Sample 'r_fc_P' (fossil coral) reveals the presence of calcite and plagioclases (Fig. 108).

6 The spectrum of *S. gaederopus* shows calcite signals [at 1091 cm^{-1} (m) and 284 cm^{-1} (vw)] and polyenes bands [at 1513 cm^{-1} (h), 1126 cm^{-1} (h), 1021 cm^{-1} (mw), 2245 cm^{-1} (m), 3020 cm^{-1} (w), 2983 cm^{-1} (s), 2621 cm^{-1} (m), 2523 cm^{-1} (w), 2144 cm^{-1} (w), 1301 cm^{-1} (w), 3712 cm^{-1} (vw), 3349 cm^{-1} (vw)].

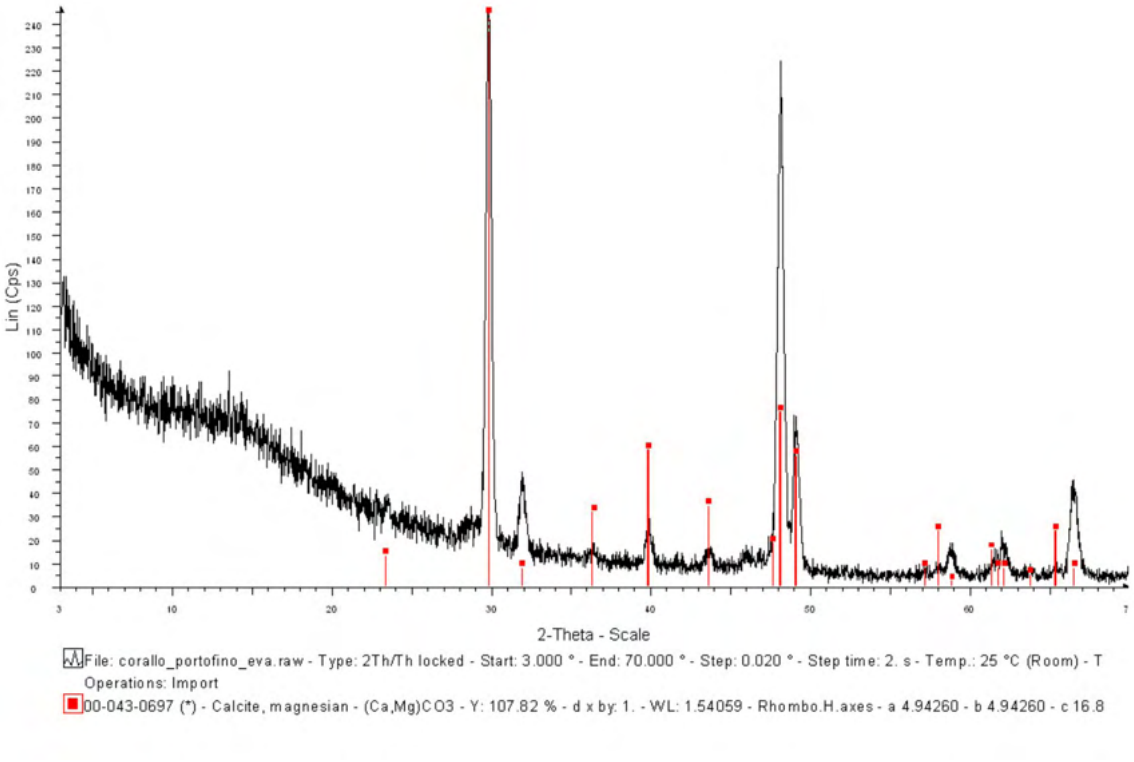
Lin (Cps)
2-Theta - Scale
File: corallo_portofino_eva.raw - Type: 2Th/Th locked - Start: 3.000 ° - End: 70.000 ° - Step: 0.020 ° - Step time: 2. s - Temp.: 25 °C (Room) - T
Operations: Import
00-043-0697 (*) - Calcite, magnesian - (Ca,Mg)CO3 - Y: 107.82 % - d x by: 1. - WL: 1.54059 - Rhombo.H.axes - a 4.94260 - b 4.94260 - c 16.8

Figure 104. μ-XRD diffractogram of 'r_Cr_L' (ligurian *C. rubrum*): Mg-calcite.

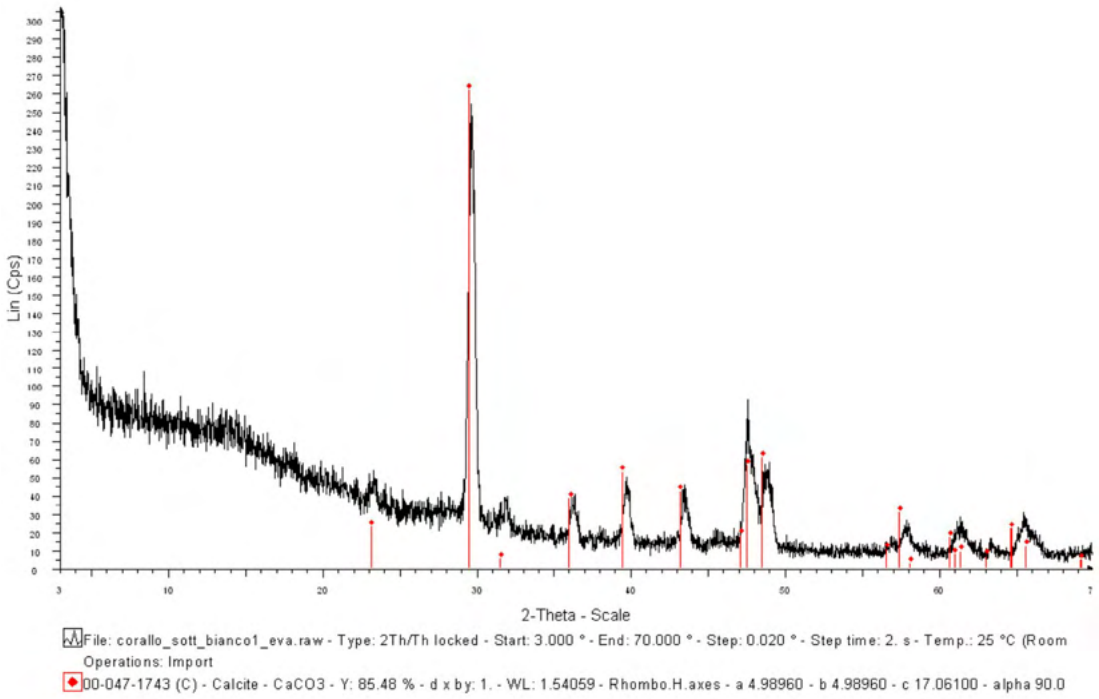
Lin (Cps)
2-Theta - Scale
File: corallo_sott_bianco1_eva.raw - Type: 2Th/Th locked - Start: 3.000 ° - End: 70.000 ° - Step: 0.020 ° - Step time: 2. s - Temp.: 25 °C (Room
Operations: Import
00-047-1743 (C) - Calcite - CaCO3 - Y: 85.48 % - d x by: 1. - WL: 1.54059 - Rhombo.H.axes - a 4.98960 - b 4.98960 - c 17.06100 - alpha 90.0

Figure 105. μ-XRD diffractograms of 'r_c_L' (Ligurian white coral): calcite.

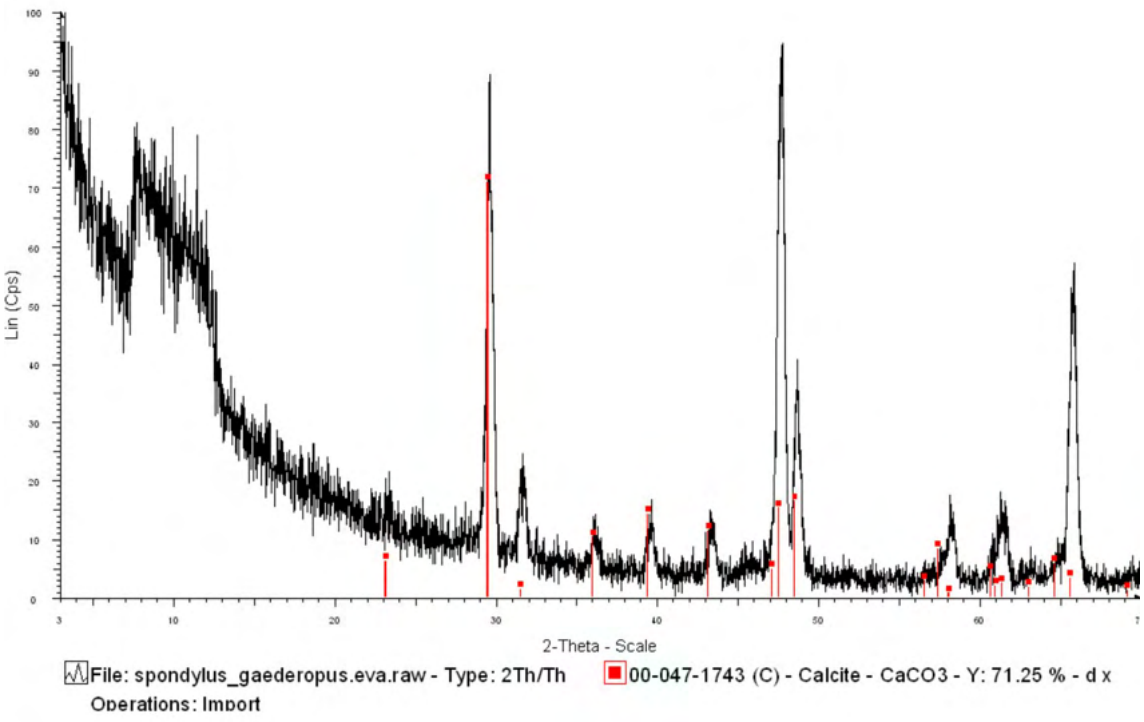
Lin (Cps)
2-Theta - Scale
File: spondylus_gaederopus.eva.raw - Type: 2Th/Th
00-047-1743 (C) - Calcite - CaCO3 - Y: 71.25 % - d x
Operations: Import

Figure 106. µ-XRD diffractograms of 'r_Sg_Sa' (*Spondylus gaederopus*): calcite.

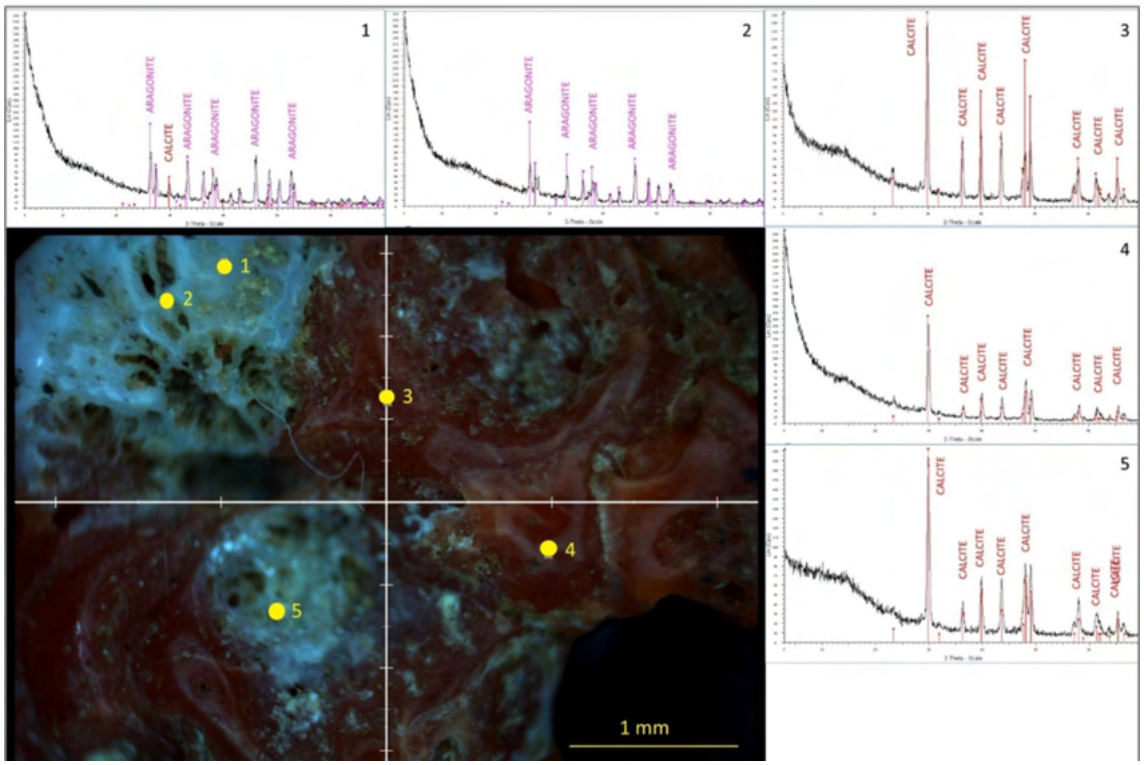

Figure 107. µ-XRD patterns collected on different areas (red or white) of 'r_Cr_Si' (*C. rubrum* from Sicily), with indication of their positions on the magnified image of the coral fragment.

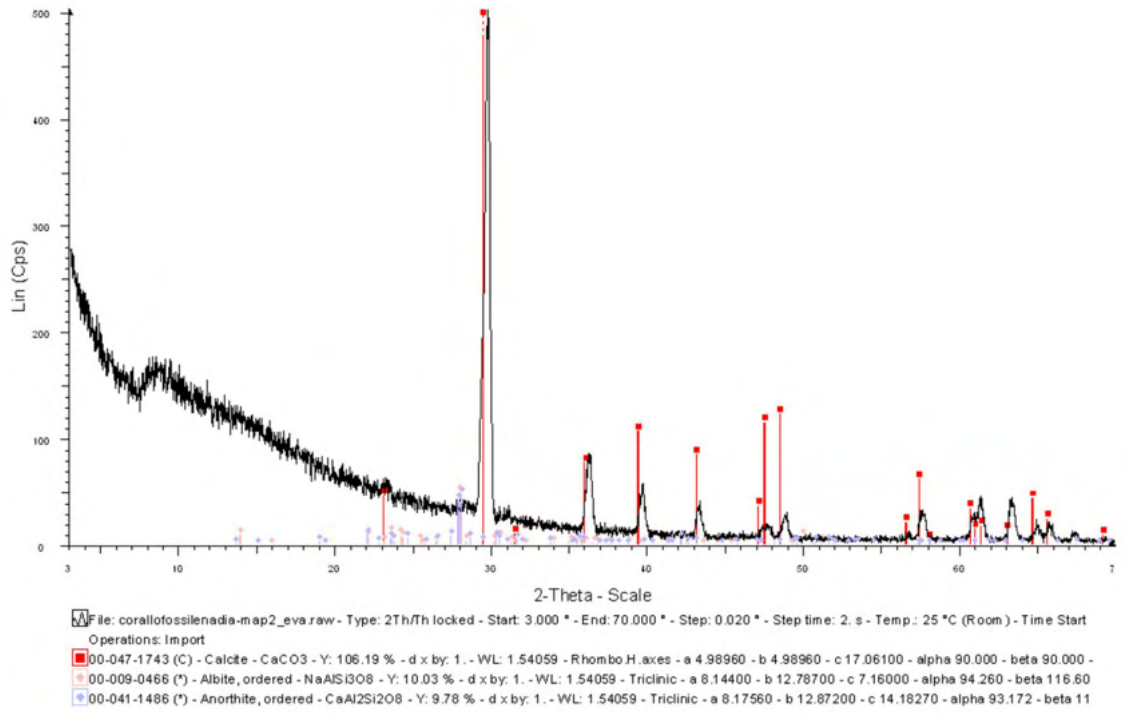
Lin (Cps)
2-Theta - Scale
File: corallofossilenadia-map2_eva.raw - Type: 2Th/Th locked - Start: 3.000 ° - End: 70.000 ° - Step: 0.020 ° - Step time: 2. s - Temp.: 25 °C (Room) - Time Start
Operations: Import
00-047-1743 (C) - Calcite - CaCO3 - Y: 106.19 % - d x by: 1. - WL: 1.54059 - Rhombo.H.axes - a 4.98960 - b 4.98960 - c 17.06100 - alpha 90.000 - beta 90.000 -
00-009-0466 (*) - Albite, ordered - NaAlSi3O8 - Y: 10.03 % - d x by: 1. - WL: 1.54059 - Triclinic - a 8.14400 - b 12.78700 - c 7.16000 - alpha 94.260 - beta 116.60
00-041-1486 (*) - Anorthite, ordered - CaAl2Si2O8 - Y: 9.78 % - d x by: 1. - WL: 1.54059 - Triclinic - a 8.17560 - b 12.87200 - c 14.18270 - alpha 93.172 - beta 11

Figure 108. µ-XRD diffractograms of 'r_fc_P' (fossil coral from Piedmont): calcite (red) and plagioclases (pink and purple).

7.1.1.5. SEM-EDS analysis

SEM-EDS analyses revealed significant differences among *C. rubrum*, white coral (r_c_L), *Spondylus gaederopus* (r_Sg_Sa) and fossil coral (r_fc_P) – on both a µ-morphological and compositional level.

The surface of 'r_Cr_L' (Ligurian *C. rubrum*), reveals presence of characteristic *C. rubrum* sclerites, µ-protuberances with a specific morphology embedded in the calcareous mass (Weinberg 1993; Vielzeuf *et al.* 2008; Fig. 109a). Such structures are not present in 'r_Cr_Si', referable to sicilian *C. rubrum* transported by sea (Fig. 109b), and not even in 'w_Cr_u', the worked specimen of unknown Mediterranean provenience. 'w_pCr_Sa', the whitish-to-pink worked sardinian coral, has a compact surface (Fig. 109c). 'r_c_L', the white Ligurian coral (Fig. 109d) shows a completely different microstructure, as does 'r_Sg_Sa' of sardinian *S. gaederopus* (Fig. 109e; Sakalauskaite *et al.* 2020). Finally, 'r_fc_P', the fossil coral, is characterised by a compact microstructure (Fig. 109f)[7].

Semi-quantitative chemical analysis by EDS identifies predominance of Ca, with variable Mg-contents in the different samples (Fig. 110): in red *C. rubrum* samples ('r_Cr_L', 'w_Cr_u' and 'r_Cr_Si') the Mg-contents vary between 11.95 and 12.25 mol% $MgCO_3$, which is consistent with literature data (Hasegawa *et al.* 2010; Floquet *et al.* 2015; Vielzeuf *et al.* 2008; 2013; Weinbauer *et al.* 2000). In sardinian withish-to-pink *C. rubrum* (w_pCr_Sa) an average Mg-content of 10.65 mol % $MgCO_3$ is found (intermediate between HMC and MMC), but highly variable between the white (9.98 mol% $MgCO_3$) and pink (12.32 mol% $MgCO_3$) areas of the coral (Fig. 110). In white ligurian coral (r_c_L) a Mg-content in the MMC range is found (10.11 mol% $MgCO_3$). In *S. gaederopus* sample (r_Sg_Sa) a 3.51 mol% $MgCO_3$ is found, compatible with LMC according to literature (Sakalauskaite *et al.* 2020). In piedmontese fossil coral (r_fc_P), an even lower Mg-amount is found (1.11 mol% $MgCO_3$).

The Mg/Ca ratio (Fig. 111) is fairly constant in the different analysed spots for samples 'w_Cr_u', 'r_Sg_Sa' and 'r_fc_P' (referable respectively to modern worked *C. rubrum* sample, *S. gaederopus* sample and fossil coral sample), while it is very variable from point to point for samples 'r_Cr_L', 'r_Cr_Si', 'w_pCr_Sa' and 'r_c_L' (referable respectively to modern unprocessed *C. rubrum*

7 For further examples Appendix 1, Fig. 225b-f.

samples, the whitish-to-pink worked coral and the white modern unprocessed coral sample).
Other minor and trace elements were also detected (Tab. 16; Figs. 112-113). For instance, Si is a probable residue of the marine sediment; in fact, it is only present in unprocessed samples. Na and Cl are abundant in samples 'r_Cr_L' and 'r_Sg_Sa', which were not cleaned after collection from seawater and probably retain salt residues. S, indicator of a biogenic origin, is abundant in samples 'r_Cr_L' (*C. rubrum*) and 'r_c_L' (white coral).

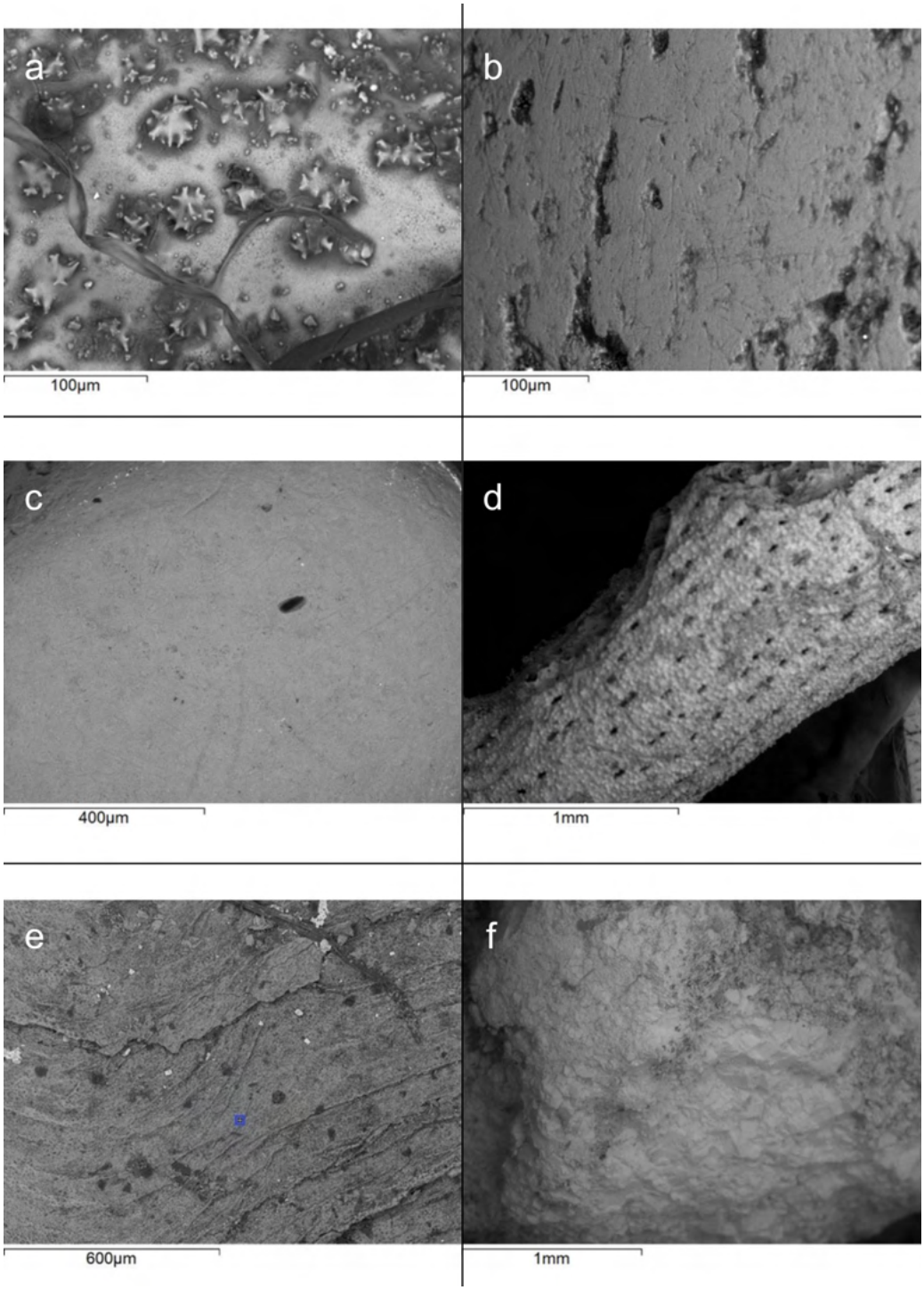

Figure 109. a) BSE-image of sample' r_Cr_L': ligurian *C. rubrum* with sclerites; b) BSE-image of sample 'r_Cr_Si': sicilian *C. rubrum* with traces of marine transport polishing; c) BSE-image of sample 'w_pCr_Sa': Sardinian polished worked whitish-to-pink *C. rubrum*; d) BSE-image of sample 'r_c_L': Ligurian white coral; e) BSE-image of sample 'r_Sg_Sa': *Spondylus gaederopus*; f) BSE-image of sample 'r_fc_P': fossil coral.

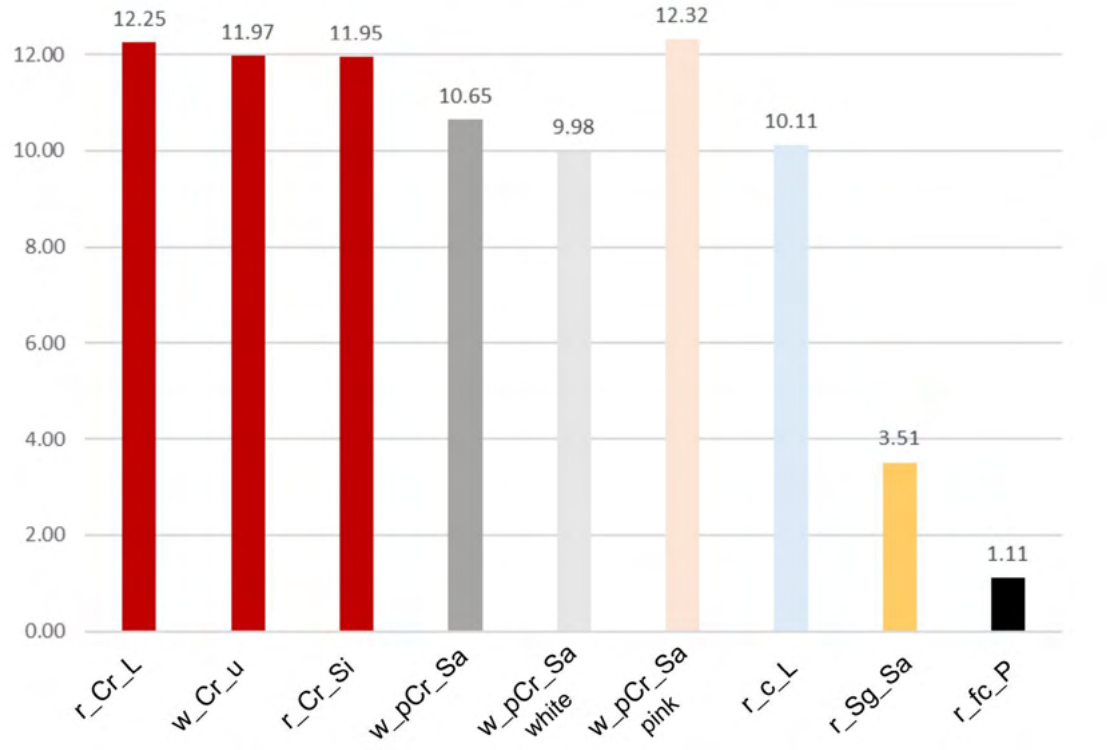

Figure 110. Mg-content (mol% $MgCO_3$) in different modern samples [r_Cr_L: unworked ligurian *C. rubrum*; w_Cr_u: worked-polished *C. rubrum*; r_Cr_Si: sicilian *C. rubrum* collected on the beach; w_pCr_Sa: sardinian pinkish-to-white worked coral; r_c_L: Ligurian white coral; r_Sg_Sa: Sardinian *S. gaederopus*; r_fc_P: Piedmont fossil coral].

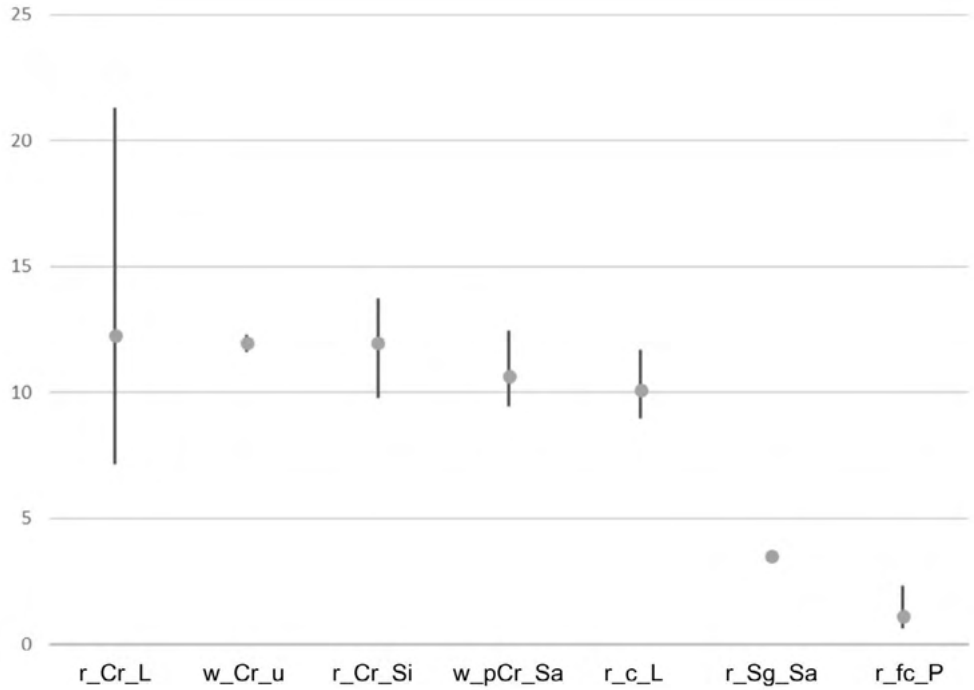

Figure 111. Mg-content variation in each sample (bar indicates the variation between minimum and maximum value) and average value (point indicates the average value of all the points of analysis on the sample) [r_Cr_l: unworked ligurian *C. rubrum*; w_Cr_u: worked-polished *C. rubrum*; r_Cr_Si: sicilian *C. rubrum* collected on the beach; w_pCr_Sa: sardinian pinkish-to-white worked coral; r_c_L: Ligurian white coral; r_Sg_Sa: Sardinian *S. gaederopus*; r_fc_P: Piedmont fossil coral].

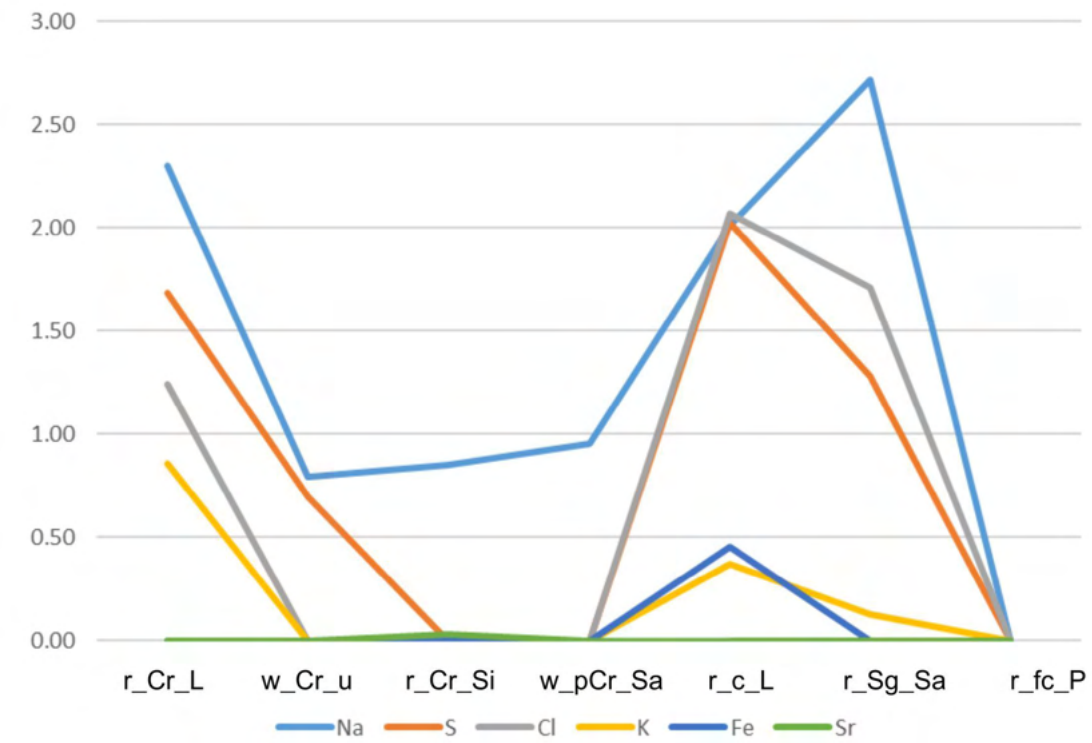

Figure 112. Graph of the occurrence of some minor elements (Na, S, Cl, K, Fe, Sr) in different samples [r_Cr_L: unworked ligurian *C. rubrum*; w_Cr_u: worked-polished *C. rubrum*; r_Cr_Si: sicilian *C. rubrum* collected on the beach; w_pCr_Sa: sardinian pinkish-to-white worked coral; r_c_L: Ligurian white coral; r_Sg_Sa: Sardinian *S. gaederopus*; r_fc_P: Piedmont fossil coral].

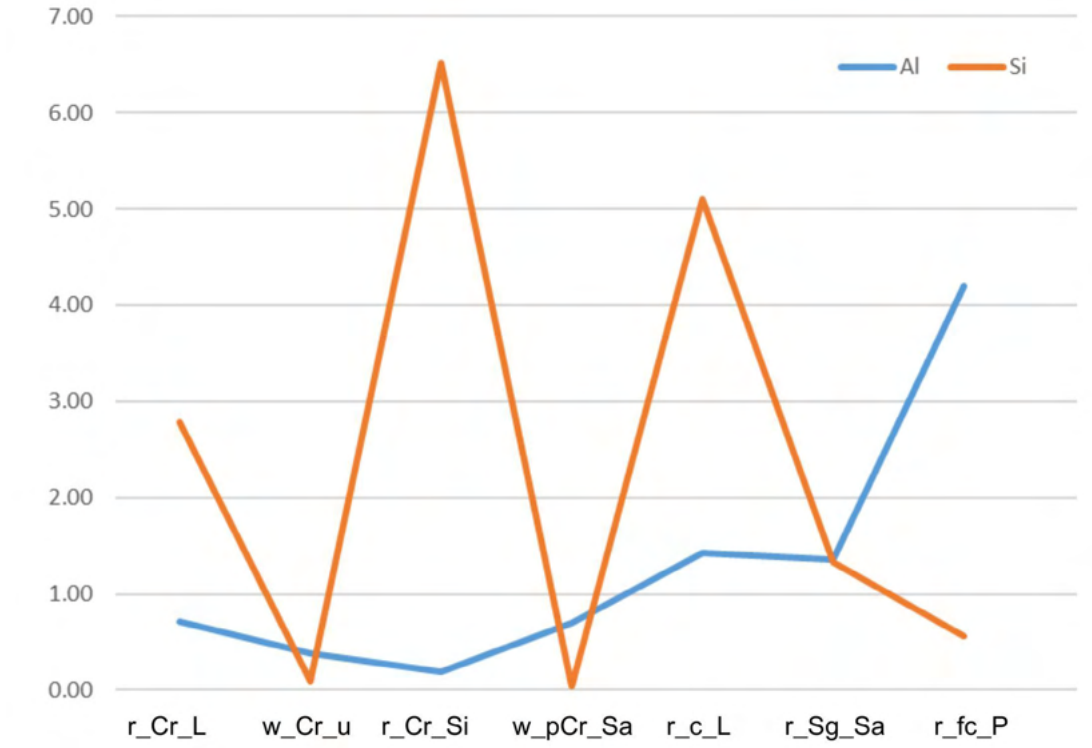

Figure 113. Graph of the occurrence of Al and Si in different samples [[r_Cr_L: unworked ligurian *C. rubrum*; w_Cr_u: worked-polished *C. rubrum*; r_Cr_Si: sicilian *C. rubrum* collected on the beach; w_pCr_Sa: sardinian pinkish-to-white worked coral; r_c_L: Ligurian white coral; r_Sg_Sa: Sardinian *S. gaederopus*; r_fc_P: Piedmont fossil coral].

Table 17 summarises the main characteristics of the various calcite materials examined, including their characteristic surface microstructures, magnesium content, and polyene presence.

7.1.2. Archaeological finds

The results reported in this paragraph refer to the analysis of 264 archaeological finds of various types, examined using the same archaeometric protocol used for the study of modern comparison samples.

7.1.2.1. Optical microscopy

It allows to detect the μ-morphologies typical of *C. rubrum* (Tab. 18; Debreuil *et al.* 2011; Fan 2018; Fürst *et al.* 2016; Perrin *et al.* 2015; Vielzeuf *et al.* 2008). In unprocessed or poorly processed artefacts, these features are well preserved (34 cases out of 46; ≈ 74%); for highly processed artefacts, their incidence is significantly lower (19 cases out of 149; ≈ 13%;). These structures are visible also when low to medium Mg-calcite (LMC/MMC) is identified by other techniques.
46 unprocessed / poorly-processed archaeological finds were examined (6 raw coral branches, 12 beads, 9 composite bow fibulae and 19 pendants). The most common features identified are longitudinal crenulations (30 cases; Fig. 114a), corresponding to the position of the gastrodermal canals in *C. rubrum*. In few cases (6 finds; Fig. 114b), concentric structures are also identified, corresponding to the growth rings of the organism (i.e. medullar region). In 3 cases, deeper furrows are visible (Fig. 114c), traces of bio attack by other organisms originating in post-depositional diagenesis or before collection on the beach (see section 7.1.1.1)[8].
In the decorations of elaborated artefacts (e.g., leech fibulae with circular insets: Ø ≈ 2 mm), garland-like morphology is the most abundant feature (17 cases; Fig. 114d), corresponding to a wavy edge visible in the cross-section of the coral branch. In one case, the presence of medullar region concentric structures is visible (Fig. 114e), while longitudinal crenulations are discernible in two cases (Fig. 114f).
Other than coral, in five cases[9] typical bone μ-morphologies are observed (Figs. 114b, 114c, 115b): mosaic morphology, cracking on the surface and μ-porosity in the inner-parts; Tappen, Peske 1970; Pokines *et al.* 2018). Two of these finds (D1667 and St. 124133) are identifiable as burnt bone remains, due to the presence of characteristic bone structures (e.g., trabeculae; Fig. 115b) and factors indicating combustion. These include their colouring and characteristic deformations, such as a mosaic of polygonal micro-fractures (Fig. 114g) and conchoid fractures (Fig. 114h; Gonçalves *et al.* 2011; Krap *et al.* 2017). In other cases, different μ-morphologies were also observed: i.e. Motto Lagone bead (T2) shows a microcrystalline structure (Fig. 115c), while a bead of unknown provenance (inv. no. MV5916) has a structure suggesting deer antler use (characteristic granulated pattern: Fig. 115d; Paral *et al.* 2007).
However, in most cases (76%: Fig. 116) optical microscope does not identify any specific morphology. In circular decorations, the whitish material often has a compact and pasty appearance (Fig. 115e), indicating either the possible use of a paste or an alteration by recrystallisation of the original material.
Metal alteration by-products often form above the whitish decoration, obliterating it completely or in part. In most cases, they form from the edge towards the core of the hole, but sometimes also from the core to the edge (Figs. 115d, 115e). They are generally greenish in colour; seldom a blue hue is also recorded (Fig. 115h)[10], sometimes erroneously interpreted as a vitreous glaze (i. e. Montebelluna, loc. Posmon). Such bluish hue recurs in the Venetic context, maybe due to a different soil composition[11].

8 For further examples see Appendix 1, Figs. 215-220.

9 Inv. no. St. 1993, St. 124133, D1667, D2109. Identification is more complex for a bead fragment (St. 18.236/CT1141; Fig. 99.a) due to the treatment of the material used to make the object; in this case, it could be either bone or deer antler.

10 Inv. no. 217, I.G. 304784, I.G. 304780, I.G. 312348, IG. 34914.

11 For further examples see Appendix 1, Figs. 219-220.

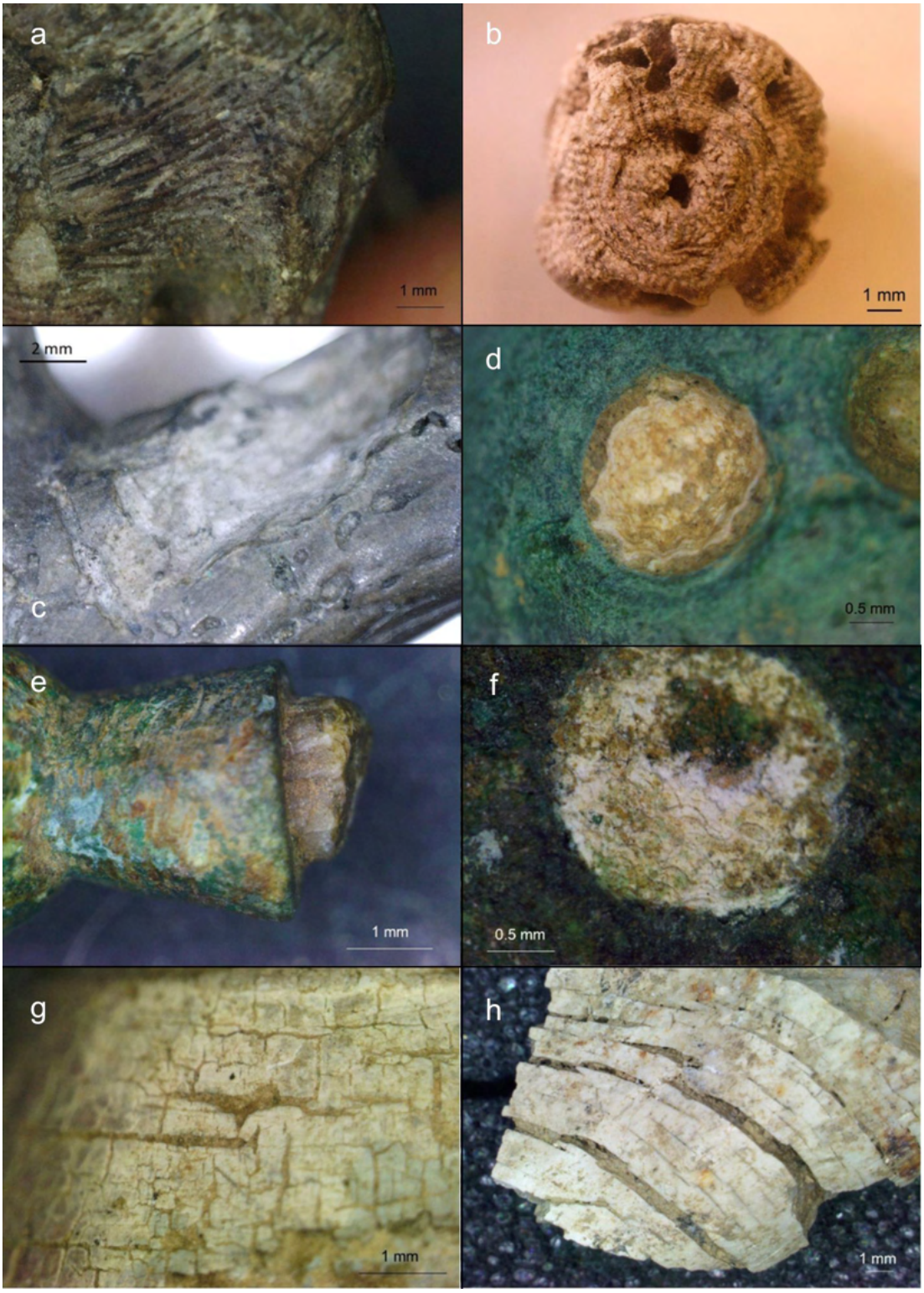

Figure 114. a) Golasecca - Longone al Segrino pendant (inv. no. D1668; Museo Giovio Como): longitudinal crenulation; b) Pieve d'Alpago, Pian della Gnela - Bead (inv. no. I.G.355534; SABAP): medullar region concentric structures; c) Golasecca - Longone al Segrino pendant (inv. no. MV103; Museo Archeologico Villa Mirabello Varese): biological attack features; d) Borgonovo V. T. - Leech fibula with circular insets (inv. no. 20.S258-2.118; Museo Archeologico della Val Tidone): garland-like morphology; e) Pontecurone - Fibula (inv. no. 23.M.380-9.6; Musei Reali Torino): crenulation; f) Castelletto Ticino - Vigevano (?) - Leech fibula with circular insets (inv. no. 946; Museo Novara): medullar region concentric structures; g) Como, Ca' Morta - Composite bow fibula (inv. no. St 1993; Museo Giovio Como): burnt bone features; h) Como, Ca' Morta - Fragments (inv. no. St. 124133; Museo Giovio Como): burnt bone features.

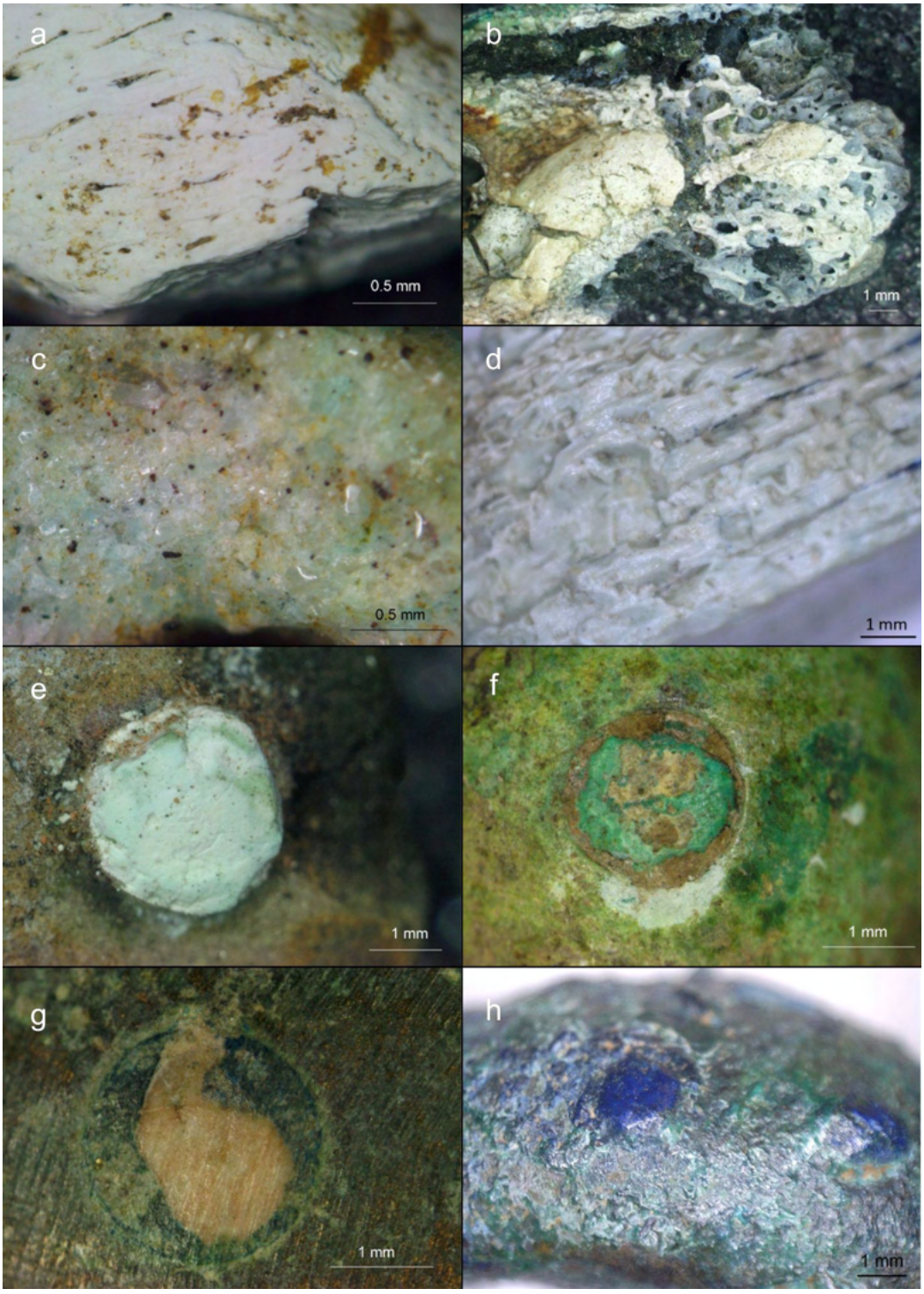

Figure 115. a) Castelletto Ticino - Bead (inv. no. CT1141; 18.236; GSAC); b) Golasecca - Fragment (inv. no. D1667; Museo Giovio Como): bone features: trabeculae; c) Motto Lagone - Bead (grave 2; Arona Museum): crystalline structure; d) Unknown provenance - Bead (inv. no. MV5916; Museo Archeologico Villa Mirabello Varese): deer antler's characteristic granulated pattern; e) Golasecca - Leech fibula with circular insets (inv. no. D2065; Museo Giovio Como): whitish inlay; f) San Bernardino di Briona - Leech fibula with circular insets (inv. no. 23-M380-9.1; Musei Reali): green metallic alteration products on the circular decoration; g) Como - Leech fibula with circular insets (inv. no. St. 57262; Museo Giovio Como): green metallic alteration products on the circular decoration; h) Montebelluna, loc. Posmon - Leech fibula with circular insets (inv. no. I.G. 304784, Montebelluna Museum): blue metallic alteration products on the circular decoration.

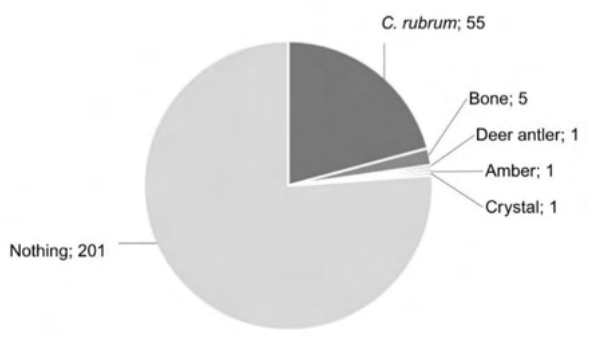

Figure 116. Graph concerning the incidence of µ-morphologies useful for material characterisation with respect to the whole archaeological record under examination.

7.1.2.2. Raman analysis

Raman analyses were carried out on almost all archaeological finds (Tab. 20) using two instruments with the same laser wavelength (see section 6.2.2.2): a bench-top µ-Raman (246 finds) and a portable-one (18). Higher fluorescence effects were recorded using the portable instrument.

In 7 cases, analyses were not performed due various reasons (e.g., artefact too large or too small). For 56 finds (21% of the record), no signal (or only fluorescence) was observed – and in 13 finds the interpretation was doubtful. In all other cases, various materials were identified – but mainly Ca-carbonate. Sometimes, aragonite and calcite were discriminated, due to the typical signals (Fig. 117).

Contextual presence of calcite (signals at 1083/1094, 714/717, 282/289 and 153/159 cm^{-1}) and polyenes (signals at 3028/3035, 2631/2638, 2530, 2253/2256, 2143/2149, 1518/1521, 1294/1298, 1134 and 1017/1020 cm^{-1}) suggests presence of *C. rubrum* (Fig. 118) (though other validations should also be done: e.g., by SEM-EDS; see section 6.2.2.5). In many cases, only the bands of calcite are visible (Fig. 119), revealing the absence of polyenes bands. At times fluorescence allows only the identification of the main $CaCO_3$ peak at ≈ 1086 cm^{-1} (Fig. 120), without discerning the different polymorphs. Calcite, aragonite and vaterite, in fact, can be distinguished basing on minor peaks position (Tab. 19; Barnard, de Waal 2006). In one case (linear decoration on a grooming tool; Fig. 121), presence of aragonite is observed (main peak at 1087 cm^{-1}, doublet at 710-706 cm^{-1} and bands at 156, 207, 271 cm^{-1}). Various strategies can be adopted to minimise fluorescence, such as baseline correction algorithms or changing the excitation laser wavelength. In this study, we opted for the green laser due to its efficacy in identifying polyenes (see section 6.2.2.2; Figs. 91-92), but a red laser would be more effective in identifying carbonate polymorphs when fluorescence hinders identification.

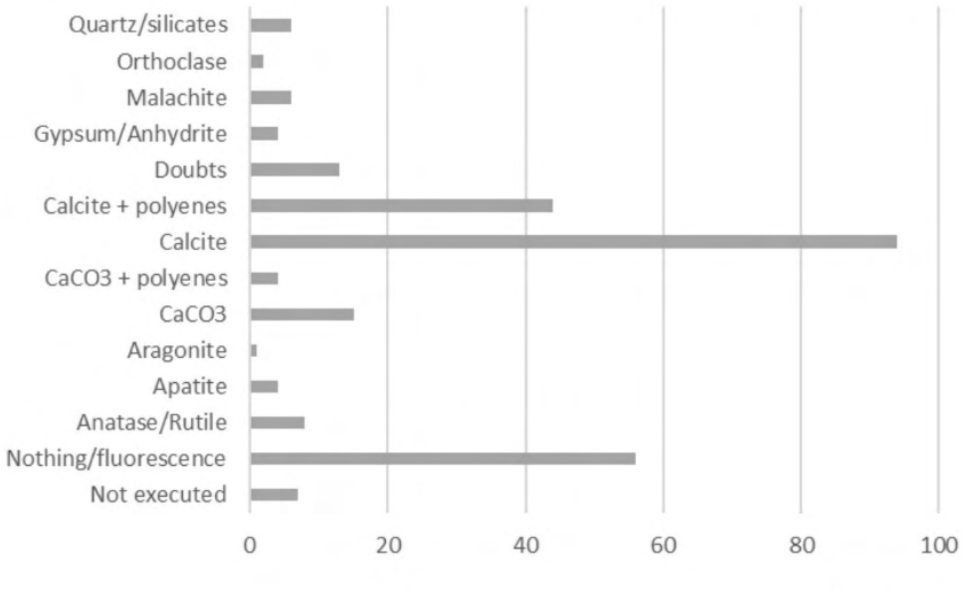

Figure 117. Inorganic compound identified by Raman analysis and abundance.

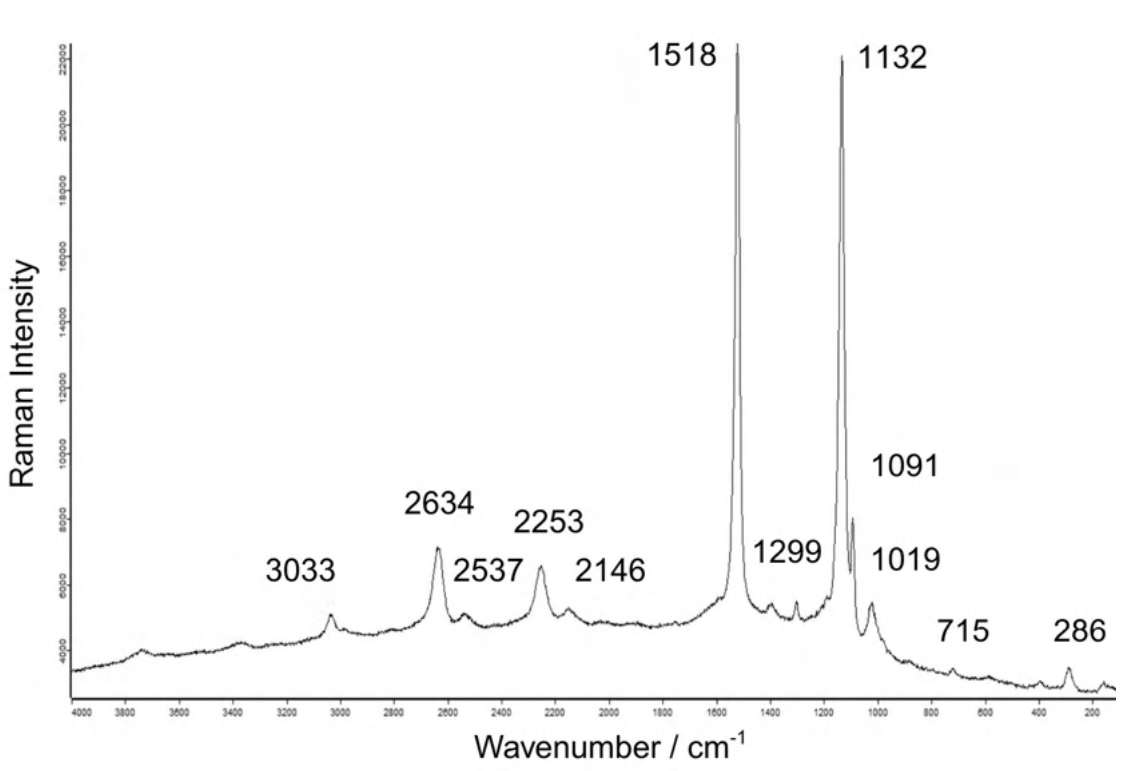

Figure 118. Raman spectrum of whitish circular decoration on Motto Lagone leech-fibula (magnification 20X, filter d 0.3): polyenes and calcite.

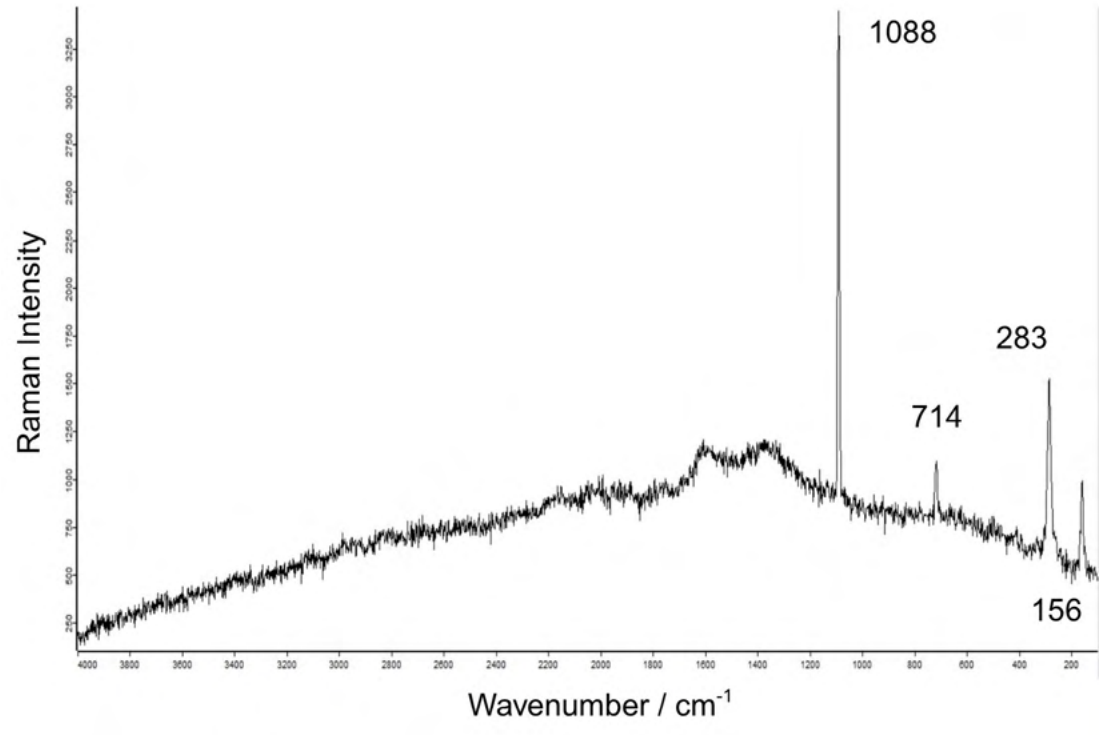

Figure 119. Raman spectrum of whitish circular decoration on Como (Ca' Morta, Rebbio, Cava Ballerini) leech fibula (inv. no. St. 879; magnification 10X, filter d 0.3): calcite.

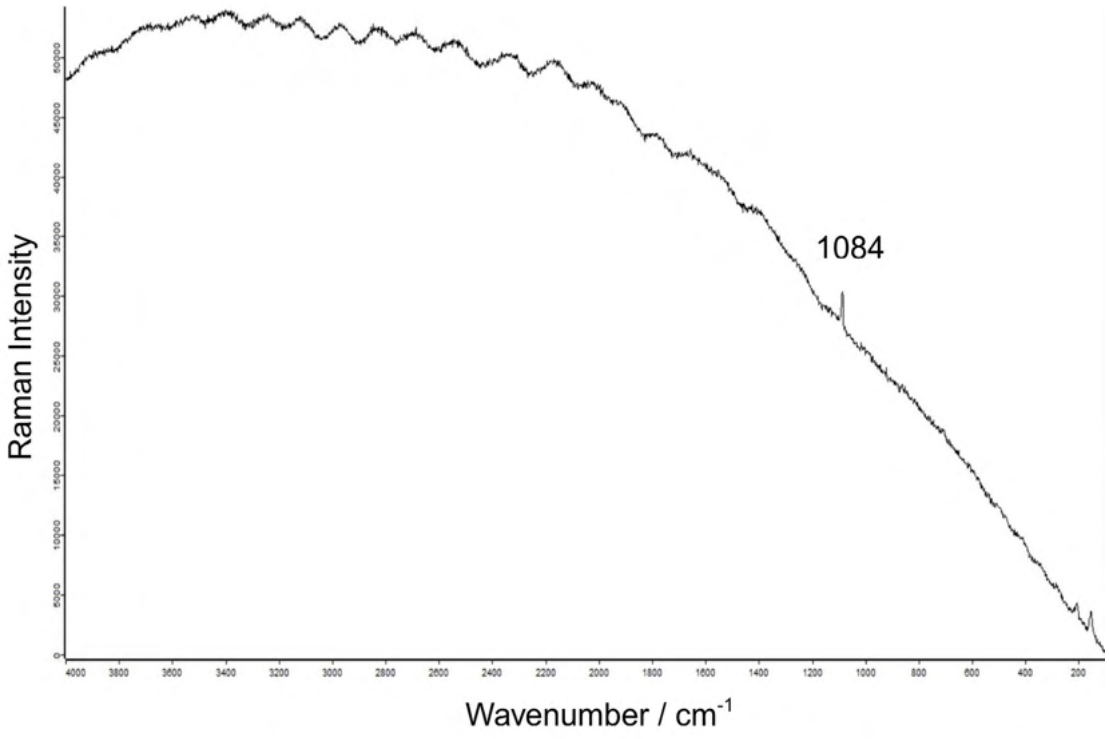

Figure 120. Raman spectrum of whitish inset on a bronze fragment from Pontecurone (AL; inv. no. 23.M.380-9.6): $CaCO_3$.

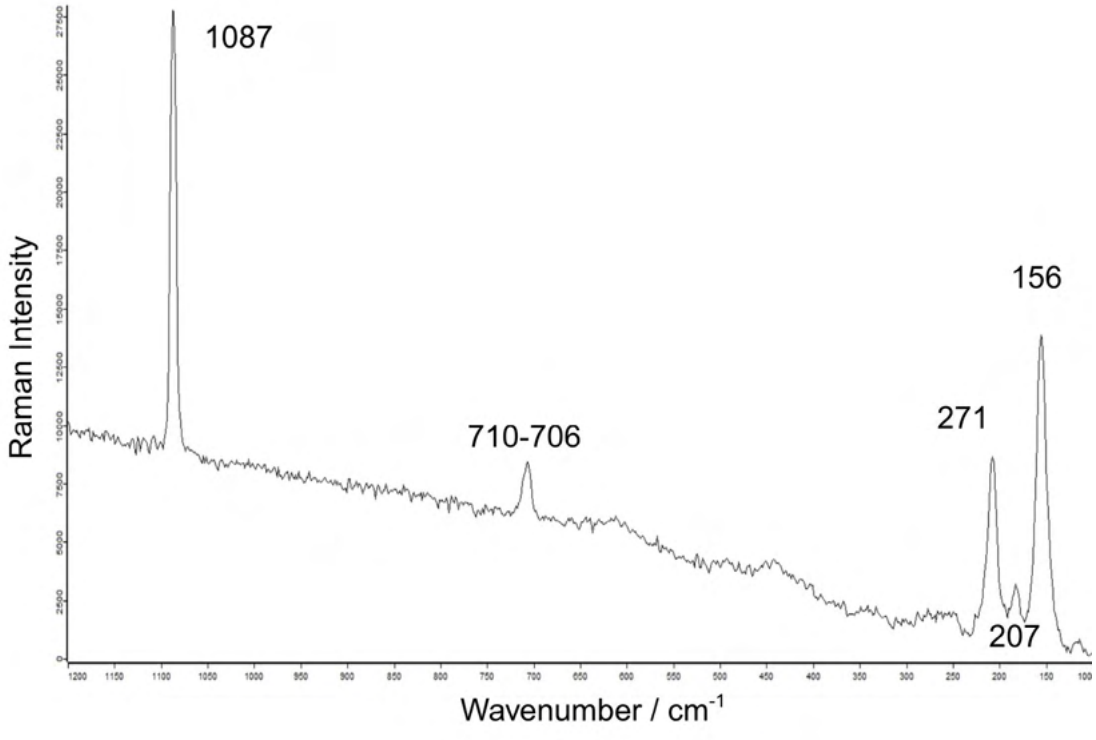

Figure 121. Raman spectrum of whitish linear decoration on a grooming tool (tweezer) from Piovego (PD; T95.10): detail of the part of interest, showing characteristic peaks of aragonite.

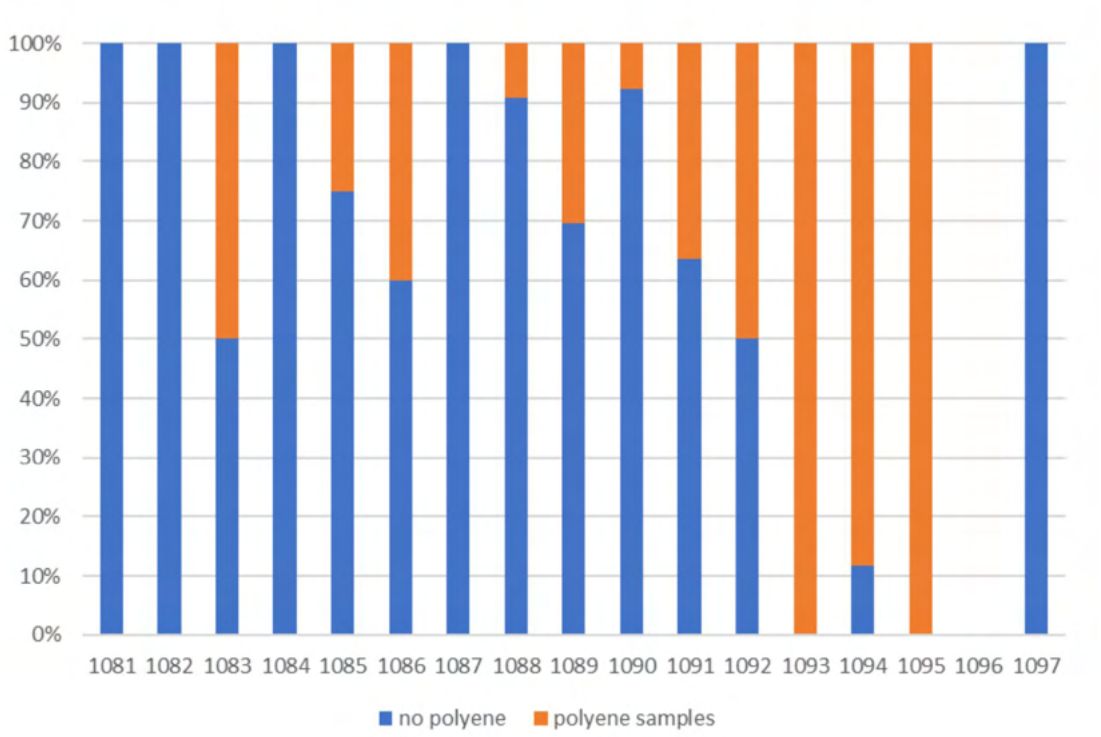

Figure 122. Graph showing the frequency of different values for the main carbonate peak (v_1) in spectra with (in red) and without (in blue) polyenes, as a percentage of the total (see Appendix 2, Tab. 38).

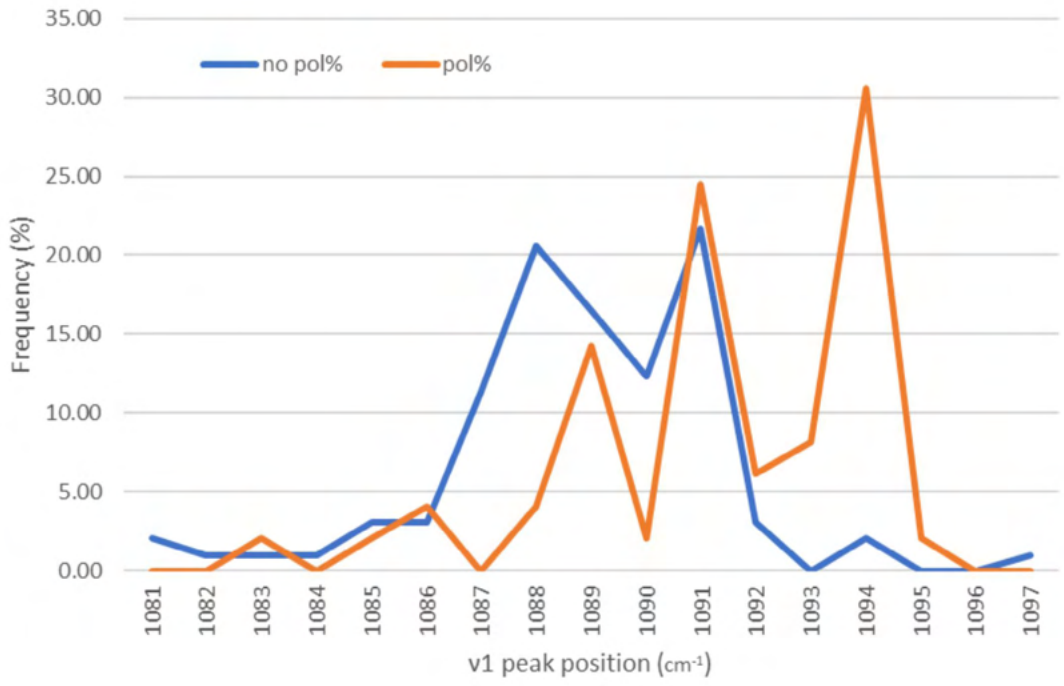

Figure 123. Graph showing the frequency of different values for the main carbonate peak (v_1) in spectra with (in red) and without (in blue) polyenes, as a percentage of the total (see Appendix 2, Tab. 38).

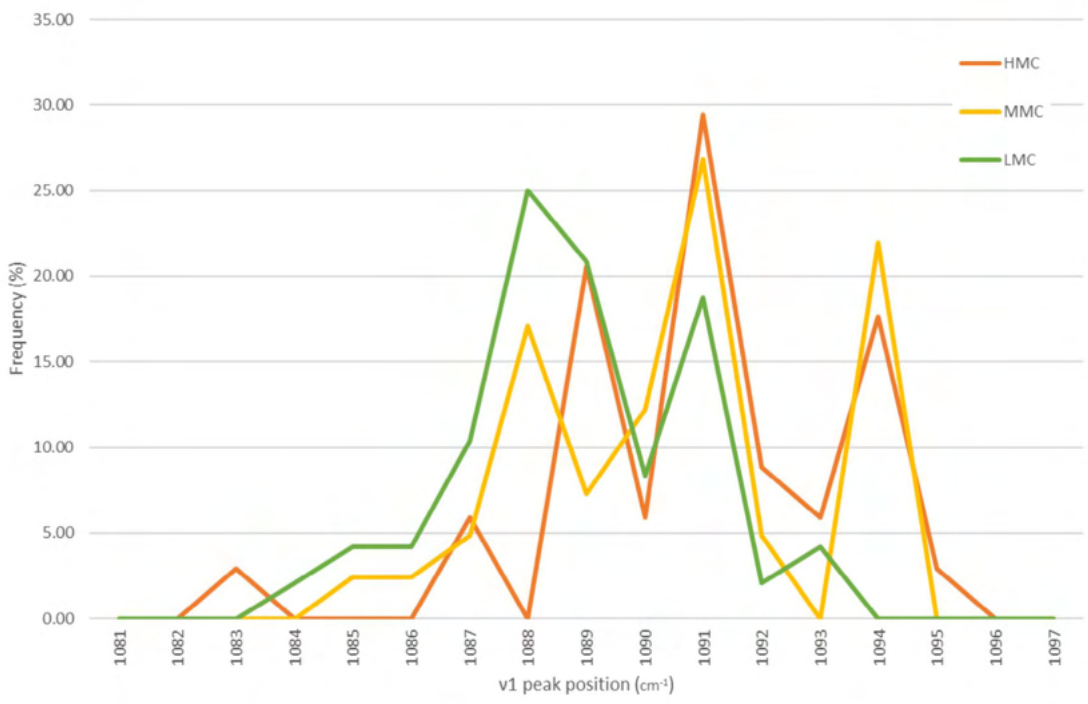

Figure 124. Graph of the frequency (as a percentage of the total) of the different values for the main carbonate peak (v_1) in the spectra of high/medium/low magnesium calcite (HMC/MMC/LMC) (see Appendix 2, Tab. 39).

The main band of Ca-carbonate shows a systematic shift at 1082 cm^{-1} in the spectra collected with the portable instrument. Conversely, in those obtained with the bench-top instrument this band has variable shifts at higher and/or lower wavenumbers (from 1081 to 1094 cm^{-1}). By processing these spectral data, the ν_1 peak of carbonate without polyenes is mostly located in the 1087-1090 cm^{-1} range, while if polyenes occur the range is 1093-1095 cm^{-1} (Figs. 122-123; Appendix 2, Tabs. 38, 40). This behaviour could also be related to a variation in the Mg-content of the carbonate (Bischoff *et al.* 1985; Borromeo *et al.* 2017; Edwards *et al.* 2005; Fürst *et al.* 2016; Macchia *et al.* 2016; Urmos *et al.* 1991), which is supported by comparative analyses performed on modern *C. rubrum* (see section 7.1.1.2). Although the trend is not so clear-cut – straight comparison with semi-quantitative SEM-EDS data on archaeological samples indicates that this band occurs at lower wavenumbers for LMC and at higher ones for MMC/HMC, (Fig. 124; Appendix 2, Tabs. 39-40). In conclusion, the exact position of the main carbonate band in Raman spectra appear to be partly related to the Mg-content, but this evidence is not so reliable to be used as a substitute for chemical analyses[12]. In some cases, calcite and anhydrite ($CaSO_4$; bands at 1010 and 497 cm^{-1}) appear together (Fig. 125), suggesting a possible alteration of calcite into gypsum ($CaSO_4 * 2H_20$; see section 7.1.4) followed by heat treatment. In one case (Fig. 126) gypsum/anhydrite were identified as the sole components (bands at 3410, 1010, 497 cm^{-1}. Sometimes, calcite and apatite [$Ca_5(PO_4)_3(Cl/F/OH)$; signals at 965, 585, 438 cm^{-1}] are present suggesting either the use of both materials in the decoration or contamination by human remains in burial conditions (Fig. 127). TiO_2, in the form of rutile (bands at 801, 614, 446, 244 cm^{-1}) or anatase (638, 516, 395, 142 cm^{-1}), was also found and related to modern highlighting of the decorations (Fig. 128).

As far as organic compounds are concerned, beeswax is sporadically identified (10 cases, some dubious) as well as pine resin or Paraloid (14 cases: signals at 2939, 1734, 1455, 812 cm^{-1}) (Fig. 129). In one case (leech fibula with insets, G-type; inv. no. St. 57244), calcite, polyenes and beeswax (2883-2846-1439-1298-1134 cm^{-1}) are detected simultaneously (Fig. 130). Beeswax could represent a binder for the decoration, but its signals are similar to those of synthetic wax. Besides, both beeswax and synthetic wax have long been used as restoration materials and, without a restoration report, it is impossible to verify their origin.

12 To see detailed data: Appendix 2, Tabs. 38-40).

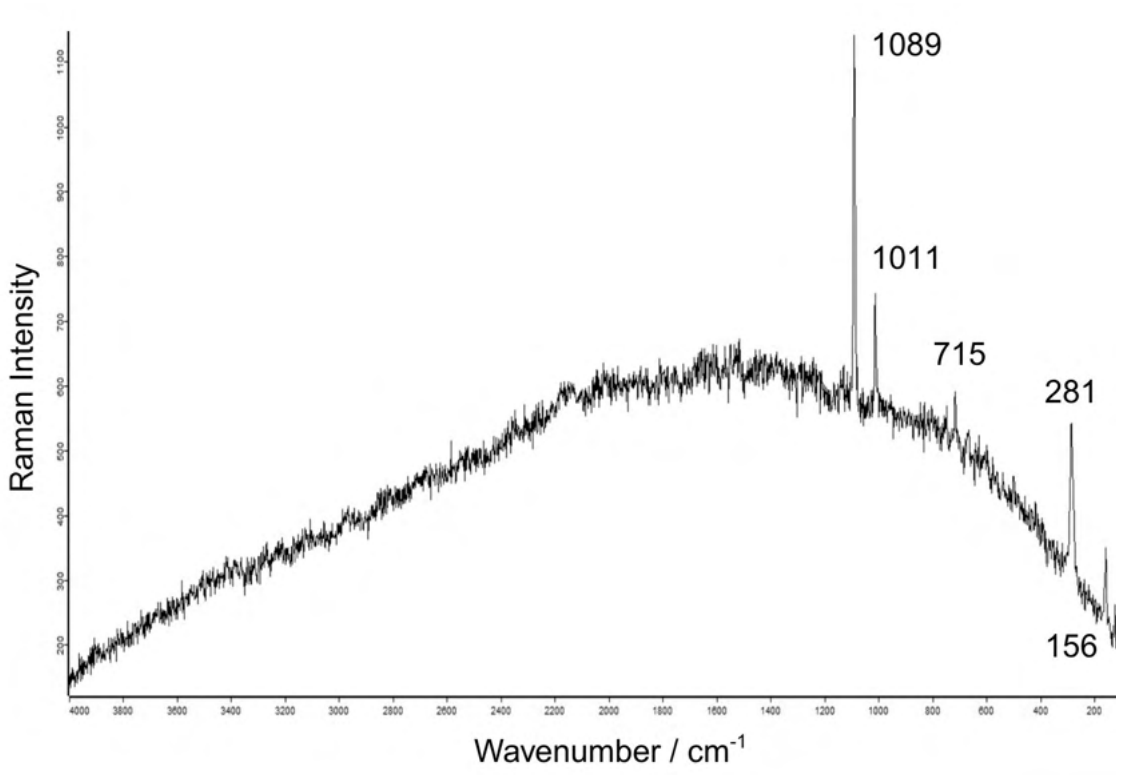

Figure 125. Raman spectrum of whitish circular decoration on Golasecca leech fibula (inv. no. D2065; magnification 10X, filter d 0.3): calcite and anhydrite.

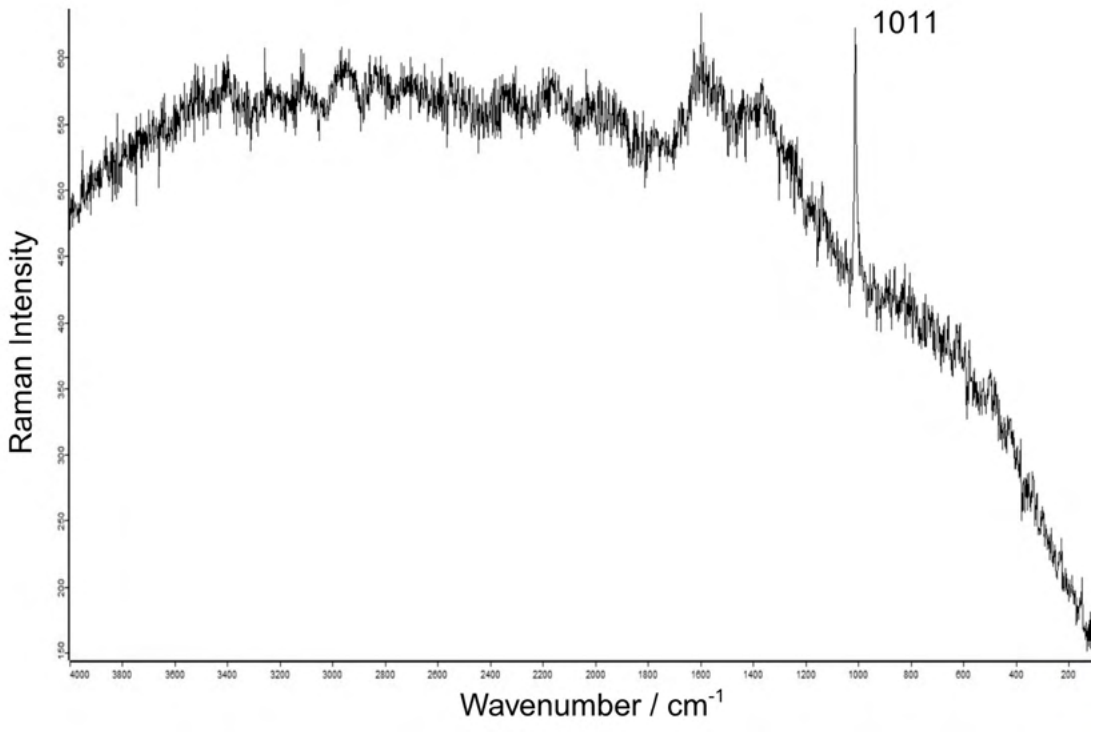

Figure 126. Raman spectrum of whitish Longone al Segrino type pendant from Como, Ca' Morta, grave 302 (inv. no. St. 33593; magnification 10X, filter d 0.3): gypsum.

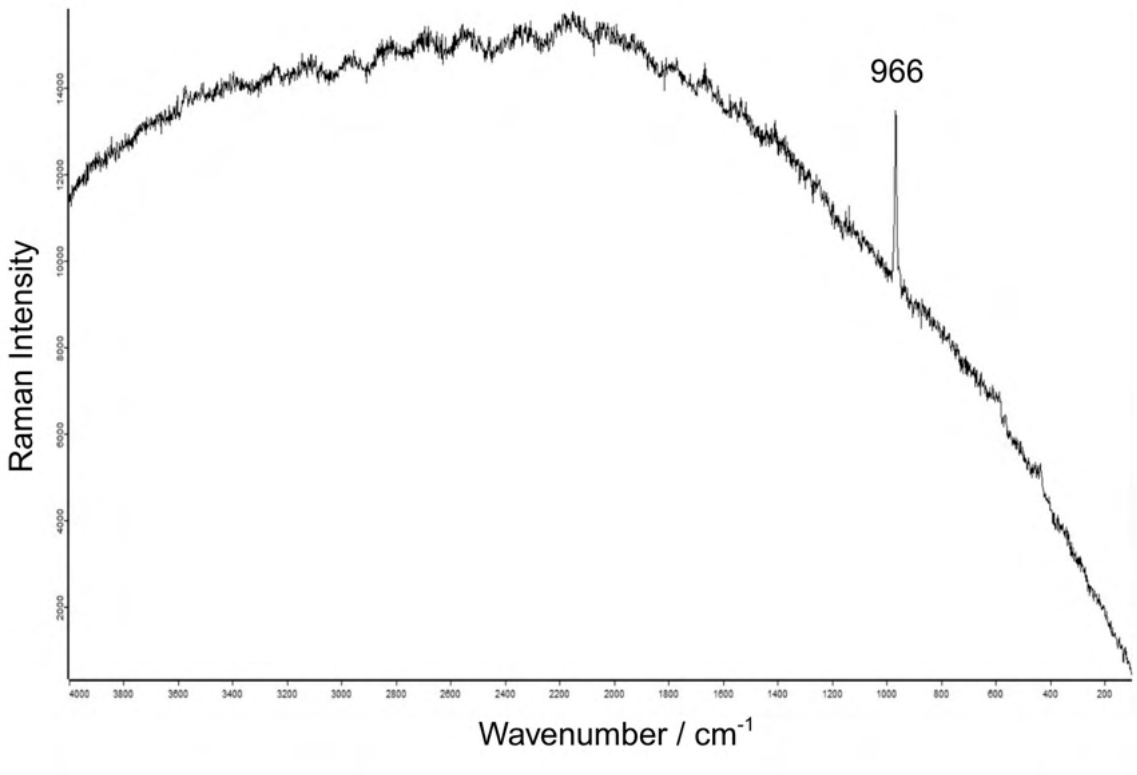

Figure 127. Raman spectrum of whitish Longone al Segrino type pendant from Como, Ca' Morta, grave 200 (inv. no. St. 124142; magnification 10X, filter d 0.3): apatite. Further points of analysis on the same find show the clear presence of calcite; the signs of apatite are probably attributable to contamination by bone tissue referable to the deceased.

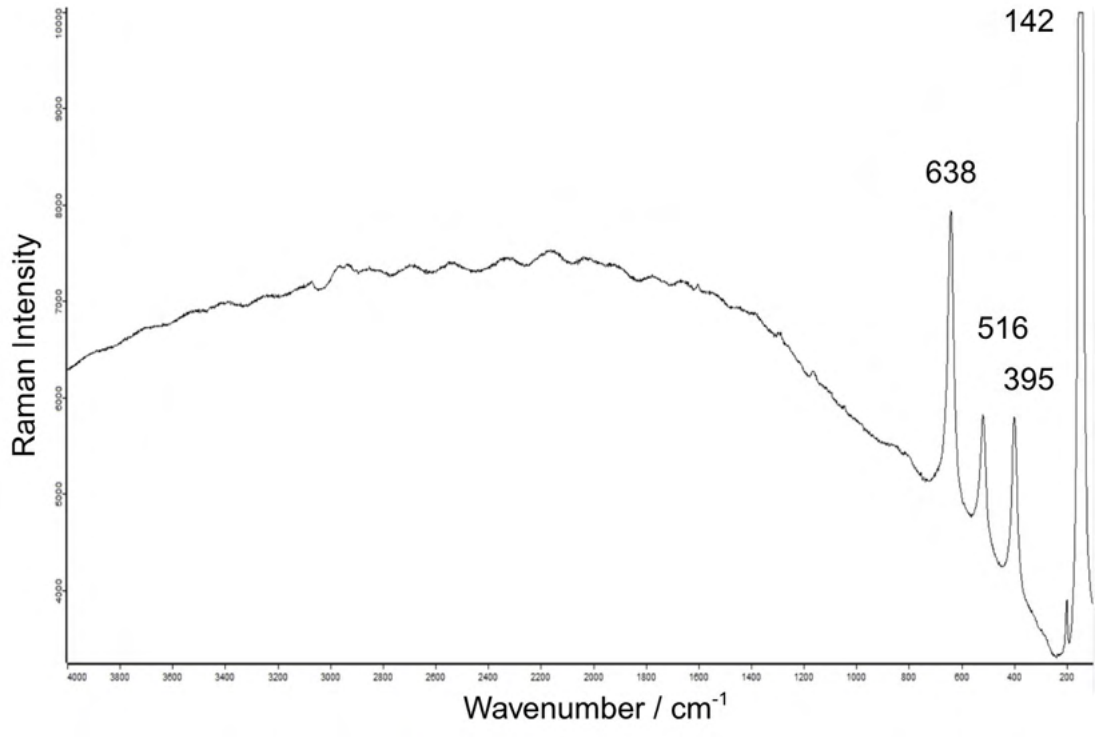

Figure 128. Raman spectrum of whitish decoration on a fibula from Parre (inv. no. 40; magnification 10X, filter d 0.3): anatase.

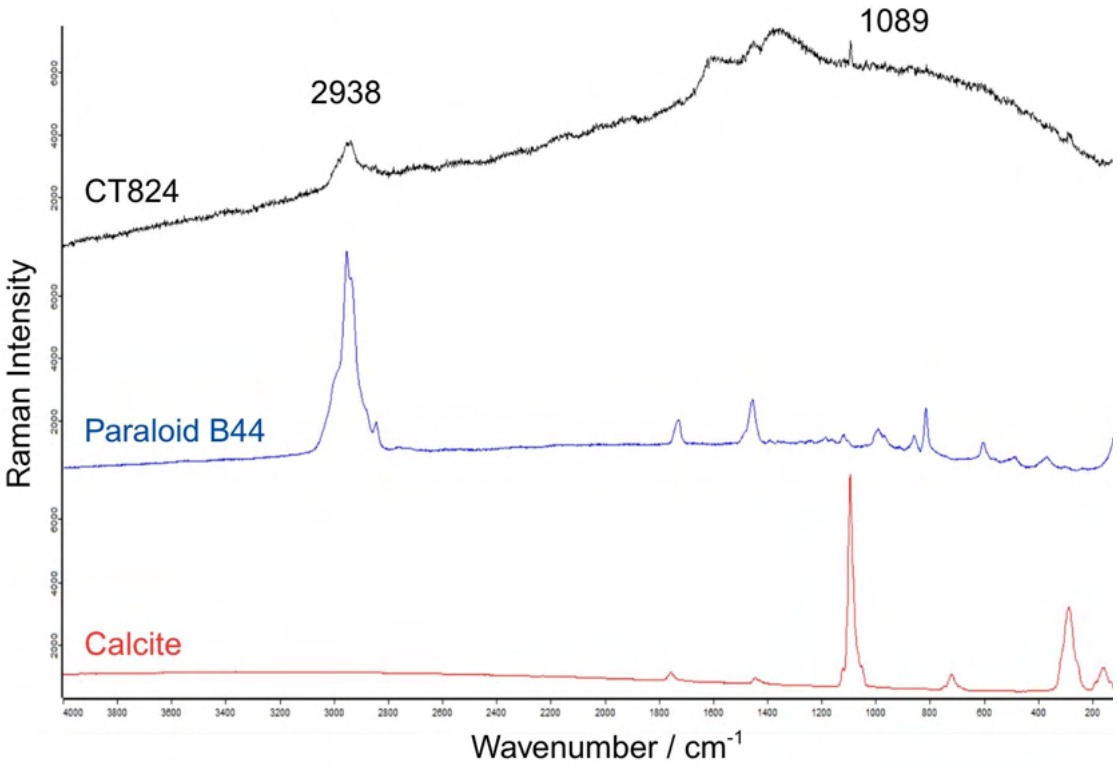

Figure 129. Comparison of Raman spectra obtained from analysis of the find CT824 in black, Paraloid B44 in blue and calcite in red; 10X magnification, D0.3 filter.

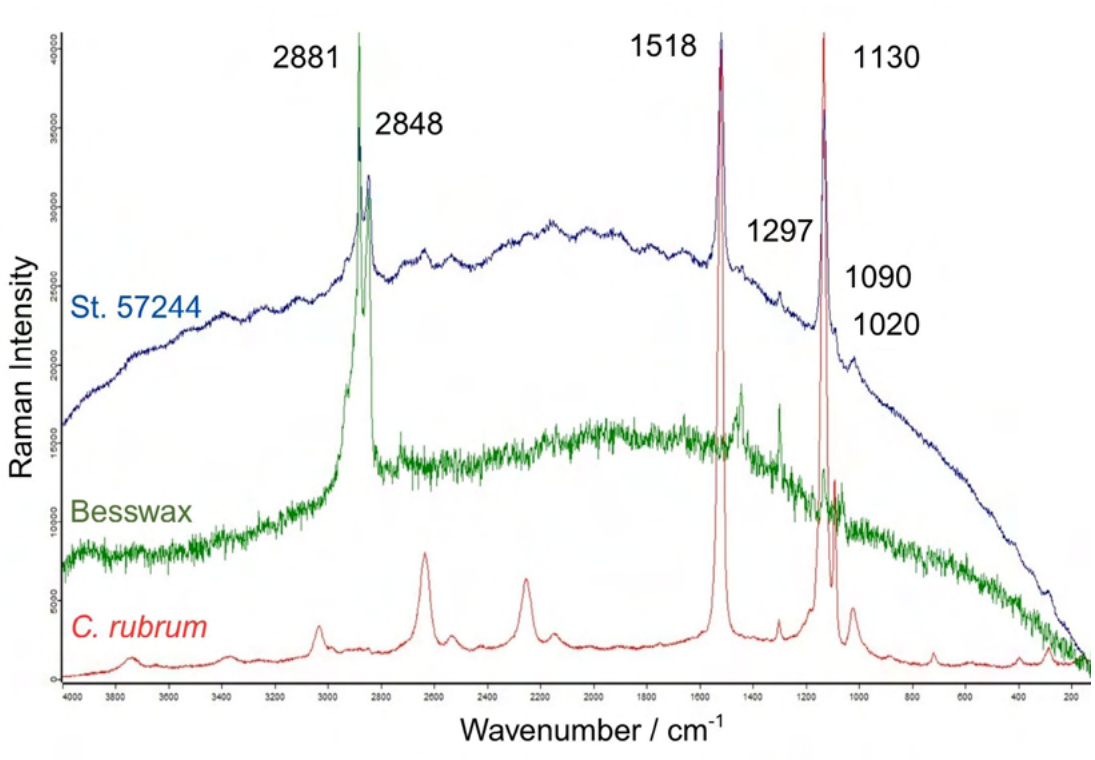

Figure 130. Comparison of Raman spectra obtained from analysis of the circular decoration of find St57244 in blue, beeswax in green and *Corallium rubrum* in red; 10X magnification, D0.3 filter.

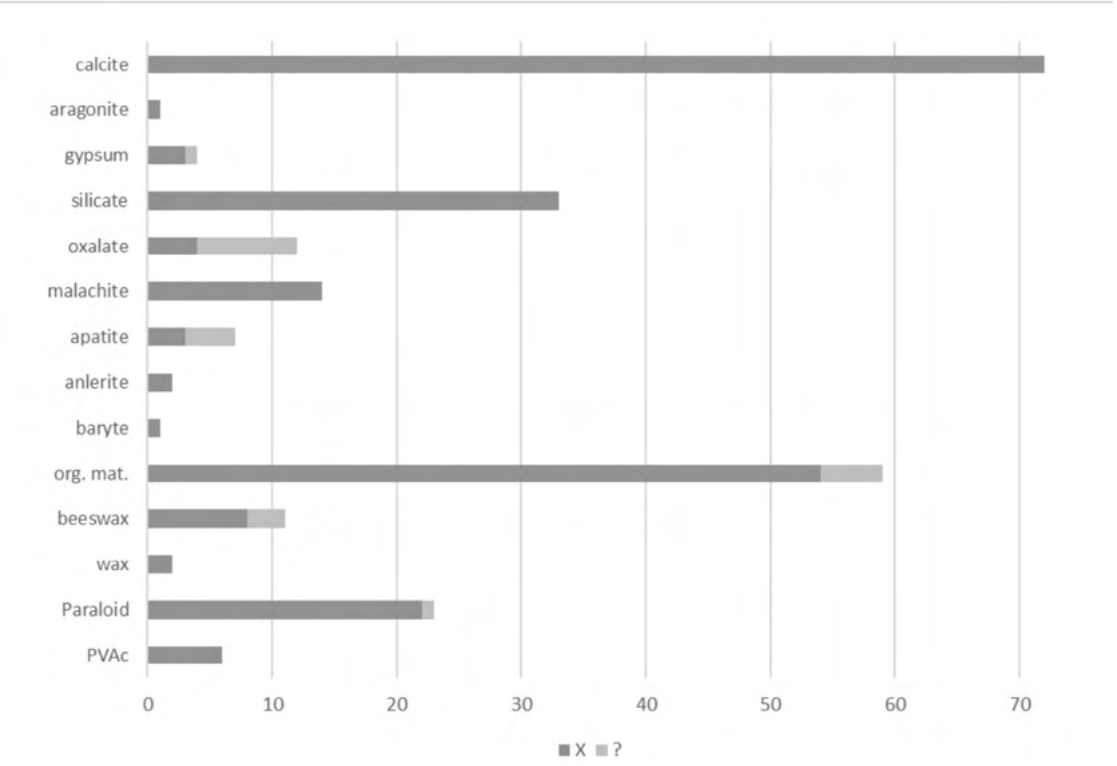

Figure 131. Compounds identified ('X') by FT-IR analysis and dubious identifications ('?').

7.1.2.3. FT-IR analysis

104 µ-samples, collected from 264 archaeological finds, were analysed. In a few cases, multiple samples were extracted from a single find, but the obtained results are comparable and will be treated uniquely.

Organic and inorganic and materials were identified (Tab. 21; Fig. 131), mostly calcite (69%), followed by quartz and silicates (32 %) and malachite [$Cu_2(CO_3)(OH)_2$; 13 %]. Aragonite is only occasional (1 case), with gypsum (3 cases), oxalates (4 cases), apatite or hydroxyapatite ($Ca_5(PO_4)_3(OH)$; 3 cases), antlerite ($Cu_3(SO_4)(OH)_4$; 2 cases) and baryte ($BaSO_4$; 1 case). Calcite, aragonite and apatite could result from decorative materials, but apatite may be also related to a bone contamination from the burial. Gypsum could indicate the presence of a pigment, as well as result from the alteration of calcite. Oxalates are also likely to be attributed to calcite alteration products. Malachite and antlerite were probably derived from alteration products of the copper alloy. Silicates, quartz and (perhaps) barite, are indicative of traces of depositional soil.

Main Ca-carbonate band is located at ≈ 1450 cm^{-1} (generally saturated in our samples), related to the C=O asymmetric stretching vibration ν3. Calcite shows signals at 2513, 1796, 1450, 876, 711 cm^{-1} (Fig. 134); aragonite at 1784, 1450, 1086, 858, 716, 713, 700 cm^{-1} (Fig. 135). The latter is distinguishable by the presence of a doublet around 700-713 cm^{-1} in our spectrum (703-708 cm^{-1}), together with other signals at 1787/1814, 1088/1118, 866/907 cm^{-1}. Calcite, in addition to the main peak, show signals at 1700/1804, 881/913, 733/750 cm^{-1} (Kaczorowska *et al.* 2003). Cu-carbonates (i.e. malachite and azurite) are characterized by CO_3^{2-} stretching bands at 1530-1350 cm^{-1}, O-C-O bending bands at 900-650 cm^{-1}, O-H stretching bands at 3700-3100 cm^{-1} ad O-H bending bands at 1100-1000 cm^{-1}.

Quartz and silicates show a strong Si-O stretching band near 1100 cm^{-1} and a Si-O absorption band at 1200-800 cm^{-1}. Quartz is identifiable by a small doublet near 790 cm^{-1} (Fig. 136). Sulfates (gypsum, baryte and anhydrite) show a strong S-O stretching band at » 1200-1050 cm^{-1} (which may split for specific sulfates) and a small band near 1000 cm^{-1} (S-O bending vibration), together with others at 700-600 cm^{-1}. Gypsum is identifiable by presence of the OH absorption band near 3500 and 1600 cm^{-1} (Derrik *et al.* 1999; Fig. 137). Hydroxyapatite (Fig. 138) is identified by bands at 3572 and 630 cm^{-1} (OH^- ion), 1460 and 875 cm^{-1} ($-CO^{3-}$), 1040, 1093 and 962 cm^{-1} (PO_4^{2-}),

plus others related to water peak (1640 and between 3250 and 3500 cm^{-1}: Farmer 1974).
Interpretation of organic signals was more complex. Peaks in the 2800-3100 cm^{-1} range are frequent and may indicate presence of organic compounds – such as binders, restoration products, contaminants or even the organic fraction of the coral, if preserved (Casanova *et al.* 2016; Derrik *et al.* 1999). Paraloid (signals at 2986, 2985, 1732, 1476, 1449, 1387, 1368, 1270, 1236, 1177, 1151, 1028, 988/976, 861/849, 754 cm^{-1}) seems to be the most abundant (21%): though its spectrum is similar to those of natural resins, in some cases it was possible to identify it by comparison with the pure Paraloid spectra (Fig. 132). Beeswax and synthetic wax have similar spectral signatures (distinguishable from a band at 1740 cm^{-1}, very intense for natural wax: Casanova *et al.* 2016) and were identified in 10% of the samples (Fig. 133). Polyvinyl acetate (PVAc), used for restoration purposes, was at times detected (6%). Signals in the 2800-3100 cm^{-1} region are perhaps traces of the organic fraction of the coral, as they also appear in spectra collected on modern corals (see section 7.1.1.2).

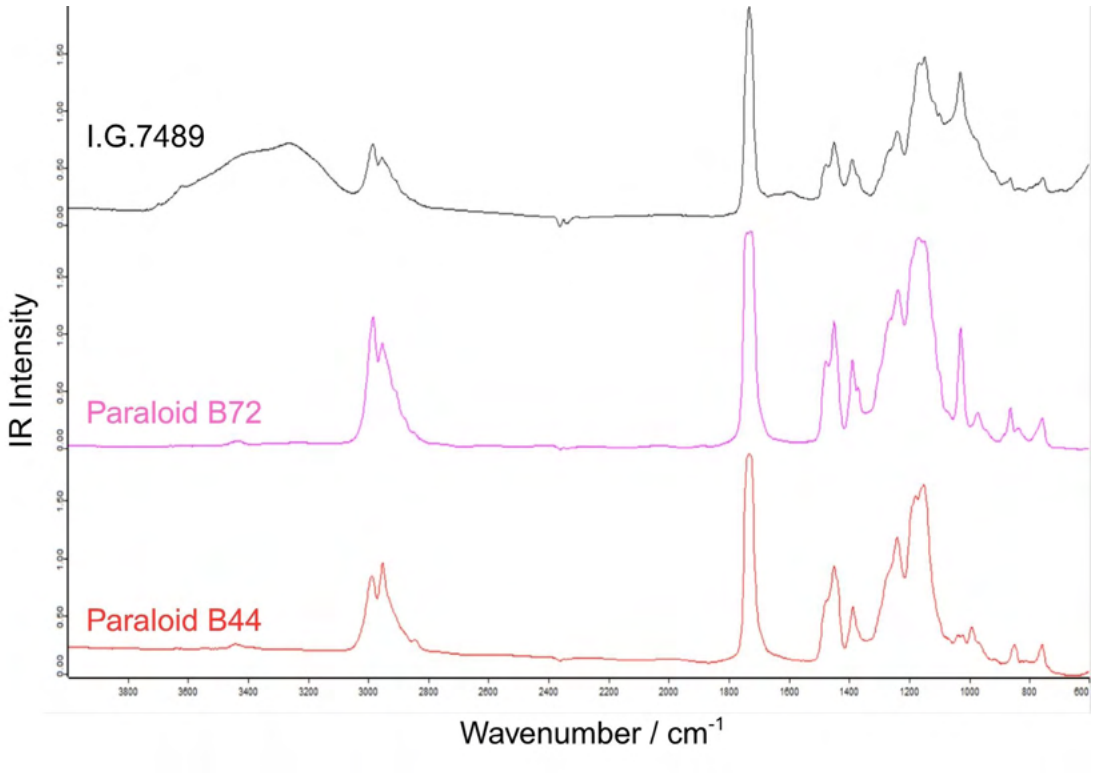

Figure 132. Comparison between FT-IR spectra of an archaeological sample (decoration of circular decoration of a leech fibula; inv. no. I.G. 7489; Montebelluna) in black and Paraloid B72 an B44 in fuchsia and red.

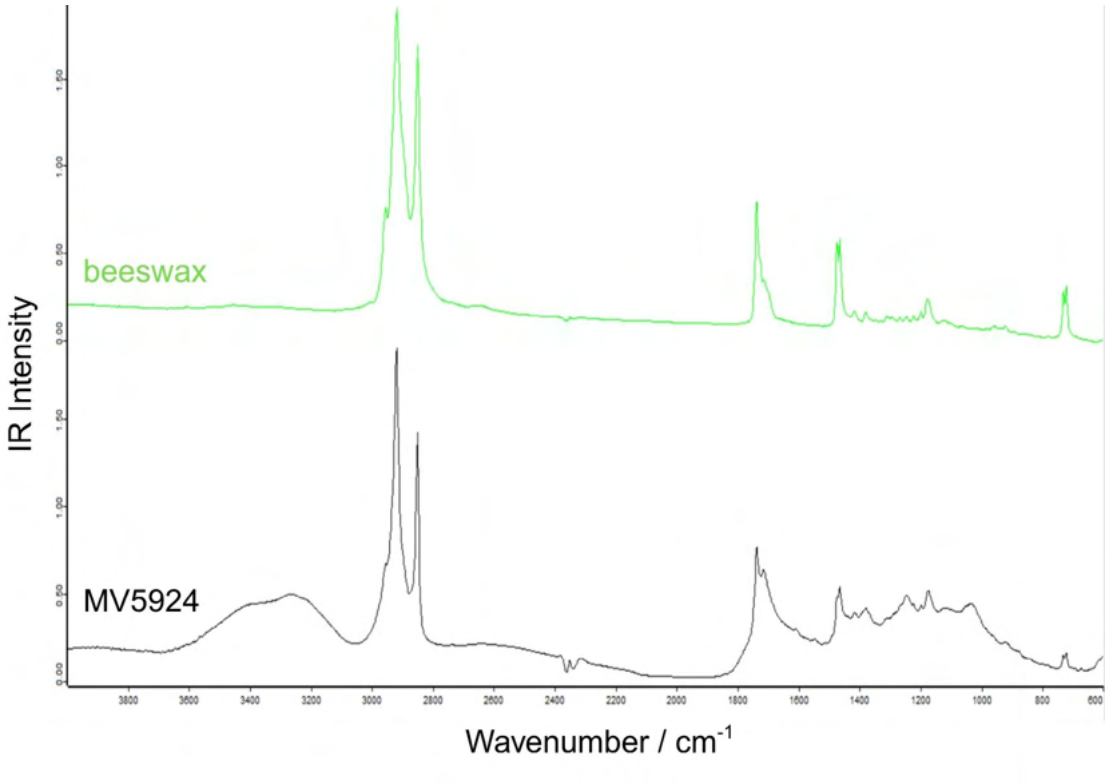

Figure 133. Comparison between FT-IR spectra of an archaeological sample (red bead; inv. no. MV5924; Varese Museum) in black and beeswax in green (comparison database).

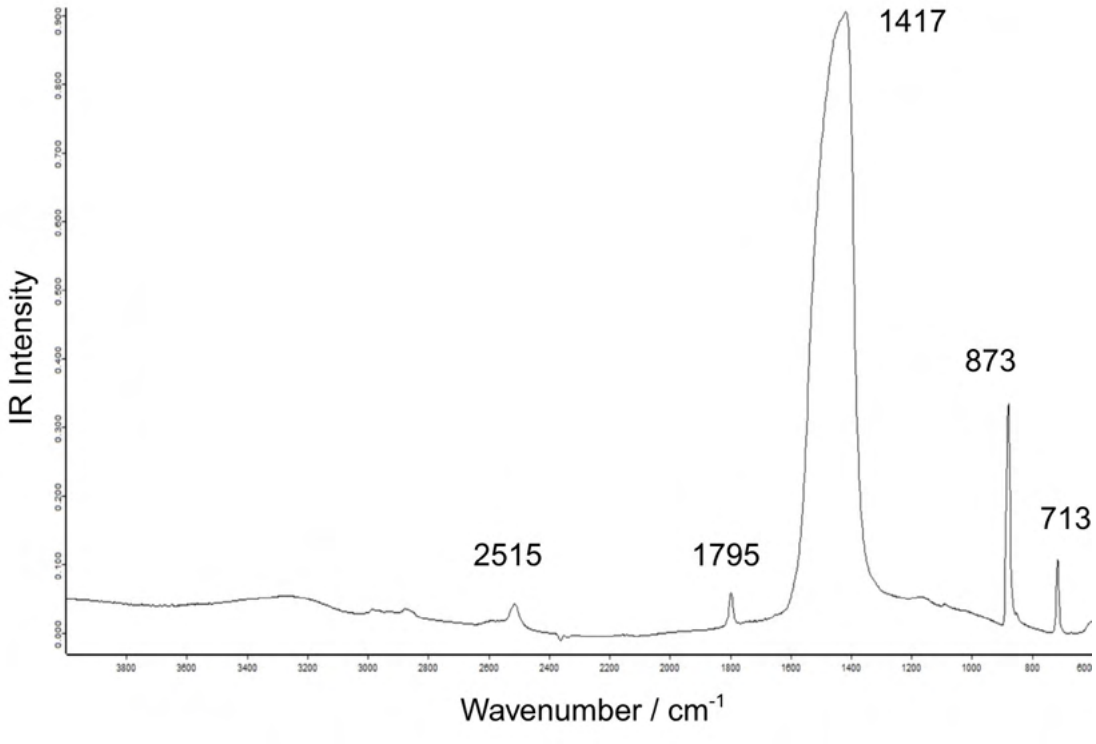

Figure 134. FT-IR spectrum of sample collected from a leech fibula with circular decoration (inv. no. 22.S288-1.205; Golasecca, loc. Galliasco): calcite.

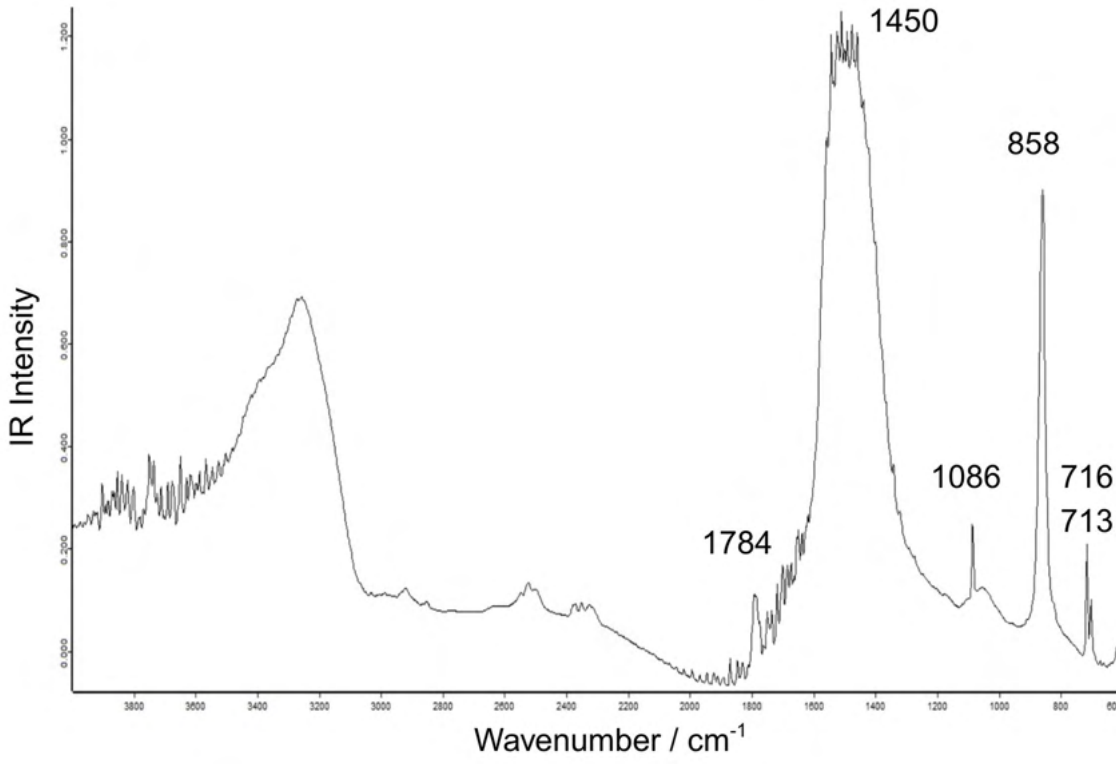

Figure 135. FT-IR spectrum of a sample collected from a grooming tool (tweezer; grave 95.10, Padova, loc. Piovego): aragonite.

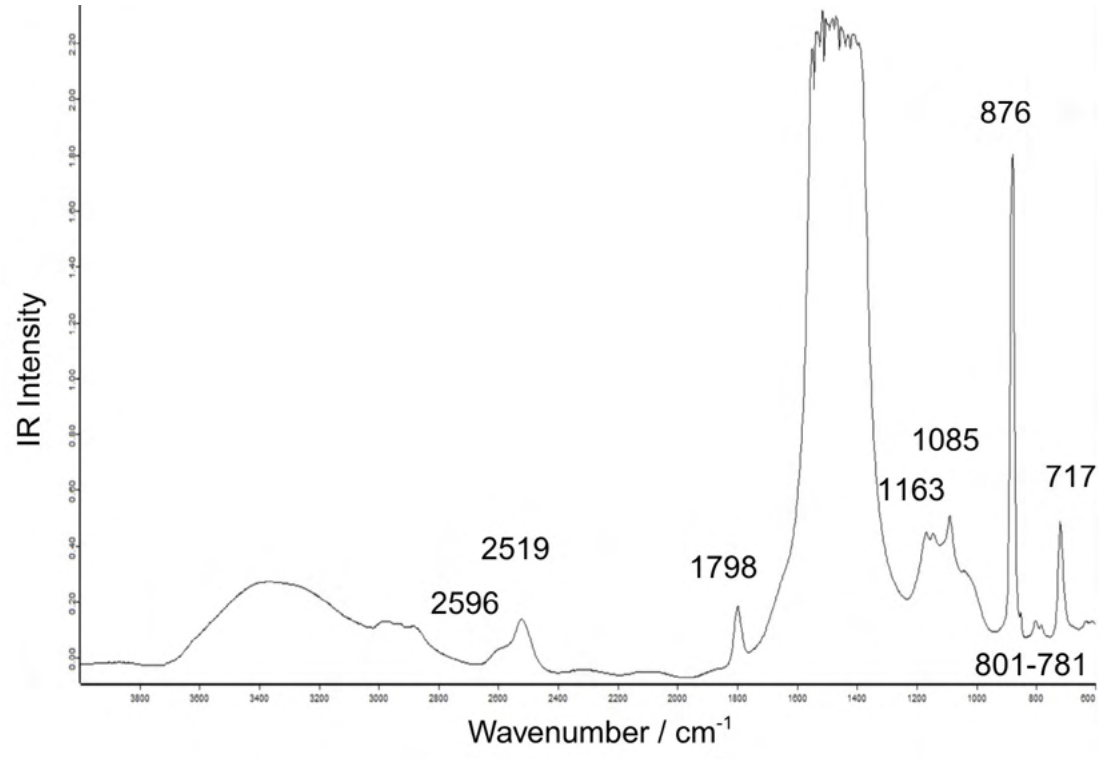

Figure 136. FT-IR spectrum of a sample collected from a bead (inv. no. I.G. 355542; Pieve d'Alpago): calcite, quartz and org. mat.

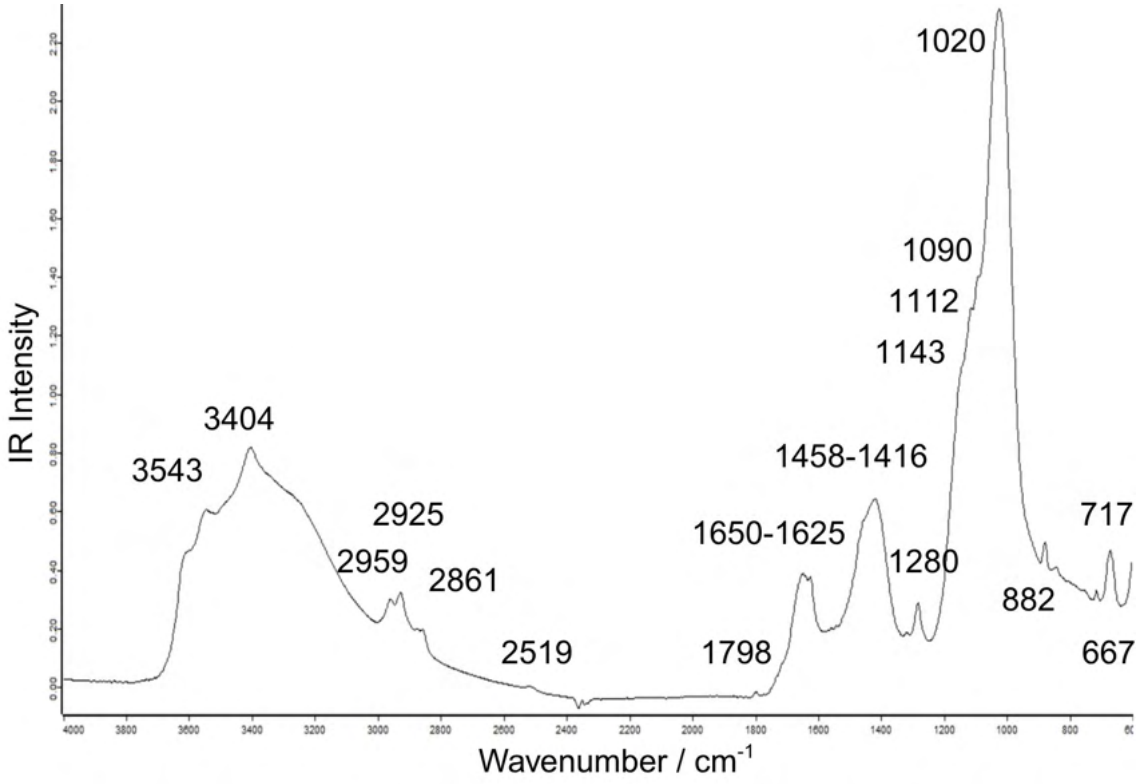

Figure 137. FT-IR spectrum of sample collected from a leech fibula with circular decoration (Collezione Bellini; Museo Civico Archeologico Sesto Calende): calcite, gypsum, silicate, org. mat.

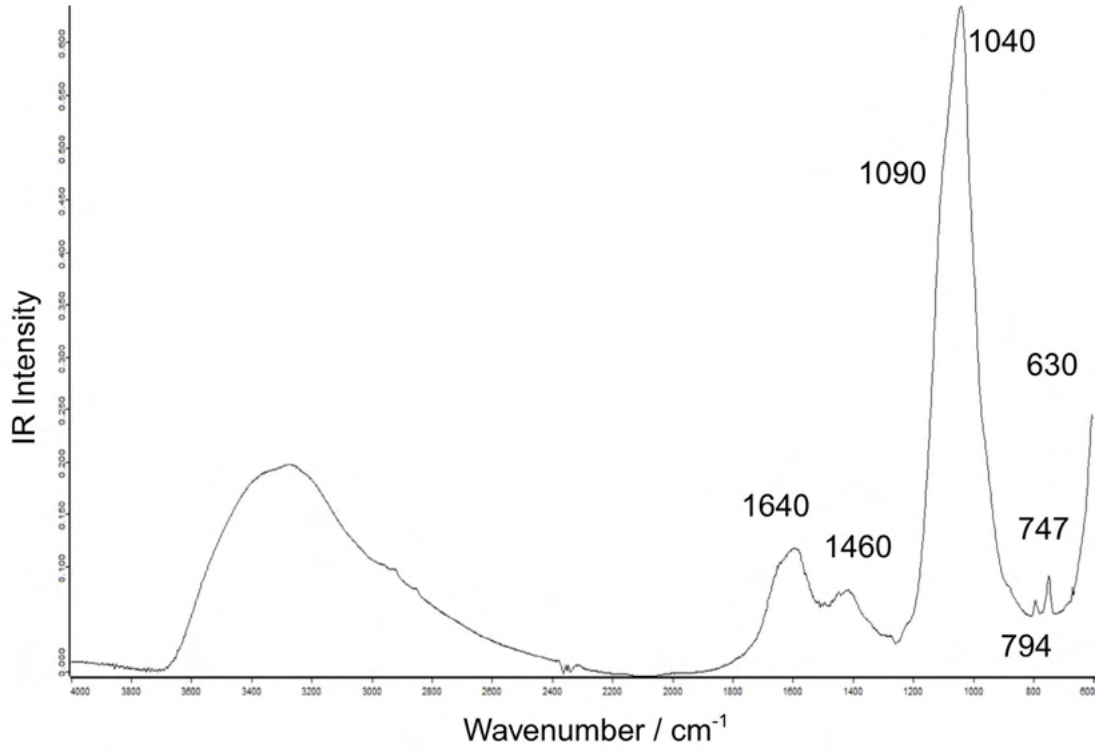

Figure 138. FT-IR spectrum of sample collected from a leech fibula with circular decoration (inv. no. St. 23751; Sesto Calende, loc. Mulini Bellaria, grave 4; Museo Civico Archeologico Sesto Calende): hydroxylapatite and organic material.

7.1.2.4. μ-XRD analysis

XRD investigation was carried out for 141 out of 264 finds (Tab. 22), mostly in μ-area mode, despite the lower quality of the resulting diffractograms – if compared to those obtained by XRPD (Fig. 139). This choice was dictated either by the need to analyse the archaeological finds preserving their integrity or, else, by the availability of μ-samples. This inevitably affected the quality of the results: μ-area data often show quite convoluted backgrounds (due to the non-flatness of the samples). Besides, the reflections intensity is non-useable for quantitative purposes. Also, in some cases a systematic shift in the reflections position is observed, impairing the data quality (Fig. 140). All these factors had to be properly considered in data interpretation.

μ-area mode analyses were carried out by using a 2 mm incident slit – which roughly corresponds to the width of the X-ray beam effectively 'bathing' the sample surface. Therefore, while analysing the tiny decorations on the artefacts as such, part of the surrounding metal support was also at times affected by the X-ray beam (see section 7.2.3). In most cases, only one spot per artefact was investigated; in others, however, several spots were investigated (e.g., due to presence of different materials). In some cases, the inadequate morphology of the sample surface (e.g. too pronounced curvature, cavities) precluded analysis.

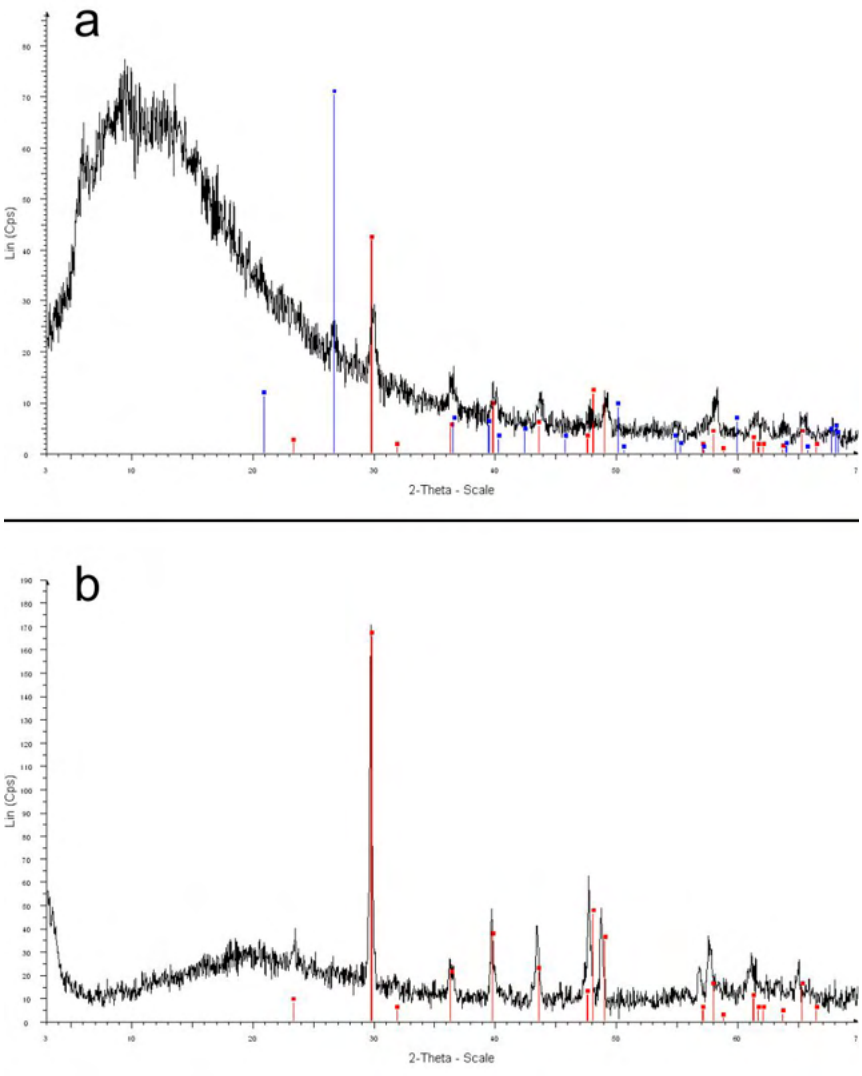

Figure 139. Comparison of diffractograms of samples collected from finds (a) inv. no. C-FR-NE/2 (Brignano Frascata, leech fibula with circular decoration) and (b) 22.S288-1.205 (Golasecca, loc. Galliasco, leech fibula with circular decoration), analysed by micro-area XRD (left) and XR Powder Diffraction (right), respectively.

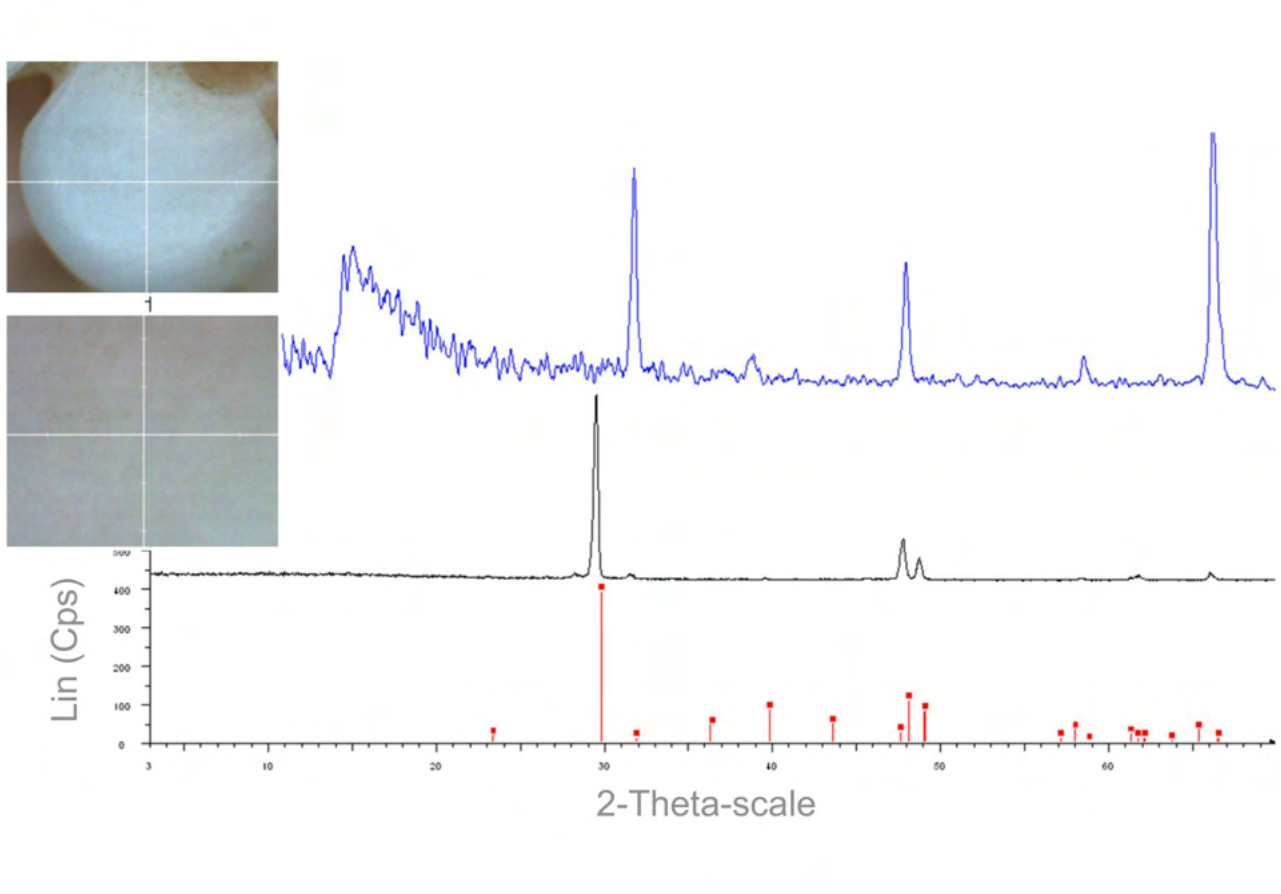

Figure 140. Comparison of diffractograms obtained from the same piece of modern *C. rubrum* (w_pCr_Sa). The object is perfectly flat on one side and worked on the other. The diffractogram obtained from the flat side (in black) is of considerably better quality and shows the presence of the Mg-calcite peaks (in red). The one collected on the worked side (in blue) shows the irregular background and a consequent shift of the calcite peaks.

In most cases, the analyses yielded interpretable qualitative results (only 11 out of 141 gave none), despite the difficulties related to the samples irregular surfaces. Presence of calcite recurs in almost all samples – either as a pure crystalline phase ($CaCO_3$: 33 cases; 1 dubious) or containing a certain amount of Mg (i.e., Mg-calcite: 29 cases; 2 dubious). Discrimination was attempted by basing on the position of the related reflections[13]. However, it has to be pointed out that by operating in µ-XRD mode, other factors may also affect a peak shift (e.g., a peculiar orientation of the crystallites in the non-pulverised sample).
In order to test their reliability, the Mg-amounts calculated by basing on the shifts of the XRD reflections were compared with those extrapolated by the EDS-semi-quantitative chemical analyses, carried out on the same objects (possibly, in the same spots: see section 7.1.2.5; Fig. 141; to see detailed data: Appendix 2, Tab. 42). As far as presence of Mg is concerned, 87% of all specimens catalogued by SEM-EDS as HMC, were also identified as Mg-calcite by XRD. Conversely, of all the samples catalogued by SEM-EDS as LMC, 75% were recognized as pure calcite by XRD. Regarding those samples identified at SEM-EDS as MMC, the situation is even more controversial: they are identified either as Mg-calcite (30%) or as pure calcite (70 %). Furthermore, in 10 out of 62 cases, presence of calcite is detected by XRD but not confirmed by SEM-EDS.
This lack of accuracy is certainly to be ascribed to the abovementioned caveats and limitations related to XRD data collection in µ-area mode on non-flat samples (i.e., Fig. 140) – which inevitably affects the exact position of the (104) reflection biasing the accurate extrapolation of the related Mg-amount. In this case, therefore,

13 For what concerns the quantification of the Mg-amount in calcite, an accurate measure of the shift affecting the (104) reflection should provide an estimate of this value (expressed as mol% $MgCO_3$: Bente *et al.* 2017; 2022; Goldsmith *et al.* 1961; Han *et al.* 2013; Pagani, Turi 1977; Ries 2011).

the measurement of the calcite (104) peak shift is not sufficient, 'per se', to achieve an accurate quantification of the Mg-amount in calcite.
In addition to calcite, other crystalline phases were also identified, including possible decorative materials and residues of the deposition soil, as well as alteration products of the metal alloy (Fig. 142; see section 7.2.4):

- dolomite [$CaMg(CO_3)_2$; Fig. 143], ankerite [$Ca(Fe^{2+},Mg)(CO_3)_2$], CaO, gypsum [Fig. 145] and portlandite [$Ca(OH)_2$], referable to different pigments or even calcite alteration products (Charola *et al.* 2007; Giustetto *et al.* 2020; Siedel, Siegesmund 2014);
- fluorapatite [$Ca_5(PO_4)_3F$], hydroxylapatite [$Ca_5(PO_4)_3(OH)$], carbonatehydroxylapatite [$Ca_5(PO_4,CO_3)_3(OH,O)$; Fig. 146], whitlockyte [$Ca_9Mg(PO_4)_6(PO_3OH)$; Fig. 147] and brushite [$Ca(PO_3OH) \cdot 2H_2O$], related to the presence of bone material in decorations or contamination by bones from the burial;
- anatase and rutile (Fig. 148), related to modern interventions;
- albite [$Na(AlSi_3O_8)$], anorthite [$Ca(Al_2Si_2O_8)$], muscovite [$KAl_2(AlSi_3O_{10})(OH)_2$], illite [$K_{0.65}Al_{2.0}[Al_{0.65}Si_{3.35}O_{10}](OH)_2$], talc [$Mg_3Si_4O_{10}(OH)_2$], cristobalite [$SiO_2$], quartz (Fig. 144), kaolinite [$Al_2(Si_2O_5)(OH)_4$], gehelenite [$Ca_2Al[AlSiO_7]$], probably residue from the deposition soil;
- wax (Fig. 149; Gaillard *et al.* 2011; Schoening 1980), referable to the use of a binder or to restoration activities.

Plagioclases (albite and anorthite) and quartz are quite common materials, presumably deriving from residues of the interment soil. Unidentified peaks are often also present (Tab. 22) – e.g., a recurring one at d=5.45-5.55 Å, for which possible presence of a restoration product was assumed.

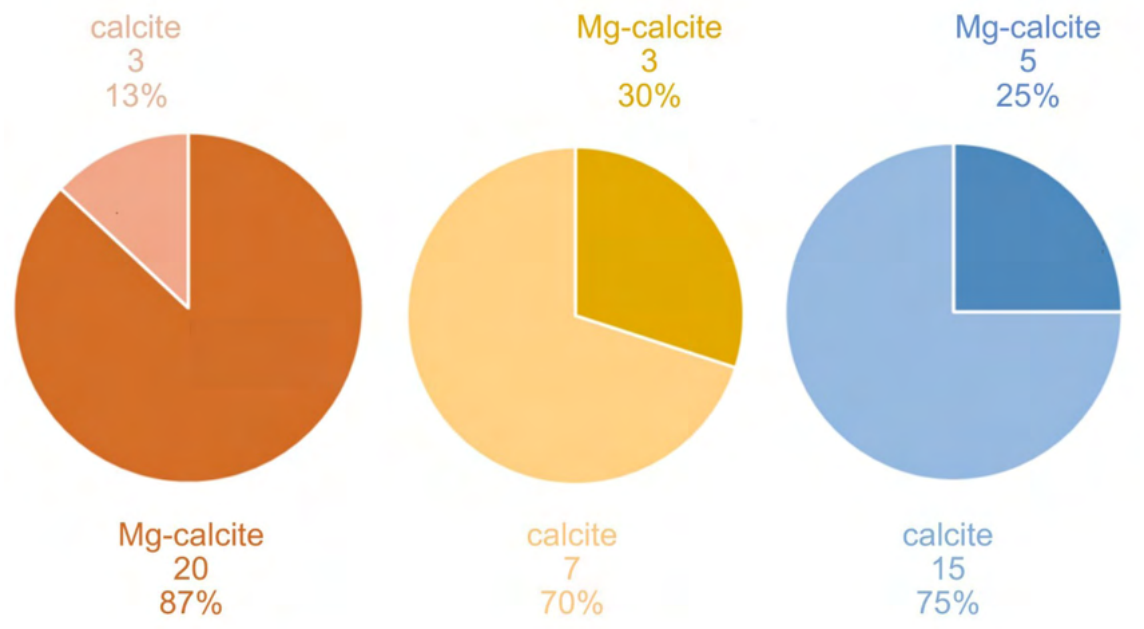

Figure 141. Correspondence percentage between SEM-EDS and μ-XRD data for HMC (in red on the left), MMC (in yellow in the centre) and LMC (in blue on the right).

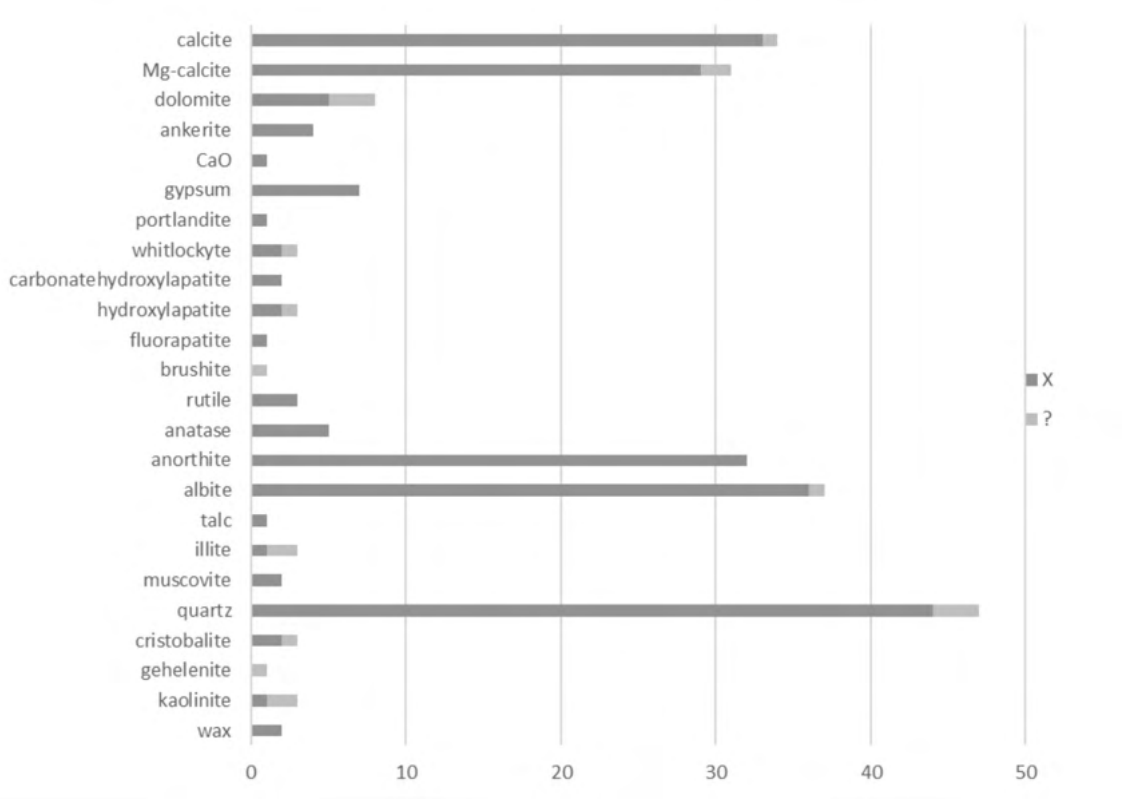

Figure 142. Identified crystalline phases (excluded bronze alteration products) and relative abundance (X = sure identification; ? = doubtful).

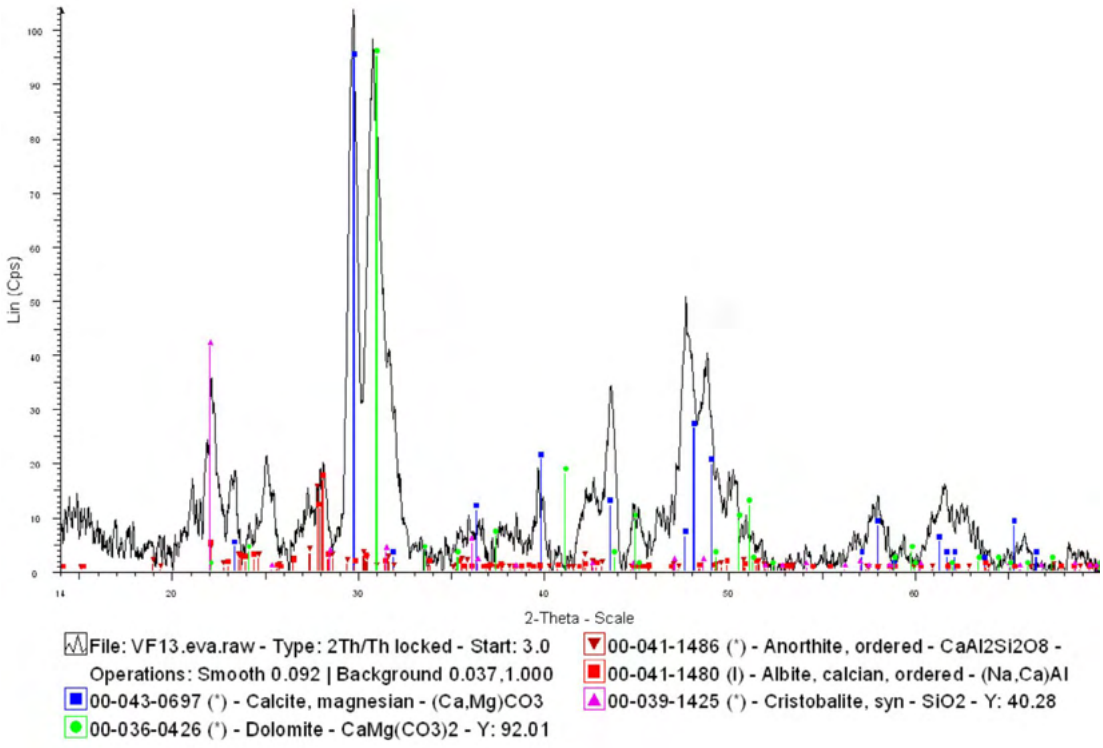
Lin (Cps)
2-Theta - Scale
File: VF13.eva.raw - Type: 2Th/Th locked - Start: 3.0
Operations: Smooth 0.092 | Background 0.037,1.000
00-043-0697 (*) - Calcite, magnesian - (Ca,Mg)CO3
00-036-0426 (*) - Dolomite - CaMg(CO3)2 - Y: 92.01
00-041-1486 (*) - Anorthite, ordered - CaAl2Si2O8 -
00-041-1480 (I) - Albite, calcian, ordered - (Na,Ca)Al
00-039-1425 (*) - Cristobalite, syn - SiO2 - Y: 40.28

Figure 143. Diffractogram portion of the sample VF13 (collected by finds St. 51877, Villa del Foro): main reflections of HMC (blue) and dolomite (green) visible, together with other crystalline phases.

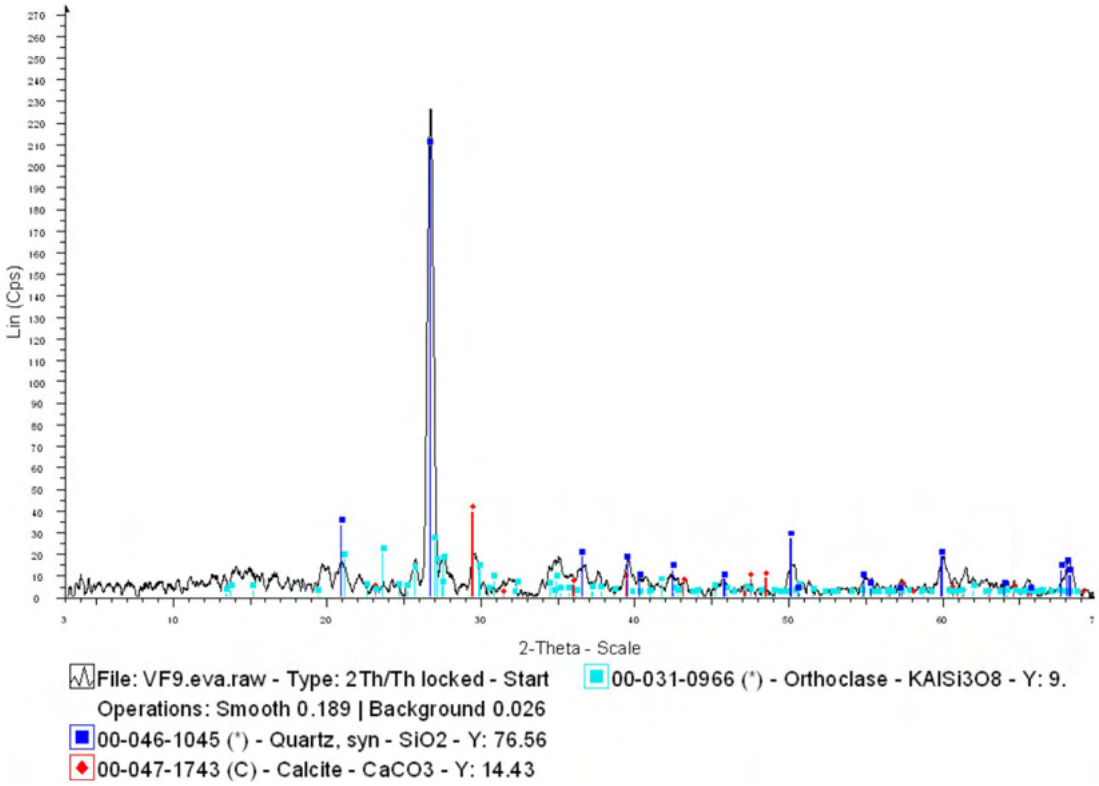
Lin (Cps)
2-Theta - Scale
File: VF9.eva.raw - Type: 2Th/Th locked - Start
00-031-0966 (*) - Orthoclase - KAlSi3O8 - Y: 9.
Operations: Smooth 0.189 | Background 0.026
00-046-1045 (*) - Quartz, syn - SiO2 - Y: 76.56
00-047-1743 (C) - Calcite - CaCO3 - Y: 14.43

Figure 144. Quartz diffractogram (blue reflex) of the sample VF9, collected from fibula inv. no. St. 66132 (Villa del Foro).

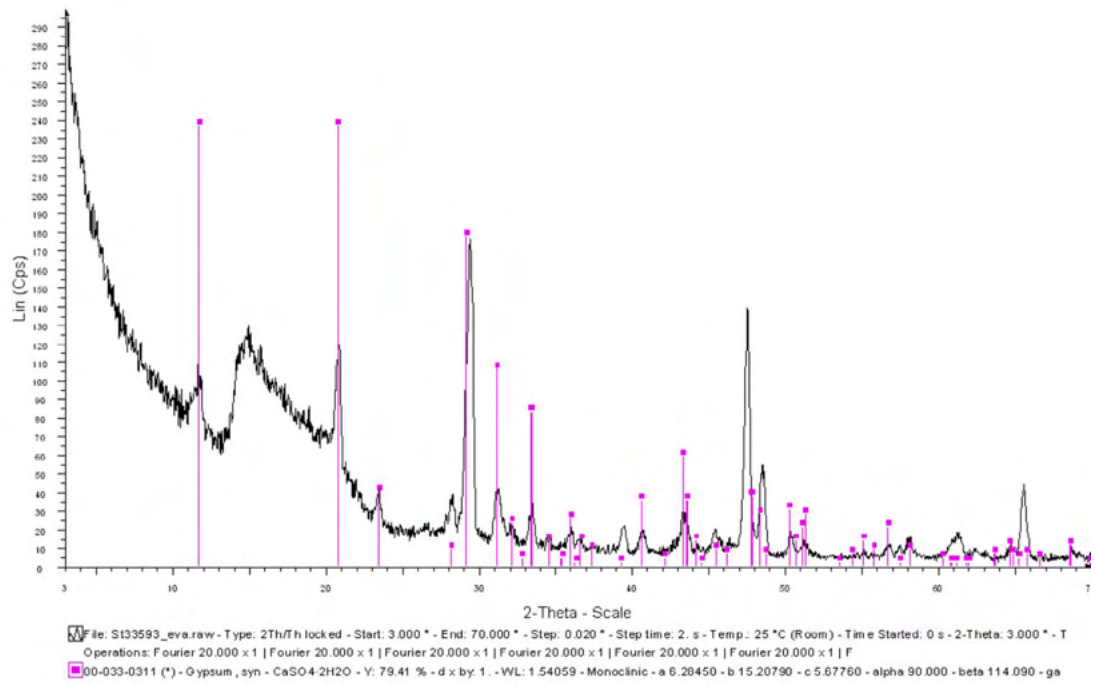
Lin (Cps)
2-Theta - Scale
File: St33593_eva.raw - Type: 2Th/Th locked - Start: 3.000 * - End: 70.000 * - Step: 0.020 * - Step time: 2. s - Temp.: 25 °C (Room) - Time Started: 0 s - 2-Theta: 3.000 * - T
Operations: Fourier 20.000 x 1 | Fourier 20.000 x 1 | Fourier 20.000 x 1 | Fourier 20.000 x 1 | Fourier 20.000 x 1 | Fourier 20.000 x 1 | F
00-033-0311 (*) - Gypsum , syn - CaSO4·2H2O - Y: 79.41 % - d x by: 1. - WL: 1.54059 - Monoclinic - a 6.28450 - b 15.20790 - c 5.67760 - alpha 90.000 - beta 114.090 - ga

Figure 145. Gypsum diffractogram of the pendant inv. no. St. 33593 (Como, grave 302).

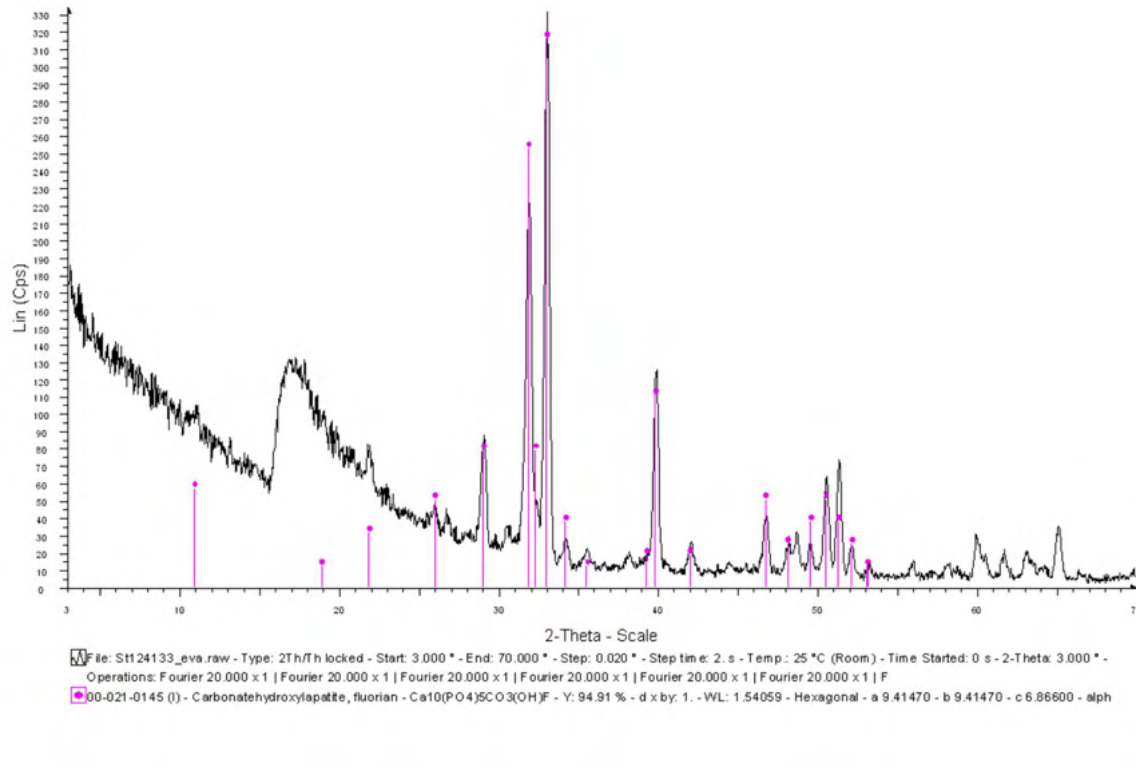
Lin (Cps)
2-Theta - Scale
File: St124133_eva.raw - Type: 2Th/Th locked - Start: 3.000 ° - End: 70.000 ° - Step: 0.020 ° - Step time: 2. s - Temp.: 25 °C (Room) - Time Started: 0 s - 2-Theta: 3.000 ° -
Operations: Fourier 20.000 x 1 | Fourier 20.000 x 1 | Fourier 20.000 x 1 | Fourier 20.000 x 1 | Fourier 20.000 x 1 | F
00-021-0145 (I) - Carbonatehydroxylapatite, fluorian - Ca10(PO4)5CO3(OH)F - Y: 94.91 % - d x by: 1. - WL: 1.54059 - Hexagonal - a 9.41470 - b 9.41470 - c 6.86600 - alph

Figure 146. Carbonate-hydroxylapatite diffractogram of the sample St. 124133 (Como, Ca' Morta) with background rise, but no peak shift.

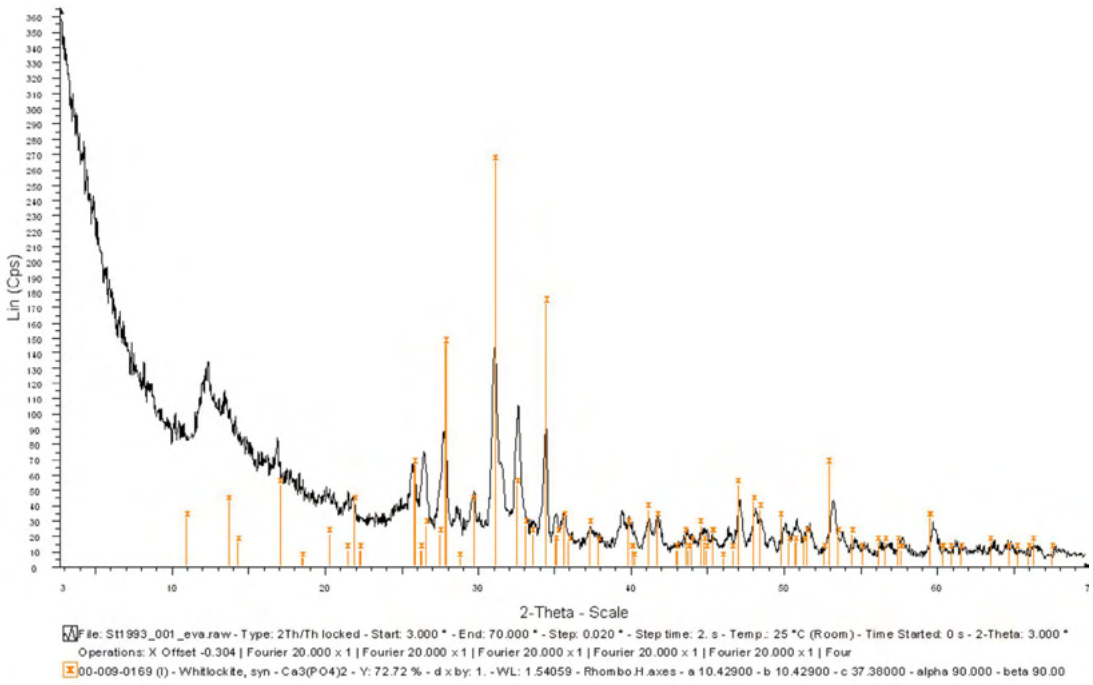
Lin (Cps)
2-Theta - Scale
File: St1993_001_eva.raw - Type: 2Th/Th locked - Start: 3.000 ° - End: 70.000 ° - Step: 0.020 ° - Step time: 2. s - Temp.: 25 °C (Room) - Time Started: 0 s - 2-Theta: 3.000 °
Operations: X Offset -0.304 | Fourier 20.000 x 1 | Fourier 20.000 x 1 | Fourier 20.000 x 1 | Fourier 20.000 x 1 | Four
00-009-0169 (I) - Whitlockite, syn - Ca3(PO4)2 - Y: 72.72 % - d x by: 1. - WL: 1.54059 - Rhombo.H.axes - a 10.42900 - b 10.42900 - c 37.38000 - alpha 90.000 - beta 90.00

Figure 147. Whitlockite diffractogram of the sample inv. no. St. 1993 (Como, Ca' Morta).

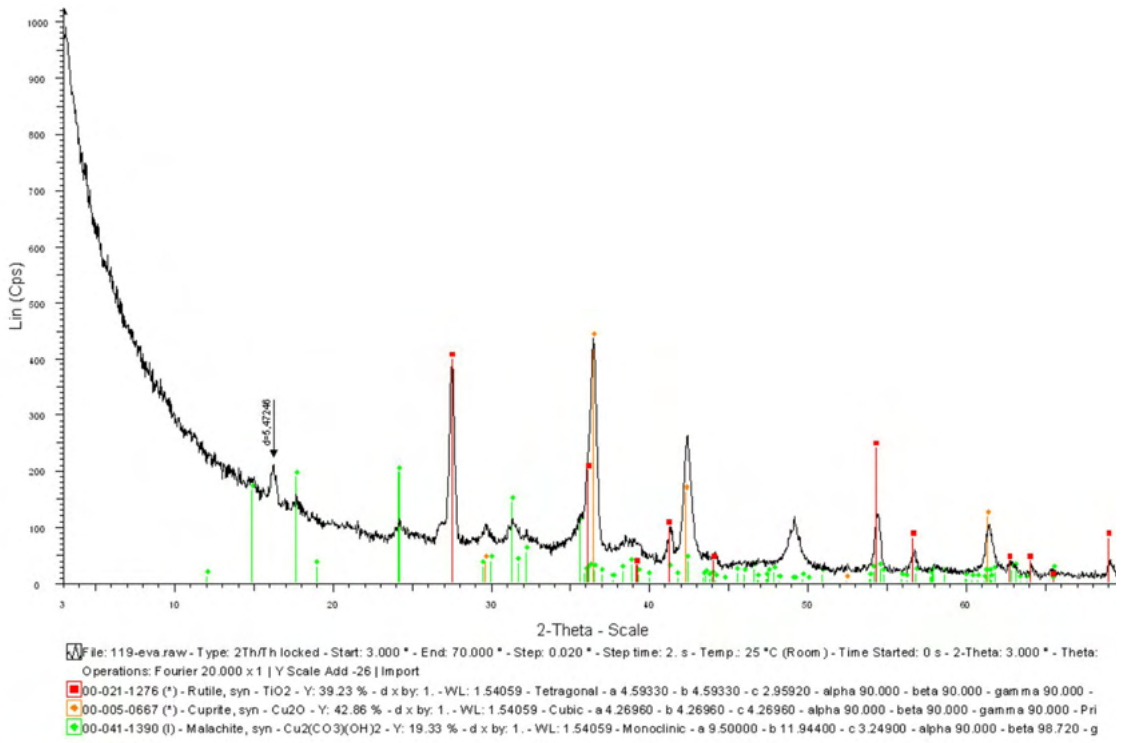
Lin (Cps)
d=5.47246
2-Theta - Scale
File: 119-eva.raw - Type: 2Th/Th locked - Start: 3.000 ° - End: 70.000 ° - Step: 0.020 ° - Step time: 2. s - Temp.: 25 °C (Room) - Time Started: 0 s - 2-Theta: 3.000 ° - Theta:
Operations: Fourier 20.000 x 1 | Y Scale Add -26 | Import
00-021-1276 (*) - Rutile, syn - TiO2 - Y: 39.23 % - d x by: 1. - WL: 1.54059 - Tetragonal - a 4.59330 - b 4.59330 - c 2.95920 - alpha 90.000 - beta 90.000 - gamma 90.000 -
00-005-0667 (*) - Cuprite, syn - Cu2O - Y: 42.86 % - d x by: 1. - WL: 1.54059 - Cubic - a 4.26960 - b 4.26960 - c 4.26960 - alpha 90.000 - beta 90.000 - gamma 90.000 - Pri
00-041-1390 (I) - Malachite, syn - Cu2(CO3)(OH)2 - Y: 19.33 % - d x by: 1. - WL: 1.54059 - Monoclinic - a 9.50000 - b 11.94400 - c 3.24900 - alpha 90.000 - beta 98.720 - g

Figure 148. Diffractogram of the fibula inv. no. 199 (Parre): in red rutile reflections, in orange cuprite reflections, in green doubtful malachite reflection.

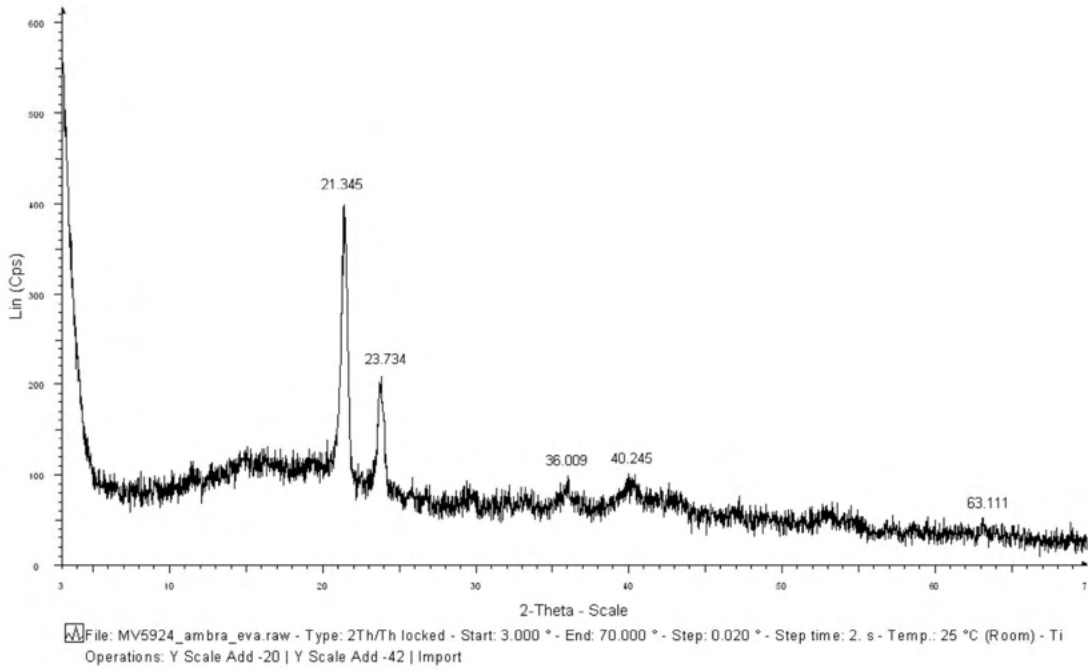
Lin (Cps)
21.345
23.734
36.009
40.245
63.111
2-Theta - Scale
File: MV5924_ambra_eva.raw - Type: 2Th/Th locked - Start: 3.000 ° - End: 70.000 ° - Step: 0.020 ° - Step time: 2. s - Temp.: 25 °C (Room) - Ti
Operations: Y Scale Add -20 | Y Scale Add -42 | Import

Figure 149. Diffractogram of the object inv. no. MV5924 (presumably amber by microscopic observation; unknown provenance, Musei Civici Villa Mirabello Varese): reflections attributable to wax (Gaillard *et al.* 2011; Schoening 1980), instead of amber (Pakutinskiene *et al.* 2007).

7.1.2.5. SEM-EDS analysis

SEM-EDS analyses were performed for almost all the analytical record, leaving out only 23 finds[14]. 241 artefacts were analysed, obtaining no interpretable results only in 12 cases, mainly due to the presence of surface protective modern products that hampered investigations (Fig. 150a)[15].

EDS semi-quantitative chemical analyses of the decorations are in general agreement with the results obtained by the other techniques (Fig. 151). A Ca-carbonate composition is mostly detected (57%; 133 finds). Conventionally, calcite with a content higher than 10.5 mol% $MgCO_3$ is defined as HMC. However, a debate exists about the specific Mg-content discriminating HMC from LMC. Some authors indicate that both LMC (0-5.5 mol% $MgCO_3$) and HMC (10.5-20 mol% $MgCO_3$) exist in nature, whereas unaltered calcites with intermediate values (5.5-10.5 mol% $MgCO_3$) do not (Borromeo *et al.* 2017; Fürst *et al.* 2016; McGregor, Gagan 2003). While interpreting our results, the following intervals were adopted (Tab. 25):

- 'CALC' = 0 mol% $MgCO_3$;
- 'LMC' = 0-5.5 mol% $MgCO_3$;
- 'MMC' = 5.5-10.5 mol% $MgCO_3$;
- 'HMC' = $MgCO_3$ > 10.5 mol%.

In the investigated record, LMC is predominant (22% of cases; 51 samples), followed by MMC (18%; 42), HMC (15%; 35) and pure calcite (CALC: 2%; 4 samples). However, the Mg-content can significantly vary – even within the same sample – in different analytical spots (Figs. 152, 153a).

Sometimes Ca and P are detected as major elements (5%; 11 samples), suggesting the occurrence of phosphates (bone materials). If Ca and S are predominant, presence of gypsum was hypothesized (2 cases). Sporadic Ti predominance was correlated with the use of White Indian Ink (3%; 8). When Cu, Sn and Pb are abundant (7%; 15), they refer to bronze alteration by-products, while predominance of Si and Al is referred to residues of the deposition ground (10 %; 23). In 17 % of the cases (39), bronze alteration by-products and soil residues were identified in combination.

If HMC is present, the decoration is likely to be made of *C. rubrum*. In its skeleton, in fact, the Mg-content ranges from 9 to 15 mol% $MgCO_3$, with a mean value of 12±1.0%. The extreme variability in the Mg-content in different analytical spots on the same sample is another occurrence compatible with this kind of material. In the *C. rubrum* calcitic skeleton, minor elements are also present (Na, S, Sr, K, P, B, Ba, Fe, Li, Mn, Pb and U: Hasegawa *et al.* 2010; Floquet *et al.* 2015; Vielzeuf *et al.* 2008; 2013; Weinbauer *et al.* 2000), which are also detected in the investigated artefacts – together with others derived from soil of bronze alteration (Na, Al, Si, P, S, Cl, K, Ti, Mn, Fe, Ni, Cu, Zn, As, Sr, Ag, Sn, Pb: Fig. 153b; Tabs. 23-24).

Sulphur (S) – a common element in marine and biogenic calcites, detected both in the inorganic and organic parts of *C. rubrum* – is abundant in both HMC and MMC, but lower in LMC. This is in agreement with a possible biogenic origin of these materials (Busenberg, Plummer 1985; Hermans 2010; Macchia *et al.* 2016; Perrin *et al.* 2017; Pingitore *et al.* 1995; Vielzeuf *et al.* 2013). Phosphorous (P) represents a marker of the organic matrix presence in biominerals (Vielzeuf *et al.* 2013) and is more abundant in HMC than in MMC and LMC. Such a depletion could indicate an occurred loss of the organic portion in the skeleton of an originally biogenic organism and, consequently, a possible alteration of the original material. Cl and Pb show similar behaviours; both can be related to the alteration of bronze (Angelini *et al.* 2009; Scott 2002).

As already done for optical microscopy, SEM also allows to investigate the finer details of these decorations – e.g., the borders of the small decorating inlays (i.e., where they are wedged in the circular hosting holes on the fibulae: Fig. 150b) and observe the μ-morphologies typical of *C. rubrum*. These are visible in separate samples as well as on intact finds, especially when there are areas with detached material. Biogenic carbonatic insets show different textures: multibranched or aghiform with various orientations (Fig. 154a), microporous and with spheroidal particles (Fig. 154b), mammellonary or cauliflower (Fig. 154c), crusty (Fig. 154d), compact (Fig. 154e). Sometimes the typical structures of *C. rubrum* are evident: crenulation (Fig. 154f), wavy, medullar features. In 2 cases (inv. no.

14 18 finds analysed only 'in situ', 1 fibula did not fit in the chamber (inv. no. D2077), 3 unnecessary analyses due to the nature of the finds (inv. no. MV5924, 2019-01-109 and 2021-01-179), 1 sample was depleted by other analyses (inv. no. St. 66120).

15 For further examples see Appendix 1, Figs. 221-223.

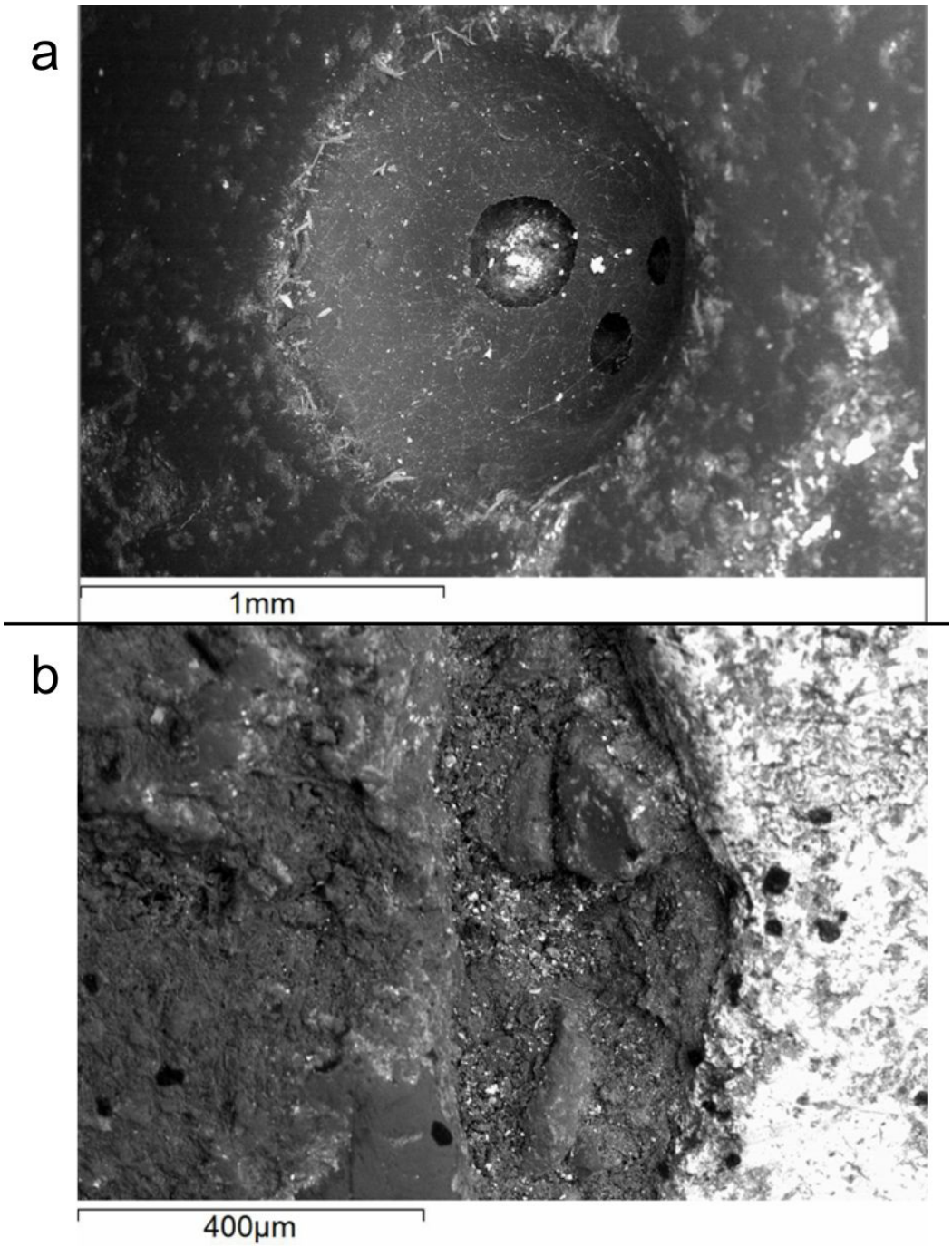

Figure 150. a) BSE-image of the decoration of pendant inv. no. St. 18711 (Pianello Val Tidone): the decoration is completely filled with a consolidant, probably Paraloid, which conceals the underlying material; b)BSE-image of a circular decoration (Motto Lagone, grave 1): detail of the presence of incoherent material standing between the inset and the border of the hole containing it.

3051-3052), the overlapping of the growth rings is clearly visible (Fig. 155e).

Non-carbonate materials show, instead, different µ-features: vitreous materials have a conchoid aspect (Fig. 155b), White Indian Ink looks like varnish (Fig. 155c), bone shows a typical microporosity (Fig. 155d), gypsum is compact in aspect (Fig. 155e). At times, peculiar details are observed: e.g., in the inv. no. D1750 pendant (Fig. 155f), some fibers are trapped in the spring[16].

16 For further examples see Appendix 1, Figs. 222-223.

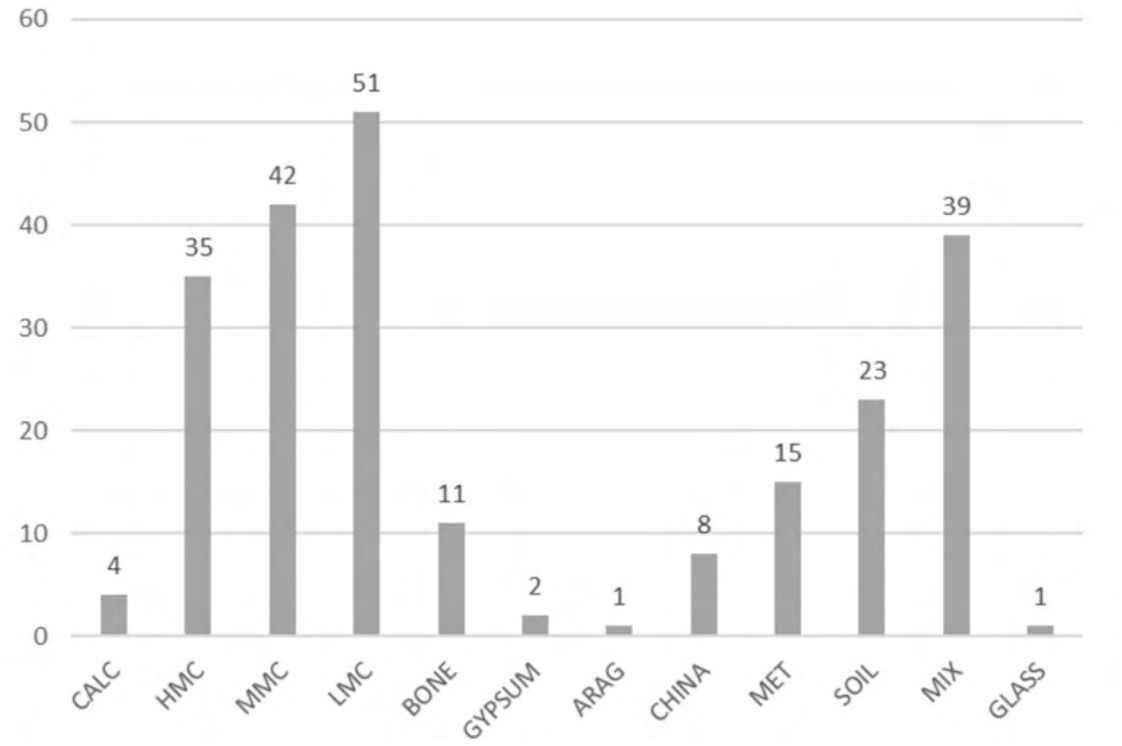

Figure 151. Macro-categories identified on the basis of major elements: 'HMC' = high-magnesian-calcite, 'MMC' = medium-magnesian-calcite, 'LMC' = low-magnesian-calcite, 'CALC' = calcite, 'BONE' = apatitic material, 'GYPSUM' = gypsum, 'ARAG' = aragonite, 'CHINA' = White Indian Ink, 'GLASS' = vitreous material, 'MET' = metal alloy and its alteration; 'SOIL' = deposition ground and 'MIX' a mixture of MET and SOIL.

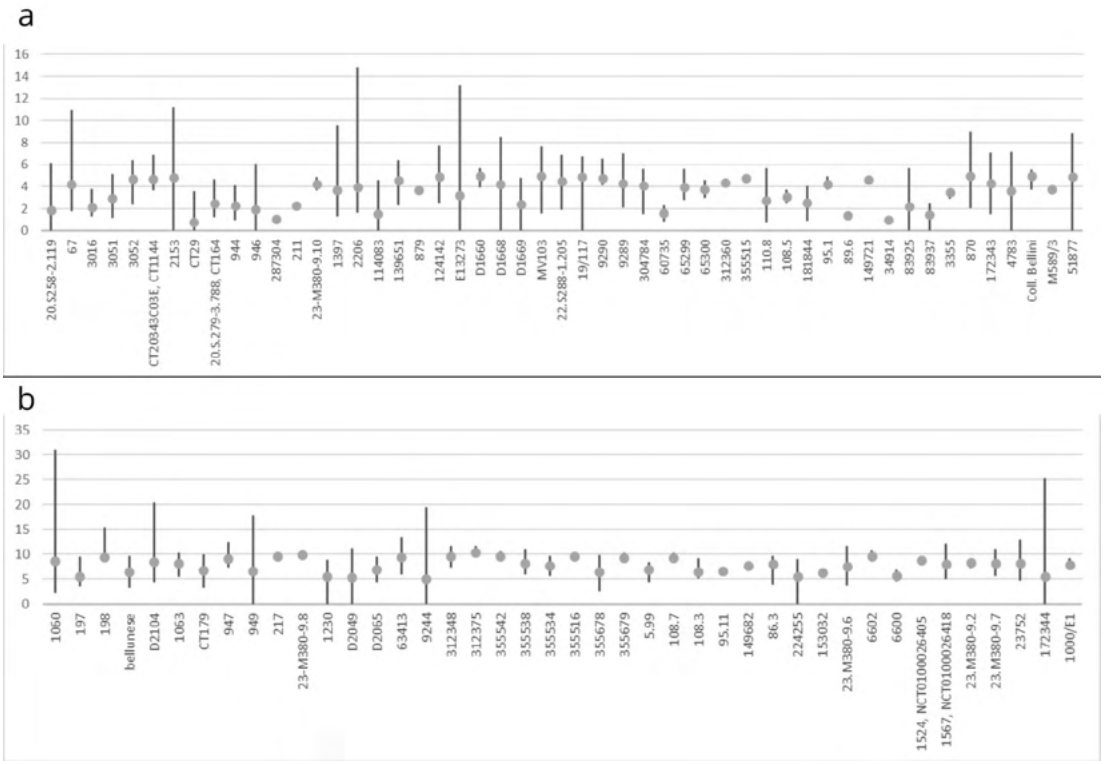

Figure 152. a) LMC samples: Mg-content variation in each sample (bar indicates the variation between minimum and maximum value) and average value (point indicates the average value of all the points of analysis on the sample); b) MMC samples: Mg-content variation in each sample (bar indicates the variation between minimum and maximum value) and average value (point indicates the average value of all the points of analysis on the sample).

Figure 153. a) HMC samples: Mg-content variation in each sample (bar indicates the variation between minimum and maximum value) and average value (point indicates the average value of all the points of analysis on the sample); b) Graph of the occurrence (as a percentage of the total) of minor elements in calcites with different Mg-content.

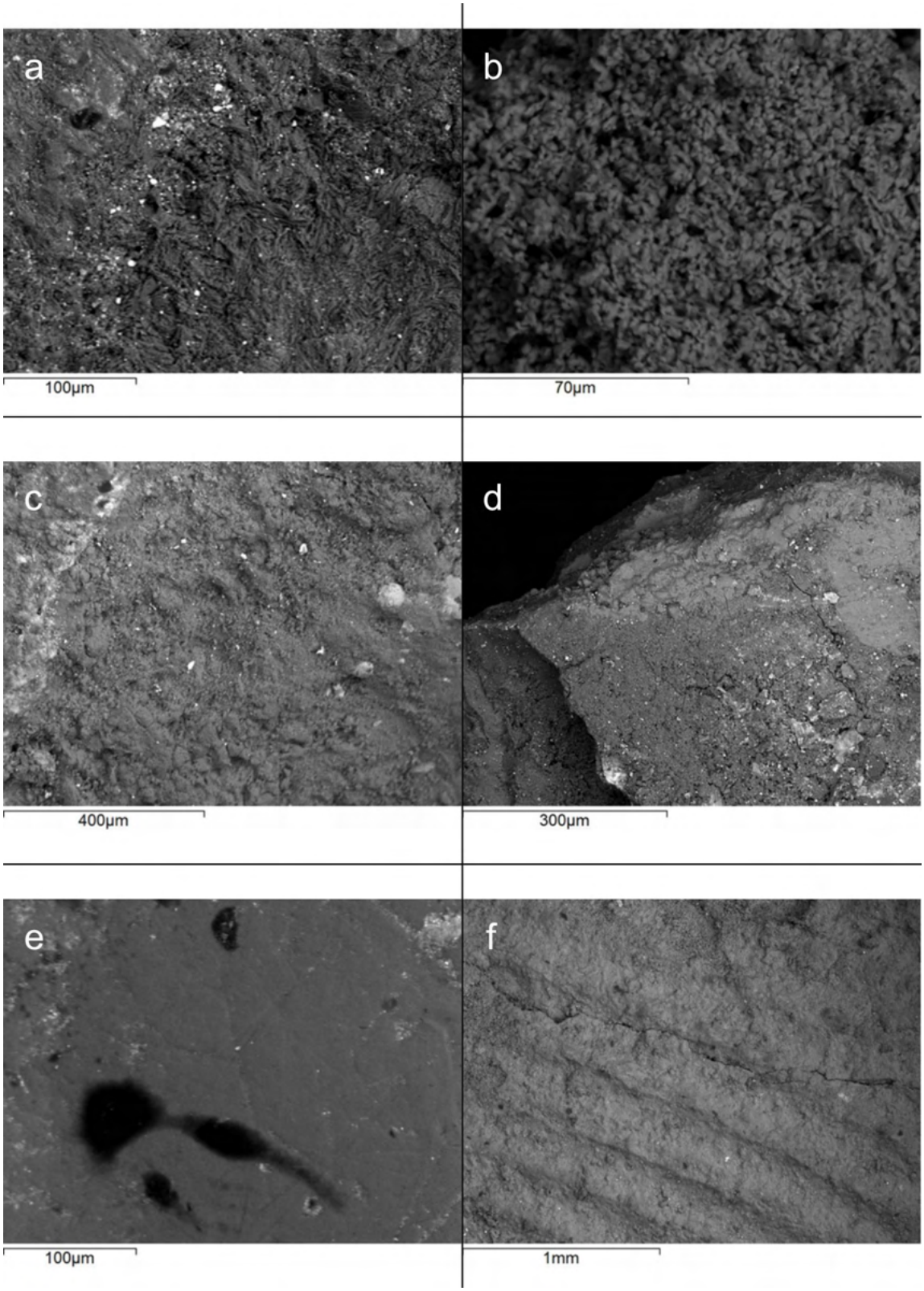

Figure 154. a) BSE-image of a circular decoration (Motto Lagone, T1): multi-branched micro-morphology; b) BSE-image of a circular decoration (Bra Museum, inv. no. M589/3): micro-porous morphology; c) BSE-image of a circular decoration (Novara Museum, inv. no. 946): mammellonary micro-morphology; d) BSE-image of a sample from a circular decoration (Brignano Frascata, inv. no. C-FR-S/2): crusty micro-morphology; e) BSE-image of a circular decoration (Motto Lagone, T1): compact micro-morphology; f) BSE-image of an element of a composite bow fibula (Brembate Sotto, inv. no. 3052): crenulation features.

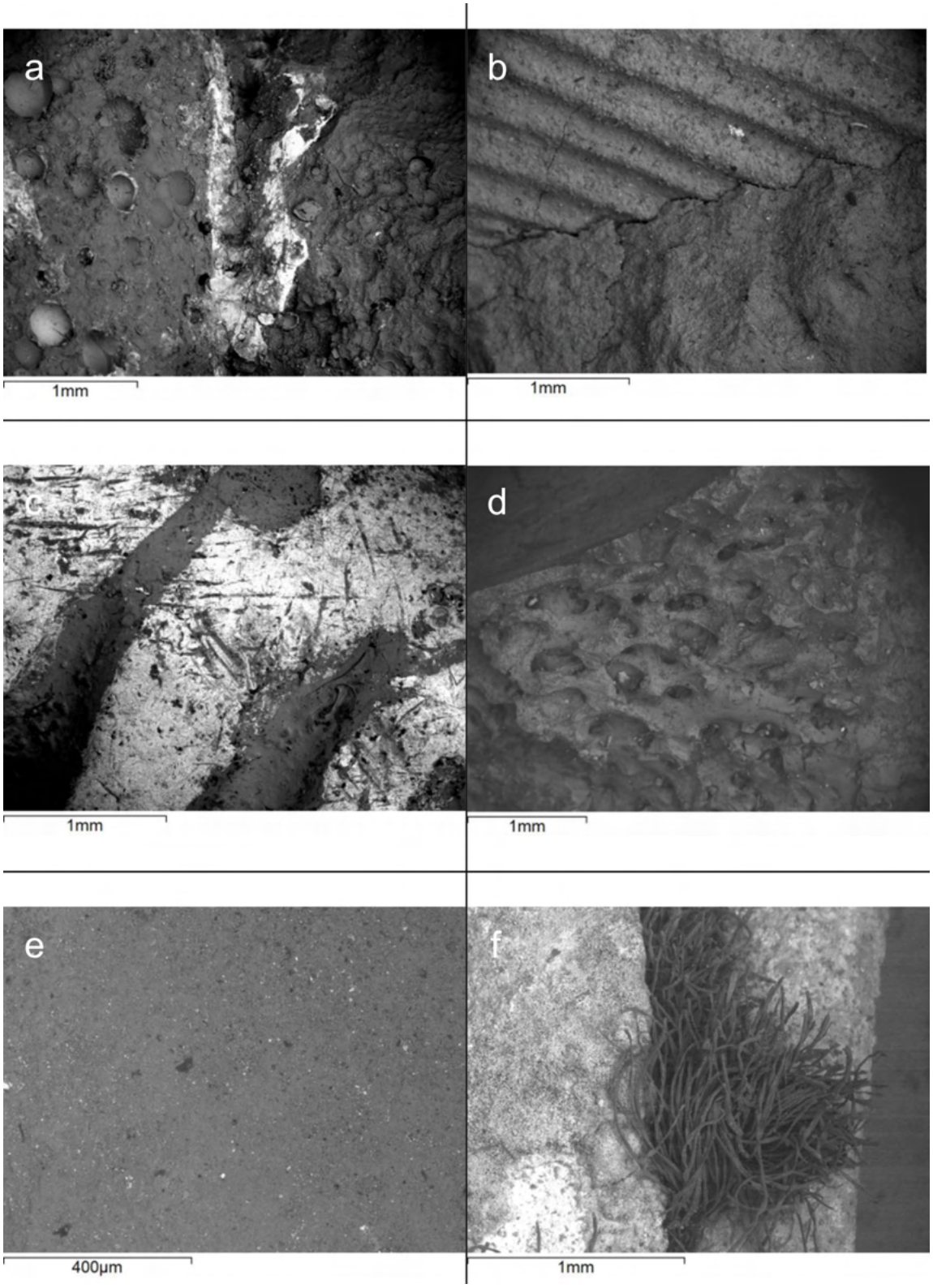

Figure 155. a) BSE-image of an element of a composite bow fibula (Brembate Sotto, inv. no. 3052): superposition of different concentric growth-rings in annular region; b) BSE-image of a vitreous bead (Castelletto Ticino, inv. no. CT14031X, CT868b): conchoid micro-morphology; c) BSE-image of the TiO_2 decoration of a fibula (Parre, inv. no. 3002): varnish aspect; d) BSE-image of a bone fragment (Golasecca, inv. no. D1667); e) BSE-image of a Longone al Segrino type pendant (Como, inv. no. St. 33593): compact micro-morphology of gypsum; f) BSE-images of Longone al Segrino type pendant (Castelletto Ticino, inv. no. D1750): detail of the presence of fibre residues trapped in the bronze rod spring.

7.1.3 Combustion experiments

Most of the analysed archaeological finds come from incineration burials. They may therefore have been burnt on the funeral pyre, but often they were placed in the grave only after cremation, as documented by the absence of traces of combustion. Some objects were, however, certainly burnt, as is evident by examining the metal surface of the artefact.
To simulate such conditions, a burning experiment was carried out in the laboratory on samples of modern *Corallium rubrum* for comparison purposes. 5 small fragments of modern *C. rubrum* (numbered: 0, 1, 2, 3, 4: Fig. 156a) were chosen and analysed by μ-Raman, SEM-EDS and FT-IR before and after combustion, to verify possible changes in the Mg-content. All analyses were performed in the same analytical conditions as those adopted for the study of the archaeological finds.
Coral samples were placed in ceramic crucibles and burnt at a constant temperature of 750°C overnight (Fig. 156b) in agreement with literature data (identifying T ≈ 600-700°C for cremated human remains found in Iron Age Piedmont contexts: Bedini, Petiti 2015). The following morning, they had lost their characteristic red colour but retained their shape. After about a week in the air at room temperature, they also lost their shape and considerably increased in volume (Figs. 156c-d). This experiment allowed recognizing the formation first of calcium hydroxide (portlandite) and then of secondary calcite. After combustion, the Mg-content decreased, according to literature (Floquet *et al.* 2015), from an average of 12 to 9 mol% $MgCO_3$, variable from sample to sample.

$$CaCO_3 \rightarrow CaO + CO_2\uparrow$$
$$CaO + H_2O \rightarrow Ca(OH)_2$$
$$Ca(OH)_2 + CO_2 \rightarrow CaCO_3 + H_2O\uparrow$$

As shown in the reaction, above the de-carbonation temperature (T > 800°C) calcite decomposes into calcium oxide (CaO), with the release of CO_2. Reacting with humidity in the air or soil, it turns into calcium hydroxide [$Ca(OH)_2$], which reacts with CO_2, leading to the recrystallisation of calcite. The de-carbonation temperature for calcite is not compatible with those identified for cremation in the Iron Age. Floquet *et al.* (2015), however, demonstrated how this temperature limit is significantly lowered in the case of the Mg-calcite constituent *C. rubrum* (550°C). The data are in good agreement with ex-situ and in-situ annealing experiments performed on *C. rubrum* by Bente *et al.* (2023).

7.1.3.1. μ-Raman analyses

Spectra were collected before combustion and then 9 months after. Before combustion, red coral shows the typical peaks of calcite (1752, 1089, 718, 280, 157 cm^{-1}) and polyenes (3746, 3376, 3034, 2633, 2533, 2256, 2144, 1520, 1299, 1132, 1022, 349 cm^{-1}). After combustion, the spectra show the signals of calcite (probably secondary), calcium hydroxide (3624, 363 cm^{-1}) and calcium oxide (3655 cm^{-1}) with variable intensity (Schmid, Dariz 2015). The amount of secondary calcite, calcium hydroxide and calcium oxide residues varies in the different samples and in different areas in the same sample, as testified by the variation in intensity of the bands (Fig. 157; Tab. 26).

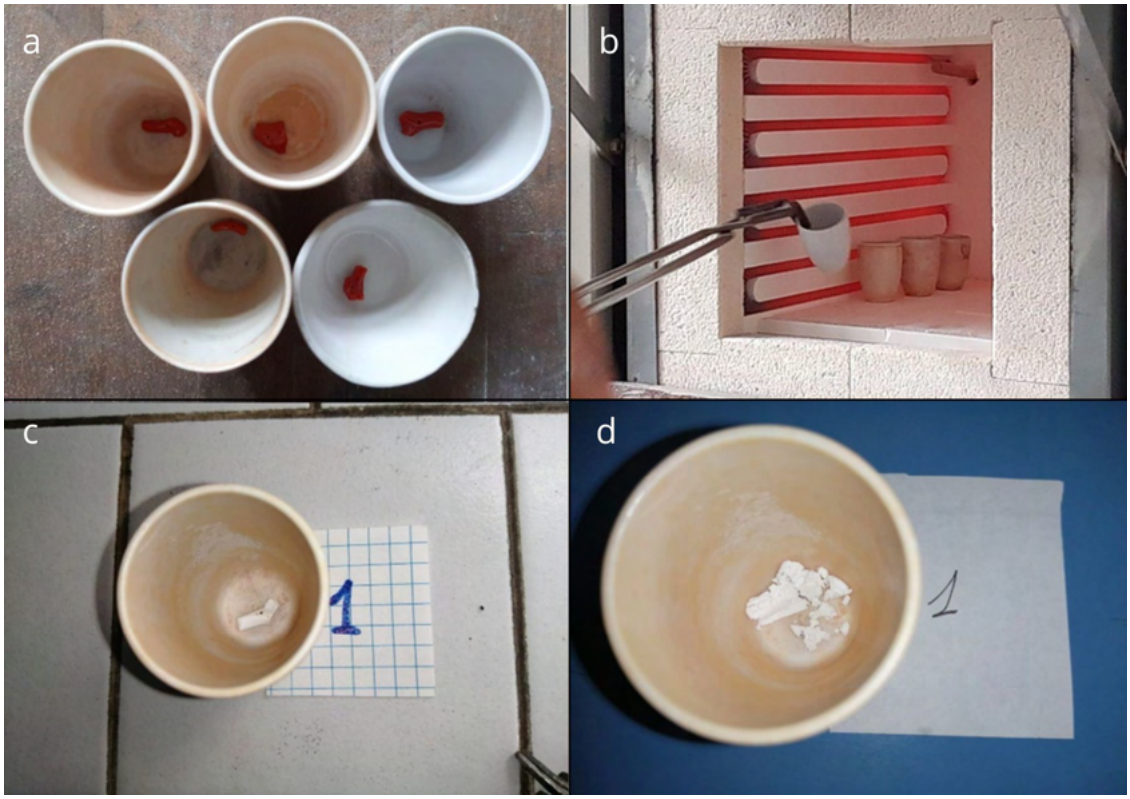

Figure 156. a) *C. rubrum* samples before heating treatment; b) Positioning in the oven; c) Sample 1 after heating treatment: appearance the day after treatment; d) Sample 1 after heating treatment: appearance after one week.

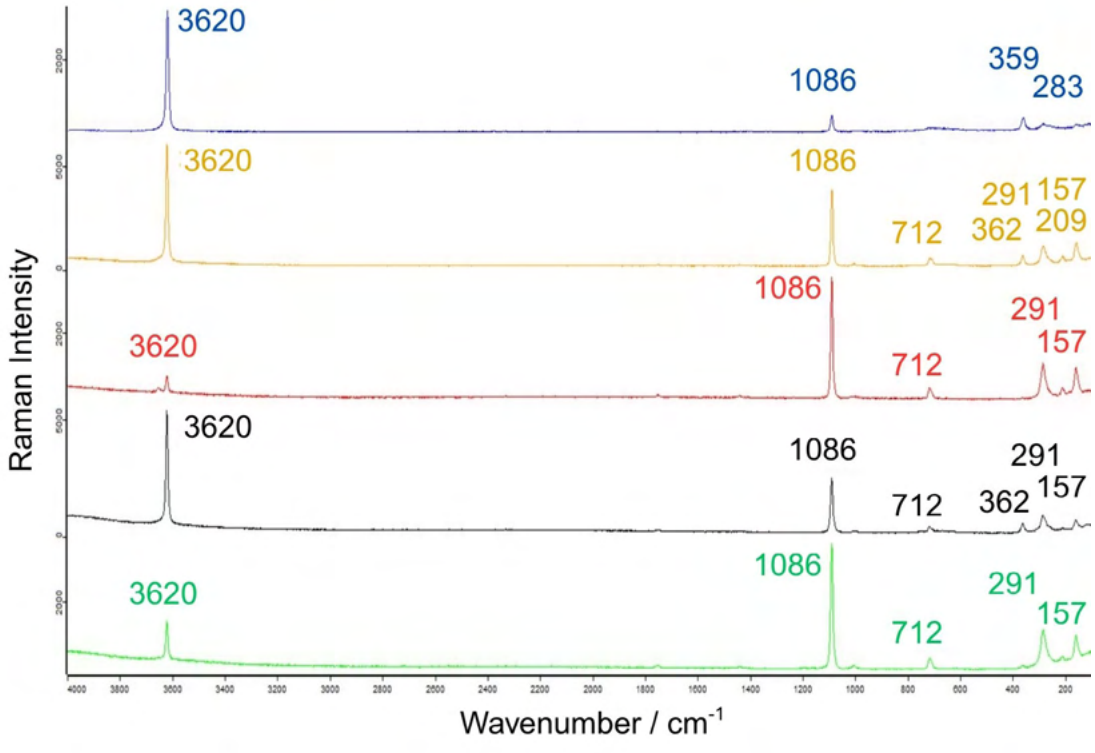

Figure 157. Comparison of the different Raman spectra of burnt corals 9 months after combustion, from top to bottom: zero (blue), one (orange), two (red), three (black), four (green).

7.1.3.2. FT-IR analyses

FT-IR analyses were performed 3 months after combustion (Tab. 27; Fig. 158). The spectra show bands of both calcite (2514, 1796, 1416, 876, 714, 671 cm^{-1}) and Ca-hydroxide (3648, 1648, 1444, 876 cm^{-1}), with variable intensity (Cizer *et al.* 2012).

7.1.3.3. SEM-EDS analyses

SEM-EDS analyses performed before combustion show a relatively homogenous Ca-based composition, with ≈ 12 mol% $MgCO_3$ and other minor elements (i.e., Na, S, Al, Si). The Mg-content slightly varies from sample to sample (Tab. 29). Post-burning analyses show a different composition, still Ca-based but with a different Mg-content. The amount of Mg undergoes a general depletion after combustion, decreasing from ≈ 12% to ≈ 9%, with slight variations in the different samples, thus affecting the Ca/Mg ratio (Tab. 28; Fig. 159). Also, other trace elements appear (i.e. K, Fe, Sr; Tab. 30) Such evidence confirms that a possible Mg-loss may occur during the burning of the artefacts on the funeral pyre.

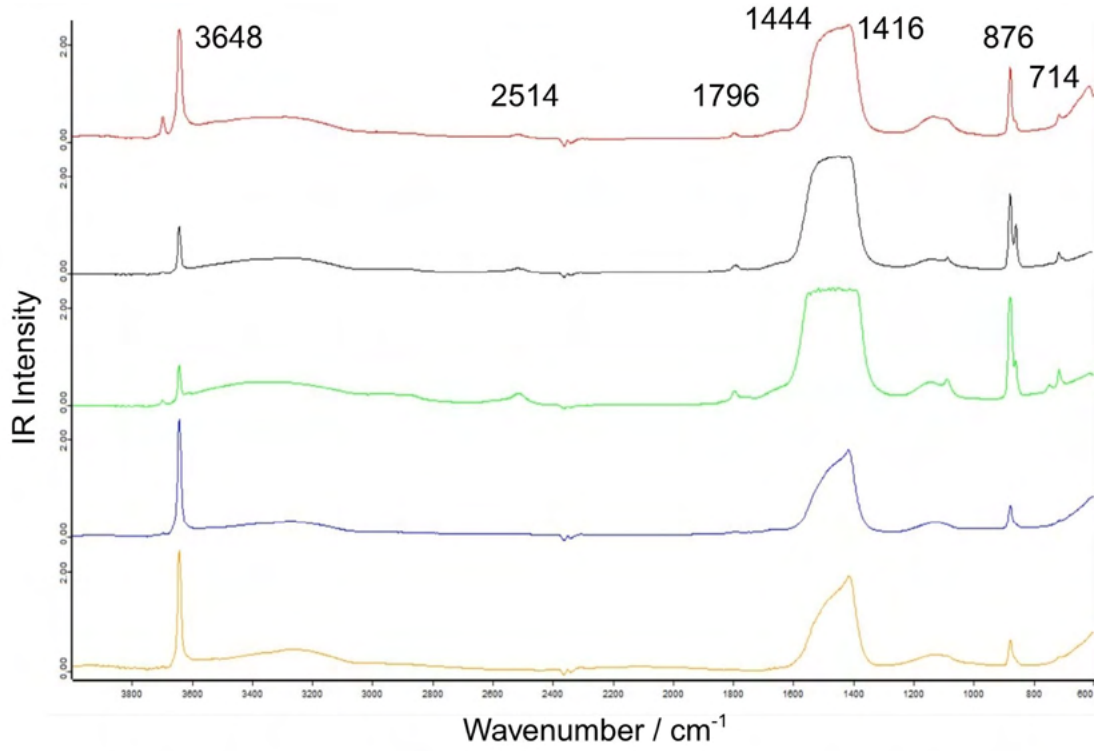

Figure 158. Comparison of different FT-IR spectra of burnt corals 3 months after combustion, from top to bottom: zero (blue), one (orange), two (red), three (black), four (green).

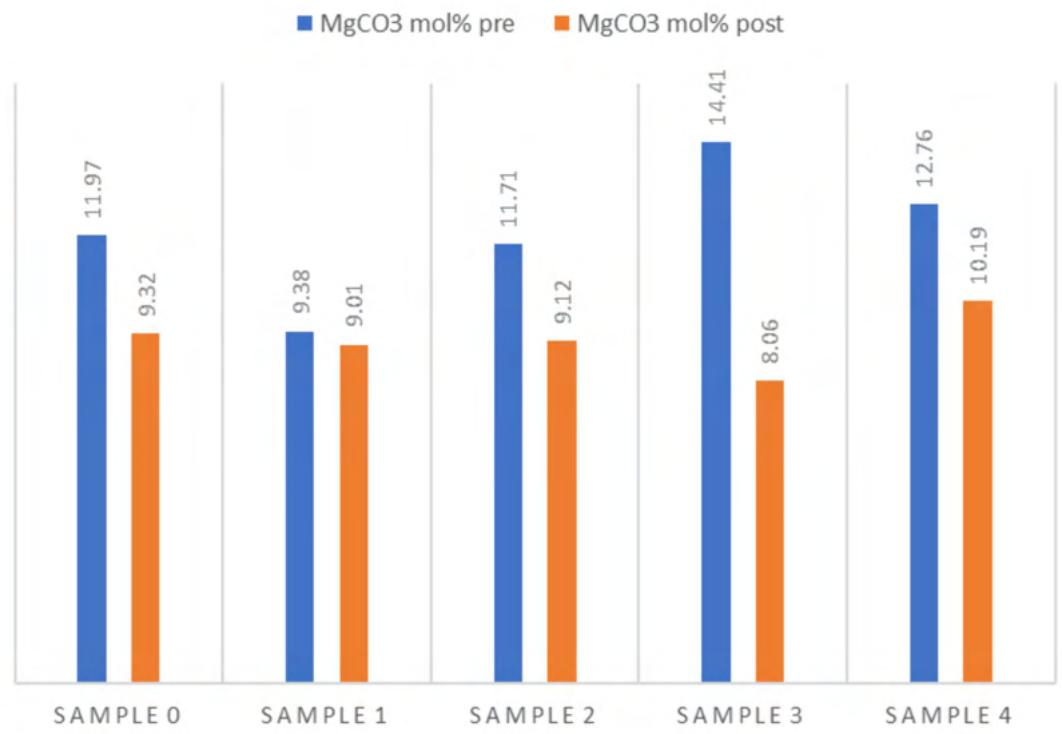

Figure 159. Graph of the variation in magnesium content in calcite before and after burning coral samples.

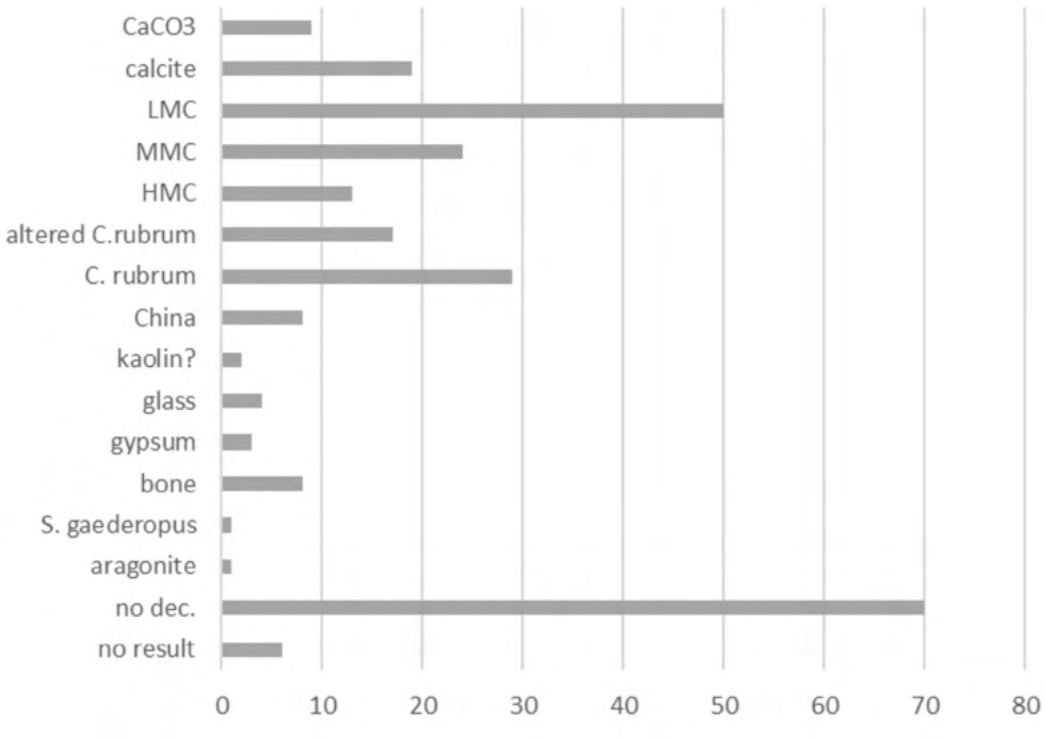

Figure 160. Different identified materials and relative abundancy.

7.1.4 Considerations

In this study, 264 archaeological finds were analysed by using three different archaeometric protocols (i.e. direct-transport, µ-sampling, 'in situ'), with variable degrees of accuracy. Among these, the most fruitful proved to be the first one, since not only it is totally non-destructive, but allows applying different techniques and analysing several sites on the artefact, enhancing the quality and reliability of the results.
The most significant outcome is that a carbonate phase represents the common factor detected in the decorations of most artefacts (163). This common aspect, however, can be declinated and contextualized in several different, multifaceted materials (red coral, pure calcite, HMC, MMC, LMC, etc: Fig. 160), each one characterized by peculiar features and origins. The reasons of these supposed differentiations are exposed hereafter – as are also the other situations, in which a carbonate phase has not been detected.
The occurrence of *C. rubrum* can be certainly acknowledged in 46 (17 %) of the analysed artefacts. This certainty is provided by the contextual presence of both calcite, with a significantly high Mg-content (HMC), and the spectral Raman features of organic red pigments (Hasegawa *et al.* 2010; Floquet *et al.* 2015; Vielzeuf *et al.* 2008; 2013; Weinbauer *et al.* 2000). More specifically, HMC is unequivocally present in 29 cases (11%), while in 17 specimens (6 %) the Mg-content is likely to be more relatable to MMC. This may be due to an incipient alteration process affecting the biogenic carbonate (in table 31 identified with altered *C. rubrum*), also in relation to the common co-occurrence of other materials (e.g., gypsum). In both cases (HMC and MMC), an extreme variability exists in the Mg-content from one analytical spot to another, in agreement with what reported in the literature for *C. rubrum* (Bente *et al.* 2023; Vielzeuf *et al.* 2008; 2013).
The archaeological artefacts for which analyses identify HMC and polyenes include both pinkish and white areas in the decorations, with no differences in the related spectral features (differently from what observed in the modern coral samples, analysed for comparison purposes).
Presence of a lower Mg-content in calcite, detected in the remaining cases, opens some problem of interpretation. Referring to the conventionally adopted values (Borromeo *et al.* 2017; Fürst *et al.* 2016; McGregor, Gagan 2003), calcite-based specimens have been divided, based on the Mg-content, in: 'CALC' = 0 mol% $MgCO_3$; 'LMC' = 0-5.5 mol% $MgCO_3$; 'MMC' = 5.5-10.5 mol% $MgCO_3$; 'HMC' = > 10.5 mol% $MgCO_3$.
In the absence of polyenes, 13 artefacts (5 %) show presence of HMC and 24 (9 %) of MMC. Besides, in 50 archaeological finds (19 %) LMC is detected, with no polyenes. Finally, 21 specimens (8 %) are made of pure calcite (in one case coupled to gypsum and in another one with bone). The absence of polyenes, as well as the Mg-depletion, may be related to heat treatment (e.g. combustion on the funeral pyre, or during a domestic fire, as in the case of the raw coral branches from Forcello di Bagnolo S. Vito, inv. no. 1060). In fact, polyenes decay at » 200°C, with consequent colour alteration (white or grey; Bente *et al.* 2023). This hypothesis may be valid for artefacts that also show clear signs of combustion in the metal parts (around 20% of those examined).
Several causes can justify a different Mg-content in calcite. For example, variations in the Mg-content could be related to the use of materials other than coral – e.g., non-biogenic carbonates. However, as far as biogenic carbonate is considered, variations in the Mg-content could also be justified by a post-depositional alteration of the metastable HMC typical of *C. rubrum*, or – else – of aragonitic materials (e.g. white corals or shells).
Both LMC and HMC can exist in nature, as far as non-biogenic calcites are concerned, while unaltered calcites with intermediate values were never found (Borromeo *et al.* 2017; Fürst *et al.* 2016; McGregor, Gagan 2003). This is the reason why when MMC is identified in an archaeological find, with or without presence of polyenes, its nature is with all due probability attributable to an alteration of an original *C. rubrum* – rather than to the use of other non-biogenic calcareous materials. Supporting this assumption, abundant S is usually found both in HMC and in MMC, indicating a probable biogenic marine origin in both cases (Busenberg, Plummer 1985; Hermans 2010; Macchia *et al.* 2016; Perrin *et al.* 2017; Pingitore *et al.* 1995; Vielzeuf *et al.* 2013). Therefore, alteration phenomena affecting an original *C. rubrum* – or even other materials – cannot be excluded. A loss in the Mg-content can be induced by meteoric diagenesis, leading to the formation of MMC, or even LMC, starting from an original HMC (typical of red coral), or even from aragonite (principal

component of deep-water-corals) (Angelini, Molin, 2015; Borromeo *et al.* 2017; Fürst *et al.* 2016; McGregor, Gagan 2003). Those artefacts in which either pure calcite, LMC or MMC are detected could therefore result from post-depositional diagenesis in the soil of an original red coral. However, though presence of MMC could be caused by diagenetic alteration, some alternative explanations – not to be completely ruled out – may also exist. These include the selection and use, by the ancient craftsmen, of white corals resulting from post-mortem diagenetic phenomena in the marine environment, or that of fossil corals[17] (Bente *et al.* 2015; 2017; Schrickel *et al.* 2013; 2014). This hypothesis is also supported by some outcomes achieved in the current study. In fact, the analysis of the modern sample of white coral 'no. 6' brought to the identification of MMC (10.11 mol% $MgCO_3$), suggesting that similar materials might also have been used in ancient times (see section 7.1.1.5). An enrichment of the comparative studies performed on modern corals for comparison purposes, especially on white Mediterranean corals, could help in shedding light upon this aspect for the future.

For what concerns the rest of the investigated record, in 70 artefacts (26 %) no decorative material was detected in the artefact's circular holes or engravings, etc., but only soil residues or metal alteration products (Fig. 160). In 6 cases (all with the 'in situ' approach), the analyses were inconclusive. In 2 cases (both La Tène fibulae[18]), the interpretation is doubtful (Figs. 74-75) since the analyses exclude the presence of Ca-carbonate material, detecting instead quartz, possible illite and kaolinite by µ-XRD. As such, they could refer to a kaolin-based decoration, or to traces of soil retained by a binder, originally applied to hold *cabochons* in other materials (e.g., coral or glass) that might have been lost (Zlámalová Cílová *et al.* 2024, pp. 59-60). Raman analyses unfortunately give no indication and further investigations are necessary for their sharp characterisation (see section 4.3.2). In 8 cases (3 %) the presence of 'White Indian Ink' was identified, surely related to a modern intervention (late 19th-early 20th century; Schrickel, Bente 2013; Fig. 161a)[19]. Vitreous material was detected in 4 cases (< 2 %), referring to beads and pendants.

In 14 cases (5 %), the analysis revealed the presence of apatite. It is sometimes exclusive and suggests that a material other than coral – probably bone – was used for decoration purposes[20]. Conversely, when apatite is accompanied by other materials (7 cases: 6 leech fibulae with circular decoration and a grooming tool), the interpretation becomes troublesome. Apatite, in fact, is detected only by certain methods; moreover, in these cases Cu (detected by EDS) is abundant, suggesting a possible contamination by both metal alteration products and bone material present in the burial. In 3 of these cases, gypsum was also detected, indicating an intervening marked post-depositional alteration, which may also have played a role in this respect.

Gypsum or anhydrite were detected in 8 cases (3 %), generally in association with calcite and/or bone – except in two cases[21]. Rather than a further decorative material, presence of these sulfates is probably due to a gradual transformation after an original coralline matrix, occurred during the artefact's interment in acidic soils. In some cases (e.g., inv. no. St. 33593) OM-observations clearly identify the canalicular µ-morphologies typical of *C. rubrum* (see Appendix 1, Fig. 217b). Transformation of Ca-carbonate into gypsum due to sulfation is a well-known process, with SO_2 and SO_4^{2-} being the most important S-sources in air and water (Charola *et al.* 2007; Siedel, Siegesmund 2014). Formation of gypsum on a calcareous matrix after weathering depends on several factors (e.g., pollutants concentration, moisture, surface heterogeneity and porosity), with a growth rate of

17 The latter would be easily identifiable with the study of C and O isotopes, because they yield very different data from modern or altered coral (Bente *et al.* 2023).

18 I.e., inv. no. St. 74974 and St. 74975, from Chiomonte (TO).

19 This is not a common practice but a specific case, brought to my attention during the survey for the identification of the analytical record: 10 fibulae from the archaeological site of Parre (BG), known for the discovery of a conspicuous bronze hoard at the end of the 19th century, displayed various linear and/or geometric decorations, marked by an unusually bright white colour.

20 In this case, the objects belong to different categories: 3 beads (one of which was probably made of deer antler), a composite bow fibula, a Late Hallstattian fibula and 3 fragments of burnt bone (mistakenly confused with decorative material, but probably part of the cremated remains).

21 I.e. a pendant 'Longone al Segrino' type (Como, Ca' Morta, grave 302, inv. no. St. 33593) and a fibula with 'occhio di dado' decoration (Parre, inv. no. 128).

few µm/year (Giustetto *et al.* 2020). Simulations were also performed on modern *C. rubrum*, which proved that a superficial gypsum film forms when treating coral with a $(Na,NH_4)_2SO_4$ solution (Bente *et al.* 2015c). Its presence in association with calcite in 4 cases[22] supports this hypothesis.

In a few cases (9, all related to an 'in situ' approach), presence of a generic Ca-carbonate was recognised by p-Raman (the only one useable in that situation), without the possibility of discriminating between calcite or aragonite (due to a marked fluorescence covering almost all signals). This further confirms that by applying a single analytical method (e.g., in the 'in situ' approach), only limited information can be obtained.

Aragonite was identified only on one artefact, i.e., in a grooming tool from the Piovego necropolis in Padua (grave 95, no. 11, tweezer). This tool is part of a more elaborate grooming set, consisting of tweezer, 'auriscalpium' and 'scalpitorium', held together by a suspension element. This exquisitely crafted bronze set has a mixed linear and circular decoration, containing insets of presumed coral. For this set, the extraction of only two micro-samples was authorised: a circular decoration on the 'scalpitorium' and the linear decoration on the tweezer were thus chosen (Fig. 161b). The analysis of the linear decoration evidenced presence of aragonite, whereas that of the circular inset revealed presence of LMC (4.21 mol% $MgCO_3$). These results open to different interpretations: 1) original aragonitic composition for both decorations (white deep-sea Mediterranean coral or shells), with alteration of circular decoration in secondary LMC; 2) use of different materials. Further analysis on other decorations on this or other similar grooming sets may help in solving such an issue.

In one case, the possible use of *Spondylus gaederopus* has been identified, indicated by presence of LMC (4,26 mol% $MgCO_3$) and polyenes. The identification of HMC and polyenes would in fact suggest the use of *C. rubrum* as a possible decorative material. Its skeleton is composed of HMC, with a $MgCO_3$ content ranging from 8-9 to 15 mol%, and polyenes. However, the low Mg content detected by SEM-EDS in this artefact, in association with the presence of polyenes, suggests the use of a portion of the upper coloured valve of *S. gaedeopus* instead.

Unfortunately, this artefact (dolphin-shaped fibulae) is not from northern but probably from southern Italy (Basilicata) and has been analysed for comparison purposes (see section 3.3.4; Fig. 162). The red eyes of two of the artefacts[23] were examined and found to be made of *C. rubrum* (9.91 mol% $MgCO_3$) in one case and of *S. gaederopus* in the other. This differentiation suggests that a degree of heterogeneity may have existed in the selection of raw material sources, possibly in relation to different coastal geographical areas.

The recurrence in the use of a particular material was also evaluated in relation to the main types of archaeological artefacts, in an attempt to understand whether the ancient artisans may have privileged the use of certain materials for producing specific types of artefacts. However, the number of objects analysed for each type varies considerably. In some cases, such as grooming tools, it is very low, whereas in others, such as leech fibulae, it is very high. An attempt was made to correlate the type of archaeological find with the raw material used. However, it is worth noting the statistical uncertainty that affects these considerations.

The different types considered were also grouped into two main macro-groups: less-processed objects, which retain clearly visible surface micro-morphologies useful for identifying the raw material (e.g., *C. rubrum*), and artefacts with highly worked coral parts, for which it is less easy to recognise characteristic surface morphologies.

For what concerns the less processed objects, a predominance of *C. rubrum* is not observed, though in some cases its typical µ-morphologies (see section 7.1.2.1) can be appreciated. It is predominant only in the rough coral branches (50% *C. rubrum*; 17% altered *C. rubrum*; 33% MMC; Fig. 163a). The greatest variability in materials is observed in beads (Fig. 163b); their composition seems to vary geographically: those from the Venetic area show a predominant Ca-carbonate composition. For this type, *C. rubrum* or altered *C. rubrum* are again predominant, respectively 8% and 42%. The situation varies for the pendants (Figs. 163c-d) as well as for the composite fibulae (Fig. 163e): the

22 I.e. inv. no. St. 72276 from Pombia, D2065 from Golasecca, 23.M380-9.2 and NCT0100026418 from San Bernardino di Briona.

23 I.e. inv. no 23-M380-9.8 (Fig. 10) and 23-M380-9.10 (Fig. 164).

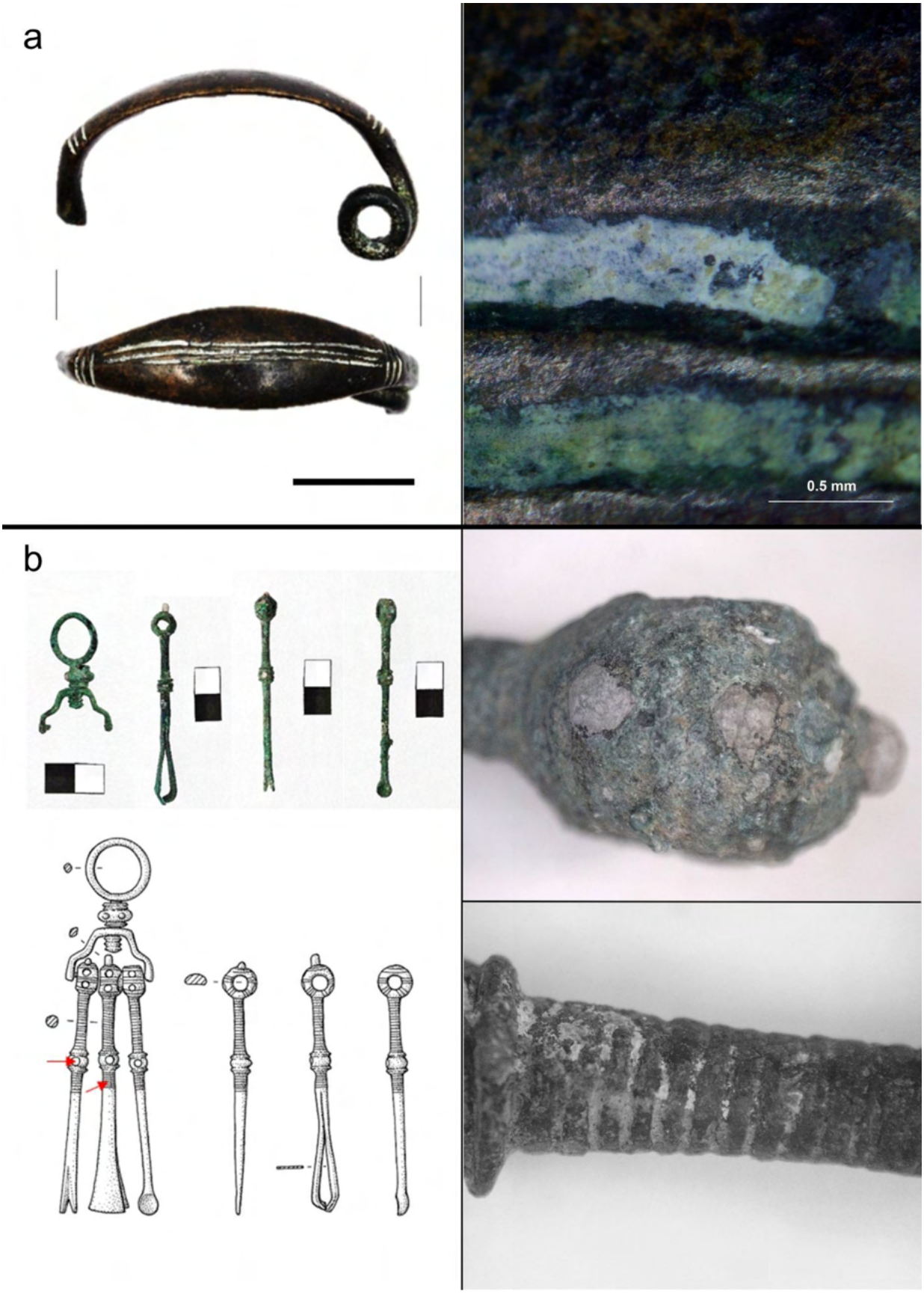

Figure 161. a) White Indian Ink decoration of fibula inv. no. 40 from Parre (Bergamo Archaeological Museum; ph. Berruto; metric reference 1 cm); b) Grooming tools set from Piovego necropolis, Padua (tomb 95, no. 10): sampling point and detail of the analysed areas (ph. Berruto; drawing modified after Gallo 2023).

analyses identified mostly carbonate material, with a predominance of LMC. As the µ-features of *C. rubrum* are often visible, a greater intervention of alteration phenomena is assumed for these materials.

The situation is similar for artefacts with highly worked coral parts. For both bucket pendants (Fig. 163f) and grooming tools (Fig. 163g), an exclusively Ca-carbonate composition is identified, with a strong predominance of LMC (50%). Some categories, such as late-Hallstattian fibulae, are poorly represented. The best represented category is that of leech fibulae with circular decoration (Fig. 163h), for which a carbonate composition is predominant again, with a few rare exceptions. For this type, there is greater variability among the materials identified, due to the larger number of finds analysed: 22% LMC, 16% *C. rubrum*, 12% calcite, 11% MMC, 6% HMC, 5% altered *C. rubrum*, 3% $CaCO_3$, 2% other materials, 23% no decoration.

An examination of the occurrence of different raw materials across artefact types did not reveal any statistically significant trends. An important finding is the association of characteristic morphologies of *C. rubrum* in some less-processed objects with the predominance of LMC in the archaeometric analysis, which is probably an indication of marked alteration phenomena. This phenomenon is most noticeable in artefacts with metal parts, such as Longone pendants and composite bow fibulae. By contrast, it does not occur in artefacts without metal parts, such as raw coral branches and beads, where archaeometric investigations mainly identify *C. rubrum* or altered *C. rubrum*. It is therefore possible to hypothesise the occurrence of alteration phenomena involving Mg depletion and polyenes loss in relation to deposition in contact with bronze. If this hypothesis were true, this data would be crucial for interpreting the results of archaeometric analyses of bronze artefacts with highly worked coral parts, such as leech fibulae, bucket pendants and grooming tools. Close contact with metal in these artefacts may have promoted post-depositional alteration, making it difficult to identify *C. rubrum* in the absence of micro-morphologies that are recognisable under an optical microscope. However, it should be noted that the corpus considered for this correlation is not homogeneous. The number of archaeological finds analysed for each type is not always comparable (e.g. 3 pendants and 133 leech fibulae). These considerations therefore remain speculative and would require further analysis to make the comparison statistically relevant.

Focusing exclusively on leech fibulae, the best represented type, an attempt was made at identifying possible trends in relation to other factors, such as: occurred combustion (Fig. 164a), typological based-chronology (Fig. 164b), year of discovery (Fig. 164c) and macro-area of origin (Fig. 164d).

Relating data to a possibly intervened combustion provides some interesting considerations (Fig. 164b). Such an event, in fact, has a certain recurrence in those leech fibulae in which LMC and/or pure calcite are found (incidence of burnt artefacts ≈ 50 %) – thus being responsible (in whole or in part) for a certain depletion in the Mg-content. Conversely, *C. rubrum* is always found on non-combusted artefacts. Also, the incidence of combustion is almost negligible for the HMC-based (1 case out of 8) and MMC-based (3 out of 15 cases) decorations. In the case of HMC, combustion may have accounted for loss of the polyenes (at T > 200°C), whereas for MMC (according to experimental data from modern coral combustion), it might have explained a gradual depletion in the Mg-content.

Figure 162. Dolphin-shaped fibula of unknown provenance (Collezione Assi, Musei Reali, Torino; inv. no. 23-M380-9.10, 4/27; ph. Berruto; metric reference 1 cm).

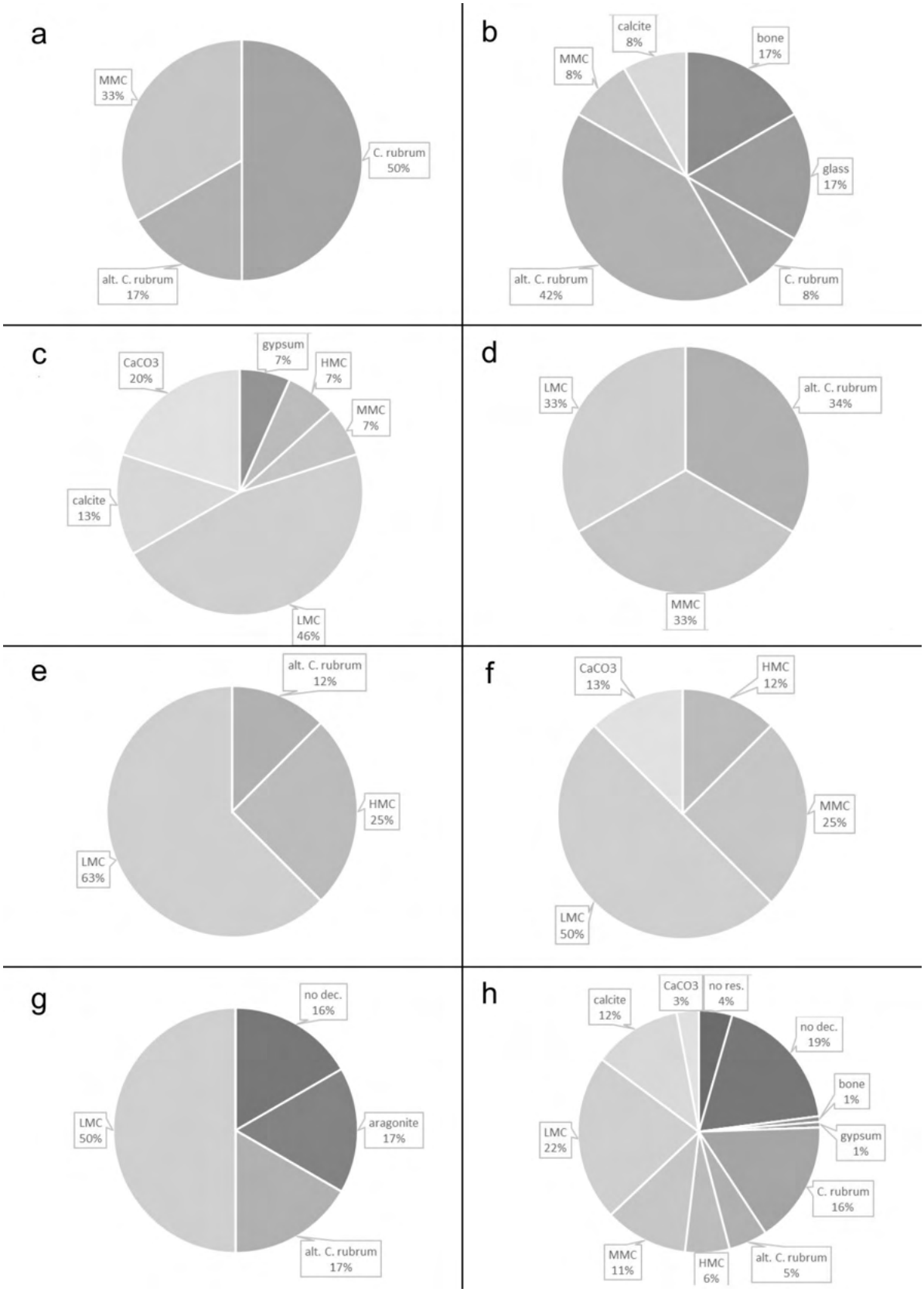

Figure 163. a) Identified materials for 6 raw coral branches; b) Identified materials for 12 analysed beads; c) Identified materials for 15 Longone al Segrino type analysed pendants; d) Identified materials for analysed 3 other pendants; e) Identified materials for 9 analysed composite fibulae; f) Identified materials for 8 analysed bucket pendants (1A type); g) Identified materials for 6 analysed grooming tools; h) Identified materials for 133 analysed leech fibulae with circular decoration.

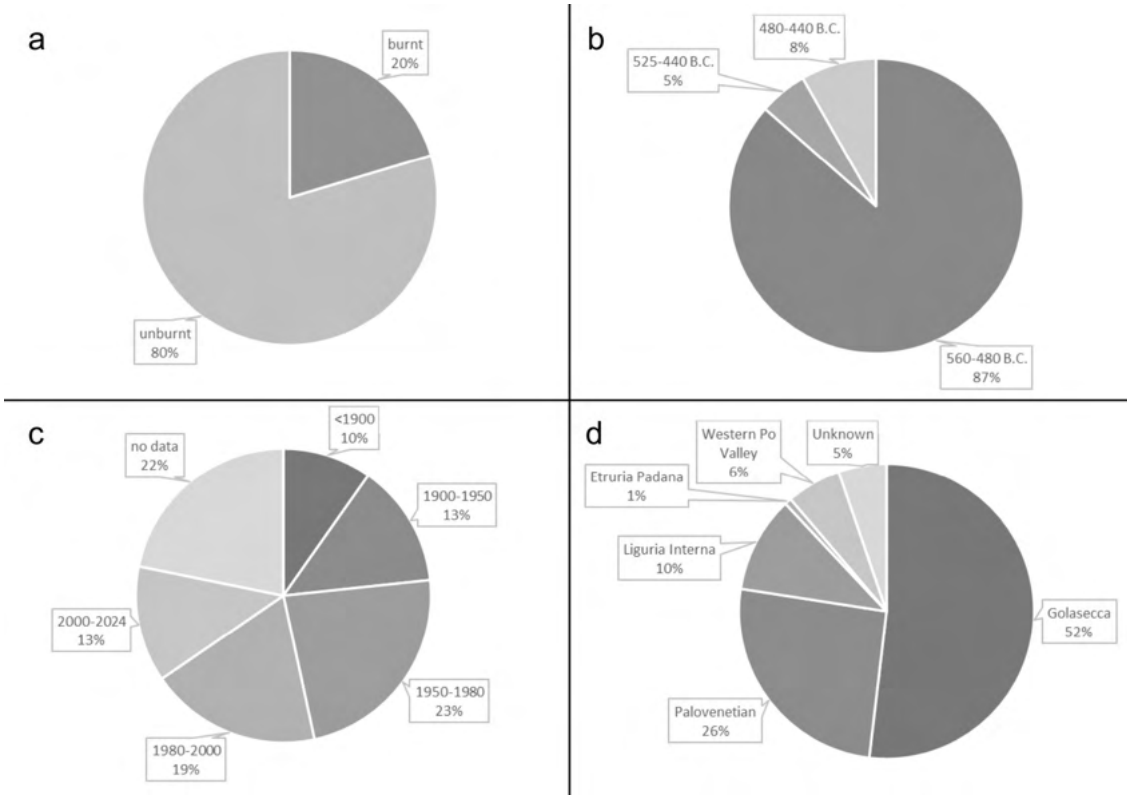

Figure 164. a) Leech-fibulae with circular decoration: percentage of burnt finds; b) Leech-fibulae with circular decoration: different artefact dates on a typological basis and relative percentages; c) Leech-fibulae with circular decoration: year of discovery and relative percentages; d) Leech-fibulae with circular decoration: geographical macro-areas of origin and relative percentages.

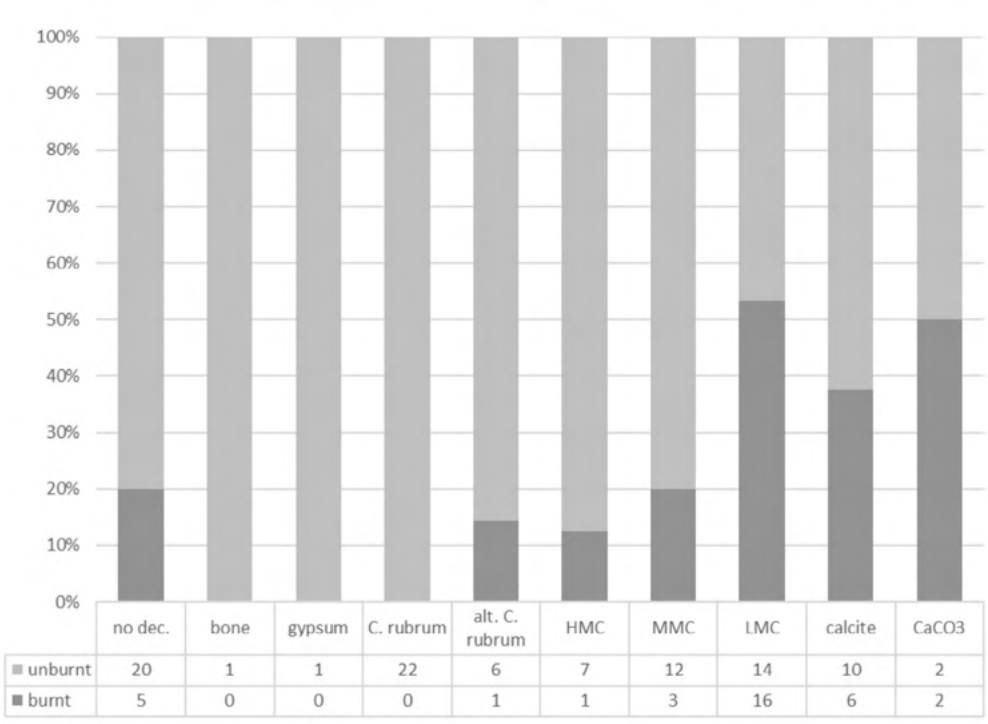
100%
90%
80%
70%
60%
50%
40%
30%
20%
10%
0%
no dec. | bone | gypsum | C. rubrum | alt. C. rubrum | HMC | MMC | LMC | calcite | CaCO3
unburnt | 20 | 1 | 1 | 22 | 6 | 7 | 12 | 14 | 10 | 2
burnt | 5 | 0 | 0 | 0 | 1 | 1 | 3 | 16 | 6 | 2

Figure 165. Graph of the quantity of burnt and unburnt artefacts by type of material identified.

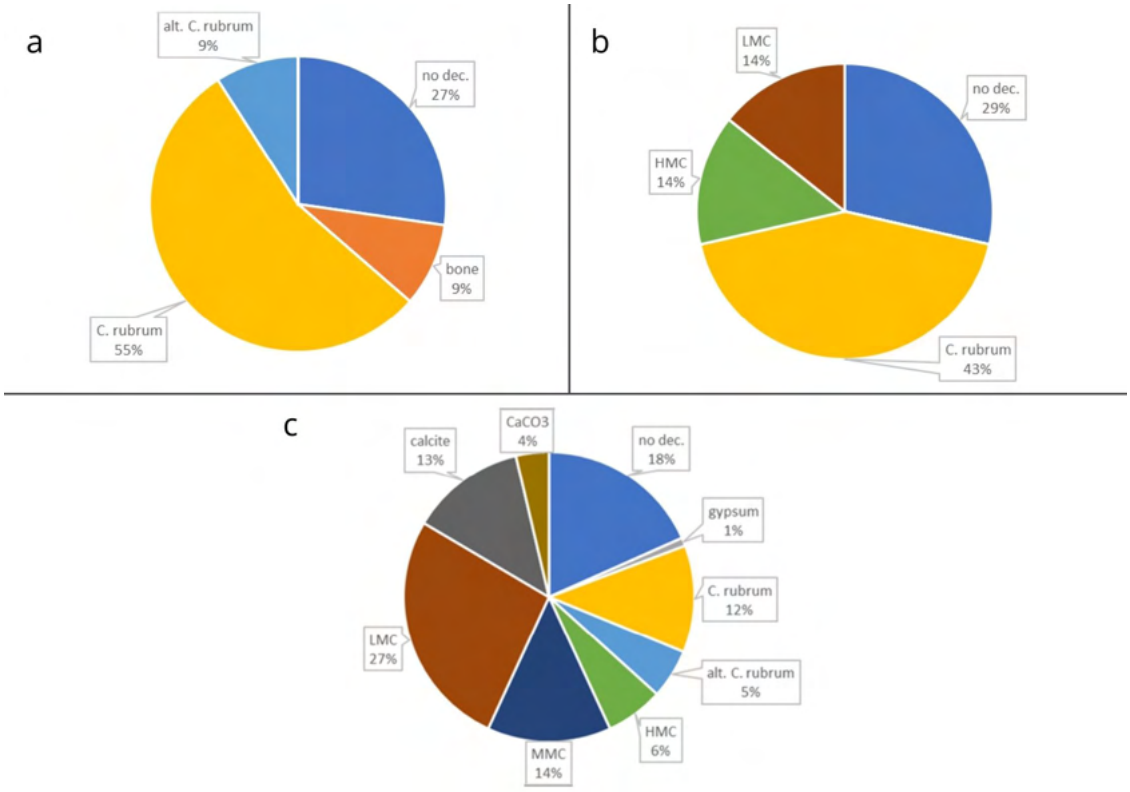

Figure 166. a) Occurrence of different materials in fibulae decorations dated to 480-440 BCE; b) Occurrence of different materials in fibulae decorations dated to 525-440 BCE; c) Occurrence of different materials in fibulae decorations dated to 560-480 BCE.

As far as chronology is concerned, another interesting trend emerges. On a typological basis, by correlating the presumed dating of the leech fibulae with the identified decorating materials, two main chronological macro-divisions (560-480 BCE and 480-440 BCE) can be individuated –plus a third overlapping phase (525-440 BCE)[24] (Tab. 31; Fig. 166). According to this trend, the following generalisations can be sketched:

- *C. rubrum* is most frequently found in the decorations of the more recent artefacts (480-440 BCE), where LMC is absent;
- Higher variations in the Mg-content characterize the oldest chronology (560-480 BCE).

However, it should be noted that the more recent finds are the less represented in the analytical record (Fig. 164b) – which might also explain the higher variability in the Mg-content of the older finds (as the number of analysed finds increases, so does the variability). In spite of this, the higher incidence of *C. rubrum* in the more recent artefacts could hint that this material became more and more used in time.

Based on the year of discovery, the leech fibulae were divided into 6 groups: i) pre-1900, ii) 1900-1950, iii) 1950-1980, iv) 1980-2000, v) 2000-today, vi) no data indication. All groups are well represented in the analytical record (Fig. 164c) and no specific trend is highlighted by comparing this data with the frequency of the different materials identified (Fig. 167).

The leech fibulae were also divided into 6 groups on the basis of the cultural affiliation to the site of origin: i) Golasecca area, ii) Venetic area, iii) Liguria Interna, iv) Etruria Padana, v) western Po valley and vi) unknown (Fig. 164d). Etruria Padana is the least represented area (only 1 fibula), while the best represented ones are the Golasecca and Este (or Venetic) cultures, with 69 and 34 analysed items respectively. Occurrence of LMC is higher in the Este culture area than in the Golasecca area, where instead calcite is well

24 The chronological classification (see section 4.2.1.4) of leech-fibulae with circular decoration is based firstly on the variants of bow decoration, identifying two macro-groups: classical type (variants A, B, C, D, E, F: 560-480 BCE) and evolved 'Palestro' type (variant G: 480-440 BCE). If the bow is not preserved, it can be referred to the foot, with three chronological subdivisions: classical type (variants P, S, V: 525-480 BCE), 'Palestro' type (variants G or GG: 480-440 BCE) and intermediate type Q (525-440 BCE).

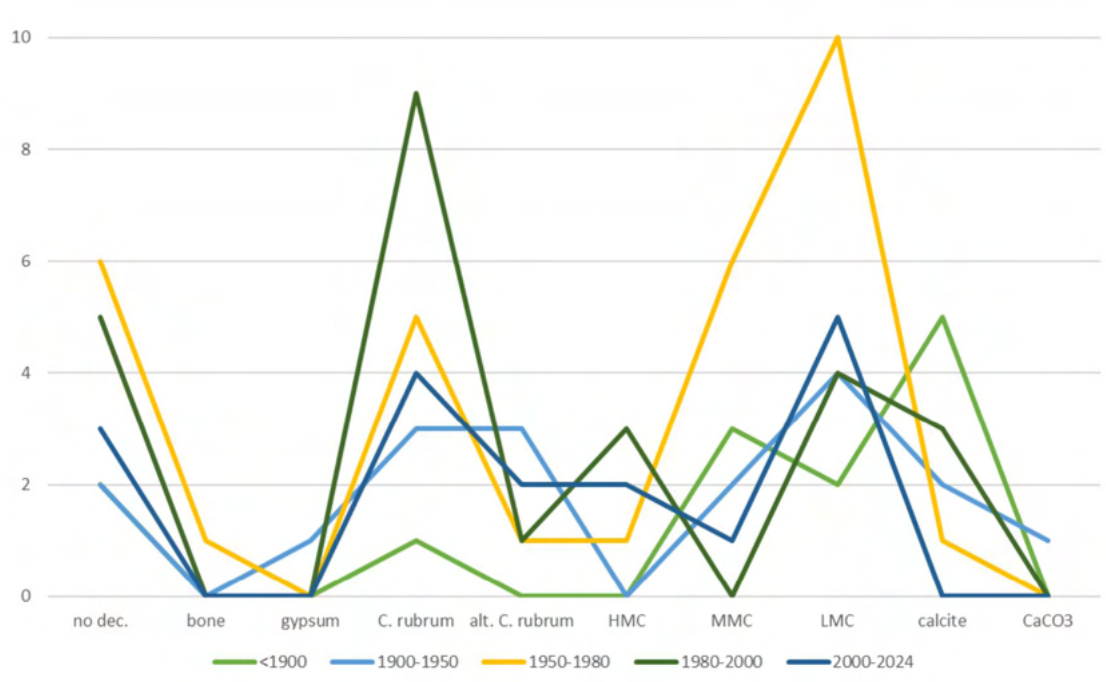

Figure 167. Occurrence of different materials in different discovery chronological ranges.

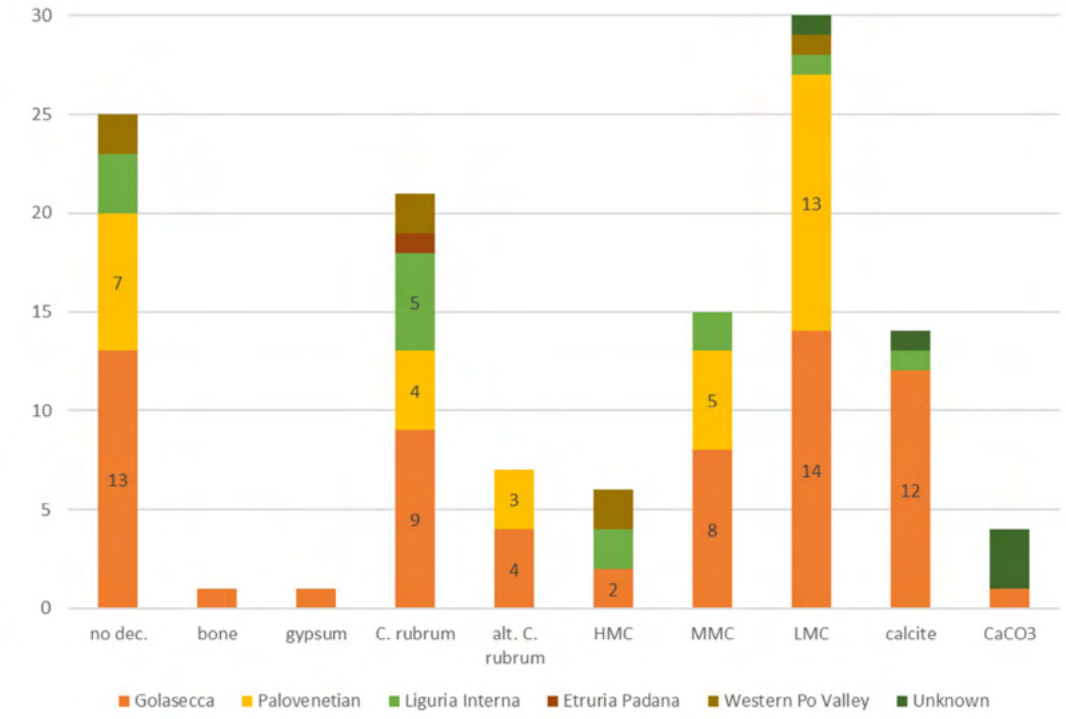

Figure 168. Frequency of different materials in different geographical macro-areas.

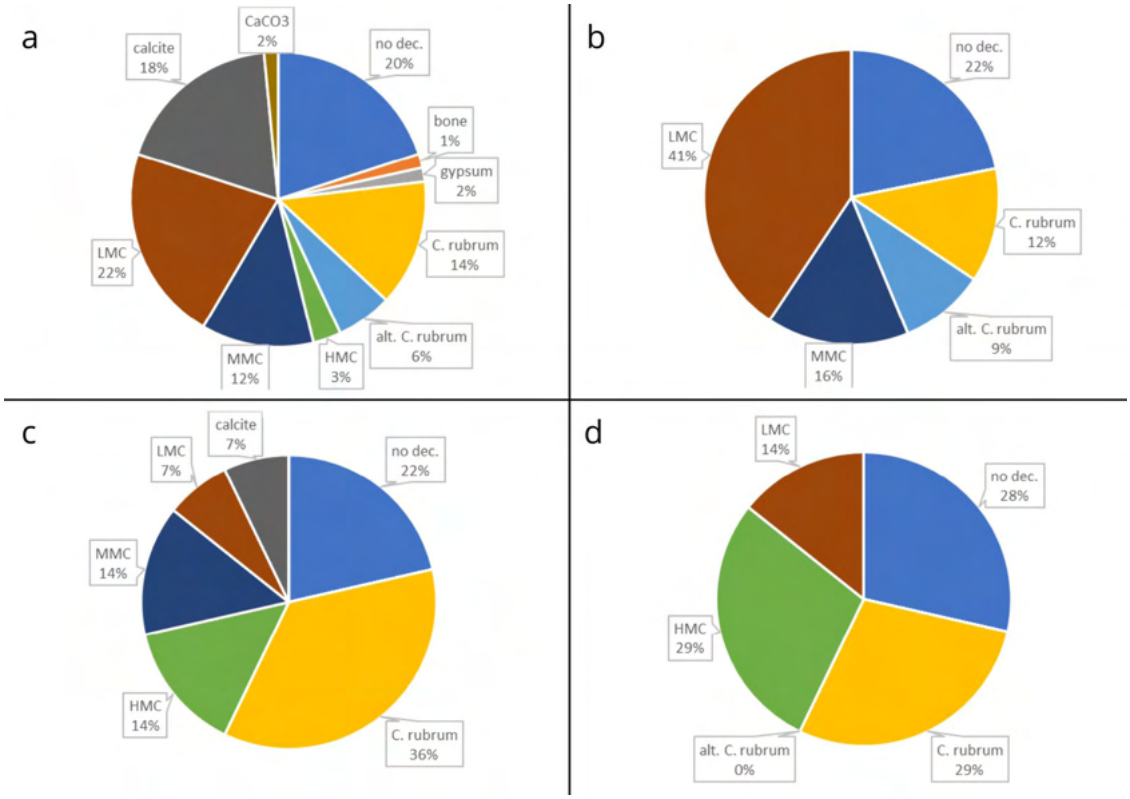

Figure 169. a) Occurrence of different materials in fibulae decorations from Golasecca area; b) Occurrence of different materials in fibulae decorations from Este area; c) Occurrence of different materials in fibulae decorations from Liguria Interna; d) Occurrence of different materials in fibulae decorations from western Po Valley.

documented. The incidence of some materials is slightly unbalanced in favour of the Venetic macro-area (i.e., altered *C. rubrum* and MMC), while the occurrence *C. rubrum* is slightly higher in the Golasecca area (Figs. 168, 169a). Some trends are also observable for 'Liguria Interna' and the western Po Valley (Figs. 168, 169c), but they are scarcely significant, due to the low number of artefacts from these areas (Fig. 164d). Based on these trends, as far as leech fibulae with circular insets (the most represented type of the dataset) are concerned, the most relevant discriminant factor concerning the use of red coral seems to be based on chronological issues. The higher incidence of *C. rubrum* has been identified in the more recent finds (480-440 BCE). This could indicate that, in the earliest phases, the use of different materials to produce these decorations was also common practice, and that the use of coral became more and more consolidated in time – maybe also favoured by a stylistic development that caused a certain evolution in the manufacture of more sophisticated – hence, more precious – objects of fine art. This hypothesis should be confirmed by extending the analytical record to a higher number of fibulae of the evolved type – which prevail in the Swiss area of the Golasecca culture.

Supporting this evidence, the case of a leech-fibula from San Bernardino di Briona (Fig. 170; inv. no. NCT0100026418; 525-480 BCE) is singular. In the decoration of this object, the use of different materials (*C. rubrum*, apatite and gypsum) is documented. If gypsum could result from an alteration of calcite (as indicated by the simultaneous presence, in one hole, of both analytical signals), apatite may indeed indicate the use of a different material. This artefact is also singular in its manufacture, since – unlike general uniformity – it has variable hole sizes (Ø 2-4 mm). As such, it could thus represent an experimentation of a sophisticated manufacturing technique in the artefact design, corroborated by the adoption of several decorating materials.

By extending the discussion to each and every type of artefact examined in our dataset, the archaeometric analyses in many cases identified LMC or MMC in poorly worked artefacts, which simultaneously retain surface traces of the μ-morphologies typical of *C. rubrum*. In these cases, any anomalous compositional variation (i.e., a lower Mg-content) should depend – with

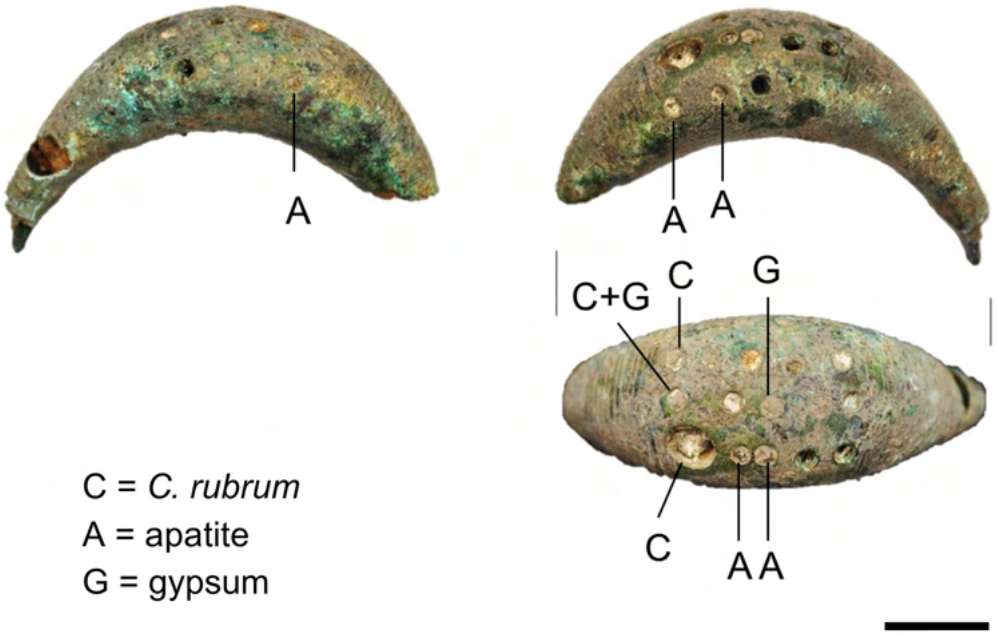

Figure 170. Leech fibula with circular decoration from San Bernardino di Briona (inv. no. NCT0100026418).

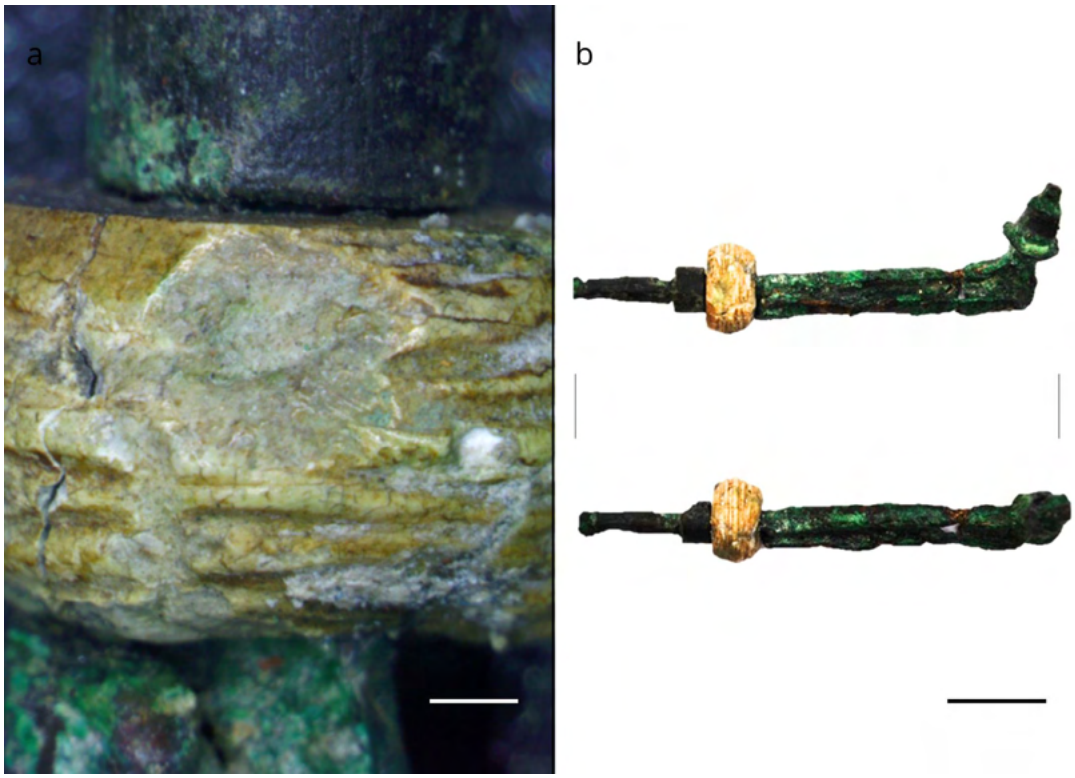

Figure 171. Bead on a composite bow fibula from Brembate Sotto (inv. no. 67): a) detail of the fracture (metric reference 1 mm); archaeological find (ph Berruto, metric reference 1 cm).

all due probability – on an occurred alteration of *C. rubrum*, which brought to Mg-depletion and denaturation of polyenes. To corroborate such interpretation, a particular situation must be described: composite bow fibula from Brembate sotto (inv. no. 67, Fig. 171) with a bead inserted in the foot. In this artefact, no specific µ-morphologies of coral were observed at the microscope, but useful suggestions came from the archaeometric results. Its chemical composition, measured by EDS, revealed presence of LMC (average 4.25 mol% $MgCO_3$) on the entire surface of the bead, further confirmed by Raman. However, presence of a small fracture allowed µ-Raman analysis of an inner portion, in which *both* polyenes and calcite were identified. Such evidence confirmed that an alteration of an original *C. rubrum* had indeed occurred, as diagenesis during burial of the artefact caused Mg-depletion, proceeding from the surface inwards and resulting in the preservation of the original composition only in the core of the object, as demonstrated in previous studies on a similar artefact from Leinbach (Bente *et al.* 2020)[25].

Finally, with regard to the organic materials, an identification was attempted comparing the related spectral features with those of modern samples and literature (Casanova *et al.* 2016; Rageot *et al.* 2019). Unfortunately, materials used as ancient binders often show spectra very similar to those of synthetic materials used nowadays for restoration purposes (having at times been used as restoration materials themselves: e.g., beeswax). It was therefore not possible to identify with certainty the presence of organic binders, also due to the absence of any data regarding the restoration history of the artefacts.

7.2 Metal surface

The results reported here refer to the analysis of 118 archaeological finds (plus 23 additional samples)[26]. Different non-invasive analytical techniques were applied in this study – i.e., µ-Raman, µ-XRD and SEM-EDS; the latter two proved to be the most effective for investigating bronze alteration products[27].

7.2.1. Optical microscopy

Optical microscopy provides information about the technological aspects (see section 8.1) and conservation purposes. The artefacts are affected by different levels of alteration, probably related to diagenetic phenomena occurring in the post-burial phase, or influenced by post-excavation life and restoration.

Generally, the metallic surface is covered by a patina of alteration of various colours, appearances and extent. At times, it has been removed (as in the artefacts from Como, via Isonzo, where microscopic examination reveals traces of heavy abrasion during restoration: Fig. 172a). Elsewhere, no intervention was done, and the alteration products are perfectly preserved (Fig. 173), sometimes even obliterating the decorations (Fig. 174; see section 7.1.2.1). Occasionally, post-excavation life alteration is visible, (e.g., growth of alteration products after restoration: Fig. 172b).

25 In the case of a fibula from the Second Iron Age (La Tène) from Leinbach (similar because it is characterised by a metal arch covered with coral beads), TEM-AEM and µ-XRD analyses detected a different composition between the surface (Mg-free calcite) and the inner part (HMC), probably resulting from interaction with meteoric water (Bente *et al.* 2020).

26 This investigation has always been performed on all the metallic artefacts transported to the University's laboratories (118), for which has been possible to collect many points of analysis. Data on metallic alteration products, obtained from µ-sample analysis, are also reported for completeness.

27 Due to the short acquisition times, many analytical spots on the artefact were acquired for µ-Raman and SEM-EDS investigations; for µ-XRD, only one spot was usually analysed; in this case, the data refer to the areas around the decorations.

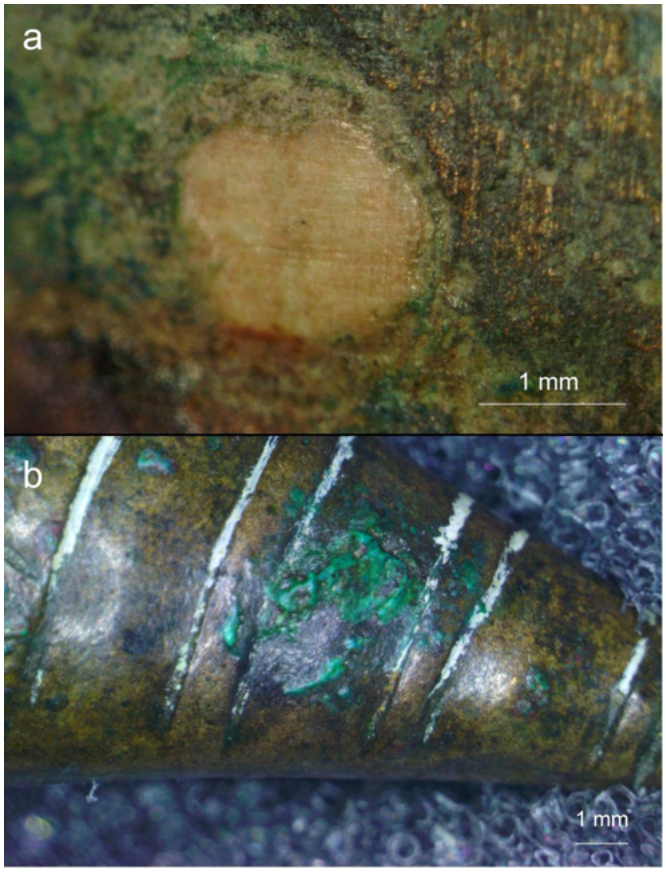

Figure 172. a) Leech fibula decoration (Como, via Isonzo; inv. no. St. 57262): heavy abrasion during restoration on both the metallic and coral parts; b) Fibula from Parre (inv. no. 49): bronze alteration products on modern White Indian Ink decoration.

Figure 173. Leech fibula with circular insets from Piovego necropolis (inv. no. 108.3): not restored artefact with marked patina (ph. Berruto; metric reference 1 cm).

Figure 174. Leech fibula with circular insets from Piovego necropolis (inv. no. 86.3a; ph. Berruto; metric reference 1 cm): detail of the bow upper part, showing an almost complete obliteration of the decoration due to presence of surface alteration products.

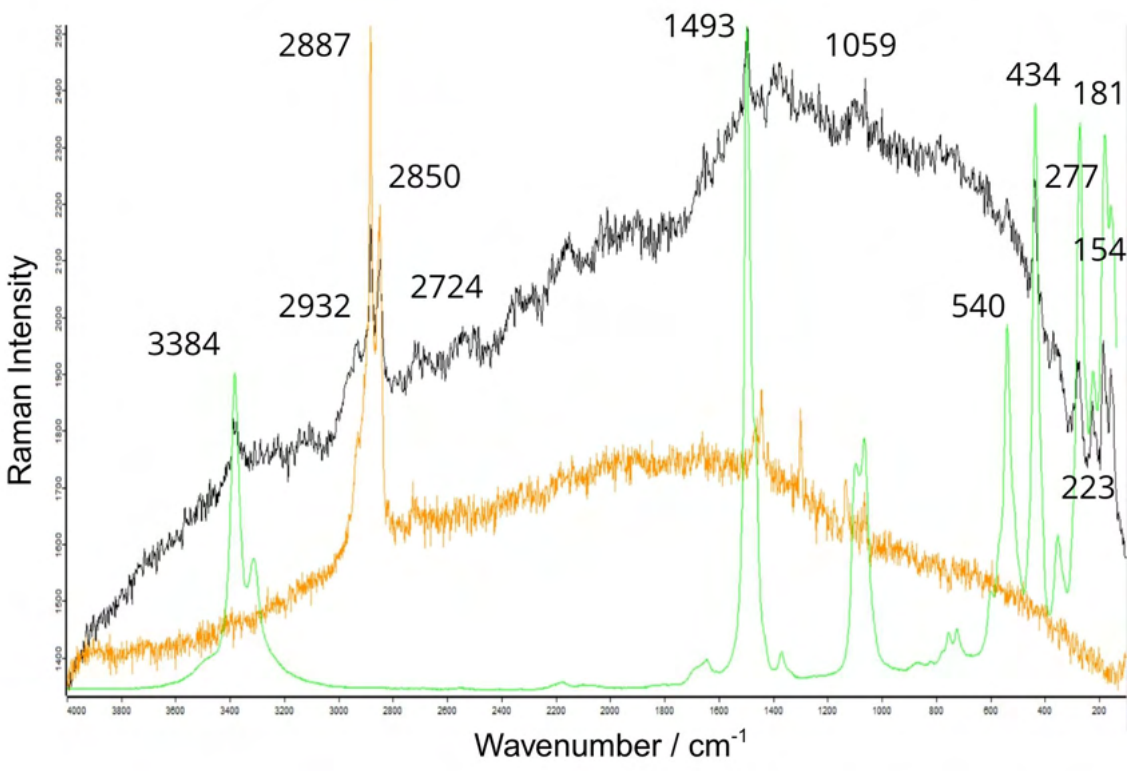

Figure 175. St. 72276 (Pombia necropolis): Raman spectrum of the metal surface analysis in black and comparison with the spectrum of beeswax (orange) and malachite (RRUFF database - malachite Zaire: Lafuente *et al*. 2015; green).

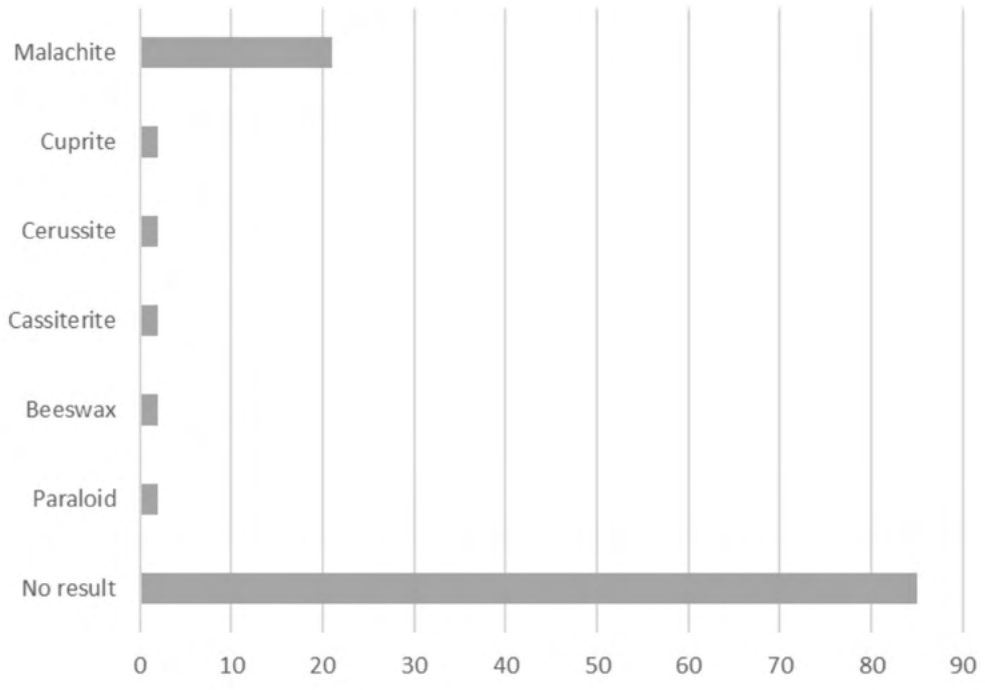

Figure 176. μ-Raman analysis results and relative abundance per number of artefacts.

7.2.2. μ-Raman analysis

They were carried out on 118 archaeological finds with preserved metallic portions, using a benchtop μ-Raman instrument. In most cases (72 %, 85 archaeological artefacts), no interpretable signal was obtained, with due exception (Fig. 176) – such as malachite (Fig. 175), cuprite (1 case each), malachite & cuprite (1), cerussite (2) and cassiterite (2). Organic compounds have also been detected, i.e., Paraloid (2 cases) and beeswax (2). For a more detailed overview, see Tab. 32.

7.2.3. μ-XRD analysis

Several crystalline phases were detected (Fig. 177; Tab. 33) related to metal alteration by-products, suggesting a possible composition for the original alloy. Copper alteration products are various (Figs. 180-184)[28], followed by tin alteration products (Fig. 187)[29], indicating that bronze is indeed the alloy forming the artefacts. Lead by-products are also present (Figs. 185-186)[30], which (as corroborated by EDS analyses: see section 7.2.5) provide interesting technological suggestions (see section 8). In some cases, reflections at d = 2.12 and 1.84 Å specifically indicate presence of bronze (Fig. 179: Asnavandi *et al.* 2013; Liao *et al.* 2018; Song, Tegus 2023) – especially in those artefacts where the surface alteration patina is reduced or absent. Moreover, the identification of mckinstryite (Ag_2S; Fig. 178) suggests presence of silver (also confirmed by EDS).

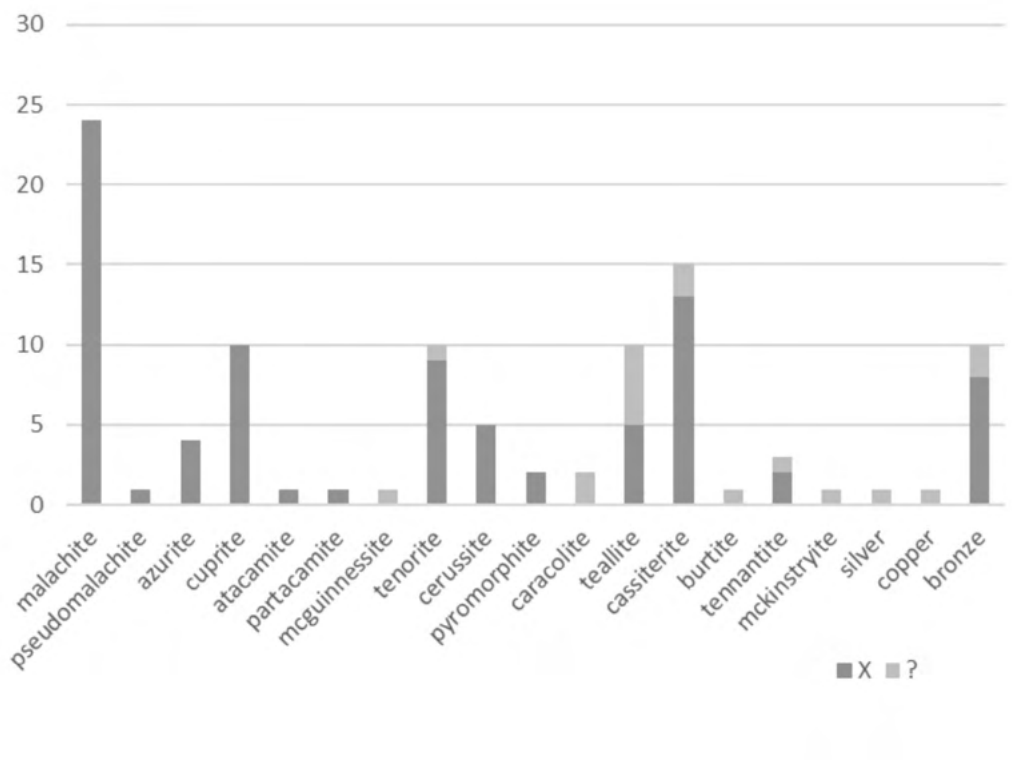

Figure 177. Identified crystalline phases (bronze alteration products) and relative abundance (X = sure identification; ? = questionable).

28 i.e. malachite [$Cu_2(CO_3)(OH)_2$], presudomalachite [$Cu_5(PO_4)_2(OH)_4$], azurite [$Cu_3(OH)_2CO_3$], cuprite (Cu_2O), atacamite [$Cu_2(OH)_3Cl$], paratacamite [(Cu, Zn, Ni, Co)$_2$(OH)$_3$Cl], mcguinnessite [(Mg,Cu)$_2$(CO$_3$)(OH)$_2$], tenorite (CuO), tennantite [$Cu_6(Cu_4Zn_2)As_4S_{13}$].

29 i.e. cassiterite (SnO_2), burtite {Ca[Sn(OH)$_6$]}.

30 i.e. teallite ($PbSnS_2$), cerussite ($PbCO_3$), pyromorphite [(PbCl)$Pb_4(PO_4)_3$], caracolite [$Na_3Pb_2(SO_4)_3Cl$].

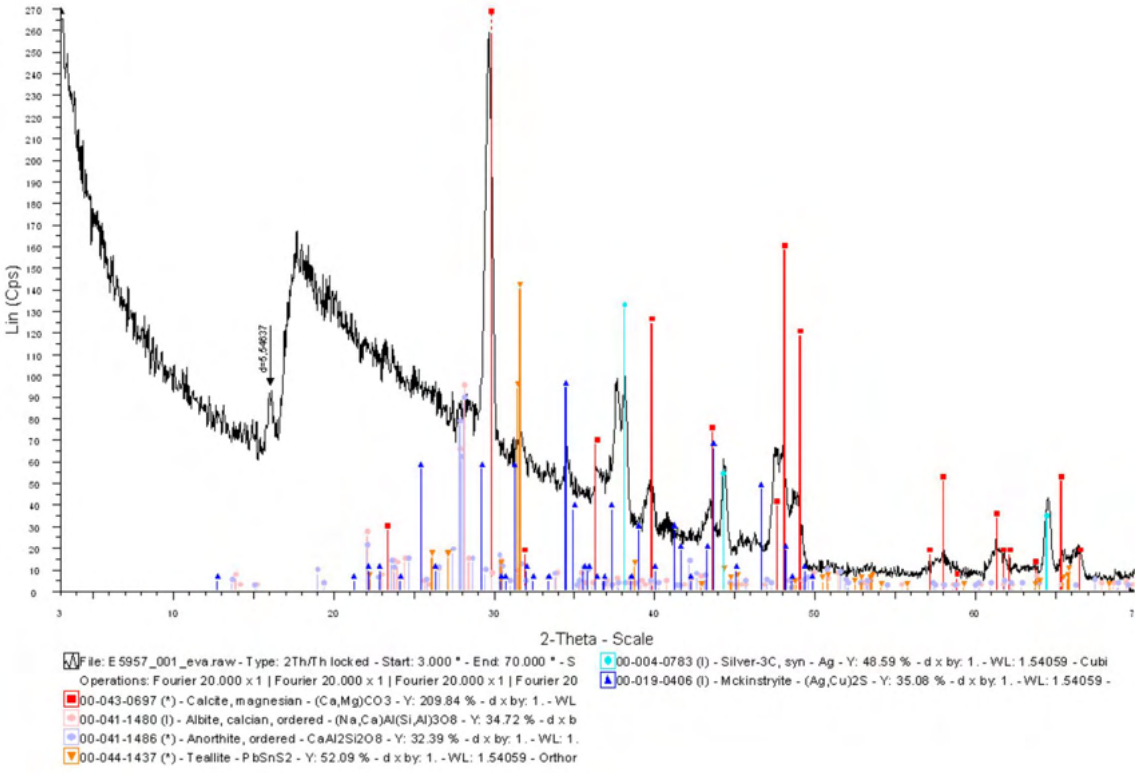
Lin (Cps)
d=5,54037
2-Theta - Scale
File: E 5957_001_eva.raw - Type: 2Th/Th locked - Start: 3.000 * - End: 70.000 * - S
Operations: Fourier 20.000 x 1 | Fourier 20.000 x 1 | Fourier 20.000 x 1 | Fourier 20
00-043-0697 (*) - Calcite, magnesian - (Ca,Mg)CO3 - Y: 209.84 % - d x by: 1. - WL
00-041-1480 (I) - Albite, calcian, ordered - (Na,Ca)Al(Si,Al)3O8 - Y: 34.72 % - d x b
00-041-1486 (*) - Anorthite, ordered - CaAl2Si2O8 - Y: 32.39 % - d x by: 1. - WL: 1.
00-044-1437 (*) - Teallite - PbSnS2 - Y: 52.09 % - d x by: 1. - WL: 1.54059 - Orthor
00-004-0783 (I) - Silver-3C, syn - Ag - Y: 48.59 % - d x by: 1. - WL: 1.54059 - Cubi
00-019-0406 (I) - Mckinstryite - (Ag,Cu)2S - Y: 35.08 % - d x by: 1. - WL: 1.54059 -

Figure 178. Diffractogram of composite fibula inv. no. E5957 (Como): Mckinstryite (blue), silver (light blue), Mg-calcite (red), teallite (orange), albite (pink), anorthite (purple).

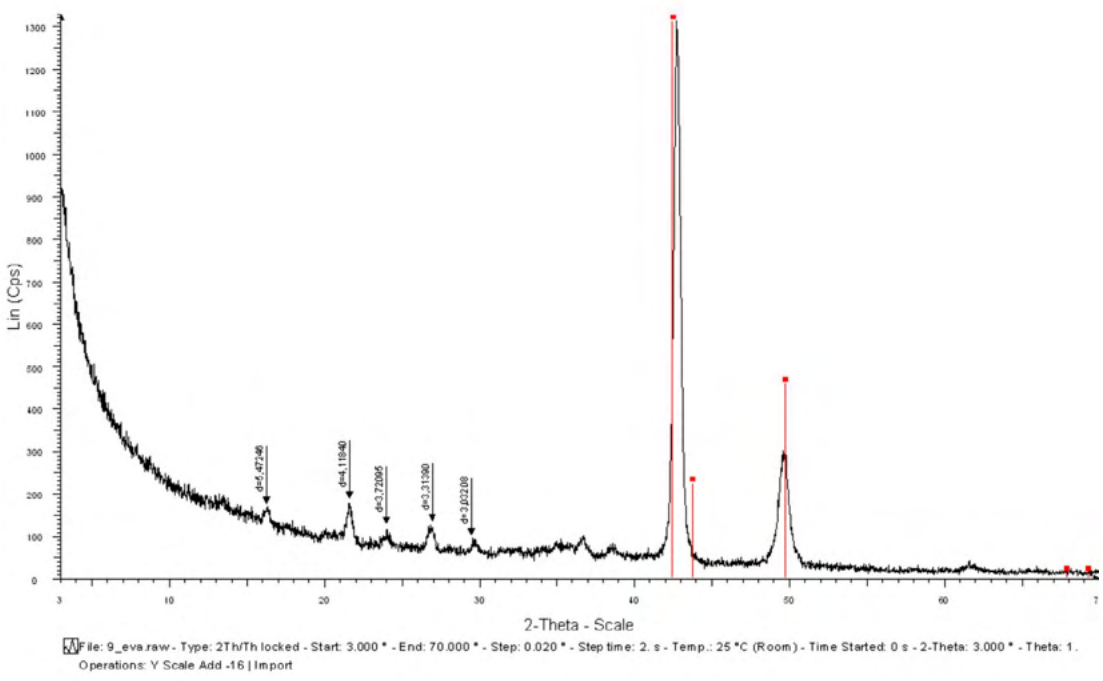
Lin (Cps)
d=5,47246
d=4,11840
d=3,72095
d=2,31390
d=2,02208
2-Theta - Scale
File: 9_eva.raw - Type: 2Th/Th locked - Start: 3.000 * - End: 70.000 * - Step: 0.020 * - Step time: 2. s - Temp.: 25 °C (Room) - Time Started: 0 s - 2-Theta: 3.000 * - Theta: 1.
Operations: Y Scale Add -16 | Import

Figure 179. Diffractogram of fibula inv. no. 9 (Parre) with linear decoration: bronze (d = 2.12 e 1.84) and unidentified reflections at d = 3.03, 3.31, 4.12 e 5.47.

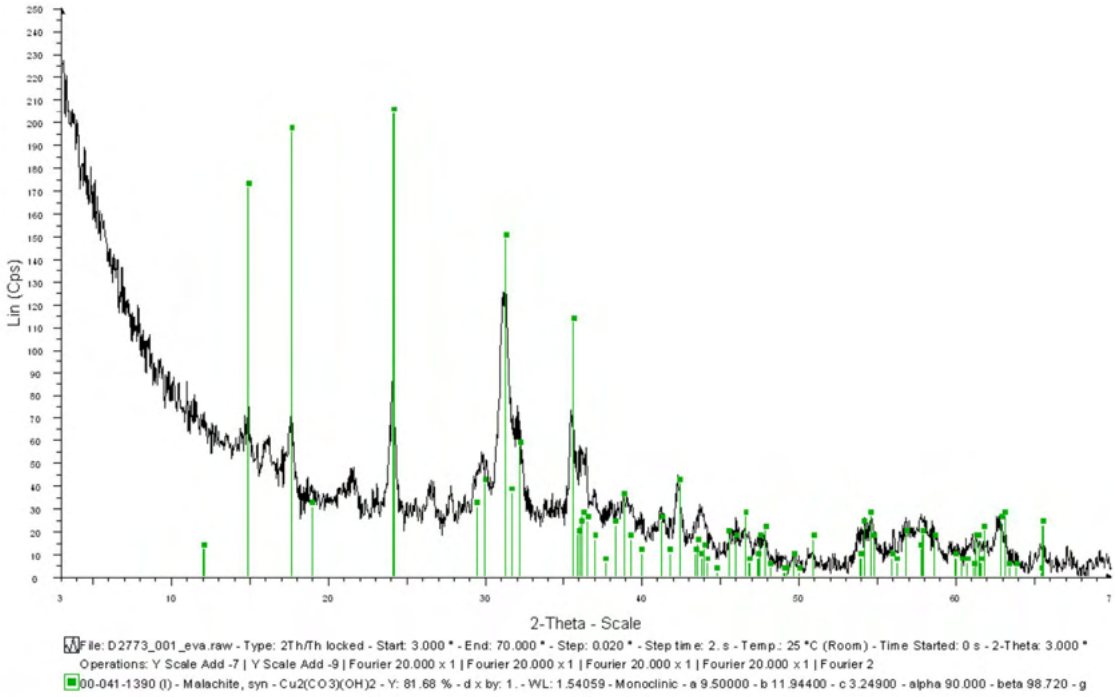
Lin (Cps)
2-Theta - Scale
File: D2773_001_eva.raw - Type: 2Th/Th locked - Start: 3.000 * - End: 70.000 * - Step: 0.020 * - Step time: 2. s - Temp.: 25 °C (Room) - Time Started: 0 s - 2-Theta: 3.000 *
Operations: Y Scale Add -7 | Y Scale Add -9 | Fourier 20.000 x 1 | Fourier 20.000 x 1 | Fourier 20.000 x 1 | Fourier 20.000 x 1 | Fourier 2
00-041-1390 (I) - Malachite, syn - Cu2(CO3)(OH)2 - Y: 81.68 % - d x by: 1. - WL: 1.54059 - Monoclinic - a 9.50000 - b 11.94400 - c 3.24900 - alpha 90.000 - beta 98.720 - g

Figure 180. Malachite diffractogram (leech fibula inv. no. D2773, Castelletto Ticino).

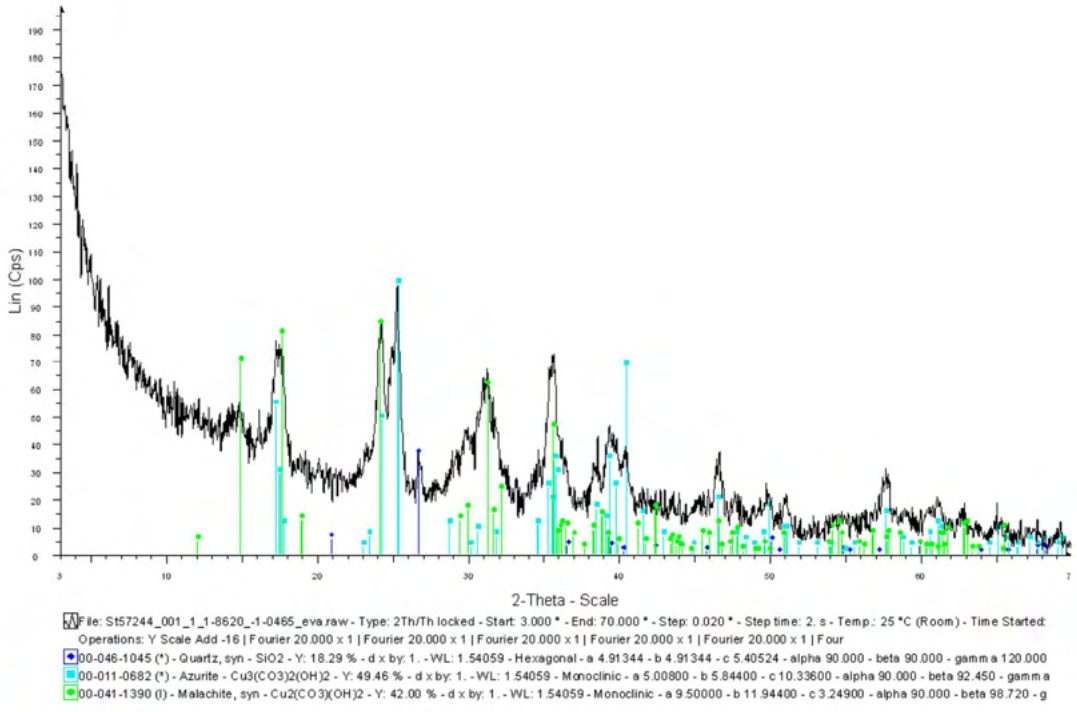
Lin (Cps)
2-Theta - Scale
File: St57244_001_1_1-8620_-1-0465_eva.raw - Type: 2Th/Th locked - Start: 3.000 * - End: 70.000 * - Step: 0.020 * - Step time: 2. s - Temp.: 25 °C (Room) - Time Started:
Operations: Y Scale Add -16 | Fourier 20.000 x 1 | Fourier 20.000 x 1 | Fourier 20.000 x 1 | Fourier 20.000 x 1 | Fourier 20.000 x 1 | Four
00-046-1045 (*) - Quartz, syn - SiO2 - Y: 18.29 % - d x by: 1. - WL: 1.54059 - Hexagonal - a 4.91344 - b 4.91344 - c 5.40524 - alpha 90.000 - beta 90.000 - gamma 120.000
00-011-0682 (*) - Azurite - Cu3(CO3)2(OH)2 - Y: 49.46 % - d x by: 1. - WL: 1.54059 - Monoclinic - a 5.00800 - b 5.84400 - c 10.33600 - alpha 90.000 - beta 92.450 - gamma
00-041-1390 (I) - Malachite, syn - Cu2(CO3)(OH)2 - Y: 42.00 % - d x by: 1. - WL: 1.54059 - Monoclinic - a 9.50000 - b 11.94400 - c 3.24900 - alpha 90.000 - beta 98.720 - g

Figure 181. Diffractogram of fibula inv. no. St. 57244 (Como, via Isonzo): azurite (light blue), malachite (green) and quartz (blue).

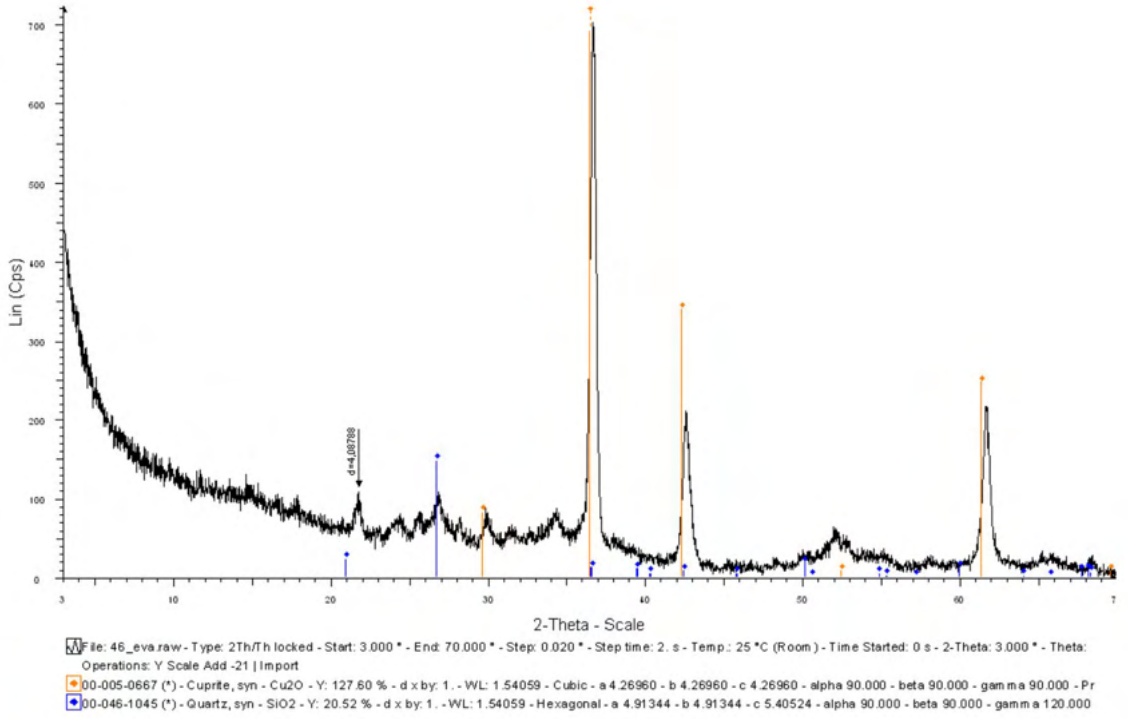
Lin (Cps)
2-Theta - Scale
File: 46_eva.raw - Type: 2Th/Th locked - Start: 3.000 ° - End: 70.000 ° - Step: 0.020 ° - Step time: 2. s - Temp.: 25 °C (Room) - Time Started: 0 s - 2-Theta: 3.000 ° - Theta:
Operations: Y Scale Add -21 | Import
00-005-0667 (*) - Cuprite, syn - Cu2O - Y: 127.60 % - d x by: 1. - WL: 1.54059 - Cubic - a 4.26960 - b 4.26960 - c 4.26960 - alpha 90.000 - beta 90.000 - gamma 90.000 - Pr
00-046-1045 (*) - Quartz, syn - SiO2 - Y: 20.52 % - d x by: 1. - WL: 1.54059 - Hexagonal - a 4.91344 - b 4.91344 - c 5.40524 - alpha 90.000 - beta 90.000 - gamma 120.000

Figure 182. Diffractogram of fibula inv. no. 46 (Parre): cuprite (orange) and doubtful quartz (blue).

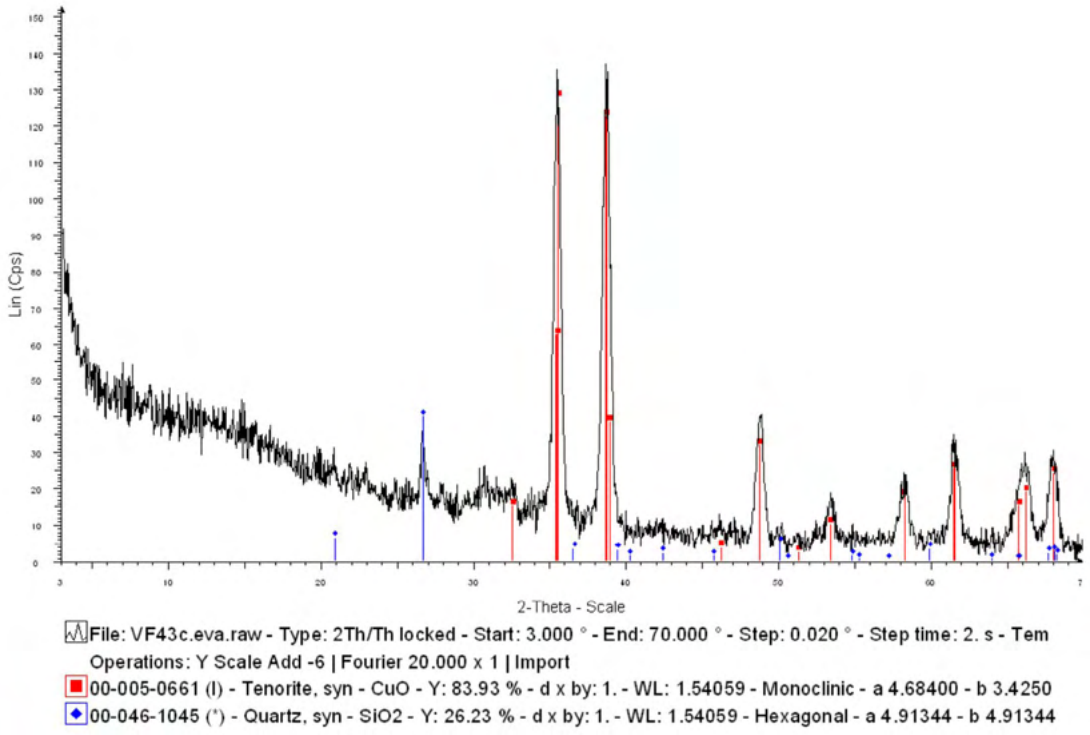
Lin (Cps)
2-Theta - Scale
File: VF43c.eva.raw - Type: 2Th/Th locked - Start: 3.000 ° - End: 70.000 ° - Step: 0.020 ° - Step time: 2. s - Tem
Operations: Y Scale Add -6 | Fourier 20.000 x 1 | Import
00-005-0661 (I) - Tenorite, syn - CuO - Y: 83.93 % - d x by: 1. - WL: 1.54059 - Monoclinic - a 4.68400 - b 3.4250
00-046-1045 (*) - Quartz, syn - SiO2 - Y: 26.23 % - d x by: 1. - WL: 1.54059 - Hexagonal - a 4.91344 - b 4.91344

Figure 183. Diffractogram of sample VF43c, collected on fibula inv. no. SP28b (Villa del Foro): tenorite (red) and quartz (blue).

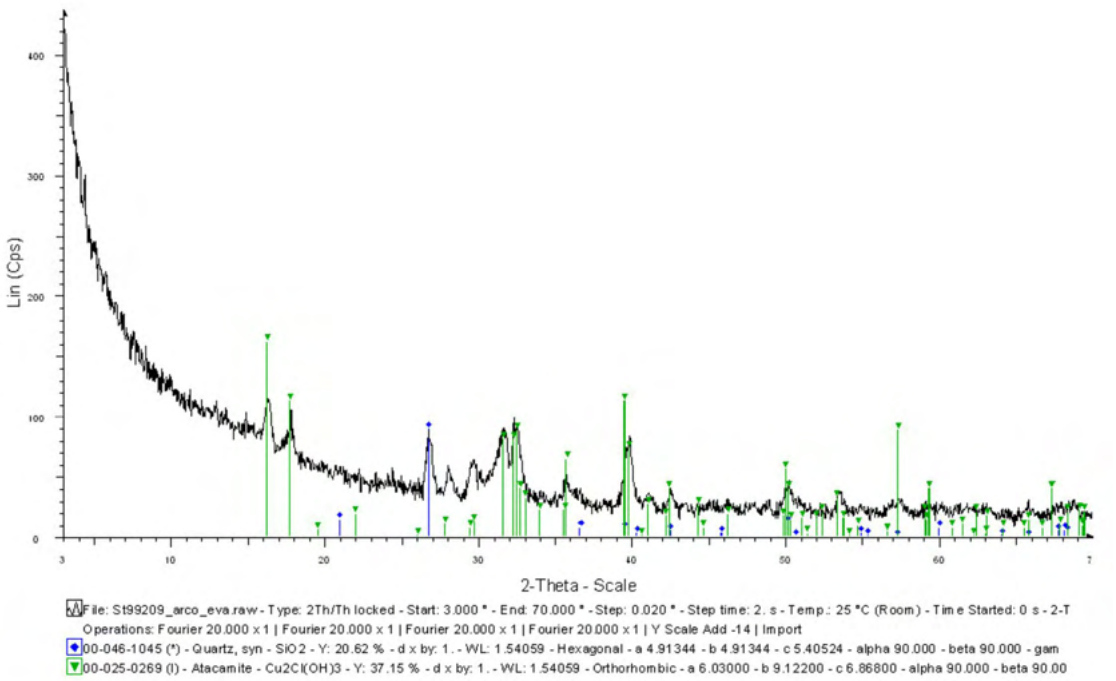
Lin (Cps)
2-Theta - Scale
File: St99209_arco_eva.raw - Type: 2Th/Th locked - Start: 3.000 ° - End: 70.000 ° - Step: 0.020 ° - Step time: 2. s - Temp.: 25 °C (Room) - Time Started: 0 s - 2-T
Operations: Fourier 20.000 x 1 | Fourier 20.000 x 1 | Fourier 20.000 x 1 | Fourier 20.000 x 1 | Y Scale Add -14 | Import
00-046-1045 (*) - Quartz, syn - SiO2 - Y: 20.62 % - d x by: 1. - WL: 1.54059 - Hexagonal - a 4.91344 - b 4.91344 - c 5.40524 - alpha 90.000 - beta 90.000 - gam
00-025-0269 (I) - Atacamite - Cu2Cl(OH)3 - Y: 37.15 % - d x by: 1. - WL: 1.54059 - Orthorhombic - a 6.03000 - b 9.12200 - c 6.86800 - alpha 90.000 - beta 90.00

Figure 184. Diffractogram of a point of the bow of the fibula inv. no. St. 99209 (Forcello di Bagnolo San Vito): atacamite (green) and quartz (blue).

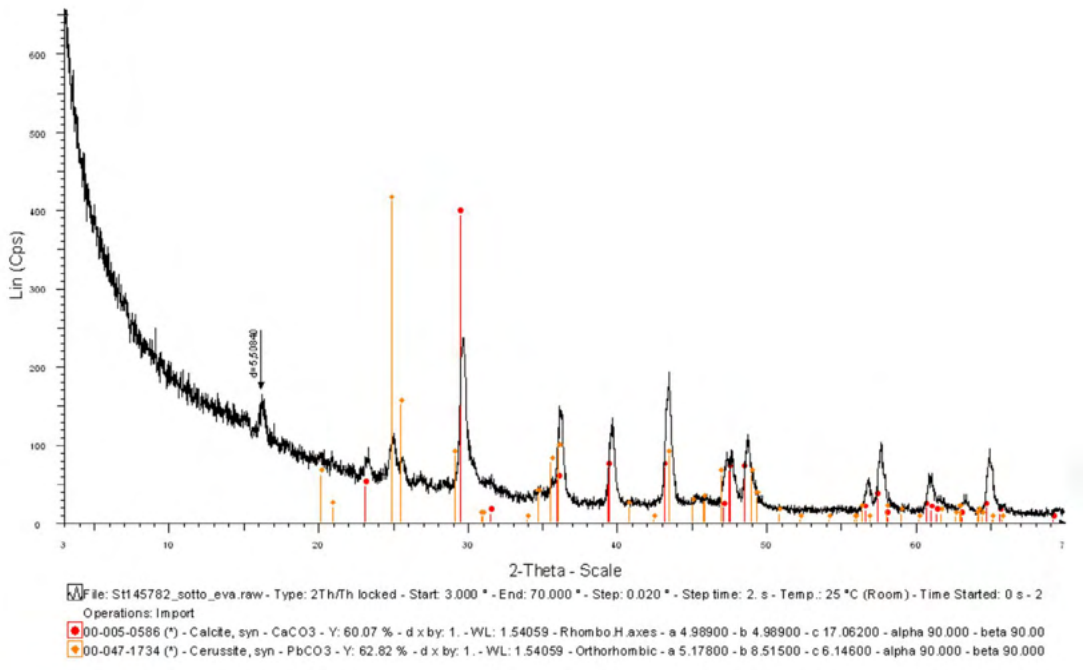
Lin (Cps)
d=5.53040
2-Theta - Scale
File: St145782_sotto_eva.raw - Type: 2Th/Th locked - Start: 3.000 ° - End: 70.000 ° - Step: 0.020 ° - Step time: 2. s - Temp.: 25 °C (Room) - Time Started: 0 s - 2
Operations: Import
00-005-0586 (*) - Calcite, syn - CaCO3 - Y: 60.07 % - d x by: 1. - WL: 1.54059 - Rhombo.H.axes - a 4.98900 - b 4.98900 - c 17.06200 - alpha 90.000 - beta 90.00
00-047-1734 (*) - Cerussite, syn - PbCO3 - Y: 62.82 % - d x by: 1. - WL: 1.54059 - Orthorhombic - a 5.17800 - b 8.51500 - c 6.14600 - alpha 90.000 - beta 90.000

Figure 185. Diffractogram of bucket pendant inv. no. St. 145782 (Forcello di Bagnolo San Vito): cerussite (orange) and calcite (red).

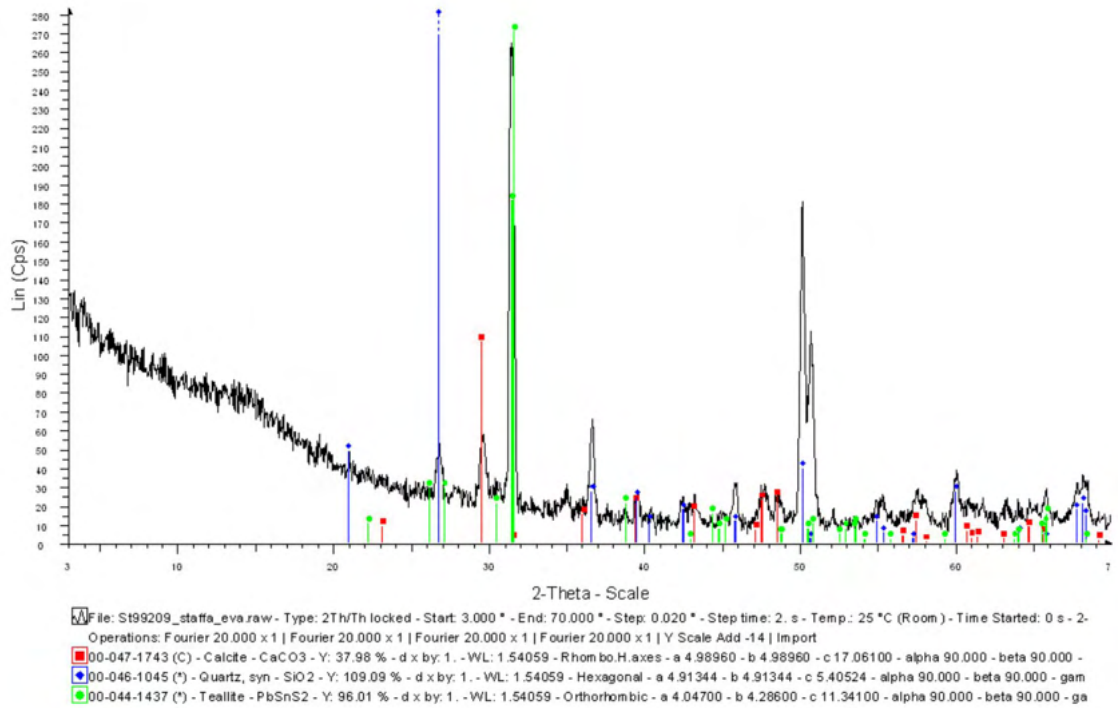
Lin (Cps)
2-Theta - Scale
File: St99209_staffa_eva.raw - Type: 2Th/Th locked - Start: 3.000 ° - End: 70.000 ° - Step: 0.020 ° - Step time: 2. s - Temp.: 25 °C (Room) - Time Started: 0 s - 2-
Operations: Fourier 20.000 x 1 | Fourier 20.000 x 1 | Fourier 20.000 x 1 | Fourier 20.000 x 1 | Y Scale Add -14 | Import
00-047-1743 (C) - Calcite - CaCO3 - Y: 37.98 % - d x by: 1. - WL: 1.54059 - Rhombo.H.axes - a 4.98960 - b 4.98960 - c 17.06100 - alpha 90.000 - beta 90.000 -
00-046-1045 (*) - Quartz, syn - SiO2 - Y: 109.09 % - d x by: 1. - WL: 1.54059 - Hexagonal - a 4.91344 - b 4.91344 - c 5.40524 - alpha 90.000 - beta 90.000 - gam
00-044-1437 (*) - Teallite - PbSnS2 - Y: 96.01 % - d x by: 1. - WL: 1.54059 - Orthorhombic - a 4.04700 - b 4.28600 - c 11.34100 - alpha 90.000 - beta 90.000 - ga

Figure 186. Diffractogram of a point on the foot of the fibula inv. no. St. 99209 (Forcello di Bagnolo San Vito): teallite (green), calcite (red) and quartz (blue).

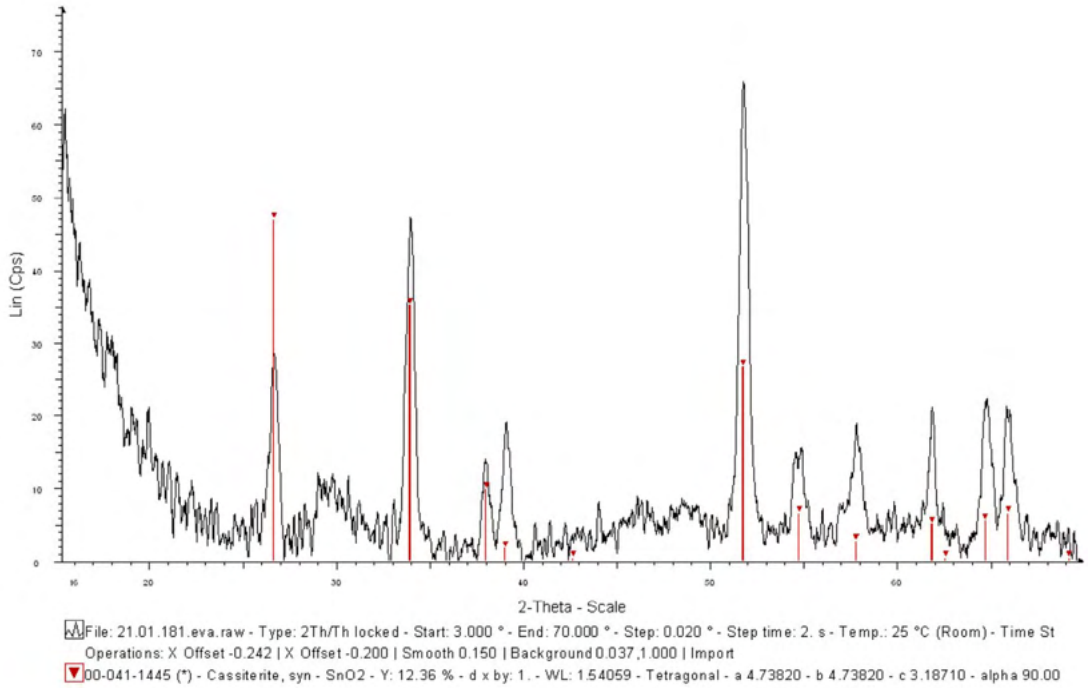
Lin (Cps)
2-Theta - Scale
File: 21.01.181.eva.raw - Type: 2Th/Th locked - Start: 3.000 ° - End: 70.000 ° - Step: 0.020 ° - Step time: 2. s - Temp.: 25 °C (Room) - Time St
Operations: X Offset -0.242 | X Offset -0.200 | Smooth 0.150 | Background 0.037,1.000 | Import
00-041-1445 (*) - Cassiterite, syn - SnO2 - Y: 12.36 % - d x by: 1. - WL: 1.54059 - Tetragonal - a 4.73820 - b 4.73820 - c 3.18710 - alpha 90.00

Figure 187. Portion of the diffractogram obtained on the fibula's foot inv. no. 2021.01.181 (Gropello Cairoli, loc. Santo Spirito): cassiterite.

7.2.4. SEM-EDS analysis

Semi-quantitative chemical EDS analyses were performed on 116 archaeological finds. Analyses were carried out on different metallic areas and then averaged, in order to obtain a meaningful composition (Tab. 37).
Data were treated separately in the case of composite artefacts (4 cases), for which, on the basis of archaeological and technological observation, the presence of several joined parts is observed or assumed: e.g. leech fibulae in which body and needle are the result of two different casting moments. This choice is dictated by the need of verifying possible compositional differences (i.e. presence/absence of Pb).
Based on the obtained data, interesting technological considerations emerge, which should be considered with caution. The investigations carried out, in fact, do not relate directly to the original alloy composition, but rather to surface analyses which are, in most cases, influenced by presence of related alteration products. The results are therefore variously influenced by the alteration processes that occurred in the deposition ground and later in the various phases of the artefacts post-excavation life (e.g., cleaning and/or restoration interventions, or conservation issues, etc.).
Copper almost systematically present in the metal alteration products, often accompanied by tin in (82% of the cases; 95 objects) and lead (66%; 77) (Figs. 188-189). Sometimes Pb is found even when Sn is not detected. In many cases, Sn and Pb amounts are quite high (in 33 cases Sn > 20 wt% and in 21 cases Pb > 20 wt%). Such an anomaly might be explained by the above-mentioned surface alteration phenomena, which may cause considerable compositional variations (Angelini *et al.* 2009; Northover 1998; Scott 2002). The high Pb content may also be the result of extreme segregation: during casting, in fact, it tends to migrate to the surface because it cools down less quickly than Cu and Sn (Charalambous *et al.* 2014; Giumlia-Mair 2003; Northover 1998).
Considering the high number of finds and their typological variety, an analysis of the data is attempted here by grouping them in functional classes. For each type, the presumed tin and lead wt% content was checked, as well as the presence of trace elements (i.e. Ni, Zn, As, Ag, Sb). Chemical analyses also identified the presence of other minor or trace elements (i.e. Na, Mg, Al, Si, P, S, Cl, K, Ca, Ti, Mn and Fe), but these are not considered hereafter, as they are likely to result from enrichment phenomena in the corrosion layer and/or related to the depositional ground (Dungworth 1996; Ingo *et al.* 2006).
It is well known that the actual composition of the alloy is directly related to the possible technological processes involved in the manufacture of the various instruments. Artefacts that involve processing after casting (e.g. hammering) will require a strong, elastic and ductile alloy (i.e. bronze with a Sn content < 10 wt%), while those that are cast-finished (e.g. with very thin or finely decorated parts) will require a very fluid alloy in casting, with high Sn content and eventually addition of Pb (Figs. 188-189[31]; Charalambous *et al.* 2014; Giumlia-Mair 1998; 2000; 2003; 2005; Giumlia-Mair *et al.* 2016; Klein, Hauptmann 1999; Northover 1998).
Based on such premises, the most significant outcome is the constant presence of lead in cast-finished artefacts and its quite total lack in those requiring post-casting working (Fig. 189). In the latter case, there are some differences between the macro-categories identified (Tab. 34): the pendants Longone-type and the composite bow fibulae are characterised by no or very low tin content (0-3/4 wt%), while this seems to be higher in the more elaborate fibulae (i.e. arch fibulae from Parre[32] and latenian fibulae from Chiomonte[33]). This difference is consistent with the technological aspects of the artefact production: lower tin contents correlate with fully hammered objects. The artefacts from Parre show a lead content < 1%, not suggesting an intentional addition.

31 As the record examined consists predominantly of cast-finished artefacts (95) and to a lesser extent post-cast worked artefacts (24), the values in the histograms have been normalised as a percentage of the total artefacts for each type (i.e. cast-finished or worked).
32 Several types of fibulae involving post-casting processing steps from the Parre (BG) deposit have been grouped in this category: i.e. arch fibula, low arch fibula, flat-arched fibula, foliate-arch fibula.
33 This category is here represented by the two Latenian folded-foot fibulae from Chiomonte (TO).

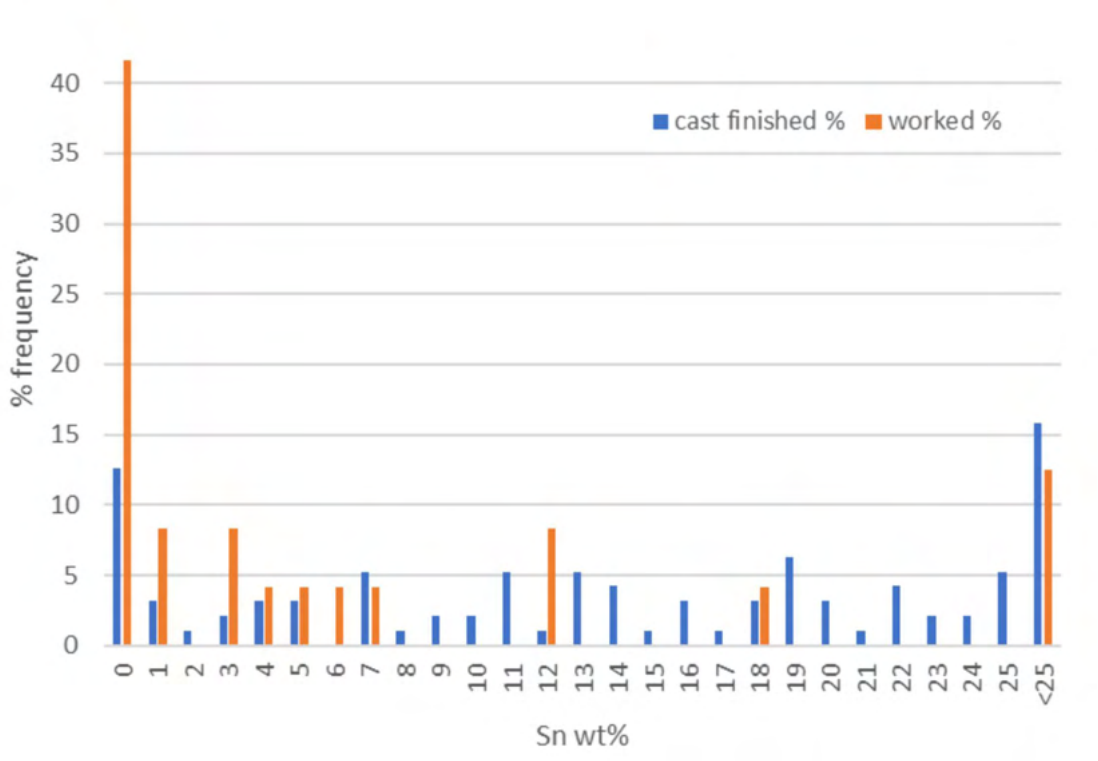

Figure 188. Sn wt% content frequency for cast-finished and worked after casting objects: each column counts the number of objects having Sn in a concentration range of 1% by weight.

The averaged Sn content of the cast-finished artefacts is generally > 10 wt%, except in the navicella fibulae (Fig. 190a; Tab. 35). A high tin content improves the castability of the alloy and is consistent with elaborate artefacts.

Leech fibulae have been subdivided according to the decoration (circular, linear, or transversal) and the features of the arch (full or with terracotta core), as these factors are likely to have an influence on the production technology. This division shows that the Pb content is actually higher in leech fibulae with a terracotta core (11-14 wt% average) than in those with full-arch (4-9 wt% average), in agreement with what expected (Fig. 190b; Tab. 35) [34]. The difference between the two types is striking and can probably be attributed to a difference in content even in the original alloy. The first type of arch is characterised by presence of a terracotta core surrounded by a thin layer of metal (≈ 1 mm thick), which requires the use of a very fluid casting alloy.

The pin, on the other hand, has to be made in a different moment and then incorporated into the fibula body. As such, it requires a different composition because it has to be worked by hammering after casting. Analysis of the 4 available pins from leech fibulae confirmed the archaeo-technological hypotheses (see section 8.1), revealing the absence of lead and a low tin content (average 5 wt%; Tab. 34).

A difference in the amount of Pb is shown also by other archaeological types (Tab. 35). The levels found in bucket pendants (average 19 wt%)[35] and Late Hallstattian fibulae[36] (average 14 wt%) are comparable to those found in leech fibulae with terracotta core. Conversely, grooming tools show lower Pb levels (average 4 wt%)[37].

34 These values are slightly high compared to what is reported in the literature, probably due to segregation or alteration phenomena (Angelini *et al.* 2009; Charalambous *et al.* 2014; Giumlia-Mair 1998).

35 Four bucket pendants were analysed, one of which was covered with Paraloid (inv. no. St. 18711) and therefore not considered.

36 Full-arch leech fibulae with transverse decoration and late-hallstattian fibulae have been grouped in this category for similarity.

37 Of the 3 grooming tools analysed, 2 showed traces of combustion. Combustion may have favoured the migration or loss of volatile elements, altering the composition even more. The Sn and Pb contents for the non-combusted artefact are 23 and 4 wt % respectively.

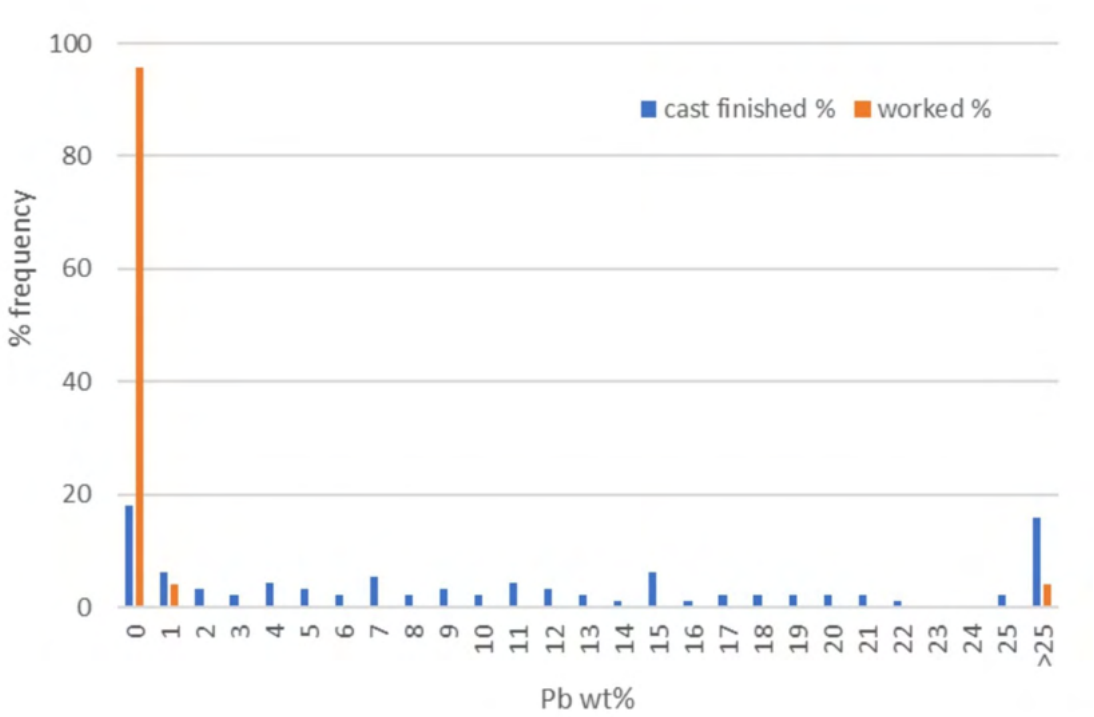

Figure 189. Pb wt% content frequency for cast-finished and worked after casting objects: each column counts the number of objects having Pb in a concentration range of 1% by weight.

The low Sn content (< 10 wt%) and almost total lack of Pb (< 1 wt%) in the navicella fibulae is surprising. From a technological point of view, this type shows several similarities with the leech fibulae with terracotta core but seems to have a very different composition. Both are in fact modelled in wax around a clay core (lost-wax technique: Giumlia-Mair 1998). Unfortunately, these data lack statistical significance, due to the low number of analysed artefacts of this type. A bigger navicella fibula (Valvaraita type; Fig. 55e) was not included in this category due to evident size differences. The Sn and Pb contents recorded in this case are 44 % and 6.74 wt% respectively; this is consistent with literature data, which state that bigger castings normally contain a higher amount of lead than those found in similar smaller objects (Giumlia-Mair 1998).

A triangular lamina pendant was also included in the analytical record, with the following values: Sn 25 wt%, Pb 19 wt% and As 0.05 wt%. The high Pb content is anomalous for a laminated object (as is the high Sn content). However, it may be related to the decoration, maybe made after casting by punching.

Presence of silver in composite bow fibulae from Como was confirmed by EDS investigations (inv. no. E5957-5958). This type of artefact is characterised by the presence of bronze and coral beads, inserted into the bronze rod arch. These coral beads are decorated with thin rods composed mainly of Ag and S; nowadays they appear black in colour, when observed at the optical microscope, but they were originally made of silver (Fig. 191). Such evidence can be interpreted with the use of additional decorative elements: for this kind of artefact, these decorative elements were usually made of gold; in this case, however, they consisted of tiny silver rods nowadays completely transformed into Ag sulphide.

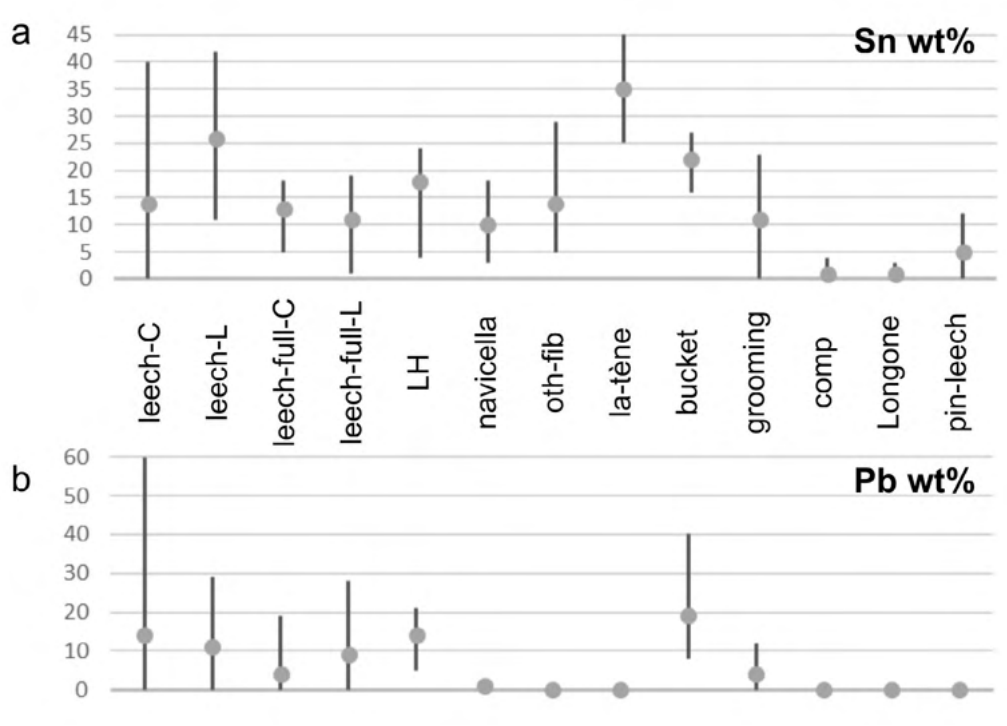

Figure 190. Sn wt% (a) and Pb wt% (b) values in different functional categories: bar indicates the variation between minimum and maximum value and point indicates the mean value (calculated on the average between the different specimens; 'Leech-core' = leech fibulae with terracotta core; 'leech full' = leech fibula with full arch; 'C' = circular decoration; 'L' = linear decoration; 'LH' = late Hallstattian fibulae; 'oth-fib' =other type of fibulae; 'comp' = composite bow fibulae).

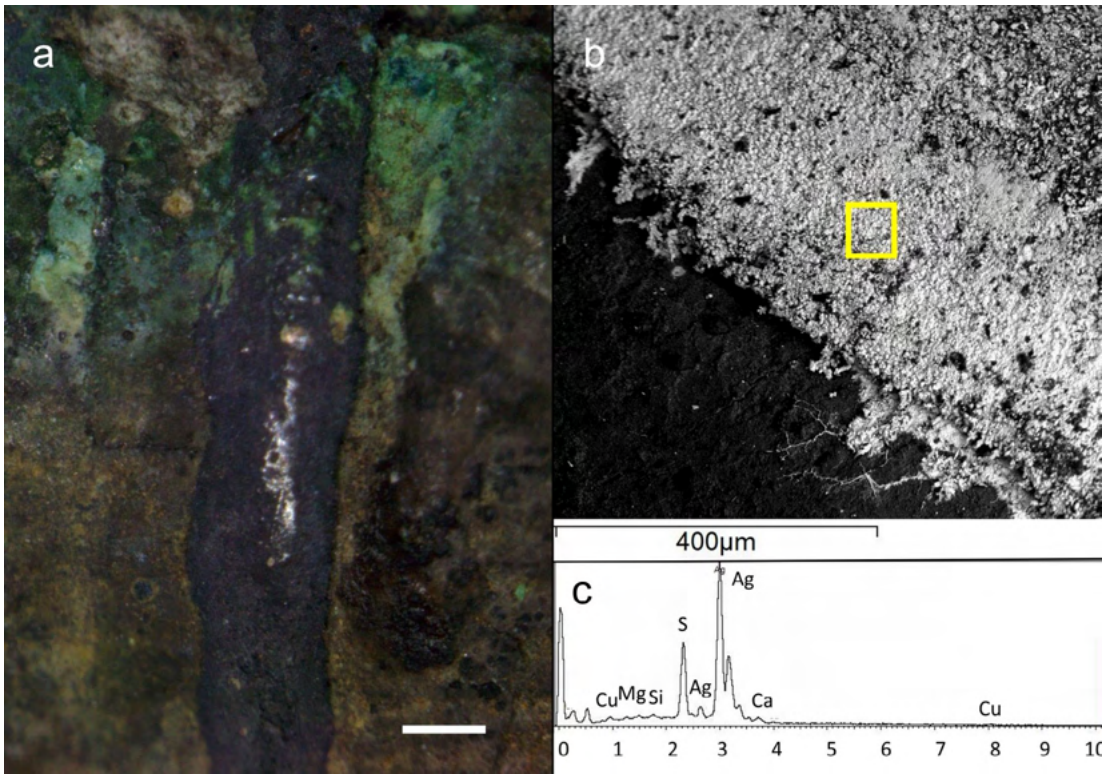

Figure 191. Silver rod on the HMC bead of the E5957 fibula: a) OM-image detail of the black band, in relief with respect to the surrounding areas (metric reference 0.5 mm); b) BSE-image of the black band (the yellow square marks the analytical spot); c) related EDS spectrum.

Trace elements have also been considered, as they can sometimes give an indication about the type of ore used for copper extraction. However, these impurities are commonly found in several deposits, often spread over large geographical areas, as they result from the same geological processes and are not homogeneous in the same outcrop. These residual phases also depend on the melting conditions, and the materials present in the furnace. For these reasons, they are often insufficient for a determination of provenance (Artioli *et al.* 2009; Dungworth 1996).
Excluding elements that are likely to be enriched from the soil, the sum of the main trace elements (i.e. Ni, Zn, As, Ag, Sb) is generally < 1 wt%, with an average value of 0.77 wt% (min. 0 and max. values 17.11 wt%) for the entire analytical record and 0.62 wt% (min. 0 and max. 7.36 wt%) for the leech fibulae with terracotta core and circular decoration. Such a limited presence of trace elements indicates that the used copper has a high degree of purity, generally associated with the most elaborated artefacts (Giumlia-Mair 1998; Dungworth 1996).
An attempt was made at correlating the presence and quantity of some trace elements (i.e. Ni, Zn, As, Ag, Sb) with the geographical area of origin of the artefacts (Fig. 192). Four geographical and cultural areas were identified: Golasecca area (95 artefacts), Liguria Interna (3), Etruria Padana (8) and Western Po Valley (9).
Arsenic is always present, with similar values in the different areas (≈ 0.32 wt%), while Sb is almost always absent[38]. All trace elements considered are present in all areas, except for Liguria Interna, where the number of samples is not statistically significant. Ni is present, with varying tenors, only in Etruria Padana (0.02 wt%) and in the Golasecca area (0.15 wt%). Zn is quite always present, with comparable values (≈ 0.04 wt%). Ag is almost always present, however with different values (Tab. 36).

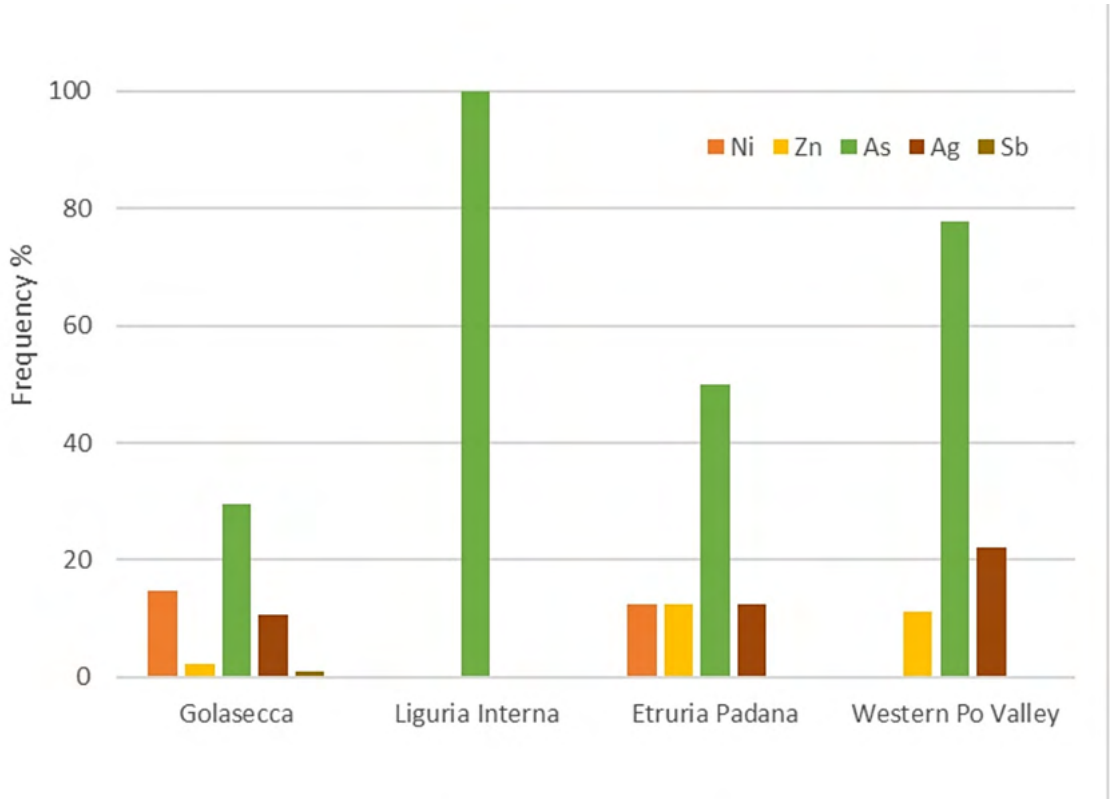

Figure 192. Frequency % of the most significant trace elements in relation to main geographical-cultural areas.

38 Sb is only attested in fibula St. 57216 from Como, Golasecca area.

7.2.5. Considerations

The analyses of the metal alloy degradation by-products seem to reveal compositional differences in relation to the different classes of objects, which may be indicative of a possible intentional control of the alloy composition in relation to the properties desired for the planned working technique. This observations are consistent with what is known for the Iron Age, according to practices that were widespread during the same period in the Upper Adriatic, Etruscan, Phoenician, Mesopotamian, Magna Graecia and Hallstatt civilisations (Giumlia-Mair 1998; 2000; 2003; 2005; 2009; Artioli *et al.* 2024; Angelini *et al.* 2009; Piccardo *et al.* 2010; Charalambous *et al.* 2014; Klein, Hauptmann 1999; Northover 1998).

Tin is found in varying amounts, generally higher in artefacts that require more fluidity during casting and no post-processing activities. Objects that require post-casting hammering have instead quite low tin contents. Tin increases elasticity, strength and ductility of the alloy up to values of 10 %; additions between 10 and 20 % increase hardness and strength but reduce ductility; above 20 % the alloy becomes fragile. Such additions also lower the melting temperature, with economic and technical advantages (Giumlia-Mair 1998; 2003).

As regards lead, the most significant outcome is just its presence. This, in addition to further lowering the melting temperature, makes the alloy more fluid and less viscous in the molten state, even at very low levels (2 wt%). In higher quantities, it increases the solidification interval, making it easier to fill complex moulds or large castings (e.g. large objects or multiple castings): channels remain in the metal structure through which the hot metal can continue to flow, ensuring that all spaces are filled correctly. It also increases the workability for post-processing operations such as cutting, drilling and punching, because it acts as an internal lubricant, but it is not compatible with hammering (e.g. sheets-metal or rods). Lead is in fact not soluble in copper and forms a compound with globules within the metal structure, points of weakness during hammering operations because lead crushes more easily than the surrounding metal (Charalambous *et al.* 2014; Giumlia-Mair 1998; 2000; 2003; Giumlia-Mair *et al.* 2016; Klein, Hauptmann 1999; Northover 1998).

In the analyses presented here, lead is generally absent in artefacts for which post-processing after casting is required and seems to have higher concentrations for more complex artefacts (e.g. leech fibulae with terracotta core), maybe indicative of an intentional addition. The arch of this type of fibula is characterised by the presence of a terracotta core surrounded by a thin layer of metal (≈ 1-2 mm thick), thus requiring the use of a very fluid casting alloy. There are also refined decorations on the surface, probably made directly on the wax model, in order to minimise the post-casting processing of the artefact and reduce the risk of breakage due to the fragility of the lead alloy.

A further significant result is the identification of compositional differences in leech fibulae between the body of the fibula (bow and foot) and the pin – with Pb being detected only in the former (11-14 wt%) – which confirms the archaeological attribution to composite objects for this type of artefacts.

8. Experimental archaeology contribution

Abstract

Il contributo dell'archeo-tecnologia allo studio delle fibule a sanguisuga con inserti circolari ha permesso di approfondire le tecnologie di produzione di questi complessi manufatti. Il lavoro, condotto con il supporto del Centro di Archeologia Sperimentale Torino (CAST), ha integrato l'analisi tecnologica (microscopica e macroscopica), radiografica e archeometrica, con attività di archeologia sperimentale. Tutte le fibule analizzate presentano caratteristiche riconducibili alla tecnica della cera persa, compatibile con la complessità interna (presenza di un'anima in argilla e spessori metallici ridotti, ≈1 mm). La variabilità dimensionale e decorativa indica produzioni individuali piuttosto che seriali. Le radiografie di 45 esemplari hanno evidenziato, in 36 casi, la presenza di anima in cotto e tracce costanti del possibile uso di supporti interni per le varie fasi di lavorazione. Inoltre il negativo in argilla delle decorazioni circolari probabilmente contribuiva al sostegno dell'anima durante la fusione, rendendo tale decorazione funzionale oltre che esteticamente gradevole.
Le prove sperimentali (32 fibule e 9 ardiglioni) hanno consentito la ricostruzione ipotetica della catena operativa: modellazione dell'anima in argilla, rivestimento con cera tramite immersioni successive, realizzazione del modello in cera (con decorazioni, fori per inserti e inserimento dell'ardiglione, preparazione dello stampo in argilla, colata del metallo dal lato della staffa, raffreddamento e rifinitura, fino all'inserimento degli inserti in corallo). L'inserimento degli inserti in corallo è stato oggetto di specifici test, mostrando che l'uso di piccoli frammenti sagomati – con o senza adesivi (cera d'api e resina di pino) – è più efficace rispetto all'uso di paste di corallo, che risultano instabili e alterate cromaticamente.

Introduction

An archaeo-technological approach was also employed to study leech fibulae with circular inlays, with essential support provided by the 'Centro di Archeologia Sperimentale Torino' (CAST).
A technological study of artefacts is fundamental for interpreting the processes that led to their production. It must inevitably begin the analysis of technological traces preserved on archaeological finds, in order to identify the different phases of manufacture, and then proceed to experimental replication and verification of the observations and hypotheses formulated (Gaj, Maestro 2023; Gaj, Burdese 2009; Fazzini 2020; Cerezer 2014; Bente, Berthold 2018; Kuijpers 2018).

8.1. Technological study

The technological study was carried out on all leech fibulae with circular insets (164) and involved both macroscopic and microscopic (optical or digital) investigation. It also used the results of the archaeometric investigations (see section 7), as well as radiography (for 45 artefacts; see section 8.2).
All examined fibulae belong to the same type, with numerous variations with regard to decoration (e.g. number of holes) and size (see section 4.2.1.4). From a technological point of view, no substantial differences were found between the type variants. The main difference lies in the presence or absence of an inner clay core, which could be inserted to economise bronze and reduce the global weight, especially in larger artefacts. Full-arch objects are less common and generally smaller in size. In undamaged artefacts, the presence or absence of an inner core can be identified from the weight of the objects. In the considered record, no fibulae are of equal size and shape, as evidenced by a detailed measurement of the different parts[1]. This suggests

1 The artefacts were weighed and measured in detail: overall length (if preserved), length of the arch, foot and pin; height of the arch; thickness of the arch; width of the arch and of the foot; diameter of the spring, the small globe, the termination and any bulges; decoration: diameter of the holes and depth (if visible), thickness of the lines.

the use of a lost-wax technique, rather than that of a bivalve matrix, as otherwise suggested by the study of similar finds from the Arbedo hoard in Switzerland (Schindler 1998b). The use of this technique appears to be the most plausible, particularly for specimens with a clay core; indeed, in a bivalve mould it would not be possible to keep the core perfectly in position by means of pins (surrounding metal thickness ≈ 1 mm; Fig. 193). The only way to achieve the required thickness is by repeatedly immersing the core in a bath of liquid wax. The presence of supports was in any case necessary to keep the core in place after the removal of the wax by heating the mould.

An examination of the artefacts reveals the constant presence of two holes on the upper face of the arch – a larger one on the spring side and a smaller one on the foot side. The first one is generally filled with metal, making it difficult to detect on the surface. A larger metal gusset is also visible on the ventral face of the bow (Figs. 194a-d). Radiographic investigations identify, on each of these details, the constant presence of an internal metal element (hole on the spring side), an elongated cavity (small hole on the foot-side; Fig. 202b) and a conical dowel (lower face). At first, we thought that these might represent three support elements of the inner core, which had been removed or cut on the surface after casting. However, no evidence of surface cutting of any pin was found. Examination of the foot often shows traces of scraping on wax in the needle holder, further supporting the hypothesis of adopting the lost-wax technique (Fig. 194e-f).

Figure 193. Section of leech fibula with circular decoration, metal thickness around the inner core is visible (inv. no. E5868, Como).

Filling such a small thickness required a very fluid alloy – i.e., with a high tin content and the addition of lead, as suggested by archaeometric investigations of metal composition of corrosion layers (see section 7.2). The pin, instead, was made separately, using a different alloy and a different processing. As such, it was inserted later into the wax model, as is clearly visible on the artefacts (Figs. 194g-h), by X-ray imaging (Fig. 202d) and consistently with all previous studies (Buson, Baldini 2003; Giumlia-Mair 1998; Schindler 1998b). It sometimes has a quadrangular or rounded section (≈ 2 mm thick) at the insertion point and spring, which is always rounded in the needle. Manufacturing probably involved casting a bar slightly thicker than ≈ 2 mm, which was hammered to give the desired shape and then curved at the spring. The creation of non-rounded, semi-finished products has considerable advantages: it is easier to make an asymmetrical bivalve matrix with only one worked valve than a symmetrical one with two perfectly matching semicircular grooves. The difference in composition between the alloy of the fibula body and that of the pin also allowed the latter to be encapsulated. In the same way, any metal support pins (whose existence was hypothesised by other studies: Buson, Baldini 2003; Giumlia-Mair 1998; 2000; Schindler 1998b), would also have been incorporated in the artefact, hindering extraction after casting.

The use of a very fluid alloy probably allows to directly replicate the decorations made on wax, both in terms of circular and linear decoration, thus reducing processing of the artefacts after casting. Examination of the decorations under the microscope often shows traces of wax elevation and corrugation (Fig. 195-197).

The holes of the circular decorations generally have a standardised diameter (≈ 2 mm), with some exceptions (lower or higher values are recorded sporadically: 1.5-3 mm: Fig. 198). They are deeper (≈ 3-4 mm) than the thickness of the metal (1 mm) and have a conical shape – visible when the coral inset is lacking. These holes were made on the wax model until the clay core was reached and then filled with a fine clay paste during mould construction. After the metal casting, during removal of the clay 'pin', their depth was increased.

This decoration is also functional in supporting the core in the mould after the wax has been removed. Its negative imprint is composed by a series of small clay 'pins' which surround the

clay core and hold it in place, together with a single pin on the ventral side, without the need for other longitudinal suspension elements.
Finally, regarding the coral inclusion, the presence of an inset is sometimes evident (Figs. 98c-d), while in other cases a pasty material seems to fill the holes (Fig. 99e), possibly also related to an alteration of the original inset. A detailed examination also revealed that sometimes the decorating material did not fill the hole completely (Fig. 200f).

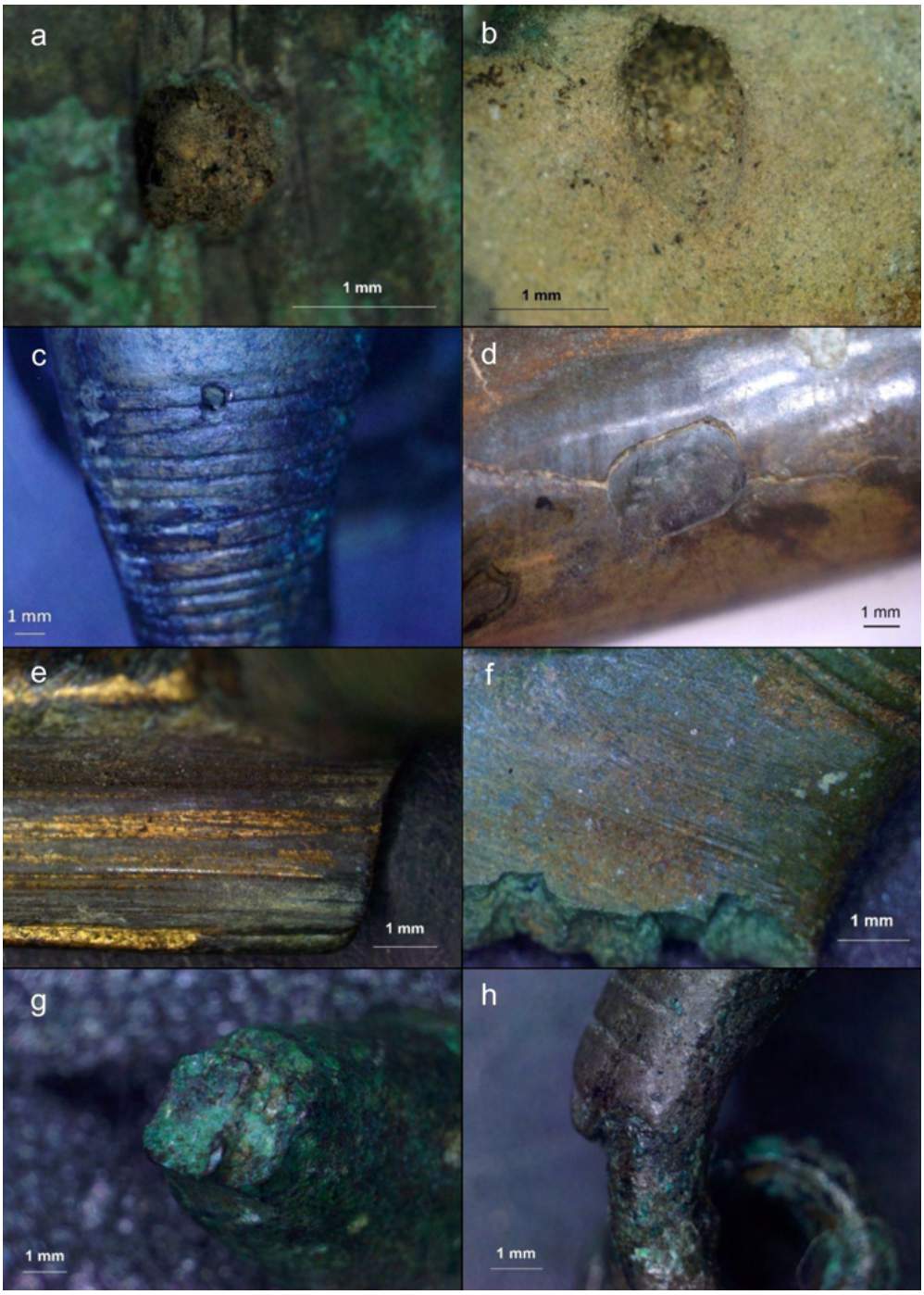

Figure 194. a) Detail of the hole at the foot-side (inv. no. D2049, Golasecca); b) Detail of the hole at the foot-side, absent metal part (inv. no. D2073, Castelletto Ticino); c) Detail of the hole at the foot-side (inv. no. D2104, Castelletto Ticino); d) Detail of the ventral-face gusset (inv. no. 6615, loc. Prà, Chies D'Alpago); e) Detail of pin support, traces of scraping on wax (inv. no. 870, San Bernardino di Briona); f) Detail of pin support, traces of scraping on wax (inv. no. 868, San Bernardino di Briona); g) Detail of the pin insertion point (inv. no. 947, Castelletto Ticino-Vigevano?); h) Detail of the pin insertion point (inv. no. CT1144, Castelletto Ticino).

Figure 195. Detail of linear decorations: white arrows = grooves/linear pattern; yellow arrows = trace of wax elevation; red arrows = trace of wax corrugation (inv. no. St. 83946, Pombia, NO).

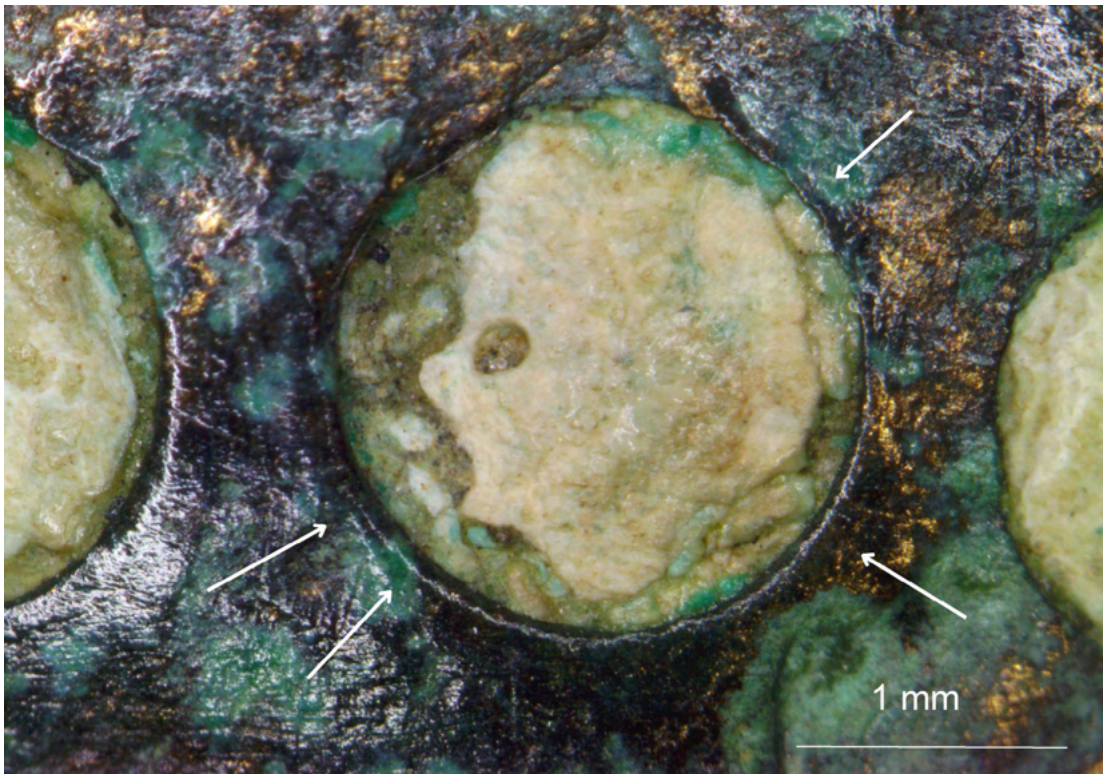

Figure 196. Detail of circular decoration: white arrows = trace of wax elevation (tomb 1, Motto Lagone, NO).

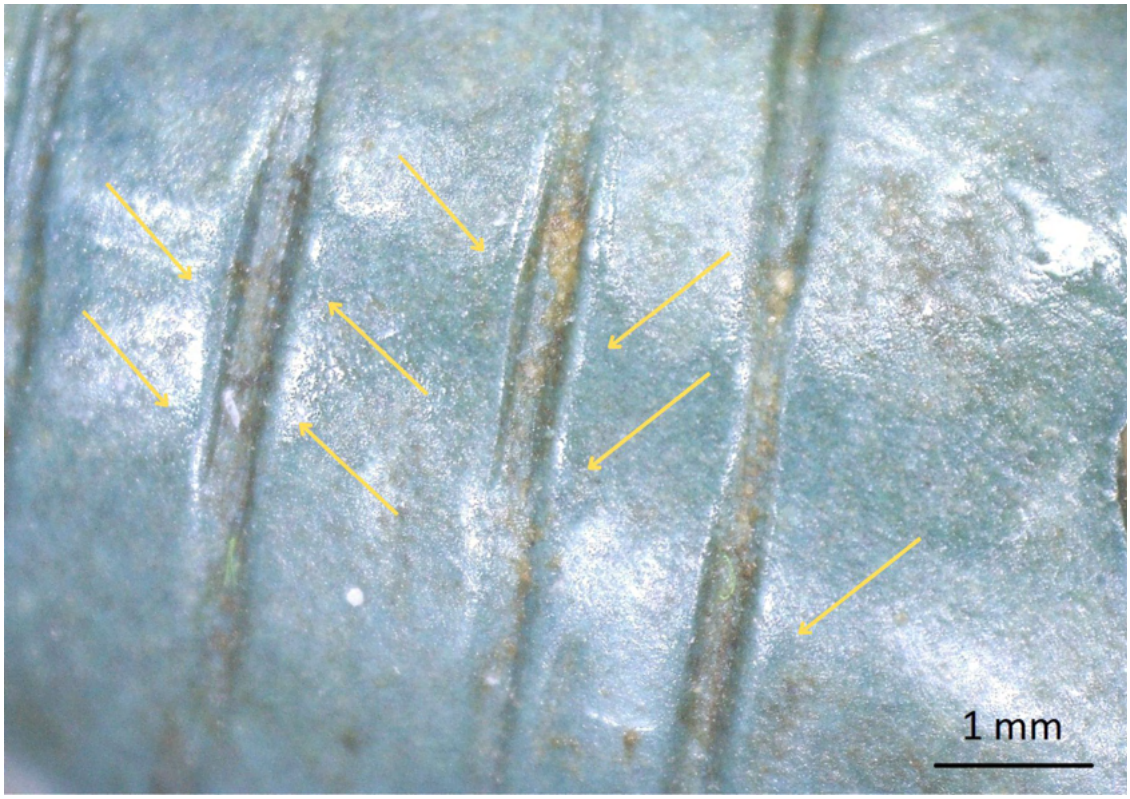

Figure 197. Detail of linear decorations: yellow arrows = trace of wax elevaton (inv. no. St. 63413, loc. Monsorino, Golasecca).

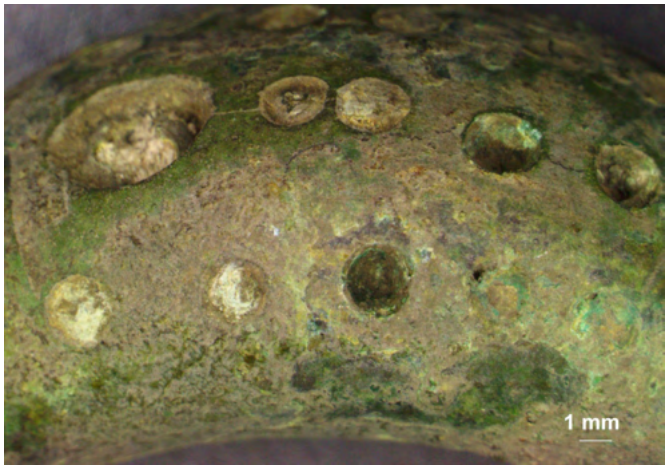

Figure 198. Detail of the circular decoration on the bow of the fibula NCT0100026418 (San Bernardino di Briona, NO): holes with several size and superpositions.

Figure 199. Clay cores with a peduncle on the ventral face (after Buson, Baldini 2003, fig. 21).

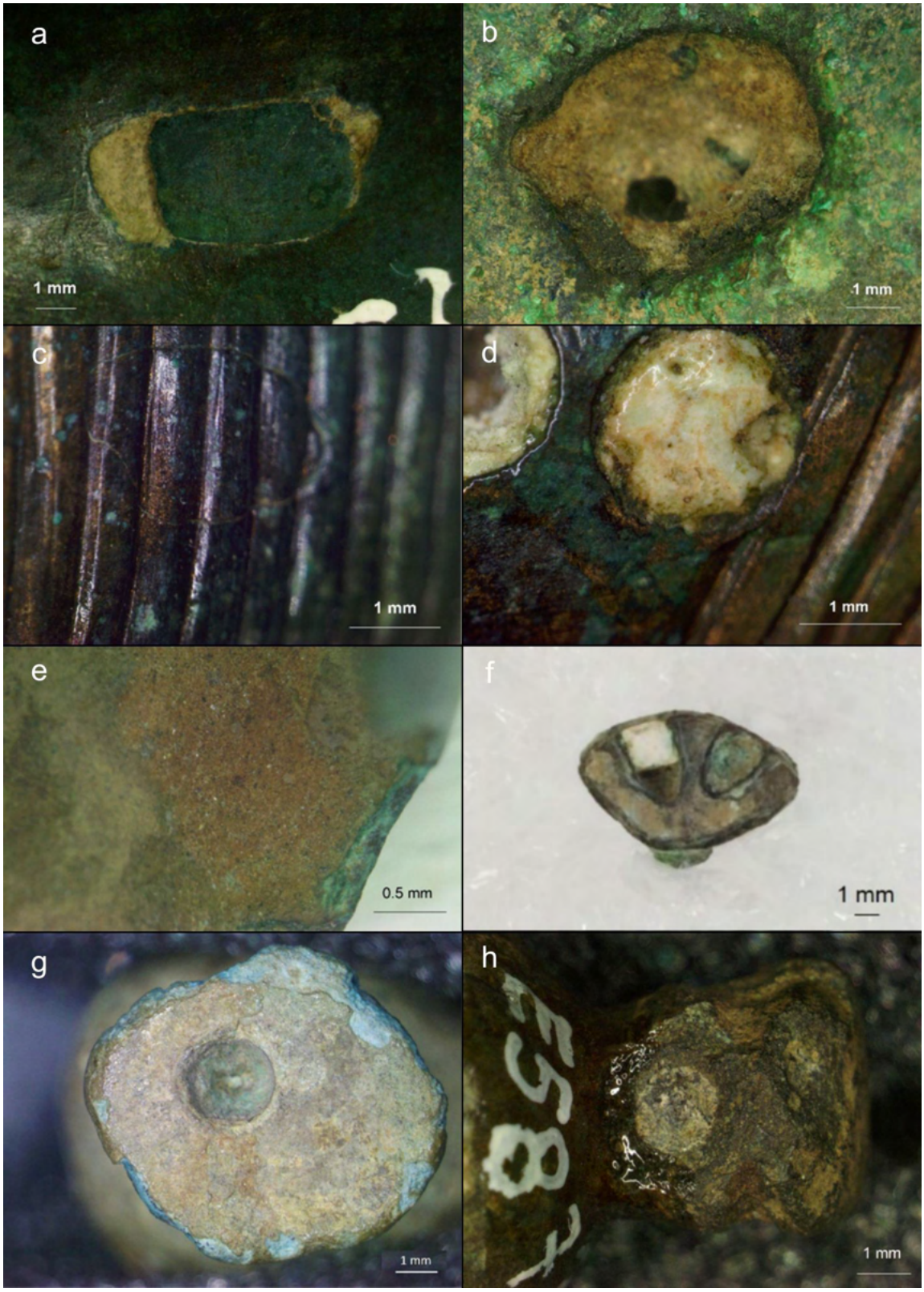

Figure 200. a) Detail of the ventral-face gusset (inv. no. St. 57216, Como); b) Detail of the ventral-face residual hole of the gusset (inv. no. E5552, Como); c) Detail of the upper face of the bow and the point of emergence of the spring-side 'support': linear decoration in continuity (tomba 1, Motto Lagone, Arona); d) Detail of the upper face of the arch: the circular decoration covers the linear one, with a wax coating (tomba 1, Motto Lagone, Arona); e) Detail of the core mixture (inv. no. St. 57220, Como); f) Section of a full-arch fibula: detail of the inset in the hole (inv. no. Sp834, Villa del Foro); g) Foot termination drilled after casting (inv. no. 23-M380-9.4, Castello di Annone); h) Coarse foot termination (probable casting funnel; inv. no. E5873, Como).

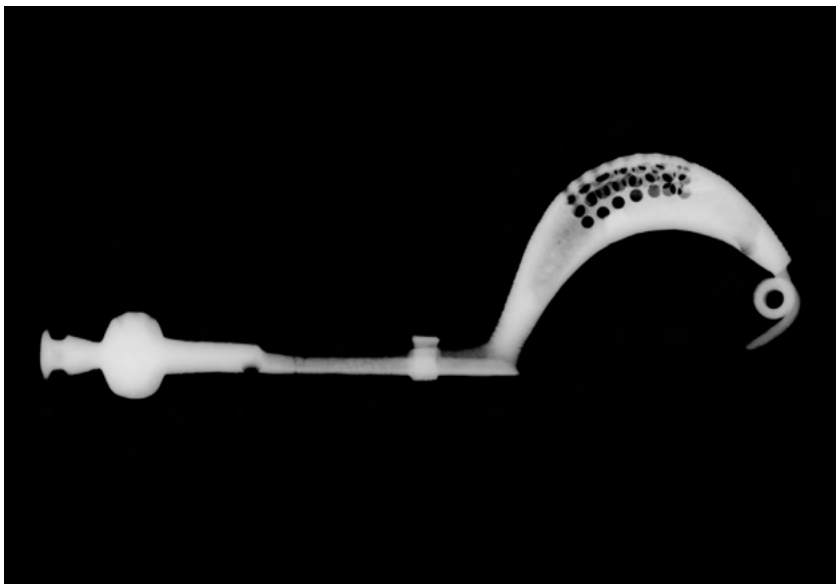

Figure 201. Leech fibula with terracotta core from Tomb 1 of Motto Lagone (Arona).

8.2. Radiographic examination

X-ray radiographies were collected on 45 leech fibulae, partly from the Como area and partly from the provinces of Varese and Novara, corresponding to the two main areas of the Golasecca culture. No substantial technological differences were found between the two groups of materials (Tab. 38).

The inspection identified the presence of a terracotta core in 36 of the examined fibulae; a full-arch was observed in six cases (Figs. 201-202b). In 4 artefacts, the insertion of the pin into the metal is observed (Fig. 202c)[2], confirming the archaeo-technological hypotheses. Such an insertion never affects the profile of the terracotta core, indicating it was made only in the wax model. Radiographs show the almost constant presence of an inner element on the upper-spring-side and another shorter one on the ventral face (Fig. 202a). The former is generally pointed and no longer than half the length of the arch. An internal element has never been found on the upper-foot-side, where the hole on the external surface of the artefact is. When the bronze coating is not preserved, an elongated void in the clay core is shown at this point – possibly the trace of a pin that is no longer present (maybe because made of perishable material; Fig. 202d)[3]. In any case, the two pivots on the upper side of the bow are always distinct and generally not aligned.

Particular circumstances were also observed, such as:

- an additional internal element on the ventral face of a fibula (one case; Fig. 202e);
- an ornithomorphic decorative element emerging from the bow of the fibula, supported by a clearly visible internal pin, perhaps having a support function (one case; Fig. 202f).

The circular decoration is clearly visible in radiography, both in the case of the presence of a terracotta core or not, as are the linear decorations. For these, the radiographic examination allows more complex decorative variants to be better appreciated – e.g., alternating relief lines of variable thickness (Fig. 202g). Such a motif was certainly made with a special tool on wax, since no similar result could be obtained directly on bronze decoration.

Fibula feet were observed in 7 cases, never with an internal core (Fig. 202h).

With regard to conservation, radiographic investigation is particularly useful for identifying micro-fractures and surface corrosion affecting the materials (e.g. St. 2208; Fig. 202i), as well as evidence of previous restoration work, including additions and the recomposition of fractures (e.g., St. 2206; Fig. 202l).

2 For further examples see Appendix 1, Figs. 227-231.

3 Any voids inside the core are visible when the outer metal cover is preserved and become detectable exclusively in its absence: specimens inv. no. D2065 e St. 83966.

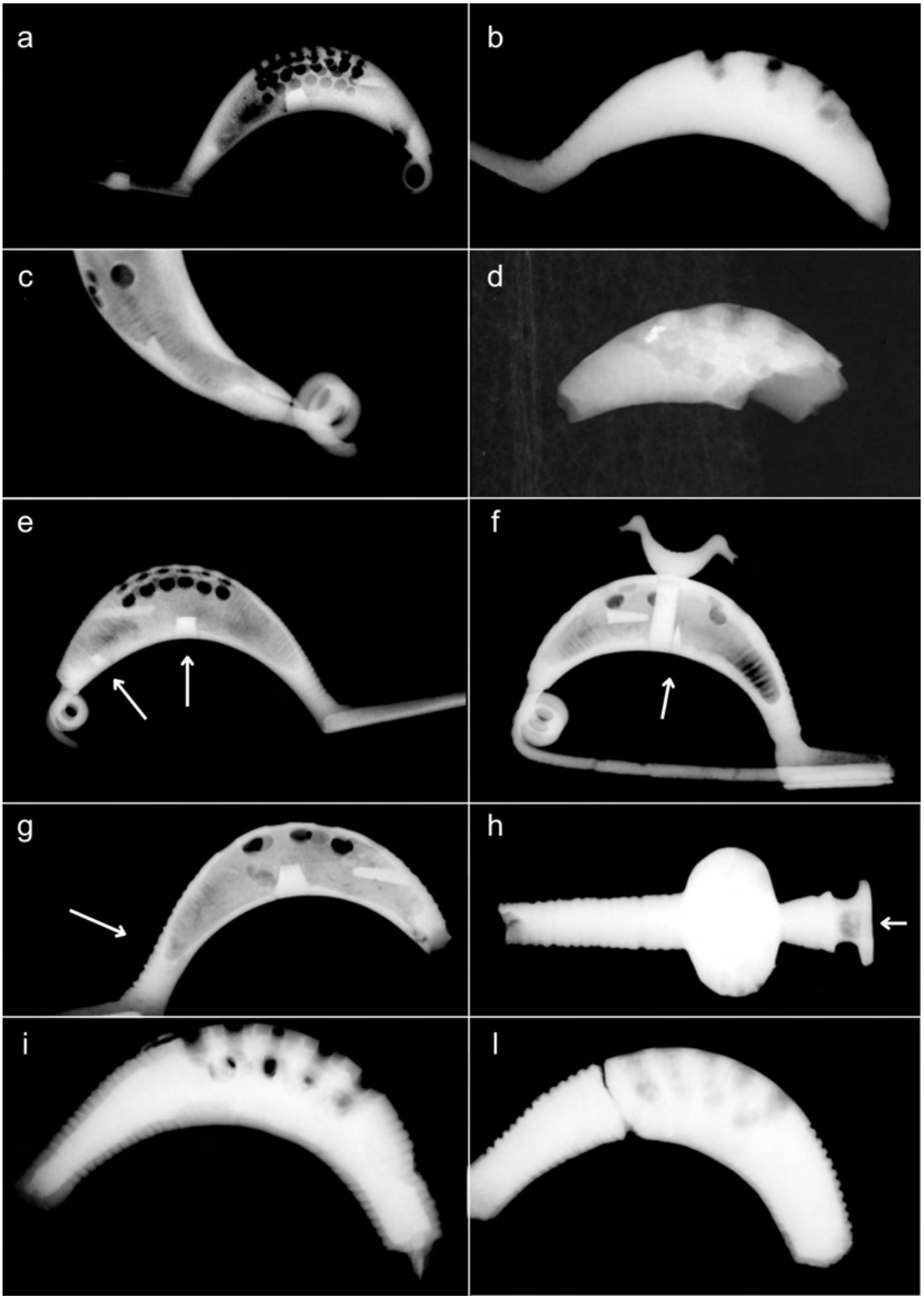

Figure 202. a) Detail of the bow with terracotta core and internal metal elements (tomb 1, Motto Lagone, Arona); b) Detail of the full-arch of the fibula inv. no. St. 114083 (Como); c) Detail of the pin insertion point in the bow body (inv. no. 944, Castelletto Ticino – Vigevano?); d) Detail of the hole left by the inner element on the upper-foot-side (D2065, Golasecca); e) Leech fibula with terracotta core with double ventral side support pin (inv. no. CT728, Castelletto Ticino); f) Leech fibula with terracotta core with orthomorphic internal element (inv. no. D2773, Castelletto Ticino); g) Alterned linear decoration (inv. no. St. 879, Como); h) Fibula foot with globe and vase-shaped final part (inv. no. St. 83937, Pombia); i) Full-arch fibula, detail of superficial corrosion (inv. no. St. 2208, Como); l) Full-arch fibula with recomposed fracture (inv. no. St. 2206, Como).

8.3. Experimental archaeology tests

A technological study of the artefacts offers multiple interpretative perspectives, inevitably revealing discrepancies that may be related to the adoption of different techniques by individual artisans. An experimental approach is therefore necessary to address and clarify these issues.
These experimental simulations were carried out by trying to reproduce the ancient technological procedures, adopting a protocol respectful of previous methodologies, materials and tools compatible with the considered period (Gaj, Maestro 2023; Gaj, Burdese 2009). Two main paths were followed, based on the data obtained from the study of the ancient artefacts: i) the placement of the insets in the decorations and ii) the bronze casting. Various experimental sessions (≈ 40 non-consecutive days) took place over the course of two years. During each session, the environmental conditions, people at work, assumptions, criticalities and results were systematically recorded. During all phases, the newly obtained artefacts were examined under an optical microscope. The results of the experimental investigations provided a considerable amount of data, while also highlighting numerous difficulties and extremely long timescales.

8.3.1. Placement and bonding of coral insets

Since the study of coral decorations is the primary aim of this project, and, consequently, the understanding of how they were set from an experimental perspective, we initially focused on this aspect, leaving aside the manufacture of the bronze components. For the sole purpose of testing the insertion and gluing methods of coral inlays, suitable test specimens were produced to simulate the morphology of the perforations. These consisted of hollow copper cylinders, 1 mm thick, which were drilled using modern tools to obtain series of holes of different diameters (2, 2.5, and 3 mm). The tubes were filled with clay to simulate the presence of a fired core; the clay was first air-dried and then fired in an electric kiln. It soon became evident that these test specimens were unsuitable for this purpose, as the fired clay tended to move within the tubes as a result of drying shrinkage (Fig. 203b).
An attempt was made at simulating the deepening of the holes in the clay, using specially prepared tools equipped with a metal tip, and consequent insertion of the coral (Figs. 203a-c). The test specimens used showed considerable problems: the terracotta core, in fact, tends to fracture inside the copper tube when deepening the holes. In those cases, in which such an operation is successful, the hole obtained is pointed, reminding those seen on the archaeological finds.
In a following stage, potential adhesives (namely birch pitch, beeswax and resin, alone and/or mixed with one another) were tested and heated (Fig. 203d). Several attempts were made, with or without adhesives, cutting the coral fragments to size (with flint or metal tools) or breaking them directly inside the holes (Figs. 203e, 204a). Small, period-compatible tweezers were also used to soak the pieces in the binder. The immersion of the coral fragments in containers of different depths was attempted, finding that the better results were obtained by using millimetric layers of adhesive (in semi-flat containers: Fig. 203f).
The production of a coral paste for filling the holes, obtained out of powders prepared by using lithic grindstones, was also attempted. These powders, however, lose their typical red colour and glossy aspect after grinding. Once mixed with beeswax, the powder even changes colour (turning to yellow-brown), making such a paste unsuitable for the purpose. An attempt was also made at producing a whitish paste by grinding the shells, but the colour obtained once the binder is added is even less suitable (Figs. 204b-f).
The possible removal of the insets from the hosting cavities was also tested to verify the adhesives tightness. Some specimens were worn for a day, so as to check consequences on their aspect. In some cases, if the inset is juxtaposed in the hosting cavity, tightness is effective even with no adhesive. Among the tested adhesives, birch pitch is the worst, both in terms of colour and tightness. Pine resin soils the metal surface. Beeswax works but has a moderate tightness. The mixture of beeswax and pine resin seems the best option, in terms of application, hold and colour rendering. If the insets are smaller than the hosting hole, a mixture of coral paste and beeswax is effective both as a bonding agent and to fill the gaps with an acceptable hue.

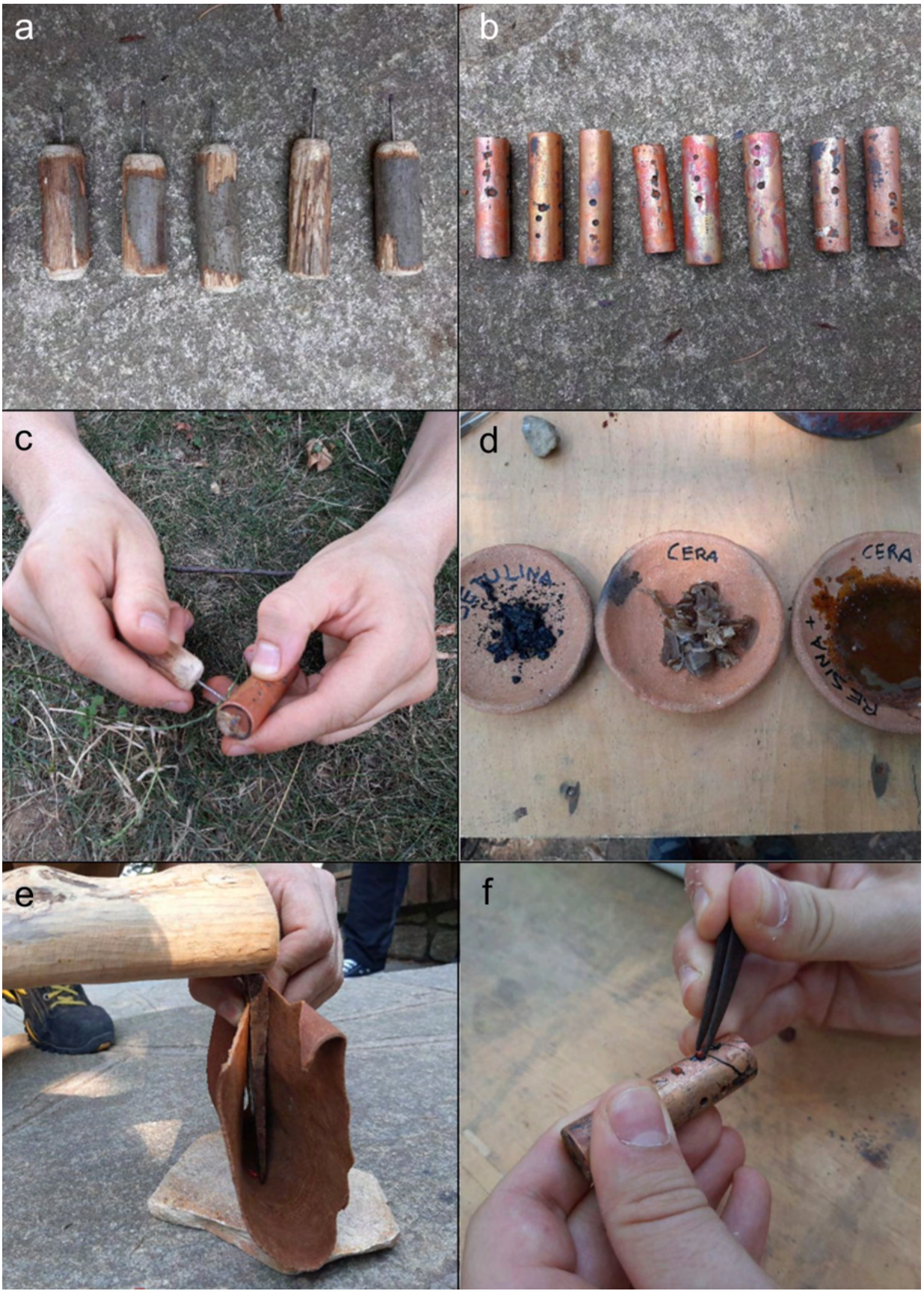

Figure 203. a) Drilling tools; b) Copper and clay tests; c) Deepening the holes in the inner core; d) Binders: birch pitch, beeswax and a mixture of beeswax and pine resin; e) Cutting tests with bronze tool; f) Insertion of the coral inset.

Figure 204. a) Cutting tests of the already inserted inset; b) Coral grinding; c) Shell grinding; d) Paste of shells and beeswax; e) Insertion of coral with binder; f) Ground coral paste (beeswax).

In addition to the aptly prepared test specimens, these experimental attempts aimed at coral insertion were also tested on leech fibulae made experimentally by casting bronze alloys (see section 8.3.2)[4]. The specimens obtained are often incomplete, but nevertheless suitable for simulations.
The adopted tools proved to perform well with the newly produced artefacts – producing a conical hole in the terracotta core akin to that observed in the decorations of the ancient archaeological finds. Since the use of coral pastes of different kinds gave unsatisfactory results, we decided to proceed with the sole insertion of small coral insets, using the previously mentioned binders. The results are similar to those already highlighted by the previous experiments. The best results are obtained when the inset is perfectly sized to fit its hosting hole. In this case, the binder is even unnecessary, the insertion being excellent with just the joint. To prevent it from being dislodged during use, it should not protrude from the fibula. If a protruding inset is used, no binder is effective in glueing it to the fibula. In this case, the exceeding part can easily be removed, once in its slot, by using a clean, light tap with a small bronze chisel. The method of causing a lever fracture at the edge of the hole sometimes does work and at times not.
Among the binders, pitch works well, especially when it is very liquid, but a very thin black layer forms around the coral. However, the hold is not so good, as the coral falls off after a short time. Pine resin alone is not effective, as it crystallises during drying, becoming fragile. Independently from temperature, it becomes solid when exposed to the air, even before reaching the fibula. Beeswax works well, but the surface of the inset becomes dirty; however, the gaps around the holes are well filled and the colour is clear. Although being a bit pasty and difficult to insert, the grip is good (but not great). The best binder is a 50%-50% mixture of wax and resin: easy to place (if sufficiently liquid), its colour is clear and has a good grip. However, liquid wax tends to settle on the surface, therefore the mixture needs to be mixed frequently. Wax can also be added after a while, as it wears off before resin.

4 Few simulations were carried out by using only tin, and others using bronze and lead bronze.

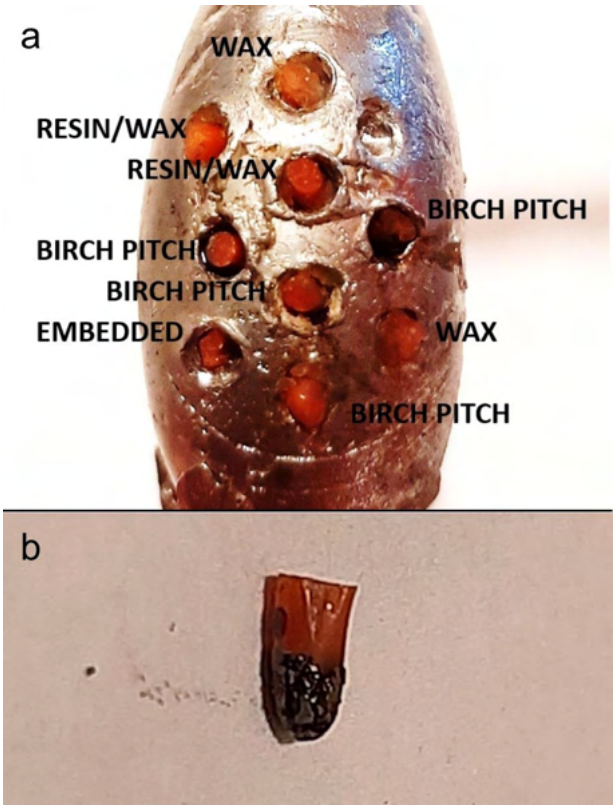

Figure 205. a) test 6: evidence of coral embedding with different binders; b) failed embedding of coral inset held by birch pitch.

8.3.2. Bronze casting

Experimental tests for the production of leech fibulae with a terracotta core by using ancient technologies and materials are still ongoing, and some hypotheses have not yet been fully developed and verified. These experiments were carried out in different steps and by performing various attempts. In the following report, we will examine the process as a whole, discussing the critical issues encountered so far and related considerations. Based on observations made on archaeological artefacts, the only possible way to manufacture these objects is the so-called 'lost wax technique'. For this reason, it is the only one attempted here: the thickness of the metal around the core, in fact, does not allow production by reusable moulds to be plausible.
The technological study on leech fibulae with a terracotta core (see sections 8.1 and 8.2) led to some general considerations:

- traces of the presence of pins are often visible in specific sites on the fibulae surface (marked as A, B and C in Fig. 206);
- radiographic investigation shows presence of internal elements in those sites marked as

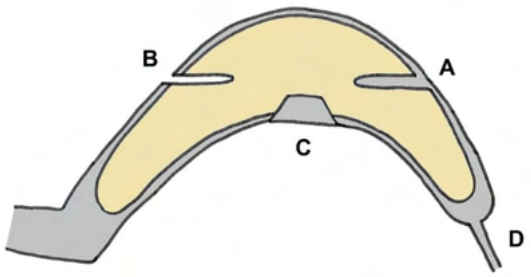

Figure 206. Attempted reconstruction of the fibula structure.

A and C, while B is always empty (Fig. 206);
- the sites marked as A and B (Fig. 206) are generally not aligned and do not deepen throughout half of the fibula body.

The first step consists in producing the clay core, then incorporated into the wax model. Different types of clay were used. Industrial clays (i.e., those used in art, to be fired in electric ovens) tend to explode when the mould is heated; to prevent this problem, a semi-pure natural clay was used instead.

Based on technological issues, pivots for the support of the clay core were located in specific sites, marked as A, B and C (Fig. 206). During firing of the mould, the release of wax would require a support to the inner core, which would otherwise move in the cavity. Various kinds of support (metallic and non-metallic, multiple or alternating, inserted in the core) were tried out (Fig. 207a).

The clay core, once exsiccated, was covered with wax, experimenting different methods (dipping, making a sheet, etc.; Figs. 207b-c). The best results are obtained by repeated immersions in a bath of liquid beeswax – but not too hot, otherwise the layer created is compromised during immersion. The pins in A and B proved to be very useful at this stage. Cooling of the wax layers was checked both in air and water, the former reducing the risk of bubble formation. The core should be rotated to obtain a uniform coverage and alternately soaked by holding it with the two pins, to avoid formation of a thicker covering on the underside. Five immersions are optimal for obtaining a wax layer of approximately 1-1.5 mm thick, compatible with what observed on the archaeological finds.

Then, the wax model of the fibula must be modelled. The bow and foot are worked and decorated separately and then joined (Fig. 207f). The bow needs a thicker wax layer at the insertion point of the needle, so that it is completely encapsulated. The decorations are made directly on the wax, consistently with the traces observed on ancient artefacts. The availability of a fluid alloy, in fact, allows for a perfect reproduction of the decorations on the wax model, reducing the need for refining the artefact after casting. For a circular decoration, a metal awl (either heated or not) can be used in the early stages. However, the wax edge around the hole is much more pronounced than that observed on the ancient finds. Removal with a blade was attempted, but the traces left on the wax are different than those observed on the archaeological finds. Hollow materials (such as wheat stalks or feathers) were thus used and found to be more suitable, since they allow the exceeding wax to be removed by slightly rotating them[5]. The traces around the hole become thus comparable to those seen on the archaeological artefacts (Fig. 207e).

To produce the linear decorations, a metal blade or wire were used, both of which swinging across the bow (hot and cold; Figs. 208a-b). Traces left by the metal blade, thin and with slight raised edges, are compatible with what observed on the archaeological artefacts. However, presence of support pins in A and B hinders the production of these linear decorations and at times makes it impossible to reproduce them (e.g. the linear decoration observed on the T1 fibula from Motto Lagone: Fig. 200c). Their removal from the wax model was then tested; wooden rather than metal pins are easier to remove.

Once the wax model is finished, the needle, equipped with an already preformed spring, is inserted into the wax in position D. The model can then be covered with the mould clay (Fig. 208c). The first layers of clay must be very liquid and purified in order to perfectly trace the decorations. The clay 'pins' – resulting from the negative mould of the circular decoration themselves – act as a support for the clay core, when the wax is removed by heating. The outer clay mould always tends to break while drying, as it shrinks around the wax model that instead

5 When some wheat is used, a new part of the stem must be cut after each hole is drilled, since the wax cannot be removed from the inside; however, the different portions have various dimensions and this does not agree with the traces found on the archaeological finds (Ø ≈ 2 mm constant). The use of feathers is more efficient, allowing for a uniform diameter; the material is also much more resistant and can be emptied several times by slight heating.

Figure 207. a) Clay cores; b) Coating a clay core with a wax sheet; c) Immersion of a clay core in a liquid wax bath; d) Making the circular decoration with a metal punch; e) Making the circular decoration with a feather; f) Foot modelling.

Figure 208. a) Metal wire for linear decoration; b) Metal blade for linear decoration; c) Filling decorations with liquid clay; d) Preparation of the mixture for the mould: clay and animal fur; e) Beeswax vents; f) Gramineous stem vents.

maintains the same size. To overcome this problem, the clay was mixed with organic material (animal hair; Fig. 208d) with excellent results.
At this stage, vents for the escape of air at the metal inlet must be inserted. Initially, these vents were made from thin wax threads – but they were difficult to apply, too thick and also difficult to remove. Hollow grass stems were successfully tried instead (Figs. 208e-f): despite their partial combustion when heating the moulds, they allowed air to pass through while hindering loss of metal and are easier to apply.
No trace about the position of the casting funnel was found on the archaeological artefacts. In our initial attempts, we placed it close to the insertion of the pin (D), but the moulds did not fill because the molten metal was restrained from passing through the reduced thickness around the core. The casting funnel was thus placed at the opposite end (the end of the foot), so that the molten metal could pass from a larger to a smaller thickness, limiting its cooling; such an expedient brought to successfully fill the moulds.
Trials on bronze casting were carried out in several stages, starting with the bow and proceeding with the rest of the fibula. An earthen furnace with two bag bellows and a single blowpipe with upper insufflation was adopted (Figs. 209a-b), and both natural clay and graphite crucibles were used – completely covered with a charcoal pile to achieve the desired temperature and reduce heat loss. Natural clay crucibles work well but can only be used for a single casting with no lid, due to the melting-casting-glazing (Fig. 209c). Graphite crucibles were used with a ceramic or metal lid (Fig. 209d), which helps in performing the casting. All tested lids are welded to the crucible and must be removed prior to casting with a sharp blow from the bottom to the top. The presence of a lid greatly facilitates the operation.
The used alloys were prepared 'ad hoc' with industrial metals. Bronze alloys with a low tin content proved not to be very fluid for filling the moulds, and alloys compatible with the data obtained from the analysis of the artefacts, containing tin and lead, were tested. For the percentages of the different metals, bibliographical data from comparable artefacts were used:

1. 87 % Cu, 10 % Sn, 3 % Pb (Charalambous *et al.* 2014);
2. 80 % Cu, 18 % Sn, 2 % Pb (Sfrecola 2021);
3. 77 % Cu, 17 % Sn, 6 % Pb.

The results obtained with the first two formulations are good; the third composition was developed in order to test whether a higher lead content favoured casting in complex moulds. For each casting, 200 g of alloy was produced: enough for a whole fibula or two bow test specimens. To obtain a flowable metal suitable for casting.
Either direct casting of the fibula or casting of an ingot were attempted. In the latter case, the colour is more uniform (Figs. 209e-f).
The moulds were never fired separately, but directly on the furnace during heating of the metal, and placed with the funnel downwards to allow the wax to escape (Figs. 209g-h). At the time of casting, they were turned upside down and held in place inside a container filled with sand. Pouring must be done quickly (in a few seconds) and continuously, to avoid creating defects (Figs. 210a-c, 210e). A large, narrow-necked casting funnel can be used to favour continuity and avoid material dispersion.
The results obtained are good, but there are still many defects in the artefacts, especially at the bow. As mentioned before, different supports (wood, metal or clay) and different positions of the vents were tested, which brought to the following considerations:

- The pin remains incorporated inside the artefact; similarly, any metal pins are also trapped and the only way to remove them is to saw them off at the surface (which is not easy);
- The internal wooden pins are charred during firing/casting and remain in the form of charcoal, preventing the passage of metal;
- A clay (rather than metal) pin can be made on the ventral side of the bow, with excellent results (it would not be possible to saw a metal pin after casting in that position);
- The presence of the clay pins in the circular decoration, together with a clay pin in C (even in the absence of pins in A and B), holds the core in place;
- The presence of the needle helps the support of the core by contact;
- The wide casting funnel prevents dispersion of the metal during casting (Fig. 210f);
- Presence of the foot promotes casting in the mould;
- Wax vents are too big and fill up with metal, which is then difficult to remove;
- Grass stem vents work well and do not let

metal through, but only air;
- Two attempts were made without venting: the metal bubbled up in the casting funnel and the moulds filled perfectly;
- Mould fractures occur almost always;
- After casting of the mould, rapid cooling in water or slow cooling in air does not seem to affect the final result;
- The firing of the moulds already takes place by placing them on the furnace, so it may not be useful to fire them.

Variables still to be verified include:
- The firing of the moulds before casting;
- The absence of vents;
- The creation of moulds out of clay and vegetable material, rather than animal hair, to verify whether fractures can be reduced.

Work was also carried out on the needles, which were cast separately using a different alloy. According to the literature, the optimal alloy for needles contains around 8-10 wt% Sn (Giumlia-Mair 1998; 2003). The alloys used in the experiments ranged between 6 and 12 wt% Sn.
Initially, a bivalve matrix made of two refractory bricks was used. The two valves were smoothed by grinding them against each other with sand (Fig. 211c). A straight groove and thin 45-degree vents were made on one of them with a bronze awl, as well as a casting funnel. The union of the two valves results in preliminary, semi-finished products with a triangular section (Fig. 211d); in the future, different shapes (e.g. quadrangles) will also be considered. The two valves are held together by a wooden clamp held by a rope (Fig. 211e). This is crucial to improve adhesion between the valves, enhancing the quality of the finished products (Figs. 211g-h).
Hammering trials were started with the aim of producing circular sections, proceeding step by step and working on the edges, alternating with the negative tampering of the semi-finished product (Figs. 212a-d). Experimentation with bending to make a spring were also attempted successfully, on fully hammered bars.
Experimental tests are still in progress. No annealing events (e.g. firing or cremation) have been simulated on finished artifacts (with the exception of laboratory simulations on modern coral: section 8.1.7), which are likely to be useful in order to identify any melting phenomena on the bronze corpus of the fibulae.

8.4 Considerations

The technological study of the leech fibulae with a terracotta core is very complex: in fact, these are composite and very elaborate artefacts, the production of which must have required considerable skills. The traces visible on the surface of the ancient artefacts and the information obtained from their radiographic observation provided various interpretations, also identifying some problems, especially in relation to the actual presence and disposition of internal supports for the clay core.
The experiments carried out (32 tests on fibulae and 9 pins) allowed certain problems to be solved and a possible production chain to be reconstructed for the manufacturing of these fibulae (see below). It must be pointed out, however, that this is a preliminary study, as the experiments are still in progress and some variables remain to be tested.
The study of archaeological artefacts revealed (Fig. 213.0):
- the presence of an internal metal element in site A, obstructed on the surface, but sometimes decipherable;
- the presence of a hole in site B;
- the presence of a metal piece in site C;
- the incorporation of the pin in site D.

Based on this evidence and experimental trials, a possible chain can be proposed for the production of leech fibulae with circular insets:
1 – Realisation of the clay core with a protuberance in C and two wooden supports in A and B (Fig. 213.1);
2 – Coverage of the core with ≈ 5 baths of beeswax (in yellow in Fig. 213.2): pins A and B are functional for immersion;
3 – Modelling the wax model, including several steps (Fig. 213.3):
- cleaning of protuberance C,
- removal of the pins in A and B,
- blocking of the larger hole in A with wax,
- drawing of the linear decoration,
- drilling of the wax at the circular decoration up to the terracotta core,
- addition of the foot;

4 – Preparation of the mould, including several steps (Fig. 213.4):
- reinsertion of the pin in B (functional for dipping in the first baths of semi-liquid clay for filling the decorations),
- insertion of the pin in D,

Figure 209. a) Two bellows melting furnace; b) Two bellows melting furnace; c) Ceramic crucible after a bronze casting; d) Graphite crucible with ceramic cap, after casting; e) Bronze ingot; f) Fibula with non-uniform colouring for direct realisation, without preliminary ingot: test specimen 19; g) Heating the moulds on the furnace during casting; h) Vertical positioning of the mould after casting (right); furnace (background); graphite crucible and metal cup (left).

Figure 210. a) Extracting the crucible from the furnace; b) Casting the bronze in the mould; c) Casting defect due to flow interruption: test 20; d) Alloy melting in progress, combustible addition; e) Casting the bronze in the mould; f) Molten bronze in the mould and vents in action; g) Breaking the clay mould with a scalpel: test 21; h) Casting defect due to incorrect filling of the gap around the inner core: test 21.

Figure 211. a) Fibula with vents originally made of beeswax: test 15; b) Casting defect due to incorrect filling of the gap around the inner core; c) Uniformity by rubbing the surface of the two valves; d) Bivalve matrix; e) Fixing the two valves before casting; f) Bronze casting; g) Pin resulting from a casting with not perfectly joined valves: presence of many casting burrs; h) Successful example, the result of the correct joining of the two shells.

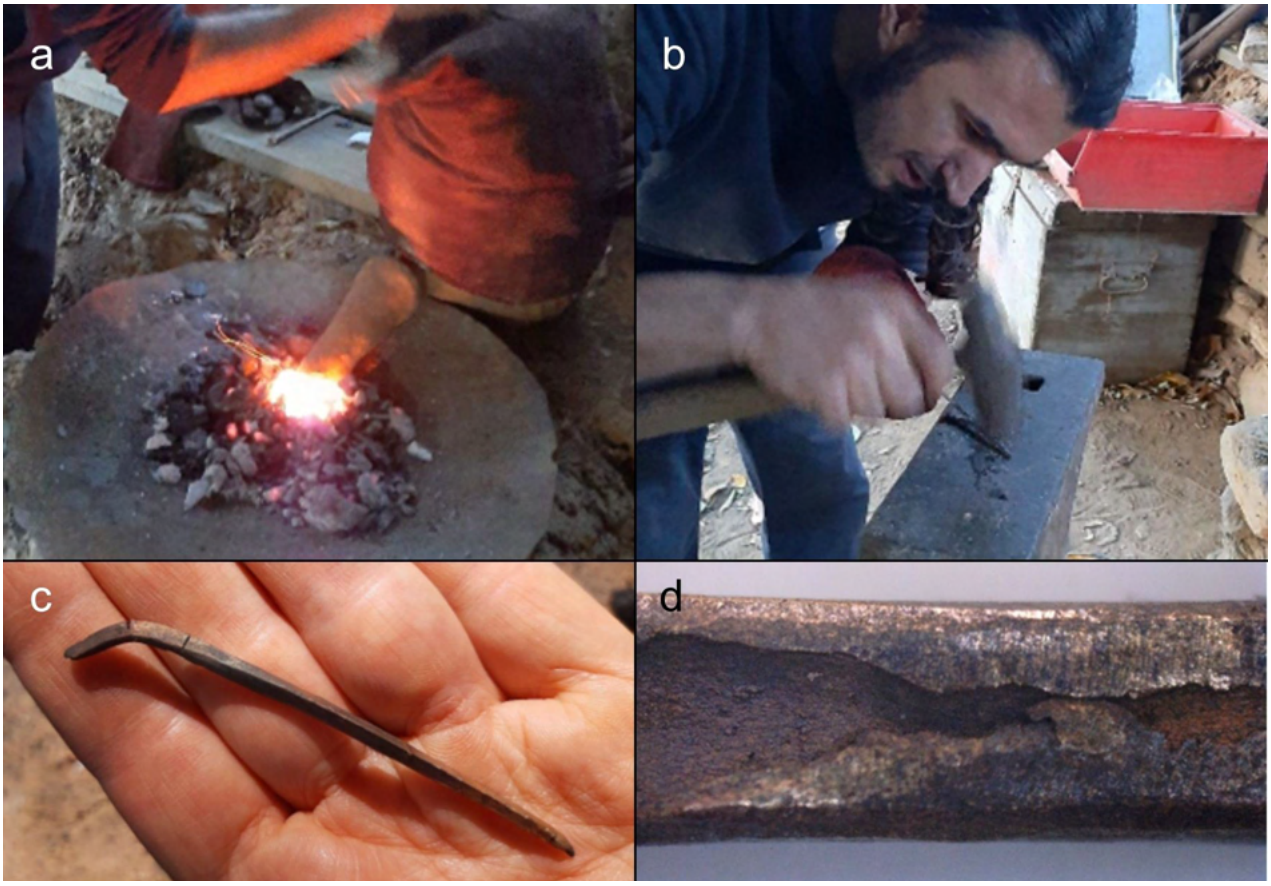

Figure 212. a) Reheating the semi-finished product by reverse tempering; b) Processing by hammering; c) Breaking defect during hammering; d) Detail of the folding of the edges of the semi-finished product.

- immersion in semi-liquid clay and partial drying,
- covering with clay to create the mould,
- drying;

5 – Wax removal by heating or partial firing of the mould: release from the foot (Fig. 213.5);
6 – Bronze casting: infusion of molten metal from the foot and incorporation of the pin (Fig. 213.6);
7 – Post processing (Fig. 213.7):

- Removal of the clay mould,
- Cleaning and deepening of the circular decoration holes and of the prominence in C;

8 – Insertion of a bronze cap in C (Fig. 213.8);
9 – Insertion of coral in circular decorations (Fig. 213.9).
Experimentation of casting by using a lead bronze alloy with a high tin content showed that the final colour of the object may have been, in ancient times, much silverier than that of classical bronze, influencing the final reconstruction of the artefact. Red-coloured coral insets are highlighted in these artefacts (Fig. 214).
Very good results were obtained about the possible procedure according to which coral insets were placed in the circular decorations. The study of the archaeological finds led to the formulation of two hypotheses: i) insertion of a coral piece or ii) filling with a paste. Experimental tests showed that the use of a paste is hardly feasible, whereas the insertion of tiny coral portions is easy – either without glue or using a mixture of beeswax and pine resin.

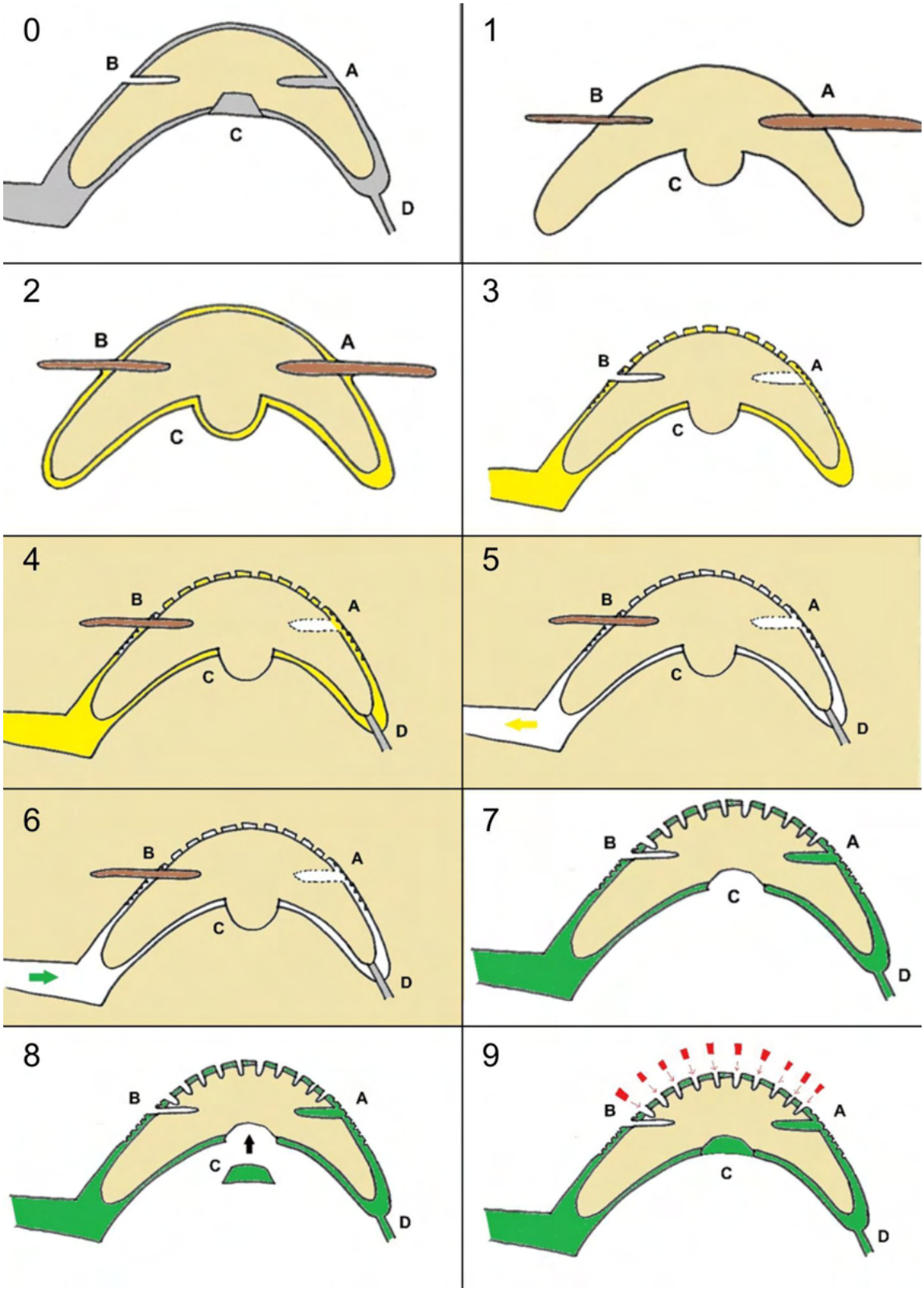

Figure 213. 0) Schematisation of observations made on archaeological artefacts; 1) Clay core; 2) Beeswax coverage; 3) Modelling the wax model; 4) Preparation of the mould; 5) Wax removal; 6) Bronze casting; 7) Mould opening; 8) Cap insertion; 9) Coral elements insertion.

Figure 214. Colour rendering of artefacts.

9. Conclusions

Abstract

Questo volume è dedicato all'analisi archeologica e archeometrica delle fibule a sanguisuga con inserti circolari, databili tra VI e V sec. a.C. e diffuse principalmente in Italia settentrionale negli areali delle culture di Golasecca e di Este. Questi manufatti bronzei presentano decorazioni circolari campite da materiale bianco, tradizionalmente interpretato come corallo rosso mediterraneo (*Corallium rubrum*). Per la loro caratterizzazione è stato sviluppato un protocollo non distruttivo multi-analitico che integra microscopia ottica, spettroscopia Raman e FT-IR, diffrazione a raggi X e SEM-EDS. Lo studio archeo-tipologico di dettaglio ha permesso l'identificazione di alcune tendenze nella manifattura di questi ornamenti, rilevando la presenza di oggetti con caratteristiche meno elaborate nell'area della Liguria interna e della Pianura Padana occidentale, probabilmente in quanto imitazioni locali dei tipi golasecchiani.
Nel record esaminato sono state incluse per confronto anche altre tipologie di reperti cronologicamente affini, accomunate dalla presenza di parti in presunto corallo, per un totale di 372 reperti esaminati nel dettaglio. Tra questi, su 264 reperti selezionati per le analisi archeometriche, solo il 17% ha mostrato segnali diagnostici certamente riferibili a *C. rubrum*, grazie alla compresenza di calcite magnesiaca (MMC-HMC) e polieni. Il 43% invece è identificabile come materiale carbonatico (calcite con vari tenori di Mg), senza polieni. In altri casi sono stati identificati materiali alternativi come osso, gesso, aragonite e *Spondylus gaederopus*, oppure è stata rilevata l'assenza di una campitura decorativa.
L'analisi metallurgica superficiale, mediante μ-XRD e SEM-EDS, ha suggerito un verosimile controllo intenzionale della lega: bronzo povero di stagno per gli oggetti che richiedevano una lavorazione post-fusione, e bronzo ricco di stagno e con tracce di piombo per i manufatti finiti in colata. La tecnologia impiegata è coerente con la fusione a cera persa, con decorazioni realizzate sul modello in cera.
Le problematiche aperte riguardano la verifica di una maggiore incidenza del *Corallium rubrum* in oggetti più recenti, la spiegazione dell'abbondanza di calcite basso magnesiaca e la possibile determinazione della provenienza del corallo.

9.1 Project overview

The main goal of the present research is the archaeometric and archaeological study of the decorations of a specific type of fibula, widespread in northern Italy during the Early Iron Age (6th - 5th century BCE), namely the leech fibula with circular insets. It is characterised by a leech shaped bow, generally with a clay core, and a long foot, ending with a small globe. Its distinctive consiste of several small circular holes, filled with a white material, traditionally identified as coral.
Coral spreads in northern Italy from the end of 8th and throughout the 7th century BCE and continues to be used until approximately the 5th century BCE. After this period, it disappears from these regions, while it remains attested north of the Alps and in southern Italy. During the Early and Middle Iron Age, this material was employed in the production of various types of ornaments in northern Italy, with a distribution mainly concentrated in two areas: the Golasecca cultural sphere and the Venetic–Este area. It is possible to identify a general evolution from less elaborated artefacts, such as the 'Longone al Segrino' pendants or the Venetic beads, towards more and more elaborated forms, such as the leech fibula with insets, or with transverse groove decoration, or the bucket pendants with 'occhio di dado' decoration. The coral decorations are generally white in colour today, with few exceptions, and the attribution to red Mediterranean coral (*Corallium rubrum*) has generally been made on the basis of the literature, by comparison with some finds that preserve red or orange hue.
In order to try to solve this incertainty in the material characterisation, a specific non-destructive protocol has been developed and applied on several archaeological artefact from northern

Italy, with a specific focus on leech fibulae with presumed coral circular insets, complemented by a comparative analysis of other Iron Age artefacts sharing similar characteristic.
This research proposes a change of perspective in the study of archeological finds and their decoration by integrating the traditional archeo-typological approach with archaeometric and archeo-technological analyses. This combined methodology aims to achieve a more comprehensive understanding of both the artefacts themselves and the cultural contexts that produced them.

9.2 Archaeotypological study: archaeological trends

The typological assessment of leech fibulae with insets, based on both published literature and unpublished artefacts from Italian collections, revealed crucial patterns in the cultural dissemination, chronological development, and regional variation of these objects. The fibulae are most commonly associated with the Este and Golasecca cultural spheres, but their distribution also includes more peripheral regions of northern and central Italy, as well as transalpine territories. Of the 421 leech fibulae with insets identified, including published and unpublished material, only 296 are preserved in Italy. This type is dated between the mid-6th and mid-5th century BCE and is traditionally subdivided into several varieties based on the number and distribution of circular holes on the bow. In this study also the conformation of the foot termination has been considered, in order to check for the presence of any chronological or geographical trends: it is generally characterised by the presence of globet, which can be round or flattened, decorated with circular insets or not, placed all around or only on the upper face; it may be accompanied by a bulge, which may be decorated; finally the foot termination may have particular shapes (i.e. pointed, swallow-tailed, vase-shaped). Eight different subtypes have been identified, with varying frequency and with different geographical and chronological distribution. The types with double or triple globet ends are mainly found in the Swiss area of the Golasecca culture, with three exceptions in the Po Valley and the Apennines, while the 'Q type', with foot with bulge before the globet, and in particular the sub-variant with flattened globet and bulge, both decorated only on the upper part ('type QB3'), is more common along the northern Apennines.
The extensive study of Italian artefacts also allowed the identification of a novel type, the leech fibulae with grooves, which can be subdivided into sub-types based on the orientation of the grooves on the bow and on the presence or absence of circular inlays alternating with the grooves. This type probably originated in the Italian context from the fusion of typical features of leech fibulae with coral inlays with those of late-Hallstattian fibulae, as it has many similarities with both. The so-called Late Hallstattian fibulae, found in Italy in few exemples, are a typical Celtic production of the HAD3-LTA period. Among this vaste production two types may have coral inlays. The presence of these fibulae in the eastern part of Italy has led some authors to suggest that the use of coral was a local elaboration of trans-Alpine types. The leech fibulae with grooves combine typical characteristics of leech fibulae, such as the morphology of the foot, the unilateral spring fused with the body of the fibula, with a type of decoration referable to the late-hallstattian fibulae with coral, which have variously folded foots and bilateral spring, inserted separately in a hole in the arch.
Based on the archaeological evidence, it is difficult to identify the locations of possible production centres. The main indicators that can be considered are the discovery of raw materials and of artefacts – particularly those clearly associated with production contexts. Regarding leech fibulae with inlays, there are some differences between artefacts produced in the Golasecca cultural area and those from Liguria Interna and the western Po valley. The former are generally more refined objects with a clay core and standardised characteristics, while the latter are similar but have specific features that suggest they may be the result of local production, such as a greater incidence of full arches, flattened lenticular or biconvex bow morphology and reduced dimensions. Consequently, it is possible to hypothesise the presence of at least two different production areas, with the first production centres linked to Golasecca, such as probably Castelletto Ticino-Sesto Calende or Gropello Cairoli or Como, and other centres (such as Villa del Foro and perhaps Brignano Frascata, San Polo d'Enza and Pianello Val Tidone), where these products were imitated less skilfully by local craftsmen. This is evidenced by the greater

incidence of full bow fibulae, which are easier to make.
Artefacts from Genoa appear to be more closely related to those from the Golasecca area, suggesting that they are not locally produced but rather represent original Golasecca items. This may be related to a raw coral trade across the Scrivia valley, as suggested by the presence of a raw coral element in the Genoa Castello excavations. In north-eastern Italy, leech fibulas with insets are mostly attributable to the oldest variants and display highly refined characteristics, as in the case of the golasecchian fibulas. These were probably manifactured in the main production centres, such as Este, Padua, Montebelluna.
Concerning the presence of raw materials for the production of these artefacts, the site of Forcello di Bagnolo San Vito is particularly noteworthy, as numerous coral fragments have been recovered there, suggesting local processing of the material. However, no direct evidence of actual production activities has been documented.

9.3 Archaeometric analysis: protocol and results

The archaeometric characterisation of presumed coral parts has been achieved with a non-destructive multi-analytical protocol, specifically designed for the characterisation of *Corallium rubrum*. This involves the use of optical microscopy, vibrational spectroscopies (μ-Raman and FT-IR with a diamond cell), μ-X-ray diffraction and scanning electron microscopy with micro-chemical analysis.
The proposed protocol enables three different archaeometric approaches ('in situ', in laboratory, μ-sampling) in the white material characterisation and is thus adaptable to the conservation requirements of museums and conservation institutions. It combines the needs for preservation of archaeological finds with the relaibility of the archaeometric investigations. The most effective approaches involve complete characterisation, either through μ-sampling or by transporting the findings to the laboratory without sampling. Both approaches use several techniques and do not require any pre-treatment; they are equally valid. The latter allows completely non-invasive multi-spot analysis. Meanwhile, μ-sampling avoids the need for transport and ensures the artefact remains on public display at the museum. The least effective approach is the 'in situ' approach, which only allows partial characterisation and involves portable Raman instrumentation and a digital microscope.
Such a versatility implies limitations in the resolution of analyses, particularly for what concerns some methods. In fact, μ-XRD investigations are strongly influenced by the surface irregularity of some samples, leading to a shift in the characteristic peaks and mostly preventing all extrapolations about correlating this shift with the chemistry of the samples. SEM-EDS analyses in low vacuum, with no surface pre-treatment of the specimens, lead to semi-quantitative results, sufficient to adequately infer the Ca/Mg ratio in calcite.
The archaeological record considered in the present research comprises all artefacts containing presumed coral parts from northern Italy that can be dated to the Iron Age. Particular focus is given to leech fibulae with insets. A review of the literature identified 534 published archaeological finds with presumed coral parts. The current location of only 436 of these is known. Of these, 372 artefacts were examined 'in situ' using a portable digital microscope and 264 were selected for archaeometric analysis based on the preservation of the presumed coral parts.
The reason for focusing on this particular type of fibula is its specific nature, as the characterisation of its small inlays requires an archaeometric approach. Their size and method of manufacture make identification by simple macroscopic observation difficult, as is often the case with raw coral branches.
Archaeometric investigations allowed the unequivocal identification of *C. rubrum* in 17 % of the analysed artefacts, due to the simultaneous identification of calcite with a medium-to-high magnesium content (MMC-HMC) and polyenes. In 43% of cases, carbonate phases (i.e., medium-high magnesian calcite, calcite with reduced or no magnesium content) were identified, but no polyenes.
The identification of low magnesian calcite (LMC) or pure calcite (29 %) raises interesting questions, as these materials could result either from the use of rock-forming carbonates (e.g. limestones or marbles) or coral skeletons subjected to post-depositional alteration processes (e.g. altered *C. rubrum* or altered white coral or fossil coral). The sporadic occurrence of gypsum

(1%) is the result of transformation from a possibly biogenic carbonate matrix after burial in acidic soils. Similarly, it seems plausible to attribute the presence of LMC to post-depositional diagenesis, rather than to the selection and use of different raw materials.
Occasionally, the performed analyses also identified different materials in the decorations – such as bone, glass, aragonite, *S. gaederopus* and White Indian Ink. However, in 29 % of the cases no adequate filler was identified.
Correlating these data with the artefact type revealed no clear trend. For leech fibulae with insets, the best-represented type, correlations with several other variables (e.g., possible combustion, year of discovery, dating, provenance) were also examined. This analysis indicated a higher occurrence of *C. rubrum* in the more recent artefacts (480–440 BCE), whereas the oldest artefacts (560–480 BCE) are characterised by calcite lacking polyenes and exhibiting greater variability in Mg content. This evidence suggests the diversified use of various materials in earliest phases, culminating in the consolidation of the use of *C. rubrum* in more recent phases. However, the record of more recent objects is less abundant than that of older ones, which may contribute to the apparent lower diversification of materials. Consequently, the chronological hypothesis should be tested by extending the analysis to Swiss artefacts, particularly those dating to GIIIA1.
Overall, the results obtained are largely consistent with previous archaeometric studies on Iron Age transalpine fibulae (Furst *et al.* 2016; Bente *et al.* 2015c; 2016; 2020; 2023). In particular, some similarities exist with the study of *Mitteldeutsche Korallenfibel*, metal-bow fibulae with coral beads, dated to the Late Iron Age and widespread in Germany and Austria (Bente *et al.* 2023). *C. rubrum*, in fact, was identified in some cases and poor-Mg-calcite or calcite in others, posing similar problems of interpretation about the origin of the latter. In this case, the integration of Raman and μ-XRD studies with μ-CT (internal density) and isotopic analyses proved to be particularly useful in identifying *C. rubrum* with a recent marine origin, excluding the use of fossil coral (Bente *et al.* 2015c; 20-23). Finally, the analogy between an Italian fibula (Brembate Sotto) and a transalpine one (Leinbach; Bente *et al.* 2020) is particularly interesting, as it reveals a compositional difference between the surface (LMC or simple calcite) and the inner part (*C. rubrum*, HMC with polyenes), indicating presence of an external alteration.

9.4 Critical issues: LMC problem

Low magnesium calcite has been identified in many cases, raising issues of interpretation regarding the origin of this material. It may in fact derive from the use of a different raw material, such as calcareous stone, or from the red coral altered by diagenesis in the soil. Another factor to consider is the potential influence of the depositional context. For instance, artefacts from incineration tombs may have been exposed to heat during funerary rituals.
Approximately 20% of artefacts composed of LMC show signs of combustion. This phenomenon could explain the loss of polyenes, which occur above 200°C, as documented in the literature. In order to verify a potential decrease in Mg content, combustion tests were performed in laboratory on modern coral at temperatures consistent with those reported by archaeological data for Iron Age funeral pyres. Measuring the Mg-content in the calcite before and after combustion revealed an effective decrease, resulting in the formation of MMC from the HMC that constitutes the coral. However, burnt archaeological finds only account for a small proportion, so this phenomenon cannot completely explain the presence of LMC.
In the considered record, *C. rubrum* is obviously never detected in burnt artefacts. These are generally associated with calcium carbonate, pure calcite or LMC, compared to MMC or HMC. An attempt was made to correlate the materials with the year of discovery, to assess whether post-excavation alterations could have influenced the results; however, no significant correlations were identified. According to literature (Borromeo *et al.* 2017; Fürst *et al.* 2016; McGregor, Gagan 2003), both LMC and HMC can exist in nature; however, unaltered calcites with intermediate values have never been found. This is why, when MMC is identified in an archaeological find, with or without polyenes, it is attributed to the alteration of an original *C. rubrum*. A loss in the Mg-content can be induced by meteoric diagenesis, leading to the formation of MMC or even LMC, starting from an original HMC (typical of red coral) or even aragonite (the main component of deep-water corals).

9.5 Critical issues: coral provenance

Regarding the provenance of ancient coral, Pliny the Elder tells us that the finest material came from the Gallic Gulf and the Sicilian Sea, near the Aeolian Islands and Trapani, as well as from Gravisca and Naples. Dioscorides and Oribasius, for their part, report that it originates from Cape Pachino, near Syracuse. In previous centuries, evidence of red coral has been documented along the coasts of the Marseille and Béziers areas, as well as in the excavations of Genoa Castello. In northern Italy, raw coral has been found in Como, Forcello and the Este area. In central and southern Italy, votive deposits have been discovered in Cagliari, Gravisca, Foce del Sele, Velia and Oria. During the Middle Ages, exploitation continued in the same areas, but new sites were also documented, such as Corsica and Sardinia from the 13th century, and North Africa from the 14th century.
Furthermore, other white corals are documented in the Mediterranean Sea. These are known as cold water corals (CWC) or, more commonly, madrepores, and are generally sporadic colonies in a state of decay or fossils. The presence of white corals in the Mediterranean Sea is of interest in the context of this study, as this material may also have been used in the production of Iron Age artefacts. However, the bathymetric distribution of CWC at greater depths is not compatible with free-diving fishing methods and they were probably not or less exploited in ancient times. Nevertheless, some evidence suggests that these corals were used in antiquity, as pointed out by medieval texts from western Provence mentioning the trade in white and red coral for use in pharmaceuticals. In the 1st century, Dioscorides wrote about red and white corals. The earliest evidence of the use of these corals was found at the Tas-Silg sanctuary in Malta. Eight fragments of the *Dendrophyllia ramea* coral were found there as a votive offering. These fragments were dated partly to the 4th century BCE and partly to the late Republican and early Imperial Roman periods.
Unfortunately, archaeometric methods currently cannot determine with certainty the sourcing areas of the coral used in these artefacts. While no specific studies exist for coral, some authors have focused on shell provenance (Bajnóczi *et al.* 2013; Bente *et al.* 2023; Claassen, Sigmann 1993; Douka 2011; Leng, Lewis 2016; Pierre 1999), mentioning two possible approaches: isotopic and trace-element analysis – both of which are, however, difficult to apply to *C. rubrum*. The main problem is that *C. rubrum* mainly come from a single basin, Mediterranean Sea. Both isotopic signature and chemical elemental fingerprints are quite stable inside the same basin. Furthermore, provenance determination on archaeological samples would require an exhaustive analysis of all possible old collection sites, for comparison purposes. In *C. rubrum* case, this assumption is not feasible, because the ancient supply sites, located at a low depth, are certainly now depleted. Modern pollution is another potential problem. Additionally, the effects of diagenesis have to be considered because calcite recrystallisation reflects the environmental conditions at the site of recrystallisation rather than the area of provenance of the material. The effective presence and extent of diagenesis might be determined: by combining XRD and SEM-EDS to assess the structural and mineralogical integrity of the material, or by the use of cathodoluminescence.

9.6 Archaeometallurgical insights

The metal surfaces of the objects were also analysed using the same protocol, which indicated variations in composition that appear to correlate with the different manufacturing processes involved in producing the artefacts. These observations, however, should be interpreted with caution, as the results are inevitably influenced by post-depositional alteration processes.
Good results were obtained with μ-XRD and SEM-EDS investigations, which identified several crystalline phases related to metal alteration products containing copper, tin and lead. The analyses revealed compositional differences in relation to the different classes of objects, suggesting a possible intentional control of the alloy composition in relation to the properties desired for the planned working technique. In particular, analysis of the metal surface alteration by-products revealed low tin content for objects requiring post-casting hammering, while, conversely, complex artefacts requiring a liquid casting alloy appear to have high levels of tin and lead.
A further significant result is the possible evidence of compositional differences in leech fibulae between the body of the fibula (bow and foot) and the pin, confirming that these objects

can be considered 'composite' artefacts. The pin and spring seem to be made of tin-poor bronze, while the bow and foot are composed of tin-rich bronze with lead. The amount of lead also appears to vary depending on the presence or absence of a clay core in the bow, with higher values in the former case. The arch of this type of fibula is characterised by the presence of a clay core coated by a thin layer of metal, thus requiring the use of a very fluid casting alloy. There are also refined decorations on the surface, probably made directly on the wax model, in order to minimise the post-casting processing of the artefact and reduce the risk of breakage due to the fragility of the lead alloy. These are composite artefacts that require a high degree of technological craftsmanship.

Trace elements have also been considered, in order to check for some suggestion about the possible ore used for copper extraction, but not significant result emerge. Excluding elements that are likely to be enriched from the soil, the sum of the main trace elements is generally minor than 1 wt%, indicating a high degree of purity for the used copper, an important technological information.

Finally, the study of two composite bow fibulae with coral beads from Como reveals the presence of a decoration with thin rods originally made of silver, now blackish in colour. For this type, these decorative elements were usually made of gold and the identification of the use of silver is of particular interest.

9.7 Archaeo-technology

The archaeo-technological study focuses on leech fibulae with inlays. No substantial differences were found between type variants. The main difference lies in the presence or absence of an inner clay core. This core could be inserted to economise bronze and reduce the global weight, especially in larger artefacts.

The fibulae in the record vary in size and shape, suggesting the use of a lost-wax technique. This technique also allows decorations to be easily created directly on the wax model, as evidenced by the traces on the edges of the linear and circular decorations found on the archaeological artefacts.

Supports were necessary to keep the core in place after the wax was removed from the mould by heating. Examination of the artefacts reveals the constant presence of two holes on the upper face of the arch: a larger one on the spring side and a smaller one on the foot side. The former is generally filled with metal, which makes it difficult to detect on the surface, and is sometimes decorated, such as in the fibula from Motto Lagone. A large metal gusset is also generally visible on the ventral side of the bow.

An in-depth radiographic examination was performed on 45 fibulae from the Golasecca area to examine their internal structure. The study revealed the constant presence of an internal metal element in the upper part of the bow that matched the hole on the spring side. It also revealed an elongated cavity in correspondence with the small hole on the foot side and a conical element on the lower face. X-rays also allowed observation of the pin insertion point in the metal part of the fibula body and never inside the clay core, together with some particular other evidences, such as the insertion of the rare ornitomorphic element.

Subsequently, experimental archaeology led to the reconstruction of a potential lost-wax production process. The data obtained from the experimental tests are consistent with the results of the archaeometric analyses conducted on the metal surface. Experimental tests on the manufacture of these bronze artefacts are ongoing and will hopefully validate the remaining identified variables.

As far as circular decorations are concerned, experimental archaeology tests proved that it is easier to frame a coral inset in the hosting cavity than to fill it with a paste, and that this produces a much better aesthetic result. Various binders were tried out, and a mixture of beeswax and pine resin was found to be the best option in terms of application, holding power and colour rendering. However, a binder is unnecessary when the inset is placed exactly in the hosting cavity.

9.8 Future perspectives

Possible future developments of this research could focus on addressing the critical issues that have been identified.

Further studies on this topic could investigate the apparently higher prevalence of *C. rubrum* in more recent artefacts. This could be achieved by expanding the sample to include a larger number of the more evolved leech fibulae with

insets, which are particularly abundant in the Swiss sector of the Golasecca culture.

The presence of calcite with different Mg-content could also be investigated using various methods, such as isotopic analysis to identify recent, altered or fossilised coral (Bente *et al.* 2023), cathodoluminescence (Moreno-Azanza *et al.* 2016), X-ray computed tomography, and TEM data on nanostructure and microstructure arrangements, as for mesocrystals and their transition and local chemical compositions. Other future developments may focus on understanding the whitening of originally red coral decorations, to be investigated through experimental simulations. This phenomenon could result from the partial or complete degradation of *C. rubrum*, interactions with burial soils (e.g., humic solutions), or heat exposure (as suggested by Bente *et al.* 2023).

The interdisciplinary, non-destructive study of the bronze and coral artefacts presented here has allowed for a comprehensive understanding of both their constituent materials and the production techniques involved in their manufacture. This research thus provides an innovative perspective on the study of these archaeological objects, linking multiple disciplines to enhance our understanding of the artefacts.

Acknowledgments

I would like to thank Marica Venturino, Eliano Diana and Roberto Giustetto for believing in this project and for their advice and support throughout all stages of its development.
I would also like to express my gratitude to Lorenzo Zamboni for his precious advice and for his editorial and revision work, and for his valuable support in finalising this volume.
I am extremely grateful also to Veronica Cicolani and Sebastian Fürst, the external evaluators, and to professor Klaus Bente, for their valuable advice and feedback
Furthermore, this research would not have been possible without the fundamental help and cooperation of the Soprintendenza officials, museum directors and curators, restorers, conservators, professors, PhD students and local volunteers, who approved, facilitated and advised in the study of archaeological materials. In particular, I would like to thank: L. Mordeglia (SABAP Biella, Novara, VCO e Vercelli); S.G. Lerma, G. Garbarino (SABAP Alessandria, Asti e Cuneo); C. Longhi (SABAP Bergamo e Brescia); L. Lamanna, C. Marastoni (SABAP Cremona, Mantova e Lodi); D. Locatelli, B. Grassi (SABAP Como, Lecco, Monza-Brianza, Pavia, Sondrio e Varese); C. Moine, A. Francesconi (SABAP Parma e Piacenza); C. Rossignoli, C. D'Incà, M.C. Vallicelli, C. Pirazzini, F. Santinon, S. Emanuele, G. Sperandio (SABAP Venezia, Belluno, Padova, Treviso); M. Rapi (University of Milan); M. Cupitò, V. Gallo (University of Padua); S. Casini (Civico Museo Archeologico di Bergamo); M. Hirose (Museo Nazionale Mantova); R. Invernizzi (Museo Archeologico Nazionale della Lomellina); E. Pagella, E. Panero, P. Petitti, F. Pepi, C. Meli (Musei Reali Torino); G. Cravero (Museo Civico Archeologico Palazzo Traversa, Bra); C. Orsenigo, G. Cossandi (Museo Civico Giovio Como); B. Cermesoni (Museo Civico Villa Mirabello Varese); G. Bolzoni (Museo Archeologico della Val Tidone); E. Poletti (Museo Archeologico di Arona); J. Colombo (Museo Fanchini di Oleggio); A. Provenzali, S. Loreto (Museo Archeologico Milano); F. Veronese (Musei Civici Padova); C. Cavalli, C. De Biasio (Museo Civico di Belluno); E. Gilli (Museo di Storia Naturale e Archeologia di Montebelluna); M. Frapporti (Mel, Borgo Valbelluna); M. Pieroni, I. Festari, G. Di Gresy (Museo Civico Novara); M. Squarzanti (Civico Museo Archeologico Sesto Calende); F. Gernetti and F. Marostegan (Gruppo Storico Archeologico Castellettese). For their willingness, although it was unfortunately ultimately not possible to study any archaeological finds, I would also like to thank: S. Ratto (SABAP Città Metropolitana Torino); N. Radi, N. Campana, L. Trigona, F. Sciamanna (SABAP Genova e La Spezia); F. Marzatico, F. Nicolis, L. Endrizzi (Provincia Autonoma di Trento); A. Pozzi (SABAP Ravenna, Forlì, Cesena e Rimini); C. Azzolini, Dr. Marco Podini (SABAP Parma e Piacenza); R. Micheli, S. Di Tonto, G. Musina (SABAP Friuli Venezia Giulia); P. Salzani, B. Bruno (SABAP Verona, Rovigo e Vicenza); N. Martinelli (Museo Storia Naturale Verona); B. Prosdocimi (Museo Nazionale di Este); G. Pellegrini (Museo Gaetano Chierici); P. Garibaldi (Museo di Archeologia Ligure a Genova); A. Azzolini, L. Dalprà, L. Dallemule (Castello del Buonconsiglio, Trento); A. Armirotti, C. De La Pierre, L. Appollonia (Regione Autonoma Valle d'Aosta); E. Drago (Musei Civici di Treviso). Thanks are also due: for the collaboration and support to M. Ruffa and to A. Monticone; for the help in contacts to F. Garbasi; for the advice to V. Cicolani and B. Demarchi.
I would like to express my deepest gratitude also to the professors, technicians, research assistants and PhD students who generously shared their knowledge and expertise in the archaeometric analysis and data interpretation. Special thanks are due to A. Lo Giudice, A. Re, E. Costa, N. Curetti, D. Bernasconi, M. Labate, A. Giordana, L. Vigorelli, F. Tansella, S. Grassini and L. Es Sebar. For teaching and support in the experimental archaeology tests, I would like to thank CAST (Centro Archeologia Sperimentale Torino), expecially in the persons of G. Gaj.
Lastly, I would be remiss in not mentioning my family, Paolo and Sophia, and my mother. Thanks to your constant support and encouragement, this work has been completed.

Editorial team statement
The editorial team has used artificial intelligence tools (ChatGPT, GPT-5 mini model) exclusively to assist with language editing and stylistic improvements. AI was not involved in the scientific content, analysis, or interpretation of the research.

Topographical index

Adda River 48
Adige River 52, 77
Adige Valley 54
Adria 37, 52, 54, 61, 88
Adriatic Sea 21, 27, 43, 53, 54, 104
Aeolian Islands, Isole Eolie 27, 40, 97
Afghanistan 41
Agde 35, 39
Ajaccio 43
Alba 51
Albania 21
Albate 60, 85
Alboran Sea 21, 22, 40
Alessandrino 45, 96
Algeria 21, 25, 31, 40
Alghero 42
Alife 33, 34
Almeria 21, 42
Altino 77, 88
Alto Verbano 48
Ameno 48
Andalusia 31
Aosta, Ospedale 56
Apennine 55, 58, 66, 90, 109, 220
Apulia - Puglia 21, 22, 29, 32, 40
Aquitaine 38
Arbedo 50, 196
Arbedo, Cerinasca 61, 101
Archipelagos of Madeira 21
Argos 30
Arles 35, 38
Armissan 29
Arona 95
Asia Minor 27, 40
Asolo 54
Astigiano 45, 96
Atlantic Ocean 21, 22
Aude 29
Aude valley 35
Austria 30, 77, 79, 82, 92, 103, 222
Auvergne-Rhône-Alpes 27
Bactrian 41
Baden-Württemberg 29, 35, 79
Baganzola 64
Bagnolo S. Vito, Forcello 34, 36, 52, 56, 61, 77, 82, 90, 124, 168, 221
Baldaria di Cologna Veneta 52
Balearic Islands 31, 32
Balkans 53, 54, 88
Baltic Sea 36
Barcelona 27
Baou de Saint-Marcel 37
Basilicata 33, 40, 170
Bavaria 92
Belbo River 51
Bellinzago Novarese 82
Bellinzona 48, 50
Belluno 53, 54, 61, 88, 109
Bergamo 48, 80
Béziers 35, 38, 39
Bisagno Valley 42
Bismantova 54, 61, 90
Bobbio 90
Böblingen district 36
Bohemia 77, 92
Bologna - Felsina 36, 52, 54, 55, 56, 64, 80, 85, 90, 92, 101
Bologna, Arnoaldi necropolis 36, 90, 92
Bologna, Certosa di Bologna necropolis 36, 90
Bologna, De Luca necropolis 36, 90
Bonifacio 41, 43,
Borgo Virgilio, Arginotto 24, 37, 90
Borgonovo V.T 66, 90
Bormida River 51
Borso del Grappa 64
Bourges 35, 37
Bourguignon-lès-Morey 35
Bragny-sur-Saône 35
Brembate sotto 60, 179, 222
Brenta valley 53
Brenta River 54
Breolungi, Mondovì 51, 81
Brescello 56
Brescia 37
Bresciano 93
Brignano Frascata 61, 86, 102, 119, 220
Broucherion Coast 41
Bruechel - Geispolsheim 35
Budapest 37
Burgos 28
Burgundy 37
Byrsa - Carthage 31
Cabo de San Antonio 42
Cademario 50
Cadore 54
Cagliari - Caralis 32, 41, 223
Cal Rjolic 27
Calferi di Stenico 61
Campania 27, 32, 36, 37, 40, 43
Campolino-Lothen 92
Canary Islands 21
Cannes 39
Canosa 33
Canton Ticino 48, 49, 61, 64, 87, 93, 95

Cape Pachino 40, 42, 223
Capri 41
Capua 32
Caralis – Cagliari 32
Carceri d'Este 66, 74
Carpi 56
Carpignano Salentino 28
Carthage 31
Casan 88
Caserta 33
Casinello 34
Castaneda 61
Castellazzo della Garolda 61, 90
Castelletto (sopra) Ticino 48, 59, 61, 64, 74, 75, 85, 102, 220
Castelletto Ticino, Cascina Riviera, Merlotitt 74
Castelletto Ticino, Motto Falco 59
Castello di Annone 51, 64, 86, 102
Castelveccana, Castello Valtravaglia 59, 85
Castelvecchio, Peveragno 51
Catalan coast 41, 87
Çatalhöyük 29
Catalonia 21, 27, 35, 39, 40
Caverna delle Arene Candide 28
Caverzano 54, 61, 75
Caverzano, Limade 54
Caverzano, Masiera-Font 75
Cervo 43
Cesseras 38
Champagne 35, 36, 79, 92
Châtillon-sur-Seine 35
Chiavari 85
Chies d'Alpago 61
China 41
Chiomonte, La Maddalena 94, 169, 188
Chiusa Pesio, Monte Cavanero 51
Cisalpine 35, 48, 56, 97
Civitavecchia 42, 43
Comasco 93
Como 37, 48-50, 56, 59-61, 66, 80, 85, 169, 179, 190, 192, 201, 220, 223, 224
Como, Albate 85
Como, Ca' Morta 60, 169
Como, Ca' Morta, Rebbio 85
Como, Ca' Morta, terreno IACP 59
Como, Prestino, via Isonzo 179
Como, Respaù 60
Como, Sant'Anna-Tre Camini 56
Concise 29
Corinth 30
Corsica 21, 27, 28, 41-43, 223
Cossano Belbo 64
Côte-d'Or 35
Courtesoult 87
Croatia 21
Cucuron 39
Cucurru S'Arriu 29
Cuggiono 60, 85
Cugnan 61
Cunardo 85
Cyclades 30
Cyprus 31
Czech Republic 35, 101
Dalmatia 37
Dalpe 61
Danube 37
Dasterru Cave 29
Défenneh 30
Delos 30
Destra Basento 34
Ditzingen-Schockingen 87
Donja Dolina 88
Dormelletto 95
Drepana 40, 97
Dürrnberg, Hallein 36, 79
Eberdingen 35
Egypt 29, 30, 40, 41
Emilia Romagna 54-56, 64, 92
Emporion - Gerona 24, 35, 39
Ensérune 39
Enza River 56
Ephesus 30
Episcopi – Hierapetras 30
Eritre 40
Esslingen 87
Este 9, 24, 45, 52, 61, 64, 74, 77, 5, 87, 88, 96, 97, 107, 175, 219-221, 223
Este, Capodaglio 64
Este, Casa di Ricovero 87
Este, Costa-Martini 74
Este, Pelà 74
Estérel 41
Etruria 36, 38, 48, 55, 85
Etruria Padana 9, 34, 45, 48, 54, 61, 77, 78, 82, 90, 96, 97, 175, 192
Europe 9, 14, 27-29, 34, 48, 54, 55, 77, 100, 108
Felsina - Bologna 52, 54, 55, 64
Finale Ligure 29
Florence 33
Foggia 24
Fondo Ruozzo sanctuary 32
Forcello di Bagnolo San Vito 34, 36, 52, 56, 61, 77, 82, 90, 124, 168, 221
France 27-30, 33, 35, 38, 77, 79, 82, 91
Frattesina di Fratta Polesine 54, 55
Fréjus 39
Frejus tunnel 94
Friulan 53, 54

Friuli Venezia Giulia 54, 88
Gaggio 90
Galliate 95
Gallic Gulf 22, 40, 45, 97, 223
Gargano 21
Gavà 27
Gazzo Veronese 52, 61, 64
Geispolsheim 35
Genoa 37, 38, 41, 42, 48, 50, 52, 86, 221, 223
Genoa, Bisagno Valley 42
Genoa, Polcevera Valley 42
Genoa, Portofranco 50
Genoa, San Silvestro 37, 86
Genova, Oppidum del colle di Castello 37, 86, 221, 223
Genova, Val Brevenna 86
Gerlingen - Obere Gerteisen 35
Germany 14, 29, 30, 35, 36, 50, 77, 79, 81, 82, 101-103
Germersheim district 35
Gerona - Emporion 24
Gironde estuary 38
Giubiasco 50
Golasecca 9, 14, 24, 27, 34-36, 45, 48-61, 64, 66, 74, 80-82, 85-87, 90, 96, 97, 101, 102, 107, 109, 119, 124, 170, 175, 177, 192, 201, 219-221, 224, 225
Golasecca, Galliasco 119
Gorduno 61
Gracarca 88
Gräfenhainichen 35
Graubünden 48, 50
Gravisca 30, 40, 45, 97, 223
Greece 21, 22, 30
Gremiasco, Guardamonte 51
Gropello Cairoli, Santo Spirito 48, 61, 66, 85, 220
Gros Ped 37
Grotta dei Piccioni di Bolognano 28
Grotta del Frate 29
Grotta della Matta 29
Grotta della Tartaruga 29
Grotte de Bringairet 29
Grotte de La Lioure 38
Grotte de la Treille 29
Grotte de Sargen en Rouergue 39
Guardamonte di Gremiasco 51
Gudo 61
Gulf of Lion 50, 51, 97
Gulf of Naples 25, 41
Gurina 88
Hadrumentum - Sousse 31
Hagia-Triada 30
Hallein 36
Hallstatt 30, 35, 48, 54, 56, 79, 88, 90, 123, 193
Hänichen 14, 35
Hawaii 43
Herakleia - Policoro 33
Hochdorf, Eberdingen 35
Hungary 29, 37
Hyères Islands 21, 40, 97
Ibiza 32
Îles d›Or, Hyères Islands 21, 40, 97
India 27, 41
Indian Ocean 41
Ionian Islands 21
Ionian Sea 22
Island of Sainte-Marguerite 39
Isontine valleys 54
Istria 37
Italy 9, 13, 14, 22, 24, 28, 30, 32, 34, 35, 37, 40-42, 45, 46, 48, 50, 52, 55, 56, 58, 61, 64, 72, 76-82, 87, 90-92, 96, 97, 100, 107-110, 116, 120, 170, 219, 220, 221, 223
Japan 43
Jászladány 29
Jász-Nagykun-Szolnok 29
Jura 37
Kaltbrunn 29, 87
Kleinkorbetha 35
Krummäcker - Weingarten 35
La Alcudia del Elche 32, 42
La Balme-les-Grottes 27
La Calle, Marsacarès-La Calle - Marsa al-Kharaz 41, 42
La Heuneburg, Herbertingen-Hundersingen 35, 87
La Serreta 27
Lago superiore di Mantova 61, 90
Lagos 21
Laigueglia 43
Lake Como 48
Lake Constance 29
Lake Maggiore 48, 50
Lama Giotta 29
Langenau 35
Languedoc - Linguadoca 27, 35, 38, 39, 45, 97
La-Rivière-Drugeon 77
Lattes 39
Lavello 33, 34
Lazio 43
Le Marduel 38, 39
Lecco 48
Leimbach 35
Les Gardies, Pignan - Oppidum des Gardies 39
Libya 21, 31
Liguria 9, 21, 27, 29, 38, 45, 50, 51, 54, 58, 64, 86, 90, 96, 97
Liguria Interna 45, 48, 50-52, 61, 64, 86, 96, 102, 175, 177, 192, 219, 220

Ligurian Gulf 41
Ligurian Sea 22, 37, 97
Lilybeo - Marsala 32
Livorno 43
Loire basin 38
Loire department 35
Lombardy 48, 49, 92
Longone al Segrino 59
Lora 28
Lower Rhine department 35
Ludwigsburg district 35
Magdalenenberg 87
Maghreb 21, 27, 41
Mailhac 29, 37, 38
Majorca 32
Mallia 30
Malpensa 48
Malta 17, 22, 31, 223
Malta, Tas Silg 17, 22, 223
Mantua, piazza Santa Barbara 90
Mantua 36, 37, 52, 90
Marduel 38, 39
Marmara Sea 29
Marsa al-Kharaz - Marsacarès-La Calle 41, 42
Marsacarès-La Calle - Marsa al-Kharaz 41, 42
Marsala - Lilybeo 32, 42
Marseille 21, 35, 37, 38, 39, 41-43, 51, 223
Marseille, Butte Saint-Laurent 37
Marseille, La Tourette 37
Marseille, place Jules Verne 37
Marseille, Tunnel de la Major 38
Martigues 39
Marzabotto 52, 54, 61, 90, 92
Massalia - Marseille 38
Mechel 61, 77, 88, 92
Mediolanum - Milan 48, 52
Mediterranean Sea 9, 18, 21, 22, 29, 30, 41, 55, 104, 223
Megara Hyblaea 30
Mel 52, 54, 64, 109
Melfi 34
Memphis 30
Mesolcina Valley 48, 49, 61
Metaponto 33
Metapontum - Metaponto 34
Milan 48, 49, 51
Milano, Museo Civico Archeologico Castello Sforzesco 114
Minusio 50, 61
Modena 56
Modenese 56, 92
Moesa valley 50
Mondovì, Breolungi 51, 81
Mont Lassois 35
Monte Arci 28
Monte Cavanero, Chiusa Pesio 51
Monte Ceneri 48, 49
Montebello Vicentino 92
Montebelluna 52, 54, 61, 109, 135, 221
Montebelluna, Posmon 135
Montecastagneto 54
Montecastello 51
Monterenzio, Monte Bibele 90
Monte Valestra 54
Montfo 38
Montlaurès 33, 38, 39
Morgongiori 28
Morocco 21, 42, 104
Most na Soci, Santa Lucia di Tolmino 53, 61, 72, 77, 88, 89, 101
Motto Lagone 135, 207, 224
Mozia 32
Naples 40-43, 97, 223
Naples, Sellaria road 43
Naucratis 30
Nébéchen 30
Nebringen necropolis 36
Neuchâtel 29
Nile 30, 41
Nonantola 56
Nora 32
Nordhouse 87
North Africa 43, 223
Novara 95, 201
Novarese 49, 94
Nubia 31, 41
Obere Gerteisen - Gerlingen 35
Olbia 35
Olius 27
Oppeano 61, 85
Ordona 24, 34
Oria 32, 223
Ospedaletto Euganeo 74
Pacific Ocean 43
Padova, CUS-Piovego 77, 82, 85, 170
Padova, vicolo San Massimo 82
Padua, Padova 52, 54, 61, 64, 77, 82, 109, 170, 221
Paestum 30, 32, 34
Palencia 28
Palestro 61, 66
Palugana, Ospedaletto Euganeo 74
Panaro River-Valley 54, 56
Pantanello necropolis 33, 34
Paramo del Las Tuerces 28
Parma 56
Parre di Sotto 80, 169, 188
Pavese 51, 61
Pavia 48, 66

Pazzallo 50
Peloponnese 30
Penon de la Gomera 42
Perachora 30
Persian Gulf 40, 41
Peveragno, Castelvecchio 51
Philippines 43
Phoenicia 30-32, 193
Piacentino 45, 90, 96
Piacenza 56, 66
Pianello V.T. 54, 82, 90, 220
Piave valley 52-54, 109
Piedmont 9, 48-52, 56, 86, 90, 94, 97, 102, 113, 164
Pieve d'Alpago, Pian della Gnela 82, 102
Pignan, Oppidum des Gardies 39
Pisa 50
Plan de la Tour 39
Pocapaglia 51
Polcevera Valley 42
Po River 34, 48, 50, 97
Policoro - Herakleia 33
Policoro, Via Avellino 33
Pollera Cave 29
Pombia 61, 170
Pompei 32
Ponte nelle Alpi, Casan 88
Ponte nelle Alpi, Cugnan 61
Pontecagnano 33
Pontecurone 86
Pontòs 39
Ponza 42
Poříčany 35
Port Conthy 29
Portmàn 42
Portofino 41
Portugal 21, 42, 104
Porza 50
Pregassona 50
Provence 22, 25, 35, 38-43, 97, 223
Pully Chamblandes 27
Punta Giglio 29
Pyrenees 35
Rapallo 37
Rasun 88
Red Sea - Mar Rosso 27, 29, 40, 41
Reggiano 56, 61, 90
Rhodes 30
Rhone 27, 38
Roma, Museo delle Civiltà, Museo Pigorini 32
Rome 32
Rottofreno 64, 90
Rubiera 56
Ruvo 34
Safforze 61
Saint Léonard, Carrière 27
Saint Vincent, Gaujac 39
Saint-Blaise 37, 38
Saint-Brès 39
Saint-Pierre-Les-Martigues 39
Saint-Raphael 41
Saint-Rome-de-Cernon 39
Salins-les-bains, Champ de Chateau 77
Salses, Le Port 39
Samos 30
San Bernardino di Briona 82, 170, 177
San Pietro island 42
San Polo d'Enza 61, 64, 82, 90, 220
San Tomio di Malo 92
San Vito lo Capo 42
Santa Lucia, Tolmino 53, 61, 72, 77
Santa Margherita Ligure 43
Sant'Angelo di Statte 28
Sant'Antioco island 42
Sant'Arcangelo 33
Sant'Ilario d'Enza, Bettolino 64
Santo Spirito, Gropello Cairoli 48, 61, 66, 85, 220
Santorso 92
Sanzeno 53
Saône department 35, 77
Saône valley 38
Samoggia River 56
Sardinia 21, 28, 29, 31, 32, 41-43, 223
Sava valley 37
Savoy 27
Schussenried 29
Sciacca 21, 43
Scrivia River-Valley 38, 49, 51, 52, 221
Secchia River-Valley 56
Serio River 48
Serravalle Scrivia 51
Servirola 56
Sesto Calende 48, 59, 60, 61, 85, 220
Sesto Calende, Gajaccio 85
Sesto Calende, Mulini Bellaria 60
Seuil des Chèvres cave 27
Sicilian Channel 20, 22
Sicilian Sea 40, 223
Sicily 21, 30-32, 41, 42
Singen 82, 87
Slovenia 53, 54, 61, 64, 77, 81, 82, 85, 87-89, 101
Soča region 53
Somma Lombardo 48
Sopraceneri, Alta Val Mesolcina 48, 61
Sottoceneri 50
Sousse - Hadrumentum 31
Spain 21, 27, 28, 32
Spina 37, 54
Sri Lanka 41

Stenico, Calferi 61
Stična 61
Stoechadae Islands, Hyères Islands 40
Strait of Gibraltar 21, 22, 42
Strait of Sicily 21
Susa Valley 94
Swiss plateau 50, 92
Switzerland 27, 29, 35, 50, 61, 64, 66, 82, 92, 196
Syracuse 40, 42, 223
Tabarka 42
Tanaro River 50, 51
Taranto 28, 33
Taranto, contrada Madre Grazia 33
Taranto, contrada Tesoro 33
Taranto, via di Palma 33
Tarquinia 30, 97
Teano 32, 34
Tharros 32
Ticino Valley 50
Torre del Greco 43
Tortona 49, 51
Toscana 45
Trapani 27, 40-43, 97, 223
Trentino Alto Adige 53, 54, 61, 92-94
Trieste karst 77
Tunisia 21, 31, 40
Turin 9, 14, 113, 116, 122
Turin, Musei Reali, Museo di Antichità di Torino 33, 59, 107
Turkey 29
Tyrrhenian Sea-coast 21, 22, 38, 50, 52, 104
Ullastret 39
Upper Isonzo 53
Vaccareccia necropolis 32
Vače 61
Valais 27, 50
Valbrevenna 61, 86
Val de Loire 37
Valdieri 51
Valsassina 48
Valtellina 48
Var department 39, 40
Varese 201
Varese, Villa Mirabello Civic Museums, Museo Civico Villa Mirabello 59
Variglie-Revigliasco 51
Vaucluse 39
Vaud 27
Veio 32
Velia 30, 223
Veneto 52-56, 78, 82, 88
Venice 43
Vera 42
Verona 52-54
Verretto 61
Verucchio 54, 55, 61, 90
Verucchio, Pozzo di Pian del Monte 90
Vho di Piadena 92
Vicentino 92
Vicenza 52-54
Villa del Foro 51, 61, 64, 72, 80, 86, 102, 119, 220
Villar Dora 94
Villaricos 32
Vix 35
Vukovar 37
Weingarten - Krummäcker 35
Zvoleněves 35

References

Acker J.G., Byrne R.H., Ben-Yaakov S., Feely R.A., Betzer P.R. 1987. The effect of pressure on aragonite dissolution rates in seawater. *Geochimica et Cosmochimica Acta* 51, pp. 2171-2175. https://doi.org/10.1016/0016-7037(87)90266-3

Adam A.M. 1996. *Le fibule di tipo celtico nel Trentino*, Patrimonio storico e artistico del Trentino 19. Trento.

Adam A.M. 1997. Gli ornamenti dell'età del Ferro in area alpina. In Endrizzi, Marzatico 1997, pp. 177-184.

Alfonsi A. 1922. Este. Scoperte archeologiche nella necropoli atestina del nord riconosciuta nel fondo Rebato. *Notizie degli Scavi di Antichità. Atti della R. Accademia dei Lincei. Memorie della Classe di scienze morali, storiche e filologiche* (1922) fasc. 1, pp. 1-54.

Amos F.F., Destine E., Ponce C.B., Evans J.S. 2010. The N-and C-terminal regions of the pearl-associated EF hand protein, PFMG1, promote the formation of the aragonite polymorph in vitro. *Crystal growth & design* 10, pp. 4211-4216. https://doi.org/10.1021/cg100363m

Angelini I., Molin G., Artioli G. 2009. L'atelier metallurgico di Monte Cavanero. Indagini chimiche e metallografiche. In Venturino Gambari 2009, pp. 107-166.

Angelini I., Molin G. 2015. Gli intarsi delle fibule e dei pendenti natura dei materiali. In Gangemi, Bassetti, Voltolini 2015, pp. 52-53.

Angiolillo M., Giusti M., Rossi L., Tunesi L. 2022. A *Dendrophyllia ramea* Population in the Ionian Sea (Central Mediterranean Sea) Threatened by Anthropogenic Impacts. *Frontiers in Marine Science* 9, *Deep-Sea Environments and Ecology*, pp. 25-32.

Angiolillo M., Bo M., Toma M., Giusti M., Salvati E., Giova A., Lagudi A., Rossi L., Collina M., Bruno F. 2023. A baseline for the monitoring of Mediterranean upper bathyal biogenic reefs within the marine strategy framework directive objectives. *Deep Sea Research Part I: Oceanographic Research Papers* 194: 103963.

Apollonia L., Volpin S. 1999. *Le analisi di laboratorio applicate ai beni artistici policromi*, I Talenti. Padova.

Archeologia a Genova 1977. Genova.

Artioli G., Angelini I., Giunti I., Omenetto P., Villa I. 2009. La provenienza del metallo degli oggetti di Monte Cavanero: considerazioni basate sugli isotopi del Pb e sulla geochimica delle mineralizzazioni cuprifere limitrofe. In Venturino Gambari 2009, pp. 167-178.

Artioli G., Fontanari A., Angelini I., Lucarelli C., Etter M., Jeppesen H.S., Shilstein S., Shalev S. 2024. The tin content of lead inclusions in ancient tin-bronze artifacts: a time-dependent process? *Applied Crystallography* 57, pp. 700-706.

Asnavandi M., Ghorbani M., Kahram M. 2013. Production of Cu–Sn–graphite–SiC composite coatings by electrodeposition. *Surface and Coatings Technology* 216, pp. 207-214. https://doi.org/10.1016/j.surfcoat.2012.11.042

Augier, L., Buchsenschutz, O., Durand, R., Filippini, A., Germinet, D., Maçon, P., Pauly, S., Pescher, B., Ralston, I.B.M., Roure, R., Salin, M., Tichit, A., Vannière, B., 2012. *Un complexe princier à l'âge du Fer: Le quartier artisanal de Port Sec Sud à Bourges (Cher).* Supplément à la Revue archéologique du centre de la France, 41. Tours.

Aurelle D., Ledoux J.-B., Rocher C., Borsa P., Chenuil A., Feral J.-P. 2011. Phylogeography of the red coral (*Corallium rubrum*): inferences on the evolutionary history of a temperate gorgonian. *Genetica* 139, pp. 855-869. https://doi.org/10.1007/s10709-011-9589-6

Aurino P. 2014. Preistoria e protostoria nel territorio astigiano. In Venturino Gambari 2014, pp. 19-32.

Bagnasco Gianni G. 1988. Contributo allo studio sulla periodizzazione della cultura di Golasecca: il momento di transizione tra le fasi IC e IIA. *Quaderni della Soprintendenza Archeologica del Piemonte* 7, pp. 13-33.

Bajnóczi B., Schöll-Barna G., Kalicz N., Siklósi Z., Hourmouziadis G.H., Ifantidis F., Kyparissi-Apostolika A., Pappa M., Veropoulidou R., Ziota C. 2013. Tracing the source of Late Neolithic Spondylus shell ornaments by stable isotope geochemistry and

cathodoluminescence microscopy. *Journal of Archaeological Science* 40, pp. 874-882. https://doi.org/10.1016/j.jas.2012.09.022

Baratti G. 2014. Lo scavo dell'Università degli Studi di Milano al castelliere del Guardamonte. In Maggi, Gorrini 2014, pp. 47-57.

Barbieri E. 2014. *Castelletto Ticino (NO). Analisi di contesti funerari golasecchiani di VII e VI secolo a.C. tra le vie Cosio, Ramacci, Aronco e Caduti per la Libertà*. Tesi di Laurea. Università degli Studi di Milano.

Barbieri E. 2019. Pendagli a secchiello golasecchiani in un contesto di abitato etrusco-padano. *LANX. Rivista della Scuola di Specializzazione in Archeologia-Università degli Studi di Milano* 27, pp. 38-62.

Barbieri E. 2023. Analisi della collezione Bellini e dei suoi reperti. *Zixu. Studi sulla cultura celtica di Golasecca* 5, pp. 13-96.

Barbin V. 2013. Application of cathodoluminescence microscopy to recent and past biological materials: a decade of progress. *Mineralogy and Petrology* 107, pp. 353-362.

Barbin V. Schvoerer, M., 1997. Cathodoluminescence géosciences. *Comptes Rendus de l'Académie des Sciences-Series IIA-Earth and Planetary Science* 325, pp. 157-169.

Barelli V. 1877. Villaggio preromano di Rondineto. *Rivista Archeologica della Provincia di Como* 11, pp. 1-32.

Barelli V. 1879. Nuove scoperte in Rondineto, comune di Breccia, dal luglio 1877 in poi. *Rivista Archeologica della Provincia di Como* 13, pp. 2-27.

Barnabei F. 1896. Tomba preromana nella necropoli settentrionale atestina. *Notizie degli Scavi di Antichità. Atti della R. Accademia dei Lincei. Memorie della Classe di scienze morali, storiche e filologiche*, Serie 5, Annata 293, Volume 4, p. 357.

Barnard W., de Waal D. 2006. Raman investigation of pigmentary molecules in the molluscan biogenic matrix. *Journal of Raman Spectroscopy* 37, pp. 342-352. https://doi.org/10.1002/jrs.1461

Barocelli P. 1926. Sepolcreti novaresi della prima età del ferro. *Bullettino di Paletnologia Italiana* I, pp. 175-194.

Barral Ph., Guillaumet J.P., Rouillère-Lambert M.J., Saracino M., Vitali D. (dir.) 2014. *Les Celtes et le nord de l'Italie. Premier et second âges du Fer*. Actes du XXXVIe colloque international de l'A.F.E.A.F. (Vérone, 17-20 Mai 2012). Dijon.

Baserga G. 1907. Necropoli preromana di Albate. *Rivista Archeologica dell'antica Provincia e Diocesi di Como*, pp. 83-100.

Baserga G. 1910. Nuove scoperte nella necropoli preromana di Albate, *Rivista Archeologica dell'Antica Provincia e Diocesi di Como*, pp. 7-46.

Baserga G. 1925. La necropoli della Ca Morta e la sua civiltà preistorica. *Rivista Archeologica dell'antica Provincia e Diocesi di Como*, pp. 39-63.

Baserga G. 1927. Altre importanti scoperte preistoriche alla Ca Morta. *Rivista Archeologica dell'antica Provincia e Diocesi di Como*, pp. 46-59.

Baserga G. 1929. Tomba con carro ed altre scoperte alla Ca Morta. *Rivista Archeologica dell'antica Provincia e Diocesi di Como*, pp. 25-44.

Bedini E., Petiti E. 2015. Primo tentativo di interpretazione sistematica dei rituali di cremazione in Piemonte tra la medio-tarda età del Bronzo e l'età del Ferro. In von Eles P., Bentini L., Poli P., Rodriguez E. (a cura di), *Immagini di uomini e di donne dalle necropoli villanoviane di Verucchio*. Atti delle Giornate di Studio dedicate a Renato Peroni. Quaderni di Archeologia dell'Emilia Romagna 34, pp. 180-186.

Belcher A.M., Wu X.H., Christensen R.J., Hansma P.K., Stucky G.D., Morse D.E. 1996. Control of crystal phase switching and orientation by soluble mollusc-shell proteins. *Nature* 381, pp. 56-58. https://doi.org/10.1038/381056a0

Bente K., Berthold C., Schrickel M., Wendling H., Ende M. 2014. White coral beads of La Tène and Hallstatt age: original color or decolorated material? *92nd Annual Meeting of the Deutsche Mineralogische Geselchaft* (DMG).Jena, 81.

Bente K., Berthold C., Dolz S., Keuper M., Gerdes A. 2015a. Archäometrische Charakterisierung von rotem Schmuckdekor historischer Ethnographica aus dem Königreich Benin (Nigeria), Tunesien und Algerien. In Gluhak T., Greiff S., Kraus K., Prange M. (Hrsg.), *Archäometrie und Denkmalpflege*. Jahrestagung (Mainz 25-28

märz 2015). Metalla Sonderheft 7. Bochum, pp. 129-130.

Bente K., Berthold C., Wirth R., Schreiber A., Keuper M. 2015b. Microstructural and chemical mechanisms of the transformation of red (*Corallium rubrum*) to white corals. doi.org/10.2312/GFZ.LIS.2015.003 84

Bente K., Koenig A., Dehn F., Krüger P., Wirth R., Hirsch D., Münster T., Berthold C. 2015c. Vergleichende computertomografische und elektronenmikroskopische Studien zu eisenzeitlicher Korallenzier. In Gluhak T., Greiff S., Kraus K., Prange M. (Hrsg.), *Archäometrie und Denkmalpflege.* Jahrestagung (Mainz 25-28 märz 2015). Metalla Sonderheft 7. Bochum, pp. 59-61.

Bente K., Berthold C., Keuper M., Wirth R. 2016. *Colour of Latène and Hallstatt period fibulae beads*.

Bente K., Berthold C., Keuper M., Gerdes A., Ansorge J., König A. 2017. Die Korallenperlenkette aus Greifswald von um 1300 – archäometrische Untersuchungen an *Corallium rubrum* aus einer mittelalterlichen Hansestadt. *Archäologische Berichte aus Mecklenburg-Vorpommern* 24, pp. 69-79.

Bente K., Berthold C. 2018. Chaine operatoire: a link between archaeology and archaeometry. In Archäometrie Und Denkmalpflege 2018: Proceedings, Jahrestagung, Kurzfassung Der Vorträge Und Poster (Hamburg, B.R. Deutschland, 20.-24. März 2018). https://doi.org/10.3204/DESY-PROC-2018-01

Bente K., Berthold C., Rauchfuß B., Wirth R., Schreiber A., Hölzig H., Panneerselvam R., Keilholz S., Poppitz D., König A. 2020. Construction and Material signatures of the Prezeworsk fibula from Leimbach (Nordhausen County, Central Germany). In Gori M. (ed.), *Resources and transformation in pre-modern societies*. International Conference (Bochum 19–21 November 2020, 11 December 2020, 15 January 2021). Metalla Sonderheft 10. Bochum. https://doi.org/10.46586/metalla.v.2020.i10

Bente K., Berthold C., Wirth R., Schreiber A., König A. 2022. Multi-methodological characterisation of medieval to early modern coral beads from a cesspit of the 'fronerei auf dem schrangen' in Lübeck (Germany). *Metalla* 26, 1, pp. 25-36. https://doi.org/10.46586/metalla.v26.2022.i1.25-36

Bente K., Berthold C., Kupka T., Beirau T., Wrzalik R., Wirth R., Schreiber A., Hölzig H., Keilholz S., Günther A., Gerdes A., König A. 2023. Explaining white/grey Iron Age coral decorations: experimental studies on *Corallium rubrum.* In Klein S., Berthold C., Berger D., Pernicka E. (Hrsg.), Jahrestagung Archäometrie und Denkmalpflege (Reiss-Engelhorn-Museen, Mannheim 28 März - 01 April 2023). Metalla Sonderheft 12. Bochum, pp. 127-129. https://doi.org/10.46586/metalla.v.2023.i12

Bentini L., von Eles P., Giumlia-Mair A., Naso A., Negrini C., Poli P., Rodriguez E., Tomedi G. 2020. Verucchio tra Mediterraneo ed Europa: circolazione di materie prime, prodotti artigianali, persone. *Rivista di Scienze Preistoriche* LXX, S1, pp. 389-399.

Bergamonti L., Bersani D., Csermely D., Lottici P.P. 2011. The nature of the pigments in corals and pearls: a contribution from Raman spectroscopy. *Spectroscopy Letters* 44, pp. 453-458. https://doi.org/10.1080/00387010.2011.610399

Bergamonti L., Bersani D., Mantovan S., Lottici P.P. 2013. Micro-Raman investigation of pigments and carbonate phases in corals and molluscan shells. *European Journal of Mineralogy* 25, pp. 845-853. https://doi.org/10.1127/0935-1221/2013/0025-2318

Berruto G. 2023. Analisi archeometriche sulla fibula a sanguisuga con inserti circolari della collezione Bellini. *Zixu. Studi sulla cultura celtica di Golasecca* 5, pp. 97-102.

Berruto G. 2025. *Technology and trade in the Early Iron Age between Europe and Mediterranean: archaeometric investigation on metal ornaments decorations.* Tesi di dottorato (XXXVI ciclo) Università di Torino.

Berruto G., Ruffa M. 2022. Il corredo di una tomba dal Galliasco di Golasecca e studio archeometrico di una fibula a sanguisuga con intarsi. *Sibrium* 36, pp. 270-291.

Berruto G., Diana E., Giustetto R. 2014. Studio archeometrico di decorazioni campite in pasta bianca su reperti preistorici e protostorici. In Venturino Gambari 2014, pp. 237-254.

Berruto G., Diana E., Giustetto, R. Venturino M. 2018. Sea treasures and ancient trade: archaeometrical investigation on Iron Age bronze fibulae with inserts. In *Venticinque Anni Di AIAr*. Abstract Book (X Congresso

Nazionale AIAr, Torino 14-17 febbraio 2018), C&D-O3.

Berruto G., Diana E., Giustetto R. 2021. Tesori del mare nella tecnologia antica: indagine archeometrica sulle fibule in bronzo con inserti in corallo. In Venturino, Giaretti 2021, pp. 551-560.

Berruto G., Costa E., Curetti N., Diana E. Giustetto R. 2023a. Archaeometric investigation of bronze Iron Age fibulae with nestled coral insets from three archaeological sites of the Piedmont region (Northwestern Italy). *Journal of Archaeological Science: Reports* 51, 104119, pp. 1-14.

Berruto G., Diana E., Giustetto R., Venturino M. 2023b. Analisi archeometriche su decorazioni campite di manufatti metallici golasecchiani: risultati preliminari. In Caramella L.A.R. (a cura di), *Dall'acqua alla terra: cambiamenti nell'occupazione del territorio*. Atti delle giornate di studi (Varese, 20 novembre - Golasecca, 21 novembre 2021), *Sibrium Atti* 1, pp. 210-227.

Berruto G., Giaretti M., Venturino M. *in press*. Brignano Frascata. Analisi archeometriche su fibule in bronzo della media età del Ferro. *Quaderni di Archeologia del Piemonte* 8.

Bertolone M. 1953. Ancora sulla II tomba di guerriero a Sesto Calende. *Sibrium* I, pp. 67-72.

Bertolone M. 1956. Tombe protostoriche a Rebbio (Como). In *Studi in Onore di Aristide Calderini e Roberto Paribeni* 3. Milano, pp. 103-114.

Bianco S. 2006. Conchiglie e corallo nella Basilicata antica. In *Coralli segreti* 2006, pp. 98-133.

Bietti Sestieri A.M. 2015. *L'Italia nell'età del Bronzo e del Ferro. Dalle palafitte a Romolo (2200-700 a.C.)*. Roma.

Bietti Sestieri A.M., Bellintani P., Salzani L., Angelini I., Chiaffoni B. 2015. Frattesina: un centro internazionale di produzione e di scambio nell'età del bronzo del Veneto. In Leonardi G., Tinè V. (a cura di), *Preistoria e protostoria del Veneto*. Studi di preistoria e protostoria 2. Padova, pp. 427-436.

Bietti Sestieri A.M., Bellintani P., Giadino C. 2019. *Frattesina: un centro internazionale di produzione e di scambio nella tarda età del Bronzo del Veneto*. Accademia Nazionale dei Lincei, Memorie della Classe di Scienze Morali Storiche e Filologiche, serie 9, volume 39, fascicolo 1. Roma.

Bischoff W.D., Sharma S.K., MacKenzie F.T. 1985. Carbonate ion disorder in synthetic and biogenic magnesian calcites: a Raman spectral study. *American Mineralogist* 70, pp. 581-589.

Bocchio G., Salzani L. 1973. I materiali preistorici e protostorici del Colle di S.Martino (Gavardo). *Annali del Museo. Notiziario di preistoria e archeologia* 11, pp. 37-60.

Bonacelli B. 1934. Gli elementi della civiltà pregallica nel Comasco. *Studi Etruschi* VIII, pp. 319-325.

Borrello M. 2001. Vous avez dit 'corail'? *Annuaire de la Société Suisse de Préhistoire et d'Archéologie* 84, pp. 191-196.

Borrello M.A., Micheli R. 2004. *Spondylus gaederopus*, gioiello dell'Europa preistorica. *Preistoria Alpina* 40, pp. 71-82.

Borrello M.A., Micheli R. 2011. *Spondylus gaederopus* in prehistoric Italy: jewels from neolithic and copper age sites. In Ifantidis, Nikolaidou 2011, pp. 25-37.

Borrello M., Bosch J., Mazzorin J., Martín A., Esteve X., Gorgoglione M., Mariéthoz F., Nadal J., Oms F.X. 2012. Les parures néolithiques en corail (*Corallium rubrum* L.) d'Europe occidentale. *Rivista di Scienze Preistoriche* LXII, pp. 67-82.

Borromeo L., Zimmermann U., Andò S., Coletti G., Bersani D., Basso D., Gentile P., Schulz B., Garzanti E. 2017. Raman spectroscopy as a tool for magnesium estimation in Mg-calcite. *Journal of Raman Spectroscopy* 48, pp. 983-992. https://doi.org/10.1002/jrs.5156

Brambilla L., Tommasini M., Zerbi G., Stradi R. 2012. Raman spectroscopy of polyconjugated molecules with electronic and mechanical confinement: the spectrum of *Corallium rubrum*. *Journal of Raman Spectroscopy* 43, pp. 1449-1458. https://doi.org/DOI 10.1002/jrs.4057

Bresc H. 2000. Peche et commerce du corail en Méditerranéede l'Antiquité au Moyen Age. In Morel *et al.* 2000, pp. 41-54.

Budd D.A. 1988. Aragonite-to-calcite transformation during fresh-water diagenesis of carbonates: Insights from pore-water chemistry. *Geological Society of America Bulletin* 100, pp. 1260-1270.

Busenberg E., Plummer L.N. 1985. Kinetic and thermodynamic factors controlling the distribution of SO32- and Na+ in calcites and selected aragonites. *Geochimica et Cosmochimica Acta* 49, pp. 713-725.

Buson S., Baldini C. 2003. Caratteristiche tecnologiche delle fibule a sanguisuga e a navicella di Este. In Formigli E. (a cura di), *Fibulae dall'età del Bronzo all'alto medioevo*. Firenze, pp. 125-139.

Butti Ronchetti F. 2012. Sulle tracce dei Comenses nell'incontro con i Romani. *Rivista Archeologica dell'antica Provincia e Diocesi di Como* 191-192, pp. 7-52.

Campi L. 1885. Il Sepolcreto di Meclo nella Naunia. *Archivio Trentino* IV, pp. 61-112.

Campi L. 1889. Scavi e scoperte fatte negli anni 1885-1886 nello stabile a Valemporga di Meclo. *Archivio Trentino* VIII, pp. 209-261.

Campi L. 1897. Uso del corallo in età preromane. *Bullettino di Paletnologia Italiana* 23, pp. 15-18.

Camporeale G. 2006. *Gli Etruschi in Provenza e il Linguadoca*. In Gori S. (a cura di), *Etruschi da Genova ad Ampurias. Atti del XXIV Convegno di Studi Etruschi ed Italici*, (Marseille-Lattes, 26 settembre-1 ottobre 2002). Pisa-Roma, pp. 1000-1008.

Cardani Vergani R., Mangani C., Voltolini D. 2011. Necropoli di Solduno (Locarno, TI): scavi UBC 1995-2002. *Annuario di archeologia svizzera* 94, pp. 61-102.

Cartier L.E., Krzemnicki M.S., Lendvay B., Meyer J.B. 2018. DNA Fingerprinting of Pearls, Corals and Ivory: A Brief Review of Applications in Gemmology. *Journal of Gemmology* 36 (2), pp. 152- 160.

Casanova E., Pelé-Meziani C., Guilminot É., Mevellec J.-Y., Riquier-Bouclet C., Vinçotte A., Lemoine G. 2016. The use of vibrational spectroscopy techniques as a tool for the discrimination and identification of the natural and synthetic organic compounds used in conservation. *Analytical Methods* 8, pp. 8514-8527. https://doi.org/10.1039/C6AY02645A

Casini S. 2000a. Ritrovamenti ottocenteschi di sepolture della cultura di Golasecca nel territorio bergamasco. *Notizie Archeologiche Bergomensi* 6, pp. 109-154.

Casini S. 2000b. Il ruolo delle donne golasecchiane nei commerci del VI-V secolo a.C. In de Marinis, Biaggio Simona 2000, pp. 75-100.

Casini S. 2011. La pratica dell'esogamia nella cultura di Golasecca. In Marchesini S. (a cura di), *Matrimoni Misti: una via per l'integrazione tra i popoli*. Atti del Convegno (Verona - Trento 1-2 dicembre 2011). Verona, pp. 65-78.

Casini S. 2014. La necropoli golasecchiana di Brembate Sotto. Revisione dei vecchi dati. In Barral *et al.* 2014, pp. 387-392.

Casini S. 2017. La necropoli golasecchiana di Brembate Sotto (Bergamo). *Notizie Archeologiche Bergomensi* 15 (2007), pp. 9-173.

Casini S. 2022. I principali insediamenti della cultura di Golasecca: un quadro d'insieme. In de Marinis R.C., Rapi M. (a cura di), *Preistoria e Protostoria in Lombardia e Canton Ticino*. Numero speciale, *Rivista di scienze preistoriche* LXXII (S2), pp. 531-562.

Casini S., de Marinis R.C., Rapi M. 2001. L'abitato protostorico di Como. In *La protostoria in Lombardia*. Atti del 3° convegno archeologico regionale (Como 22-24 ottobre 1999), Como, pp. 97-140.

Casini S., Chaume B. 2014. Indices de mobilité au Premier âge du Fer entre le sud et le nord des Alpes. In Barral *et al.* 2014, pp. 231-250.

Castelfranco P. 1900. Corredo da toeletta di Rebbio (Como). *Bullettino di Paletnologia Italiana* 26, pp. 24-33.

Castiglioni E., Rottoli M. 2015. I materiali organici dalle sepolture: carboni dei roghi, le offerte alimentari, i tessuti e gli altri resti. In Gangemi, Bassetti, Voltolini 2015, pp. 219-234.

Catarsi M., Dall'Aglio P.L. 1987. Il territorio piacentino dall'età del bronzo alla Romanizzazione. Ipotesi sulla formazione dell'ethnos ligure. In Vitali 1987, pp. 405-414.

Cattaneo-Vietti R., Cicogna F. 1994. Il corallo rosso: una risorsa mediterranea. In Cicogna F., Cattaneo-Vietti R. (a cura di), *Il corallo rosso in Mediterraneo: arte, storia e scienza - red coral in the Mediterranea Sea: Art, history and science*. Roma, pp. 3-9.

Cerezer J.F. 2014. Ceramic technology: fragments of an experimental process. In Cura S., Cerezer J.F., Gurova M., Santander B., Oosterbeek L., Cristóvão J. (eds.), *Technology and Experimentation in Archaeology*.

Proceedings of the XVI World Congress of the International Union of Prehistoric and Protohistoric Sciences, BAR International Series, pp. 57-63.

Cerri R. 2011. Catalogo dei reperti e delle strutture. Via del Maneggio, scavi 2001-2003. In Gambari, Cerri 2011, pp. 83-158.

Chaabane S., Montagn P., López Corre M., Kallel N., Taviani M., Ziveri P. 2014. Skeletal architecture and geochemical investigation of the Mediterranean red coral *Corallium rubrum* from depth-contrasting populations. In *4ème Forum de l'eau : Ressources en eau : effets des changements climatiques et perspectives.*

Chaabane S., López Correa M., Montagna P., Kallel N., Taviani M., Linares C., Ziveri P. 2016. Exploring the oxygen and carbon isotopic composition of the Mediterranean red coral (*Corallium rubrum*) for seawater temperature reconstruction. *Marine Chemistry* 186, pp. 11-23. https://doi.org/10.1016/j.marchem.2016.07.001

Charalambous A., Kassianidou V., Papasavvas G. 2014. A compositional study of Cypriot bronzes dating to the Early Iron Age using portable X-ray fluorescence spectrometry (pXRF). *Journal of archaeological science* 46, pp. 205-216.

Charola A.E., Pühringer J., Steiger M. 2007. Gypsum: a review of its role in the deterioration of building materials. *Environmental Geology* 52, pp. 339-352. https://doi.org/10.1007/s00254-006-0566-9

Chaume B. 2001. *Vix et son territoire à l'âge du fer: fouilles du mont Lassois et environnement du site princier*. Mergoil.

Chazottes M.A. 2018. Approvisionnement, circulation, transformation et usage du corail en Provence occidentale (XIII-XVI siècles). *Rives méditerranéennes* 57, pp. 129-156. https://doi.org/10.4000/rives.5773

Chen S., Vahur S., Teearu A., Juus T., Zhilin M., Savchenko S., Oshibkina S., Asheichyk V., Vashanau A., Lychagina E., Kashina E., German K., Dubovtseva E., Kriiska A., Leito I., Oras E. 2022. Classification of archaeological adhesives from Eastern Europe and Urals by ATR-FT-IR spectroscopy and chemometric analysis. *Archaeometry* 64, pp. 227-244. https://doi.org/10.1111/arcm.12686

Cherici A. 1999. Amuleti nei corredi funebri paleoveneti e dell'Italia antica. In Paoletti O., Tamagno Perna L. (a cura di), *Protostoria e storia del 'venetorum angulus'*. Atti del XX convegno di studi etruschi ed italici (Portogruaro-Quarto d'Altino-Este-Adria, 16-19 Ottobre 1996). Pisa-Roma, pp. 169-216.

Chiaramonte Trerè C., Baratti G. 2016. L'insediamento d'altura del Guardamonte tra IV e III secolo a.C. Considerazioni a fronte dei recenti scavi. In Govi 2016, pp. 555-579.

Chieco Bianchi A.M. (a cura di) 1981, *Padova Preromana*. Catalogo della mostra (Padova 27 giugno - 15 novembre 1976). Padova.

Chieco Bianchi A.M. 1988. I Veneti. In *Italia omnium terrarum alumna. La civiltà dei Veneti, Reti, Liguri, Celti, Piceni, Umbri, Latini, Campani e Iapigi.* Milano, pp. 3-98.

Chieco Bianchi A.M., Calzavara L., De Min M., Tombolani M. 1976. *Proposta per una tipologia delle fibule di Este*. Biblioteca di Studi Etruschi 9. Firenze.

Chung S.N., Lee K., Feely R.A., Sabine C.L., Millero F.J., Wanninkhof R., Bullister J.L., Key R.M., Peng T.-H. 2003. Calcium carbonate budget in the Atlantic Ocean based on water column inorganic carbon chemistry. *Global Biogeochemical Cycles* 17, no. 4, 1093, pp. 1-16. doi: 10.1029/2002GB002001

Ciampoltrini G. 1993. Ricerche sugli insediamenti liguri dell'Alta Valle del Serchio. *Bollettino di Archeologia, Soprintendenza Archeologia Toscana* 19-20-21, pp. 39-70.

Cicogna F. 2000. Il corallo rosso del Mediterraneo (*Corallium rubrum*): pesca e legislazione per una corretta gestione della risorsa. In Morel *et al.* 2000, pp. 69-78.

Cicolani V. 2017. *Passeurs des Alpes. La culture de Golasecca entre Méditerranée et Europe continentale à l'âge du Fer*. Paris.

Cicolani V. 2021. Piccoli bronzi e metallurgia in lega di rame. In Venturino, Giaretti 2021, pp. 527-550.

Cicolani V., Berruto G. 2017. L'ornementation des fibules de Ligurie interne: approches typologiques et archéometriques pour l'étude des faciès d'Italie nord-occidentale. In Marion S., Deffressigne S., Kaurin J., Bataille G. (dir.), *Production et proto-industrialisation aux âges du Fer*, Actes du XXXIXe colloque international de l'A.F.E.A.F. (Nancy 13-17 mai 2015). Bordeaux, pp. 411-419.

Cicolani V., Gambari F.M. 2021. Des chefs guerriers aux seigneurs des terres et du commerce : les ”princes” de la zone occidentale de la culture de Golasecca entre VIIe et Ve s. a.C. In Brun P., Chaume B., Sacchetti F. (éd.), *Vix et le phénomène princier*, Actes du colloque de Châtillon (2016), Pessac, pp. 191-205. https://una-editions.fr/vix-et-le-phenomene-princier

Cicolani V., Huet T. 2019. Essai de modélisation des échanges et des réseaux de circulation dans les Alpes centrales au premier âge du Fer. In Deschamps M., Costamagno S., Milcent P.Y., Pétillon J.M., Renard C., Valdeyron N. (éd.), *La conquête de la montagne: des premières occupations humaines à l'anthropisation du milieu*. Paris, pp. 1-23. https://doi.org/10.4000/books.cths.7827

Cicolani V., Zamboni L. 2023. Alpine connections: Iron age mobility in the Po valley and the circum-alpine regions. In Fernández-Götz M., Nimura C., Stockhammer P.W., Cartwright R. (eds.), *Rethinking migrations in late prehistoric Eurasia.* Proceedings of the British Academy, 254. Oxford, pp. 258–279

Cicolani V., Huet T., Zamboni L. 2024. Modélisation des interactions en Italie du Nord au premier âge du Fer: de la circulation de parures aux réseaux d'influences culturelles. *Bulletin de la Société préhistorique française*, 121 (2), pp. 307-330.

Cizer Ö., Rodriguez-Navarro C., Ruiz-Agudo E., Elsen J., Van Gemert D., Van Balen K. 2012. Phase and morphology evolution of calcium carbonate precipitated by carbonation of hydrated lime. *Journal of Materials Science* 47, 16, pp. 6151-6165. https://doi.org/10.1007/s10853-012-6535-7

Claassen C., Sigmann S. 1993. Sourcing Busycon artifacts of the eastern United States. *American Antiquity* 58, pp. 333-347. https://doi.org/10.2307/281974

Colonna G. 1979. Scavi e scoperte. *Studi Etruschi*, serie III, volume XLVII, pp. 463-536.

Conradin E. 1978. Das spathallstattische Urnengraberfeld Tamins-Unterm Dorf in Grabunden. *Jahrbuch der Schweizerischen Gesellschaft für Ur- und Frühgeschichte* 61, pp. 65-156.

Coralli segreti 2006. *Coralli segreti. Immagini e miti dal mare tra Oriente ed Occidente*. Catalogo della mostra (Museo Archeologico Nazionale della Basilicata "Dinu Adamesteanu", Potenza 22 giugno - 30 ottobre 2006). Lavello.

Costantini F., Aurelle D., Ledoux J.-B., Abbiati M. 2016. Population genetic structure of *Corallium rubrum* in the Mediterranean Sea: diversity, phylogeography, and bathymetric patterns. In Goffredo S., Dubinsky Z. (eds), *The Cnidaria, past, present and future. The world of Medusa and her sisters*, pp. 717-728. https://doi.org/10.1007/978-3-319-31305-4

Costanza S. 2006. Lu bonu magisterio. Pesca e artigianato del corallo. In Ravazza 2006, pp. 33-42.

Courel B., Schaeffer P., Féliu C., Thomas Y., Adam P. 2018. Birch bark tar and jewellery: the case study of a necklace from the Iron Age (Eckwersheim, NE France). *Journal of Archaeological Science: Reports* 20, pp. 72-79. https://doi.org/10.1016/j.jasrep.2018.04.016

Courtois J.-C. 1968. La stratigraphie de Sainte-Colombe (Hautes-Alpes). *Bulletin de la Société préhistorique française* 65, pp. 154-160. https://doi.org/10.3406/bspf.1968.9008

Damiani I., Maggiani A., Pellegrini E., Saltini A.C., Serges A. 1992, *L'età del Ferro nel Reggiano. I materiali delle collezioni dei Civici Musei di Reggio Emilia*, Cataloghi dei Civici Musei 12. Reggio Emilia.

D'Arpa C., Di Patti C. 2006. I coralli, una storia lunga cinquecento milioni di anni. In *Coralli segreti* 2006, pp. 23-40.

Dauphin Y. 2006. Mineralizing matrices in the skeletal axes of two Corallium species (Alcyonacea). Comparative *Biochemistry and Physiology Part A: Molecular & Integrative Physiology* 145, pp. 54-64. https://doi.org/10.1016/j.cbpa.2006.04.029

D'Souza S.M., Alexander C., Carr S.W., Waller A.M., Whitcombe M.J., Vulfson E.N. 1999. Directed nucleation of calcite at a crystal-imprinted polymer surface. *Nature* 398, pp. 312-316. https://doi.org/10.1038/18636

Davis K.J., Dove P.M., De Yoreo J.J. 2000. The role of Mg2+ as an impurity in calcite growth. *Science* 290, pp. 1134-1137.

Debreuil J., Tambutté S., Zoccola D., Segonds N., Techer N., Marschal C., Allemand D., Kosuge S., Tambutté É. 2011. Specific organic matrix characteristics in skeletons of

Corallium species. *Marine Biology* 158, pp. 2765-2774.

Demarchi A., Ferrero L., Padovan S. 2007. Il Museo Civico di Palazzo Traversa a Bra: i reperti archeologici della Collezione di Don Giuseppe Tornatore. *Quaderni della Soprintendenza archeologica del Piemonte* 22, pp. 73-86.

Demarchi B., O'Connor S., de Lima Ponzoni A., de Almeida Rocha Ponzoni R., Sheridan A., Penkman K., Hancock Y., Wilson J. 2014. An Integrated Approach to the Taxonomic Identification of Prehistoric Shell Ornaments. *PLOS ONE* 9, e99839, pp. 1-12. https://doi.org/10.1371/journal.pone.0099839

Demarchi B., Boano R., Ceron A., Bello F.D., Favero-Longo S.E., Fiddyment S., Marochetti E.F., Mangiapane G., Mattonai M., Pennacini C., Ribechini E., Woolley J., Zilberstein G., Righetti P.G. 2020. Never boring: Non-invasive palaeoproteomics of mummified human skin. *Journal of Archaeological Science* 119, 105145, pp. 1-12. https://doi.org/10.1016/j.jas.2020.105145

de Marinis R.C. 1974. La situla di Trezzo (Milano). *Varia Archaeologica* I, pp. 67-85.

de Marinis R.C. 1981. Il periodo Golasecca III A in Lombardia. *Studi Archeologici* I, pp. 41-284.

de Marinis R.C. (a cura di) 1986. *Gli Etruschi a nord del Po*. Catalogo della mostra (Mantova, Palazzo Ducale, Galleria dell'Estivale, 21 settembre 1986 - 12 gennaio 1987). Mantova.

de Marinis R.C. 1986a. I commerci dell'Etruria con i paesi a nord del Po dal IX al VI secolo a.C. In de Marinis 1986, 1, pp. 52-80.

de Marinis R.C. 1986b. Fibule tardohallstattiane occidentali. In de Marinis 1986, 1, pp. 243-245.

de Marinis R.C. 1987. Fibule tardohallstattiane occidentali dell'abitato etrusco del Forcello (Bagnolo S. Vito). In Vitali 1987, pp. 89-99.

de Marinis R.C. 1988a. Le popolazioni alpine di stirpe retica. In *Italia omnium terrarum alumna. La civiltà dei Veneti, Reti, Liguri, Celti, Piceni, Umbri, Latini, Campani e Iapigi.* Milano, pp. 101-158.

de Marinis R.C. 1988b. Liguri e celto-liguri. In *Italia omnium terrarum alumna. La civiltà dei Veneti, Reti, Liguri, Celti, Piceni, Umbri, Latini, Campani e Iapigi.* Milano, pp. 159-262.

de Marinis R.C. 1991a. I Celti golasecchiani. In *I Celti.* Catalogo della mostra a Palazzo Grassi (Venezia). Milano, pp. 93-102.

de Marinis R.C. 1991b. La stratigrafia dell'abitato del Forcello di Bagnolo S. Vito e i rapporti cronologici con le culture dell'area circumalpina. *Archeologia Classica* 43, pp. 237-259.

de Marinis R.C. 1992. Tomba con situla bronzea dal Lazzaretto di Golasecca. *Sibrium* XXI (1990-1991), pp. 157-200.

de Marinis R.C. 1997. Il corallo nella Preistoria e Protostoria dell'Italia settentrionale. In Endrizzi, Marzatico 1997, pp. 153-160.

de Marinis R.C. 2000. Il corallo nella cultura di Golasecca. In Morel *et al.* 2000, pp. 159-175.

de Marinis R.C. 2007. Le relazioni degli etruschi del Forcello con i Veneti, Reti e Celti. In de Marinis R.C., Rapi M. (a cura di), *L'abitato etrusco del Forcello di Bagnolo S. Vito (Mantova): le fasi arcaiche*. Firenze, pp. 203-212.

de Marinis R.C. 2009a. La culture de Golasecca : une histoire de plusieurs siècles. In Lorre, Cicolani 2009, pp. 39-44.

de Marinis R.C. 2009b. Signes de pouvoir et de richesse à Golasecca : du monde des morts à celui des vivants. In Lorre, Cicolani 2009, pp. 45-53.

de Marinis R.C. 2009c. La Necropoli Mulini Bellaria di Sesto Calende (scavi 1977-1980). In de Marinis *et al.* 2009, pp. 431-454.

de Marinis R.C. 2009d. Le tombe del Golasecca IA 2 da Sesto Calende via Carera. In de Marinis *et al.* 2009, pp. 386-393.

de Marinis R.C. 2009e. Le tombe del Golasecca IB e IC dalle località Mulini e Impiove di Sesto Calende. In de Marinis *et al.* 2009, pp. 394-405.

de Marinis R.C. 2009f. Sesto Calende, la seconda tomba di guerriero. In de Marinis *et al.* 2009, pp. 162-203.

de Marinis R.C. 2009g. Sesto Calende, loc. Cascina Gajaccio: tomba del Golasecca II B. In de Marinis *et al.* 2009, pp. 204-206.

de Marinis R.C. 2009h. Una tomba del Golasecca IIA da La Castiona di Sesto Calende. In de Marinis *et al.* 2009, pp. 412-415.

de Marinis R.C. 2009i. Presualdo, Rastrel Rosso e Brivio, tombe del Golasecca I e II. In de Marinis *et al.* 2009, pp. 416-430.

DE MARINIS R.C. 2009l. La collezione di antichità di Golasecca di Carlo Ermes Visconti. In DE MARINIS *et al*. 2009, pp. 637-644.

DE MARINIS R.C. 2010. Materiali della cultura di Golasecca conservati al Musée des Antiquités Nationales di Saint-Germain-en-Laye. *Notizie Archeologiche Bergomensi* 16 (2008), pp. 21-65.

DE MARINIS R.C. 2019. Sui riti funerari della cultura di Golasecca. *IpoTESI di Preistoria* 11, pp. 1-56. https://doi.org/10.6092/issn.1974-7985/9894

DE MARINIS R.C., BIAGGIO SIMONA S. (a cura di) 2000. *I Leponti tra mito e realtà*. Raccolta di saggi in occasione della mostra. Locarno.

DE MARINIS R.C., CASINI S. 2020. The Early Iron Age protourbanisation along the Ticino River and around Como. In ZAMBONI *et al.* 2020, pp. 243-256.

DE MARINIS R.C., CASINI S., RAPI M. 2017. Il contributo del Forcello alla cronologia della transizione tardo Hallstatt–antico La Tène. In Piana Agostinetti P. (a cura di), *I Celti d'Italia. I Celti dell'età di La Tène a sud della Alpi.* Atti del convegno internazionale (Roma 16-17 dicembre 2010). Biblioteca di studi etruschi 59. Roma, pp. 13-41.

DE MARINIS R.C., GAMBARI F.M. 2005. La cultura di Golasecca dal X agli inizi del VII secolo a.C.: cronologia relativa e correlazioni con altre aree culturali. In Bartoloni G., Delpino F. (a cura di), *Oriente e occidente: metodi e discipline a confronto. Riflessioni sulla cronologia dell'età del Ferro in Italia*. Atti dell'incontro di studi (Roma 30-31 ottobre 2003). *MEDITERRANEA* I. Roma, pp. 197-225.

DE MARINIS R.C., GŭSTIN M. 1975. Qualche considerazione sulla cronologia e diffusione delle fibule semilunate. *Preistoria Alpina* 11, pp. 237-253.

DE MARINIS R.C., MASSA S., PIZZO M. (a cura di) 2009. *Alle origini di Varese e del suo territorio. Le Collezioni Del Sistema Archeologico Provinciale*, Bibliotheca Archaeologica 44. Roma.

DE MARINIS R.C., ROFFIA E. 1979. Scavi e scoperte, 35. Sesto Calende (Varese). *Studi Etruschi*, serie III, volume XLVII, pp. 521-523.

DE MARINIS R.C., SPADEA G. 2005 (a cura di), *I Liguri: un antico popolo europeo tra Alpi e Mediterraneo*. Milano.

DEODATO A. 2013. Processi di trasformazione nelle comunità del Basso Verbano nella seconda età del ferro: i centri di Dormelletto e Oleggio (NO). *Bollettino dell'Associazione archeologica ticinese* 25, pp. 18-23. https://doi.org/10.5169/seals-391560

DE ROMANIS F. 2000. Esportazioni di corallo mediterraneo in india nell'età ellenistico-romana. In MOREL *et al.* 2000, pp. 211-216.

DERRIK M.R., STULIK D., LANDRY J.M. 1999. *Infrared spectroscopy in Conservation Science, Scientific tool for conservation*. Los Angeles.

DI MAIO P., GAMBARI F.M., GERNETTI F., PIROTTO S., SQUARZANTI M. 2001. I corredi ed i reperti. In GAMBARI 2001, pp. 25-92.

DONEDDU G. 2006. La pesca del corallo tra Liguria, Corsica e Sardegna. In RAVAZZA 2006, pp. 43-52.

DOUKA K. 2011. The contribution of archaeometry to the study of prehistoric marine shells. In IFANTIDIS, NIKOLAIDOU 2011 pp. 171-180.

DUNGWORTH D.B. 1996. The production of copper alloys in Iron Age Britain. *Proceedings of the Prehistoric Society* 62, pp. 399-421.

EDWARDS H.G., VILLAR S.E.J., JEHLICKA J., MUNSHI T. 2005. FT-Raman spectroscopic study of calcium-rich and magnesium-rich carbonate minerals. *Spectrochimica Acta Part A: Molecular and Biomolecular Spectroscopy* 61, pp. 2273-2280.

EERKENS J.W., ROSENTHAL J.S., SPERO H.J., SHIRAKI R., HERBERT G.S. 2007. Shell bead sourcing: a comparison of two techniques on *Olivella biplicata* shells and beads from western north America. In Glascock M.D., Speakman R.J., Popelka-Filcoff R.S. (eds.), *Archaeological chemistry: analytical techniques and archaeological interpretation.* Washington DC, pp. 167-193.

ENDRIZZI L., MARZATICO F. (a cura di) 1997. *Ori Delle Alpi.* Catalogo della mostra (Trento, Castello Del Buonconsiglio, 20 giugno - 9 novembre 1997), Quaderni della Sezione Archeologica Castello Del Buonconsiglio - Monumenti e Collezioni Provinciali 6. Trento.

ENGLAND J., CUSACK M., PATERSON N.W., EDWARDS P., LEE M.R., MARTIN R. 2006. Hyperspectral cathodoluminescence imaging of modern and fossil carbonate shells. *Journal of Geophysical Research: Biogeosciences* 111, pp. 2-10.

Faget D., Vielzeuf D. 2018. Le vase et le microscope: origines et développement d'une connaissance scientifique du corail rouge de Méditerranée (XVIe XXIe siècle), *Rives mediterraneennes* 57, pp. 157-180.

Fan L. 2018. Precious Coral. In Duque Beltran C., Tello Camacho E. (eds.), *Corals in a Changing World*, pp. 51-72. http://dx.doi.org/10.5772/intechopen.73149

Farmer W.C. 1974. *The infrared spectra of mineral*. London.

Faudino V., Ferrero L., Giaretti M., Venturino Gambari M. 2014. Celti e Liguri. Rapporti tra la cultura di Golasecca e la Liguria interna nella prima Età del Ferro. In Barral *et al.* 2014, pp. 17-20.

Fazzini F. 2020. L'Archeologia Sperimentale e la metallurgia del bronzo in Italia: storia degli studi e problematiche. *Archeologie sperimentali. Temi, metodi, ricerche* 1, pp. 100-107.

Feely R.A., Sabine C.L., Lee K., Berelson W., Kleypas J., Fabry V.J., Millero F.J. 2004. Impact of anthropogenic CO_2 on the $CaCO_3$ system in the oceans. *Science* 305, pp. 362-366. https://doi.org/10.1126/science.1097329

Feely R.A., Sabine C.L., Hernandez-Ayon J.M., Ianson D., Hales B. 2008. Evidence for upwelling of corrosive' acidified' water onto the continental shelf. *Science* 320, pp. 1490-1492. https://doi.org/10.1126/science.1155676

Fernandes R., Maia L., Couri M., Costa L.A., De Oliveira L.F. 2015. Raman spectroscopy as tool in differentiating conjugated polyenes from synthetic and natural sources. *Spectrochimica acta. Part A, Molecular and biomolecular spectroscopy* 134C, pp. 434-441. https://doi.org/10.1016/j.saa.2014.06.022

Ferrero L., Rubat Borel F. 2017. Fibule protostoriche pugliesi dalla Collezione Giovanni Battista Assi al Museo di Antichità di Torino. In Radina F. (a cura di), *Preistoria e Protostoria della Puglia*. Atti della XLVII Riunione Scientifica Preistoria e Protostoria della Puglia (Ostuni, 9-13 ottobre 2012). Studi di Preistoria e Protostoria 4. Firenze, pp. 1025-1032.

Feugère M. 2000. Le corail à l'époque romaine. In Morel *et al*. 2000, pp. 205-210.

Filocamo G. 2000. L'artigianato del corallo: approvvigionamenti, lavorazione e mercato. In Morel *et al*. 2000, pp. 23-36.

Floquet N., Vielzeuf D., Ferry D., Ricolleau A., Heresanu V., Perrin J., Laporte D., Fitch A.N. 2015. Thermally induced modifications and phase transformations of red coral Mg-calcite skeletons from infrared spectroscopy and high resolution synchrotron powder diffraction analyses. *Crystal Growth & Design* 15, pp. 3690-3706. https://doi.org/10.1021/acs.cgd.5b00291

Frey O.H. 1969. *Die Entstehung der Situlenkunst: Studien zur figürlich verzierten Toreutik von Este*. Römisch-Germanische Forschungen 31. Berlin.

Fogolari G. 1975. La protostoria delle Venezie. In Rittatore Vonwiller F., Fogolari G. (a cura di), *Popoli e civiltà dell'Italia antica* 4. Roma, pp. 61-222.

Fogolari G., Frey O.H. 1965. Considerazioni tipologiche e cronologiche sul II e III periodo atestino. *Studi Etruschi*, serie II, volume XXXIII, pp. 237-293.

Freiwald A., Beuck L., Rüggeberg A., Taviani M., Hebbeln D., Participants R.M.C.M.-1 2009. The white coral community in the central Mediterranean Sea revealed by ROV surveys. *Oceanography* 22, pp. 58-74.

Frey O.H. 1971. Fibeln vom westhallstättischen typus aus dem gebiet südlich der Alpen: zum problem der keltischen wanderung. In Società Archeologica Comense (a cura di), *Oblatio. Raccolta di studi di antichità e arte in onore di Aristide Calderini*. Como, pp. 555-586.

Frey O.H. 1991. La formazione della cultura di La Tène nel V secolo a.C. In *I Celti.* Catalogo della mostra a Palazzo Grassi (Venezia). Milano, pp. 127-145.

Fürst S. 2014. Korallen am Übergang zur Frühlatènezeit – Zum wissenschaftlichen Potential eines problematischen Schmuckmaterials. In Hornung S. (hg.), *Produktion distribution-ökonomie: siedlungs- und wirtschaftsmuster der latene zeit*. Akten des internationalen kolloquiums in Otzenhausen. Bonn, pp. 41-66.

Fürst S., Muller K., Paris C., Bellot-Gurlet L., Pare C., Reiche I. 2014. Neue Identifizierungsstrategie eisenzeitlicher Korallen anhand optischer und Ramanspektroskopischer Charakteristiken. *Berliner Beiträge zur Archäometrie, Kunsttechnologie und Konservierungswissenschaft* 22, pp. 25-36.

Fürst S., Müller K., Gianni L., Paris C., Bellot-Gurlet L., Pare C., Reiche I. 2016. Raman Investigations to Identify *Corallium rubrum* in Iron Age Jewelry and Ornaments. *Minerals* 6, 56, pp. 1-23. https://doi.org/10.3390/min6020056

Gaillard Y., Mija A., Burr A., Darque-Ceretti E., Felder E., Sbirrazzuoli N. 2011. Green material composites from renewable resources: Polymorphic transitions and phase diagram of beeswax/rosin resin. *Thermochimica Acta* 521, pp. 90–97. https://doi.org/10.1016/j.tca.2011.04.010

Gaj G., Burdese S. 2009. Analisi tecnologica e indagine sperimentale. In Venturino Gambari 2009, pp. 201-222.

Gaj G., Maestro O. 2023. Archeologia Sperimentale: un approccio sistematico alla disciplina. *Archeologie Sperimentali. Temi, Metodi, Ricerche* IV, pp. 8-20.

Gallo V. 2023. *La necropoli della piena età del ferro del CUS-Piovego a Padova. Analisi del contesto e proposta di scansione in fasi*. Tesi di dottorato. Università di Padova.

Gambacurta G., Ruta Serafini A. 2019. *I Celti e il Veneto. Storie di culture a confronto.* Ricerche 7. Bologna.

Gambari F.M. 1984. Castelletto Ticino, tombe golasecchiane (Notiziario Novara). *Quaderni della Soprintendenza Archeologica del Piemonte* 3, pp. 262-263.

Gambari F.M. 1987. La necropoli di San Bernardino di Briona: revisione critica alla luce dei risultati preliminari dei nuovi scavi. *Quaderni della Soprintendenza Archeologica del Piemonte* 6, pp. 63-95.

Gambari F.M. 1998. Gli insediamenti e la dinamica del popolamento nell'età del Bronzo e nell'età del Ferro. In Mercando L, Venturino Gambari M. (a cura di), *Archeologia in Piemonte. La Preistoria* 1. Torino, pp. 129-146.

Gambari F.M. (a cura di) 2001. *La birra e il fiume. Pombia e le vie dell'ovest Ticino tra VI e V secolo a.C.* Catalogo della mostra (Oleggio, Museo civico etnografico "C.G. Fanchini", 21 aprile - 31 ottobre 2001). Torino.

Gambari F.M. 2014. La media età del Ferro nella valle del Tanaro tra Etruschi e primi arrivi transalpini. In Venturino Gambari 2014, pp. 33-38.

Gambari F.M. 2019a. Cronologia e storia. I riscontri archeologici e toponomastici delle vicende legate alla istruzione di Caruscum/Carystum. In Venturino M. (a cura di), *Le ceneri degli Statielli. La necropoli della seconda età del Ferro di Montabone.* Acquae Statiellae - Studi di Archeologia 4. Genova, pp. 11-22.

Gambari F.M. 2019b. De transitu Gallorum haec accepimus. Cronologia, fonti e modelli narrativi dei passi liviani sull'arrivo dei Galli, alla luce dell'archeologia. *Preistoria Alpina* 49bis, pp. 55-63.

Gambari F.M. 2022. Modelli di fondazione e nascita dei centri protourbani nella cultura di Golasecca. *Rivista di scienze preistoriche* LXXII, pp. 621-635.

Gambari F.M., Cerri R. (a cura di) 2011. *L'alba della città. Le prime necropoli del centro protourbano di Castelletto Ticino*. Novara.

Gambari F.M., Rubat Borel F. 2011. Les Gaulois des deux versants des Alpes. In Jospin J.P., Dalaine L. (dir.), *Hannibal et les Alpes. Une traversée, un mythe*. Catalogue de l'exposition (Grenoble, Musée dauphinois 21 aprile 2011 – 2 luglio 2012). Gollion, pp. 59-67.

Gambari F.M., Venturino Gambari M. 1997. Gli oggetti di ornamento in Piemonte. In Endrizzi, Marzatico 1997, pp. 333-340.

Gangemi G. 2015. L'inquadramento cronologico e culturale del territorio. In Gangemi, Bassetti, Voltolini 2015, pp. 25-28.

Gangemi M. 2006. La pesca del corallo nelle 'Relazioni' della Marina Mercantile Italiana (1885-1930). In Ravazza 2006, pp. 77-116.

Gangemi G., Bassetti M., Voltolini D. (a cura di) 2015. *Le Signore dell'Alpago. La necropoli preromana di 'Pian de la Gnela'. Pieve d'Alpago (Belluno)*. Treviso.

Gerdes A., Bente K., Berthold C. 2015. Sr-und B-isotopie zum korallendekor latene-und hallstatt zeitlicher fibeln und korrelierbare objecte. In Gluhak T., Greiff S., Kraus K., Prange M. (Hrsg.), *Archäometrie und Denkmalpflege.* Jahrestagung (Mainz 25-28 märz 2015). Metalla Sonderheft 7. Bochum, pp. 47-48.

Ghirardini G. 1897. La situla italica primitiva studiata specialmente in Este. *Monumenti Antichi della Reale Accademia dei Lincei* VII, pp. 5-200.

Ghirardini G. 1901. La situla italica primitiva studiata specialmente in Este. *Monumenti*

Antichi della Reale Accademia dei Lincei X, pp. 5-222.

Giaretti M. 2001. L'età del Ferro. In Venturino Gambari 2001, pp. 137-160.

Giaretti M. 2014. Fibule e oggetti di ornamento personale dell'età del ferro. In Venturino Gambari 2014, pp. 381-383.

Giorcelli Bersani S., Venturino M. (a cura di) 2021. *I liguri e Roma. Un popolo tra archeologia e storia*. Atti del convegno (Acqui Terme 31 maggio - 1 giugno 2019). Studi e ricerche sulla Gallia Cisalpina 29. Roma.

Giordani N. 2008. Attestazioni dalla seconda età del Ferro all'Altomedioevo nel Modenese. In Bernabò Brea M., Valloni R. (a cura di), *Archeologia ad alta velocità in Emilia. Indagini geologiche e archeologiche lungo il tracciato ferroviario*. Atti del convegno (Parma 9 giugno 2003). Firenze, pp. 201-210.

Giumlia-Mair A. 1998. Studi metallurgici sui bronzi della necropoli di S. Lucia-Most na Soči. *Aquileia Nostra* 69, pp. 29-136.

Giumlia-Mair A. 2000. Bronze technology in the eastern subalpine region between Final Bronze Age and Early Iron Age. In Giumlia-Mair A. (ed.), *Ancient Metallurgy between Oriental Alps and Pannonian Plain.* Workshop (Trieste 29-30 October 1998). Quaderni dell'Associazione nazionale per Aquileia 8. Trieste, pp. 77-91.

Giumlia-Mair A. 2003. Evoluzione tecnica e formale nella produzione di fibule e spilloni tra il IX e il IV sec. a.C. nell'area Alpino-Orientale. In Formigli E. (a cura di), *Fibulae dall'età del Bronzo all'alto medioevo*. Firenze, 49-58.

Giumlia-Mair A. 2005. Copper and Copper Alloys in the Southeastern Alps: An Overview. *Archaeometry* 47, pp. 275-292. https://doi.org/10.1111/j.1475-4754.2005.00202.x

Giumlia-Mair A. 2009. Ancient Metallurgical traditions and connections around the Caput Adriae. *Journal of Mining and Metallurgy B: Metallurgy* 45, pp. 149-163.

Giumlia-Mair A., Stefan L., Gilmour B., Degasperi N., Bellintani P. 2016. L'officina metallurgica dell'età del Ferro di Zambana 'El Vato' (TN) (Scavi 2010–2011). Analisi e prime considerazioni sui reperti in lega di rame e in ferro e sui resti di strutture pirotecnologiche. *Archeologia delle Alpi* 2, pp. 49-72.

Giustetto, R. 2008. Analisi dei componenti su frammenti ceramici. In Gambari F.M. (a cura di), *Taurini sul confine. Il Bric San Vito di Pecetto nell'età del Ferro*. Beinasco, pp. 119-122.

Giustetto R., Diana E., Berruto G., Silenzi F. 2012. Studio archeometrico di decorazioni campite in pasta bianca e rossa su ceramiche preistoriche piemontesi. *Quaderni della Soprintendenza Archeologica del Piemonte* 27, pp. 61-76.

Giustetto R., Berruto G., Diana E., Costa E. 2013. Decorated prehistoric pottery from Castello di Annone (Piedmont, Italy): Archaeometric study and pilot comparison with coeval analogous finds. *Journal of Archaeological Science* 40, pp. 4249-4263. https://doi.org/10.1016/j.jas.2013.06.012

Giustetto R., Pastero L., Aquilano D. 2020. Potential effects of the shape of gypsum aggregates on the early sulfation of marble and travertine, *Journal of Building Engineering* 32, 101794, pp. 1-10. https://doi.org/10.1016/j.jobe.2020.101794

Goldsmith J.R., Graf D.L., Heard H.C. 1961. Lattice constants of the calcium magnesium carbonates. *The american mineralogist* 46, pp. 453-457.

Gonçalves D., Thompson T.J.U., Cunha E. 2011. Implications of heat-induced changes in bone on the interpretation of funerary behaviour and practice. *Journal of Archaeological Science* 38, pp. 1308-1313. https://doi.org/10.1016/j.jas.2011.01.006

Govi E. (a cura di) 2016. *Il mondo etrusco e il mondo italico di ambito settentrionale prima dell'impatto con Roma.* Atti del convegno di Studi Etruschi e Italici, Sezione Etruria padana e Italia settentrionale (Bologna 28 febbraio-1 marzo 2013).

Grassi B. 2014. Rito e costume funerario: corredi dell'età del Ferro dalla località Mulini di Sesto Calende. In Grassi B., Pizzo M. (a cura di), *Gallorum insubrum fines. Ricerche e progetti archeologici nel territorio di Varese*. Atti della giornata di studio (Varese, Villa Recalcati 29 gennaio 2010). Roma, p. 111-134.

Grassi B. 2017. Strutture funerarie e riti golasecchiani: la necropoli di via Moncenisio a Sesto Calende (VA) - (scavi 1995-1996), *Zixu. Studi sulla cultura celtica di Golasecca* 2, pp. 11-152.

Grassi B., Mangani C., 2016 (a cura di). *Nel bosco degli antenati. La necropoli del Monsorino di Golasecca (scavi 1985-86)*. Sesto Fiorentino.

Grassi B., Mangani C. 2021. I reperti (La necropoli di via Montrucco a Sesto Calende). *Zixu. Studi sulla cultura celtica di Golasecca* 4, pp. 47-74.

Grellet-Tinner G., Corsetti F., Buscalioni A. 2010. The importance of microscopic examinations of eggshells: Discrimination of bioalteration and diagenetic overprints from biological features. *Journal of Iberian Geology* 36, pp. 181-192.

Grillo M.C., Goldberg W.M., Allemand D. 1993. Skeleton and sclerite formation in the precious red coral *Corallium rubrum*. *Marine Biology* 117, pp. 119-128. https://doi.org/10.1007/BF00346433

Güggisberg M.A. 2004. *Die Hydria von Grächwil: zur Funktion und Rezeption mediterraner Importe in Mitteleuropa im 6. und 5. Jahrhundert V. Chr*. Akten Internationales Kolloquium anlässlich des 150. Jahrestages der Entdeckung der Hydria von Grächwil durch das Institut für Archäologie des Mittelmeerraumes der Universität Bern (Bern, Bernisches Historisches Museum 5, 12-13 Oktober 2001).

Hall, A., Kennedy, W.J. 1967. Aragonite in Fossils. *Proceedings of the Royal Society of London. Series B, Biological Sciences* 168, pp. 377-412.

Han N., Blue C.R., De Yoreo J.J., Dove P.M. 2013. The Effect of Carboxylates on the Mg Content of Calcites that Transform from ACC. *Procedia Earth and Planetary Science* 7, pp. 223-227. https://doi.org/10.1016/j.proeps.2013.03.224

Harmelin J.G. 2000. Le corail rouge de Méditerranée : quelques aspects de sa biologie et de son écologie. In Morel *et al.* 2000, pp. 11-22.

Hasegawa H., Rahman M.A., Luan N.T., Maki T., Iwasaki N. 2012. Trace elements in Corallium spp. as indicators for origin and habitat. *Journal of Experimental Marine Biology and Ecology* 414, pp. 1-5. https://doi.org/10.1016/j.jembe.2012.01.005

Hermans J. 2010. *Incorporation du magnésium dans les squelettes calcitiques des échinodermes et des éponges hypercalcifiées*. Thèse doctorale. Université Libre de Bruxelles.

Hermary A. 2000. Le corail dans le monde grec antique : les témoignages archéologiques. In Morel *et al.* 2000, pp. 135-138.

Hirose M., Lamanna L. 2015. La necropoli golasecchiana di via Ardeatine a Castelletto Ticino. Analisi dei corredi e del contenuto delle urne alla luce degli esami TC. *Quaderni della Soprintendenza Archeologica del Piemonte* 30, pp. 87-115.

Ifantidis F., Nikolaidou M. (eds.) 2011. *Spondylus in prehistory. New data and approaches. Contributions to the archaeology of shell technologies.* Oxford.

Ingo G.M., de Caro T., Riccucci C., Angelini E., Grassini S., Balbi S., Bernardini P., Salvi D., Bousselmi L., Çilingiroglu A., Gener M., Gouda V.K., Al Jarrah O., Khosroff S., Mahdjoub Z., Al Saad Z., El-Saddik W., Vassiliou P. 2006. Large scale investigation of chemical composition, structure and corrosion mechanism of bronze archeological artefacts from Mediterranean basin. *Applied Physics A* 83, pp. 513-520. https://doi.org/10.1007/s00339-006-3550-z

Iozzo M. 2013. Una fibula tarantina a delfino. In Bruni S., Cianferoni G.C. (a cura di), *Dósis d'olíge te phíle te: studi per Antonella Romualdi*. Firenze, pp. 357-370.

Kaczorowska B., Hacura A., Kupka T., Wrzalik R., Talik E., Pasterny G., Matuszewska A. 2003. Spectroscopic characterization of natural corals. *Analytical and bioanalytical chemistry* 377, pp. 1032-1037. https://doi.org/10.1007/s00216-003-2153-1

Kellnert R.A. 2003. Spettroscopia infrarossa e Raman. In Kellnert R.A., Mermet J.M., Otto M., Widmer H.M. (a cura di), *Chimica analitica*. Napoli, pp. 570-594.

Keuper M., Bente K., Berthold C., Nickel K.G. 2014. Ramanspektroskopische Differenzierung von organischen Pigmenten in biomineralischem Verbund. In *92nd Annual Meeting of the Deutsche Mineralogische Geselchaft*. Jena, p. 80.

Keuper M., Bente K., Berthold C., Wendling H., Teschner U., Münster T., Hirsch D., Wirth R. 2015. Provenance and Colour of La Tène

and Hallstatt period fibulae beads - analytics and experimental treatments. *GNAA Meeting*. Mainz.

Kiefert L., Karampelas S. 2011. Use of the Raman spectrometer in gemmological laboratories. *Spectrochimica Acta Part A: Molecular and Biomolecular Spectroscopy* 80, pp. 119-124.

Klein S., Hauptmann A. 1999. Iron Age Leaded Tin Bronzes from Khirbet Edh-Dharih, Jordan. *Journal of Archaeological Science* 26, pp. 1075-1082. https://doi.org/10.1006/jasc.1999.0412

Krap T., van de Goot F.R.W., Oostra R.-J., Duijst W., Waters-Rist A.L. 2017. Temperature estimations of heated bone: A questionnaire-based study of accuracy and precision of interpretation of bone colour by forensic and physical anthropologists. *Legal Medicine* 29, pp. 22-28. https://doi.org/10.1016/j.legalmed.2017.08.001

Kruta V. 1978. Celtes de cispadane et transalpins aux IVe et IIIe siècles avant notre ère : données archéologiques. *Studi Etruschi* XLVI, pp. 150-174.

Kruta V. 1986. Le corail, le vin et l'Arbre de vie : observations sur l'art et la religion des Celtes du Ve au Ier siècle avant J.C. *Études celtiques* 23, pp. 7-32. https://doi.org/10.3406/ecelt.1986.1811

Kruta V. 1987. Il corallo, il vino e l'albero della vita: apporti peninsulari allo sviluppo della civiltà di La Tène. In Vitali 1987, pp. 23-33.

Kruta V. 1991. I Celti della prima espansione storica (IV secolo a.C.). In *I Celti.* Catalogo della mostra a Palazzo Grassi (Venezia). Milano, pp. 194-213.

Kruta V., Moucha, V. 2018. Une fibule ornithomorphe du début du V e siècle avant J.-C. au musée de Slaný (Bohême). *Archeologické Rozhledy* 70.1, pp. 67-90.

Kruta-Poppi L. 1975. Les Celtes à Marzabotto (province de Bologne). *Études celtiques* 14, pp. 345-376. https://doi.org/10.3406/ecelt.1975.1543

Kruta-Poppi L. 1977. Les vestiges laténiens de la région de Modène. *Études celtiques* 15, pp. 425-439. https://doi.org/10.3406/ecelt.1977.1588

Kuijpers M.H. 2018. A Sensory Update to the Chaîne Opératoire in Order to Study Skill: Perceptive Categories for Copper-Compositions in Archaeometallurgy. *Journal of archaeological method and theory* 25, pp. 863-891.

Kupka T., Lin H.M., Stobińsk, L., Chen C.-H., Liou W.-J., Wrzalik R., Flisak Z., 2009. Experimental and theoretical studies on corals. I. Toward understanding the origin of color in precious red corals from Raman and IR spectroscopies and DFT calculations. *Journal of Raman Spectroscopy* 41, pp. 651-658. https://doi.org/10.1002/jrs.2502

Lafuente B., Downs R.T., Yang H., Stone N. 2015. 1. The power of databases: The RRUFF project. In Armbruster T., Danisi R.M. (eds.), *Highlights in Mineralogical Crystallography*. Berlin, pp. 1-30.

Landolfi M. 1987. Presenze galliche nel Piceno a sud del fiume Esino. In Vitali 1987, pp. 443-468.

Ledoux J.B., Mokhtar-Jamaï K., Roby C., Féral J.-P., Garrabou J., Aurelle D. 2010. Genetic survey of shallow populations of the Mediterranean red coral [*Corallium rubrum* (Linnaeus, 1758)]: new insights into evolutionary processes shaping nuclear diversity and implications for conservation. *Molecular Ecology* 19, pp. 675-690. https://doi.org/10.1111/j.1365-294X.2009.04516.x

Ledoux J.B., Aurelle D., Féral J.-P., Garrabou J. 2013. Molecular forensics in the precious Mediterranean red coral, *Corallium rubrum*: testing DNA extraction and microsatellite genotyping using dried colonies. *Conservation Genetics Resources* 5, pp. 327-330.

Ledoux J.B., Antunes A., Haguenauer A., Pratlong M., Costantini F., Abbiati M., Aurelle D. 2016. Molecular forensics into the sea: how molecular markers can help to struggle against poaching and illegal trade in precious corals?. In Goffredo S., Dubinsky Z. (eds.), *The Cnidaria, past, present and future. The world of Medusa and her sisters*, pp. 729-745.

Leicht M. 1871. Avanzi preistorici nel bellunese. In Fogolari G. (a cura di), *I Paleoveneti alpini. Protostoria del bellunese e del cadore*. Atesa Antichità 2. Reggello.

Lendvay B., Cartier L.E., Gysi M., Meyer J.B., Krzemnicki M.S., Kratzer A., Morf N.V. 2020. DNA fingerprinting: an effective tool for taxonomic identification of precious corals in

jewelry. *Scientific Reports* 10, 8287, pp. 1-12. https://doi.org/10.1038/s41598-020-64582-4

Leng M.J., Lewis J.P. 2016. Oxygen isotopes in Molluscan shell: applications in environmental archaeology. *Environmental Archaeology* 21, pp. 295-306.

Lerat L. 1966. Franche-Comté. *Gallia* 24, pp. 345-375.

Leurini L. 2000. Il corallo nei testi greci e latini. In Morel *et al.* 2000, pp. 81-98.

Liao X., Cao F., Zhang J. 2018. Effect of sulphate on the corrosion behavior of bronze under a chloride-containing thin electrolyte layer. *Materials and Corrosion* 69. https://doi.org/10.1002/maco.201810132

Liverino B., 1989, *Red Coral jewel of the sea*. Bologna.

Locatelli D., Manessi P., Nascimbene A. 2003. Santa Maria in Colle - Scavi 153, 1959, 1960, 1962 - I corredi - Catalogo. *Archaiologhia - Quaderni del Museo di Storia Naturale e Archeologia di Montebelluna* I, pp. 51-122.

Longhi A. 1882. Continuazione delle scoperte archeologiche nella Valtravaglia. *Rivista Archeologica dell'antica Provincia e Diocesi di Como* 21, 19-39.

Lorre C., Cicolani V. (dir.) 2009. *Golasecca du commerce e des hommes à l'age du fer (VIII-V siècle av. J.C.), Catalogue de l'exposition* (Saint-Germain-en-Laye 27 novembre - 26 avril 2010). Paris.

Lucke W. 1962. *Die Situla in Providence (Rhode Island): ein Beitrag zur Situlenkunst des Osthallstattkreises*. Römisch-germanische Forschungen 26. Berlin.

Macchia M., Resta V., Quarta G., Calcagnile L. 2016. Precious coral non-destructive characterization by Raman and XRF spectroscopy. *X-Ray Spectrometry* 45, pp. 281-287. https://doi.org/10.1002/xrs.2703

Maggi S., Gorrini M.E. (a cura di) 2014. *Casteggio e l'antico: 25 anni di studi e ricerche archeologiche in Provincia di Pavia*, Atti del convegno di studi (Casteggio, 19 ottobre 2013). Sesto Fiorentino.

Magni A. 1907. La necropoli gallica di Pianezzo nel Canton Ticino. *Rivista Archeologica dell'antica Provincia e Diocesi di Como* 53-55, pp. 3-82.

Maia L.F., Fleury B.G., Lages B.G., Barbosa J.P., Pinto Â.C., Castro H.V., de Oliveira V.E., Edwards H.G., de Oliveira L.F. 2010. Identification of reddish pigments in octocorals by Raman spectroscopy. *Journal of Raman Spectroscopy* 42, pp. 653-658. https://doi.org/10.1002/jrs.2758

Maier F. 1957. Geometrisch verzierte Gürtelbleche aus Gräbern der späten Hallstattzeit von Singen am Hohentwiel (Ldkr. Konstanz). *Germania* 35, 3/4, pp. 249-265. https://doi.org/10.11588/ger.1957.44134

Maier F. 1958. Zur Herstellungstechnik und Zierweise der späthallstattzeitlichen Gürtelbleche Südwestdeutschlands. *Bericht der Römisch-Germanischen Kommission* 39, pp. 131-249.

Mangani C. 2016. Corallo al Monsorino? In Grassi, Mangani 2016, pp. 131-132.

Mangani C., Minarini L. 1998. La necropoli di Cerinasca d'Arbedo (Arbedo-Castione TI): nuove osservazioni sulla stratigrafia orizzontale. *Archeologia Svizzera* 21, pp. 77-79.

Mangani C., Minarini L. 2000. La necropoli di Cerinasca d'Arbedo. In de Marinis, Biaggio Simona 2000, pp. 259-269.

Mansfeld G. 1973. *Die Fibeln der Heuneburg, 1950-1970. Ein Beirtrag zur Geschichte der Spathallstattfibeln*. Heuneburgstudien II. Berlin.

Mantovani G. 1890. Brembate-Sotto: nuove scoperte nel sepolcreto preromano presso la via provinciale. *Notizie degli Scavi di Antichità. Atti della R. Accademia dei Lincei. Memorie della Classe di scienze morali, storiche e filologiche*, Serie 4, Annata 287, Volume 8, pp. 52-63.

Marastoni S. 2006. Virtù magiche e terapeutiche del corallo. In *Coralli segreti* 2006, pp. 51-65.

Marchesetti C. 1893. Scavi nella necropoli di Santa Lucia del Dr. Carlo Marchesetti (1885-1892). *Bollettino della Società Adriatica di Scienze Naturali in Trieste* 15, pp. 3-334.

Marzatico F. 2014. L'età del Ferro in area alpina centro-orientale. In Roncador, Nicolis 2014, pp. 11-28.

Marzatico F. 2019. I Reti e i popoli delle Alpi orientali. *Preistoria Alpina* 49bis, pp. 73-82.

Mastrocinque A. 2006. Le origini del corallo: tra religione, mito e magia. In *Coralli segreti* 2006, pp. 41-50.

McGregor H.V., Gagan M.K. 2003. Diagenesis and geochemistry of Porites corals from Papua New Guinea: Implications for paleoclimate reconstruction. *Geochimica et Cosmochimica Acta* 67, pp. 2147-2156. https://doi.org/10.1016/S0016-7037(02)01050-5

Meeks D. 2000. Le corail dans l'Egypte ancienne. In Morel *et al.* 2000, pp. 99-117.

Melli P. 2007. *Genova preromana. Una città portuale del Mediterraneo tra il VII e il III secolo a.C.* Genova.

Melli P. 2017. *Genaua Kainua Genua Ianua: Genova. Le molte vite di una città portuale dal Neolitico al VII secolo d.C.* Sestri Levante.

Melli P. 2021. Tra le Alpi e il Tirreno. La Liguria e il basso Piemonte tra VII e V secolo a.C. In Venturino, Giaretti 2021, pp. 65-80.

Merlin J.C. 1985. Resonance Raman spectroscopy of carotenoids and carotenoid-containing systems. *Pure and Applied Chemistry* 57, pp. 785-792.

Merlin J.C. Delé-Dubois, M.L., 1986. Resonance Raman characterization of polyacetylenic pigments in the calcareous skeleton. *Comparative Biochemistry and Physiology Part B: Comparative Biochemistry* 84, pp. 97-103.

Micheli R. 2004. Gli ornamenti in conchiglia del Neolitico dell'Italia settentrionale. *Preistoria Alpina* 40.1, pp. 53-70.

Micheli R. 2012. Personal ornaments, Neolithic groups and social identities: some insights into northern Italy. *Documenta Praehistorica* 39, pp. 227-256. https://doi.org/10.4312/dp.39.16

Miedico C. 2011 (a cura di), *Armille, fibule e castoni. Ornamenti e gioielli nella provincia di Varese dalla Preistoria al Medioevo*. Catalogo della mostra (mostra diffusa: Civici Musei e Parchi Archeologici di Angera, Arsago Seprio, Castelseprio, Sesto Calende; 22 settembre - 30 ottobre 2011).

Milanese M. 1987. *Scavi nell'Oppidum preromano di Genova: Genova-S. Silvestro 1*. Studia Archaeologica 48. Roma, pp. 1-385.

Millotte J.P. 1975. Franche-Comté. *Gallia Préhistoire* 18, pp. 583-600.

Mollo Mezzena R. 1997. L'età del Bronzo e l'età del Ferro in Valle d'Aosta. In *La Valle d'Aosta nel quadro della Preistoria e Protostoria dell'arco alpino centro-occidentale*. Atti della XXXI Riunione Scientifica (Courmayeur 2-5 giugno 1994). Firenze, pp. 139-223.

Morel J.P. 2000. Le corail dans l'Occident phénico-punique. In Morel *et al.* 2000, pp. 121-134.

Morel J.P. 2006. Il corallo nell'antico Egitto e nel mondo greco, fenicio-punico, romano e asiatico. In *Coralli segreti* 2006, pp. 65-78.

Morel J.P., Rondi-Costanzo C., Ugolini D. (a cura di), *Corallo di ieri - Corallo di oggi*. Atti del convegno (Ravello Villa Rufolo 13-15 dicembre 1996). Travaux Du Centre Camille Jullian 25. Bari.

Morelli N. 1888. Antichi manufatti metallici rinvenuti nella Liguria. *Bullettino di Paletnologia Italiana* 14, pp. 8-19, tavv. I-II.

Moreno-Azanza M., Bauluz B., Canudo J.I., Gasca J.M., Torcida Fernández-Baldor F. 2016. Combined Use of Electron and Light Microscopy Techniques Reveals False Secondary Shell Units in Megaloolithidae Eggshells. *PLOS ONE 11*, e0153026, pp. 1-17. https://doi.org/10.1371/journal.pone.0153026

Morico G. 1987. Il pozzo di Pian del Monte. Le fibule. In Bermond Montanari G. (a cura di), *La formazione della città in Emilia Romagna. Prime esperienze urbane attraverso le nuove scoperte archeologiche*. Catalogo della mostra (Bologna, Museo Civico Archeologico, 26 settembre 1987- 24 gennaio 1988). Bologna, pp. 263-272.

Mostra dell'Etruria Padana e della città di Spina. 1960. Catalogo della mostra (Bologna Palazzo dell'Archiginnasio, 12 settembre - 31 ottobre 1960). Bologna.

Mucci A. 1983. The solubility of calcite and aragonite in seawater at various salinities, temperatures, and one atmosphere total pressure. *American Journal of Science*, 283, pp. 780-799.

Musellius M.I. 1756. *Antiquitatis reliquiae collectae Veronae*.

Nagy P. 2012. *Castaneda GR. Die Eisenzeit im Misox*. Bonn, Habelt.

Nascimbene A. 1999. *Caverzano di Belluno: aspetti e problemi di un centro dell'età del Ferro nella media Valle del Piave*. Quaderni della Società per la Preistoria e Protostoria della Regione Friuli-Venezia Giulia 7. Trieste.

Nascimbene A. 2009. *Le Alpi Orientali nell'età del Ferro (VII-V secolo a.C.).* Udine.

Northover P. 1998. Annex 1: Analysis of copper alloy metalwork from Arbedo TI. In Schindler 1998b.

Orejas C., Gori A., Jiménez C., Rivera J., Kamidis N., Abu Alhaija R., Lo Iacono C. 2019. Occurrence and distribution of the coral Dendrophyllia ramea in Cyprus insular shelf: Environmental setting and anthropogenic impacts. *Deep Sea Research Part II: Topical Studies in Oceanography, Revisiting the Eastern Mediterranean: Recent knowledge on the physical, biogeochemical and ecosystemic states and trends* 164.1, pp. 190-205. https://doi.org/10.1016/j.dsr2.2019.04.006

Ortalli J. 2020. Archaeology of Early Felsina. The Birth of a Villanovan City. In Zamboni *et al*. 2020, pp. 91-108.

Ortalli J., Curina R., Trocchi T. 2024. *Racconti dalla città: trasformazioni urbane e mutamenti sociali nella Bologna preromana. L'abitato villanoviano e orientalizzante di Felsina*. Bologna.

Padovan S., Thirault E. 2007. *Pionieri delle Alpi. Chiomonte e Sollières dal Neolitico alle invasioni galliche*. Torino.

Pagani M., Turi A. 1977. Analisi mineralogica quantitativa per diffrazione a raggi X di sedimenti carbonatici attuali: applicazione ai sedimenti della laguna di Porto Cesareo (penisola salentina). *Atti della Società toscana di scienze naturali residente in Pisa. Memorie* 104, pp. 104-121.

Pakutinskiene I., Kiuberis J., Bezdicka P., Senvaitiene J., Kareiva A. 2007. Analytical characterization of Baltic amber by FTIR, XRD and SEM. *Canadian Journal of Analytical Sciences and Spectroscopy* 52, pp. 287-293.

Paral V., Witter K., Tonar Z. 2007. Microscopic examination of ground sections – a simple method for distinguishing between bone and antler? *International Journal of Osteoarchaeology* 17, pp. 627-634. https://doi.org/10.1002/oa.912

Pare C.F.E. 1989. Ein zweites Fürstengrab von Apremont 'La Motte aux Fées' (Arr. Vesoul, Dép. Haute-Saône). Untersuchungen zur Späthallstattkultur im ostfranzösischen Raum. *Jahrbuch des Römisch-Germanischen Zentralmuseums Mainz* 36, pp. 411-472. https://doi.org/10.11588/jrgzm.1989.2.76657

Parker J.E., Thompson S.P., Lennie A.R., Potter J., Tang C.C. 2010. A study of the aragonite-calcite transformation using Raman spectroscopy, synchrotron powder diffraction and scanning electron microscopy. *CrystEngComm* 12, pp. 1590-1599. https://doi.org/10.1039/B921487A

Pauli L. 1971. *Studien zur Golasecca Kultur*. München.

Pauli L. 1975. *Keltisker Volkglaube. Amulette und Sonderbestattungen am Durrnberg bei Hallein und im eisenszeitlichen Mitteleuropa*. München.

Peroni R. 1976. La 'koinè adriatica e il suo processo di formazione. *Jadranska obala u protohistoriji*, Dubrovnik 1972 (1976), pp. 95-114.

Peroni R., Carancini G.L., Coretti Irdi P., Ponzi Bonomi L., Rallo A., Saronio Masolo P., Serra Ridgway F.R. 1975. *Studi sulla cronologia delle civiltà di Este e Golasecca.* Origines. Firenze.

Perrin F. 2000. L'origine de la mode du corail méditerranéen (*Corallium rubrum* L.) chez les peuples celtes : essai d'interprétation. In Morel *et al*. 2000, pp. 193-203.

Perrin C., Smith D.C. 2007. Decay of skeletal organic matrices and early diagenesis in coral skeletons. *Comptes Rendus Palevol* 6, pp. 253-260. https://doi.org/10.1016/j.crpv.2007.02.003

Perrin J., Vielzeuf D., Ricolleau A., Dallaporta H., Valton S., Floquet N. 2015. Block-by-block and layer-by-layer growth modes in coral skeletons. *American Mineralogist* 100, pp. 681-695.

Perrin J., Rivard C., Vielzeuf D., Laporte D., Fonquernie C., Ricolleau A., Cotte M., Floquet 2017. The coordination of sulfur in synthetic and biogenic Mg calcites: The red coral case. *Geochimica et Cosmochimica Acta* 197, pp. 226-244. https://doi.org/10.1016/j.gca.2016.10.017

Piccardo P., Amendola R., Ervas A. 2010. Metallographic investigation and experimental replication of an Etruscan bronze mirror. *Historical metallurgy* 44, pp. 10-14.

Piccinno L. 2006. Le popolazioni liguri e la pesca del corallo nel Mediterraneo. In Ravazza 2006, pp. 117-136.

Pierre C. 1999. The oxygen and carbon isotope distribution in the Mediterranean water masses. *Marine geology* 153, pp. 41-55.

Pigorini L. 1896. Uso del corallo nelle età preromane. *Bullettino di Paletnologia Italiana* 22, pp. 305-306.

Pingitore N.E., Meitzner G., Love K.M. 1995. Identification of sulfate in natural carbonates by x-ray absorption spectroscopy. *Geochimica et Cosmochimica Acta* 59, pp. 2477-2483. https://doi.org/10.1016/0016-7037(95)00142-5

Pisani Dossi A. 1908. Tre tombe della prima età del Ferro a Longone al Segrino. *Rivista Archeologica dell'antica Provincia e Diocesi di Como* 56-8, pp. 3-12.

Pokines J.T., Faillace K., Berger J., Pirtle D., Sharpe M., Curtis A., Lombardi K., Admans J. 2018. The effects of repeated wet-dry cycles as a component of bone weathering. *Journal of Archaeological Science: Reports* 17, pp. 433-441. https://doi.org/10.1016/j.jasrep.2017.11.025

Poggiani Keller R., Rondini P. 2020. Bergamo and Parre during the Iron Age: Early Urbanization and the Alpine World. In Zamboni *et al.* 2020, pp. 275-298.

Pomey P. 2000. Un témoignagerécent sur la peche au corail à Marseille à l'époque archaiche. In Morel *et al.* 2000, pp. 37-40.

Prosdocimi A.L. 1891. Este. Nuove scoperte nella necropoli atestina presso Santo Stefano. *Notizie degli Scavi di Antichità. Atti della R. Accademia dei Lincei. Memorie della Classe di scienze morali, storiche e filologiche*, Serie 4, Annata 288, Volume 9, pp. 175-191.

Prosdocimi A.L. 1893. S. Maria di Carceri: antichità preromane scoperte presso la chiesa dell'abbazia. *Notizie degli Scavi di Antichità. Atti della R. Accademia dei Lincei. Memorie della Classe di scienze morali, storiche e filologiche*, Serie 5, Annata 290, Volume 1, pp. 396-403.

Prosdocimi A.L. 1896. Scoperta di una tomba preromana nella necropoli settentrionale atestina. *Notizie degli Scavi di Antichità. Atti della R. Accademia dei Lincei. Memorie della Classe di scienze morali, storiche e filologiche*, Serie 5, Annata 293, Volume 4, pp. 302–316.

Purpura G. 2005. Osservazioni sulla pesca del corallo rosso nell'antichità. *Archaeologia Maritima Mediterranea* 2, pp. 93-106.

Quek Z.B.R., Huang D. 2022. Application of phylogenomic tools to unravel anthozoan evolution. *Coral Reefs* 41, pp. 475-495. https://doi.org/10.1007/s00338-021-02072-3

Quercia A. 2008. Il corallo nei santuari del Mediterraneo antico. Il caso di Tas Silg. (Malta). In D'Andria F., de Grossi Mazzorin J., Fiorentino G. (a cura di), *Uomini, piante e animali nella dimensione del sacro*. Atti del seminario di studi di bioarcheologia (Cavallino 2002). Beni Archeologici, conoscenza e tecnologia. Quaderno 6. Santo Spirito, pp. 201-208.

Quirino T. 2011. Le case FI e F II del Forcello di Bagnolo S. Vito (MN): analisi preliminare di due abitazioni etrusche di fine VI secolo a.C. *Notizie Archeologiche Bergomensi* 19, pp. 379-390.

Rageot M., Théry-Parisot I., Beyries S., Lepère C., Carré A., Mazuy A., Filippi J.-J., Fernandez X., Binder D., Regert M. 2019. Birch bark tar production: Experimental and biomolecular approaches to the study of a common and widely used prehistoric adhesive. *Journal of Archaeological Method and Theory* 26, pp. 276-312.

Rageth J. 1997. Oggetti d'ornamento dei Grigioni. In Endrizzi, Marzatico 1997, pp. 243-256.

Rageth J. 2000. Kleine Urgeschichte Graubündens. *Archäologie der Schweiz* 23, pp. 32-46.

Rahman M.A., Oomori T., Wörheide G. 2011. Calcite formation in soft coral sclerites is determined by a single reactive extracellular protein. *Journal of Biological Chemistry* 286, pp. 31638-31649.

Railsback L.B. 2006. *Some fundamentals of mineralogy and geochemistry*. On-line book, quoted from: www. gly. uga. edu/railsback 387.

Rapi M. 2008. Un pendaglio ad anatrelle golasecchiano al Museo di Brescia. *Notizie Archeologiche Bergomensi* 16, pp. 67-73.

Rauchfuss B. 2016. Korallenfibel aus Siedlungsgrube. *Archäologie in Deutschland* 3, p. 53.

Raynaud C., Roux J.C., Columeau P., Tendille C. 1983. L'oppidum des Gardies à Pignan (Hérault). *Documents d'Archéologie Méridionale* 6, pp. 23-65.

Ravaglia M. 2000. La Valle Leventina e la Val di Blenio nell'età del Ferro. In de Marinis, Biaggio Simona 2000, pp. 279-297.

Ravazza N. (a cura di) 2006. *Un fiore dagli abissi. Il corallo: pesca, storia, economia, leggenda, arte*. Atti del convegno (San Vito Lo Capo, 11-13 ottobre 2002). San Vito Lo Capo.

Regert M., Rodet-Belarbi I., Mazuy A., Dantec G.L., Dessì R.M., Briz S.L., Henry A., Rageot M. 2019. Birch-bark tar in the Roman world: the persistence of an ancient craft tradition? *Antiquity* 93, pp. 1553-1568. https://doi.org/10.15184/aqy.2019.167

Ricci S. 1897. Palestro. Tomba preromana scoperta fuori dell'abitato. *Notizie degli Scavi di Antichità. Atti della R. Accademia dei Lincei. Memorie della Classe di scienze morali, storiche e filologiche*, Serie 5, Annata 294, Volume 5, pp. 1-6.

Ries J.B. 2011. Skeletal mineralogy in a high-CO2 world. *Journal of Experimental Marine Biology and Ecology* 403, pp. 54-64.

Rittatore F. 1947. Sepolcreti piemontesi dell'età del Ferro (contributo alla conoscenza della Civiltà di Golasecca). *Rassegna Storica del Seprio* VII, pp. 11-13.

Rizzini P. 1910. Illustrazione dei Civici Musei di Brescia. Catalogo dei bronzi. *Commentari dell'Ateneo di Brescia*, pp. 265-370.

Roncador R., Nicolis F. (a cura di) 2014. *Antichi popoli delle Alpi. Sviluppi culturali durante l'età del Ferro nei territori alpini centro-orientali*. Atti della giornata di studi internazionale (Sanzeno 1 Maggio 2010). Trento.

Roncoroni F. 2005. *La Cultura di Golasecca nella Collezione Garovaglio: l'area occidentale*, AIS (Archeologia dell'Italia Settentrionale) 10. Como.

Rondi-Costanzo C., Ugolini D. 2000. Le corail dans le bassin nord-occidental de la Mediterranée entre le VI et le II s. av. J.-C. In Morel *et al.* 2000, pp. 177-191.

Rondini P., Zamboni L. 2020. Verucchio: The Iron Age Settlement. In Zamboni *et al.* 2020, pp. 71-90.

Ruffa M. 1998. La necropoli protostorica di Dorbié Superiore - Castelletto Ticino. *Quaderni della Soprintendenza Archeologica del Piemonte* 15, pp. 11-39.

Ruffa M. 1999. Tre fermagli di cintura da Castelletto Ticino (NO). *Quaderni della Soprintendenza Archeologica del Piemonte* 16, pp. 29-36.

Ruffa M. 2001. L'abitato golasecchiano di Cascina Rivera a Castelletto Ticino. *Quaderni della Soprintendenza Archeologica del Piemonte* 18, pp. 13-28.

Ruffa M. 2010. Produzione metallurgica a S. Spirito-Gropello Cairoli (PV). *Notizie Archeologiche Bergomensi* 18, pp. 99-131.

Ruffa M. 2021. Golasecchiani o Liguri? Una comunità composita a Gropello Cairoli (PV). In Giorcelli Bersani, Venturino 2021, pp. 355-363.

Ruta Serafini A. 1984. Celtismo nel Veneto: materiali archeologici e prospettive di ricerca. *Études celtiques* 21, pp. 7-33. https://doi.org/10.3406/ecelt.1984.1752

Ruta Serafini A. 1997. Veneto - Età del Ferro. In Endrizzi, Marzatico 1997, pp. 543-546.

Sabine C.L., Key R.M., Feely R.A., Greeley D. 2002. Inorganic carbon in the Indian Ocean: Distribution and dissolution processes. *Global Biogeochemical Cycles* 16 (4), 1067, pp. 1-18. https://doi.org/10.1029/2002GB001869

Sakalauskaite J., Andersen S., Biagi P., Borrello M., Cocquerez T., Colonese A.C., Dal Bello F., Girod A., Heumüller M., Koon H., Mandili G., Medana C., Penkman K., Plasseraud L., Schlichtherle H., Taylor S., Tokarski C., Thomas J., Wilson J., Demarchi B. 2019. 'Palaeoshellomics' reveals the use of freshwater mother-of-pearl in prehistory. *eLife Sciences* 8, e45644, pp. 1-65. https://doi.org/10.7554/eLife.45644

Sakalauskaite J., Marin F., Pergolizzi B., Demarchi B. 2020a. Shell palaeoproteomics: first application of peptide mass fingerprinting for the rapid identification of mollusc shells in archaeology. *Journal of Proteomics* 227, 103920, pp. 1-10. https://doi.org/10.1016/j.jprot.2020.103920

Sakalauskaite J., Plasseraud L., Thomas J., Albéric M., Thoury M., Perrin J., Jamme F., Broussard C., Demarchi B., Marin F. 2020b. The shell matrix of the European thorny oyster, *Spondylus gaederopus*: microstructural and molecular characterization. *Journal of Structural Biology* 211, 107497, pp. 1-17. https://doi.org/10.1016/j.jsb.2020.107497

Salvati E., Tunesi L., Molinari A. 2004. Presence of the Scleractinian *Dendrophyllia ramea* in the shallow waters of Mediterranean Morocco (Al Hoceima, Alboran Sea). *Rapport Communication internationale Mer Méditerranéen* 37, p. 547.

Salzani L. 1976. Scavi e Scoperte, 24. Gazzo Veronese (Verona). *Studi Etruschi*, serie III, volume XLIV, pp. 417-425.

Sandberg P.A. 1983. An oscillating trend in Phanerozoic non-skeletal carbonate mineralogy. *Nature* 305, pp. 19-22. https://doi.org/10.1038/305019a0

Saronio P. 1970. La necropoli di Castello Valtravaglia (VA). *Sibrium* X, pp. 109-151.

Schembri P.J., Dimech M., Camilleri M., Page R. 2007. Living deep-water Lophelia and Madrepora corals in Maltese waters (Strait of Sicily, Mediterranean Sea). *Cahiers de Biologie Marine*, 48, pp. 77-83.

Schindler M.P. 1997. Nuove ricerche sul ripostiglio di bronzi del V sec. a.C. di Arbedo, Canton Ticino (Svizzera). In *La Valle d'Aosta nel quadro della Preistoria e Protostoria dell'arco alpino centro-occidentale*. Atti della XXXI Riunione Scientifica (Courmayeur 2-5 giugno 1994). Firenze, pp. 514-520.

Schindler M.P. 1998a. Il ripostiglio di bronzi del V sec. a. C. di Arbedo. *Bollettino dell'Associazione archeologica ticinese* 10, pp. 10-15.

Schindler M.P., 1998b (ed.), *Der Depotfund von Arbedo TI und die Bronzedepotfunde des Alpenraums vom 6. bis zum 4. Jh. v.Chr. - Il ripostiglio di Arbedo TI e i ripostigli di bronzi della regione alpina dal VI all'inizio del IV sec. a.C*. Antiqua 30. Basel.

Schindler M.P., de Marinis R.C. 2000. L'età del Ferro nel Canton Ticino e nella Mesolcina. In de Marinis, Biaggio Simona, pp. 159-183.

Schmid T., Dariz P. 2015. Shedding light onto the spectra of lime: Raman and luminescence bands of CaO, Ca $(OH)_2$ and $CaCO_3$. *Journal of Raman Spectroscopy* 46, pp. 141-146.

Schmid-Sikimić B. 2000a. Edelkoralle in der Adria. Zur Frage der Korallenficherei und des Korallenhandels in der Eisenzeit. In Morel *et al.* 2000, pp. 147-158.

Schmid-Sikimić B. 2000b. An den Wegen über die Alpen. Minusio und Mesocco: Referenzorte der älteren Eisenzeit in der Südschweiz. In de Marinis, Biaggio Simona 2000, pp. 215-244.

Schmid-Sikimić B. 2002. Mesocco Coop (GR). *Eisenzeitlicher Bestattungsplatz im Brennpunkt zwischen Sud und Nord*. Universitätsforschungen zur prähistorischen Archäologie 88.

Schmid-Sikimić B., Bigler B. 2005. Von Süden in den Norden und wieder zurück : Wege über die Alpen - Aktuelles zur Eisenzeitforschung im Kanton Zug. *Archéologie suisse* 28, pp. 6-19. https://doi.org/10.5169/seals-21019

Schoening F.R.L. 1980. The X-ray diffraction pattern and deformation texture of beeswax. *South African Journal of Science* 76, pp. 262-265.

Schrickel M., Bente K. 2013. Bedeutung und Bedeutungsverlust roter Korallen: Archäologische und aturwissenschaftliche Studien zu eisenzeitlichen Fibeln. In Meller H. (hrsg.), *Rot - Die Archäologie Bekennt Farbe. 5. Mitteldeutscher Archäologentag. Tagungen Landesmus.* Vorgesch 10 (Halle/S. 2013), pp. 341-352.

Schrickel M., Bente K., Fleischer F., Franz A. 2013. Importation ou imitation du corail à la fin de l'âge du Fer? Première approche par analyses du matériau. In Colin A., Verdin F. (dir.), *L'âge du Fer en Aquitaine et Sur Ses Marges. Mobilité des Hommes, Diffusion des Idées, Circulation des Biens dans L'espace Européen à L'âge du Fer*. Actes du 35e colloque international de l' A.F.E.A.F. (Bordeaux, 2-5 juin 2011). *Aquitania* Supplement 30, Bordeaux, pp. 753-759.

Schrickel M., Bente K., Berthold C., Grill W., Teschner U., Sarge C., Hoppe T. 2014. Vergleichende archaometrische untesuchungen an mitteldeuschen korallenfibeln. Fragestellungen und methodischer uberblick. *Universitätsforschungen zur prähistorischen Archäologie Band Aus dem Institut für Vor- und Frühgeschichte der Universität Mainz* 258, pp. 67-91.

Schvoerer M., Bechtel F., N'Guyen P.H., Clastre J., Villeneuve G. 2000. Repères afin de caractériser ou dater les coraux anciens. In Morel *et al.* 2000, pp. 225-235.

Scott D.A. 2002. *Copper and bronze in art: corrosion, colorants, conservation*. Los Angeles.

Sfrecola S. 2021. Analisi archeometriche sull'anima in cotto di fibule a sanguisuga. In Venturino, Giaretti 2021, pp. 561-564.

Siedel H., Siegesmund S. 2014. Characterization of Stone Deterioration on Buildings. In Siegesmund, S., Snethlage, R. (eds.), *Stone in Architecture: Properties, Durability*, Berlin, Heidelberg, pp. 349-414. https://doi.org/10.1007/978-3-642-45155-3_6

Simoni P. 1964. Gavardo dalla preistoria alla romanità: dieci anni di indagine archeologica. *Annali del Museo. Notiziario di preistoria e archeologia (Civico Museo Gruppo Grotte Gavardo)* 3, pp. 1-55.

Sirago M. 2006. La città del corallo. Attività marinare, commercio e artigianato a Torre del Greco in età moderna. In Ravazza 2006, pp. 53-76.

Skeates R. 1993. Mediterranean coral: its use and exchange in and around the alpine region during the later Neolithic and copper age. *Oxford Journal of Archaeology* 12, pp. 281-292.

Smith C.P., McClure S.F., Eaton-Magaña S., Kondo D.M., 2007. Pink-to-red coral: a guide to determining origin of color. *Gems & Gemology* 43, pp. 4-15.

Song Z., Tegus O. 2023. The Corrosion Properties of Bronze Alloys in NaCl Solutions. *Materials* 16, 5144, pp. 1-13. https://doi.org/10.3390/ma16145144

Sordi M. 1986. Etruschi e Celti nella pianura padana: analisi delle fonti antiche. In de Marinis 1986, 1, pp. 111-115.

Sormani M.A. 2013 (2011-2012). La necropoli protostorica di Gudo, Canton Ticino: dall'epoca del Bronzo alla seconda età del Ferro. *Rivista Archeologica dell'antica Provincia e Diocesi di Como* 193-194, pp. 5-160.

Spagnolo Garzoli G. 2009 (a cura di), *I celti di Dormelletto*. Verbania.

Squarzanti M. 2009. La collezione Bellini. In de Marinis *et al*. 2009, pp. 371-375.

Squarzanti M. 2017. Modi e mode dell'abbigliamento nell'area prealpina golasecchiana. In Miedico C., Tassinari G. (a cura di), *Nei panni degli altri: costumi e accessori inconsueti nella Lombardia antica*. Varese, pp. 11-24.

Squarzanti M. 2021. Le tombe del 1932 (?) di Sesto Calende, via Montrucco (area SIAI). *Zixu. Studi sulla cultura celtica di Golasecca*, pp. 113-124.

Stanley S.M., Hardie L.A. 1998. Secular oscillations in the carbonate mineralogy of reef-building and sediment-producing organisms driven by tectonically forced shifts in seawater chemistry. *Palaeogeography, Palaeoclimatology, Palaeoecology* 144, pp. 3-19. https://doi.org/10.1016/S0031-0182(98)00109-6

Stephenson A.E., DeYoreo J.J., Wu L., Wu K.J., Hoyer J., Dove P.M. 2008. Peptides enhance magnesium signature in calcite: Insights into origins of vital effects. *Science* 322, pp. 724-727. https://doi.org/10.1126/science.1159417

Tagliente M. 2006. Coralli segreti. Immagini e miti dal mare tra Oriente ed Occidente. In *Coralli segreti* 2006, pp. 11-19.

Tamassia A.M. 1979. Scavi e scoperte, 35. Roncoferraro (Mantova). *Studi Etruschi*, serie III, volume XLVII, pp. 520-521.

Tansella F., Vigorelli L., Ricchiardi G., Re A., Bonizzoni L., Grassini S., Staropoli M., Lo Giudice A. 2022. X-ray Computed tomography analysis of historical woodwind instruments of the late eighteenth century. *Journal of Imaging* 8, pp. 1-13. https://doi.org/10.3390/jimaging8100260

Tappen N.C., Peske G.R. 1970. Weathering Cracks and Split-Line Patterns in Archaeological Bone. *American Antiquity* 35, pp. 383-386. https://doi.org/10.2307/278350

Taviani M. 1997. L'uomo e il corallo. In Endrizzi, Marzatico 1997, pp. 151-152.

Taviani M., Freiwald A., Zibrowius H. 2005. Deep coral growth in the Mediterranean Sea: an overview. In Freiwald A., Murray R.J. (eds.), *Cold-water corals and ecosystems*. Berlin, pp. 137-156.

Tessmann B. 2007. Körbchenanhänger im Süden – Göritzer Bommeln im Norden1. Eine vergleichende Studien zu einem späthallstattzeitlichen Anhängertyp. In M. Blečić, M. Črešnar, B. Hänsel, A. Hellmuth, E. Kaiser, C. Metzner-Nebelsick (eds.), *Scripta praehistorica in honorem Biba Teržan*, Situla 44, pp. 667-694.

Teržan B., de Marinis R.C. 2018. The Northern Adriatic. In Haselgrove C., Rebay- Salisbury K., Wells P.S. (eds.), *The Oxford Handbook of the European Iron Age*. Oxford. 10.1093/ oxfordhb/ 9780199696826.013.32

Tombolani M. 1987. Materiali di tipo La Tène da Altino. In Vitali 1987, pp. 171-189.

Tori L., Carlevaro E., della Casa P., Pernet L., Schmid-Sikimic B. 2010. *La necropoli di Giubiasco (TI), 3. Le tombe dell'età del Bronzo, della prima età del Ferro e del La Tène antico e medio. La sintesi.* Zürich.

Trainito E., Baldacconi R. 2016. *Coralli del Mediterraneo*. Cornaredo.

Ugolini D. 2006a. Il corallo tra il VII e il II sec. a.C. lungo le coste della Catalogna e della Gallia. In *Coralli segreti* 2006, pp. 78-87.

Ugolini D. 2006b. Il corallo antico in Italia. In *Coralli segreti* 2006, pp. 89-98.

Ugolini D., Rondi-Costanzo C., Perrin F., D'andria F., Mastronuzzi G. 2000. Le corail dans le monde indigène préromain d'Italie méridionale. In Morel *et al.* 2000, pp. 139-146.

Urmos J., Sharma S.K., Mackenzie F.T. 1991. Characterization of some biogenic carbonates with Raman spectroscopy. *American Mineralogist* 76, pp. 641-646.

Vanzini R. 2018. Alle origini di Felsina. L'abitato villanoviano della Fiera. *Ocnus. Quaderni della Scuola di Specializzazione in Beni Archeologici* 26, pp. 19-39.

Vanzini R. 2023. *La formazione di Felsina/ Bologna tra Bronzo finale e prima Età del Ferro*, DISCI. Archeologia 32. Bologna.

Venturino Gambari M. (a cura di) 2001. *Dai Bagienni a Bredulum. Il pianoro di Breolungi tra archeologia e storia*, Quaderni della Soprintendenza Archeologica del Piemonte (Monografie) 9. Torino.

Venturino Gambari M. 2001a. Il pianoro di Breolungi tra l'età del Bronzo finale e l'età del Ferro. In Venturino Gambari 2001, pp. 13-30.

Venturino Gambari M. (a cura di) 2009. *Il ripostiglio del Monte Cavanero di Chiusa di Pesio*. Alessandria.

Venturino Gambari M. (a cura di) 2014. *La memoria del passato. Castello di Annone tra archeologia e storia.* ArcheologiaPiemonte 2. Alessandria.

Venturino Gambari M. 2014a. Lungo le vie di Annone. Preistoria e Protostoria a Castello di Annone. In Venturino Gambari 2014, pp. 39-69.

Venturino M. 2024. Celti, Liguri ed Etruschi: il Piemonte nell'età del Ferro. In *Gli Etruschi nella Valle del Po*. Atti del XXX Convegno Nazionale di Studi Etruschi ed Italici (Bologna 23-25 giugno 2022). Atti di Convegni 30. Roma, 837-857. https://doi.org/10.26406/AC30

Venturino Gambari M., Roncaglio M., Cazzulo M., Scarrone F. 2014. Pontecurone, località Cascina Torre. Tracce di frequentazione dalla preistoria al Medioevo. *Quaderni della Soprintendenza Archeologica del Piemonte* 29, pp. 110-115.

Venturino M., Giaretti M. (a cura di) 2021. *Villa del Foro. Un emporio ligure tra Etruschi e Celti*. Archeologia Piemonte 8. Genova.

Verger S. 2006a. La grande tombe de Hochdorf, mise en scène funéraire d'un 'cursus honorum' tribal hors pair. *Siris* 7, pp. 5-44.

Verger S. 2006b. A propos des vieux bronzes du dépôt d'Arbedo. Essai de séquençage d'un ensemble complexe. In Bataille G., Guillaumet J.-P. (dir.), *Les depots metalliques au second age du Fer en Europe temperee*. Actes de la table ronde, Glux-en-Glenne (Bibracte, 13-14 octobre 2004). Bibracte, 11, pp. 23-55.

Vidale M. 2001. On the exploitation of corals in the Indus tradition. *South Asian archaeology* 1, pp. 316-325.

Vidale M., Pignatti J., Langella L., Guida G. 2015. Symbols at War. The Impact of *Corallium rubrum* in the Indo-Pakistani Subcontinent. In Narchi N., Leimar Price L. (eds.), *Ethnobiology of Corals and Coral Reefs*. Berlin, pp. 59-72.

Vielzeuf D., Garrabou J., Baronnet A., Grauby O., Marschal C. 2008. Nano to macroscale biomineral architecture of red coral (*Corallium rubrum*). *American Mineralogist* 93, pp. 1799-1815. https://doi.org/10.2138/am.2008.2923

Vielzeuf D., Garrabou J., Gagnon A., Ricolleau A., Adkins J., Günther D., Hametner K., Devidal J.-L., Reusser E., Perrin J. 2013. Distribution of sulphur and magnesium in the red coral. *Chemical Geology* 355, pp.13-27. http://dx.doi.org/10.1016/j.chemgeo.2013.07.008

Vigorelli L. 2023. *Dimensional measurements with X-ray Computed Tomography and application to Cultural Heritage.* PhD Thesis. Politecnico di Torino.

Viollier D. 1907. Etude sur les fibules de l'age du fer trouvées en Suisse: essai de typologie et de chronologie; epoque gauloise. *Indicateur des Antiquités suisses* IX band, 2 heft, pp. 8-22.

Vitali D. (a cura di) 1987. *Celti ed Etruschi nell'Italia centro-settentrionale dal V secolo alla romanizzazione.* Atti del Colloquio

internazionale (Bologna 12-14 aprile 1985), Imola.

Vitali D. 1991. I Celti in Italia. In *I Celti.* Catalogo della mostra, Palazzo Grassi (Venezia). Milano, pp. 220-235.

Vitali D. 2014. I Celti d'Italia (IV-I secolo a.C.) tra identità e assimilazioni. In Lamberg-Karlovsky C.C, Genito B., Cerasetti B (eds.), *'My Life is like the Summer Rose' Maurizio Tosi e l'Archeologia come modo di vivere. Papers in honour of Maurizio Tosi for his 70th birthday.* BAR International Series 2690. Oxford, pp. 733-754.

Vitri S. 1997. Gli oggetti di ornamento tra il I sec. a.C. e la prima età imperiale: influssi culturali e romanizzazione. In Endrizzi, Marzatico 1997, pp. 564-569.

Vitri S., Corazza S., Righi G. 2014. L'area alpina friulana nell'età del Ferro: lo stato delle conoscenze. In Roncador, Nicolis 2014, pp. 229-244.

Voltolini D. 2019. Presualdo di Sesto Calende: prime considerazioni a partire dalle tombe del recupero 1997. *Zixu. Studi sulla cultura celtica di Golasecca* 3, pp. 47-56.

von Eles Masi P. 1986. *Le fibule dell'Italia settentrionale*. Prähistorische Bronzefunde XIV. 5. München.

Weber S. 1925. Sanzeno. *Studi trentini* VI, pp. 188-189.

Weinbauer M.G., Brandstätter F., Velimirov B. 2000. On the potential use of magnesium and strontium concentrations as ecological indicators in the calcite skeleton of the red coral (*Corallium rubrum*). *Marine Biology* 137, pp. 801-809.

Weinberg S. 1994. Il corallo rosso e la ricerca scientifica nei secoli. In Cicogna, Cattaneo-Vietti 1994, pp. 37-60.

Welc F., Nebelsick L., Metzner- Nebelsick C., Balzer I., Vanzetti A., Grassi B. 2020. The first results of geophysical prospections using the ADC method on the proto-urban settlement site of Como, Spina Verde. In Zamboni *et al.* 2020, pp. 257-2 74.

Windler A. 2019. The use of *Spondylus gaederopus* during the Neolithic of Europe. *Journal of Open Archaeology Data* 7, pp. 1-5. https://doi.org/10.5334/joad.59

WoRMS Editorial Board 2024. World Register of Marine Species. Available from https://www.marinespecies.org at VLIZ. https://doi.org/10.14284/170

Yoshioka S., Kitano Y. 1985. Transformation of aragonite to calcite through heating. *Geochemical Journal* 19, pp. 245-249.

Zamboni L. 2018. *Sepolture arcaiche della pianura emiliana. Il riconoscimento di una società di frontiera*. Reditus (Riflessioni di archeologia) 1. Roma.

Zamboni L. 2021a. Passaggio in Liguria: L'insediamento dell'età del Ferro sull'altura del Castello di Serravalle Scrivia. In Giorcelli Bersani, Venturino 2021, pp. 271-280.

Zamboni L. 2021b. The Urbanization of Northern Italy: Contextualizing Early Settlement Nucleation in the Po Valley. *Journal of Archaeological Research* 29, pp. 387-430.

Zamboni L. 2022. Do you think we are Etruscans? Recognition issues in the 6th century BCE Po valley. In Saccoccio F., Vecchi E. (eds.), *Who do you think you are? Ethnicity in the Iron Age mediterranean*. Accordia specialist studies on the Mediterranean 8. London, pp. 77-96.

Zamboni L. 2025. I Celti nella valle del Po. Mobilità, visibilità e modelli interpretativi. In Chiappelloni P., Storchi P. (a cura di), *Piacenza, Etruria. Il Fegato di Piacenza, gli Etruschi e gli altri popoli antichi in Emilia occidentale*. Bologna, pp. 33-58.

Zamboni L., Fernández-Götz M., Metzner-Nebelsick C. (eds.) 2020. *Crossing the alps. Early urbanism between northern Italy and central Europe (900-400 BC)*. Leiden.

Zibrowius H., Taviani M. 2005. Remarkable sessile fauna associated with deep coral and other calcareous substrates in the Strait of Sicily, Mediterranean Sea. In Freiwald A., Murray R.J. (eds.), *Cold-water corals and ecosystems*. Berlin, pp. 807-819.

Zlámalová Cílová Z., Čisťakova V., Brychová V., Lapčák L., Březinová G., Kmječ T., Matoušková Š., Čižmářová H. 2024. Non-metallic decorative inlays in La Tène jewellery - contribution of archaeometry to the understanding of production technologies. *Archaeological and Anthropological Science* 16, p. 60. https://doi.org/10.1007/s12520-024-01963-0

Appendix 1 – Supplementary Figures

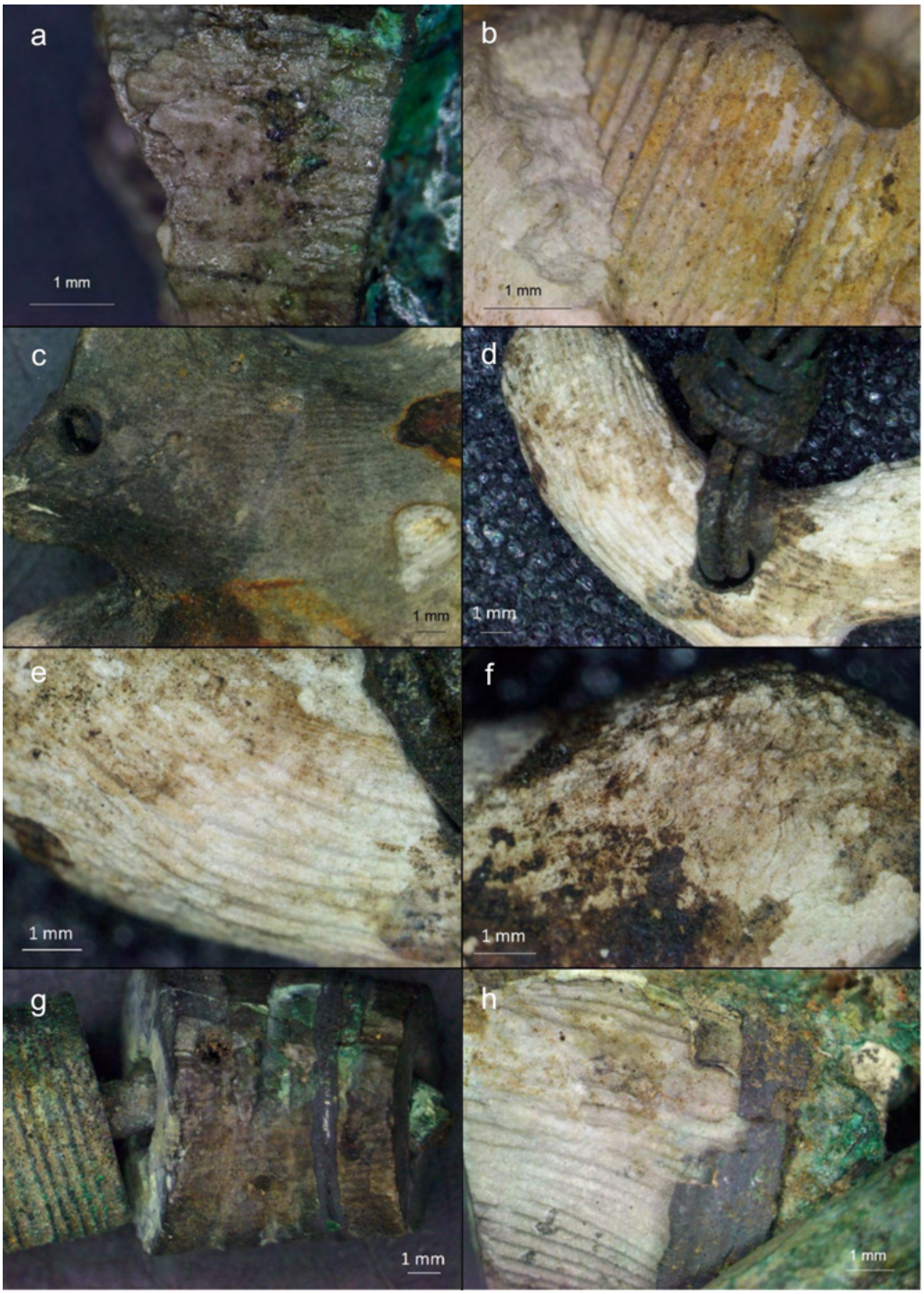

Figure 215. a) Crenulation (Castelletto Ticino, Motto d'Egro; Longone al Segrino pendant; inv. no. CT179; GSAC); b) Crenulation (Brembate Sotto; composite bow fibula; inv. no. 3051; Museo Civico Archeologico Bergamo); c) Crenulation (Golasecca; Longone al Segrino pendant; inv. no. D1669; Museo Giovio Como); d) Crenulation (Castelletto Ticino; Longone al Segrino pendant; inv. no. D1750; Museo Giovio Como); e) Crenulation (Castelletto Ticino; Longone al Segrino pendant; inv. no. D1750; Museo Giovio Como); f) Medullar region concentric structures (Castelletto Ticino; Longone al Segrino pendant; inv. no. D1750; Museo Giovio Como); g) Crenulation (Como, Respaù; composite bow fibula; inv. no. E5957; Museo Giovio Como); h) Crenulation (Como, Respaù; composite bow fibula; inv. no. E5958; Museo Giovio Como).

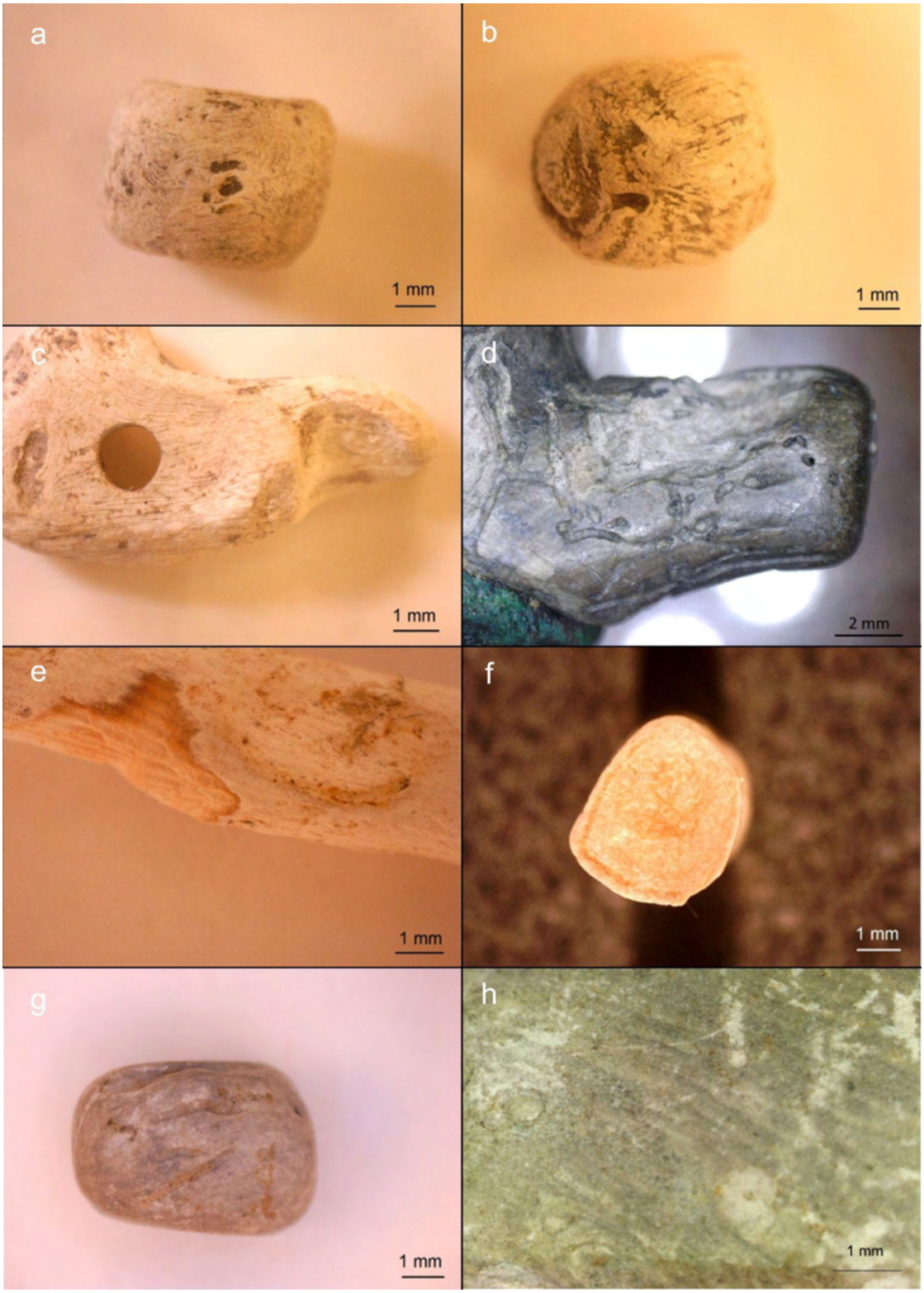

Figure 216. a) Medullar region concentric structures (Pieve d'Alpago; bead; inv. no. I.G.355538; SABAP); b) Medullar region concentric structures (Pieve d'Alpago; bead; inv. no. I.G. 355542; SABAP); c) Crenulation and medullar region concentric structures (Pieve d'Alpago; bead; inv. no. I.G. 355679; SABAP); d) Bio-attack (Golasecca; Longone al Segrino pendant; inv. no. MV103; Museo Civico Archeologico Villa Mirabello Varese); e) Crenulation (Piovego, grave 5.99; UNIPD); f) Medullar region concentric structures (Piovego, grave 5.99; UNIPD); g) Bio-attack (Piovego, grave 110.13; UNIPD); h) Crenulation (Como, Ca' Morta; composite bow fibula; inv. no. St. 1230; Museo Giovio Como).

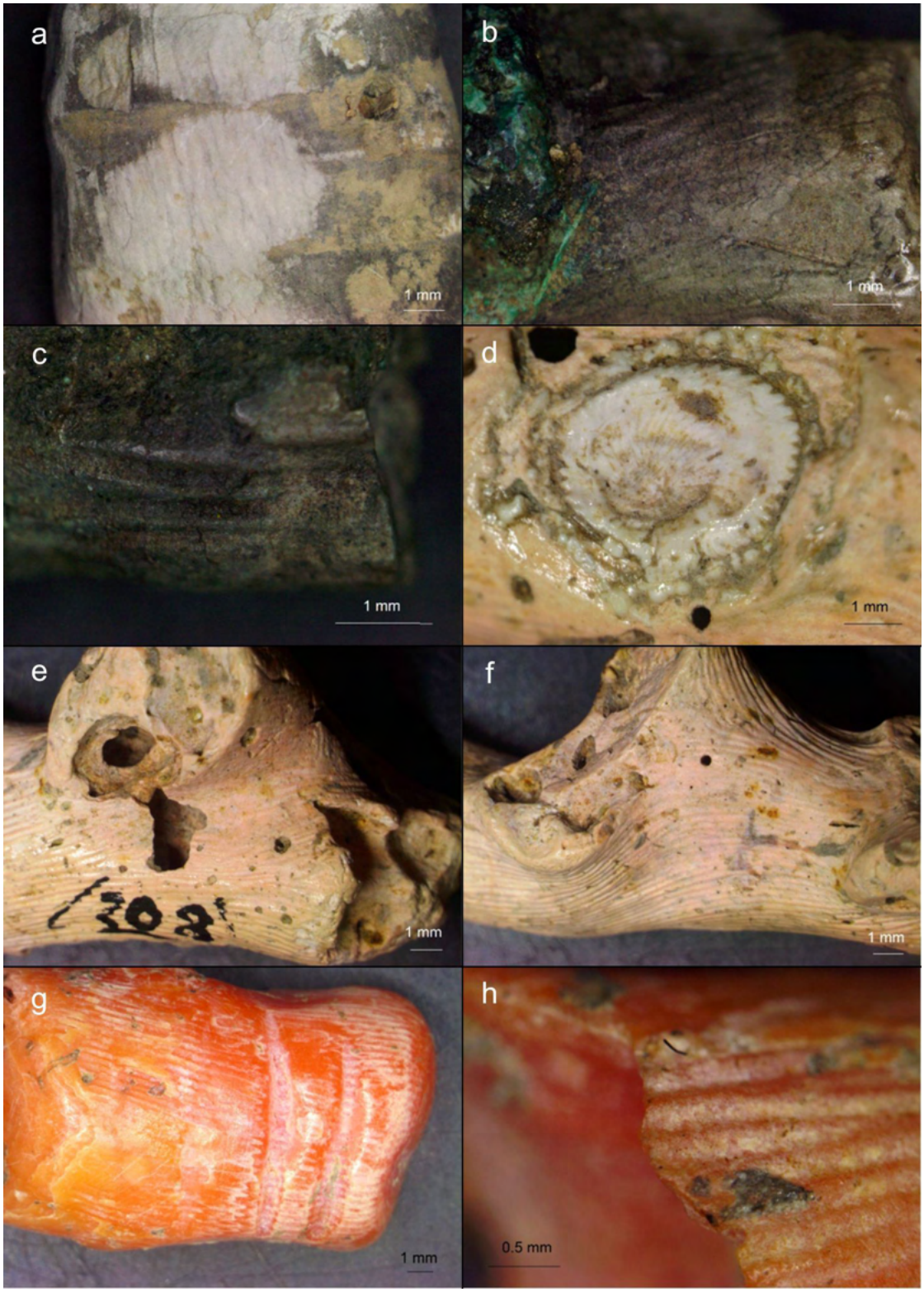

Figure 217. a) Crenulation (Como, Ca' Morta; composite bow fibula; inv. no. St 1397; Museo Giovio Como); b) Crenulation (Como, Ca' Morta; Longone al Segrino Pendant; inv. no. St33593; Museo Giovio Como); c) Crenulation (Como, Ca' Morta; Longone al Segrino Pendant; inv. no. St. 33594; Museo Giovio Como); d) Shell (Forcello di Bagnolo San Vito; inv. no. St.78799; Museo Nazionale Mantova); e) Crenulation and bio-attack (Forcello di Bagnolo San Vito; inv. no. St.78799; Museo Nazionale Mantova); f) Crenulation (Forcello di Bagnolo San Vito; inv. no. St.78799; Museo Nazionale Mantova); g) Crenulation (Forcello di Bagnolo San Vito; inv. no. St. 78797; Museo Nazionale Mantova); h) Crenulation (Forcello di Bagnolo San Vito; inv. no. St. 78798; Museo Nazionale Mantova).

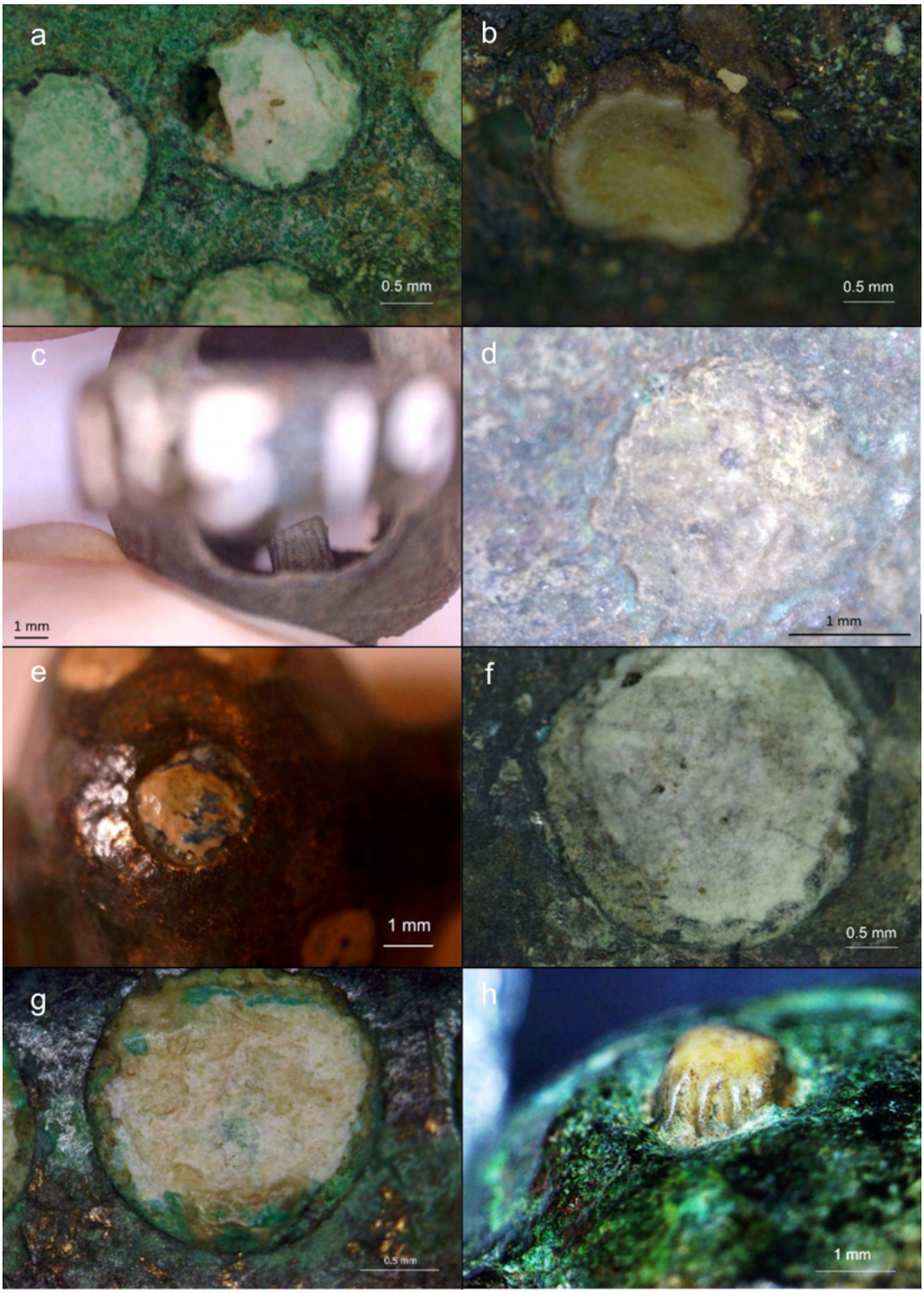

Figure 218. a) Garland-like morphology (Borgonovo V. T., leech fibula with circular insets; inv. no. 20.S258-2.119; Museo Archeologico della Valle Tidone); b) Garland-like morphology (Borgonovo V. T., leech fibula with circular insets; inv. no. 20.S258-2.171; Museo Archeologico della Valle Tidone); c) Crenulation (Golasecca, bucket pendant; inv. no. A.4858; Musei Civici Milano); d) Garland-like morphology (Golasecca, Lazzaretto, leech fibula with circular insets; inv. no. A.17519; Musei Civici Milano); e) Garland-like morphology (Cavarzano, Masiera, leech fibula with circular insets; inv. no. 217; Museo Civico Belluno); f) Garland-like morphology (Golasecca, leech fibula with circular insets; inv. no. D2049; Museo Giovio Como); g) Garland-like morphology (Motto Lagone - grave 1, leech fibula with circular insets; Museo Archeologico Arona); h) Garland-like morphology (Pianello V. T., leech fibula with circular insets; inv. no. St. 200191; Museo Archeologico della Valle Tidone).

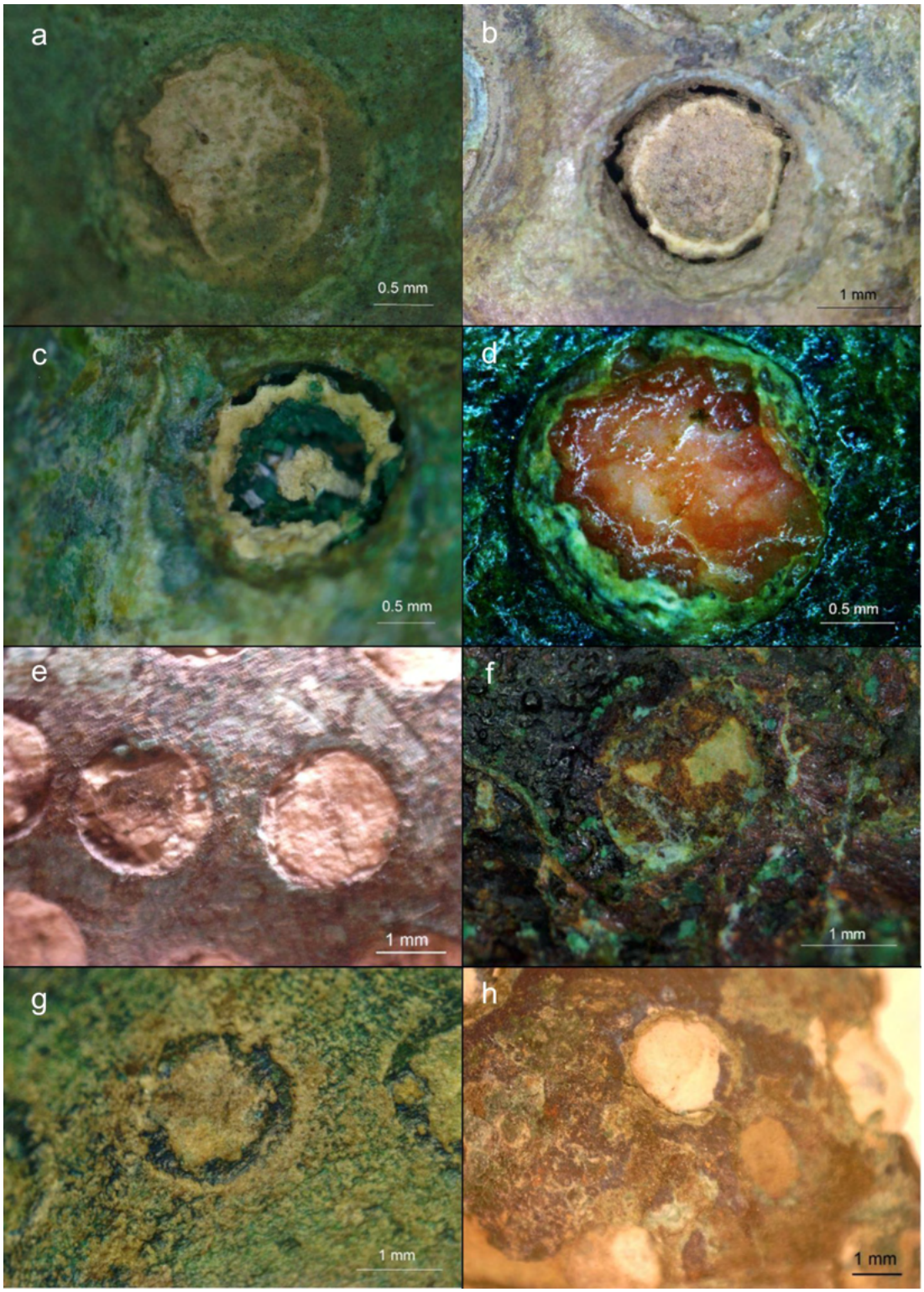

Figure 219. a) Garland-like morphology (Como, leech fibula with circular insets; inv. no. St. 57210; Museo Giovio Como), b) Garland-like morphology (Villa del Foro, leech fibula with circular insets; inv. no. St. 66132; Musei Reali Torino); c) Garland-like morphology (Pombia, leech fibula with circular insets; inv. no. St. 83946; Museo Fanchini Oleggio); d) Garland-like morphology (Mantova, leech fibula with circular insets; inv. no. St. 169519; Museo Nazionale Mantova); e) Unknown provenance; Leech fibula with circular insets (inv. no. MV589/3; Bra Museum): whitish inlays; f) Golasecca; Leech fibula with circular insets (inv. no. D2059; Museo Giovio Como): green metallic alteration products on the circular decoration; g) Como; Leech fibula with circular insets (inv. no. St.57244; Museo Giovio Como): green metallic alteration products on the circular decoration; h) Piovego, Padua; Leech fibula with circular insets (inv. no. I.G. 34914, UNIPD): blue metallic alteration products on the circular decoration.

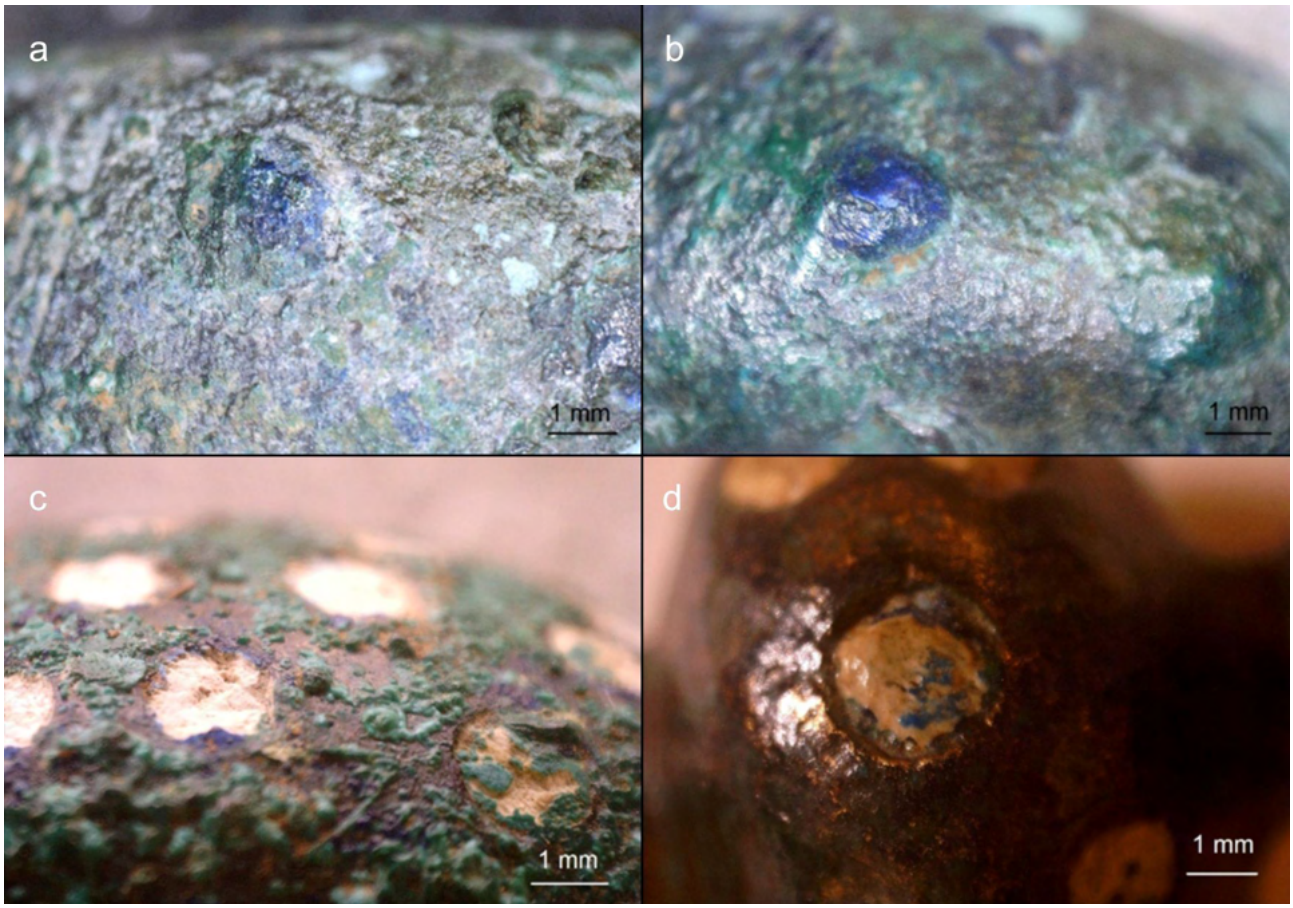

Figure 220. a) Montebelluna, loc. Posmon; Leech fibula with circular insets (inv. no. I.G. 304780, Montebelluna Museum): blue metallic alteration products on the circular decoration; b) Montebelluna, loc. Posmon; Leech fibula with circular insets (inv. no. I.G. 304784, Montebelluna Museum): blue metallic alteration products on the circular decoration; c) Pieve d'Alpago; Leech fibula with circular insets (inv. no. I.G. 312348, SABAP): blue metallic alteration products on the circular decoration; d) Cavarzano, Masiera; Leech fibula with circular insets (inv. no. 217, Museo Civico Belluno): blue metallic alteration products on the circular decoration.

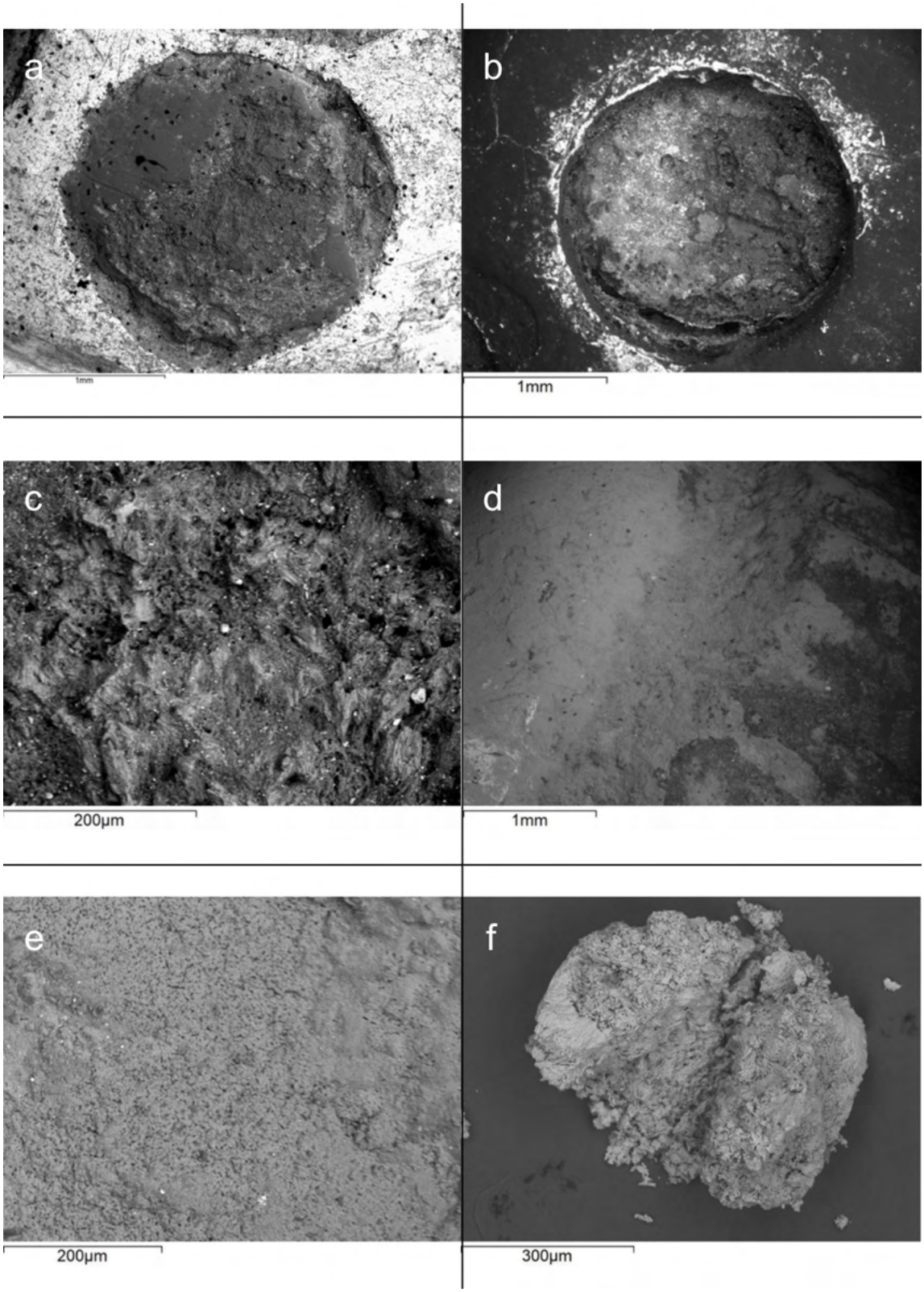

Figure 221. a) BSE-image of a circular decoration (Motto Lagone, T1); b) BSE-image of a circular decoration with high presence of Paraloid on the metal surface (Motto Lagone, T1); c) BSE-image of a circular decoration (Motto Lagone, T1): multi-branched micro-morphology; d) BSE-image of a pendant surface (Brembate Sotto, inv. no. 3016): garland-like wavy structure; e) BSE-image of an element of a composite bow fibula (Brembate Sotto, inv. no. 3052): micro-porous morphology; f) BSE-image of a sample from a circular decoration (Brignano Frascata, inv. no. C-FR-NE/2): multi-branched micro-morphology.

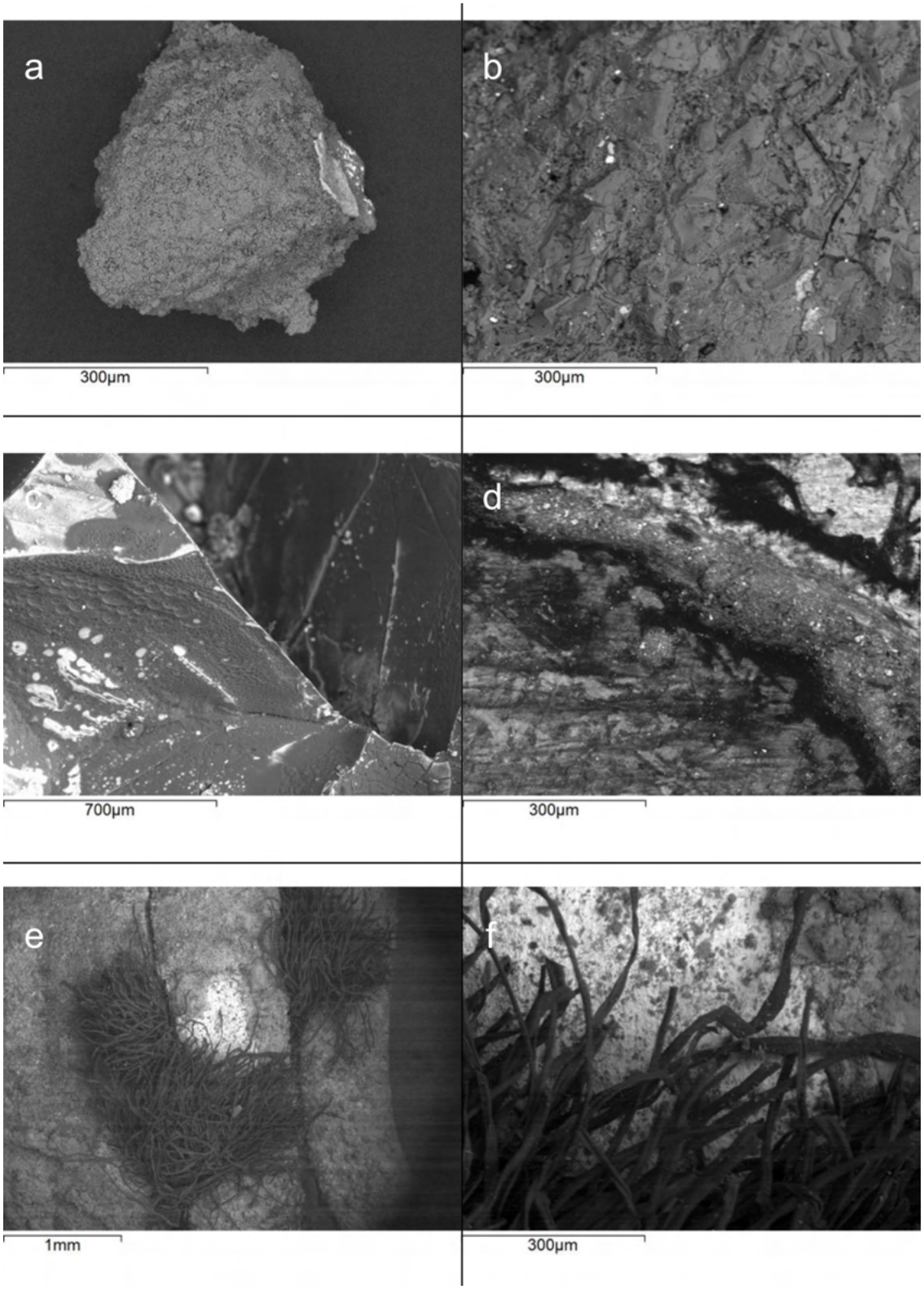

Figure 222. a) BSE-image of a sample from a circular decoration (Brignano Frascata, inv. no. C-FR-NE/2): mammellonary micro-morphology; b) BSE-image of a vitreous bead (Motto Lagone, grave 1): conchoid micro-morphology: c) BSE-image of a vitreous bead (Castelletto Ticino, inv. no. CT14031X, CT868c): high presence of Paraloid on the surface; d) BSE-image of a circular decoration (Como, via Isonzo, inv. no. St.57220): detail of the presence of incoherent material standing between the inset and the border of the hole containing it; e) BSE-images of Longone al Segrino type pendant (Castelletto Ticino, inv. no. D1750): detail of the presence of fibre residues trapped in the bronze rod spring; f) BSE-images of Longone al Segrino type pendant (Castelletto Ticino, inv. no. D1750): detail of the presence of fibre residues trapped in the bronze rod spring.

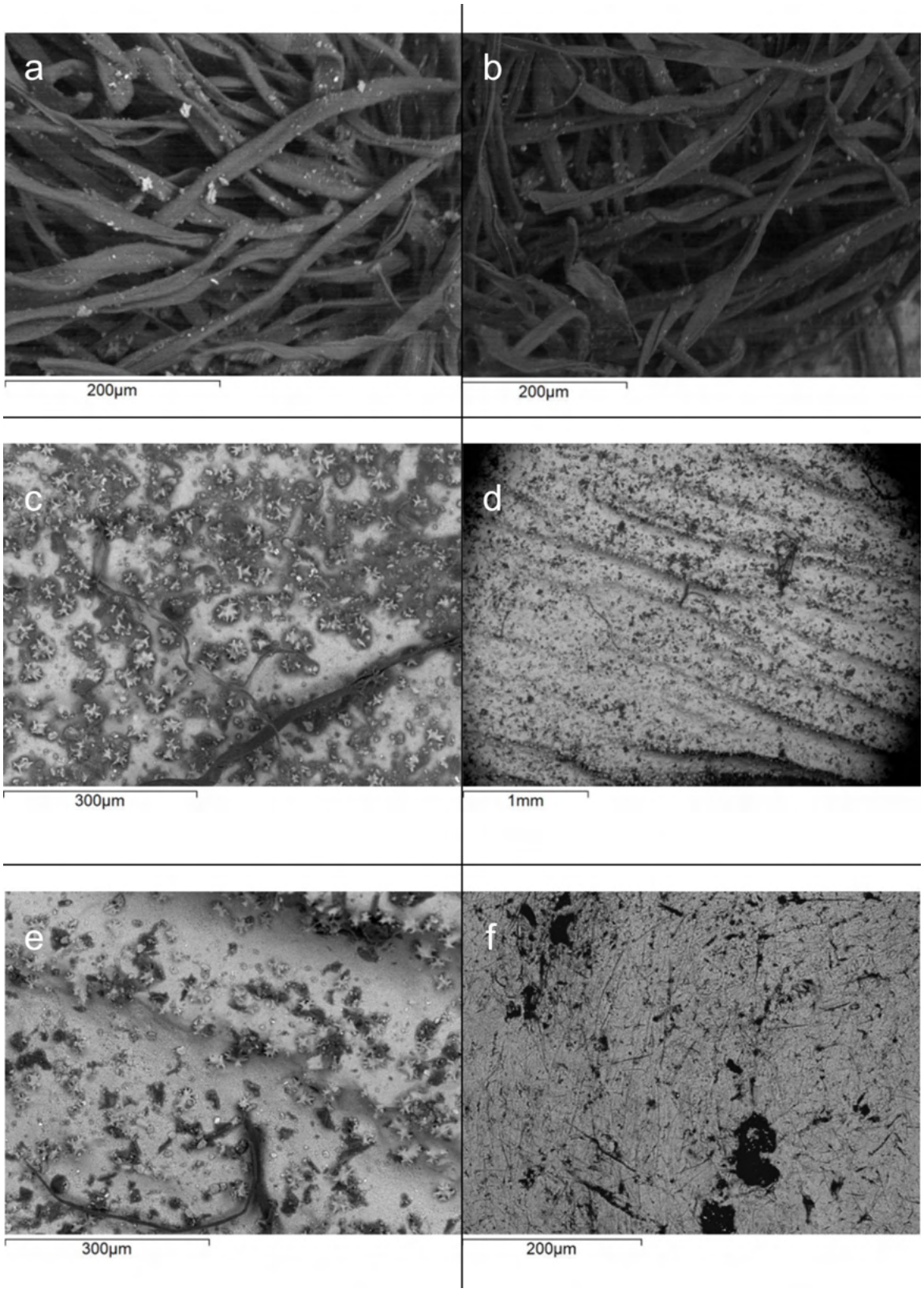

Figure 223. a) BSE-images of Longone al Segrino type pendant (Castelletto Ticino, inv. no. D1750): detail of the presence of fibre residues trapped in the bronze rod spring; b) BSE-images of Longone al Segrino type pendant (Castelletto Ticino, inv. no. D1750): detail of the presence of fibre residues trapped in the bronze rod spring; c) BSE-image of 'r_Cr_L': ligurian *C. rubrum* with sclerites.; d) BSE-image of 'r_Cr_L': ligurian *C. rubrum* with crenulations; e) BSE-image of 'r_Cr_L': ligurian *C. rubrum* with sclerites; f) BSE-image of 'w_Cr_u': polished worked *C. rubrum*.

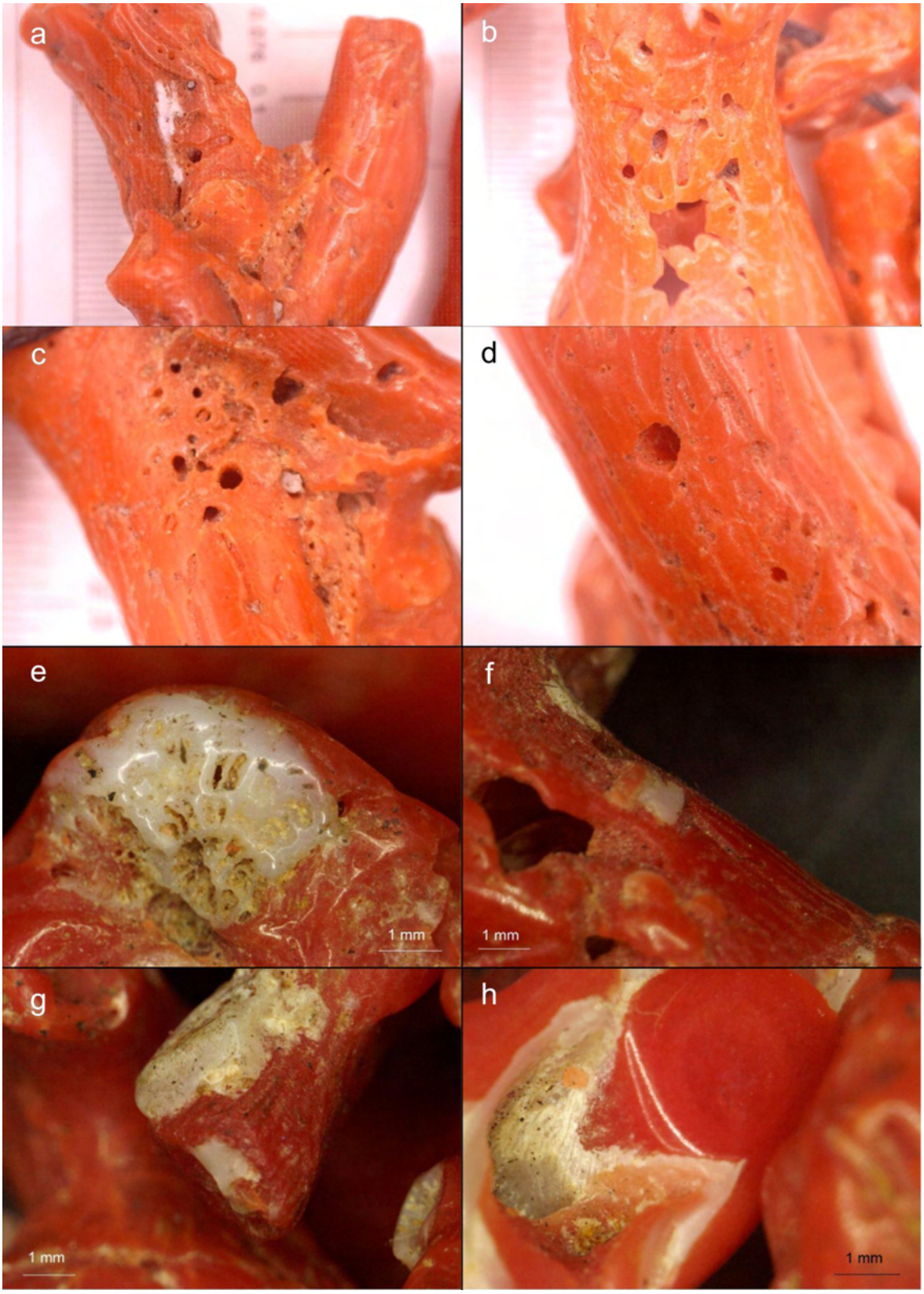

Figure 224. a) Traces of biogenic attack by other organisms (*C. rubrum*, 'r_Cr_Si'); b) Traces of biogenic attack by other organisms (*C. rubrum*, 'r_Cr_Si'); c) Surface smoothing due to marine transport and races of biogenic attack (*C. rubrum*, 'r_Cr_Si'); d) Surface smoothing due to marine transport and races of biogenic attack (*C. rubrum*, 'r_Cr_Si'); e) Surface smoothing due to marine transport (*C. rubrum*, 'r_Cr_Si'); f) Surface smoothing due to marine transport (*C. rubrum*, 'r_Cr_Si'); g) Surface concretions (*C. rubrum*, 'r_Cr_Si'); h) Surface smoothing due to marine transport *C. rubrum*, 'r_Cr_Si').

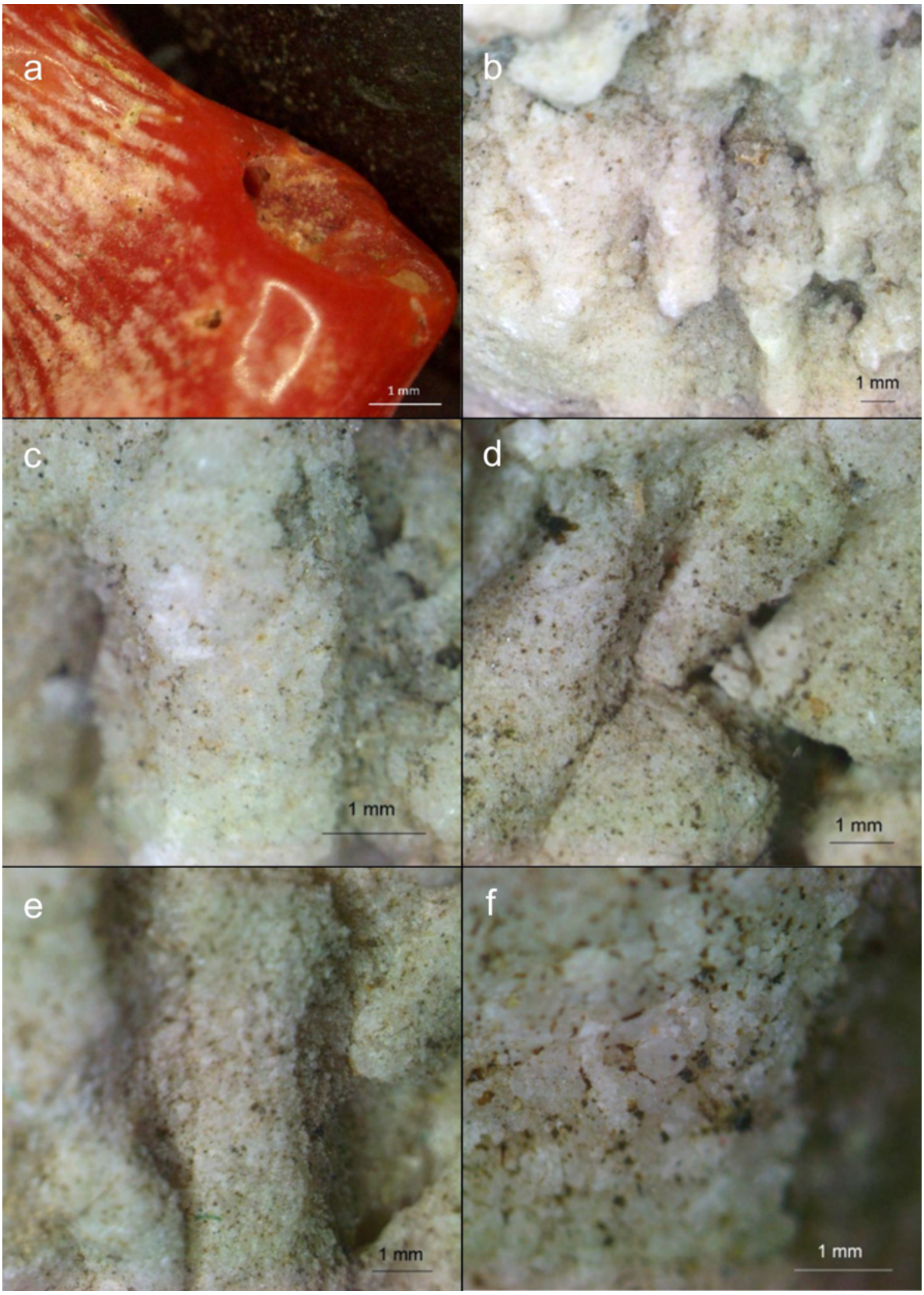

Figure 225. a) Surface smoothing due to marine transport (*C. rubrum*, 'r_Cr_Si'); b) Elongated µ-structures and a grainy, compact surface (fossil Piedmontese coral, 'r_fc_P'); c) Elongated µ-structures and a grainy, compact surface (fossil Piedmontese coral, 'r_fc_P'); d) Elongated µ-structures and a grainy, compact surface (fossil Piedmontese coral, 'r_fc_P'); e) Elongated µ-structures and a grainy, compact surface (fossil Piedmontese coral, 'r_fc_P'); f) Elongated µ-structures and a grainy, compact surface (fossil Piedmontese coral, 'r_fc_P').

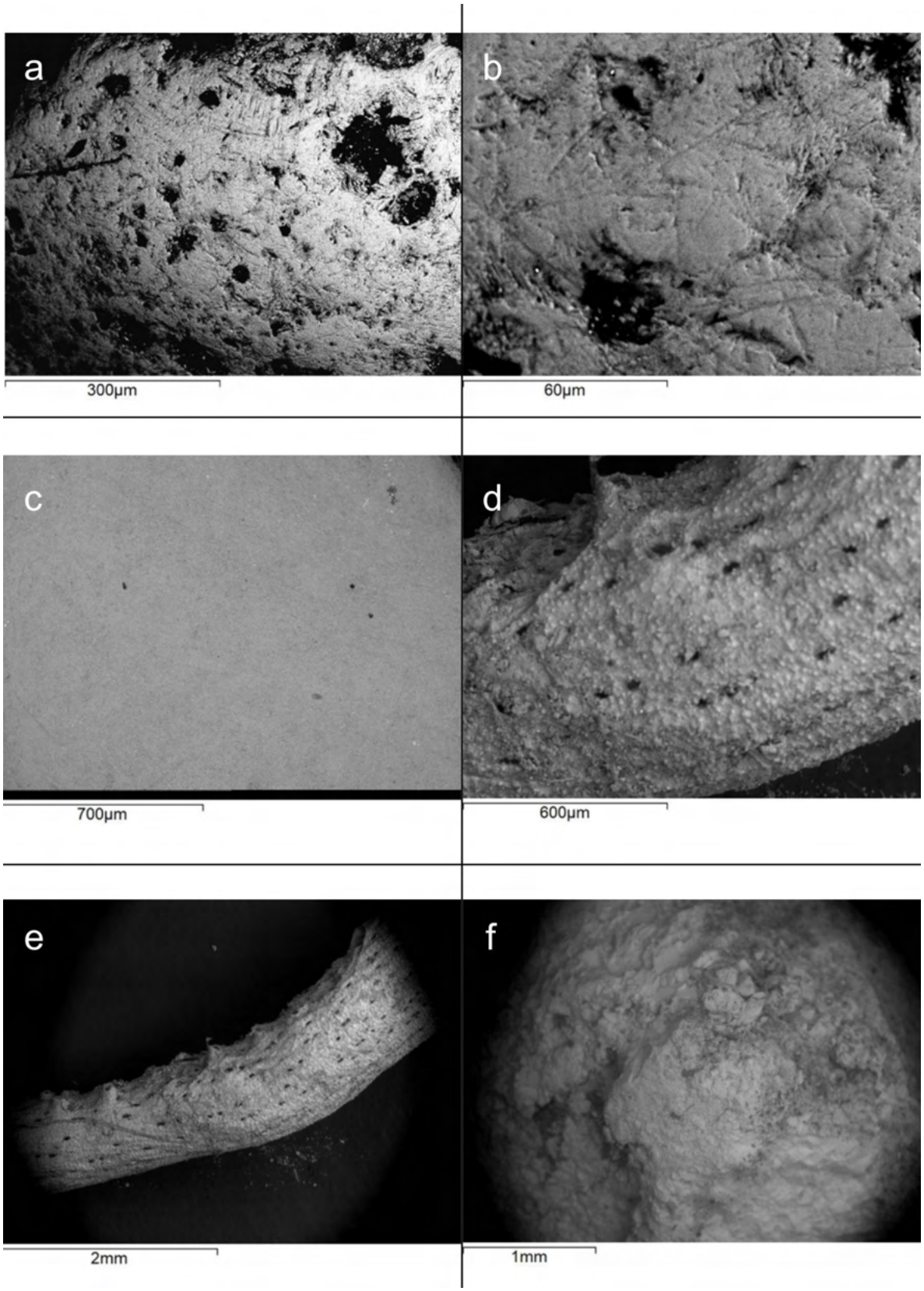

Figure 226. a) BSE-image of 'r_Cr_Si': sicilian *C. rubrum* with traces of marine transport polishing; b) BSE-image of 'r_Cr_Si': sicilian *C. rubrum* with traces of marine transport polishing; c) BSE-image of 'w_pCr_Sa': Sardinian polished worked whitish-to-pink *C. rubrum*; d) BSE-image of 'r_c_L': Ligurian white coral; e) BSE-image of 'r_c_L': Ligurian white coral; f) BSE-image of 'r_fc_P': fossil coral.

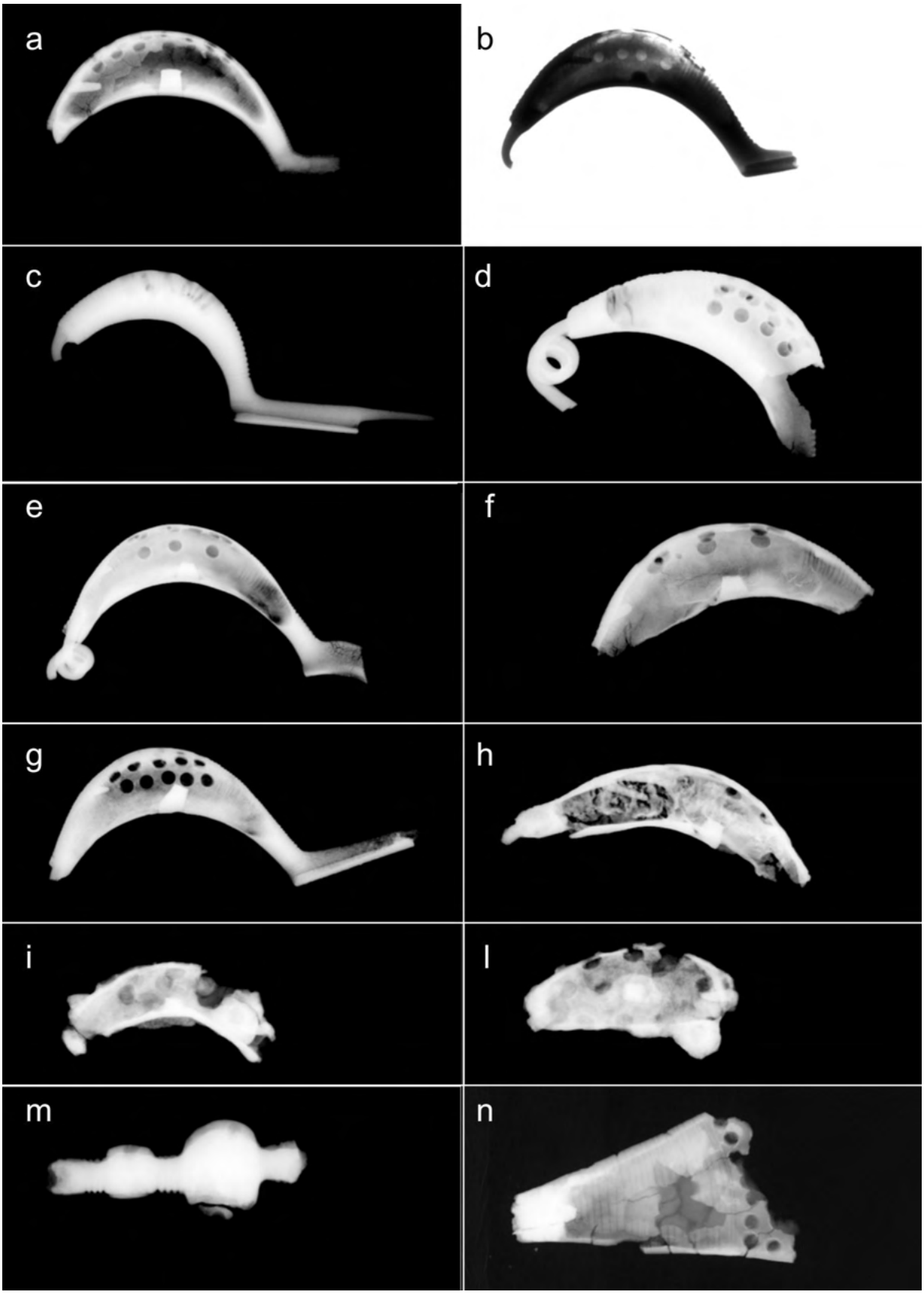

Figure 227. a) Radiography of inv. no. 868; b) Radiography of inv. no. 197; c) Radiography of inv. no. 870; d) Radiography of inv. no. 198; e) Radiography of inv. no. 944; f) Radiography of inv. no. 946; g) Radiography of inv. no. 947; h) Radiography of inv. no. 949; i) Radiography of inv. no.St.83925; l) Radiography of inv. no. St. 83925; m) Radiography of inv. no. St. 83946; n) Radiography of inv. no. St. 83946.

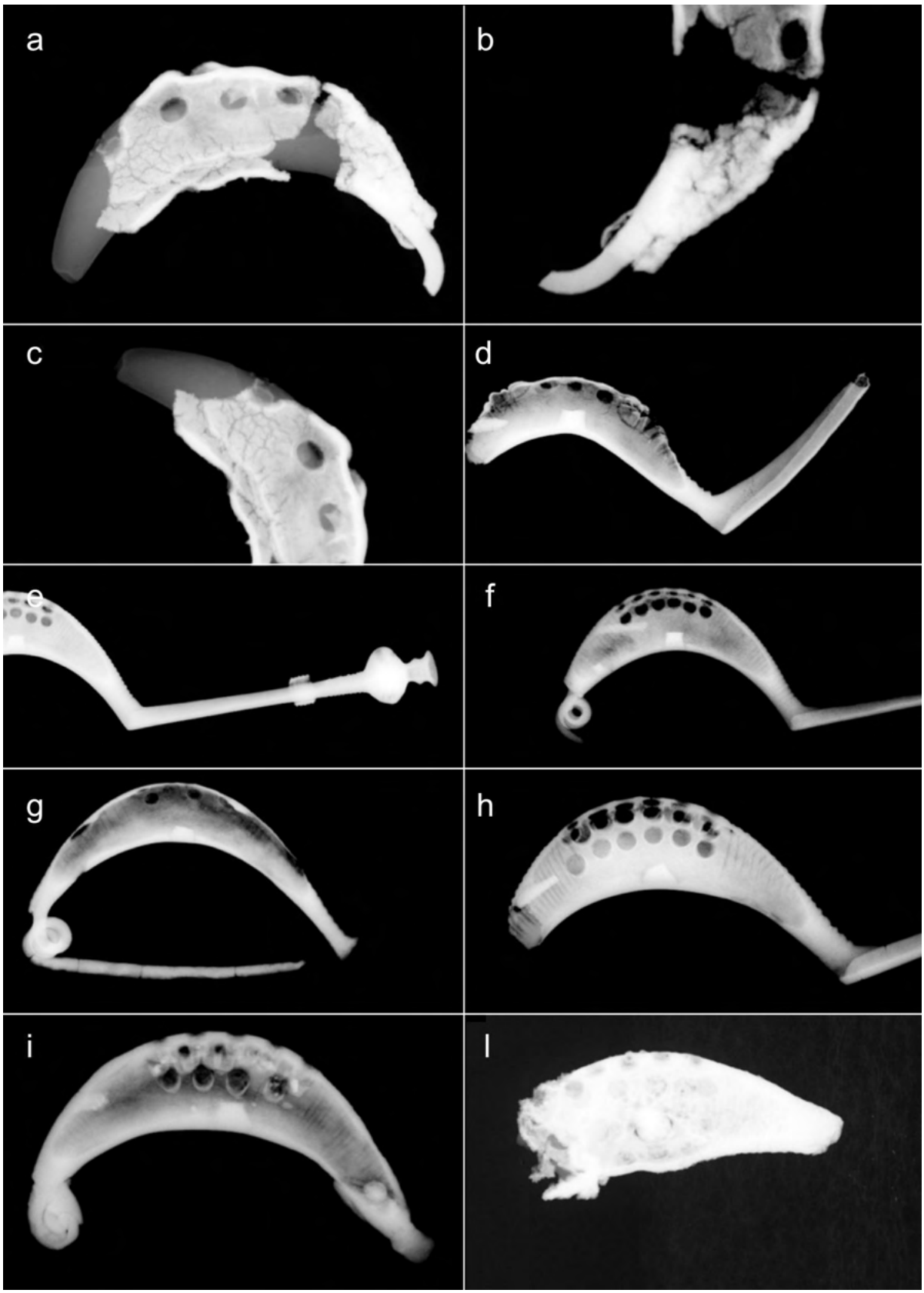

Figure 228. a) Radiography of inv. no. St. 83966, b) Radiography of inv. no.St. 83966, pin; c) Radiography of inv. no. St. 83966; d) Radiography of inv. no. CT29; e) Radiography of inv. no. CT728; f) Radiography of inv. no. CT728; g) Radiography of inv. no. CT1144; h) Radiography of inv. no. D2049; i) Radiography of inv. no. D2059; l) Radiography of inv. no. D2064.

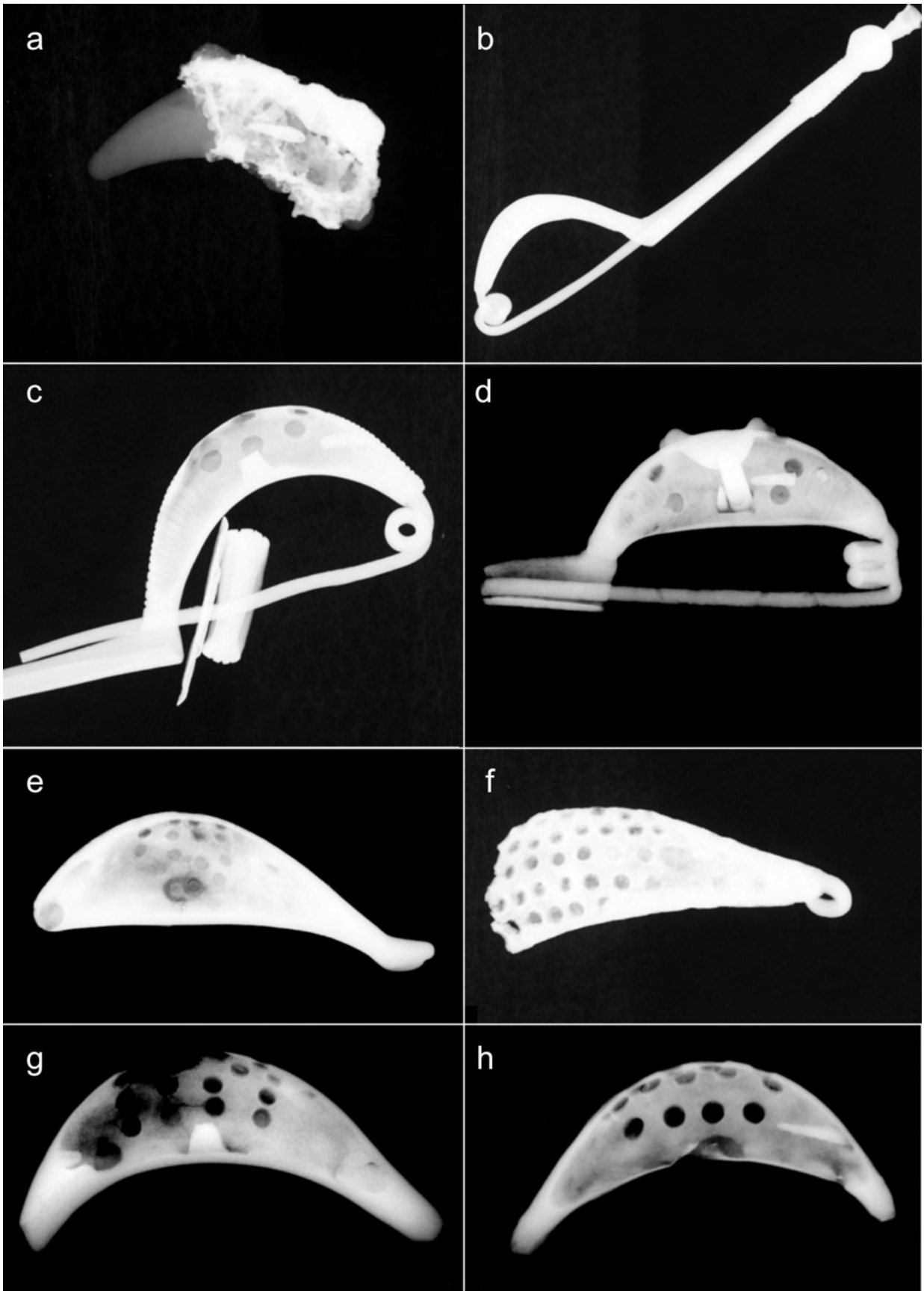

Figure 229. a) Radiography of inv. no. D2073; b) Radiography of inv. no. D2077; c) Radiography of inv. no. D2104; d) Radiography of inv. no. D2773; e) Radiography of inv. no. E5552; f) Radiography of inv. no. E5553; g) Radiography of inv. no. E5667; h) Radiography of inv. no. E5865.

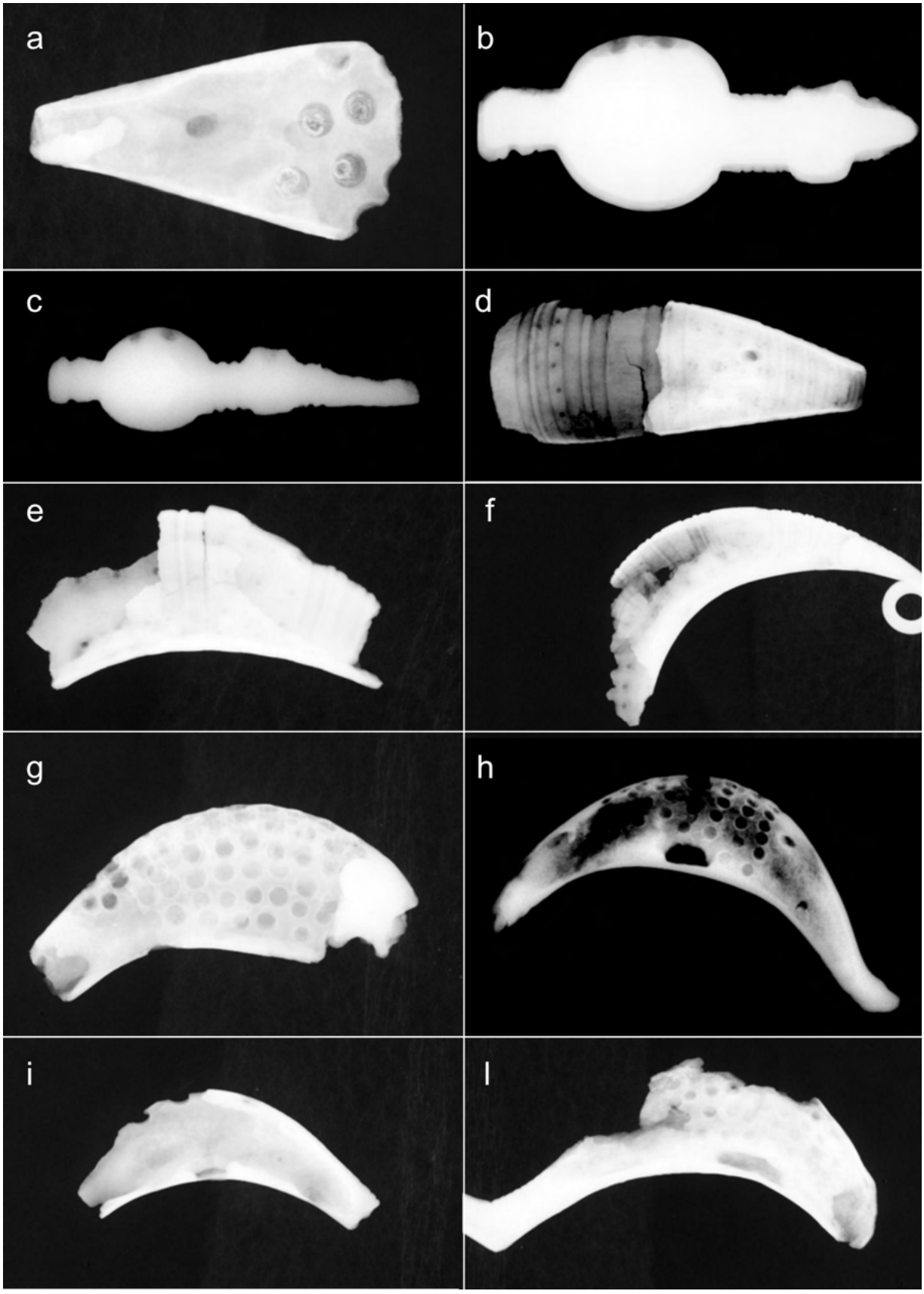

Figure 230. a) Radiography of inv. no. E5868; b) Radiography of inv. no. E5873; c) Radiography of inv. no. E13225; d) Radiography of inv. no. St.864; e) Radiography of inv. no. St.864; f) Radiography of inv. no. St.865; g) Radiography of inv. no. St. 57210; h) Radiography of inv. no. St. 57244; i) Radiography of inv. no. St. 57220; l) Radiography of inv. no. St. 57250.

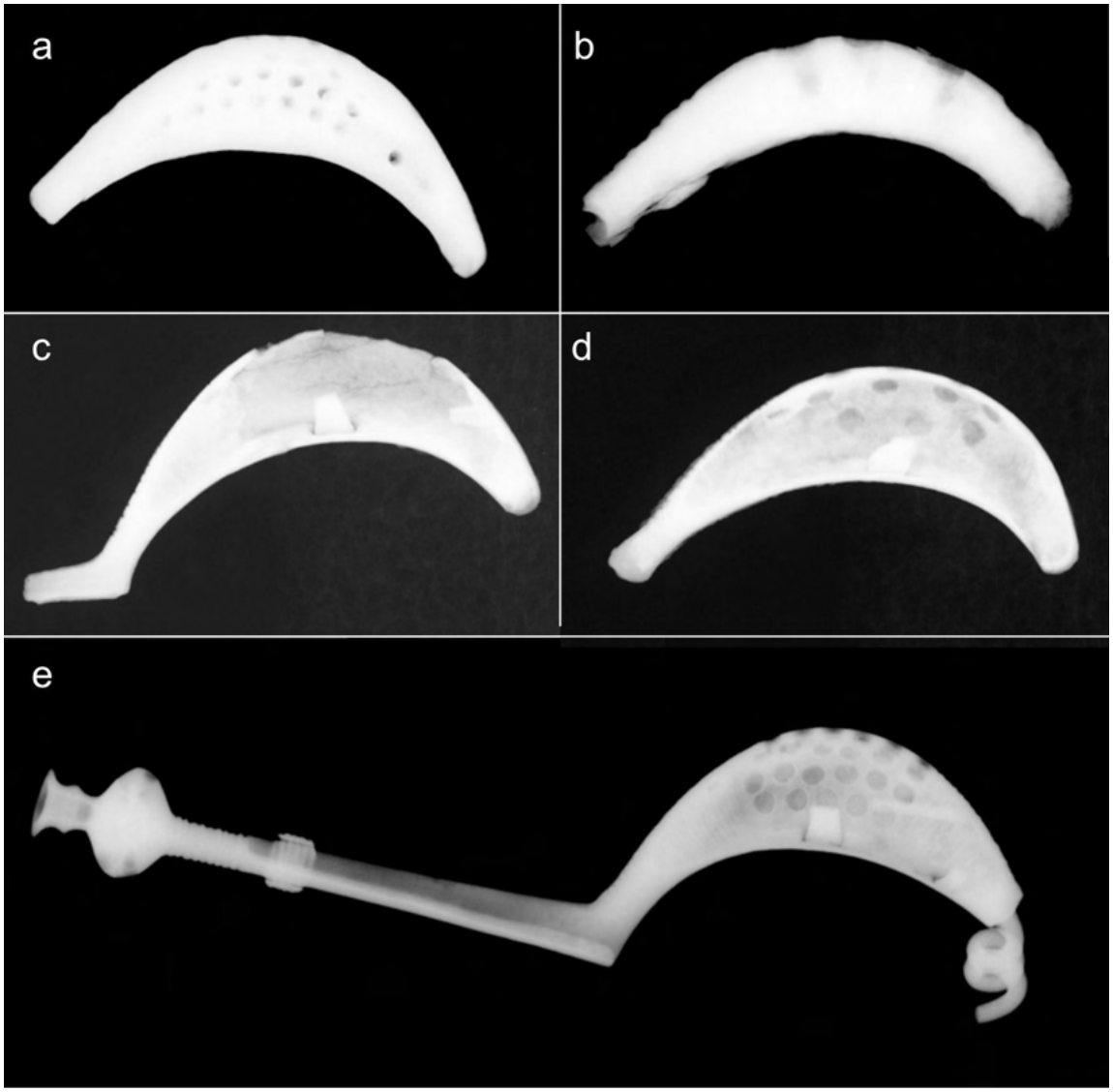

Figure 231. a) Radiography of inv. no. St. 57262; b) Radiography of inv. no. St. 114084; c) Radiography of inv. no. St. 139651; d) Radiography of inv. no. St. 139652; e) Radiography of inv. no. CT728.

Appendix 2 – Tables

Archaeological site	Site typology	Excavation data	Tomb	Inv.	Num.	Chronology	Country	Region	Location	Literature	Considered
Genova, Oppidum del colle di Castello	settlement	excavation, area Q1			2	middle 5th c. BCE	I	LI		Melli 2021, p. 75, f. 48; Milanese 1987, pp. 155, 352, 380, n. 243	N
Como, Albate	burial	1903, excavation			2		I	LO		Baserga 1907, pp. 86-87	D
Como, Ca' Morta	burial	Asnaghi donation		E13273	3	7th-5th c. BCE	I	LO	C-MC	Thanks to dr. Grassi, dr. Orsenigo and dr. Cossandi for the notice	A
Forcello di Bagnolo San Vito	settlement	excavation, sect. V-W 10-11		98797	1		I	LO	M-MN	de Marinis 1987a, pp. 89-90, f. 2; 1997, p. 157	A
Forcello di Bagnolo San Vito	settlement	excavation, sect. V-W 10-11		98798	1		I	LO	M-MN	de Marinis 1987a, pp. 89-90, f. 2; 1997, p. 157	A
Forcello di Bagnolo San Vito	settlement	excavation, sect. V-W 10-11		98799	1		I	LO	M-MN	de Marinis 1987, pp. 89-90, f. 2 1997, p. 157	A
Forcello di Bagnolo San Vito	settlement	excavation, room 3		1060	multiple	515-495 BCE	I	LO	BSV	Barbieri 2019, p. 46; Quirino 2011, p. 388, f. 8	A
Golasecca				A0.9.28598, br487	1	late 8th-7th c. BCE	I	LO	M-MCA	de Marinis 1997, p. 154, note 15; 2000, p. 163, note 21	A
Mantova, Borgo Virgilio, loc. Arginotto	burial	excavation	T 5	169394	1		I	LO	M-MN	Thank's to dr. Hirose and dr. Lamanna for the notice	L
Este, Ricovero	burial	1961	T 3		21	625-525 BCE	I	V		Cherici 1999, p. 182	N
Este, Ricovero	burial		T 200		31	575-525 BCE	I	V		Cherici 1999, pp. 178, 181	N
Este, Ricovero	burial	1897	T 149		21	675-575 BCE	I	V		Cherici 1999, p. 181	N
Este, Ricovero	burial		T 234		multiple		I	V		Fogolari, Frey 1965, f. 5.8	N
Este, Ricovero	burial	1897	T 155		1	675-575 BCE	I	V		Cherici 1999, p. 181	N
Piovego	burial	1970-1980	T 5	5,99	1	6th-5th c. BCE	I	V	P-UNIPD	Gallo 2023	A
Bologna, Arnoaldi	burial						I	ER		de Marinis 1997, p. 157	N
Bologna, Certosa	burial						I	ER		de Marinis 1997, p. 157	N
Bologna, De Luca	burial	1875-1876					I	ER		de Marinis 1997, p. 157	N
Trüllikon	burial				1	late 6th c. BCE	Sw			Cicolani, Huet 2019; Schmid-Sikimic, Bigler 2005; Schmid-Sikimic, 2002, f. 9.8	N
Marseille, La Tourette	settlement					6th c. BCE	Fr			Rondi-Costanzo, Ugolini, 2000, p. 177; Purpura 2005, pp. 97-98; Ugolini 2006a, pp. 80-81	N
Marseille, La Butte Saint-Laurent	settlement					6th c. BCE	Fr			Rondi-Costanzo, Ugolini 2000, p. 177; Purpura 2005, pp. 97-98; Ugolini 2006a, pp. 80-81	N
Marseille, port Jules Verne	shipwreck	1993, excavation				6th c. BCE	Fr			Rondi-Costanzo, Ugolini 2000, p. 177; Pomey 2000; Purpura 2005, pp. 97-98; Ugolini 2006a, pp. 80-81	N
Saint-Blaise	settlement					6th c. BCE	Fr			Rondi-Costanzo, Ugolini 2000, pp. 178-179	N

Table 1. Raw coral distribution in northern Italy and across the Alps between the 7th and 6th century BCE. The table shows, for each artefact, the site of discovery, type of site and excavation data, country and region, inventory number, chronology, location, literature and an indication of optical and/or archaeometric examinations [A = analysed; L= looked; N = not searched; D = missing, impossible to found]. Abbreviations were used for the locations of preservation and the country of discovery – as reported in the Introduction. A geographical order of listing was adopted for the artefacts: State, Region from west to east (e.g. Piedmont, Liguria, Lombardy, Emilia Romagna, Veneto) and Municipality (alphabetical order).

Archaeological site	Site typology	Excavation data	Tomb	Inv.	Chronology	Country	Region	Location	Literature	Considered
Castelletto Ticino	burial	1878		D1750; 72	late 8th-7th c. BCE	I	P	C-MC	Grassi, Mangani 2021, p. 81; Roncoroni 2005, p. 73, n. 172, t. 18.172.	A
Castelletto Ticino	burial	1876, Marazzini's excavation, (Fabretti)	T12		late 8th-early 7th c. BCE	I	P	MRT	de Marinis 1997, p. 154; 2000, pp. 159, 163; Grassi, Mangani 2021, p. 80; Pauli 1971, t. 13-4; Peroni *et al.* 1975, pp. 218, 220, 230	D
Castelletto Ticino	burial	1876, Marazzini's excavation, (Fabretti)	T50			I	P	MRT	de Marinis 2000, p. 173, nota.19; Grassi, Mangani 2021, p. 81; Pauli 1971, t. 26-5	D
Castelletto Ticino	burial	1876, Marazzini's excavation, (Fabretti)	T48		late 8th-early 7th c. BCE	I	P	MRT	de Marinis 1997, p. 154; Pauli 1971, t. 13-4; Peroni *et al.* 1975, pp. 218, 220, 230	D
Castelletto Ticino, loc. Motto d'Egro	burial	1993, Ficcarelli's delivery	T10/1993	20.S.279-3.788, CT164; CT14288-E4		I	P	CT-GSAC		A
Castelletto Ticino, loc. Motto Falco	burial	GSAC discovery	T1	CT179		I	P	CT-GSAC		A
Castelletto Ticino, via del Maneggio	burial	GSAC excavation: US163A-16	T04/01	91374, CT824 cod 14253	750-675 BCE	I	P	CT-GSAC	Cerri 2011, p. 93-94, f. 52.22; Grassi, Mangani 2021, p. 79.	A
Castelletto Ticino, proprietà Amodio	burial	1998, excavation: US103	T		late 8th-early 7th c. BCE	I	P	CT-GSAC	Grassi, Mangani 2021, p. 80; Barbieri 2014-2015, pp. 66-69, t. IV-14.	L
Castelletto Ticino?				A0.9.28560, b622		I	P	M-MCA		A
Castelletto Ticino, via del Maneggio	burial	2001, GSAC excavation	T07/01	91387	825-675 BCE	I	P	CT-GSAC	Cerri 2011, p. 98, f. 58.4; Grassi, Mangani 2021, p. 79	L
Castelveccana, Castello Valtravaglia	burial	excavation	T XX		late 8th-7th c. BCE	I	LO		de Marinis 2000, p. 163; Longhi 1882, p. 32, t. II, XX.7; Grassi, Mangani 2021, p. 81; Peroni *et al.* 1975, pp. 218, 220, 230	D
Castelveccana, Castello Valtravaglia	burial	excavation	T XXIX		late 8th-7th c. BCE	I	LO		de Marinis 2000, p. 163; Longhi 1882, p. 32, t. II, XX.8; Grassi, Mangani 2021, p. 80; Peroni *et al.* 1975, pp. 218, 220, 230	D
Como, Ca' Morta, terreno IACP	burial	1979	T302	33593, E5271	7th c. BCE	I	LO	C-MC	Casini 2011, p. 67, nota 11; Casini, Chaume 2012, p. 232; de Marinis 1997, p. 154; 2000, pp. 159-162, f. 2.7; de Marinis, Gambari 2004, t. 12; Grassi, Mangani 2021, p. 79;	A
Como, Ca' Morta, terreno IACP	burial	1979	T302	33594, E5272	7th c. BCE	I	LO	C-MC	Casini 2011, p. 67, nota 11; de Marinis 1997, p. 154; 2000, pp. 159-162, f. 2.9; de Marinis, Gambari 2005, t. 12; Casini, Chaume 2012, p. 232; Grassi, Mangani 2021, p. 79	A
Como, Ca' Morta, terreno IACP	burial	1979	T302		7th c. BCE	I	LO	C-MC	Casini 2011, p. 67, nota 11; Casini, Chaume 2012, p. 232; de Marinis 1997, p. 154; 2000, pp. 159-162, f. 2.8; Grassi, Mangani 2021, p. 79	L
Como, Ca' Morta, Cava Frangi	burial	1928	TI/1928		late 8th-early 7th c. BCE	I	LO		Baserga 1929, p. 27, f. 5; Bonacelli, 1934, p. 320; Cherici 1999, p. 197; de Marinis 1997, p. 154; 2000, pp. 159-163; Grassi, Mangani 2021, p. 79; Peroni *et al.* 1975, pp. 218, 220, p. 230	D
Como, Ca' Morta, Cava Frangi	burial	1928	TI/1928		late 8th-early 7th c. BCE	I	LO		Baserga 1929, p. 27, f. 6; Bonacelli 1934, p. 320; Cherici 1999, p. 197; de Marinis 1997, p. 154; 2000, pp. 159-163; Grassi, Mangani 2021, p. 79; Peroni *et al.* 1975, pp. 218, 220, p. 230	D
Como, Ca' Morta, Rebbio	burial	1953, Rittatore's excavation	T200	124142, E4491	750-675 BCE	I	LO	C-MC	de Marinis 1997, p. 154; 2000, pp. 159-162, f. 3; Grassi, Mangani 2021, p. 79	A
Como, Ca' Morta, loc. Ronchetti	burial	1953, Casartelli's survey				I	LO		Peroni *et al.* 1975, pp. 218, 220, 230; Bertolone 1956, p. 111, f. 7-14	D
Golasecca				A0.9.28600	late 8th-7th c. BCE	I	LO	M-MCA	de Marinis 1997, p. 154, note 15; 2000, p. 163, nota 21	A

Table 2 - List of findings for the Longone al Segrino type pendant

Archaeological site	Site typology	Excavation data	Tomb	Inv.	Chronology	Country	Region	Location	Literature	Considered
Golasecca				A0.9.28592, br537	late 8th-7th c. BCE	I	LO	M-MCA	de Marinis 1997, p. 154, note 15; 2000, p. 163, nota 21	A
Golasecca	burial			D1667; 29		I	LO	C-MC	Roncoroni 2005, t. 18, n. 176	A
Golasecca	burial			D1668; 30		I	LO	C-MC	Roncoroni 2005, t. 18, n. 171	A
Golasecca	burial			D1669; 31		I	LO	C-MC	Roncoroni 2005, t. 18, n. 175	A
Golasecca		1871, De Mortillet's acquisition		Inv. 17184	late 8th-7th c. BCE	I	LO	SGL-MAN	de Marinis 1997, p. 154, note 15; 2000, p. 163, note 21; 2010, p. 55, f. 14.1; Grassi, Mangani 2021, p. 81	N
Golasecca				MV 103	late 8th-7th c. BCE	I	LO	V-MC	Marinis 1997, p. 154, note 15; 2000, p. 163, note 21	A
Golasecca					late 8th-7th c. BCE	I	LO	M-MCA	Marinis 1997, p. 154, note 15; 2000, p. 163, note 21	D
Golasecca					late 8th-7th c. BCE	I	LO	M-MCA	Marinis 1997, p. 154, note 15; 2000, p. 163, note 21	D
Golasecca					late 8th-7th c. BCE	I	LO	B-IB	Marinis 1997, p. 154, note 15; 2000, p. 163, note 21	N
Golasecca					late 8th-7th c. BCE	I	LO		Marinis 1997, p. 154, note 15; 2000, p. 163, note 21	D
Golasecca					late 8th-7th c. BCE	I	LO		Marinis 1997, p. 154, note 15; 2000, p. 163, note 21	D
Golasecca					late 8th-7th c. BCE	I	LO		Peroni *et al.* 1975, pp. 218, 220, 230	D
Golasecca, loc. Monsorino		Giani Colletion		1		I	LO		Grassi, Mangani 2016, p. 110, f. 164, t. XLIII.4; 2021, p. 81	D
Longone al Segrino	burial	1894, Pisani Dossi recovery	TIII		late 8th-early 7th c. BCE	I	LO	C-CPD	de Marinis 1997, p. 154; 2000, pp. 159, 163, f. 5.13; Pisani Dossi 1908, pp. 10-11, f. 7 up; Grassi, Mangani 2021, p. 79	N
Longone al Segrino	burial	1894, Pisani Dossi recovery	TIII		late 8th-early 7th c. BCE	I	LO	C-CPD	de Marinis 2000, pp. 159, 163, f. 5.14; 1997, p. 154; Pisani Dossi 1908, pp. 10-11, f. 7 up; Grassi, Mangani 2021, p. 79	N
Longone al Segrino	burial	1894, Pisani Dossi recovery	TIII		late 8th-early 7th c. BCE	I	LO	C-CPD	de Marinis 2000, pp. 159, 163, f. 5.15; 1997, p. 154; Pisani Dossi 1908, pp. 10-11, f. 7 up; Grassi, Mangani 2021, p. 79	N
Longone al Segrino	burial	1894, Pisani Dossi recovery	TIII		late 8th-early 7th c. BCE	I	LO	C-CPD	de Marinis 2000, pp. 159, 163, f. 5.16; 1997, p. 154; Pisani Dossi 1908, pp. 10-11, f. 7 up; Grassi, Mangani 2021, p. 79	N
Longone al Segrino	burial	1894, Pisani Dossi recovery	TIII		late 8th-early 7th c. BCE	I	LO	C-CPD	de Marinis 2000, pp. 159, 163, f. 5.17; 1997, p. 154; Pisani Dossi 1908, pp. 10-11, f. 7 up; Grassi, Mangani 2021, p. 79	N
Longone al Segrino	burial	1894, Pisani Dossi recovery	TIII		late 8th-early 7th c. BCE	I	LO	C-CPD	de Marinis 2000, pp. 159, 163, f. 5.18; 1997, p. 154; Pisani Dossi 1908, pp. 10-11, f. 7 up; Grassi, Mangani 2021, p. 79	N
Sesto Calende, loc. Presualdo	burial	1997	T2		late 8th-early 7th c. BCE	I	LO		Grassi, Mangani 2021, p. 80; Voltolini 2019, pp. 49, 52, t. II.19	D
Sesto Calende, Molini di Mezzo	burial	1966	T	12782	late 8th-early 7th c. BCE	I	LO	SC-MC	Grassi, Mangani 2021, p. 79; de Marinis 2009e, pp. 400-411	D
Sesto Calende, via Moncenisio	burial	1995-1996, excavation	T15	172343	7th c. BCE	I	LO	SC-MC	Grassi, Mangani 2021, p. 79; Grassi 2017, pp. 85-91, t. 37, f. 131-135	A
Sesto Calende, via Moncenisio	burial	1995-1996, excavation	T15	172344	7th c. BCE	I	LO	SC-MC	Grassi, Mangani 2021, p. 79; Grassi 2017, pp. 85-91, t. 37, f. 131-135	A
Sesto Calende, via Moncenisio	burial	1995-1996, excavation	T15		7th c. BCE	I	LO	SC-MC	Grassi, Mangani 2021, p. 79; Grassi 2017, pp. 85-91, t. 37, f. 131-135	L
Sesto Calende, via Moncenisio	burial	1995-1996, excavation	T22		late 8th-early 7th c. BCE	I	LO	SC-MC	Grassi, Mangani 2021, p. 79	L
Sesto Calende, via Montrucco	burial	1932, Rittatore's discovery	T2 (oT3 Rittatore)	4783	7th c. BCE	I	LO	SC-MC	Miedico 2011; Grassi, Mangani 2021, p. 80; de Marinis 2009d, f. 11; Squarzanti 2017, f. 1; 2021, pp. 115, 117, 120-121, t. 3, f. 4	A
Sesto Calende, via Montrucco	burial	2003, excavation: US103b6-7	T1	18.S288-3.47-48	7th c. BCE	I	LO	SC-MC	Grassi, Mangani 2021, pp. 47-50, t. 15.5-6, f. 42, 47-48	L
Sesto Calende, via Sempione	burial	2005, excavation	T101	162117	late 8th-early 7th c. BCE	I	LO		Grassi 2014, pp. 114-122, 129, f. 14, 19; Grassi, Mangani 2021, p. 79	D
Golasecca - Sesto C.		Visconti Collection				I	LO	SL-CV	Grassi, Mangani 2021, p. 81; de Marinis 2009h, pp. 640-641, f. 6-5	N

(Table 2 — continued)

Archaeological site	Site typology	Excavation data	Tomb	Inv.	Type	Chronology	Country	Region	Location	Literature	Considered
Brembate Sotto	burial			67	1	525-480 BCE	I	LO	B-MA	Casini 2017, p. 22, fig. 11, n. 26; von Eles Masi 1986, t. 112. 1343	A
Brembate Sotto	burial	excavation	T 12	3051; M214-215-217	2	480-440 BCE	I	LO	B-MA	Casini 2014, p. 391; 2017, pp. 67, 117, f. 69, n. 344; de Marinis 1981, pp. 137-140, t. 19-10 ; 2000, p. 170	A
Brembate Sotto	burial	excavation	T 12	3052; M214-215-217	2	480-440 BCE	I	LO	B-MA	Casini 2014, p. 391 ; 2017, pp. 67, 117, f. 69, n 344; de Marinis 2000, p. 170	A
Cardano					2	480-440 BCE	I	LO		de Marinis 1981, p. 224, t. 68-14	A
Como, Albate	burial	1908-1909, Baserga's recovery	T XII	E16519	1	early 6th c. BCE	I	LO	C-MC	Baserga 1910, p. 17 ; de Marinis 1997, p. 155; 2000, pp. 165-166, f. 6.3-6	L
Como, Ca' Morta	burial	1955	T 4	E17707	1	550-525 BCE	I	LO	C-MC	de Marinis 1997, p. 155; 2000, p. 166, f. 7.8-10	L
Como, Ca' Morta	burial	1926, acquisition	T VIII/1926 o Tomba dell'Elmo	960; E3350	2	480-440 BCE	I	LO	C-MC	de Marinis 1981, p. 224, t. 31-6 ; 2000, p. 170; Baserga 1927, pp. 51	L
Como, Ca' Morta	burial	1927	T 1	979; E3369	2	5th-4th c. BCE	I	LO		Baserga 1927, p. 53, f. 24; de Marinis 1981, p. 224	D
Como, Ca' Morta	burial	1959, Rittatore's excavation	T 116	1397; E3787	2	480-440 BCE	I	LO	C-MC	de Marinis 1981, p. 224, t. 24-6 ; 2000, p. 170	A
Como, Ca' Morta	burial		Tomba del Carro		2	480-440 BCE	I	LO		de Marinis 1981, p. 224, t. 28-10; 2000, p. 170	D
Como, Ca' Morta	burial			1230; E3620	2	480-440 BCE	I	LO	C-MC	Bertolone 1956, p. 111, f. 7.18	A
Como, Ca' Morta	burial	1959, Rittatore's excavation	T 122	1490; E3908	1	525-480 BCE	I	LO	C-MC	de Marinis 1997, p. 155; de Marinis 2000, pp. 166-169, f. 8.12-13	L
Como, Ca' Morta	burial	1959, Rittatore's excavation	T 122	1519; E3937	1	525-480 BCE	I	LO	C-MC	de Marinis 1997, p. 155; de Marinis 2000, pp. 166-169, f. 8.14-19	L
Como, Ca' Morta	burial	1959, Rittatore's excavation	T 131	1993; E4022		675-600 BCE	I	LO	C-MC		A
Como, Ca' Morta	burial	1975, Rittatore's excavation	T 248	23283/86; E5150		550-525 BCE	I	LO	C-MC	de Marinis 1997, p. 155; 2000, p. 166	L
Como, Ca' Morta	burial	1953, Casartelli' survey					I	LO		Bertolone 1956, p. 111, f. 7.6	D
Como, Ca' Morta	burial	1953, Casartelli' survey					I	LO		Bertolone 1956, p. 111, f. 7.19	D
Como, Respaù	burial	Dono Amedeo		E5957; 460	2	480-440 BCE	I	LO	C-MC	de Marinis 1981, p. 224 ; 2000, pp. 170-171, f.11 sx	A
Como, Respaù	burial	Dono Amedeo		E5958	2	480-440 BCE	I	LO	C-MC	de Marinis 1981, p. 224 ; 2000, pp. 170-171, f. 11 dx	A
Cuggiono	burial				2	480-440 BCE	I	LO		de Marinis 1981, p. 224, t. 7-19; 2000, p. 170	D
Golasecca, Lazzaretto	burial	1886, Castelfranco's excavation	Tomba della situla del Lazzaretto	195	1	525-480 BCE	I	LO	M-MCA	de Marinis 1992, pp. 161-162, f. 2.5	N
Golasecca, Lazzaretto	burial	1886, Castelfranco's excavation	Tomba della situla del Lazzaretto	195	1	525-480 BCE	I	LO	M-MCA	de Marinis 1992, pp. 161-162, f. 2.7	N
Sesto Calende, loc. Presualdo		1994					I	LO	SC-CMA	Miedico 2011	L
Sesto Calende, Mulini Bellaria	burial	1977, excavation	T 4 del tripode		1	525-480 BCE	I	LO	SC-CMA	de Marinis 2000, p. 169 ; 2009, p. 443, f. 14.4; 2019, p. 32-33, f. 24.2; de Marinis, Roffia 1979, pp. 521-523	L
Sesto Calende, Mulini Bellaria	burial	1977, excavation	T 4 del tripode		1	525-480 BCE	I	LO	SC-CMA	de Marinis 2000, p. 169; 2009c, p. 443; 2019, p. 32; de Marinis, Roffia 1979, pp. 521-523	L
Sesto Calende, Mulini Bellaria	burial	1977, excavation	T 4 del tripode		1	525-480 BCE	I	LO	SC-CMA	de Marinis 2000, p. 169; 2009c, p. 443; 2019, p. 32; de Marinis, Roffia 1979, pp. 521-523	L
Sesto Calende, Mulini Bellaria	burial	1977, excavation	T 4 del tripode		1	525-480 BCE	I	LO	SC-CMA	de Marinis 2000, p. 169; 2009c, p. 443; 2019, p. 32; de Marinis, Roffia 1979, pp. 521-523	L
Trezzo d'Adda	burial	1848	Tomba della Situla		1	525-480 BCE	I	LO	M-MCA	de Marinis 1974, pp. 68-70, n. 8, t. 2.5-6; 1997, p. 155; 2000, p. 166	N
Pazzallo	burial		T 1		2	480-440 BCE	Sw			de Marinis 1981, p. 224	N

Table 3. List of findings for 'Coral composite bow fibula' type.

Area	Region/Province	Variety (bow)						
		A	B	C	D	E	F	G
Golasecca area	Novara, Vercelli, Como	X	X	X	X	X	X	X
	Pavia							X
	Switzerland	X	X	X	X	X		X
	Bergamo							X
Ligurian area	Coastal Liguria				X			X
	Liguria interna	X			X			X
	Reggio Emilia	X	X			X		X
Etruscan area	Modena					X		
	Mantova	X	X	X				X
	Piacenza	X						X
	Verucchio							X
	Toscana							X
Venetic area	Este-Padova	X	X	X		X		X
	Verona	X	X				X	
	Belluno	X	X	X		X	X	X
Rhaetian area	Trentino		X	X				X
Upper Adriatic	Friuli					X		
	Slovenia	X				X		
Picenum	Marche					X		
Transalpine area	Liechtenstein							X
	Polony	X						

Table 4. Distribution of types of arch decoration in different regions (for variety G 'Palestro' foot fragments with similar characteristics were also considered, i.e., types Q, GG e GGG).

Archaeological site	Site typology	Excavation data	Tomb	Inv.	Preserved parts	Bow type	Foot type	Chronology	Country	Region	Location	Literature	Web sources	Considered
Aosta?		sporadic			B	A		560-525 BCE	I	A		Mollo Mezzena 1997, p. 193, 198, t. 27.10		N
Bellinzago	burial	1956, Apostolo donation		197; 1561	B	B			I	P	N-MC	Pauli 1971, p. 157, t. 42,22; von Eles Masi 1986, p. 165, t. 125.1541		A
Bellinzago		1956, Apostolo donation		198; 1562	B	C			I	P	N-MC	von Eles Masi 1986, p. 166, t. 126.1563		A
Brignano Frascata C-FR-NE		1970, Nebiacolombo, survey		C-FR-NE/1	F		QB4*	525-480 BCE	I	P	MRT	Faudino *et al.* 2014, p. 132, f. 7.3; Cicolani, Berruto 2017, p. 414, f. 2; Berruto *et al.* 2023, f. 1		A

Table 5. List of findings for the type leech fibula with circular decoration; abbreviations: in column 'Preserved parts' B indicates the bow, F the foot and T the whole fibula; in column 'Bow type' and in 'Foot type' the variants identified above; chronology refers to that reported in the literature and is indicated only where present (for a calculated chronological indication based on the typology presented here see Tab. 30); in column 'Web sources' the number refers to the link indicated in the footnote below[1].

1 Nos. 1-22: http://www.lombardiabeniculturali.it/reperti-archeologici/schede (1: /1m060-03349/; 2: /1m060-01287/; 3: /1m060-01289/; 4: /1m060-00171/; 5: /1m060-01711/; 6: /1m060-01712/; 7: /1m060-01839/; 8: /1m060-01840/; 9: /1m140-00290/; 10: /1m140-00291/; 11: /1m060-01374/; 12: /1m060-01375/; 13: /1m130-00441/; 14: /1m130-00444/; 15: /1m130-00449/; 16: /1m060-02761/; 17: /1m130-00133/; 18: /1m130-00134/; 19: /1m130-00243/; 20: /1m130-00244/; 21: /1m130-00245/; 22: /1m060-02159/); nos. 23-24: https://musee-archeologienationale.fr/phototheque/oeuvres (23: /fibule-a-arc-cintre-renfle-a-sanguisuga_alliage-cuivreux_moule-technique; 24: /fibule-a-sanguisuga_alliage-cuivreux_corail-matiere); nos 25-29: website no longer available at https://www.comune.re.it/catalogomuseo/musei.nsf/; no. 30: http://www.archeoagordo.it/n%2027/avanzi_preistorici_nel_bellunese.htm; nos. 31-32: https://sammlung.nationalmuseum.ch/de/list?searchText=sanguisugafibel&detailID=33389; no. 33: http://www.smb-digital.de/eMuseumPlus?service=ExternalInterface&module=collection&objectId=2446591&viewType=detailView

Archaeological site	Site typology	Excavation data	Tomb	Inv.	Preserved parts	Bow type	Foot type	Chronology	Country	Region	Location	Literature	Web sources	Considered
Brignano Frascata C-FR-NE		1970, Nebiacolombo, survey		C-FR-NE/2	T	D	V2*	525-480 BCE	I	P	MRT	Faudino *et al.* 2014, p. 132, f. 7.1; Cicolani, Berruto 2017, p. 414, f. 2; Berruto *et al.* 2023, f. 1		A
Brignano Frascata C-FR-NE		1970, Nebiacolombo, survey		C-FR-NE/3	F		QB3*	525-480 BCE	I	P	MRT	Faudino *et al.* 2014, p. 132, f. 7.2; Cicolani, Berruto 2017, p. 414, f. 2; Berruto *et al.* 2023, f. 1		A
Castelletto Ticino	burial	1877		D2073; 2	B	C		560-525 BCE	I	P	C-MC	von Eles Masi 1986, p. 168, t. 129.1595; Roncoroni 2005, t. 11, n. 91		A
Castelletto Ticino	burial	1878		D2077; 9	T	0*	V0*	560-525 BCE	I	P	C-MC	von Eles Masi 1986, t. 137.1720; Roncoroni 2005, t. 12, n. 100		A
Castelletto Ticino	burial	1878		D2104; 97	T	A	P	560-525 BCE	I	P	C-MC	von Eles Masi 1986, p. 168, t. 129.1592; Roncoroni 2005, t. 11, n. 88		A
Castelletto Ticino	burial	1877		D2773; 64	B	A-P		560-525 BCE	I	P	C-MC	von Eles Masi 1986, n. 1459, t. 119.1459; Roncoroni 2005, t. 11, n. 89, f. 21		A
Castelletto Ticino	burial	1876, Fabretti acquisition, Marazzini excavation	T 34	23.M380-9.5; SN1092	B	C		480-440 BCE	I	P	MRT	Bagnasco Gianni 1988, p. 17, t. VI.5; Pauli 1971, p. 146, t. 20.8; Peroni *et al.* 1975, pp. 200-201 (tipo 54.8), 211		A
Castelletto Ticino	burial	1876, Fabretti acquisition, Marazzini excavation	T 48	2140	B	A		560-525 BCE	I	P	MRT	Barocelli 1926, p. 188; Pauli 1971, p. 139-140, 149, t. 25.26; Peroni *et al.* 1975, pp. 200-201 (tipo 54.8), 212; von Eles Masi 1986, p. 165, t. 124.1531		A
Castelletto Ticino	burial	1876, Fabretti acquisition, Marazzini excavation	T 48	2153	F		V1*	525-480 BCE	I	P	MRT	Pauli 1971, p. 139-140, 149, t. 25.16; Peroni *et al.* 1975, pp. 200-201 (tipo 54.8), 212		A
Castelletto Ticino - Vigevano?				944	B	A			I	P	N-MC			A
Castelletto Ticino - Vigevano?				946; 1011	B	A			I	P	N-MC			A
Castelletto Ticino - Vigevano?				947; 1013	B	C			I	P	N-MC			A
Castelletto Ticino - Vigevano?				949; 1010	B	A			I	P	N-MC			A
Castelletto Ticino, loc. Bosco del Monte		1905, GSAC		CT29; B4D	B	A			I	P	CT-GSAC			A
Castelletto Ticino, loc. Cascina Brua, Via Ardeatine	burial	2009/2010, excavation, GSAC	T 13	CT20343C03E; 18.214; CT1144	B	A		560-525 BCE	I	P	CT-GSAC	Hirose, Lamanna 2015, pp. 104-105, f. 13.1		A

(Table 5 — continued)

Archaeological site	Site typology	Excavation data	Tomb	Inv.	Preserved parts	Bow type	Foot type	Chronology	Country	Region	Location	Literature	Web sources	Considered
Castelletto Ticino, loc. Cascina Riviera, Merlotitt	settlement	1986-88, excavation: US210		210/230	T			5th c. BCE	I	P	CT-GSAC	Ruffa 1999, p. 31, t. VI.7; Ruffa 2001, p. 17		N
Castelletto Ticino, loc. Dorbié Superiore	burial	1987, excavation	T 2	62324	B			late 6th c. BCE	I	P	MRT	Ruffa 1998, p. 15-16, t. II.7		L
Castelletto Ticino, via Valsesia	burial	2002, GSAC	T 1	20.S.279.3.780; cod.20212-G6; CT728	T	C	V2*		I	P	CT-GSAC			A
Castello di Annone	settlement	1988-2010		23.M380-9.4; SP-F16	F		QB4*	525-480 BCE	I	P	MRT	Faudino *et al.* 2014, p. 132, f. 7.9; Berruto *et al.* 2014, p. 238, f. 227; 2023, f. 1; Cicolani, Berruto 2017, p. 414, f. 2; Giaretti 2014, p. 382, f. 342.5, 343		A
Motto Lagone	burial		T 1		T	D	V2*	early 5th. c. BCE	I	P	A-MAA	Gambari 2001, p. 93, note 1; Casini 2014, p. 388		A
Pombia, loc. Monticello, propr. Planca	burial	1993, excavation	T 1	83925	B	A		560-525 BCE	I	P	O-MCF	Di Maio *et al.* 2001, pp. 30-33, f. 17.14		A
Pombia, loc. Monticello, propr. Planca	burial	1993, excavation	T 2	72276-72277	T	A-E	V0	560-525 BCE	I	P	MRT	Di Maio *et al.* 2001, pp. 35-37, f. 19.12, t. 10		A
Pombia, loc. Monticello, propr. Planca	burial	1993, excavation	T 4	83937	F		V2*	525-490/480 BCE	I	P	O-MCF	Di Maio *et al.* 2001, pp. 40-41, f. 26.7		A
Pombia, loc. Monticello, propr. Planca	burial	1993, excavation	T 8	83946	T	G	QB3*	525-490/480 BCE	I	P	O-MCF	Di Maio *et al.* 2001, p. 43, f. 30.2		A
Pombia, loc. Quara, propr. Baù	burial	1994-1995, excavation		83966	B	A		560-525 BCE	I	P	O-MCF	Di Maio *et al.* 2001, pp. 49-50, f. 35.B.6, t. 15		A
Pontecurone		2012, excavation: Area2, US26, S3		23.M380-9.6; 6599; RR12	F		V0*	600-475 BCE	I	P	MRT-MAT	Venturino Gambari *et al.* 2014, p. 111, f. 22.4		A
Ponte nelle Alpi - Cugnan	burial	1936		6626; 3355	B	A		550-525 BCE	I	P	B-MC	von Eles Masi 1986, p. 165, t. 124.1532; Nascimbene 2009, pp. 280-281, t. V.3		A
San Bernardino di Briona	burial	1918-1919, excavation, Barocelli		868; 198	B	A			I	P	N-MC	Pauli 1971, p. 156-157, t. 36, n. 26		A
San Bernardino di Briona	burial	1918-1919, excavation, Barocelli		870	B*	A			I	P	N-MC	Pauli 1971, p. 156-157, t. 36, n. 27		A

(Table 5 — continued)

Archaeological site	Site typology	Excavation data	Tomb	Inv.	Preserved parts	Bow type	Foot type	Chronology	Country	Region	Location	Literature	Web sources	Considered
San Bernardino di Briona	burial	1984	T 1		B	A		560-525 BCE	I	P		Gambari 1987, p. 80, t. XXVIc		D
San Bernardino di Briona	burial	1918-1919, excavation, Barocelli			B	A			I	P	MRT	Pauli 1971, t. 41.2 dx-IV; von Eles Masi 1986, p. 165, t. 124.1530		D
San Bernardino di Briona	burial	1918-1919, excavation, Barocelli		NCT0100026405	B	A			I	P	MRT	Pauli 1971, t. 41.2 sx-III; von Eles Masi 1986, p. 164, t. 123.1524		A
San Bernardino di Briona	burial	1918-1919, excavation, Barocelli		NCT0100026418	B	C			I	P	MRT	Pauli 1971, t. 41.2 sx-II; von Eles Masi 1986, p. 166, t. 127.1567		A
San Bernardino di Briona	burial	1918-1919, excavation, Barocelli		NCT0100026417	B	A			I	P	MRT	Pauli 1971, t. 41.2 sx-IV; von Eles Masi 1986, p. 164, t. 123.1514		A
San Bernardino di Briona	burial	1918-1919, excavation, Barocelli		NCT0100026415	B	A			I	P	MRT	Pauli 1971, t. 41.2 dx.V; von Eles Masi 1986, pp. 165-6, t. 125.1547		A
San Bernardino di Briona	burial	1918-1919, excavation, Barocelli			F		V2		I	P		Pauli 1971, p. 156-157, t. 36, n. 18		D
San Bernardino di Briona	burial	1918-1919, excavation, Barocelli		23.M380-9.2	F		V1*		I	P	MRT	Pauli 1971, t. 41.3 up		A
San Bernardino di Briona	burial	1918-1919, excavation, Barocelli		23.M380-9.1	F		V1*		I	P	MRT	Pauli 1971, t. 41.3 down		A
Villa del Foro				RS154	F		*		I	P	MRT			A
Villa del Foro				1000/E1	B	A		560-525 BCE	I	P	MRT	Berruto *et al.* 2021, p. 552, f. 337; 2023, f. 1; Cicolani 2021, p. 533, f. 323; Faudino *et al.* 2014, p. 132, f. 7.5		A
Villa del Foro		1980-1990, sporadic, Oberti		SP 27	B	A		560-525 BCE	I	P	MRT	Berruto *et al.* 2021, p. 552, f. 337; 2023, f. 1; Cicolani 2021, p. 533, f. 323		A
Villa del Foro		1980-1990, sporadic, Oberti		66132; SP688	B*	A-var		560-525 BCE	I	P	MRT	Berruto *et al.* 2021, p. 552, f. 337; 2023, f. 1; Cicolani 2021, p. 533, f. 323; Cicolani, Berruto 2017, p. 414, f. 2; Faudino *et al.* 2014, p. 132, f. 7.8		A
Villa del Foro		1980-1990, sporadic, Oberti		51877	B	A		560-525 BCE	I	P	MRT	Berruto *et al.* 2021, p. 552, f. 337; Berruto 2023, f. 1; Cicolani 2021, p. 533, f. 323; Faudino *et al.* 2014, p. 132, f. 7.7		A

(Table 5 — continued)

Archaeological site	Site typology	Excavation data	Tomb	Inv.	Preserved parts	Bow type	Foot type	Chronology	Country	Region	Location	Literature	Web sources	Considered
Villa del Foro		1980-1990, sporadic, Oberti		SP 215	B*				I	P	MRT	Berruto *et al.* 2021, p. 552, f. 337; 2023, f. 1; Cicolani 2021, p. 533, f. 323		A
Villa del Foro		1980-1990, sporadic, Oberti		SP 28b	F		V2*	525-490/480 BCE	I	P	MRT	Berruto *et al.* 2021, p. 552, f. 337; 2023, f. 1; Cicolani 2021, p. 533, f. 323		A
Villa del Foro		1980-1990, sporadic, Oberti		51878; SP696	B*	A-bis		6th. c. BCE	I	P	MRT	Berruto *et al.* 2021, p. 552, f. 337; 2023, f. 1; Cicolani 2021, p. 533, f. 323		A
Villa del Foro		1980-1990, sporadic, Oberti		SP 834 a	B*	A-bis		6th. c. BCE	I	P	MRT	Berruto *et al.* 2021, p. 552, f. 337; 2023, f. 1; Cicolani 2021, p. 533, f. 323		A
Villa del Foro		1980-1990, sporadic, Oberti			F		QB	480-440 BCE	I	P	MRT	Cicolani 2021, p. 538, f. 324, 22		N
Genova, Oppidum del colle di Castello	settlement	1960, excavation: sett.SZ 80 IX f		79707	B	G		525-490/480 BCE	I	LI	G-SABAP	I Liguri 2005, p. 323, V.2.19; Melli 2007, p. 50		N
Genova, Oppidum del colle di Castello	settlement	1960, excavation: sett GN		35849	F		V2	525-490/480 BCE	I	LI	G-SABAP	Archeologia a Genova 1977, p. 22, f. 24; Casini 2000b, p. 87, n. 15; I Liguri 2005, p. 323, V.2.20		N
Genova, Oppidum del colle di Castello	settlement	1997, excavation: US2220		97839	F		QB3	480-440 BCE	I	LI	G-SABAP	I Liguri 2005, p. 323, V.2.21		N
Genova, Val Brevenna				285	B	D			I	LI	G-MAP	Casini 2000b, p. 87, n. 21; von Eles Masi 1986, p. 167, t. 127.1574		N
unknown (provincia di Varese)		early XX c., Don G. Tornatore acquisition, Bertolone donation		M0585/3	B	C			I	LO	Bra	Demarchi *et al.* 2007, p. 82, t. XXII.3		A
Casteggio						G		480-440 BCE	I	LO		Casini 2000b, p. 88, n. 32		N
Castellazzo della Garolda, Roncoferraro		1977-1978, Zanoni recovery			B	A			I	LO		de Marinis 2000, p. 170; Tamassia 1979, pp. 520-521, t. LXXXII.b		D
Castello Valtravaglia	burial	1888, Longhi donation		E13651	B			600-480 BCE	I	LO	C-MC	Saronio 1970, pp. 140-141	1	L
Colle San Martino, Gavardo		1957-1960, excavation, Gruppo Grotte Gavardo			B				I	LO	G-MA	Simoni 1964, p. 47 dx; Bocchio-Salzani 1973-1974, pp. 48, 60, t. IX.116		N
Como, Ca' Morta	burial	1963, Rittatore	T 177	2206; E4385	B*	B		525-480 BCE	I	LO	C-MC	von Eles Masi 1986, pp. 166, t. 126.1555	2	A
Como, Ca' Morta	burial	1963, Rittatore	T 177	2208; E4387	B*	B		525-480 BCE	I	LO	C-MC	von Eles Masi 1986, pp. 166, t. 126.1554	3	A

(Table 5 — continued)

Archaeological site	Site typology	Excavation data	Tomb	Inv.	Preserved parts	Bow type	Foot type	Chronology	Country	Region	Location	Literature	Web sources	Considered
Como, Ca' Morta	burial	1928	T II/1928		B	A		560-525 BCE	I	LO		Baserga 1929, p. 28, f. 8; Peroni *et al.* 1975, pp. 200-201 (tipo 54.7), 211		D
Como, Ca' Morta	burial	1963	T 177		T	G		480-440 BCE	I	LO		Peroni *et al.* 1975, pp. 200-201 (tipo 54.8), 211		D
Como, Ca' Morta	burial	1964	T 187		T	G		480-440 BCE	I	LO		Peroni *et al.* 1975, pp. 200-201 (tipo 54.8), 211		D
Como, Ca' Morta, Rebbio	burial	1926, Ballerini donation	T VI/1926-27	879; E3269	T	A-F	V0	550-480 BCE	I	LO	C-MC	Baserga 1927, p. 50; Peroni *et al.* 1975, pp. 200-201 (tipo 54.7), 211; von Eles Masi 1986, p. 167, t. 128.1580	4	A
Como, Ca' Morta, Rebbio	burial	1976, excavation, Rittatore	T 264	139671; E4804	B	A		525-480 BCE	I	LO	C-MC		5	L
Como, Ca' Morta, Rebbio	burial	1976, excavation, Rittatore	T 264	139672; E4805	B	A		525-480 BCE	I	LO	C-MC		6	L
Como, Ca' Morta, Rebbio	burial	1975, excavation, Rittatore	T 256	139651; E4932	B	A		525-480 BCE	I	LO	C-MC		7	A
Como, Ca' Morta, R ebbio	burial	1975, excavation, Rittatore	T 256	139652; E4933	B	A		525-480 BCE	I	LO	C-MC		8	A
Como, Ca' Morta, Rebbio	burial	1969, excavation, Rittatore	T 238	114083; E5384	B*	A		550-525 BCE	I	LO	C-MC		9	A
Como, Ca' Morta, Rebbio	burial	1969, excavation, Rittatore	T 238	114084; E5385	B*	A-bis		550-525 BCE	I	LO	C-MC		10	A
Como, Ca' Morta, Rebbio	burial	1964, excavation, Rittatore	T 187	124087; E4471				525-480 BCE	I	LO	C-MC	von Eles Masi 1986, p. 185, t. 144.1860	11	L
Como, Ca' Morta, Rebbio	burial	1964, excavation, Rittatore	T 187	124088; E4472	B	B		525-480 BCE	I	LO	C-MC	von Eles Masi 1986, pp. 166, t. 126.1552; p. 185, t. 144.1858	12	L
Como, Ca' Morta, Rondineto	burial	Galli donation	T Galli	E5865; 418	B	A		480-410 BCE	I	LO	C-MC	Barelli 1879, t. II.u; Peroni *et al.* 1975, pp. 200-201 (tipo 54.8), 211	13	A
Como, Ca' Morta, Rondineto		Galli donation		E5868; 422	B	B		600-480 BCE	I	LO	C-MC		14	A
Como, Ca' Morta, Rondineto		1892		E5873; 423	F		QB4	550-440 BCE	I	LO	C-MC	Barelli 1877, pp. 1-32	15	A

(Table 5 — continued)

Archaeological site	Site typology	Excavation data	Tomb	Inv.	Preserved parts	Bow type	Foot type	Chronology	Country	Region	Location	Literature	Web sources	Considered
Como, Civiglio-Pregosa	burial	1973-1974, excavation, Frigerio	T 1	E17022	T	A	S	525-480 BCE	I	LO	C-MC		16	D
Como, dintorni				E5552; 61	B	G		480-410 BCE	I	LO	C-MC		17	A
Como, dintorni				E5553; 61	B	G		480-410 BCE	I	LO	C-MC		18	A
Como, dintorni				E5667; 68	B	C		525-480 BCE	I	LO	C-MC	von Eles Masi 1986, p. 166, t. 126.1564	19	A
Como, dintorni				E5668; 68	B	B		525-480 BCE	I	LO	C-MC	von Eles Masi 1986, p. 166, t. 125.1548	20	L
Como, dintorni				E5669; 68	B	E		525-480 BCE	I	LO	C-MC	von Eles Masi 1986, p. 167, t. 128.1578	21	L
Como, Prestino, via Isonzo	settlement	1981, excavation		57210	B	G		475-410 BCE	I	LO	C-MC			A
Como, Prestino, via Isonzo	settlement	1981, excavation		57216	B	A		475-410 BCE	I	LO	C-MC			A
Como, Prestino, via Isonzo	settlement	1981, excavation		57220	B	A		475-410 BCE	I	LO	C-MC			A
Como, Prestino, via Isonzo	settlement	1981, excavation		57244	B	G		475-410 BCE	I	LO	C-MC			A
Como, Prestino, via Isonzo	settlement	1981, excavation		57250	B	G		475-410 BCE	I	LO	C-MC			A
Como, Prestino, via Isonzo	settlement	1981, excavation		57262	B	G		475-410 BCE	I	LO	C-MC			A
Como, Rebbio				A0.9.5822; br869	B	G			I	LO	M-MCA			A
Como, Rebbio	burial			A0.9.27537; 750	B	A			I	LO	M-MCA	von Eles Masi 1986, p. 165, t. 124.1538		A
Como, Rebbio, Villa Giovio		1927, donation		E13225	F		QB4	480-440 BCE	I	LO	C-MC		22	A
Como/Milano, dintorni				MAN20475.01	B*	A-bis		6th-5th c. BCE	I	LO	SGL-MAN	Cicolani 2017, p. 101, f. 68; Lorre, Cicolani 2009, p. 91	23	N
Como/Milano, dintorni				MAN20475.03	T	G	QB4*	5th c. BCE	I	LO	SGL-MAN	Cicolani 2017, p. 102, f. 69	24	N
Forcello di Bagnolo San Vito					B	G			I	LO		Colonna 1979, t. LXXVII.b; de Marinis 2000, p. 173, note 40		D
Gaggio					B	A-E			I	LO		Giordani, 2008, f. 1		N
Gazzo Veronese, Colombara	burial				B	B			I	LO		Salzani 1976, pp. 418, 421, f. 12.5; von Eles Masi 1986, pp. 166, t. 125.1551A		D
Gazzo Veronese, Colombara	burial				B	B-F			I	LO		von Eles Masi 1986, p. 168, t. 128.1585A		D
Gazzo Veronese, Dosso del Pol	burial	excavation			T*	A-var	V1		I	LO		Salzani 1976, pp. 422, 425, f. 16.4		N

(Table 5 — continued)

Archaeological site	Site typology	Excavation data	Tomb	Inv.	Preserved parts	Bow type	Foot type	Chronology	Country	Region	Location	Literature	Web sources	Considered
Golasecca	burial			A0.9.4858; 554; br616	B	C			I	LO	M-MCA	von Eles Masi 1986, p. 166, t. 126.1565		A
Golasecca	burial			A0.9.4908; br427a	B	C-F			I	LO	M-MCA	von Eles Masi 1986, p. 168, t. 128.1586		A
Golasecca	burial			A0.9.28258; br444b	B	A			I	LO	M-MCA	von Eles Masi 1986, p. 165, t. 124.1534		A
Golasecca	burial			A.9.4922; br508d	B	A			I	LO	M-MCA	von Eles Masi 1986, p. 165, t. 124.1537		A
Golasecca	burial			A0.9.28865; br427b	B	A-F			I	LO	M-MCA	von Eles Masi 1986, p. 164, t. 123.1515		A
Golasecca	burial			A0.9.4842; br570, 1673	T	A-F	TA		I	LO	M-MCA	von Eles Masi 1986, p. 168, t. 129.1593		A
Golasecca				A0.9.4810	T	A	V0		I	LO	M-MCA			A
Golasecca	burial			br508c	B	C			I	LO	M-MCA	von Eles Masi 1986, p. 166, t. 126.1561		D
Golasecca	burial			br618	T	A-F			I	LO	M-MCA	von Eles Masi 1986, p. 167, t. 128.1583		D
Golasecca	burial			D 2059; 7/2	B	C		525-490/480 BCE	I	LO	C-MC	Roncoroni 2005, t. 11, n. 93		A
Golasecca	burial			D 2064; 7/2	B	C		6th c. BCE	I	LO	C-MC	Roncoroni 2005, t. 11, n. 94		A
Golasecca	burial			D 2065; 7/2	B	A		6th c. BCE	I	LO	C-MC	Roncoroni 2005, t. 11, n. 90		A
Golasecca	burial			D2049; 6	B	C		525-490/480 BCE	I	LO	C-MC	Roncoroni 2005, t. 11, n. 92; von Eles Masi 1986, pp. 166, t. 125.1551		A
Golasecca	burial	1873, Bertrand acquisition		20806	F		V1*		I	LO	SGL-MAN	de Marinis 2010, p. 55, f. 14.3		N
Golasecca	burial	1873, Bertrand acquisition		20806	B	C			I	LO	SGL-MAN	de Marinis 2010, p. 55, f. 14.4		N
Golasecca	burial			MV4062	T	A			I	LO	V-MC	von Eles Masi 1986, p. 164, t. 124.1526		A
Golasecca	burial				T	A	V0*		I	LO		von Eles Masi 1986, p. 164, t. 123.1521		D
Golasecca	burial				B	C			I	LO	Bre	von Eles Masi 1986, p. 166, t. 126.1557		N
Golasecca	burial				B	C			I	LO	Bre	von Eles Masi 1986, p. 166, t. 127.1568		N
Golasecca	burial				B	D			I	LO		von Eles Masi 1986, p. 167, t. 127.1572		D
Golasecca					T	C-F	V2*	525-490/480 BCE	I	LO	B-IB	de Marinis 2000, p. 170, f. 9		N
Golasecca				A0.9.28288; br641	F		V2*		I	LO	M-MCA			A
Golasecca ?				637	B	C			I	LO	M-MCA	von Eles Masi 1986, p. 166, t. 126.1559		D
Golasecca ?					T	C			I	LO	M-MCA	von Eles Masi 1986, p. 166, t. 126.1560		D
Golasecca ?					T	B-E			I	LO	V-MC	von Eles Masi 1986, p. 167, t. 127.1576		D

(Table 5 — continued)

Archaeological site	Site typology	Excavation data	Tomb	Inv.	Preserved parts	Bow type	Foot type	Chronology	Country	Region	Location	Literature	Web sources	Considered
Golasecca, Lazzaretto	burial	1886, excavation, Castelfranco	Tomba della situla del Lazzaretto	188	B	A			I	LO	M-MCA	de Marinis 1992, pp. 161-162, f. 3.1; von Eles Masi 1986, p. 164, t. 124.1527		N
Golasecca, Lazzaretto	burial	1886, excavation, Castelfranco	Tomba della situla del Lazzaretto	189	B	A			I	LO	M-MCA	de Marinis 1992, pp. 161-162, f. 3.2; von Eles Masi 1986, p. 165, t. 124.1528		N
Golasecca, Lazzaretto	burial	1886, excavation, Castelfranco	Tomba della situla del Lazzaretto	190	B	A			I	LO	M-MCA	de Marinis 1992, pp. 161-162, f. 3.4; von Eles Masi 1986, p. 168, t. 129.1594		N
Golasecca, loc. Galliasco	burial	1964, excavation, Dajelli, seizure	T 25.8.1964		T	C	V2*	525-490/480 BCE	I	LO	M-SABAP	de Marinis 2010, p. 49, note 222, p. 51, f. 11.1; Berruto, Ruffa 2022, p. 274, f. 2		A
Golasecca, Monsorino	burial	1985-1986, excavation	T 39	63413	T	A	V0*	525-490/480 BCE	I	LO	V-MC	Grassi, Mangani2016, p. 83, f. 111, t. XXVII.5; de Marinis 2019, p. 11, f. 5.5		A
Golasecca, Monsorino	burial	1985	T 16		T			525-490/480 BCE	I	LO		Grassi, Mangani2016, p. 79		D
Golasecca?				A0.9.5961; 86; 538	T	A	V0*		I	LO	M-MCA	von Eles Masi 1986, p. 164, t. 123.1522		A
Golasecca?	burial			A0.9.28164; br476	B	B			I	LO	M-MCA	von Eles Masi 1986, p. 165, t. 125.1545		A
Golasecca?		1917, Corbetta donation		A0.9.35542	B	A			I	LO	M-MCA	von Eles Masi 1986, p. 165, t. 124.1535		A
Golasecca?				A0.9.32750; 42, 2065	B	B			I	LO	M-MCA	von Eles Masi 1986, p. 164, t. 123.1520		A
lago superiore di Mantova						A			I	LO		de Marinis 2000, p. 170; Nascimbene 2009, p. 135, n. 23		D
Malgesso				MV4025	T	C			I	LO	V-MC	von Eles Masi 1986, p. 166, t. 126.1558		A
Mantova, piazza Santa Barbara		2013, excavation		169519	B	C			I	LO	M-MN			A
Palestro	burial	1894, acquisition			T	G	GG	480-440 BCE	I	LO	MRT	Ricci 1897, pp. 1-6; Peroni *et al.* 1975, pp. 200-201 (tipo 54.8), 211		D
Rivoltella	burial			60047	T	C			I	LO	MUCIV	von Eles Masi 1986, p. 167, t. 127.1569		N
Santo Spirito, Gropello Cairoli	settlement	1979, Pace recovery		2019.01.112	F		GG2*	480-440 BCE	I	LO	MANL	Ruffa 2010, pp. 111-112, f. 8.49		A
Sesto Calende	burial	1928	T 3	12436; 980/23	B	A-F			I	LO	V-MC	Bertolone 1953-1954, t. XXXV.2; Peroni *et al.* 1975, pp. 200-201 (tipo 54.8), 212; von Eles Masi 1986, p. 167, t. 128.1582		A
Sesto Calende	burial	1928	T di Guerriero B	12437	B	A			I	LO	V-MC	von Eles Masi 1986, p. 164, t. 123.1517		A

(Table 5 — continued)

Archaeological site	Site typology	Excavation data	Tomb	Inv.	Preserved parts	Bow type	Foot type	Chronology	Country	Region	Location	Literature	Web sources	Considered
Sesto Calende, Mulini Bellaria	burial	1977, excavation	T 4 “del tripode”	23751	B	G		525-490/480 BCE	I	LO	SC-MC	de Marinis 1988b, f. 179; 2009c, pp. 432-444, f. 14.1; 2019, p. 32, f. 24.3; de Marinis, Roffia1979, pp. 521-523		A
Sesto Calende, Mulini Bellaria	burial	1977, excavation	T 4 “del tripode”	23752	B	G		525-490/480 BCE	I	LO	SC-MC	de Marinis 2009c, pp. 432-444, f. 14.2; 2019, p. 32, f. 24.4; de Marinis, Roffia1979, pp. 521-523		A
unknown		Bellini’s collection			B	C-F		525-490/480 BCE	I	LO	SC-MC	Barbieri 2023, pp. 80-81, f. 150, t. 137; Berruto 2023, pp. 97-102; Squarzanti 2009		A
Verretto								525-490/480 BCE	I	LO	PV-MC	de Marinis 2000, p. 170; Casini 2000b, p. 87, n. 30		N
Bismantova				11954	B	A		480-440 BCE	I	ER	RE-MGC	Damiani *et al.* 1992, pp. 128, 308, t. LXII, n. 932; de Marinis 2000, p. 173, note 40; Casini 2000b, p. 88, n. 44	25	N
Bismantova				11990	F		QB3	480-440 BCE	I	ER	RE-MGC	Damiani *et al.* 1992, pp. 129, 308, t. LXII, n. 937; de Marinis 2000, p. 173, note 40; Casini 2000b, p. 88, n. 53	26	N
Bismantova				11992	F		QB3	480-440 BCE	I	ER	RE-MGC	Damiani *et al.* 1992, pp. 129, 308, t. LXII, n. 935; de Marinis 2000, p. 173, note 40; Casini 2000b, p. 88, n. 53	27	N
Bismantova				11993	F		QB3	480-440 BCE	I	ER	RE-MGC	Damiani *et al.* 1992, pp. 129, 308, t. LXII, n. 938; de Marinis 2000, p. 173, note 40; Casini 2000b, p. 88, n. 53	28	N
Bobbio		Perrando, sporadic			F		QB4		I	ER		Casini 2000b, p. 88, n. 36; Catarsi, dall’Aglio 1987, p. 407, f. 2.8; Morelli 1888, p. 19, t. I, n. 2		N
Borgonovo V.T., loc. Acquedotto di Castelnuovo		2020, sporadic		20.S258-2.118	F		V4	early 6th-5th c. BCE	I	ER	P-MAVT	Thanks to dr. Moine and dr. Bolzoni for the notice		A
Borgonovo V.T., loc. Acquedotto di Castelnuovo		2020, sporadic		20.S258-2.119	F		QB3	early 6th-5th c. BCE	I	ER	P-MAVT	Thanks to dr. Moine and dr. Bolzoni for the notice		A
Borgonovo V.T., loc. Bilegno		2020, sporadic		20.S258-2.171	F		V2	early 6th-5th c. BCE	I	ER	P-MAVT	Thanks to dr. Moine and dr. Bolzoni for the notice		A
Borgonovo V.T, loc. Bilegno		2020, sporadic		20.S258-2.172	F		GG2*	480-440 BCE	I	ER	P-MAVT	Thanks to dr. Moine and dr. Bolzoni for the notice		A
Marzabotto									I	ER		de Marinis 2000, p. 170		N
Pianello V.T., area nuovo cimitero		1999, sporadic		201255	F		QB3	late 6th.-early 5th c. BCE	I	ER	P-MAVT	Thanks to dr. Moine and dr. Bolzoni for the notice		A

(Table 5 — continued)

Archaeological site	Site typology	Excavation data	Tomb	Inv.	Preserved parts	Bow type	Foot type	Chronology	Country	Region	Location	Literature	Web sources	Considered
Pianello V.T., loc. Arcello		1999, sporadic		200191	F		V4	late 6th.-early 5th c. BCE	I	ER	P-MAVT	Thanks to dr. Moine and dr. Bolzoni for the notice		A
Rottofreno, loc. Cascina Rondinino		2014, sporadic		259507	B*	A-var		6th-5th. c. BCE	I	ER	P-MAVT	Thanks to dr. Moine and dr. Bolzoni for the notice		A
San Polo d'Enza				11989	F		QB3	480-440 BCE	I	ER	RE-MGC	Damiani *et al.* 1992, pp. 129-308, t. LXII, n. 941; de Marinis 2000, p. 173, note 40; Casini 2000b, p. 88, n. 44	29	N
San Polo d'Enza				21275	F		QB3		I	ER	MUCIV	Damiani *et al.* 1992, pp. 129, 308, t. LXII.940		N
San Polo d'Enza					B	A			I	ER	RE-MGC	Damiani *et al.* 1992, pp. 128, 307, t. LXI.926		N
San Polo d'Enza					B	A			I	ER	RE-MGC	Damiani *et al.* 1992, pp. 128, 307, t. LXI.927		N
San Polo d'Enza					B	B			I	ER	RE-MGC	Damiani *et al.* 1992, pp. 128, 307, t. LXI.928		N
San Polo d'Enza					F		V3		I	ER	RE-MGC	Damiani *et al.* 1992, pp. 128, 307, t. LXI.929		N
San Polo d'Enza					F		V3		I	ER	RE-MGC	Damiani *et al.* 1992, pp. 128, 307, t. LXI.930		N
San Polo d'Enza					T	A-P	V0		I	ER	RE-MGC	Damiani *et al.* 1992, pp. 128, 222, 307, f. 10, t. LXI.931		N
San Polo d'Enza					B	A-var			I	ER	RE-MGC	Damiani *et al.* 1992, pp. 129, 308, t. LXII.933		N
San Polo d'Enza					F		QB3		I	ER	RE-MGC	Damiani *et al.* 1992, pp. 129, 226, 308, f. 13, t. LXII.934		N
San Polo d'Enza					F		QB3		I	ER	RE-MGC	Damiani *et al.* 1992, pp. 129, 308, t. LXII.936		N
San Polo d'Enza					F		QB3		I	ER	RE-MGC	Damiani *et al.* 1992, pp. 129, 308, t. LXII.939		N
Verucchio, Pozzo di Pian del Monte	cultual	1960-1970		4459	B	G		525-440 BCE	I	ER	V-MCA	de Marinis 2000, p. 173, note 40; Casini 2000b, p. 88, n. 63; Morico 1987, pp. 270-273, f. 176.9		N
Verucchio, Pozzo di Pian del Monte	cultual	1960-1970		5776	B	G		480-440 BCE	I	ER	V-MCA	Bentini *et al.* 2020, pp. 396-397, f. 13; de Marinis 2000, p. 173, note 40; Casini 2000b, p. 88, n. 63; Morico 1987, pp. 270-273, f. 176.10		N
Adria									I	V		de Marinis 2000, p. 170		N

(Table 5 — continued)

Archaeological site	Site typology	Excavation data	Tomb	Inv.	Preserved parts	Bow type	Foot type	Chronology	Country	Region	Location	Literature	Web sources	Considered
Borso del Grappa, Cassanego	burial	sporadic	T 1	259929	B	A-bis-L		7th-5th c. BCE	I	V	P-SABAP	Endrizzi, Marzatico 1997, p. 556, n. 85; Serafini 1997, p. 545, f. 5,5; Nascimbene 2009, p. 134, n. 3		N
Borso del Grappa, Cassanego	burial	sporadic	T 1	259931	T	A	V0	7th-5th c. BCE	I	V	P-SABAP	Endrizzi, Marzatico 1997, p. 545, f. 5,8, p. 556, n. 87		N
Carceri d'Este	burial		T30		T	A	R		I	V	E-MNA	von Eles Masi 1986, p. 185, t. 144.1859		N
Caverzano	burial	1865, excavation	T 3	211	T	A-E			I	V	B-MC	Nascimbene 1999, pp. 44-46, f. 8, n. 60; von Eles Masi 1986, p. 165, t. 124.1533		A
Caverzano, Limade		1996, sporadic		287304; 17412	T	D	V2	late 6th c. BCE	I	V	B-MC	Nascimbene 2009, pp. 302-306, t. XIII, n. 1		A
Caverzano	burial	1865, excavation		217, 3312	F		V2*	late 6th c. BCE	I	V	B-MC	Nascimbene 1999, pp. 44-47, f. 8, num. 63		A
Caverzano	burial	1865, excavation	T 3	205	B	C			I	V	B-MC	Nascimbene 1999, pp. 44-45, f. 8, n. 59; von Eles Masi 1986, p. 166, t. 126.1556		D
Caverzano	burial	1885, excavation		193	B	A			I	V	B-MC	von Eles Masi 1986, p. 165, t. 124.1529		D
Caverzano	burial	1885, excavation	T 3	206	B	A			I	V	B-MC	Nascimbene 1999, pp. 44-45, f. 8, n. 57		D
Caverzano	burial	1865, excavation				A			I	V	B-MC	von Eles Masi 1986, p. 164, t. 124.1525		D
Caverzano	burial				T	G			I	V		Leicht 1871, f. 10; Nascimbene 1999, pp. 44-46, f. 8, n. 62; von Eles Masi 1986, p. 168, t. 129.1590	30	D
Caverzano	burial	1865			B	B			I	V		Leicht 1871, f. 2; Nascimbene 1999, pp. 44-45, f. 8, n. 58; von Eles Masi 1986, pp. 166, t. 125.1550		D
Caverzano, necropoli della vigna	burial	1887, Zanussi donation		21180	B	F			I	V	MUCIV	Nascimbene 1999, pp. 44-46, f. 8, n. 61; von Eles Masi 1986, pp. 167-168, t. 128.1584		N
Chies d'Alpago	burial	1935		6615; 3344	T	A	V0*	late 6th c. BCE	I	V	B-MC	Nascimbene 2009, pp. 267-269, t. I.2; von Eles Masi 1986, n. 1523		A
Chies d'Alpago	burial	1935		6600		E			I	V	B-MC	von Eles Masi 1986, p. 167, t. 127,1577		D
Chies d'Alpago	burial	1935		6614		E			I	V	B-MC	Nascimbene 2009, pp. 267-269, t. I.1; von Eles Masi 1986, p. 167, t. 127.1575		D
Este	burial			1898	T	A-bis	V0		I	V	E-MNA	von Eles Masi 1986, p. 163, t. 122.1507		N
Este	burial	sporadic		9628	T	A-bis-L	V0		I	V	E-MNA	Chieco Bianchi *et al.* 1976, pp. 19, 39, t. 13.12; von Eles Masi 1986, p. 168, t. 129.1596		N

(Table 5 — continued)

Archaeological site	Site typology	Excavation data	Tomb	Inv.	Preserved parts	Bow type	Foot type	Chronology	Country	Region	Location	Literature	Web sources	Considered
Este	burial			2083	T	B			I	V	E-MNA	von Eles Masi 1986, p. 165, t. 125.1546		N
Este	burial		T Palazzina		T	G	QB3	480-440 BCE	I	V	MUCIV	Peroni *et al.* 1975, pp. 39-40 (tipo 6.9), 48, t. XIV, 2; von Eles Masi 1986, p. 165, 168, t. 125-1540, 129, 1591		N
Este	burial				T			700-350 BCE	I	V	MUCIV	Cherici 1999, p. 181; Pigorini 1896, p. 305		N
Este (?)					T	A-F	V0		I	V	E-MNA	Fogolari 1975, pp. 98, 101, f. 8.5		N
Este, Benvenuti	burial		T 106	5432	T	G	V2		I	V	E-MNA	von Eles Masi 1986, p. 168, t. 129.1589		N
Este, Benvenuti	burial		T 106	5433	T	G	V2		I	V	E-MNA	von Eles Masi 1986, p. 168, t. 129.1588		N
Este, Benvenuti	burial		T 108	5459	B	A		late 6th c. BCE	I	V	E-MNA	von Eles Masi 1986, p. 163, t. 122.1508A		N
Este, Benvenuti	burial		T 108	5460	B	A		late 6th c. BCE	I	V	E-MNA	von Eles Masi 1986, p. 163, t. 122.1508		N
Este, Benvenuti	burial	1879-1880	T 98		B	A			I	V		Frey 1969, pp. 20-21, f. 8.8; Fogolari, Frey 1965, pp. 279-280, f. 15.17; Peroni *et al.* 1975, pp. 38-40 (tipo6.5), 47		N
Este, Benvenuti	burial		T 103		T	C	V3		I	V	E-MNA	Chieco Bianchi *et al.* 1976, pp. 19, 39, note 114, t. 13.9; Ghirardini, 1897, col. 114, tomb 50, nn. 990-991		N
Este, Canevedo	burial			3857	T	B	V0		I	V	E-MNA	von Eles Masi 1986, p. 165, t. 124.1539		N
Este, Canevedo	burial			3858	T	A	V1		I	V	E-MNA	von Eles Masi 1986, p. 165, t. 124.1539A		N
Este, Capodaglio	burial		T 35	3145, 2819	T	A-var	V3	480-440 BCE	I	V	E-MNA	Chieco Bianchi *et al.* 1976, pp. 19, 39, t. 13.10; Frey 1971, f. 10.2; Ghirardini 1901, col. 65, tomb 1108, n. 2935; Peroni *et al.* 1975, pp. 39-40 (tipo 6.9), 48; Mostra dell'Etruria Padana e della città di Spina, 1960, pp. 396-397, n. 1242, t. CXXXI		N
Este, Capodaglio	burial	1878	T 31		F		V3	480-440 BCE	I	V	E-MNA	Casini 2000b, p. 89, n. 99; Fogolari, Frey 1965, pp. 237-293, f. 18.4; Frey 1969, p. 99, t. 33.3; Peroni *et al.* 1975, pp. 39-40 (tipo 6.9), 48		N
Este, Casa Muletti Prosdocimi	burial		T 251			G		525-350 BCE	I	V		Casini 2000b, p. 90, n. 110; Cherici 1999, p. 181		N
Este, Ricovero	burial	1887	T 147	6706	B	A			I	V	E-MNA	von Eles Masi 1986, p. 163, t. 122.1509		N
Este, Ricovero	burial		T 180	7157	B	A		late 6th c. BCE	I	V	E-MNA	Cherici 1999, p. 181; von Eles Masi 1986, p. 164, t. 123.1519		N
Este, Ricovero	burial		T 205	7408	T	A-F	V0	525-450 BCE	I	V	E-MNA	Cherici 1999, p. 182; von Eles Masi 1986, p. 167, t. 128.1581		N

(Table 5 — continued)

Archaeological site	Site typology	Excavation data	Tomb	Inv.	Preserved parts	Bow type	Foot type	Chronology	Country	Region	Location	Literature	Web sources	Considered
Este, Ricovero	burial	1891, Riccoboni/ Prosdocimi	T 205	7409	T	A-E	V0*	6th c. BCE	I	V	E-MNA	Chieco Bianchi *et al.* 1976, pp. 19, 39, t. 13.8; Prosdocimi 1891, p. 179, tomb 1, n. 17; von Eles Masi 1986, p. 167, t. 128.1579		N
Este, Ricovero	burial	1891, Riccoboni/ Prosdocimi	T 205	7410	B	A			I	V	E-MNA	von Eles Masi 1986, p. 164, n. 1513, t. 123.1513; Prosdocimi 1891, p. 179, n. 19		N
Este, Ricovero	burial	1891, Riccoboni/ Prosdocimi	T 1		T				I	V		Prosdocimi 1891, p. 179, n. 18		N
Este, Ricovero	burial	1891, Riccoboni/ Prosdocimi	T 2		B				I	V		Prosdocimi 1891, p. 184, n. 22		N
Este, Ricovero	burial	1891, Riccoboni/ Prosdocimi	T 2		T				I	V		Prosdocimi 1891, p. 184, n. 23		N
Este, Ricovero	burial	1891, Riccoboni/ Prosdocimi	T 2		T				I	V		Prosdocimi 1891, p. 184, n. 24		N
Este, Ricovero	burial		T 212					525-450 BCE	I	V		Cherici 1999, p. 182		N
Este, Ricovero	burial								I	V		Cherici 1999, p. 181		N
Mel	burial				B	A			I	V	P-SABAP	Fogolari 1975, p. 121, t. 56.3		D
Mel		1961	T 31	9244	B	A		late 6th c. BCE	I	V	MAM	Nascimbene 2009, p. 135		A
Mel		1961	T 33	9290	B	A-E		late 6th.-early 5th c. BCE	I	V	MAM	Nascimbene 2009, p. 135		A
Mel			T 38	9289	B	A		late 6th c. BCE	I	V	MAM	Nascimbene 2009, p. 135		A
Mel		1962	T 55	43328	B	A	V0	6th. c. BCE	I	V	MAM	Nascimbene 2009, p. 135		L
Mel			T 38	9271	T	miniaturistica	V0	late 6th. c. BCE	I	V	MAM	Nascimbene 2009, p. 135		A
Monte Loffa	settlement				B	A			I	V		von Eles Masi 1986, p. 164, t. 123.1517A		D
Montebelluna, loc. Posmon	burial	2001	T 118	304784	B	A		6th. c. BCE	I	V	M-MSNA	de Marinis 2000, p. 170		A
Montebelluna, loc. Posmon	burial	2001	T 118	304780	B	A-bis		6th. c. BCE	I	V	M-MSNA	de Marinis 2000, p. 170		A
Montebelluna, loc. Santa Maria in Colle		1962, sporadic		147145	B	A			I	V	M-MSNA	von Eles Masi 1986, p. 164, t. 123.1516		A

(Table 5 — continued)

Archaeological site	Site typology	Excavation data	Tomb	Inv.	Preserved parts	Bow type	Foot type	Chronology	Country	Region	Location	Literature	Web sources	Considered
Montebelluna, loc. Santa Maria in Colle	burial	1959	T 6	7489	B	A		late 6th.-early 5th c. BCE	I	V	M-MSNA	Locatelli *et al.* 2003, p. 85, 88, t. 12, n. 4; Nascimbene 2009, p. 135, n. 28; von Eles Masi 1986, p. 164, t. 123.1518		A
Montebello	burial					B			I	V	P-SABAP	Nascimbene 2009, p. 135, n. 29		N
Montebello	burial					A			I	V	P-SABAP	Nascimbene 2009, p. 135, n. 30		N
Oppeano					B	B			I	V		von Eles Masi 1986, pp. 166, t. 125.1549		D
Padova, vicolo Ognissanti	burial		T XXIX	60735	B	A-P		late 6th c. BCE	I	V	P-MC	von Eles Masi 1986, p. 157, t. 119.1459A		A
Padova, vicolo Ognissanti	burial		T XXXVII		F		V4*	late 6th c. BCE	I	V	P-MC			A
Padova, vicolo Ognissanti	burial	1910	T XXXVIII		B	A		late 6th c. BCE	I	V	P-MC	Frey 1969, p. 100, t. 34.28; Peroni *et al.* 1975, pp. 38-40 (tipo6.5), 47; von Eles Masi 1986, p. 164, t. 123.1519A		L
Padova, vicolo San Massimo	burial	1911, excavation, Civic Museum	T XVI	65296	T	A-E	V0	late 6th c. BCE	I	V	P-MC	Chieco Bianchi 1981, pp. 274-275, t. 65A.6; von Eles Masi 1986, p. 167, t. 128.1579A		L
Palugana	burial	1896, acquisition, Soranzo		22101; 56472	T	A	V0*	late 6th c. BCE	I	V	MUCIV	Frey 1969, pp. 98-99, t. 34.1; 1971, f. 9.4; Peroni *et al.* 1975, pp. 38-40 (tipo6.5), 47, t. XVII.1; von Eles Masi 1986, p. 163-164, t. 122.1510		N
Pieve d'Alpago, Pian della Gnela	burial	2004, excavation	T 10	312348; MS 10/31-32 44-45	T	C	V4	late 6th.-early 5th c. BCE	I	V	SABAP-PD	Angelini, Molin 2015, pp. 52-53, f. 1a, 2a; Gangemi *et al.* 2015, pp. 41-42, 45-46, 56, 105, n. 9		A
Pieve d'Alpago, Pian della Gnela	burial	2004, excavation	T 10	312349 - MS 10/40	T	A-E	V0	late 6th.-early 5th c. BCE	I	V	SABAP-PD	Gangemi *et al.* 2015, pp. 41-42, 45-46, 57, n. 10		A
Pieve d'Alpago, Pian della Gnela	burial	2007, excavation	T 11	355517 - MS 11/17	B	C			I	V	SABAP-PD	Angelini, Molin 2015, pp. 52-53; Gangemi *et al.* 2015, pp. 63, 67, 73, n. 7, t. IV.2, XX.dx		A
Pieve d'Alpago, Pian della Gnela	burial	2007, excavation	T 11	355516 - MS 11/19	T	C	P		I	V	SABAP-PD	Gangemi *et al.* 2015, pp. 63, 67, 72, n. 6, t. IV.2.dx, XX down-sx		A
Pieve d'Alpago, Pian della Gnela	burial	2007, excavation	T 11	355515 - MS 11/8	B	A-E			I	V	SABAP-PD	Gangemi *et al.* 2015, pp. 63, 67, 72, n. 5		A
Piovego	burial	1970-1980	T 110	110,4	B	A		6th-5th. c. BCE	I	V	UNIPD	Gallo 2023		L
Piovego	burial	1970-1981	T 108	108,3	T	A	V0	6th-5th. c. BCE	I	V	UNIPD	Gallo 2023		A
Piovego	burial	1970-1982	T 97	181844; 97.5	B	A		6th-5th. c. BCE	I	V	UNIPD	Gallo 2023		A
Piovego	burial	1970-1983	T 97	181843; 97.6	B	A		6th-5th. c. BCE	I	V	UNIPD	Gallo 2023		A
Piovego	burial	1970-1984	T 89	89,6	B	A-E		6th-5th. c. BCE	I	V	UNIPD	Gallo 2023		A

(Table 5 — continued)

Archaeological site	Site typology	Excavation data	Tomb	Inv.	Preserved parts	Bow type	Foot type	Chronology	Country	Region	Location	Literature	Web sources	Considered
Piovego	burial	1970-1985	T 79	224255; 79.7	B	B-E		6th-5th. c. BCE	I	V	UNIPD	Gallo 2023		A
Piovego	burial	1970-1986	T 62	224358; 62.3	B	A		6th-5th. c. BCE	I	V	UNIPD	Gallo 2023		A
Piovego	burial	1970-1987	T 53	224201; 53.4	B	A		6th-5th. c. BCE	I	V	UNIPD	Gallo 2023		A
Piovego	burial	1970-1988	T 5	5,73	B	A-bis		6th-5th. c. BCE	I	V	UNIPD	Gallo 2023		A
Piovego	burial	1970-1989	T 22	153032; 22.7	T	C	V2*	6th-5th. c. BCE	I	V	UNIPD	Gallo 2023		A
Piovego	burial	1970-1990	T 29	149721; 29.5	B	A-E		6th-5th. c. BCE	I	V	UNIPD	Gallo 2023		A
Piovego	burial	1970-1991	T 47	34914; 47.13	B	A		6th-5th. c. BCE	I	V	UNIPD	Gallo 2023		A
Piovego	burial	1970-1994	T 110	110,4	B	A		6th-5th. c. BCE	I	V		Gallo 2023		L
Podenzoi, Castellavazzo	burial	1968, sporadic	T	287321; 3581	T	A-E	V0	late 6th. c. BCE	I	V	B-MC	Nascimbene 2009, pp. 287-289, t. VIII, n. 4		L
Safforze	burial	1939		6599; 3328	T	A	V0	late 6th. c. BCE	I	V	B-MC	Endrizzi, Marzatico 1997, p. 554, f. 13, n. 76; Nascimbene 2009, pp. 297-298, t. XI, n. 3; von Eles Masi 1986, p. 164, t. 122.1511		L
Safforze	burial	1939		6602; 3329	F	G	V4*		I	V	B-MC	Nascimbene 2009, pp. 297-298, t. XI, n. 4		A
Safforze	burial	1939		6600; 3331	B	A-E			I	V	B-MC	Nascimbene 2009, pp. 297-298, t. XI, n. 5		A
Treviso?				165	T	G	V2*		I	V	T-MC	von Eles Masi 1986, p. 168, t. 129.1587		N
Altino, Fornasotti	burial	1977	T 2	AL. 15133	B	A		late 6th-early 5th c. BCE	I	V	A-MAN	Casini 2000b, p. 90, n. 122; Tombolani 1987, p. 171, 175, f. 1.5		N
Pozzuolo del Friuli	settlement					E		525-450 BCE	I	FVG		Nascimbene 2009, p. 135, n. 35		N
Pozzuolo del Friuli	burial		T 3			E			I	FVG		Nascimbene 2009, p. 135, n. 36		N
Mechel	cultual			3541	F			6th c. BCE	I	T	T-CB	Taviani, 1997, p. 152, f. 2, p. 477, n. 848		N
Mechel	cultual			3541	T	C	V2	6th c. BCE	I	T	T-CB	Adam 1996, p. 77, t. II.36; de Marinis 2000, p. 170; Taviani 1997, p. 152, f. 1, p. 477, n. 847		N
Mechel	cultual			9275	T				I	T	I-TLF	Adam 1996, p. 78, note 1		N
Mechel	cultual			1344; 2342	T	B	V1*		I	T	T-CB	Adam 1996, p. 77, 79, t. II,35; Campi 1885, pp. 101-102, t. VI.3; 1897, p. 16; Cherici 1999, p. 182		N
Mechel? O Veneto?				5509	F				I	T	I-TLF	Adam 1996, p. 78, note 1		N
Mechel? O Veneto?				14148/1	F				I	T	I-TLF	Adam 1996, p. 78, note 1		N
Mechel? O Veneto?				14148/2	F				I	T	I-TLF	Adam 1996, p. 78, note 1		N

(Table 5 — continued)

Archaeological site	Site typology	Excavation data	Tomb	Inv.	Preserved parts	Bow type	Foot type	Chronology	Country	Region	Location	Literature	Web sources	Considered
Stenico, loc. Calferi	cultual	1978-1981, excavation		1196	F		V2	525-490/480 BCE	I	T	S-CS	Adam 1996, p. 77, t. II.37; de Marinis 2000, p. 170		N
San Romano in Garfagnana, Monte Pisone	settlement	1984, excavation SABAP; saggio C, US9			B	G		early 5th. c. BCE	I	TO		Casini 2000b, p. 87, n. 5; Ciampoltrini 1993, pp. 40-54, f. 18.9		N
Orvieto, necropoli del Crocefisso del tufo	burial		T 10						I	U		de Marinis 2000, p. 173, note 40		N
Sirolo-Numana, Magnalardo	burial		T 3		T	E			I	M		Nascimbene 2009, p. 136, n. 47		N
unknown				A0.9.28550	B	A					M-MCA			A
unknown		Corbetta donation		A0.9.35543	B	A					M-MCA	von Eles Masi 1986, p. 165, t. 124.1536		L
unknown				A0.9.35028	B	A					M-MCA			A
unknown				A0.9.35039	F		V1*				M-MCA			A
unknown				A0.9.4916	B	C-F					M-MCA			A
unknown				A0.9.28250	F		V2*				M-MCA			A
unknown				A0.9.28047	F		V1*				M-MCA			A
unknown				br436	B	B					M-MCA	von Eles Masi 1986, p. 165, t. 125.1542		D
unknown				br436b	B	B					M-MCA	von Eles Masi 1986, p. 165, t. 125.1544		D
unknown				br90	T	A	S				M-MCA	von Eles Masi 1986, p. 164, t. 123.1512		D
unknown				16	B	D					Bre	Musellius 1756, pp. 29, 112, t. LII.3; Rizzini 1910, p. 345, n. 16; von Eles Masi 1986, p. 167, t. 127.1571		N
unknown				60046	B	D					MUCIV	von Eles Masi 1986, p. 167, t. 127.1573		N
unknown					B	C-F					MRT	von Eles Masi 1986, p. 168, t. 128.1585		D
unknown				A0.9.35026	B	C					M-MCA	von Eles Masi 1986, p. 166, t. 127.1566		L
unknown				A0.9.35025; 90	B	C					M-MCA	von Eles Masi 1986, p. 167, t. 127.1570		L
unknown				A0.9.35514; br686; 89	B	C								L
unknown	burial			A0.9.4920; br508b	B	C					M-MCA	von Eles Masi 1986, p. 166, t. 126.1562		L
unknown				A0.9.28295; br483a	B	B					M-MCA	von Eles Masi 1986, p. 165, t. 125.1543		L
unknown				A0.9.18077	B	C								L

(Table 5 — continued)

Archaeological site	Site typology	Excavation data	Tomb	Inv.	Preserved parts	Bow type	Foot type	Chronology	Country	Region	Location	Literature	Web sources	Considered
unknown				A0.9.28296; br483	B	B					M-MCA	von Eles Masi 1986, p. 165, t. 125.1544A		L
unknown	burial			A0.9.28297; 1583; br546	B	B					M-MCA	von Eles Masi 1986, pp. 166, t. 126.1553		L
Arbedo	Ripostiglio	1946, sporadic		46/425	B	D		480-440 BCE	Sw			Lorre, Cicolani 2009, p. 121, f. 1; Schindler 1997, p. 515, f. 1		N
Arbedo	Ripostiglio	1946, sporadic			F		GG	480-440 BCE	Sw			Lorre, Cicolani 2009, p. 121, f. 1; Schindler 1997, p. 515, f. 1		N
Arbedo	Ripostiglio	1946, sporadic		437		A			Sw			Schmid-Sikimić 2002, p. 299		N
Arbedo	Ripostiglio	1946, sporadic		438		A			Sw			Schmid-Sikimić 2002, p. 299		N
Arbedo	Ripostiglio	1946, sporadic		439		A			Sw			Schmid-Sikimić 2002, p. 299		N
Arbedo	Ripostiglio	1946, sporadic		440		A			Sw			Schmid-Sikimić 2002, p. 299		N
Arbedo	Ripostiglio	1946, sporadic		441		A			Sw			Schmid-Sikimić 2002, p. 299		N
Arbedo	Ripostiglio	1946, sporadic		442		A			Sw			Schmid-Sikimić 2002, p. 299		N
Arbedo	Ripostiglio	1946, sporadic		444		A			Sw			Schmid-Sikimić 2002, p. 299		N
Arbedo	Ripostiglio	1946, sporadic		445		A			Sw			Schmid-Sikimić 2002, p. 299		N
Arbedo	Ripostiglio	1946, sporadic		436		A			Sw			Schmid-Sikimić 2002, p. 299		N
Arbedo	Ripostiglio	1946, sporadic		435		B-C			Sw			Schmid-Sikimić 2002, p. 300		N
Arbedo	Ripostiglio	1946, sporadic		449		B-C			Sw			Schmid-Sikimić 2002, p. 300		N
Arbedo	Ripostiglio	1946, sporadic		453		B-C			Sw			Schmid-Sikimić 2002, p. 300		N
Arbedo	Ripostiglio	1946, sporadic		456		B-C			Sw			Schmid-Sikimić 2002, p. 300		N
Arbedo, Castione	burial		T 13		T	D	P		Sw			Schmid-Sikimić 2002, pp. 158-159, f. 7.6-D.2, tab. 7.1		N
Arbedo, Castione	burial		T 2	12926	T	D	V2		Sw			Schmid-Sikimić 2002, p. 159, tab. 7.1		N
Arbedo, Castione	burial		T 3	12931	T	B	V1		Sw			Schmid-Sikimić 2002, p. 159, tab. 7.1		N
Arbedo, Castione	burial		T 3	12931	B	A			Sw			Schmid-Sikimić 2002, p. 159, tab. 7.1		N
Arbedo, Castione	burial		T 5	12944	T	B	V2		Sw			Schmid-Sikimić 2002, p. 159, tab. 7.1		N
Arbedo, Castione	burial		T 11	12980	T	B	V1		Sw			Schmid-Sikimić 2002, p. 159, tab. 7.1		N
Arbedo, Castione	burial		T 11	12980	T	D	V2		Sw			Schmid-Sikimić 2002, p. 159, tab. 7.1		N
Arbedo, Castione	burial		T 12	12985	T	D	P		Sw		Z-LM	Schmid-Sikimić 2002, pp. 158-159, 300, f. 7.6-D.1, tab. 7.1		N
Arbedo, Castione	burial		T 12	12985	T	D	P		Sw		Z-LM	Schmid-Sikimić 2002, pp. 158-159, 300, f. 7.6-D.1, tab. 7.1		N
Arbedo, Cerinasca	burial			12317	T	G	QB2	480-440 BCE	Sw		Z-LM	Schimid-Sikimić 2000b, pp. 218-219, f. 1		N

(Table 5 — continued)

Archaeological site	Site typology	Excavation data	Tomb	Inv.	Preserved parts	Bow type	Foot type	Chronology	Country	Region	Location	Literature	Web sources	Considered
Arbedo, Cerinasca	burial		T 3	11894	B	A			Sw		Z-LM	Schmid-Sikimić 2002, p. 159, tab. 7.1		N
Arbedo, Cerinasca	burial	1896-1897, excavation, Migliorati-Ulrich	T 12	A-12985	T	D	P		Sw		Z-LM	de Marinis 2000, p. 170; Ravaglia 2000, p. 281	31	N
Arbedo, Cerinasca	burial	1896-1897, excavation, Migliorati-Ulrich	T 49		T	G	GG	480-440 BCE	Sw		Z-LM	de Marinis 2000, p. 170; Mangani, Minarini 2000, p. 261, f. 2; Ravaglia 2000, p. 281		N
Arbedo, Cerinasca	burial		T 56		T		V2	525-490/480 BCE	Sw		Z-LM	Ravaglia 2000, p. 291		N
Arbedo, Cerinasca	burial	1896-1897, excavation, Migliorati-Ulrich	T 71	12272	T	E	V0		Sw		Z-LM	de Marinis 2000, p. 170; Mangani, Minarini 1998, pp. 77-79, f. 6 up; Ravaglia 2000, p. 281; Schmid-Sikimić 2002, p. 159, tab. 7.1		N
Arbedo, Cerinasca	burial	1896-1897, excavation, Migliorati-Ulrich	T 71	12272	T	B	V0		Sw		Z-LM	de Marinis 2000, p. 170; Mangani, Minarini 1998, pp. 77-79, f. 6 down; Ravaglia 2000, p. 281; Schmid-Sikimić 2002, p. 159, tab. 7.1		N
Arbedo, Cerinasca	burial		T 72	12275	B	B			Sw		Z-LM	Schmid-Sikimić 2002, p. 159, tab. 7.1		N
Arbedo, Cerinasca	burial		T 73	12279	B	E			Sw		Z-LM	Schmid-Sikimić 2002, p. 159, tab. 7.1		N
Arbedo, Cerinasca	burial		T 73	12279	T	B	V0		Sw		Z-LM	Schmid- Sikimić 2002, p. 10, f. 2.2B; p. 224, f. 9.6; p. 159, tab. 7.1		N
Arbedo, Cerinasca	burial	1896-1897, excavation, Migliorati-Ulrich	T 77		T	G	S1		Sw		Z-LM	de Marinis 2000, p. 170; Ravaglia 2000, p. 281; Mangani, Minarini 1998, pp. 77-79, f. 4 up		N
Arbedo, Cerinasca	burial	1896-1897, excavation, Migliorati-Ulrich	T 77		T	G	S2		Sw		Z-LM	de Marinis 2000, p. 170; Ravaglia 2000, p. 281; Mangani, Minarini 1998, pp. 77-79, f. 4 down		N
Arbedo, Cerinasca	burial		T 78	12305	T	E	V1		Sw		Z-LM	Schmid-Sikimić 2002, p. 159, tab. 7.1		N
Arbedo, Cerinasca	burial		T 78	12305	T	D-G	V2		Sw		Z-LM	Schmid-Sikimić 2002, p. 159, tab. 7.1		N
Arbedo, Cerinasca	burial		T 80		T	D	QB2		Sw		Z-LM	Schmid- Sikimić 2002, p. 224, f. 9.6		N
Arbedo, Cerinasca	burial	1896-1897, excavation, Migliorati-Ulrich	T 84	12338	T	G	GG	480-440 BCE	Sw		Z-LM	de Marinis 2000, p. 170; Ravaglia 2000, p. 281	32	N
Arbedo, Cerinasca	burial		T 85	12342	T	B	V2		Sw		Z-LM	Schmid-Sikimić 2002, p. 159, tab. 7.1		N
Arbedo, Cerinasca	burial		T 85	12342	T	D	V2		Sw		Z-LM	Schmid-Sikimić 2002, p. 159, tab. 7.1		N

(Table 5 — continued)

Archaeological site	Site typology	Excavation data	Tomb	Inv.	Preserved parts	Bow type	Foot type	Chronology	Country	Region	Location	Literature	Web sources	Considered
Arbedo, Cerinasca	burial		T 87	12352	T	D	V2		Sw		Z-LM	Schmid-Sikimić 2002, p. 159, tab. 7.1		N
Arbedo, Cerinasca	burial		T 87	12352	T	D	V2		Sw		Z-LM	Schmid-Sikimić 2002, p. 159, tab. 7.1		N
Arbedo, Cerinasca	burial		T 91	12376	T	B	V1		Sw		Z-LM	Schmid-Sikimić 2002, p. 159, tab. 7.1		N
Arbedo, Cerinasca	burial		T 95	12393	B	D-G			Sw		Z-LM	Schmid-Sikimić 2002, p. 159, tab. 7.1		N
Arbedo, Cerinasca	burial		T 96	12400	T	B	V1		Sw		Z-LM	Schmid-Sikimić 2002, p. 159, tab. 7.1		N
Arbedo, Cerinasca	burial		T 96	12400	T	D-G	V1		Sw		Z-LM	Schmid-Sikimić 2002, p. 159, tab. 7.1		N
Arbedo, Cerinasca	burial		T 96	12400	T	D-G	V2		Sw		Z-LM	Schmid-Sikimić 2002, p. 159, tab. 7.1		N
Arbedo, Cerinasca	burial	excavation	T 97			G		480-440 BCE	Sw		Z-LM	Ravaglia 2000, p. 286		N
Arbedo, Cerinasca	burial		T 102	12428	T	B	V2		Sw		Z-LM	Schmid-Sikimić 2002, p. 159, tab. 7.1		N
Arbedo, Cerinasca	burial		T 102	12428	T	D-G	V2		Sw		Z-LM	Schmid-Sikimić 2002, p. 159, tab. 7.1		N
Arbedo, Cerinasca	burial		T 158		T	G	GGG	480-440 BCE	Sw		Z-LM	Schmid-Sikimić 2002, p. 223, f. 9.4		N
Baar	settlement					G		480-440 BCE	Sw			Cicolani 2017, p. 110		N
Cademario, Forcora									Sw			Schmid-Sikimić 2002, p. 33		N
Castaneda, Dorf	burial		T XLIX	III.C.127f	T	G	GGG	480-440 BCE	Sw		C-RM	de Marinis 2000 pp. 170, 173, note 44; Taviani 1997, p. 152; p. 246, n. 29		N
Castaneda, Haus Luzzi	burial	1976	T 76-2	CaL 76/20-6	T	G	GGG	480-440 BCE	Sw		C-ADGH	Taviani 1997, p. 152; p. 246, n. 27		N
Castaneda, Haus Luzzi	burial	1976	T 76-2		T	G	GGG	480-440 BCE	Sw			de Marinis 2000 pp. 170, 173, note 44; Taviani 1997, p. 152; p. 244, f. 15		N
Castaneda, Haus Luzzi	burial	1976	T 1		T	G	QB3	480-440 BCE	Sw			Rageth, 2000, f. 24.3		N
Castaneda, Haus Luzzi	burial	1976	T 1		T	G	QB3	480-440 BCE	Sw			Rageth, 2000, f. 24.4		N
Castaneda, Haus Luzzi	burial	1976	T 1		T	G	QB3	480-440 BCE	Sw			Rageth, 2000, f. 24.5		N
Castaneda, Haus Luzzi	burial	1976	T 1		T	G	QB3	480-440 BCE	Sw			Rageth, 2000, f. 24.6		N
Castaneda, Haus Luzzi	burial	1976	T 1		B	G		480-440 BCE	Sw			Rageth, 2000, f. 24.7		N
Castaneda, Haus Luzzi	burial	1976	T 1		B	G		480-440 BCE	Sw			Rageth, 2000, f. 24.8		N
Castione	burial		T 12		T				Sw			Lorre, Cicolani 2009, p. 55, f. 4		N
Chur, Areal Ackermann	settlement	1970-1974			F	G		480-440 BCE	Sw			Casini 2000b, p. 91, n. 165; Cicolani 2017, p. 110		N

(Table 5 — continued)

Archaeological site	Site typology	Excavation data	Tomb	Inv.	Preserved parts	Bow type	Foot type	Chronology	Country	Region	Location	Literature	Web sources	Considered
Chur, Markthallenplatz	settlement	1964-1968			F			480-440 BCE	Sw			Casini 2000b, p. 91, n. 169; Conradin, 1978, f. 75.8; Schmid-Sikimić̀h, 2002, p. 232		N
Chur, Markthallenplatz	settlement	1964-1968			F	G		480-440 BCE	Sw			Conradin, 1978, f. 75.14; Schmid-Sikimić̀h, 2002, p. 232		N
Claro, Alla Monda	burial		T 12	12757					Sw		C-ADGH	Schmid-Sikimić 2000b, p. 237		N
Claro, Alla Monda	burial		T 12	12759					Sw		C-ADGH	Schmid-Sikimić 2000b, p. 237		N
Claro, Alla Monda	burial		T 13	12765					Sw		C-ADGH	Schmid-Sikimić 2000b, p. 237		N
Dalpe, Vidresco	burial	1958, impresa Dotti	T 1		T	G	GG	480-440 BCE	Sw		B-CG	de Marinis 2000, p. 170; Ravaglia 2000, pp. 281-283, f. 1, n. 2		N
Gorduno	burial		T 1		B	A			Sw			de Marinis 2000, p. 170; Ravaglia 2000, p. 281; Schmid-Sikimić 2002, pp. 160, 299, f. 7.7		N
Gorduno	burial		T 2	12619		A			Sw			de Marinis 2000, p. 170; Ravaglia 2000, p. 281; Schmid-Sikimić 2002, p. 159, tab. 7.1		N
Gudo	burial	1910, excavation, Ortelli	T 79		T	G			Sw		B-CG	Baserga 1910, p. 21; de Marinis 2000, p. 170; Ravaglia 2000, p. 281		N
Gudo	burial	1910, excavation, Ortelli	T 79		T	G			Sw		B-CG	Baserga 1910, p. 21; de Marinis 2000, p. 170; Ravaglia 2000, p. 281		N
Gudo	burial	1910, excavation, Ortelli	T 85						Sw		B-CG	Baserga 1910, p. 21; de Marinis 2000, p. 170; Ravaglia 2000, p. 281		N
Gudo	burial	1910, excavation, Ortelli	T 96						Sw		B-CG	Baserga 1910, p. 21; de Marinis 2000, p. 170; Ravaglia 2000, p. 281		N
Gudo	burial	1910, excavation, Ortelli	T 119						Sw		B-CG	Baserga 1910, p. 23; de Marinis 2000, p. 170; Ravaglia 2000, p. 281		N
Gudo	burial	1910, excavation, Ortelli	T 119						Sw		B-CG	Baserga 1910, p. 23; de Marinis 2000, p. 170; Ravaglia 2000, p. 281		N
Gudo	burial	1910, excavation, Ortelli	T 119						Sw		B-CG	Baserga 1910, p. 23; de Marinis 2000, p. 170; Ravaglia 2000, p. 281		N

(Table 5 — continued)

Archaeological site	Site typology	Excavation data	Tomb	Inv.	Preserved parts	Bow type	Foot type	Chronology	Country	Region	Location	Literature	Web sources	Considered
Gudo	burial	1910, excavation, Ortelli	T 195						Sw		B-CG	Baserga 1910, p. 24; de Marinis 2000, p. 170; Ravaglia 2000, p. 281		N
Gudo	burial	1910, excavation, Ortelli	T 214						Sw		B-CG	Baserga 1910, p. 25; de Marinis 2000, p. 170; Ravaglia 2000, p. 281		N
Gudo	burial	1910, excavation, Ortelli	T 281		T	G		480-440 BCE	Sw		B-CG	Baserga 1910, pp. 28, 100, 111, f. 89; de Marinis 2000, p. 170; Ravaglia 2000, p. 281		N
Ludiano, Borgo di Motto	burial	1926, Senaggia			T	absent	V4*	525-490/480 BCE	Sw			Ravaglia, 2000, p. 290, f. 7, n. 4		N
Mesocco-Coop	burial	1969	T 4	2	T	C	QA4*		Sw			Schmid-Sikimić 2002, pp. 63, 68, 159, f. 3.20.17, tab. 7.1		N
Mesocco-Coop	burial	1969	T 9	239	T	B-E	V1	525-490/480 BCE	Sw		C-ADGH	Lorre, Cicolani 2009, p. 101; Rageth 2000, f. 23; Schmid-Sikimić 2000, p. 237-238, f. 19.1; 2002, pp. 81-82, 159, f. 3.35.62, tab. 7.1		N
Mesocco-Coop	burial	1969	T 11		T*	A-bis	V0		Sw			Schmid-Sikimić 2000b, p. 232, f. 14.B.1; 2002, pp. 90, 92, f. 3.45, n. 98		N
Mesocco-Coop	burial	1969	T 11		B*	A-bis			Sw			Schmid-Sikimić 2000b, p. 232, f. 14.B.2; 2002, pp. 92- 93, f. 3.45, n. 99		N
Minusio, loc. Ceresol	burial	1941-1942	T 14		T	G	SB2		Sw		L-MCA	de Marinis 2000, p. 170; Ravaglia 2000, p. 281; Schmid-Sikimić 2000b, pp. 221-223, f. 6.B.5; 2002, p. 36, f. 2.21-B.5		N
Minusio, loc. Ceresol	burial	1941-1942	T 14		T	G	SB2		Sw		L-MCA	de Marinis 2000, p. 170; Ravaglia 2000, p. 281; Schmid-Sikimić 2000b, pp. 221-223, f. 6.B.6; 2002, p. 36, f. 2.21-B.6		N
Minusio, loc. Ceresol	burial		T 16	41/79	T	A	V0*		Sw			Schmid-Sikimić 2002, pp. 33, 159, f. 2.19.4, tab. 7.1		N
Minusio, loc. Ceresol	burial		T 16	41/82	T	A	V0*		Sw			Schmid-Sikimić 2002, pp. 33, 159, f. 2.19.5, tab. 7.1		N
Minusio, loc. Ceresol	burial		T 16	41/83	B	A			Sw			Schmid-Sikimić 2002, pp. 33, 159, f. 2.19.6, tab. 7.1		N
Osco	burial	XIX c.	T 97		T	G		480-440 BCE	Sw			Ravaglia 2000, p. 286		N
Pianezzo, loc. Carabella	burial	1905, excavation	T 22		T	G	GGG2	480-440 BCE	Sw		L-M	Magni 1907, t. VI, up-sx		N
Pianezzo, loc. Carabella	burial	1905, excavation	T 22		T	G	GGG2	480-440 BCE	Sw		L-M	Magni 1907, t. VI, up-center		N

(Table 5 — continued)

Archaeological site	Site typology	Excavation data	Tomb	Inv.	Preserved parts	Bow type	Foot type	Chronology	Country	Region	Location	Literature	Web sources	Considered
Solduno	burial	2002, excavation	T 1		T	G	GGG2	480-440 BCE	Sw			Cardani Vergani *et al.* 2011, p. 81, t. XVII.1		N
Tamins-Unterm Dorf	burial	1964-1966	T 56	P1968.157	F		GG1*	480-440 BCE	Sw		Z-LM	Casini 2000b, p. 91, n. 161-2; Cicolani 2017, p. 110; Conradin 1978, p. 88, f. 31, 20.4; Lorre, Cicolani 2009, p. 116, f. 1, tomb 56; Schmid-Sikimić, 2002, p. 232, f. 2.11		N
Tamins-Unterm Dorf	burial	1964-1966			B	D			Sw		Z-LM	Conradin 1978, f. 30.2; Casini 2000b, p. 91, n. 163; Lorre, Cicolani 2009, p. 116, f. 1; Schmid-Sikimić 2002, f. 10.18.2		N
Zugo					B	A			Sw			Schmid-Sikimić, Bigler 2005, f. 5 center		N
Gamsen	settlement				F	G		480-440 BCE	F			Cicolani 2017, p. 110		N
Eschen, Malanser	settlement							525-480 BCE	Li			Casini 2000b, p. 93, n. 241		N
Balzers	burial					G		480-440 BCE	Li			Cicolani 2017, p. 110		N
Balzers	burial					G		480-440 BCE	Li			Cicolani 2017, p. 110		N
Balzers	burial					G		480-440 BCE	Li			Cicolani 2017, p. 110		N
Balzers	burial					G		480-440 BCE	Li			Cicolani 2017, p. 110		N
Balzers	burial				F	G		480-440 BCE	Li			Cicolani 2017, p. 110		N
Poland, Masurian Lake District		1896		PM Pr D 211	B	A			Po		B-MVF	Thanks to dr. Cicolani for the notice	33	N
Poland, Masurian Lake District		1896							Po			Thanks to dr. Cicolani for the notice		D
Libna	burial	1893	tum. I, T 30			E		late 6th c. BCE	Sl			Nascimbene 2009, p. 136, n. 52		N
Santa Lucia di Tolmino	burial		T 638			A			Sl			Schmid-Sikimić 2002, p. 299		N
Santa Lucia di Tolmino	burial		T 706			A			Sl			Schmid-Sikimić 2002, p. 299		N
Santa Lucia di Tolmino	burial		T 1245			A			Sl			Schmid-Sikimić 2002, p. 299		N
Santa Lucia di Tolmino	burial		T 1927			A			Sl			Schmid-Sikimić 2002, p. 299		N
Santa Lucia di Tolmino	burial		T 2080			A			Sl			Schmid-Sikimić 2002, p. 299		N
Santa Lucia di Tolmino	burial		T 2083			A			Sl			Schmid-Sikimić 2002, p. 299		N
Santa Lucia di Tolmino	burial		T 2229			A			Sl			Schmid-Sikimić 2002, p. 299		N

(Table 5 — continued)

Archaeological site	Site typology	Excavation data	Tomb	Inv.	Preserved parts	Bow type	Foot type	Chronology	Country	Region	Location	Literature	Web sources	Considered
Santa Lucia di Tolmino	burial		T 2229			A			Sl			Schmid-Sikimić 2002, p. 299		N
Santa Lucia di Tolmino	burial					A			Sl			Schmid-Sikimić 2002, p. 299		N
Santa Lucia di Tolmino	burial		T 716						Sl			Schmid-Sikimić 2000b, p. 237; de Marinis 2000, p. 170		N
Santa Lucia di Tolmino	burial		T 1014		T	A	V0		Sl			Marchesetti 1893, t. XV.4; Adam 1996, p. 78, note 6		N
Santa Lucia di Tolmino	burial		T 256		T	A-E	V0		Sl			Marchesetti 1893, t. XV.16		N
Stična									Sl			de Marinis 2000, p. 170		N
Vače									Sl			de Marinis 2000, p. 170		N

(Table 5 — continued)

Archaeological site	Site typology	Excavation data	Tomb	Inv.	Type	Chronology	Country	Region	Location	Literature	Considered
Castelletto Ticino, loc. Cascina Riviera, Merlotitt	settlement	1986-88, excavation: US 210		210/230	L	480-440 BCE	I	P	CT-GSAC	Ruffa 1999, p. 31, t. VI.7; 2001, p. 17	N
Castelletto Ticino, Via Sivo	burial	1983				6th c. BCE	I	P	MRT	Gambari 1984 pp. 262-263, t. LXXXIV.B.4	A
Brembate Sotto	burial	1888, Mantovani recovery		65; M22		525-480 BCE	I	LO	B-MA	Casini 2017, p. 22, f. 11, n. 26; von Eles Masi 1986, t. 142.1833	A
Brunate							I	LO	C-MC	von Eles Masi 1986, p. 184, t. 143.1838	N
Malgesso							I	LO	V-MC	von Eles Masi 1986, p. 184, t. 142.1835	N
Bellunese							I	V	B-MC		A
Carceri d'Este	burial	1893, discovery					I	V		Cherici 1999, p. 182; Prosdocimi 1893, p. 401, f. 8	N
Carceri d'Este	burial	1893	T 48		L		I	V	E-MNA	Frey 1969, p. 21, t. 28.10; Lucke 1962, f. 5.3; Peroni *et al.* 1975, pp. 39-40, 48; Prosdocimi 1893, p. 401, f. 7; von Eles Masi 1986, p. 184, t. 143.1840	N
Caverzano	burial	1865, excavation		3294		late 6th-early 5th c. BCE	I	V	B-MC	Nascimbene 1999, pp. 48-50, f. 9, n. 70	N
Caverzano	burial			94			I	V	B-MC	von Eles Masi 1986, p. 184, t. 142.1837	N
Caverzano, loc. Masiera-Font	burial	1865, excavation				450 BCE	I	V		Nascimbene 1999, pp. 80-82, f. 16, n. 164; Leicht 1871, f. 13	D
Este, Costa-Martini	burial		T 43		C	late 6th-early 5th c. BCE	I	V	E-MNA	Peroni *et al.* 1975, pp. 39-40, 48; Frey 1969, f. 9.4; Chieco Bianchi *et al.* 1976, pp. 19, 39, t. 13.11	N
Este, Costa-Martini	burial		T 43		C		I	V		Peroni *et al.* 1975, pp. 39-40, 48; Frey 1969, f. 9.5	N
Este, Pelà	burial	1877	T 14		R	525-450 BCE	I	V	E-MNA	Chieco Bianchi *et al.* 1976, p. 20, note 118; Cherici 1999, p. 182; Frey 1969, p. 21, t. 29.1; Fogolari, Frey 1965, pp. 281-282, f. 16.1; Peroni *et al.* 1975, pp. 39-40, 48; von Eles Masi 1986, p. 186, t. 144.1861	N

Table 6. List of findings for the type: leech fibula with transverse grooves [in column 'type': R = variety with swallow-tailed end; L = variety with longitudinal grooves; C = varietà with grooves alternated to circular inlays].

Archaeological site	Site typology	Excavation data	Tomb	Inv.	Type	Chronology	Country	Region	Location	Literature	Considered
Este, Pelà	burial	1877	T 14		R	525-450 BCE	I	V	E-MNA	Chieco Bianchi *et al.* 1976, p. 20, note 118; Frey 1969, p. 21, t. 29.2; Fogolari, Frey 1965, pp. 281-282, f. 16.2; Peroni *et al.* 1975, pp. 39-40, 48; von Eles Masi 1986, p. 186, t. 144.1862	N
Oppeano							I	V	V-MCSN	von Eles Masi 1986, p. 184, t. 143.1837A	D
Palugana	burial	1896, Soranzo acquisition	T Palugana	22096; 56469	C		I	V	MUCIV	Frey 1969, pp. 98-99, t. 34.5; 1971, f. 9.3; Peroni *et al.* 1975, pp. 39-40 (tipo6.7), 48, t.XVII, 5; von Eles Masi 1986, p. 184, t. 143.1839	N
Ponte nelle Alpi, Cugnan	burial	1936	T	IG 6627; 3356			I	V	B-MC	Nascimbene 2009, pp. 280-281, t. V, n. 2; von Eles Masi 1986, p. 184, t. 142.1834	N
Ponte nelle Alpi, Cugnan	burial	1936	T	IG 6628; 3357			I	V	B-MC	Nascimbene 2009, pp. 280-281, t. V, n. 1; von Eles Masi 1986, p. 184, t. 142.1836	N
Mechel	cultual	1885/86		6105			I	T	T-CB	Adam 1996, pp. 34, 46, 47, t. I.4	N
Santa Lucia di Tolmino	burial		T 1430		R		Sl			Marchesetti 1893, t.XV.12	N
Tamins-Unterm Dorf	burial	1964-1966	T 46	P1968.153			Sw		Z-LM	Conradin 1978, ff. 29, 30.1; Schmid-Sikimić 2002, fig. 10.34.5	N

(Table 6 — continued)

Archaeological site	Site typology	Excavation data	Tomb	Inv.	Type	Chronology	Country	Region	Location	Literature	Considered
Forcello di Bagnolo San Vito	settlement	survey		99211	B3	5th c. BCE	I	LO	BSV	Adam 1996, p. 41, f. 3.g; de Marinis 1987a, pp. 91-92, 94, 95, ff. 4.b, 5.11; 1987b, p. 245, n. 334, f. 146.2; 2007, p. 209, f. 130.10; 2010, f. 13.15; de Marinis *et al.* 2017, p. 35, f. 7.1; Kruta, Moucha 2018, p. 82, n. 29; Nascimbene 2009, p. 156	A
Golasecca	burial			1608; 38/454B	A1	late 6th-early 5th c. BCE	I	LO	M-MCA	de Marinis 1987b, p. 243; 2010, p. 55, f. 14.5b; Frey 1971, p. 377, list 1, f. 3.6; Nascimbene 2009, p. 156	N
Golasecca	burial	1873, Bertrand acquisition		20808	A1	late 6th-early 5th c. BCE	I	LO	SGL-MAN	Adam 1996, p. 43; de Marinis 1987a, p. 96, f. 6; 2010, p. 55, f. 14.5a; Kruta, Moucha 2018, p. 82, n. 13; Nascimbene 2009, p. 156	N
Monterenzio, Monte Bibele	settlement				A1	late 6th-early 5th c. BCE	I	ER		Adam 1996, p. 43, n. 25; de Marinis 1987b, p. 243; Kruta, Moucha 2018, p. 83, n. 34	N
Altino, Fornasotti	burial	1977	T 2	15134	B1	late 6th-early 5th c. BCE	I	V	A-MAN	Adam 1996, 45, n. 30; de Marinis 1987b, p. 243; Kruta, Moucha 2018, p. 82, n. 33, f. 4; Nascimbene 2009, p. 156; Tombolani 1987, p. 171, 175, f. 1.6	N
Altino, Fornasotti	burial	1977	T 2	15135	B1	late 6th-early 5th c. BCE	I	V	A-MAN	Adam 1996, 45, n. 30; de Marinis 1987b, p. 243; Kruta, Moucha 2018, p. 82, n. 33, f. 4; Nascimbene 2009, p. 156; Tombolani 1985, p. 171, 175, f. 1.7	N
Altino, Fornasotti	burial	1977	T 2	15140	A2	late 6th-early 5th c. BCE	I	V	A-MAN	Adam 1996, 45, n. 30; de Marinis 1987b, p. 243; Kruta, Moucha 2018, p. 82, n. 33, f. 4; Nascimbene 2009, p. 156; Tombolani 1985, p. 171, 175, f. 2.15	N
Altino, Fornasotti	burial	1977	T 2	15141	A2	late 6th-early 5th c. BCE	I	V	A-MAN	Adam 1996, 45, n. 30; de Marinis 1987b, p. 243; Kruta, Moucha 2018, p. 82, n. 33, f. 4; Nascimbene 2009, p. 156; Tombolani 1985, p. 171, 175, f. 2.16	N
Archi di Castelrotto	settlement	1978-1981, excavation			B2	early 5th c. BCE	I	V		Adam 1996, p. 41, 43, n. 23, f. 3.g; de Marinis 1987a, p. 96, f. 7b; 1987b, p. 243; Kruta, Moucha 2018, p. 82, n. 27; Nascimbene 2009, p. 156	N

Table 7. List of findings for the late Hallstattian ornithomorphic fibula [in column 'type': A1 = transversal grooves decoration; A2 = longitudinal grooves decoration; A3 = no grooves decoration; A4 = grooves alternated with circular holes decoration; B1 = transversal grooves decoration; B2 = longitudinal grooves decoration; B3 = linear decoration].

Archaeological site	Site typology	Excavation data	Tomb	Inv.	Type	Chronology	Country	Region	Location	Literature	Considered
Carceri d'Este	burial		T 38		A1	450-425 BCE	I	V	E-MNA	Adam 1996, p. 41, 43, n. 27, f. 3.c; de Marinis 1987a, p. 95, f. 5.4; Frey 1971, p. 376, 378, lista 1-2, f. 2.1; Kruta, Moucha 2018, p. 82, n. 31; Nascimbene 2009, p. 156	N
Caverzano, loc. Masiera	burial	1878		284	B1	475 BCE	I	V	B-MC	Adam 1996, p. 41, n. 29, f. 3.d; de Marinis 1987a, p. 95, f. 5.7; Frey 1971, p. 376, 378, lista 1-2, f. 2.5; Kruta, Moucha 2018, p. 82, n. 30; Nascimbene 1999, pp. 79-80, f. 16, num. 159; 2009, p. 156	L
Padova, vicolo Ognissanti	burial		T 38		A1	late 6th-early 5th c. BCE	I	V	P-MC	Adam 1996, n. 28, f. 3.b; de Marinis 1987a, p. 95, f. 5.1; Frey 1969, p. 100, t. 34.29; 1971, p. 377, 378, list 1-2, f. 2.6; Kruta, Moucha 2018, p. 83, n. 32; Nascimbene 2009, p. 156; Rapi 2008, p. 70	N
Padova, CUS-Piovego	burial	1977, excavation	T 95	95,11	A1		I	V	UNIPD	Gallo 2023	A
Padova, CUS-Piovego	burial	1977, excavation	T 126	126,6	J		I	V	UNIPD	Gallo 2023	N
Padova, CUS-Piovego	burial	1977, excavation	T 127	127,64	A1		I	V	UNIPD	Gallo 2023	L
San Giorgio di Valpolicella, loc. Torre	settlement	survey			A1		I	V		Adam 1996, p. 43, n. 24; Kruta, Moucha 2018, p. 83, n. 28; Nascimbene 2009, p. 157	N
Mechel	cultual			226	A3		I	T	M-MC	Adam 1996, p. 43, n. 21, t. I.2; Kruta, Moucha 2018, p. 83, n. 25; Nascimbene 2009, p. 156	N
Mechel	cultual	1892-1897, acquisition		14050	J		I	T	I-TLF	Adam 1996, p. 43, n. 21; Kruta, Moucha 2018, p. 83, n. 25, f. 3; Nascimbene 2009, p. 156	N
Sanzeno	settlement			13676	A1		I	T	I-TLF	Adam 1996, p. 43, n. 22; Frey 1971, p. 377, list 1, t. I.1; Kruta, Moucha 2018, p. 84, n. 26; Nascimbene 2009, p. 158	N
Monte di Medea, Gorizia	burial						I	FVG	G-MPSA	Adam 1996, p. 45, n. 31; Kruta, Moucha 2018, p. 83	N
Numana-Sirolo, area Davanzali-Circolo	burial		T VIII, Circolo delle Fibule		A1	599-400 BCE	I	M	A-MANM	Adam 1996, p. 45, n. 6; Landolfi 1987, p. 447; Kruta 1978, pp. 149-174, p. 151, nota 8; Kruta, Moucha 2018, p. 84, n. 37, f. 5; Kruta-Poppi 1975, p. 348, f. 2c; Nascimbene 2009, p. 156	N
Dürrnberg							A			Adam 1996, p. 43; Kruta, Moucha 2018, p. 82, n. 24; Nascimbene 2009, p. 158; Pare 1989, p. 469, list 9, f. 23	N
Salzburg, Hellbrunnerberg	settlement			256/76	A1		A			Adam 1996, p. 41, 43, n. 18, f. 3.f; Kruta, Moucha 2018, p. 83, n. 23; Nascimbene 2009, p. 158	N
Salzburg, Hellbrunnerberg	settlement			260/70	A1		A			Adam 1996, p. 43; Kruta, Moucha 2018, p. 83, n. 23; Nascimbene 2009, p. 158	N
Salzburg, Hellbrunnerberg	settlement			283/77	A2		A			Adam 1996, p. 43, n. 18, f. 3f; Kruta, Moucha 2018, p. 83, n. 23; Nascimbene 2009, p. 158	N
Bragny sur Saone	settlement				A1	Ha D3	F			Adam 1996, p. 43, n. 3; Kruta, Moucha 2018, p. 82, n. 5; Lorre, Cicolani 2009, 131, fig. 2-1; Nascimbene 2009, p. 157	N
Bragny sur Saone	settlement				A1	Ha D3	F			Adam 1996, p. 43, n. 3; Pare 1989, p. 469; Kruta, Moucha 2018, p. 82, n. 5; Lorre, Cicolani 2009, 131, fig. 2-1; Nascimbene 2009, p. 156	N
Chassey-le-Camp	settlement				A1	Ha D3	F			Adam 1996, p. 43, n. 2; Kruta, Moucha 2018, p. 82, n. 4; Nascimbene 2009, p. 157	N
Chouilly, Les Jogasses	burial		T 106		A1	500 BCE	F			Adam 1996, p. 43, n. 1; Kruta, Moucha 2018, p. 82, n. 2; Nascimbene 2009, p. 156	N
Chouilly, Les Jogasses	burial		T 157		A3	500 BCE	F			Adam 1996, p. 43, n. 1, f. 3a; Kruta, Moucha 2018, p. 82, n. 2; Nascimbene 2009, p. 156	N
Chouilly, Les Jogasses	burial		T 185		A3	500 BCE	F			Adam 1996, p. 43, n. 1, f. 3a; Kruta, Moucha 2018, p. 82, n. 2; Nascimbene 2009, p. 156	N
Courcelles-en-Montagne	burial		tum. la Motte Saint-Valentin				F			Kruta, Moucha 2018, p. 82, n. 3, f. 6	N

(Table 7 — continued)

Archaeological site	Site typology	Excavation data	Tomb	Inv.	Type	Chronology	Country	Region	Location	Literature	Considered
Dompierre-les-Tilleuls	burial	1979/1980 (Bichet)	tum. de Planquecet n. 3 (or 2?)		A3		F			Adam 1996, p. 43, n. 8a; Kruta, Moucha 2018, p. 82, n. 10; Nascimbene 2009, p. 157	N
Fay-en-Montagne	burial	1965, Vuillemey excavation	tum.		A1		F			Adam 1996, p. 43, n. 6; Lerat 1966, p. 362, f. 25; Kruta, Moucha 2018, p. 82, n. 6	N
Ivory, Foret des Moidons	burial		tum. des Moidons-Papillard		A1	HA IIb	F			Adam 1996, p. 43, n. 4; Frey 1971, p. 379, lista 2, f. 6.2; Kruta, Moucha 2018, p. 83, n. 7; Nascimbene 2009, p. 158	N
La Rivière-Drugeon	burial		tum. du Grand Communal n. 3		J		F			Adam 1996, p. 43, n. 7; Kruta, Moucha 2018, p. 83, n. 11; Lerat 1966, p. 352, f. 10.8	N
La Rivière-Drugeon	burial				J		F			Adam 1996, p. 43; Lerat, 1966, p. 352, f. 10.8bis	N
Orpierre, Ste-Colombe	settlement	1966, excavation: sond.A, quadr.A-B, liv.II, 0,6m prof.		SC 17	A4	late 6th-early 5th c. BCE	F		SGL-MAN	Adam 1996, p. 43, n. 10; Courtois 1968, pp. 154-160, ff. 1.2, 2; Kruta, Moucha 2018, p. 83, n. 12; Nascimbene 2009, p. 157	N
Pignan, Oppidum des Gardies	oppidum	1974, excavation Direction Régionale des Antiquités Historique: zona I, strato 4			A2	early 5th c. BCE	F			Adam 1996, p. 43, n. 28, f. 3b; Kruta, Moucha 2018, p. 83, n. 1; Nascimbene 2009, p. 158; Raynaud *et al.* 1983, pp. 39-59, ff. 17-39.6	N
Salins-les-bains, Champ de Chateau	settlement			50883	J	550-500 BCE	F		SGL-MAN	Adam 1996, p. 43, n. 5; Kruta, Moucha 2018, p. 83, n. 8; Lorre, Cicolani 2009, p. 157; Nascimbene 2009, p. 158	N
Salins-les-bains, Champ de Chateau	settlement			69561	A1	550-500 BCE	F		SGL-MAN	Adam 1996, p. 43, n. 5; Kruta, Moucha 2018, p. 83, n. 8; Lorre, Cicolani 2009, p. 157; Nascimbene 2009, p. 158	N
Vuillecin, Cottaroz	burial	1974, Bichet	tum. 1 Cotaroz		A1		F			Adam 1996, p. 43, n. 8; Kruta, Moucha 2018, p. 84, n. 9; Millotte 1975, p. 595, f. 22; Nascimbene 2009, p. 158	N
Baiersdorf	burial		Mark Forst tumulus	1962-776	B1	5th c. BCE	G			Adam 1996, p. 43, n. 15; de Marinis 1987a, p. 95, f. 7a; Kruta, Moucha 2018, p. 82, n. 20; Nascimbene 2009, p. 158	N
Heideneim-Mergelstetten	burial	1847	tum. Scheiterhau	A3357			G		WL	Adam 1996, p. 43; Kruta, Moucha 2018, p. 82, n. 19; Nascimbene 2009, p. 158	N
Herbertingen-Hundersingen-Heuneburg	settlement				A1	late 6th-early 5th c. BCE	G			Adam 1996, p. 43, n. 13; Kruta 1986, p. 8, f. 1; 1987, p. 24, f. 1; Kruta, Moucha 2018, p. 83, n. 17; Nascimbene 2009, p. 158	N
Herbertingen-Hundersingen	settlement				A1	late 6th-early 5th c. BCE	G			Adam 1996, p. 43, n. 13; Kruta, Moucha 2018, p. 83, n. 17	N
Herbertingen-Hundersingen	burial		tum. Giessubel		B2		G			Kruta, Moucha 2018, p. 83, n. 18, f. 9b	N
Hettingen-Inneringe	burial	1849-1854	tum.				G			Adam 1996, p. 43, n. 12; Kruta, Moucha 2018, p. 83, n. 16	N
Markstetten	burial		tum.				G			Kruta, Moucha 2018, p. 83, n. 22	N
Muhlacker, Heidenwäldle	burial		tum. 4, T 5				G			Adam 1996, p. 43, n. 14a; Kruta, Moucha 2018, p. 83, n. 15, f. 9a	N
Schwenderod	burial		tum. 1	95/187			G		M-PS	Adam 1996, p. 43, n. 16; Kruta, Moucha 2018, p. 84, n. 21; Nascimbene 2009, p. 158	N
Singen	burial	1953	T 53/6, fossa 4		A3		G		S-H	Adam 1996, p. 43, n. 11; Kruta, Moucha 2018, p. 84, n. 14; Maier 1957, p. 225, f. 3.B7; 1958, p. 228, t. 59.37	N
Slany				5372		6th c. BCE	G		S-VM	Adam 1996, p. 43, n. 17; Kruta 1986, p. 9; Kruta, Moucha 2018, p. 84, n. 35, f. 1; Nascimbene 2009, p. 158	N
Libna	burial	1893	T 30	65802	A2	late 6th c. BCE	Sl			Adam 1996, p. 41, 45, f. 3.e; Kruta, Moucha 2018, p. 83, n. 38; Nascimbene 2009, p. 159	N

(Table 7 — continued)

Archaeological site	Site typology	Excavation data	Tomb	Inv.	Type	Chronology	Country	Region	Location	Literature	Considered
Libna	burial	1893	T 30	65802	A2	late 6th c. BCE	Sl			Kruta, Moucha 2018, p. 83, n. 38; Nascimbene 2009, p. 159	N
Libna	burial	1889-1890	T K		A2	late 6th-early 5th c. BCE	Sl			Kruta, Moucha 2018, p. 83, n. 38; Nascimbene 2009, p. 159	N
Libna	burial	1889-1890	T K		A2	late 6th-early 5th c. BCE	Sl			Kruta, Moucha 2018, p. 83, n. 38; Nascimbene 2009, p. 159	N
Santa Lucia di Tolmino			T XIX	30250	A1	late 6th-early 5th c. BCE	Sl		T-MCSA	de Marinis 1987b, p. 243; Frey 1971, pp. 373, 378-379, list 2, f. 11.3; Nascimbene 2009, p. 159	N
Santa Lucia di Tolmino	burial	Marchesetti	T 1358				Sl			Adam 1996, p. 45, n. 32; Kruta, Moucha 2018, p. 83, n. 36	N
Santa Lucia di Tolmino	burial	Marchesetti	T 1430				Sl			Adam 1996, p. 45, n. 32; Kruta, Moucha 2018, p. 83, n. 36	N
Santa Lucia di Tolmino	burial	Marchesetti	T 1940		A1		Sl			Adam 1996, p. 45, n. 32; Kruta, Moucha 2018, p. 83, n. 36; Nascimbene 2009, p. 159	N
Santa Lucia di Tolmino	burial	Marchesetti	T 2435				Sl			Adam 1996, p. 45, n. 32; Kruta, Moucha 2018, p. 83, n. 36	N
Santa Lucia di Tolmino	burial	Szombathy	T 619		A1		Sl			Kruta, Moucha 2018, p. 83, n. 36	N

(Table 7 — continued)

Archaeological site	Site typology	Excavation data	Inv.	Chronology	Location	Literature	Considered
Bologna, Certosa	burial					Frey, 1971, pp. 355, 357, abb. 2.14-15, taf. 1.7-8	N
Forcello di Bagnolo San Vito	settlement	2004, excavation: R 18 f 19, US 1497	99210	500-440 BCE	M-MN	de Marinis 2007, pp. 208-209, f. 130.5; 2010, f. 13.10 ; de Marinis *et al.* 2017, p. 30, f. 6.9	A
Forcello di Bagnolo San Vito	settlement	excavation: US 1893	RR1272	495-475 BCE	BSV	de Marinis *et al.* 2017, p. 32, f. 6.10	A
Marzabotto				525-480 BCE	M-M	Adam 1996, p. 79, note 12; Kruta-Poppi 1975, p. 349, f. 2c	N
Mechel	cultual	1888/89	1349; 2342	5th c. BCE	T-CB	Adam 1996, p. 34, t. I.8; Campi 1889, p. 218; Frey 1971, p. 377, list 1, f. 3.5	N
Mechel	cultual		1571/6	5th c. BCE	T-CB	Adam 1996, p. 35, t.I.6	N
San Polo d'Enza				475-400 BCE	RE-MGC	Damiani *et al.* 1992, pp. 131-310, t. LXIV, n. 967; de Marinis 1987, p. 95, f. 5.15; Frey 1971, p. 377, lista 1, f. 2.9	N

Table 8. Italian distribution of the type: coral *Fußzierfibel* F1.

Archaeological site	Site typology	Excavation data	Tomb	Inv.	Chronology	Location	Literature	Considered
Bressanone / Brixen							Adam 1996, p. 39, n. 17	N
Caverzano, loc. Masiera-Font	burial			3294		B-MC	Nascimbene 1999, pp. 80-82, f. 16, n. 166	N
Como, Ca' Morta, Rebbio	burial	1953, Casartelli survey					Bertolone 1956, p. 111, f. 7.5	D
Este, Muletti	burial		T 250	8319	late 6th-early 5th c. BCE	E-MNA	Adam 1996, p. 47, n. 7; de Marinis 1987, p. 95, f. 5.5; Frey 1971, p. 376, list 1, f. 2.2	N
Forcello di Bagnolo San Vito	settlement	excavation: W 10 b 19, US 2		99209	5th c. BCE	M-MN	de Marinis 1986b, f. 146.6; 1987, p. 91-92, f. 4.f; 1997, p. 157; 2007, p. 209, f. 130.8; 2010, f. 13.11; de Marinis *et al.* 2017, p. 34, f. 6.11	A
Forcello di Bagnolo San Vito	settlement	excavation: US 344		145959	5th c. BCE	BSV	de Marinis *et al.* 2017, p. 33, f. 6.14	A
Gazzo Veronese, Dosso del Pol							Adam 1996, p. 39, n. 19	N
Mechel	cultual				late 6th-early 5th c. BCE		Adam 1996, p. 34, t. I.1	N
Mechel	cultual	1885/86		6105/32		T-CB	Adam 1996, pp. 34, 46, 47, t. I.5	N
Palugana	burial	1896, Soranzo acquisition		22098		MUCIV	Frey 1969, pp. 98-99, t. 34.2; 1971, p. 377, lista 1, f. 9.2; Peroni *et al.* 1975, p. 175 (n.6), t. XVII.3	N
San Lorenzo di Sebato, Sonnenburg		1986, discovery					Adam 1996, p. 39, n. 15	N
Sanzeno		1920		7568; MN9528	5th c. BCE	T-CB	Adam 1996, pp. 34, 46, t. I.3; Weber 1925, p. 188	N
Sirolo-Numana	burial		T 22		late 6th-early 5th c. BCE		de Marinis 1987, p. 95, f. 5.3; Frey 1971, p. 366, note 35; Landolfi 1987, p. 447	N
Vandoies di Sopra / Obervintl							Adam 1996, p. 39, n. 16	N

Table 9. Italian distribution of the type: *Fußzierfibel* F2.

Archaeological site	Excavation data	Inv.	Type	Chronology	Country	Location	Literature
Villa del Foro	1994, sporadic, Oberty recovery	66120; SP691	Navicella	late 7th-6th c. BCE	I	MRT	Faudino *et al.* 2014, p. 129, f. 4.4
Val Varaita, Sampeyre-Mandam	sac. Perini donation	E17738 (1985)	Valvaraita	480-425 BCE	I	C-MC	Faudino *et al.* 2014, pp. 129-131, f. 5.3; Peroni *et al.* 1975, pp. 200-201, type 54.7, 211; Rittatore 1947, p. 3, f. 2.1
Parre di Sotto	1883, Mantovani recovery	48	Navicella	475 BCE	I	B-MA	de Marinis, Gŭstin 1975, p. 248, f. 10sx-center; Poggiani Keller, Rondini 2020, pp. 288-289, f. 17.9B
Parre di Sotto	1883, Mantovani recovery	49	Navicella	475 BCE	I	B-MA	de Marinis, Gŭstin 1975, p. 248, f. 10sx/center; Poggiani Keller, Rondini 2020, pp. 288-289, f. 17.9B
Parre di Sotto	1883, Mantovani recovery	119	Navicella	475 BCE	I	B-MA	de Marinis, Gŭstin 1975, p. 248, f. 10sx/center; Poggiani Keller, Rondini 2020, pp. 288-289, f. 17.9B

Table 10. List of analysed find belonging to the type 'Navicella fibulae'.

Archaeological site	Site type	Excavation data	Tomb	Inv.	Chronology	Country	Region	Location	Literature	Considered
Bellinzago					525-480 BCE	I	P		Barbieri 2019, p. 45; Pauli 1971, t. 42.19; Teßmann 2007, f. 6.4, n. 4, pp. 672, 682	D
San Bernardino di Briona	Funerario	excavation: tum. XXII/4		23.M380-9.7; 8986-8987	525-480 BCE	I	P	MRT		A
Forcello di Bagnolo San Vito	Abitato	excavation: US.885; sett.R18; q. n. 17		145782; RR581	525-480 BCE	I	LO	BSV	Barbieri 2019, pp. 45, 46, 50, 53, 56, f. 10.1, 11.1; de Marinis 2007, p. 205, f. 129.6; 2010, f. 14.1; de Marinis *et al.* 2017, p. 32	A
Golasecca, loc. Lazzaretto	Funerario	1886, Castelfranco's discovery	Tomba VIII, o Tomba della situla del Lazzaretto	A0.9.17519; 205bis	525-480 BCE	I	LO	M-MCA	Barbieri 2019, p. 45; de Marinis 1992, p. 175, f. 3.8; 2007, p. 205; 2010, f. 14.2; Teßmann 2007, f. 4.3, n. 7, pp. 680-681	A
Caverzano, loc. Masiera	Funerario	1878, excavation		3321	late 6th-5th c. BCE	I	V	B-MC	Barbieri 2019, p. 46; Nascimbene 1999, pp. 111-119, f. 24, n. 283; Teßmann 2007, f. 6.5, n. 5, pp. 672, 682	D
Padova, vicolo San Massimo	Funerario	1911, excavation	T XVI	65299	late 6th c. BCE	I	V	P-MC	Barbieri 2019, p. 46; Chieco Bianchi 1981, pp. 274-275, t. 65A.8; Teßmann 2007, f. 6.11, n. 12, pp. 672, 682	A
Padova, vicolo San Massimo	Funerario	1911, excavation	T XVI	65300	late 6th c. BCE	I	V	P-MC	Barbieri 2019, p. 46; Chieco Bianchi 1981, pp. 274-275, t. 65A.9; Teßmann 2007, f. 6.12, n. 13, pp. 672, 682	A
Pieve d'Alpago, Pian della Gnela	Funerario	2004, excavation	T10	312360;	6th-5th c. BCE	I	V	P-SABAP	Angelini, Molin 2015, pp. 52-53, f. 1b, 2b; Gangemi *et al.* 2015, pp. 43, 46-47, 57, n. 17	L
Pieve d'Alpago, Pian della Gnela	Funerario	2004, excavation	T10	312361	6th-5th c. BCE	I	V	P-SABAP	Angelini, Molin 2015, pp. 52-53, f. 1b, 2b; Gangemi *et al.* 2015, pp. 43, 46-47, 57, n. 17	L
Pieve d'Alpago, Pian della Gnela	Funerario	2004, excavation	T10	365548	6th-5th c. BCE	I	V	P-SABAP	Angelini, Molin 2015, pp. 52-53, f. 1b, 2b; Gangemi *et al.* 2015, pp. 43, 46-47, 57, n. 17	L
Pieve d'Alpago, Pian della Gnela	Funerario	2007, excavation	T11	355517	6th-5th c. BCE	I	V	P-SABAP	Gangemi *et al.* 2015, pp. 63, 67, 73, n. 7, t. IV.2	L
Pieve d'Alpago, Pian della Gnela	Funerario	2007, excavation	T11	355517	6th-5th c. BCE	I	V	P-SABAP	Gangemi *et al.* 2015, pp. 63, 67, 73, n. 7, t. IV.2	L
Pieve d'Alpago, Pian della Gnela	Funerario	2007, excavation	T11	355517	6th-5th c. BCE	I	V	P-SABAP	Gangemi *et al.* 2015, pp. 63, 67, 73, n. 7, t. IV.2	L
Piovego	Funerario	1970-1980	T110	110,8	late 6th-5th c. BCE	I	V	P-UNIPD	Gallo 2023	A

Table 11. List of findings for the type: bucket pendant 1A with 'occhio di dado' decoration.

Archaeological site	Site type	Excavation data	Tomb	Inv.	Chronology	Country	Region	Location	Literature	Considered
Piovego	Funerario	1970-1980	T110	110,8	late 6th-5th c. BCE	I	V	P-UNIPD	Gallo 2023	L
Piovego	Funerario	1970-1980	T110	110,8	late 6th-5th c. BCE	I	V	P-UNIPD	Gallo 2023	L
Piovego	Funerario	1970-1980	T108	108,5	late 6th-5th c. BCE	I	V	P-UNIPD	Gallo 2023	A
Piovego	Funerario	1970-1980	T86	86,3	late 6th-5th c. BCE	I	V	P-UNIPD	Gallo 2023	A
Piovego	Funerario	1970-1980	T86	86,3	late 6th-5th c. BCE	I	V	P-UNIPD	Gallo 2023	L
Piovego	Funerario	1970-1980	T86	86,3	late 6th-5th c. BCE	I	V	P-UNIPD	Gallo 2023	L
Piovego	Funerario	1970-1980	T86	86,3	late 6th-5th c. BCE	I	V	P-UNIPD	Gallo 2023	L
Santa Lucia, Tolmino	Funerario		T388		6th-5th c. BCE	Sl			Marchesetti 1983, t. XVI.12	N
Santa Lucia, Tolmino	Funerario		T388		6th-5th c. BCE	Sl			Marchesetti 1983, t. XVI.12	N
Santa Lucia, Tolmino	Funerario		T2227		6th-5th c. BCE	Sl			Barbieri 2019, p. 46; Teßmann 2007, f. 6.19, n. 23, pp. 672	N
Santa Lucia, Tolmino	Funerario		T558		6th-5th c. BCE	Sl			Marchesetti 1893, t.XI.2	N
Santa Lucia, Tolmino	Funerario		T558		6th-5th c. BCE	Sl			Marchesetti 1893, t. XI.2	N
Santa Lucia, Tolmino	Funerario		T558		6th-5th c. BCE	Sl			Marchesetti 1893, t. XI.2	N
Singen	Funerario		T53/6, fossa 1		5th c. BCE	G		S-H	Barbieri 2019, p. 46; Maier 1957, f. 3.B7; 1958, p. 228, t. 59.7	N

(Table 11 — continued)

Archaeological site	Site type	Excavation data	Tomb	Inv.	Type	Material	Coral insets	Chronology	Country	Region	Location	Literature	Considered
Ameno	Burial		T 54	9621-9624	set of grooming tools	Fe		6th c. BCE	I	P	MRT-MAT	Pauli 1971, p. 138, t. 9.8	N
Castelletto Ticino		1877		D2049	set of grooming tools	Fe			I	P	C-MC	Roncoroni 2005, n. 227, t. 22	N
Castelletto Ticino		1878		D918	auriscalpium	B		late 7th-early 6th c. BCE	I	P	C-MC	Roncoroni 2005, n. 229, t. 22	N
Castelletto Ticino		1877		D980	tweezer	B		late 6th-early 5th c. BCE	I	P	C-MC	Roncoroni 2005, n. 230, t. 22	N
Castelletto Ticino		1887, acquisition		1063	tweezer	B	X		I	P	N-MC		A
Castelletto Ticino				D996	scalpitorium	B			I	P	C-MC	Roncoroni 2005, n. 233, t. 22	N
Castelletto Ticino, loc. Bosco del Monte		1877		D917	auriscalpium	B		late 7th-early 6th c. BCE	I	P	C-MC	Roncoroni 2005, n. 228, t. 22	N
Pombia	Burial	1987	T 1		auriscalpium	B		late 6th-early 5th c. BCE	I	P		Di Maio *et al.* 2001, p. 25, n. 12, f. 11.12; Roncoroni 2005, p. 47	N
Pombia, loc. Quara	Burial	1995	T 18		set of grooming tools	Fe		6th c. BCE	I	P		DI Maio *et al.* 2001, pp. 80-81, f. 85-5; Roncoroni 2005, p. 46	N
Pontecurone		2012, excavation: Area2, US56		St. 6602; RR24	tweezer	B		600-475 BCE	I	P	MRT	Venturino Gambari *et al.* 2014, p. 111, f. 22.9	A
Chiavari	Burial				20 grooming tools				I	LI		Zamboni 2018, p. 187	N
Castelveccana, Castello Valtravaglia	Burial		T XI		grooming tool	Fe		7th c. BCE	I	LO		Peroni *et al.* 1975, pp. 220-221, 231	N
idem	Burial		T XXVI		grooming tool	Fe		7th c. BCE	I	LO		Peroni *et al.* 1975, pp. 220-221, 231	N
idem	Burial		T XXVII		grooming tool	Fe		7th c. BCE	I	LO		Peroni *et al.* 1975, pp. 220-221, 231	N
idem	Burial		T XXVIII		grooming tool	Fe		7th c. BCE	I	LO		Peroni *et al.* 1975, pp. 220-221, 231	N
idem	Burial		T XXXI		grooming tool	Fe		7th c. BCE	I	LO		Peroni *et al.* 1975, pp. 220-221, 231	N
idem	Burial		T XXXVI		grooming tool	Fe		7th c. BCE	I	LO		Peroni *et al.* 1975, pp. 220-221, 231	N
idem	Burial		T XXXIX		grooming tool	Fe		7th c. BCE	I	LO		Peroni *et al.* 1975, pp. 220-221, 231	N
idem	Burial		T XLII		grooming tool	Fe		7th c. BCE	I	LO		Peroni *et al.* 1975, pp. 220-221, 231	N

Table 12. List of findings for the type: grooming tool [in ‘Material’ column: B = bronze; Fe = iron; Ag/Au = silver and gold; in ‘Coral insets’ column, the presence of an X indicates the presence of a coral decoration]

Archaeological site	Site type	Excavation data	Tomb	Inv.	Type	Material	Coral insets	Chronology	Country	Region	Location	Literature	Considered
Como, Albate	Burial		T VII		scalpitorium	B		late 7th-early 6th c. BCE	I	LO		Baserga 1910, p. 10, f. 5; Peroni *et al.* 1975, pp. 220-221, 231; Roncoroni 2005, p. 47	N
Como, Ca' Morta	Burial		T 24		set of grooming tools	B			I	LO		Peroni *et al.* 1975, pp. 220-221, 230, f. 61.1	N
Como, Rebbio	Burial			E18652	set of grooming tools	Ag-Au			I	LO	C-MC	Baserga 1925, pp. 40-41, f. 88-89; Castelfranco, 1900, f. 2; Peroni *et al.* 1975, pp. 220-221, 231; Roncoroni 2005, p. 47	N
Cuggiono					tweezer	B		6th c. BCE	I	LO		de Marinis 1981, t. 5.27; Peroni *et al.* 1975, pp. 220-221, 231	N
Cunardo					grooming tool	B			I	LO		Peroni *et al.* 1975, pp. 220-221, 231	N
Garlasco, cascina Bonifica	Burial	1985	T		tweezer	B				LO		de Marinis 1986a, pp. 69, 88, n. 170, f. 29.9	N
Garlasco, cascina Bonifica	Burial	1985	T		grooming tool	B				LO		de Marinis 1986a, pp. 69, 88, n. 170, f. 29.10	N
Golasecca	Burial			D1660; 11	tweezer	B	X	late 6th-early 5th c. BCE	I	LO	C-MC	Roncoroni 2005, n. 231, t. 22	A
Golasecca		1878		D1056	tweezer	B		6th c. BCE	I	LO	C-MC	Roncoroni 2005, n. 232, t. 22	N
Golasecca, Monsorino	Burial			St. 63393	grooming tool	B		late 6th-early 5th c. BCE	I	LO	V-MC	Grassi, Mangani 2016, p. 77, f. 92, t. XXIV.4	N
Palestro					set of grooming tools	B			I	LO		Castelfranco 1900, f. 1; Cicolani 2017, pp. 155-158; Roncoroni 2005, p. 47	N
Santo Spirito, Gropello Cairoli	Settlement	1950-'60-'70, discovery: capanna del fabbro		2019.01.117	grooming tool	B	X	early 5th c. BCE	I	LO	MANL	Ruffa 2010, pp. 115-116, 125, f. 10.110	A
Sesto Calende		1928	T1		grooming tool	B		6th c. BCE	I	LO		Peroni *et al.* 1975, pp. 220-221, 231	N
Sesto Calende, loc. Gajaccio	Burial	1926	T a		grooming tool	B			I	LO		Peroni *et al.* 1975, pp. 220-221, 231; Roncoroni 2005, p. 47	N
Sesto Calende, loc. Gajaccio	Burial	1945	T		set of grooming tools	B		late 6th-early 5th c. BCE	I	LO		de Marinis 2009g, pp. 204-206, f. 2.4-6; Grassi, Mangani 2016, p. 77	N
Sesto Calende, Mulini Bellaria	Burial	1977-1980	T 11		grooming tool	B		late 6th-early 5th c. BCE	I	LO		de Marinis 2009c, pp. 450-451, f. 24.6; Grassi, Mangani 2016, p. 77	N
Sesto Calende, loc. Presualdo	Burial		T 14		grooming tool	Fe		6th c. BCE	I	LO		Roncoroni 2005, p. 46	N
Sesto Calende, via Sculati	Burial	1983	T 14		scalpitorium	Fe		late 6th-early 5th c. BCE	I	LO		de Marinis 2009i, pp. 420-423, f. 10.7	N
Trezzo	Burial		T situla		set of grooming tools	Fe		late 6th-early 5th c. BCE	I	LO		de Marinis 1974, t. 3-5; Roncoroni 2005, p. 46	N
Verdello					scalpitorium	B			I	LO		Casini 2000a, p. 6, f. 5; Cicolani 2017, pp. 155-158	N
Bismantova				S 27/191	scalpitorium	B			I	ER		Damiani *et al.* 1992, p. 170, t. LXXXVI-LXXXVII, n. 1357	N
Bismantova				S 27/223	auriscalpium	B			I	ER		Damiani *et al.* 1992, p. 170, t. LXXXVI-LXXXVII, n. 1359	N
Cacciola					auriscalpium	B			I	ER		Damiani *et al.* 1992, p. 170, t. LXXXVI-XXXVII, n. 1360	N
San Polo				S37/449	scalpitorium	B			I	ER		Damiani *et al.* 1992, p. 170, t. LXXXVI-LXXXVII, n. 1355	N

(Table 12 — continued)

Archaeological site	Site type	Excavation data	Tomb	Inv.	Type	Material	Coral insets	Chronology	Country	Region	Location	Literature	Considered
Torretta di Campegine					scalpitorium	B		middle 6th. c. BCE	I	ER		Zamboni 2018, p. 187, f. 107.4	N
San Polo				S 37/445	auriscalpium	B			I	ER		Damiani *et al.* 1992, p. 170, t. LXXXVI-LXXXVII, n. 1358	N
Torretta di Campegine					auriscalpium	B		middle 6th. c. BCE	I	ER		Zamboni 2018, p. 187, f. 107.2	N
San Polo				S 44/20	tweezer	B			I	ER		Damiani *et al.* 1992, p. 170, t. LXXXVI-LXXXVII, n. 1361	N
San Polo				S 43/198	tweezer	B			I	ER		Damiani *et al.* 1992, p. 170, t. LXXXVI-LXXXVII, n. 1362	N
San Polo				S 37/443	tweezer	B			I	ER		Damiani *et al.* 1992, p. 170, t. LXXXVI-LXXXVII, n. 1363	N
Torretta di Campegine					tweezer	B		middle 6th. c. BCE	I	ER		Zamboni 2018, p. 187-188, f. 107.6	N
San Polo				S 37/442	tweezer	B			I	ER		Damiani *et al.* 1992, p. 170, t. LXXXVI-LXXXVII, n. 1364	N
Sant'Ilario-Fornaci	Burial		T 3	S 99	scalpitorium	B		525-480 BCE	I	ER		Damiani *et al.* 1992, p. 170, t. LXXXVI-LXXXVII, n. 1356; Zamboni 2018, pp. 187-188, f. 107.3	N
Sant'Ilario-Bettolino	Burial		T 5		set of grooming tools	B		middle 6th. c. BCE	I	ER		Zamboni 2018, p. 187, f. 107.1	N
Torretta di Campegine					scalpitorium	B		middle 6th. c. BCE	I	ER		Zamboni 2018, p. 187-188, f. 107.5	N
Torretta di Campegine					tweezer	B		middle 6th. c. BCE	I	ER		Zamboni 2018, p. 187-188, f. 107.7	N
Bologna									I	ER		Zamboni 2018, p. 187	N
Padova, Piovego	Burial	1970-'80	T95	95,1	set of grooming tools	B	X	6th-5th c. BCE	I	V	UNIPD	Gallo 2023	A
Este Benvenuti			T 96						I	V		Zamboni 2018, p. 187	N
Este Benvenuti			T 98						I	V		Zamboni 2018, p. 187	N
Este Benvenuti			T 296						I	V		Zamboni 2018, p. 187	N
Este Muletti			T 254						I	V		Zamboni 2018, p. 187	N
Oppeano									I	V		Zamboni 2018, p. 187	N
Arbedo Molinazzo	Burial		T 51		grooming tool	B			Sw			Cicolani 2017, pp. 155-158	N
Cademario	Burial		T 25		grooming tool	B			Sw			Cicolani 2017; Roncoroni 2005	N
Castaneda, Haus Luzzi	Burial	1976	T 1		set of grooming tools	B	X	early 5th c. BCE	Sw			Cicolani 2017, pp. 155-158; Rageth 2000, f. 24, n. 10-11; Roncoroni 2005	N
Castaneda, Haus Luzzi	Burial	1976	T 1		set of grooming tools	B	X	early 5th c. BCE	Sw			Rageth 2000, f. 24, n. 10-11; Cicolani 2017, pp. 155-158; Roncoroni 2005	N
Cerinasca d'Arbedo	Burial		T 77		grooming tool	B	X	early 5th c. BCE	Sw			Cicolani 2017, pp. 155-158; Roncoroni 2005, p. 47	N
Claro	Burial		T 25		grooming tool	B			Sw			Roncoroni 2005, p. 47	N
Gamsen	Settlement				scalpitorium	B		8th-6th c. BCE	Sw			Cicolani 2017, pp. 155-158	N
Gamsen	Settlement				auriscalpium	B		6th c. BCE	Sw			Cicolani 2017, pp. 155-158	N
Gamsen	Settlement				auriscalpium	B		late 6th-early 5th c. BCE	Sw			Cicolani 2017, pp. 155-158	N
Gamsen	Settlement				tweezer	B		late 7th-early 6th c. BCE	Sw			Cicolani 2017, pp. 155-158	N
Minusio	Burial		T 16		set of grooming tools	B			Sw			Schmid-Sikimić 2002, p. 34, f. 2.19	N
Trun	Settlement				tweezer	B			Sw			Cicolani 2017, pp. 155-158	N
Vaz, Albula	Settlement				tweezer	B		6th-5th c. BCE	Sw			Cicolani 2017, pp. 155-158	N
Bourges					scalpitorium	B	X	early 5th c. BCE	F			Cicolani 2017, pp. 155-158	N
Chilly-sur-Salins	Burial		tum B		grooming tool	B		late 6th-early 5th c. BCE	F			Cicolani 2017, pp. 155-158	N

(Table 12 — continued)

Roquefort-sur Soulzon	Burial				tweezer	B		6th-5th c. BCE	F			Cicolani 2017, pp. 155-158	N
Hochdorf					scalpitorium	Fe			G			Cicolani 2017, pp. 155-158	N
La Heuneburg				1484	scalpitorium	Fe			G			Cicolani 2017, pp. 155-158	N
Pfaffenwald	Burial		tum 11		set of grooming tools	B	X	middle 5th c. BCE	G			Cicolani 2017, pp. 155-158	N
Unknown		Collection Bertrand		20490	set of grooming tools	B		late 6th-early 5th c. BCE			SGL-MNA	Cicolani 2017, pp. 154-155, f. 127; Lorre, Cicolani 2009, pp. 90-91	N

(Table 12 — continued)

Archaeological site	Site typology	Excavation data	Tomb	Inv.	Type	Num.	Chronology	Country	Region	Location	Literature	Considered
Brembate Sotto	burial	1889, Nievo-Mantovani's excavation	T 8	3046; M124	Pendant/branch	1	late 6th-early 4th c. BCE	I	LO	B-MA	Casini 2017, pp. 55, 143, f. 35-81, n. 264; Cherici 1999, p. 197; de Marinis 1981, pp. 129-132, 224, t. 16-2; Mantovani 1890, p. 62, n. 124	A
Forcello di Bagnolo San Vito	settlement	excavation		98797	bead	1		I	LO	M-MN	de Marinis 1987a, pp. 89-90, f. 2; 1997, p. 157	A
Lot de Regaggin - Castelletto?				A0.9.2681	bead	1		I	LO	M-MCA		N
Este, Alfonsi	burial		T 3		bead	1	450-350 BCE	I	V		Cherici 1999, p. 181	N
Este, Alfonsi	burial	1907	T 13		bead	6	575-525 BCE	I	V		Cherici 1999, p. 181; Schmid-Sikimić 2002, p. 219, tab. 9.1	N
Este, Benvenuti	burial	1879-1880	T 124		bead	multiple	575-525 BCE	I	V	E-MNA	Cherici 1999, p. 182; Fogolari, Frey 1965, p. 277, f. 14,1; Frey 1969, p. 97, t. 22.2	N
Este, Benvenuti	burial	1880	T 126		bead	9	625-575 BCE	I	V	E-MNA	Cherici 1999, p. 182; Fogolari, Frey 1965, p. 269, f. 8.2; Frey 1969, p. 96, t. 19.3; Schmid-Sikimić 2002, p. 219, tab. 9.1	N
Este, Benvenuti	burial	1880	T 126		bead	multiple	625-575 BCE	I	V	E-MNA	Cherici 1999, p. 182; Fogolari, Frey 1965, p. 269, f. 8.2; 1969, p. 96, t. 19.3	N
Este, Capodaglio	burial		T38		bead	6		I	V		Fogolari, Frey 1965, pp. 289, 292	N
Este, Capodaglio	burial	1878			bead	6	450-350 BCE	I	V		Cherici 1999, p. 182; Ghirardini 1901, n. 2642	N
Este, Rebato	burial	1907-1909	T 1		bead	1	700-350 BCE	I	V		Cherici 1999, p. 182; Alfonsi 1922, p. 4	N
Este, Rebato	burial	1907-1909	T 3		bead	multiple	575-450 BCE	I	V		Cherici 1999, p. 182; Alfonsi 1922, p. 7	N
Este, Rebato	burial	1907-1909	T 13		bead	4	575-525 BCE	I	V		Cherici 1999, p. 182; Alfonsi 1922, p. 9	N
Este, Rebato	burial	1907-1909	T 76		bead	24	800-700 BCE	I	V		Cherici 1999, p. 182; Alfonsi 1922, p. 25	N
Este, Rebato	burial	1907-1909	T 218		bead	multiple	525-450 BCE	I	V		Cherici 1999, p. 182; Alfonsi 1922, p. 52	N
Este, Rebato	burial	1907-1909	T 1		pierced branch	1	700-350 BCE	I	V		Cherici 1999, p. 182; Alfonsi 1922, p. 4	N
Este, Ricovero	burial		T 205		bead	7	525-450 BCE	I	V		Cherici 1999, p. 182; Schmid-Sikimić 2002, p. 219, tab. 9.1	N
Este, Ricovero	burial	1895	T 232		bead	34	575-525 BCE	I	V	E-MNA	Barnabei 1896, p. 357; Cherici 1999, p. 182; Frey 1969, p. 97, t. 26.2; Prosdocimi 1896, p. 311-312; Schmid-Sikimić 2002, p. 219, tab. 9.1	N
Este, Ricovero	burial		T 234		bead	1	700-675 BCE	I	V		Schmid-Sikimić 2002, p. 219, tab. 9.1	N
Este, Ricovero	burial		T 18		bead	3	700-675 BCE	I	V		Schmid-Sikimić 2002, p. 219, tab. 9.1	N
Este, Ricovero	burial		T 155		bead	1	675-625 BCE	I	V		Schmid-Sikimić 2002, p. 219, tab. 9.1	N
Este, Ricovero	burial		T 149		bead	21	675-625 BCE	I	V		Schmid-Sikimić 2002, p. 219, tab. 9.1	N
Este, Ricovero	burial	1961	T 3		bead	21	625-575 BCE	I	V		Schmid-Sikimić 2002, p. 219, tab. 9.1	N

Table 13. List of findings for the types: bead, pendant and pierced branch.

Archaeological site	Site typology	Excavation data	Tomb	Inv.	Type	Num.	Chronology	Country	Region	Location	Literature	Considered
Este, Ricovero	burial		T 200		bead	4	625-575 BCE	I	V		Schmid-Sikimić 2002, p. 219, tab. 9.1	N
Este, Ricovero	burial		T 127		bead	16	575-525 BCE	I	V		Schmid-Sikimić 2002, p. 219, tab. 9.1	N
Este, Ricovero	burial		T 13		bead	75	525-450 BCE	I	V		Schmid-Sikimić 2002, p. 219, tab. 9.1	N
Este, Ricovero	burial		T 200		bead	1	575-525 BCE	I	V		Cherici 1999, pp. 178, 181	N
Gazzo Veronese, Colombara	burial	Discovery			bead	multiple		I	V		Cherici 1999, p. 182; Salzani 1976, pp. 419, 421, f. 13.11	N
Gazzo Veronese, Dosso del Pol	burial	excavation			bead	multiple		I	V		Cherici 1999, p. 182; Salzani 1976, p. 425	N
Ospedaletto	burial		Tomba Palugana		bead	1	525-450 BCE	I	V		Schmid-Sikimić 2002, p. 219, tab. 9.1	N
Pieve d'Alpago, Pian della Gnela	burial	2004, exacavation	T 10	IG 312375	bead	2		I	V	P-SABAP	Angelini, Molin 2015, pp. 52-53, f. 1c-2c; Castiglioni, Rottoli 2015, pp. 224-225, f. 18-19; Gangemi *et al.* 2015, p. 44, num. 33	A
Pieve d'Alpago, Pian della Gnela	burial	2007, excavation	T 11	IG 355542	bead	1		I	V	P-SABAP	Gangemi *et al.* 2015, pp. 63, 74, n. 36	A
Pieve d'Alpago, Pian della Gnela	burial	2007, excavation	T 11	IG 355538, 355540, 355542-45, 355548, 355550-355552, 355554-355556	bead	13		I	V	P-SABAP	Gangemi *et al.* 2015, pp. 63, 74, n. 34	A
Pieve d'Alpago, Pian della Gnela	burial	2007, excavation	T 11	IG 355534	bead	1		I	V	P-SABAP	Gangemi *et al.* 2015, pp. 63, 74, n. 33	A
Pieve d'Alpago, Pian della Gnela	burial	2007, excavation	T 11	IG 355539	bead	1		I	V	P-SABAP	Gangemi *et al.* 2015, pp. 66, 74, n. 37	L
Pieve d'Alpago, Pian della Gnela	burial	2007, excavation	T 11	IG 355546, 355557	bead	2		I	V	P-SABAP	Gangemi *et al.* 2015, pp. 63, 74, n. 38	L
Pieve d'Alpago, Pian della Gnela	burial	2007, excavation	T 11	IG 355547, 355549, 355553, 355556, 355558	bead	5		I	V	P-SABAP	Gangemi *et al.* 2015, pp. 63, 74, n. 35	L
Pieve d'Alpago, Pian della Gnela	burial	2007, excavation	T 11	IG 355652	bead	1		I	V	P-SABAP	Gangemi *et al.* 2015, p. 63, n. 55	L
Pieve d'Alpago, Pian della Gnela	burial	2007, excavation	T 11	IG 355656, 355657	bead	2		I	V	P-SABAP	Gangemi *et al.* 2015, p. 63, n. 56	L
Pieve d'Alpago, Pian della Gnela	burial	2007, excavation	T 12	IG 355675	bead	4		I	V	P-SABAP	Gangemi *et al.* 2015, pp. 83, 94, n. 43	L
Pieve d'Alpago, Pian della Gnela	burial	2007, excavation:	T 12	IG 355678	bead	4		I	V	P-SABAP	Gangemi *et al.* 2015, pp. 83, 94, n. 43	A
Pieve d'Alpago, Pian della Gnela	burial	2007, excavation	T 12	IG 355679	bead	4		I	V	P-SABAP	Gangemi *et al.* 2015, pp. 83, 94, n. 43	A
Pieve d'Alpago, Pian della Gnela	burial	2007, excavation	T 12	IG 355676, 355680-355686, 355699, 355700	bead	31		I	V	P-SABAP	Gangemi *et al.* 2015, pp. 83, 94, n. 42	L

(Table 13 — continued)

Archaeological site	Site typology	Excavation data	Tomb	Inv.	Type	Num.	Chronology	Country	Region	Location	Literature	Considered
Pieve d'Alpago, Pian della Gnela	burial	2007, excavation	T 12	IG 355687	bead	5		I	V	P-SABAP	Gangemi *et al.* 2015, pp. 83, 94, n. 44	L
Piovego	burial	1970-1980	T 110	110,13	bead	1	6th-5th c. BCE	I	V	P-UNIPD	Gallo 2023	A
Piovego	burial	1970-1980	T 108	108,7	pendant	1	6th-5th c. BCE	I	V	P-UNIPD	Gallo 2023	A
Piovego	burial	1970-1980	T 25	149682; 25.23	pendant	1	6th-5th c. BCE	I	V	P-UNIPD	Gallo 2023	A
unknown				MV5916	bead	1		?	?	V-MC	-	A
Dürrnberg					bead			A			Schmid-Sikimić 2002, p. 220, tab. 9.2	N
Hallstatt					bead			A			Schmid-Sikimić 2002, p. 220, tab. 9.2	N
Courtesoult	burial		T 27		bead	multiple	560-520 BCE	F			Schmid-Sikimić 2002, p. 221, nota 34	N
Courtesoult	burial		T 28		pierced branch	multiple	560-520 BCE	F			Schmid-Sikimić 2002, p. 221, nota 33	N
Harthouse					bead			F			Schmid-Sikimić 2002, p. 220, tab. 9.2	N
Maegstub					bead			F			Schmid-Sikimić 2002, p. 220, tab. 9.2	N
Nordhouse			T A		bead	1	6th-5th c. BCE	F			Schmid-Sikimić 2002, p. 221, nota 41	N
Nordhouse			tum.		pin-head	1	6th c. BCE	F			Schmid-Sikimić 2002, p. 221, nota 38	N
Ohlungen					bead			F			Schmid-Sikimić 2002, p. 220, tab. 9.2	N
Schirrheinerweg					bead			F			Schmid-Sikimić 2002, p. 220, tab. 9.2	N
Ditzingen-Schockingen					bead	1	6th-5th c. BCE	G			Schmid-Sikimić 2002, p. 221, nota 41	N
Ditzingen-Schockingen					pin-head	1	6th c. BCE	G			Schmid-Sikimić 2002, p. 221, nota 40	N
Esslingen			T 1		bead	1	6th-5th c. BCE	G			Schmid-Sikimić 2002, p. 221, nota 41	N
Hochdorf, Eberdingen					bead			G			Schmid-Sikimić 2002, p. 220, tab. 9.2	N
Königsbrück					bead			G			Schmid-Sikimić 2002, p. 220, tab. 9.2	N
La Heuneburg, Herbertingen-Hundersingen	Settlement				bead	1	630-550 BCE	G			Schmid-Sikimić 2002, p. 221, nota 32	N
La Heuneburg, Herbertingen-Hundersingen	Settlement				pierced branch	1	630-550 BCE	G			Schmid-Sikimić 2002, p. 221, nota 31	N
Magdalenenberg, Villingen-Schwenningen	burial		T 122		bead	7	630-550 BCE	G			Schmid-Sikimić 2002, p. 221, nota 29	N
Mühlacker					bead			G			Schmid-Sikimić 2002, p. 220, tab. 9.2	N
Singen	burial	1953	T 53/6, fossa 4		bead	30		G		S-H	Maier 1957, p. 225, f. 3.B7; Pauli 1975, p. 254, f. 3A.1-32	N
Singen	burial	1953	T 53/6, fossa 4		pendant	1	560-520 BCE	G		S-H	Maier 1957, p. 225, f. 3.B7; Pauli 1975, p. 254, f. 3A.34	N
Singen	burial	1953	T 53/6, fossa 4		pendant	1	560-520 BCE	G		S-H	Maier 1957, p. 225, f. 3.B7; Pauli 1975, p. 254, f. 3A.33	N
Altheim-Heiligkreuztal			tum. 6 Hohmichele		bead	1	6th-5th c. BCE	G			Schmid-Sikimić 2002, p. 221, nota 36	N
Kaltbrunn	burial	1864	tum.		bead	24	630-550 BCE	Sw			Schmid-Sikimić 2002, p. 221, nota 30	N
Kaltbrunn					pin-head	1	6th c. BCE	Sw			Schmid-Sikimić 2002, p. 221, nota 39	N

(Table 13 — continued)

Conservation locations	A-MAA	B-MA	B-MC	Bra	BSV	C-MC	CT-GSAC	MAM	M-MCA	M-MN	M-MSNA	MRT	M-SABAP	N-MC	O-MCF	P-MAVT	P-MC	P-SABAP	P-UNIPD	SC-MC	MANL	V-MC
Examined finds	4	18	13	1	5	62	16	5	42	7	4	63	1	11	25	9	6	15	27	8	22	8
Analysed finds	2	18	9	1	5	47	10	4	18	7	4	52	1	9	4	9	4	13	21	6	12	8

Table 14. Details of the number of archaeological artefacts examined with a portable digital microscope or analysed with an archaeometric protocol at the different conservation locations.

	Approaches	**Description**	**Analytical techniques**
1	Totally non-destructive complete approach	transport of archaeological finds to the laboratories of the University of Turin required	OM, μ-Raman, μ-XRD, SEM-EDS
2	Micro-invasive complete approach	Micro-sampling required, without moving the artefacts	OM, μ-Raman, FT-IR, μ-XRD, SEM-EDS
3	Totally non-invasive partial approach	No movement or sampling of artefacts required	OM, Raman portable

Table 15. Proposed analytical approaches to Soprintendenze and Museums.

	Na	**Mg**	**Al**	**Si**	**S**	**Cl**	**K**	**Ca**	**Fe**	**Sr**	**O**
r_Cr_L	2,30	4,49	0,71	2,79	1,69	1,24	0,86	34,08	0,00	0,00	51,85
w_Cr_U	0,80	5,67	0,38	0,09	0,70	0,00	0,00	41,73	0,00	0,00	50,64
r_Cr_Si	0,85	5,74	0,00	0,20	0,49	0,00	0,00	42,27	0,00	0,05	50,41
w_pCr_Sa	0,95	5,09	0,00	0,00	0,70	0,00	0,04	42,76	0,00	0,00	50,45
r_c_L	2,01	3,38	1,42	5,10	2,02	2,07	0,37	29,87	0,45	0,00	53,30
r_Sg_Sa	2,71	1,43	1,35	1,34	1,28	1,71	0,13	39,34	0,00	0,00	50,72
r_fc_P	0,00	0,45	4,19	0,56	0,00	0,00	0,00	43,48	0,00	0,00	51,33

Table 16. Results of the semi-quantitative chemical analysis: average values [r_Cr_L: unworked ligurian *C. rubrum*; w_Cr_u: worked-polished *C. rubrum*; r_Cr_Si: sicilian *C. rubrum* collected on the beach; w_pCr_Sa: sardinian pinkish-to-white worked coral; r_c_L: Ligurian white coral; r_Sg_Sa: Sardinian S. *gaederopus*; r_fc_P: Piedmont fossil coral].

	Surface μ-features	**Mg-content (mol% $MgCO_3$)**	**Polyenes presence**
C. rubrum	longitudinal crenulations, bifurcations	11.95-12.25	X
S. gaederopus	squamae	3,51	X
white coral		9.98-10.11	
fossil coral	granular surface	1,11	

Table 17. Summary table of the characteristic features of the various modern calcite materials examined.

Archaeological site	Inv. no.	Type	Crenulation	Garland	Medullar	Bioattack	Location
Bagnolo S. Vito - Forcello	98797	Raw	X				M-MN
Bagnolo S. Vito - Forcello	98798	Raw	X				M-MN
Bagnolo S. Vito - Forcello	98799	Raw	X			X	M-MN
Bagnolo S. Vito - Forcello	camp. 1060	Raw	X				M-SABAP
Bellinzago Novarese, loc. Valle Briga	198	Leech-C		X			N-MC
Borgonovo V.T.	20.S258-2.118	Leech-C		X			P-MAVT
Borgonovo V.T.	20.S258-2.119	Leech-C		X			P-MAVT
Borgonovo V.T.	20.S258-2.171	Leech-C		X			P-MAVT
Brembate sotto	3051	Comp	X				B-MA
Brembate sotto	3052	Comp	X				B-MA
Castelletto Ticino	D 1750, 72	Pend	X		X		C-MC
Castelletto Ticino	1063	Groom					N-MC
Castelletto Ticino, Motto d'Egro, v. Beati	20.S.279-3.788	Pend	X				CT-GSAC
Castelletto Ticino, Motto Falco	NO	Pend	X				CT-GSAC
Castelletto Ticino-Vigevano?	944	Leech-C		X			N-MC
Castelletto Ticino-Vigevano?	946	Leech-C		X	X		N-MC
Caverzano-località Masiera	217	Leech-C		X			B-MC
Como, Ca' Morta, Cava Butti	1397	Comp	X				C-MC
Como, Ca' Morta, Rebbio, Cava Bianchi	124142	Pend	X				C-MC
Como, Ca' Morta, Rebbio, loc. Ronchetti, Fondo Porciani e Cattaneo	1230	Comp	X				C-MC
Como, Ca' Morta, terreno IACP a nord di via Cecilio	33593	Pend	X				C-MC
Como, Ca' Morta, terreno IACP a nord di via Cecilio	33594	Pend	X				C-MC
Como, Ca' Morta	E13273	Comp	X				C-MC
Como, Prestino, via Isonzo	57210	Leech-C		X			C-MC
Como, Respaù, Monte Olimpino	E5957, 460 (1892)	Comp	X				C-MC
Como, Respaù, Monte Olimpino	E5958	Comp	X				C-MC
Golasecca	D 1668, 30	Pend	X				C-MC
Golasecca	D 1669, 31	Pend	X				C-MC
Golasecca	D 2049, 6	Leech-C		X			C-MC
Golasecca	A0.9.4858	Leech-C		X			M-MCA
Golasecca	A0.9.28600	Pend	X				M-MCA
Golasecca	A0.9.28592	Pend	X				M-MCA
Golasecca	A0.9.28602	Pend	X				M-MCA
Golasecca	NO	Pend	X			X	V-MC
Golasecca, loc. Lazzaretto	A0.9.17519	Bucket-P	X				M-MCA
Mantova, p.zza Santa Barbara	169519	Leech-C		X			M-MN

Table 18. List of archaeological finds with characteristic features of *C. rubrum* (alphabetically ordered according to the name of the archaeological site; 'type' column: bucket-P = bucket pendants; comp = composite bow fibula; groom = grooming tools; leech-C = leech fibula with circular decoration; pend = pendant and Longone al Segrino pendants; raw = raw coral branches; 'location' column = see section 4.5).

Archaeological site	Inv. no.	Type	Crenulation	Garland	Medullar	Bioattack	Location
Motto Lagone	T1	Leech-C		X			A-MAA
Pianello V.T.	200191	Leech-C		X			P-MAVT
Pieve d'Alpago, Pian della Gnela	355542	Bead			X		P-SABAP
Pieve d'Alpago, Pian della Gnela	355538	Bead			X		P-SABAP
Pieve d'Alpago, Pian della Gnela	355534	Bead	X		X		P-SABAP
Pieve d'Alpago, Pian della Gnela	355678	Bead	X				P-SABAP
Pieve d'Alpago, Pian della Gnela	355679	Bead			X		P-SABAP
Piovego	NO	Raw	X		X		P-UNIPD
Piovego	NO	LH		X			P-UNIPD
Piovego	149682	Pend	X				P-UNIPD
Piovego	153032	Leech-C		X			P-UNIPD
Piovego	NO	Bead				X	P-UNIPD
Pombia, loc. Monticello, propr. Planca	83946	Leech-C		X			O-MCF
Pontecurone, loc. Cascina Torre	23.M380-9.6	Leech-C	X				MRT
Sesto Calende, Mulini Bellaria	23752	Leech-C		X			SC-MC
Sesto Calende, via Moncenisio	172343	Pend	X				SC-MC
Sesto Calende, via Moncenisio	172344	Raw	X				SC-MC
Sesto Calende, via Montrucco	4783	Pend	X				SC-MC
Villa del Foro	66132	Leech-C		X			MRT

(Table 18 — continued)

$CaCO_3$ polymorph	ν_4	ν_1	lattice
Vaterite	738-750 cm^{-1}	1086 cm^{-1}	
Aragonite	700-705 cm^{-1}		205-271 cm^{-1}
Calcite	711 cm^{-1}		281 cm^{-1}

Table 19. Raman peaks position for Ca-carbonate polymorphs.

Archaeological site	Inv. no.	Type	Location	Decoration	Analysis	$CaCO_3$	Aragonite	Calcite	Polyenes	Apatite	Anhydrite/ gypsum	Cuprite	Tenorite	Malachite	Quartz/ silicates	Beeswax	Paraloid/ resin	Anatase/ Rutile
Bagnolo S. Vito - Forcello	145782	Bucket-P	M-MN	C	D			x										
Bagnolo S. Vito - Forcello	RR 745	Bucket-P	M-MN	C	D													
Bagnolo S. Vito - Forcello	98797	Raw	M-MN	G	D			x	x									
Bagnolo S. Vito - Forcello	98798	Raw	M-MN	G	D			x	x									
Bagnolo S. Vito - Forcello	98799	Raw	M-MN	G	D			x	x									
Bagnolo S. Vito - Forcello	99210	LH	M-MN	T	D													
Bagnolo S. Vito - Forcello	RR 1272	LH	M-MN	T	D													
Bagnolo S. Vito - Forcello	99209	LH	M-MN	T	D			x										
Bagnolo S. Vito - Forcello	1060	Raw	M-MN	G	D			x										
Bagnolo S. Vito - Forcello	145959	LH	M-MN	T	D											?		
Bagnolo S. Vito - Forcello	99211	LH	M-MN	C	D			x	x									
Bellinzago Novarese, loc. Valle Briga	197	Leech-C	N-MC	C	D			x										
Bellinzago Novarese, loc. Valle Briga	198	Leech-C	N-MC	C	D			x								x		
bellunese	bellunese	Leech-T	B-MC	T	S													
Borgonovo V.T.	20.S258-2.118	Leech-C	P-MAVT	C	D			x	x									
Borgonovo V.T.	20.S258-2.119	Leech-C	P-MAVT	C	D			x		x								
Borgonovo V.T.	20.S258-2.171	Leech-C	P-MAVT	C	D			x								x		
Borgonovo V.T.	20.S258-2.172	Leech-C	P-MAVT	C	D	x			x							?		
Brembate sotto	65	Leech-T	B-MA	T	D													
Brembate sotto	67	Comp	B-MA	G	D			x	x									
Brembate sotto	3016	Pend	B-MA	G	D			x										
Brembate sotto	3051	Comp	B-MA	G	D			x										
Brembate sotto	3052	Comp	B-MA	G	D			x										
Brignano Frascata	C-FR-NE/1	Leech-C	MRT	C	S			x	x									
Brignano Frascata	C-FR-NE/2	Leech-C	MRT	C	S			x	x									
Brignano Frascata	C-FR-NE/3	Leech-C	MRT	C	S			x	x									
Brignano Frascata	C-FR-S/2	Leech-L	MRT	C	S									x	x			
Castelletto Ticino	91374	Pend	CT-GSAC	G	D			x		x							x	
Castelletto Ticino	18,236	Bead	CT-GSAC	G	D					x								
Castelletto Ticino	CT20343C03E	Leech-C	CT-GSAC	C	D			x										
Castelletto Ticino	D 1750, 72	Pend	C-MC	G	D			x										

Table 20. Raman analysis results (alphabetically ordered according to the name of the archaeological site; 'type' column: bucket-P = bucket pendants; comp = composite bow fibula; groom = grooming tools; leech-C = leech fibula with circular decoration; pend = pendant and Longone al Segrino pendants; raw = raw coral branches; 'location' column: see section 4.5; 'Dec.' column: 'G' = general, 'T' = transversal grooves, 'C' = circular, 'L' = linear, 'O' = occhio di dado; 'Analysis' column: 'I' = in situ, 'D' = direct, 'S' = sampled).

Archaeological site	Inv. no.	Type	Location	Decoration	Analysis	$CaCO_3$	Aragonite	Calcite	Polyenes	Apatite	Anhydrite/ gypsum	Cuprite	Tenorite	Malachite	Quartz/ silicates	Beeswax	Paraloid/ resin	Anatase/ Rutile
Castelletto Ticino	D2073, 2	Leech-C	C-MC	C	D			x										
Castelletto Ticino	D2077, 9	Leech-C	C-MC	C	D													
Castelletto Ticino	D2104, 97	Leech-C	C-MC	C	D			x									x	
Castelletto Ticino	D2773, 64	Leech-C	C-MC	C	D													
Castelletto Ticino	23.M380-9.5	Leech-C	MRT	C	D			x										
Castelletto Ticino	2140	Leech-C	MRT	C	D													
Castelletto Ticino	2153	Leech-C	MRT	C	S			x	x									
Castelletto Ticino	1063	Groom	N-MC	C	D			x	x	x								
Castelletto Ticino, Bosco del Monte	CT29 B4D	Leech-C	CT-GSAC	C	D			x									x	
Castelletto Ticino, Motto d'Egro	20.S.279-3.788; CT164	Pend	CT-GSAC	G	D			x										
Castelletto Ticino, Motto Falco	CT179	Pend	CT-GSAC	G	D			x									x	
Castelletto Ticino, v. Aronco	CT14031X; CT868a	Other	CT-GSAC	G	D													
Castelletto Ticino, v. Aronco	CT14031X; CT868b	Bead	CT-GSAC	G	D												x	
Castelletto Ticino, v. Aronco	CT14031X; CT868c	Other	CT-GSAC	G	D												x	
Castelletto Ticino, v. Valsesia	20.S.279.3.780; CT728	Leech-C	CT-GSAC	C	D			x									x	
Castelletto Ticino, Via Sivo	23.M380-9.3	Leech-T	MRT	C	D													
Castelletto Ticino-Vigevano?	944	Leech-C	N-MC	C	D			x										
Castelletto Ticino-Vigevano?	946	Leech-C	N-MC	C	D			x										
Castelletto Ticino-Vigevano?	947	Leech-C	N-MC	C	D			x										
Castelletto Ticino-Vigevano?	949	Leech-C	N-MC	C	D			x										
Castello di Annone	23.M380-9.4	Leech-C	MRT	C	D			x										
Caverzano-località Limade	287304	Leech-C	B-MC	C	S			x										
Caverzano-località Masiera	217	Leech-C	B-MC	C	S			x	x									
Caverzano-località Masiera	211	Leech-C	B-MC	C	S			x										
Chies D'Alpago, località Prà	3344	Leech-C	B-MC	C	S			x	x									
Chiomonte, La Maddalena	74795	LaTène	MRT	C	D													
Chiomonte, La Maddalena	74794	LaTène	MRT	C	D													
Coll. Assi	23-M380-9.8	Dolphin	MRT	C	D			x	x									
Coll. Assi	23-M380-9.9	Dolphin	MRT	C	D													
Coll. Assi	23-M380-9.10	Dolphin	MRT	C	D			x	x									
Como, Ca' Morta, Cava Butti	1397	Comp	C-MC	G	D			x										
Como, Ca' Morta, Cava dalla Zuanna	2206	Leech-C	C-MC	C	D			x							x			

(Table 20 — continued)

Archaeological site	Inv. no.	Type	Location	Decoration	Analysis	$CaCO_3$	Aragonite	Calcite	Polyenes	Apatite	Anhydrite/ gypsum	Cuprite	Tenorite	Malachite	Quartz/ silicates	Beeswax	Paraloid/ resin	Anatase/ Rutile
Como, Ca' Morta, Cava dalla Zuanna	2208	Leech-C	C-MC	C	D										?			
Como, Ca' Morta, Rebbio	1993	Comp	C-MC	G	D					x								
Como, Ca' Morta, Rebbio	114083	Leech-C	C-MC	C	D			x										
Como, Ca' Morta, Rebbio	114084	Leech-C	C-MC	C	D			x										
Como, Ca' Morta, Rebbio	124133	Other	C-MC	G	D					?								
Como, Ca' Morta, Rebbio	139651	Leech-C	C-MC	C	D			x										
Como, Ca' Morta, Rebbio	139652	Leech-C	C-MC	C	D			x										
Como, Ca' Morta, Rebbio, Cava Ballerini	879	Leech-C	C-MC	C	D			x										
Como, Ca' Morta, Rebbio, Cava Bianchi	124142	Pend	C-MC	G	D			x		?								
Como, Ca' Morta, Rebbio, Cava Manzoni	864	Other	C-MC	O	D										x			
Como, Ca' Morta, Rebbio, Cava Manzoni	865	Other	C-MC	O	D													
Como, Ca' Morta, Rebbio, loc. Ronchetti	1230	Comp	C-MC	G	D			x										
Como, Ca' Morta, Rondineto	E5868, 422 (1892)	Leech-C	C-MC	C	D			x										
Como, Ca' Morta, Rondineto	E5873, 423 (1892)	Leech-C	C-MC	C	D													
Como, Ca' Morta, Rondineto	E5865, 418 (1892)	Leech-C	C-MC	C	D													
Como, Ca' Morta, terreno IACP	33593	Pend	C-MC	G	D						x							
Como, Ca' Morta, terreno IACP	33594	Pend	C-MC	G	D			x										
Como, Ca' Morta	E13273	Comp	C-MC	G	D			x										
Como, dintorni	E5552, 61 (1892)	Leech-C	C-MC	C	D													
Como, dintorni	E5553, 61 (1892)	Leech-C	C-MC	C	D													
Como, dintorni	E5667, 68 (1892)	Leech-C	C-MC	C	D													
Como, Prestino, via Isonzo	57210	Leech-C	C-MC	C	D			x	x									
Como, Prestino, via Isonzo	57216	Leech-C	C-MC	C	D			x	x									
Como, Prestino, via Isonzo	57220	Leech-C	C-MC	C	D			x	x									
Como, Prestino, via Isonzo	57244	Leech-C	C-MC	C	D			x	x							x		
Como, Prestino, via Isonzo	57250	Leech-C	C-MC	C	D			x	x									
Como, Prestino, via Isonzo	57262	Leech-C	C-MC	C	D			x	x									
Como, Rebbio, Villa Giovio	E13225	Leech-C	C-MC	C	D			x	x									

(Table 20 — continued)

Archaeological site	Inv. no.	Type	Location	Decoration	Analysis	$CaCO_3$	Aragonite	Calcite	Polyenes	Apatite	Anhydrite/ gypsum	Cuprite	Tenorite	Malachite	Quartz/ silicates	Beeswax	Paraloid/ resin	Anatase/ Rutile
Como, Respaù, Monte Olimpino	E5957, 460 (1892)	Comp	C-MC	G	D			x										
Como, Respaù, Monte Olimpino	E5958	Comp	C-MC	G	D			x										
Golasecca	D 1660, 11	Groom	C-MC	C	D			x										
Golasecca	D 1667,29	Other	C-MC	G	D					?								
Golasecca	D 1668, 30	Pend	C-MC	G	D			x										
Golasecca	D 1669, 31	Pend	C-MC	G	D			x										
Golasecca	D 2049, 6	Leech-C	C-MC	C	D			x										
Golasecca	D 2059, 7/2	Leech-C	C-MC	C	D													
Golasecca	D 2064, 7/2	Leech-C	C-MC	C	D			x										
Golasecca	D2065, 7/2	Leech-C	C-MC	C	D			x			x							
Golasecca	MV103	Pend	V-MC	G	S			x										
Golasecca	A0.9.4858	Leech-C	M-MCA	C	I													
Golasecca	A0.9.28600	Pend	M-MCA	G	I	x												
Golasecca	A0.9.28598	Pend	M-MCA	G	I	x												
Golasecca	A0.9.28599	Other	M-MCA	G	I	x												
Golasecca	A0.9.28592	Pend	M-MCA	G	I			x										
Golasecca	A0.9.28602	Pend	M-MCA	G	I	x												
Golasecca	A0.9.4908	Leech-C	M-MCA	C	I													
Golasecca	A0.9.4842	Leech-C	M-MCA	C	I			x										
Golasecca	MV4062	Leech-C	V-MC	C	S	x												
Golasecca, loc. Galliasco	22.S288-1.205	Leech-C	M-SABAP	C	S			x										
Golasecca, loc. Lazzaretto	A0.9.17519	Bucket-P	M-MCA	C	I	x												
Golasecca, loc. Monsorino	63413	Leech-C	V-MC	C	S			x	x									
Golasecca?	A0.9.5961	Leech-C	M-MCA	C	I													
Golasecca?	A0.9.28164	Leech-C	M-MCA	C	I													
Golasecca?	A0.9.35542	Leech-C	M-MCA	C	I	x												
Gropello Cairoli	19/108	Leech-L	MANL	L	D													
Gropello Cairoli	19/109	Leech-L	MANL	L	D													
Gropello Cairoli	19/110	Leech-L	MANL	L	D													
Gropello Cairoli	19/111	Leech-L	MANL	L	D													
Gropello Cairoli	19/112	Leech-C	MANL	C	D	x			x									
Gropello Cairoli	19/114	Leech-L	MANL	L	D													
Gropello Cairoli	19/115	Leech-L	MANL	L	D										x			

(Table 20 — continued)

Archaeological site	Inv. no.	Type	Location	Decoration	Analysis	$CaCO_3$	Aragonite	Calcite	Polyenes	Apatite	Anhydrite/ gypsum	Cuprite	Tenorite	Malachite	Quartz/ silicates	Beeswax	Paraloid/ resin	Anatase/ Rutile
Gropello Cairoli	19/117	Groom	MANL	C	D	x												
Gropello Cairoli	21/178	Leech-L	MANL	L	D													
Gropello Cairoli	21/179	Leech-L	MANL	L	D													
Gropello Cairoli	21/180	Leech-L	MANL	L	D							?						
Gropello Cairoli	21/181	Leech-L	MANL	L	D							?						
Malgesso	MV4025	Leech-C	V-MC	C	S	x											?	
Mantova - p.zza Santa Barbara	169519	Leech-C	M-MN	C	D			x	x									
Mel	9244	Leech-C	MAM	C	S			x										
Mel	9290	Leech-C	MAM	C	S			x										
Mel	9289	Leech-C	MAM	C	S			x										
Mel	9271	Leech-C	MAM	C	S											x	x	
Montebelluna, loc. Posmon	304784	Leech-C	M-MSNA	C	S			x						x				
Montebelluna, loc. Posmon	304780	Leech-C	M-MSNA	C	S										x			
Montebelluna, Casa Tesser	147145	Leech-C	M-MSNA	C	S													
Montebelluna, Casa Tesser	7489	Leech-C	M-MSNA	C	S													
Motto Lagone	T1	Leech-C	A-MAA	C	D			x	x									
Motto Lagone	T2	Bead	A-MAA	G	D										x			
Padova, vicolo Ognissanti	60735	Leech-C	P-MC	C	S			x										
Padova, vicolo Ognissanti	term staffa	Leech-C	P-MC	C	S			x								x	x	
Padova, vicolo San Massimo	65299	Bucket-P	P-MC	C	S			x									x	
Padova, vicolo San Massimo	65300	Bucket-P	P-MC	C	S	?											x	
Parre, loc. Castello	9	Leech-L	B-MA	L	D													
Parre, loc. Castello	40	other	B-MA	L	D													x
Parre, loc. Castello	41	Other	B-MA	L	D											?		x
Parre, loc. Castello	45	Other	B-MA	L-C	D													x
Parre, loc. Castello	46	Other	B-MA	L	D													x
Parre, loc. Castello	48	Navic	B-MA	L	D													x
Parre, loc. Castello	49	Navic	B-MA	L	D													x
Parre, loc. Castello	119	Navic	B-MA	L	D													x
Parre, loc. Castello	128	Other	B-MA	O	D						x					?		
Parre, loc. Castello	3002	Other	B-MA	L	D													
Parre, loc. Castello	3564	Leech-L	B-MA	L	D													
Parre, loc. Castello	3565	Leech-L	B-MA	L	D													

(Table 20 — continued)

Archaeological site	Inv. no.	Type	Location	Decoration	Analysis	$CaCO_3$	Aragonite	Calcite	Polyenes	Apatite	Anhydrite/ gypsum	Cuprite	Tenorite	Malachite	Quartz/ silicates	Beeswax	Paraloid/ resin	Anatase/ Rutile
Parre, loc. Castello	3569	Leech-L	B-MA	L	D			x										
Pianello V.T. (PC)	18711	Bucket-P	P-MAVT	C	D													
Pianello V.T. (PC)	18878	other	P-MAVT	C	D													
Pianello V.T. (PC)	200191	Leech-C	P-MAVT	C	D			x										
Pianello V.T. (PC)	201255	Leech-C	P-MAVT	C	D					?	?							
Pieve d'Alpago, Pian della Gnela	312348	Leech-C	P-SABAP	C	S			x	x									
Pieve d'Alpago, Pian della Gnela	312349	Leech-C	P-SABAP	C	S									x				
Pieve d'Alpago, Pian della Gnela	312360	Leech-C	P-SABAP	C	S			x										
Pieve d'Alpago, Pian della Gnela	312375	Bead	P-SABAP	G	S			x										
Pieve d'Alpago, Pian della Gnela	355677	Bead	P-SABAP	G	S			x	x									
Pieve d'Alpago, Pian della Gnela	355542	Bead	P-SABAP	G	S			x	x									
Pieve d'Alpago, Pian della Gnela	355538	Bead	P-SABAP	G	S			x	x									
Pieve d'Alpago, Pian della Gnela	355534	Bead	P-SABAP	G	S			x	x									
Pieve d'Alpago, Pian della Gnela	355517	Leech-C	P-SABAP	C	S			x	x									
Pieve d'Alpago, Pian della Gnela	355516	Leech-C	P-SABAP	C	S			x	x									
Pieve d'Alpago, Pian della Gnela	355515	Leech-C	P-SABAP	C	S													
Pieve d'Alpago, Pian della Gnela	355678	Bead	P-SABAP	G	S			x	x									
Pieve d'Alpago, Pian della Gnela	355679	Bead	P-SABAP	G	S			x	x									
Piovego	5,99	Raw	P-UNIPD	G	S			x	x									
Piovego	110,8	Bucket-P	P-UNIPD	C	S			x										
Piovego	108,7	Pend	P-UNIPD	G	S			x										
Piovego	108,5	Bucket-P	P-UNIPD	C	S			x										
Piovego	108,3	Leech-C	P-UNIPD	C	S			x										
Piovego	181844	Leech-C	P-UNIPD	C	S			x									?	
Piovego	181843	Leech-C	P-UNIPD	C	S													
Piovego	95,11	LH	P-UNIPD	C	S			x										
Piovego	149682	Pend	P-UNIPD	G	S			x	x									
Piovego	95,1	Groom	P-UNIPD	L	S		x											
Piovego	95,1	Groom	P-UNIPD	C	S			x										
Piovego	89,6	Leech-C	P-UNIPD	C	S			x										
Piovego	86,3	Bucket-P	P-UNIPD	C	S			x										
Piovego	224255	Leech-C	P-UNIPD	C	S			x										
Piovego	224358	Leech-C	P-UNIPD	C	S													
Piovego	224201	Leech-C	P-UNIPD	C	S	x												

(Table 20 — continued)

Archaeological site	Inv. no.	Type	Location	Decoration	Analysis	$CaCO_3$	Aragonite	Calcite	Polyenes	Apatite	Anhydrite/ gypsum	Cuprite	Tenorite	Malachite	Quartz/ silicates	Beeswax	Paraloid/ resin	Anatase/ Rutile
Piovego	5,73	Leech-C	P-UNIPD	C	S			x	x									
Piovego	153032	Leech-C	P-UNIPD	C	S			x										
Piovego	149721	Leech-C	P-UNIPD	C	S			x										
Piovego	34914	Leech-C	P-UNIPD	C	S			x										
Piovego	110,13	Bead	P-UNIPD	G	S	x												
Pombia, loc. Monticello	72276-72277	Leech-C	MRT	C	D			x								x		
Pombia, loc. Monticello	83925	Leech-C	O-MCF	C	D			x									?	
Pombia, loc. Monticello	83937	Leech-C	O-MCF	C	D			x									?	
Pombia, loc. Monticello	83946	Leech-C	O-MCF	C	D													
Pombia, loc. Quara	83966	Leech-C	O-MCF	C	D			x									x	
Ponte nelle Alpi-Casan	3366	Other	B-MC	C	S			x	x									
Ponte nelle Alpi-Cugnan	3355	Leech-C	B-MC	C	S			x										
Pontecurone	23.M380-9.6	Leech-C	MRT	C	D	x												
Pontecurone	RR24	Groom	MRT	L	S									x				
Rottofreno	259507	Leech-C	P-MAVT	C	D													
Safforze	6602	Leech-C	B-MC	C	S			x	x									
Safforze	6600	Leech-C	B-MC	C	S			x										
San Bernardino di Briona	868	Leech-C	N-MC	C	D													
San Bernardino di Briona	870	Leech-C	N-MC	C	D			x										
San Bernardino di Briona	NCT0100026405; 1524	Leech-C	MRT	C	D			x										
San Bernardino di Briona	NCT0100026418; 1567	Leech-C	MRT	C	D			x	x	x								
San Bernardino di Briona	NCT0100026417; 1514	Leech-C	MRT	C	D						x							
San Bernardino di Briona	NCT0100026415; 1547	Leech-C	MRT	C	D													
San Bernardino di Briona	23.M380-9.1	Leech-C	MRT	C	D	x			x	?								
San Bernardino di Briona	23.M380-9.2	Leech-C	MRT	C	D			x	x									
San Bernardino di Briona	23.M380-9.7	Bucket-P	MRT	C	D			x										
Sesto Calende, asilo	12437	Leech-C	V-MC	C	S			x										
Sesto Calende, asilo	12436	Leech-C	V-MC	C	S			x										
Sesto Calende, Mulini Bellaria	23751	Leech-C	SC-CMA	C	S						?							
Sesto Calende, Mulini Bellaria	23752	Leech-C	SC-CMA	C	S			x	x									

(Table 20 — continued)

Archaeological site	Inv. no.	Type	Location	Decoration	Analysis	$CaCO_3$	Aragonite	Calcite	Polyenes	Apatite	Anhydrite/ gypsum	Cuprite	Tenorite	Malachite	Quartz/ silicates	Beeswax	Paraloid/ resin	Anatase/ Rutile
Sesto Calende, via Moncenisio	172343	Pend	SC-CMA	G	S			x										
Sesto Calende, via Moncenisio	172344	Raw	SC-CMA	G	S			x										
Sesto Calende, via Montrucco	4783	Pend	SC-CMA	G	S			x										
Unknown	A0.9.28550	Leech-C	M-MCA	C	I													
Unknown	A0.9.35028	Leech-C	M-MCA	C	I	x												
Unknown	A0.9.35039	Leech-C	M-MCA	C	I													
Unknown	A0.9.4916	Leech-C	M-MCA	C	I	x												
Unknown	A0.9.28250	Leech-C	M-MCA	C	I	x												
Unknown	A0.9.28047	Leech-C	M-MCA	C	I			x										
Unknown	D2109	Other	C-MC	G	D					x								
Unknown	MV5924	Other	V-MC	G	S													
Unknown	MV5916	Bead	V-MC	G	S					x								
Unknown	Coll. Bellini	Leech-C	SC-CMA	C	S													
Unknown	M589/3	Leech-C	Bra	C	S			x										
Val Varaita, Sampeyre-Mandam	E17738	Navic	C-MC	O	D													
Villa del Foro	1000/E1	Leech-C	MRT	C	S			x										
Villa del Foro	SP 55	Leech-L	MRT	L	S													
Villa del Foro	SP 56a	Leech-L	MRT	L	S													
Villa del Foro	SP 27	Leech-C	MRT	C	S			x	x									
Villa del Foro	66132	Leech-C	MRT	C	S													
Villa del Foro	66131	Leech-L	MRT	L	S			x	x									
Villa del Foro	51877	Leech-C	MRT	C	S			x	x									
Villa del Foro	RS154	Leech-C	MRT	C	S									x				
Villa del Foro	RS/SP 134	Leech-L	MRT	L	S									x				
Villa del Foro	RS 135	Leech-L	MRT	L	S													
Villa del Foro	RS 160	Leech-L	MRT	L	S													
Villa del Foro	RS/SP 72	Leech-L	MRT	L	S									x				
Villa del Foro	RS 819	Leech-L	MRT	L	S													
Villa del Foro	RS 822	Other	MRT	L	S													
Villa del Foro	SP 140 b	Leech-L	MRT	L	S													
Villa del Foro	SP159	Leech-L	MRT	L	S													
Villa del Foro	SP 16	Leech-L	MRT	L	S										x			
Villa del Foro	SP16	Leech-C	MRT	C	S													

(Table 20 — continued)

Archaeological site	Inv. no.	Type	Location	Decoration	Analysis	$CaCO_3$	Aragonite	Calcite	Polyenes	Apatite	Anhydrite/ gypsum	Cuprite	Tenorite	Malachite	Quartz/ silicates	Beeswax	Paraloid/ resin	Anatase/ Rutile
Villa del Foro	SP 217	Leech-L	MRT	C	S													
Villa del Foro	SP 224	Leech-L	MRT	C	S													
Villa del Foro	SP28b	Leech-C	MRT	C	S													
Villa del Foro	St66120; SP691	Navic	MRT	L	S													
Villa del Foro	51878	Leech-C	MRT	C	S			x					x					
Villa del Foro	SP 834 a	Leech-C	MRT	C	S			x	x									
Villa del Foro	SP93	Leech-L	MRT	C	S													
Villa del Foro	SP 97	Leech-L	MRT	L	S										x			
Villa del Foro	SP98	Leech-L	MRT	L	S													
Villa del Foro, San Damiano	SP 23b	Other	MRT	C	S													

(Table 20 — continued)

Archaeological site	Inv. no.	Type	Location	Decoration	calcite	aragonite	gypsum	silicate/quartz	oxalate	malachite	apatite/ hyroxylapatite	antlerite	baryte	Organic	Paraloid	wax	beeswax	PVAc
Unknown	MV5924	Other	V-MC	G													x	
Unknown	MV5916	Bead	V-MC	G							x			x	x			
Unknown	Coll. Bellini	Leech-C	SC-MC	C	x		x	x			?						?	
Unknown	M589/3	Leech-C	Bra	C	x										?			
bellunese	bellunese	Leech-T	B-MC	T	x												?	
Brignano Frascata	C-FR-NE/1	Leech-C	MRT	C	x		?	x		x								x
Brignano Frascata	C-FR-NE/2	Leech-C	MRT	C	x		x	x										
Brignano Frascata	C-FR-NE/3	Leech-C	MRT	C	x		x	x										
Brignano Frascata	C-FR-S/2	Leech-L	MRT	C				x	x	x				x				

Table 21. FT-IR results for the 104 analysed samples (alphabetically ordered according to the name of the archaeological site; ‘type’ column: bucket-P = bucket pendants; comp = composite bow fibula; groom = grooming tools; leech-C = leech fibula with circular decoration; pend = pendant and Longone al Segrino pendants; raw = raw coral branches; ‘location’ column: : see section 4.5; ‘Dec.’ column: ‘G’ = general, ‘T’ = transversal grooves, ‘C’ = circular, ‘L’ = linear, ‘O’ = occhio di dado; ‘Analysis’ column: ‘I’ = in situ, ‘D’ = direct, ‘S’ = sampled): ‘x’ = presence of the material, ‘?’ = doubt.

Archaeological site	Inv. no.	Type	Location	Decoration	calcite	aragonite	gypsum	silicate/quartz	oxalate	malachite	apatite/ hyroxylapatite	antlerite	baryte	Organic	Paraloid	wax	beeswax	PVAc
Castelletto Ticino	2153	Leech-C	MRT	C	x			x							x			
Caverzano, loc. Limade	287304	Leech-C	B-MC	C	x									x				
Caverzano, loc. Masiera	217	Leech-C	B-MC	C	x										x			
Caverzano, loc. Masiera	211	Leech-C	B-MC	C	x										x		x	
Chies D'Alpago, loc. Prà	3344	Leech-C	B-MC	C	x			x									?	
Golasecca	MV103	Pend	V-MC	G	x									x				
Golasecca	MV4062	Leech-C	V-MC	C							?							
Golasecca, loc. Galliasco	22.S288-1.205	Leech-C	M-SABAP	C	x													
Golasecca, loc. Monsorino	63413	Leech-C	V-MC	C	x									x	x			
Malgesso	MV4025	Leech-C	V-MC	C						x						x		
Mel	9244	Leech-C	MAM	C	x										x			
Mel	9290	Leech-C	MAM	C	x												x	
Mel	9289	Leech-C	MAM	C	x												x	
Mel	9271	Leech-C	MAM	C	x					x							x	
Montebelluna, loc. Posmon,	304784	Leech-C	M-MSNA	C						x								
Montebelluna, loc. Posmon,	304780	Leech-C	M-MSNA	C				x	x									
Montebelluna, Casa Tesser	147145	Leech-C	M-MSNA	C				x							x			
Montebelluna, Casa Tesser	7489	Leech-C	M-MSNA	C											x			
Padova, vicolo Ognissanti	60735	Leech-C	P-MC	C	x										x			
Padova, vicolo Ognissanti	term staffa	Leech-C	P-MC	C	x									x				
Padova, San Massimo	65299	Bucket-P	P-MC	C	x									x			x	
Padova, San Massimo	65300	Bucket-P	P-MC	C	x												x	
Pieve d'Alpago, Pian della Gnela	312348	Leech-C	P-SABAP	C	x									x				
Pieve d'Alpago, Pian della Gnela	312349	Leech-C	P-SABAP	C						x								
Pieve d'Alpago, Pian della Gnela	312360	Leech-C	P-SABAP	C	x						?			x				
Pieve d'Alpago, Pian della Gnela	312375	Bead	P-SABAP	G	x									x				
Pieve d'Alpago, Pian della Gnela	355677	Bead	P-SABAP	G	x			x						x				
Pieve d'Alpago, Pian della Gnela	355542	Bead	P-SABAP	G	x			x						x				
Pieve d'Alpago, Pian della Gnela	355538	Bead	P-SABAP	G	x									x				
Pieve d'Alpago, Pian della Gnela	355534	Bead	P-SABAP	G	x									x				
Pieve d'Alpago, Pian della Gnela	355517	Leech-C	P-SABAP	C	x									x				
Pieve d'Alpago, Pian della Gnela	355516	Leech-C	P-SABAP	C	x									x				

(Table 21 — continued)

Archaeological site	Inv. no.	Type	Location	Decoration	calcite	aragonite	gypsum	silicate/quartz	oxalate	malachite	apatite/ hyroxylapatite	antlerite	baryte	Organic	Paraloid	wax	beeswax	PVAc
Pieve d'Alpago, Pian della Gnela	355515	Leech-C	P-SABAP	C	x						?			x				
Pieve d'Alpago, Pian della Gnela	355678	Bead	P-SABAP	G	x									x				
Pieve d'Alpago, Pian della Gnela	355679	Bead	P-SABAP	G	x									x				
Piovego	5,99	Raw	P-UNIPD	G	x										x			
Piovego	110,8	Bucket-P	P-UNIPD	C	x										x			
Piovego	108,7	Pend	P-UNIPD	G	x									x				
Piovego	108,5	Bucket-P	P-UNIPD	C	x									x				
Piovego	108,3	Leech-C	P-UNIPD	C	x									x				
Piovego	181844	Leech-C	P-UNIPD	C	x										x			
Piovego	95,11	LH	P-UNIPD	C	x													
Piovego	149682	Pend	P-UNIPD	G	x										x			
Piovego	95,1	Groom	P-UNIPD	L		x												
Piovego	95,1	Groom	P-UNIPD	C	x													
Piovego	89,6	Leech-C	P-UNIPD	C	x										x			
Piovego	86,3	Bucket-P	P-UNIPD	C	x										x			
Piovego	224255	Leech-C	P-UNIPD	C	x													
Piovego	224358	Leech-C	P-UNIPD	C						x								
Piovego	224201	Leech-C	P-UNIPD	C	x									x				
Piovego	5,73	Leech-C	P-UNIPD	C	x									x				
Piovego	153032	Leech-C	P-UNIPD	C	x									x				
Piovego	149721	Leech-C	P-UNIPD	C	x													
Piovego	34914	Leech-C	P-UNIPD	C	x									x				
Piovego	110,13	Bead	P-UNIPD	G	x			x						x				
Ponte nelle Alpi, loc. Casan	3366	Other	B-MC	C	x									x				
Ponte nelle Alpi, loc. Cugnan	3355	Leech-C	B-MC	C	x										x			
Pontecurone	RR24	Groom	MRT	L				x	x	x				x				
Safforze	6602	Leech-C	B-MC	C	x										x			
Safforze	6600	Leech-C	B-MC	C	x								x				x	
Sesto Calende, loc. asilo	12437	Leech-C	V-MC	C						x						x		
Sesto Calende, loc. asilo	12436	Leech-C	V-MC	C											x			
Sesto Calende, loc. Mulini Bellaria	23751	Leech-C	SC-MC	C							x							

(Table 21 — continued)

Archaeological site	Inv. no.	Type	Location	Decoration	calcite	aragonite	gypsum	silicate/quartz	oxalate	malachite	apatite/hyroxylapatite	antlerite	baryte	Organic	Paraloid	wax	beeswax	PVAc
Sesto Calende, loc. Mulini Bellaria	23752	Leech-C	SC-MC	C	x						x			x				
Sesto Calende, via Moncenisio	172343	Pend	SC-MC	G	x										x			
Sesto Calende, via Moncenisio	172344	Raw	SC-MC	G	x										x			
Sesto Calende, via Montrucco	4783	Pend	SC-MC	G	x									x				
Villa del Foro	1000/E1	Leech-C	MRT	C	x					x				x				
Villa del Foro	SP 55	Leech-L	MRT	L	x									x				
Villa del Foro	SP 56a	Leech-L	MRT	L								x		x				
Villa del Foro	SP 27	Leech-C	MRT	C	x			x				x		x				
Villa del Foro	66132	Leech-C	MRT	C	x			x						x				
Villa del Foro	66131	Leech-L	MRT	L	x			x						x				
Villa del Foro	51877	Leech-C	MRT	C	x			x						x				x
Villa del Foro	RS154	Leech-C	MRT	C	x			x		x				x				x
Villa del Foro	RS/SP 134	Leech-L	MRT	L				x						x				
Villa del Foro	RS 135	Leech-L	MRT	L				x						x				
Villa del Foro	RS 160	Leech-L	MRT	L						x				x				
Villa del Foro	RS/SP 72	Leech-L	MRT	L				x						x				
Villa del Foro	RS 819	Leech-L	MRT	L	x			x						x				
Villa del Foro	RS 822	Other	MRT	L				x						x				
Villa del Foro	SP 140 b	Leech-L	MRT	L				x						x				
Villa del Foro	SP159	Leech-L	MRT	L				x	?					x				
Villa del Foro	SP 16	Leech-L	MRT	L				x						x				
Villa del Foro	SP16	Leech-C	MRT	C					?	x				x				
Villa del Foro	SP 217	Leech-L	MRT	C				x	?					x				
Villa del Foro	SP 224	Leech-L	MRT	C				x	?					?				
Villa del Foro	SP28b	Leech-C	MRT	C	x			x		x				?				x
Villa del Foro	St66120; SP691	Navic	MRT	L				x	?					x				
Villa del Foro	51878	Leech-C	MRT	C	x									x				
Villa del Foro	SP 834 a	Leech-C	MRT	C	x									?				
Villa del Foro	SP93	Leech-L	MRT	C				x	?					x				
Villa del Foro	SP 97	Leech-L	MRT	L				x	?					?	x			x
Villa del Foro	SP98	Leech-L	MRT	L				x	?					?	x			x
Villa del Foro, San Damiano	SP 23b	Other	MRT	C	x			x	x					x				

(Table 21 — continued)

Archaeological site	Inv. no.	Type	Location	Decoration	Analysis	non attrib d=	calcite	Mg-calcite	dolomite	ankerite	CaO	gypsum	portlandite	fluorapatite	hydroxylapatite	carbonatehydroxylapatite	whitlockyte	brushite	anatase	rutile	talc	albite	anorthite	muscovite	illite	cristobalite	quartz	kaolinite	gehelenite	wax
Forcello	1060	Raw	M-MN	G	D		h																							
Forcello	98798	Raw	M-MN	G	D			h																						
Forcello	99209	LH	M-MN	T	D		w																				w			
Forcello	99210	LH	M-MN	T	D																									
Forcello	99211	LH	M-MN	C	D	5,51		m																						
Forcello	145782	BucketP	M-MN	C	D	5,51	m																							
Forcello	145959	LH	M-MN	T	D	5,47																					h			
Forcello	98797	Raw	M-MN	G	D	5,46		h														w								
Forcello	98799	Raw	M-MN	G	D			h																						
Forcello	RR 1272	LH	M-MN	T	D	2,98																					m			
Forcello	RR 745	BucketP	M-MN	C	D																									
Brembate	65	Leech-T	B-MA	T	D	5,57																					?			
Brembate	67	Comp	B-MA	G	D		h																							
Brembate	3016	Pend	B-MA	G	D		h																				w			
Brembate	3051	Comp	B-MA	G	D	2.90, 3.58	h																							
Brembate	3052	Comp	B-MA	G	D		h																							
Brignano F	C-FR-NE/1	Leech-C	MRT	C	S			h												w		w	w	w	w		w			
Brignano F	C-FR-NE/2	Leech-C	MRT	C	S			h																						
Brignano F	C-FR-NE/3	Leech-C	MRT	C	S			h																						
Brignano F	C-FR-S/2	Leech-L	MRT	C	S																	w	w							
CastellettoTic.	D1750	Pend	C-MC	G	D			h																			w			
CastellettoTic.	D2073	Leech-C	C-MC	C	D	2.6, 5.55	m																							
CastellettoTic.	D2077	Leech-C	C-MC	C	D			h														w	w							
CastellettoTic.	D2104	Leech-C	C-MC	C	D	5,46	h															w	w							
CastellettoTic.	D2773	Leech-C	C-MC	C	D																									
CastellettoTic.	2140	Leech-C	MRT	C	S																									
CastellettoTic.	2153	Leech-C	MRT	C	S		h																							
Castello di Annone	23.M380-9.4	Leech-C	MRT	C	D		m			w																	?			
Chiomonte	74795	LaTène	MRT	C	D	3.379,6.02																			?		m	?		
Chiomonte	74794	LaTène	MRT	C	D																				?		h	?		
Como	1397	Comp	C-MC	G	D		h															w	w							

Table 22. XRD results (excluded bronze alteration products: see paragraph 7.2.3) for the 141 analysed samples (alphabetically ordered according to the name of the archaeological site; 'type' column: bucketP = bucket pendants; comp = composite bow fibula; groom = grooming tools; leech-C = leech fibula with circular decoration; pend = pendant and Longone al Segrino pendants; raw = raw coral branches; 'location' column: : see paragraph 4.5; 'Dec.' column: 'G' = general, 'T' = transversal grooves, 'C' = circular, 'L' = linear, 'O' = occhio di dado; 'Analysis' column: 'I' = in situ, 'D' = direct, 'S' = sampled; reflex intensity: 'h' = high; 'm' =medium; 'w' = weak; '?' = doubt).

Archaeological site	Inv. no.	Type	Location	Decoration	Analysis	non attrib d=	calcite	Mg-calcite	dolomite	ankerite	CaO	gypsum	portlandite	fluorapatite	hydroxylapatite	carbonatehydrox-ylapatite	whitlockyte	brushite	anatase	rutile	talc	albite	anorthite	muscovite	illite	cristobalite	quartz	kaolinite	gehelenite	wax
Como	2206	Leech-C	C-MC	C	D	5,51	h																				m			
Como	1993	Comp	C-MC	G	D												m													
Como	124133	Other	C-MC	G	D										h															
Como	139651	Leech-C	C-MC	C	D		h																				w			
Como	139652	Leech-C	C-MC	C	D																						w			
Como	879	Leech-C	C-MC	C	D	5,53	m															w	w							
Como	124142	Pend	C-MC	G	D		h															w	w				w			
Como	865	Other	C-MC	O	D																						w			
Como	1230	Comp	C-MC	G	D	2.00, 5.55	h															w	w							
Como	E5868,	Leech-C	C-MC	C	D			h																			w			
Como	E5873,	Leech-C	C-MC	C	D	1.45, 1.48, 1.50, 1.54, 1.56, 1.59, 1.64, 1.87																								
Como	33593	Pend	C-MC	G	D							h																		
Como	33594	Pend	C-MC	G	D		h					w	h									w	w				w			
Como	E13273	Comp	C-MC	G	D	3.51, 4.27, 5.10, 6.04	h															w	w				w			
Como	E5552	Leech-C	C-MC	C	D	5.47, 11.50			m																		m			
Como	E5553	Leech-C	C-MC	C	D	5,49																					m			
Como	E5667	Leech-C	C-MC	C	D	4.15, 5.54			w													w	w				h			
Como, Isonzo	57210	Leech-C	C-MC	C	D	3,2		m																			w			
Como, Isonzo	57216	Leech-C	C-MC	C	D			h														w	w							
Como, Isonzo	57220	Leech-C	C-MC	C	D	5,51		m																						
Como, Isonzo	57244	Leech-C	C-MC	C	D	5,46																					w			
Como, Isonzo	57250	Leech-C	C-MC	C	D	5,62		m																						
Como, Isonzo	57262	Leech-C	C-MC	C	D	5,51		h																						
Como	E13225	Leech-C	C-MC	C	D																									
Como	E5957	Comp	C-MC	G	D	5,55		h														w	w							
Como	E5958	Comp	C-MC	G	D			h														w	w							
Golasecca	D1660	Groom	C-MC	C	D	5,55	h																							
Golasecca	D1668	Pend	C-MC	G	D		h															w	w							
Golasecca	D1669	Pend	C-MC	G	D	5,47	h															w	w				w			
Golasecca	D2049	Leech-C	C-MC	C	D	5,48	h															w	w							

(Table 22 — continued)

Archaeological site	Inv. no.	Type	Location	Decoration	Analysis	non attrib d=	calcite	Mg-calcite	dolomite	ankerite	CaO	gypsum	portlandite	fluorapatite	hydroxylapatite	carbonatehydrox-ylapatite	whitlockyte	brushite	anatase	rutile	talc	albite	anorthite	muscovite	illite	cristobalite	quartz	kaolinite	gehelenite	wax
Golasecca	D2059	Leech-C	C-MC	C	D	1.54, 2.47, 2.53, 3.69, 5.02, 11.5	w																							
Golasecca	D2064	Leech-C	C-MC	C	D	3.37, 4.33, 5.57	m																							
Golasecca	D2065	Leech-C	C-MC	C	D	5.56, 9.68						w																		
Golasecca	MV103	Pend	V-MC	G	S			h																						
Golasecca	MV4062	Leech-C	V-MC	C	S										?		?													
Golasecca	22.S288-1.205	Leech-C	SABAP VA	C	S			h																						
Golasecca	63413	Leech-C	V-MC	C	S			h																						
Gropello Cairoli	19/108	Leech-L	MANL	L	D	2.97, 5.59																								
Gropello Cairoli	19/109	Leech-L	MANL	L	D	5,61																								
Gropello Cairoli	19/110	Leech-L	MANL	L	D	5,51																					w			
Gropello Cairoli	19/111	Leech-L	MANL	L	D	5,53																								
Gropello Cairoli	19/112	Leech-C	MANL	C	D	5,44																								
Gropello Cairoli	19/114	Leech-L	MANL	L	D	2,95																								
Gropello Cairoli	19/115	Leech-L	MANL	L	D	1.76, 2.30, 4.66																								
Gropello Cairoli	19/117	Groom	MANL	C	D	1.67, 1.75, 2.49																								
Gropello Cairoli	21/178	Leech-L	MANL	L	D																									
Gropello Cairoli	21/179	Leech-L	MANL	L	D	2.10, 4.20																								
Gropello Cairoli	21/180	Leech-L	MANL	L	D																									
Gropello Cairoli	21/181	Leech-L	MANL	L	D																									
Malgesso	MV4025	Leech-C	V-MC	C	S	2.61, 2.89, 3.69																								
Mantova	169519	Leech-C	M-MN	C	D			h																						
Parre	9	Leech-L	B-MA	L	D	3.03, 3.31, 4.12, 5.47																								
Parre	40	other	B-MA	L	D	5,49													m											
Parre	41	Other	B-MA	L	D	5,49													m											
Parre	45	Other	B-MA	L	D														h								w			
Parre	46	Other	B-MA	L	D	4,09																					w			
Parre	48	Navic	B-MA	L	D	2.47, 4.13													w											
Parre	49	Navic	B-MA	L	D	4,09													m								w			

(Table 22 — continued)

Archaeological site	Inv. no.	Type	Location	Decoration	Analysis	non attrib d=	calcite	Mg-calcite	dolomite	ankerite	CaO	gypsum	portlandite	fluorapatite	hydroxylapatite	carbonatehydrox-ylapatite	whitlockyte	brushite	anatase	rutile	talc	albite	anorthite	muscovite	illite	cristobalite	quartz	kaolinite	gehelenite	wax
Parre	119	Navic	B-MA	L	D	5,47														h										
Parre	128	Other	B-MA	O	D	5.45, 9.25						m																		
Parre	3002	Other	B-MA	L	D	5,47														h										
Parre	3564	Leech-L	B-MA	L	D	5,45																								
Parre	3565	Leech-L	B-MA	L	D	2.83, 5.47																					m			
Parre	3569	Leech-L	B-MA	L	D		w																				m			
Pombia	72276-72277	Leech-C	MRT	C	D	1.76, 2.36, 2.63						w															w			
Pontecurone	RR24	Groom	MRT	L	S																	w	w							
S. Bernardino di Briona	1524	Leech-C	MRT	C	D	2.37, 2.61, 3.72, 4.76	m			m	w																w			
S. Bernardino di Briona	1567	Leech-C	MRT	C	D			?				w															w			
S. Bernardino di Briona	1514	Leech-C	MRT	C	D	3.67, 5.03, 5.98						m			m							w								
S. Bernardino di Briona	23.M380-9.1	Leech-C	MRT	C	D	2,96																?					?			
Sesto Calende	12437	Leech-C	V-MC	C	S		h			m								?				w	w							m
Sesto Calende	12436	Leech-C	V-MC	C	S		?																							
Sesto Calende	23751	Leech-C	SC-MC	C	S	4.31, 6.81																								
Sesto Calende	23752	Leech-C	SC-MC	C	S			h														w	w				m			
Sesto Calende	172343	Pend	SC-MC	G	S			h														w	w							
Sesto Calende	172344	Raw	SC-MC	G	S	6.41, 10.99	h															w	w							
Sesto Calende	4783	Pend	SC-MC	G	S			h														w	w							
Unknown	M589/3	Leech-C	Bra	C	S		h																							
Unknown	D2109	Other	C-MC	G	D	5,56										h														
Unknown	bellini	Leech-C	SC-MC	C	S																									
Unknown	MV5924	Other	V-MC	G	S																									h
Unknown	MV5916	Bead	V-MC	G	S									w																
Val Varaita	E17738	Navic	C-MC	O	D																									
Villa del Foro	1000/E1	Leech-C	MRT	C	S		h																							
Villa del Foro	SP 55	Leech-L	MRT	L	S																					w				
Villa del Foro	SP 56a	Leech-L	MRT	L	S				w																	w				
Villa del Foro	SP 27	Leech-C	MRT	C	S			h													w	w		w			w			
Villa del Foro	66132	Leech-C	MRT	C	S		w																				h			

(Table 22 — continued)

Archaeological site	Inv. no.	Type	Location	Decoration	Analysis	non attrib d=	calcite	Mg-calcite	dolomite	ankerite	CaO	gypsum	portlandite	fluorapatite	hydroxylapatite	carbonatehydroxylapatite	whitlockyte	brushite	anatase	rutile	talc	albite	anorthite	muscovite	illite	cristobalite	quartz	kaolinite	gehelenite	wax
Villa del Foro	66132	Leech-C	MRT	C	D	1.42, 1.86, 2.57, 3.29, 4.55																								
Villa del Foro	66131	Leech-L	MRT	L	S			h																						
Villa del Foro	51877	Leech-C	MRT	C	S			h	h													w	w			?				
Villa del Foro	RS154	Leech-C	MRT	C	S																								?	
Villa del Foro	RS/SP134	Leech-L	MRT	L	S	1.98, 3.53			w													w	w				m			
Villa del Foro	RS 135	Leech-L	MRT	L	S																						w			
Villa del Foro	RS 160	Leech-L	MRT	L	S																	w	w				w			
Villa del Foro	RS/SP 72	Leech-L	MRT	L	S				?								m													
Villa del Foro	RS 819	Leech-L	MRT	L	S		w															w	w				m			
Villa del Foro	RS 822	Other	MRT	L	S				?							h														
Villa del Foro	SP 140 b	Leech-L	MRT	L	S																	w	w							
Villa del Foro	SP159	Leech-L	MRT	L	S																	w					m			
Villa del Foro	SP 16	Leech-L	MRT	L	S																									
Villa del Foro	SP16	Leech-C	MRT	C	S			?														w	w				h			
Villa del Foro	SP 217	Leech-L	MRT	C	S					w												w	w				w			
Villa del Foro	SP 224	Leech-L	MRT	C	S				?																					
Villa del Foro	SP28b	Leech-C	MRT	C	S																									
Villa del Foro	St66120	Navic	MRT	L	S																	w	w				w			
Villa del Foro	51878	Leech-C	MRT	C	S			h																						
Villa del Foro	SP 834 a	Leech-C	MRT	C	S			m																						
Villa del Foro	SP93	Leech-L	MRT	C	S																						m			
Villa del Foro	SP 97	Leech-L	MRT	L	S	2,16																						w		
Villa del Foro	SP98	Leech-L	MRT	L	S	1,46																								
Villa del Foro, San Damiano	SP 23b	Other	MRT	C	S	1,72																h	h				w			

(Table 22 — continued)

	Na	Al	Si	P	S	Cl	K	Ti	Mn	Fe	Ni	Cu	Zn	As	Sr	Ag	Sn	Pb
HMC	18,00	30,00	30,00	29,00	31,00	23,00	23,00	4,00	2,00	32,00	1,00	29,00	0,00	2,00	0,00	3,00	12,00	21,00
MMC	18,00	30,00	36,00	23,00	40,00	14,00	17,00	4,00	3,00	36,00	3,00	35,00	0,00	1,00	0,00	0,00	13,00	14,00
LMC	10,00	39,00	46,00	28,00	35,00	13,00	22,00	5,00	1,00	39,00	1,00	46,00	1,00	1,00	1,00	1,00	10,00	14,00
CAL	0,00	2,00	4,00	3,00	2,00	1,00	0,00	0,00	0,00	1,00	0,00	4,00	0,00	0,00	0,00	0,00	0,00	1,00
TOT	46,00	101,00	116,00	83,00	108,00	51,00	62,00	13,00	6,00	108,00	5,00	114,00	1,00	4,00	1,00	4,00	35,00	50,00

Table 23. Table on the occurrence of minor elements in calcites with different Mg-content: indication of the number of objects reporting the presence of the different elements.

	Na	Al	Si	P	S	Cl	K	Ti	Mn	Fe	Ni	Cu	Zn	As	Sr	Ag	Sn	Pb
HMC	51,00	86,00	86,00	83,00	89,00	66,00	66,00	11,00	5,70	91,00	2,90	83,00	0,00	5,70	0,00	8,60	34,00	60,00
MMC	43,00	71,00	86,00	55,00	95,00	33,00	40,00	9,50	7,10	86,00	7,10	83,00	0,00	2,40	0,00	0,00	31,00	33,00
LMC	20,00	76,00	90,00	55,00	69,00	25,00	43,00	9,80	2,00	76,00	2,00	90,00	2,00	2,00	2,00	2,00	20,00	27,00
CAL	0,00	50,00	100,00	75,00	50,00	25,00	0,00	0,00	0,00	25,00	0,00	100,00	0,00	0,00	0,00	0,00	0,00	25,00
TOT	35,00	77,00	88,00	63,00	82,00	39,00	47,00	9,80	4,50	82,00	3,80	86,00	0,80	3,00	0,80	3,00	27,00	38,00

Table 24. Table on the occurrence (as a percentage of the total) of minor elements in calcites with different Mg-content.

Archaological site	Inv. no.	Type	Location	Decoration	Analysis	Interpr.	Elem.
Bagnolo S. Vito - Forcello	145782	Bucket-P	M-MN	C	D	HMC	HMC 10,57% Mg (8,76-12,82%) Ca + Na, Mg, Al, Si, P, S, Cl, K, Fe, Cu, Pb
Bagnolo S. Vito - Forcello	RR745	Bucket-P	M-MN	C	D	MIX	Si, Cu + Al, P, Ca, Sn + Mg, Fe, Pb + S, Cl, K, As
Bagnolo S. Vito - Forcello	98797	Raw	M-MN	G	D	HMC	HMC 12,51% Mg (6,91-15,46%) Ca + Mg + Na, Al, Si, P, S, Cl, K, Ti, Mn, Fe
Bagnolo S. Vito - Forcello	98798	Raw	M-MN	G	D	HMC	HMC 10,78% Mg (3,14-15,52%) Ca + Mg, Al, Si + Na, P, S, Cl, K, Fe, Mo
Bagnolo S. Vito - Forcello	98799	Raw	M-MN	G	D	HMC	HMC 11,21% Mg (8,37-13,14%) Ca + Mg + Na, Al, Si, P, S, Cl, K, Fe, Cu
Bagnolo S. Vito - Forcello	99210	LH	M-MN	T	D	-	-
Bagnolo S. Vito - Forcello	RR1272	LH	M-MN	T	D	MIX	P, Ca, Fe, Cu + Mg, Al, Si, K, Sn, Pb
Bagnolo S. Vito - Forcello	99209	LH	M-MN	T	D	MIX	Si, Cu + Al, Ca + Mg, P, S, Cl, K, Mn, Fe, Pb
Bagnolo S. Vito - Forcello	1060	Raw	M-MN	G	D	MMC	MMC 8,67% Mg (2,10-31,02%) Ca + Si + Mg, Al, Fe + Na, P, S, Cl, K, Ti, Mn, Ni, Cu, Sn, Pb
Bagnolo S. Vito - Forcello	145959	LH	M-MN	T	D	-	-
Bagnolo S. Vito - Forcello	99211	LH	M-MN	C	D	HMC	HMC 12,77% Mg (4,29-18,96%) Ca + Na, Mg, Al, Si, P, S, Cl, K, Fe, Cu, Sn, Ob
Bellinzago Novarese	197	Leech-C	N-MC	C	D	MMC	MMC 5,57% Mg (3,59-9,58%) Ca, Mg + Na, Al, Si, P, S, Cl, K, Fe, u, Sn, Pb
Bellinzago Novarese	198	Leech-C	N-MC	C	D	MMC	MMC 9,44% Mg (8,51-15,46%) Ca, Mg + Al, Si, P, S, Cl, K, Ti, Fe, Cu, Sn, Pb
bellunese	bellunese	Leech-T	B-MC	T	S	MMC	MMC 6,45% (3,28-9,63%) Ca + Mg, Al, Si, S, Cl, Fe, Cu, Sn
Borgonovo V.T.	20.S258-2.118	Leech-C	P-MAVT	C	D	HMC	HMC 17,6% Mg (8,02-27,99%) Ca + Si + Mg, Al, Fe, Cu + P, S, K, Ti, Sn, Pb
Borgonovo V.T.	20.S258-2.119	Leech-C	P-MAVT	C	D	LMC	LMC 1,84% Mg (0-6,14%) Ca + Si, Cu, Pb + Mg, Al, P, Cl, K, Ti, Fe, As, Sn
Borgonovo V.T.	20.S258-2.171	Leech-C	P-MAVT	C	D	HMC	HMC 13,27% Mg (1,97-39,35%) Ca, Si + Al + Mg, Fe, Cu + P, S, Cl, K, Ti, Pb
Borgonovo V.T.	20.S258-2.172	Leech-C	P-MAVT	C	D	SOIL	Si + Al + Mg, K, Ca, Fe, Cu + Na, P, S, Cl, Ti, Sn, Pb
Brembate sotto	65	Leech-T	B-MA	T	D	MIX	Si, Cu, Sn, Pb + Mg, Al, S, Cl,Ca, Fe
Brembate sotto	67	Comp	B-MA	G	D	LMC	LMC 4,25 % Mg (1,76-10,91) Ca, Mg + Na, Mg, Al, Si, P, S, Cl, K, Fe, Cu, Ag
Brembate sotto	3016	Pend	B-MA	G	D	LMC	LMC 2,12 % Mg (1,32-3,80%) Ca, Mg + Na, Al, Si, P, S, Cl, K, Fe, Cu
Brembate sotto	3051	Comp	B-MA	G	D	LMC	LMC 2,98 % Mg (1,14-5,13%) Ca, Mg + Na, Al, Si, P, S, Cl, K, Ti, Fe, Cu
Brembate sotto	3052	Comp	B-MA	G	D	LMC	LMC 4,70 % Mg (2,35-6,43%) Ca, Mg + Na, Al, Si, S, K, Fe, Cu
Brignano Frascata	C-FR-NE/1	Leech-C	MRT	C	S	HMC	HMC 10,38% Mg (9,36-11,01%) Ca + Mg, Al, Si, S, K, Fe, Cu
Brignano Frascata	C-FR-NE/2	Leech-C	MRT	C	S	HMC	HMC 11,48% Mg (7,32-15,05%) Ca + Na, Mg, Al, S
Brignano Frascata	C-FR-NE/3	Leech-C	MRT	C	S	HMC	HMC 11,43% Mg (0-23,06%) Ca + Mg, Al, Si, P, S, Fe, Cu, Sn, Pb
Brignano Frascata	C-FR-S/2	Leech-L	MRT	C	S	MIX	Mg, Al, Si, P, K, Ca, Fe, Cu, Sn, Pb

Table 25. SEM-EDS results (excluded bronze alteration products: see section 7.2.5) for the 241 analysed samples (alphabetically ordered according to the name of the archaeological site; 'type' column: bucket-P = bucket pendants; comp = composite bow fibula; groom = grooming tools; leech-C = leech fibula with circular decoration; pend = pendant and Longone al Segrino pendants; raw = raw coral branches; 'location' column: : see section 4.5; 'Dec.' column: 'G' = general, 'T' = transversal grooves, 'C' = circular, 'L' = linear, 'O' = occhio di dado; 'Analysis' column: 'I' = in situ, 'D' = direct, 'S' = sampled; 'Interpretation' column: 'HMC' = high-magnesian-calcite, 'MMC' = medium-magnesian-calcite, 'LMC' = low-magnesian-calcite, 'CALC' = calcite, 'BONE' = apatitic material, 'GYPSUM' = gypsum, 'ARAG' = aragonite, 'CHINA' = White Indian Ink, 'GLASS' = vitreous material, 'MET' = metal alloy and its alteration; 'SOIL' = deposition ground and 'MIX' a mixture of MET and SOIL).

Archaological site	Inv. no.	Type	Location	Decoration	Analysis	Interpr.	Elem.
Castelletto Ticino	91374, CT824	Pend	CT-GSAC	G	D	SOIL	Si, Al, Ca + Na, Mg, P, S, Cl, K, Ti, Fe, Cu
Castelletto Ticino	18.236, CT1141	Bead	CT-GSAC	G	D	BONE	Ca, P + Al, Cl
Castelletto Ticino	CT20343C03E, CT1144	Leech-C	CT-GSAC	C	D	LMC	LMC 4,73% Mg (3,64-6,9%) Ca, Cu, Si + Mg, Al, P, S, Sn
Castelletto Ticino	D1750	Pend	C-MC	G	D	HMC	HMC 11,27% Mg (9,33-13,02%) Ca + Mg, Al, Si, K, Fe
Castelletto Ticino	D2073	Leech-C	C-MC	C	D	MIX	Si, Ca, Cu + Mg, Al, P, K, Mn, Fe, Sn, Pb
Castelletto Ticino	D2104	Leech-C	C-MC	C	D	MMC	MMC 8,5% Mg (4,4-20,4%) Ca, Cu + Mg, Al, Si, P, S, Cl, K, Fe, As, Sn, Pb
Castelletto Ticino	D2773	Leech-C	C-MC	C	D	MIX	Si, Cu + Mg, Al, S, Cl, K, Ca, Fe, Zn, Sn
Castelletto Ticino	23.M380-9.5, SN1092	Leech-C	MRT	C	D	SOIL	Si, Ca + Mg, Al, P, S, Fe, Cu
Castelletto Ticino	2140	Leech-C	MRT	C	D	MIX	Si, Cu + Mg, Al, P, S, Cl, Ca, Fe
Castelletto Ticino	2140	leech-C	MRT (TO)	C	S	MIX	Mg, Al, Si, Ca, Cu
Castelletto Ticino	2153	Leech-C	MRT	C	S	LMC	LMC 4,86% Mg (0-11,20%) Ca + Mg, Al, P, Cu, Pb
Castelletto Ticino	1063	Groom	N-MC	C	D	MMC + BONE	BONE (P, Cu + Mg, Al, Si, S, Cl, K, Ca, Fe, Sn) MMC 8,15% Mg (5,46-10,21%) Ca + Mg, Al, Si, P, S, Cl, K, Cu, Sn, Ob
Castelletto Ticino, Bosco del Monte	CT29	Leech-C	CT-GSAC	C	D	LMC	LMC 0,79% Mg (0-3,57%) Ca + Mg, Al, Si, P, S, Cl, K, Fe, Cu, Sn
Castelletto Ticino, Motto d'Egro	20.S.279-3.788, CT164	Pend	CT-GSAC	G	D	LMC	LMC 2,46% Mg (1,26-4,70%) Ca + Mg, Al, Si, P, S, Mn, Fe, Cu, Sr, Sn
Castelletto Ticino, Motto Falco	CT179	Pend	CT-GSAC	G	D	MMC	MMC 6,75% Mg (3,24-10,05%) Ca + Mg, Si, Al + Na, P, S, Cl, K, Fe, Cu
Castelletto Ticino, v. Aronco	CT14031X, CT868a	Other	CT-GSAC	G	D	MIX	Al, Si, Cu + Mg, S, Ca, Fe
Castelletto Ticino, v. Aronco	CT14031X, CT868b	Bead	CT-GSAC	G	D	MIX	Si, Cu + Na, Mg, Al, P, S, Cl, Ca, Fe, Sn
Castelletto Ticino, v. Aronco	CT14031X, CT868c	Other	CT-GSAC	G	D	MIX	Si, Cu + Mg, Al, P, S, Cl, Ca, Fe, Sn
Castelletto Ticino, v. Valsesia	20.S.279.3.780	Leech-C	CT-GSAC	C	D	HMC	HMC 11,19% Mg (0-27,3%) Ca, Cu, Si + Mg, Al, P, S, Cl, K, Fe, Sn, Pb
Castelletto Ticino, Via Sivo	23.M380-9.3	Leech-T	MRT	C	D	MIX	Al, Si, P, Cu, Sn
Castelletto Ticino-Vigevano?	944	Leech-C	N-MC	C	D	LMC	LMC 2,25% Mg (0,98-4,15%) Ca, Mg + Mg, Al, Si, P, S, Cl, K, Fe, Cu, Zn, Sn
Castelletto Ticino-Vigevano?	946	Leech-C	N-MC	C	D	LMC	LMC 1,92% Mg (0-6,10%) Ca, Si + Mg, Al, P, S, K, Fe, Cu
Castelletto Ticino-Vigevano?	947	Leech-C	N-MC	C	D	MMC	MMC 9,13% Mg (7,38-12,52%) Ca, Mg, Al, Si, P, S, Cl, Fe, Cu, Pb
Castelletto Ticino-Vigevano?	949	Leech-C	N-MC	C	D	MMC	MMC 6,62% Mg (0-17,75%) Ca, Si, Cu + Mg, Al, P, S, K, Mn, Fe, Sn, Pb
Castello di Annone	23.M380-9.4	Leech-C	MRT	C	D	HMC	HMC 11,58% Mg (0-35,48%) Ca + Si, Cu + Mg, Al, P, Cl, K,Fe, As, Sn, Pb
Caverzano-località Limade	287304	Leech-C	B-MC	C	S	LMC	LMC 1,04% Mg (0,79-1,30%) Ca + Na, Mg, Al, Si, P, Fe, Cu, Sn, Pb
Caverzano-località Masiera	217	Leech-C	B-MC	C	S	MMC	MMC 9,66% Mg (9,66%) Ca + Mg + Si, S, Fe, Ni, Cu
Caverzano-località Masiera	211	Leech-C	B-MC	C	S	LMC	LMC 2,25% Mg (2,25%) Ca + Mg, Si, Fe
Chies D'Alpago, località Prà	3344	Leech-C	B-MC	C	S	MIX	Si, Ca, Fe, Cu + Na, Mg, Al, P, S, Cl, K, Ti, Ba, Pb
Chiomonte, La Maddalena	74795	LaTène	MRT	C	D	SOIL	Al, Si + Mg, K, Fe, Na + P, S, Ca, Ti, Cu
Chiomonte, La Maddalena	74794	LaTène	MRT	C	D	SOIL	Al, Si + Na, Mg, P, K, Ca, Ti, Fe, Cu
Coll. Assi	23-M380-9.8	Dolphin	MRT	C	D	MMC	MMC 9,91% Mg (9,7-10,12%) Ca + Na, Mg, Al, Si, P, S, Cl, K, Fe
Coll. Assi	23-M380-9.9	Dolphin	MRT	C	D	-	-
Coll. Assi	23-M380-9.10	Dolphin	MRT	C	D	LMC	LMC 4,26% Mg (3,66-4,86%) Ca + Mg, Al, Si, P, S, Cl, K, Fe
Como, Ca' Morta, Cava Butti	1397	Comp	C-MC	G	D	LMC	LMC 3,69% Mg (1,28-9,61%) Ca + Mg, Al, Si, S, K, Fe, Cu
Como, Ca' Morta, Cava dalla Zuanna	2206	Leech-C	C-MC	C	D	LMC	LMC 3,99% Mg (1,67-14,86%) Ca + Na, Mg, Al, Si, P, S, Cl, K, Ti, Fe, Cu, Sn
Como, Ca' Morta, Cava dalla Zuanna	2208	Leech-C	C-MC	C	D	MET	Cu + Mg, Al, Si, S, Ag
Como, Ca' Morta, Rebbio	1993	Comp	C-MC	G	D	BONE	P, Ca + Na, Mg, Al, Si, S, Cl, K, Ti, Fe, Cu, Sn
Como, Ca' Morta, Rebbio	114083	Leech-C	C-MC	C	D	LMC	LMC 1,53% Mg (0-4,6%) Ca + Mg, Si, Cu, Sn

(Table 25 — continued)

Archaological site	Inv. no.	Type	Location	Decoration	Analysis	Interpr.	Elem.
Como, Ca' Morta, Rebbio	114084	Leech-C	C-MC	C	D	CALC	Ca + Si, Cu
Como, Ca' Morta, Rebbio	124133	Other	C-MC	G	D	BONE	P, Ca + Na, Mg, Al, Si, S, K, Fe
Como, Ca' Morta, Rebbio	139651	Leech-C	C-MC	C	D	LMC	LMC 4,54% Mg (2,31-6,84%) Ca + Mg, Al, Si, Fe, Cu
Como, Ca' Morta, Rebbio	139652	Leech-C	C-MC	C	D	SOIL	Si + Al, Cu + Mg, P, S, K, Ca, Ti, Fe
Como, Ca' Morta, Rebbio	879	Leech-C	C-MC	C	D	LMC	LMC 3,68% Mg (3,40-3,97%) Ca + Mg, Al, Si, P, S, Cu
Como, Ca' Morta, Rebbio	124142	Pend	C-MC	G	D	LMC	LMC 4,9% Mg (2,52-7,77%) Ca + Na, Mg, Al, Si, P, S, Cl, K, Fe, Cu
Como, Ca' Morta, Rebbio	864	Other	C-MC	O	D	MET	Cu + Al, Si + Mg, P, S, Ca, Fe, Sn
Como, Ca' Morta, Rebbio	865	Other	C-MC	O	D	MIX	Al, Si, Cu, Sn + Na, Mg, , S, K, Ca, Ti, Fe, Pb
Como, Ca' Morta, Rebbio	1230	Comp	C-MC	G	D	MMC	MMC 5,55% Mg (0-8,89%) Ca + Na, Mg, Al, Si, P, S, Cl, K, Ti, Fe, Cu
Como, Ca' Morta, Rondineto	E5868	Leech-C	C-MC	C	D	HMC	HMC 16,1% Mg (11,5-19,9%) Ca + Na, Mg, Al, Si, P, S, Cl, K, Fe, Cu, Sn, Pb
Como, Ca' Morta, Rondineto	E5873	Leech-C	C-MC	C	D	MET	Cu, Sn, Pb + Al, Si, P, Fe
Como, Ca' Morta, Rondineto	E5865	Leech-C	C-MC	C	D	MIX	Si, Cu + Mg, Al, P, Cl, K, Ca, Fe
Como, Ca' Morta, terreno IACP	33593	Pend	C-MC	G	D	GYPSUM	S, Ca + Mg, Al, Si, Cl, K, Fe, Cu
Como, Ca' Morta, terreno IACP	33594	Pend	C-MC	G	D	MET	Cu + Si, S, Ca + Mg, Al, P, Cl, K, Mn, Fe, Sn
Como, Ca' Morta	E13273	Comp	C-MC	G	D	LMC	LMC 3,22% Mg (0-13,21%) Ca + Si, Cu + Mg, Al, P, S, Fe
Como, dintorni	E5552	Leech-C	C-MC	C	D	MIX	Cu, Si + Mg, Al, P, S, Cl, K, Ca, Fe, As, Sn
Como, dintorni	E5553	Leech-C	C-MC	C	D	SOIL	Si + Mg, Al, S, K, Ca, Fe, Cu
Como, dintorni	E5667	Leech-C	C-MC	C	D	MIX	Si, Cu + Mg, Al, S, Cl, K, Ca, Fe
Como, Prestino, via Isonzo	57210	Leech-C	C-MC	C	D	HMC	HMC 13,64% Mg (11,31-15,11%) Ca + Na, Mg, Al, Si, P, S, Cl,K, Fe, Cu, Ag, Sn, Pb
Como, Prestino, via Isonzo	57216	Leech-C	C-MC	C	D	HMC	HMC 12,7% Mg (4,85-18,3%) Ca + Mg, Al, Si, P, S, Cl, K, Fe, Cu, Pb
Como, Prestino, via Isonzo	57220	Leech-C	C-MC	C	D	HMC	HMC 17,84% Mg (16,25-19,65%) Ca + Mg, Al, Si, P, S, Cl, Fe, Cu, Sn, Pb
Como, Prestino, via Isonzo	57244	Leech-C	C-MC	C	D	MET	Cu + Na, Mg, Al, Si, P, S, Cl, K, Ca, Fe, Pb
Como, Prestino, via Isonzo	57250	Leech-C	C-MC	C	D	HMC	HMC 11,0% Mg (2,55-16,30%) Ca + Mg, Si + Na, Al, P, S, Fe, Cu, Pb
Como, Prestino, via Isonzo	57262	Leech-C	C-MC	C	D	HMC	HMC 18,81% Mg (17,17-19,99%) Ca + Na, Mg, Al, Si, P, S, Cl, K, Fe, Cu, Sn, Pb
Como, Rebbio, Villa Giovio	E13225	Leech-C	C-MC	C	D	MIX	Si, Cu + Mg, Al, S, K, Ca, Fe, Pb
Como, Respaù, Monte Olimpino	E5957	Comp	C-MC	G	D	HMC	HMC 14,09% Mg (5,87-29,77) Ca + Na, Mg, Al, Si, P, S, Cl, K, Fe, Cu, Ag
Como, Respaù, Monte Olimpino	E5958	Comp	C-MC	G	D	HMC	HMC 19,57% Mg (12,24-28,43%) Ca + Mg, Al, Si, P, S, Cl, K, Fe, Cu, Ag
Golasecca	D1660	Groom	C-MC	C	D	LMC	LMC 4,96% Mg (3,92-5,70%) Ca, Mg + Al, Si, P, S, K, Cu
Golasecca	D1667	Other	C-MC	G	D	BONE	BONE Ca, P + Na, Mg, Al, Si, S, Cl, K, Fe, Cu
Golasecca	D1668	Pend	C-MC	G	D	LMC	LMC 4,25% Mg (0-8,5%) Ca + Mg, Al, Si, S, Cl
Golasecca	D1669	Pend	C-MC	G	D	LMC	LMC 2,39% Mg (0-4,78%) Ca + Mg, Si, P, S, K, Fe
Golasecca	D2049	Leech-C	C-MC	C	D	MMC	MMC 5,33% Mg (0-11,26%) Ca + Mg, Al, Si, P, S, K, Ti, Fe, Cu, Sn, Pb
Golasecca	D2059	Leech-C	C-MC	C	D	CALC	calcite (Ca + Al, Si, P, Cu, Pb)
Golasecca	D2064	Leech-C	C-MC	C	D	MIX	Si, Ca, Cu + Mg, Al, P, S, Pb
Golasecca	D2065	Leech-C	C-MC	C	D	MMC	MMC 6,89% Mg (4,63-9,15%) Ca + Mg, Al, Si, S, K, Fe, Cu
Golasecca	MV103	Pend	V-MC	G	S	LMC	LMC 4,99% Mg (1,59-7,65%) Ca + Mg, Al, Si, S, Cu
Golasecca	MV4062	Leech-C	V-MC	C	S	MIX	Si, Cu + Mg, Al, P, S K, Ca, Ti, Fe
Golasecca, loc. Galliasco	22.S288-1.205	Leech-C	SABAP VA	C	S	LMC	LMC 4,5% Mg (1,93-6,88%) Ca + Mg, Al, Si, P, Cu, Pb
Golasecca, loc. Monsorino	63413	Leech-C	V-MC	C	S	MMC	MMC 9,5% Mg (5,84-13,43%) Ca + Mg, Al, Si, P, S, K, Mn, Fe, Cu, Pb

(Table 25 — continued)

Archaological site	Inv. no.	Type	Location	Decoration	Analysis	Interpr.	Elem.
Gropello Cairoli	19/108	Leech-L	MANL	L	D	-	-
Gropello Cairoli	19/110	Leech-L	MANL	L	D	-	-
Gropello Cairoli	19/111	Leech-L	MANL	L	D	-	-
Gropello Cairoli	19/112	Leech-C	MANL	C	D	HMC	HMC 16,32% Mg (0-56,77%) Ca + Mg, Al, Si, P, S, Cl, K, Fe, Cu, As, Sn, Pb
Gropello Cairoli	19/114	Leech-L	MANL	L	D	-	-
Gropello Cairoli	19/115	Leech-L	MANL	L	D	-	-
Gropello Cairoli	19/117	Groom	MANL	C	D	LMC	LMC 4,88% Mg (0-6,79%) Ca + Mg, Al, Si, P, S, K, Ca, Fe, Cu, Sn, Pb
Gropello Cairoli	21/178	Leech-L	MANL	L	D	-	-
Gropello Cairoli	21/180	Leech-L	MANL	L	D	-	-
Gropello Cairoli	21/181	Leech-L	MANL	L	D	-	-
Malgesso	MV4025	Leech-C	V-MC	C	S	MIX	Ca, Cu + Mg, Al, Si, S, P, Cl, K, Fe, Ba
Mantova	169519	Leech-C	M-MN	C	D	HMC	HMC 11,52% Mg (8,14-12,96%) Ca + Mg + Na, Al, Si, P, S, Cl, Fe, Cu, Pb
Mel	9244	Leech-C	MAM	C	S	MMC	MMC 5,07% Mg (0-19,49%) Ca + Na, Mg, Al, Si, S, Cl, K, Ti, Fe, Cu
Mel	9290	Leech-C	MAM	C	S	LMC	LMC 4,74% Mg (4,12-6,58%) Ca + Mg, Fe, Cu + Si, Pb
Mel	9289	Leech-C	MAM	C	S	LMC	LMC 4,29% Mg (2,12-7%) Ca + Mg, Si, S, Fe, Cu
Mel	9271	Leech-C	MAM	C	S	SOIL	Al, Si + Na, Mg, P, S, Cl, K, Ca, Ti, Fe
Montebelluna, loc. Posmon	304784	Leech-C	M-MSNA	C	S	LMC	LMC 4,09% Mg (1,49-5,63%) Ca + Al, Si, Fe, Cu + Mg, P, S, K, Pb
Montebelluna, loc. Posmon	304780	Leech-C	M-MSNA	C	S	MET	Cu + Mg, Al, Si, P, Ca, Fe, Pb
Montebelluna, Casa Tesser	147145	Leech-C	M-MSNA	C	S	MIX	Al, Si, P, Fe, Cu, Sn + Mg, S, Ca, Ag
Montebelluna, Casa Tesser	7489	Leech-C	M-MSNA	C	S	SOIL	Al, Si + Mg, P, Ca, Fe, Cu + Mg, S, K, Ti, Sn
Motto Lagone	T1	Leech-C	A-MAA	C	D	HMC	HMC 11,65% Mg (8,08-15,91%) Ca, Mg + Na, Si, P, S, Cl, K, Mn, Fe, Cu, Sn, Pb
Motto Lagone	T2	Bead	A-MAA	G	D	GLASS	Si, O + Fe, Zr + Na, Mg, Al, P, S, Cl, K, Ca, Ti, Cu, Sn
Padova, vicolo Ognissanti	60735	Leech-C	P-MC	C	S	LMC	LMC 1,59% Mg (0,85-2,33%) Ca + Cu + Mg, Al, Fe, Pb
Padova, vicolo Ognissanti	term staffa	Leech-C	P-MC	C	S	HMC	HMC 10,54% Mg (8,03-14,25%) Ca + Cu + Mg, P, S, Cl, Fe
Padova, vicolo San Massimo	65299	Bucket-P	P-MC	C	S	LMC	LMC 3,96% Mg (2,75-5,60%) Ca + Mg, Al, Si, S, K, Fe, Cu, Sn
Padova, vicolo San Massimo	65300	Bucket-P	P-MC	C	S	LMC	LMC 3,79% Mg (2,96-4,62%) Ca + Na, Mg, Al, Si, S, K, Fe, Cu
Parre, loc. Castello	9	Leech-L	B-MA	L	D	SOIL	Si, Al
Parre, loc. Castello	40	other	B-MA	L	D	CHINA	Ti + Na, Mg, Al, Si, S, Cl, K, Ca, Fe, Cu, Sn
Parre, loc. Castello	41	Other	B-MA	L	D	CHINA	Ti + Mg, Al, Si, S, K, Ca, Fe, Cu, Sn
Parre, loc. Castello	45	Other	B-MA	L	D	CHINA	Ti (linear) + Na, Mg, Al, Si, P, S, Cl, K, Ca, Fe, Ni, Cu
Parre, loc. Castello	46	Other	B-MA	L	D	CHINA	Ti + Mg, Al, Si, S, K, Ca, Cu
Parre, loc. Castello	48	Navic	B-MA	L	D	CHINA	Ti + Na, Mg, Al, Si, S, Cl K, Ca, F, Cu, Sn
Parre, loc. Castello	49	Navic	B-MA	L	D	CHINA	Ti + Na, Mg, Al, Si, S, K, Ca, Cr, Fe, Cu
Parre, loc. Castello	119	Navic	B-MA	L	D	CHINA	Ti + Mg, Al, Si, P, S, Cl, K, Ca, Cu, Sn
Parre, loc. Castello	128	Other	B-MA	O	D	SOIL	Mg, Si, Al + P, S, Cl, K, Ca, Fe, Cu, Sn
Parre, loc. Castello	3002	Other	B-MA	L	D	CHINA	Ti + Mg, Al, Si, P, S, Cl,K, Ca, Fe, Cu, Sn
Parre, loc. Castello	3564	Leech-L	B-MA	L	D	MIX	Al, Si, Cu + Mg, P, S, Cl, K,Ca, Ti, Fe, Ni
Parre, loc. Castello	3565	Leech-L	B-MA	L	D	MIX	Cu, Si, Al + Mg, P, S, Cl, K, Ca, Fe, Ni
Parre, loc. Castello	3569	Leech-L	B-MA	L	D	HMC	HMC 16,20 % Mg (8,81-22,80%) Ca, Mg + Na, Al,Si,P, S, Cl, K, Ti, Fe, Ni, Cu

(Table 25 — continued)

Archaological site	Inv. no.	Type	Location	Decoration	Analysis	Interpr.	Elem.
Pianello V.T.	18711	Bucket-P	P-MAVT	C	D	MIX	Al, Si, Cl, K, Ca, Cu, Pb
Pianello V.T.	18878	other	P-MAVT	C	D	MIX	Si, Cu, Sn, Pb + Al, Ca, Fe + Mg, P, K, Ti
Pianello V.T.	200191	Leech-C	P-MAVT	C	D	HMC	HMC 14,17% Mg (11,96-16,42%) Ca + Mg + Na, Al, Si, P, S, Cl, K, Fe, Cu
Pianello V.T.	201255	Leech-C	P-MAVT	C	D	MET	Cu, Sn, Pb + Na, Al, Si, P, S, Cl, K, Ca, Fe, As
Pieve d'Alpago, Pian della Gnela	312348	Leech-C	P-SABAP	C	S	MMC	MMC 9,51% Mg (7,39-11,64%) Ca + Mg, S, Fe, Cu, Pb
Pieve d'Alpago, Pian della Gnela	312349	Leech-C	P-SABAP	C	S	SOIL	Si + Al, Fe, Cu + Mg, P, K, Ca, Ti
Pieve d'Alpago, Pian della Gnela	312360	Leech-C	P-SABAP	C	S	LMC	LMC 4,39% Mg - Ca + Cu + Mg, Si, P, Fe, Pb
Pieve d'Alpago, Pian della Gnela	312375	Bead	P-SABAP	G	S	MMC	MMC 10,32% Mg (9,29-11,62%) Ca + Na, Mg, S, Fe, Cu
Pieve d'Alpago, Pian della Gnela	355677	Bead	P-SABAP	G	S	SOIL	Si, Ca + Mg, Al, K, Fe, Cu + P, S, Ti
Pieve d'Alpago, Pian della Gnela	355542	Bead	P-SABAP	G	S	MMC	MMC 9,65% Mg (8,73-10,58%) Ca + Mg + Na, Al, Si, S, Fe, Cu
Pieve d'Alpago, Pian della Gnela	355538	Bead	P-SABAP	G	S	MMC	MMC 8,24% Mg (5,89-11,07%) Ca + Na, Mg, Al, Si, S, Fe, Cu
Pieve d'Alpago, Pian della Gnela	355534	Bead	P-SABAP	G	S	MMC	MMC 7,73% Mg (5,58-9,73%) Ca + Na, Mg, Al, Si, P, S, Fe, Cu
Pieve d'Alpago, Pian della Gnela	355517	Leech-C	P-SABAP	C	S	HMC	HMC 10,67% Mg (6,65-15,06%) Ca + Mg + Na, S, Fe, Cu, Pb
Pieve d'Alpago, Pian della Gnela	355516	Leech-C	P-SABAP	C	S	MMC	MMC 9,64% Mg (9,45-9,84%) Ca + Mg + Al, Si, S, Fe, Cu
Pieve d'Alpago, Pian della Gnela	355515	Leech-C	P-SABAP	C	S	LMC	LMC 4,78% Mg - Ca+ Cu + Mg, Si, S, Fe
Pieve d'Alpago, Pian della Gnela	355678	Bead	P-SABAP	G	S	MMC	MMC 6,53% Mg (2,46-9,8%) Ca + Mg + Na, Al, Si, S, Fe
Pieve d'Alpago, Pian della Gnela	355679	Bead	P-SABAP	G	S	MMC	MMC 9,33% Mg (8,36-10,30%) Ca + Mg + Na, Al, Si, S, Fe
Piovego	5,99	Raw	P-UNIPD	G	S	MMC	MMC 6,98% Mg (4,39-8,38%) Ca + Mg + Na, Al, Si, S, K, Fe, Cu, Sn
Piovego	110,8	Bucket-P	P-UNIPD	C	S	LMC	LMC 2,76% Mg (0,73-5,68%) Ca + Na, Mg, Al, Si, S, K, Ti, Fe, Cu
Piovego	108,7	Pend	P-UNIPD	G	S	MMC	MMC 9,32% Mg (8,70-10,34%) Ca + Na, Mg, Si, S, Fe
Piovego	108,5	Bucket-P	P-UNIPD	C	S	LMC	LMC 3,09% (2,48-3,70%) Ca + Mg, Al, Si, P, S, K, Fe, Ni, Cu
Piovego	108,3	Leech-C	P-UNIPD	C	S	MMC	MMC 6,47% Mg (5,07-9,23%) Ca + Mg, Si, P, S, Cl, Fe, Cu
Piovego	181844	Leech-C	P-UNIPD	C	S	LMC	LMC 2,52% Mg (0,91-4,07%) Ca + Fe + Mg, Si, S, Cu, Pb
Piovego	181843	Leech-C	P-UNIPD	C	S	SOIL	Na, Cl, K, Ca + Al, Si, S, Fe
Piovego	95,11	LH	P-UNIPD	C	S	MMC	MMC 6,61% Mg (6,20-7,02%) Ca + Na, Mg, Al, Si, S, Cl, K, Fe, Cu
Piovego	149682	Pend	P-UNIPD	G	S	MMC	MMC 7,67% Mg (6,93-8,21%) Ca + Mg + Na, Al, Si, S, Fe
Piovego	95,1	Groom	P-UNIPD	L	S	ARAG	Ca + Al, Si, Fe, Cu
Piovego	95,1	Groom	P-UNIPD	C	S	LMC	LMC 4,21% Mg (3,74-4,93%) Ca + Mg, Fe, Pb
Piovego	89,6	Leech-C	P-UNIPD	C	S	LMC	LMC 1,37% Mg (1,05-1,68%) Ca + Cu + Mg, Al, Si, Fe, Pb
Piovego	86,3	Bucket-P	P-UNIPD	C	S	MMC	MMC 7,96% Mg (3,85-9,69%) Ca + Mg + Si, S, Fe, Cu
Piovego	224255	Leech-C	P-UNIPD	C	S	MMC	MMC 5,60% Mg (0-9,01%) Ca + Mg, Si, S, Fe, Cu
Piovego	224358	Leech-C	P-UNIPD	C	S	MET	Pb + Fe, Cu + Al, Si, P, Ca, As
Piovego	224201	Leech-C	P-UNIPD	C	S	HMC	HMC 11,03% Mg (10,45-11,61%) Ca + Mg + Na, S, Fe, Cu
Piovego	5,73	Leech-C	P-UNIPD	C	S	HMC	HMC 11,54% Mg (9,92-13,17%) Ca + Mg, Al, Si, P, S, K, Fe Cu, Pb
Piovego	153032	Leech-C	P-UNIPD	C	S	MMC	MMC 6,32% Mg (5,65-6,66%) Ca + Mg, Fe, Cu + Si, S
Piovego	149721	Leech-C	P-UNIPD	C	S	LMC	LMC 4,61% Mg (4,28-4,95%) Ca + Mg, Fe, Cu
Piovego	34914	Leech-C	P-UNIPD	C	S	LMC	LMC 1,03% Mg (0,92-1,16%) Ca + Mg, Fe, Cu
Piovego	110,13	Bead	P-UNIPD	G	S	SOIL	Si, Ca + Na, Mg, Al, P, K, Ti, Fe, Cu
Pombia, loc. Monticello	72276-72277	Leech-C	MRT	C	D	MET	Cu + Mg, Al, Si, P, K, Ca, Fe, Pb
Pombia, loc. Monticello	83925	Leech-C	O-MCF	C	D	LMC	LMC 2,2% Mg (0-5.7%) Ca + P, Cu + Na, Al, Si, S, K, Fe

(Table 25 — continued)

Archaological site	Inv. no.	Type	Location	Decoration	Analysis	Interpr.	Elem.
Pombia, loc. Monticello	83937	Leech-C	O-MCF	C	D	LMC	LMC 1,47% Mg (0-2.5%) Ca + Mg, Al, Si, Ca, Fe, Cu, Pb
Pombia, loc. Monticello	83946	Leech-C	O-MCF	C	D	MIX	Si, Cu + Al, P, Ca, Fe, As, Sn, Pb
Pombia, loc. Quara	83966	Leech-C	O-MCF	C	D	CALC	Ca + Al, Si, P, S, Fe, Cu
Ponte nelle Alpi-Casan	3366	Other	B-MC	C	S	HMC	HMC 11,66% Mg (10,65-12,68%) Ca + Mg + Na, Al, Si, P, S, Fe, Cu, Pb
Ponte nelle Alpi-Cugnan	3355	Leech-C	B-MC	C	S	LMC	LMC 3,46% Mg (2,92-3,77%) Ca + Mg, Al, Si, P, S, Fe, Cu
Pontecurone	23.M380-9.6	Leech-C	MRT	C	D	MMC	MMC 7,48% Mg (3,77-11,74%) Ca + Si + Mg, Al, P, K, Fe, Cu, Sn
Pontecurone	RR24	Groom	MRT	L	S	MIX	Al, Si, Ca, Cu, Sn
Rottofreno	259507	Leech-C	P-MAVT	C	D	SOIL	Si + Al, Ca, Cu + Mg, P, K, Ti, Fe, Zn, Pb
Safforze	6602	Leech-C	B-MC	C	S	MMC	MMC 9,64% Mg (8,59-10,69%) Ca + Mg + Na, S, Fe, Pb
Safforze	6600	Leech-C	B-MC	C	S	MMC	MMC 5,72% Mg (4,57-6,87%) Ca + Mg, S, Fe
San Bernardino di Briona	868	Leech-C	N-MC	C	D	MIX	Al, Si, Cu, Sn + Mg, P, Fe, Ag, Pb
San Bernardino di Briona	870	Leech-C	N-MC	C	D	LMC	LMC 4,98% Mg (2,02-8,98%) Ca, Mg + Al, Si, P, S, Cl,K, Fe, Cu
San Bernardino di Briona	1524, NCT0100026405	Leech-C	MRT	C	D	MMC	MMC 8,86% Mg (8,56-9,17%) Ca + Si, Cu + Mg, Al, P, S, Fe, Sn
San Bernardino di Briona	1567, NCT0100026418	Leech-C	MRT	C	D	MMC	MMC 8% Mg (4,92-12,14%) (Ca + Mg, Al, Si, P, S, Cu, Pb); BONE (P, Ca + Al, Si, Cu + Mg, Si, Cl, Fe, As); GYPSUM (S, Ca + P, Cu + Al, Si, Cl, Fe, Sn)
San Bernardino di Briona	1514, NCT0100026417	Leech-C	MRT	C	D	BONE	BONE Ca, P + Al, Cu, Pb + S, As
San Bernardino di Briona	1547, NCT0100026415	Leech-C	MRT	C	D	MIX	Si, Cu + Mg, Al, P, S, Ca, Fe, Sn, Pb
San Bernardino di Briona	23.M380-9.1	Leech-C	MRT	C	D	BONE	BONE Ca, P + Al, Cu, Pb + S, As
San Bernardino di Briona	23.M380-9.2	Leech-C	MRT	C	D	MMC	MMC 8,38% Mg (7,24-8,93%) Ca + Na, Mg, P, S, Cu
San Bernardino di Briona	23.M380-9.7	Bucket-P	MRT	C	D	MMC	MMC 8,21% Mg (5,53-11,12%) Ca + Cu + Mg, Al, Si, P, S, Sn, Pb
Sesto Calende, asilo	12437	Leech-C	V-MC	C	S	BONE	Ca, P + Mg, Al, Si, Cu + S, Cl, K, Fe, Sn, Pb
Sesto Calende, asilo	12436	Leech-C	V-MC	C	S	MIX	Si, P + Mg, Al, K, Ca, Fe, Cu
Sesto Calende, Mulini Bellaria	23751	Leech-C	SC-MC	C	S	MIX	P, Ca, Cu + Al + Mg, S, Cl, K, Fe, Pb
Sesto Calende, Mulini Bellaria	23752	Leech-C	SC-MC	C	S	MMC + BONE	MMC 8,11% Mg (4,63-12,97%) Ca + Mg, Al, P, S, K, Cu, Pb; BONE Ca, P, Cu + Mg, Al, S, Cl, K, Pb
Sesto Calende, via Moncenisio	172343	Pend	SC-MC	G	S	LMC	LMC 4,32% Mg (1,50-7,09%) Ca + Mg, Al, Si, S, K, Fe, Cu
Sesto Calende, via Moncenisio	172344	Raw	SC-MC	G	S	MMC	MMC 5,6% Mg (0-25,25%) Ca + Mg, Al, Si, P, Fe, Ni, Cu
Sesto Calende, via Montrucco	4783	Pend	SC-MC	G	S	LMC	LMC 3,61% Mg (0-7,14%) Ca + Mg, Al, Si, S, Cu
Unknown	D2109	Other	C-MC	G	D	BONE	Ca, P + Na, Mg, Si, S, Cl, K, Ti, Mn, Fe, Cu, Zn
Unknown	MV5916	Bead	V-MC	G	S	BONE	Ca, P
Unknown	Coll. Bellini	Leech-C	SC-MC	C	S	LMC	LMC 4,95% Mg (3,71-5,53%) Ca + Mg, Al, Si, S, Cu
Unknown	M589/3	Leech-C	Bra	C	S	LMC	LMC 3,73 % Mg Ca, Mg + Al, Si, P, S, Cu
Val Varaita	E17738	Navic	C-MC	O	D	SOIL	Si + Mg, Al, P, S, K, Ca, Tl, Fe, Cu, Sn, Pb
Villa del Foro	1000/E1	Leech-C	MRT	C	S	MMC	MMC 7,84% Mg (6,99-9,27%) Ca + Mg, Si, P, S, Cl, Fe, Cu, Pb
Villa del Foro	SP 55	Leech-L	MRT	L	S	MIX	Si, Cu + Al, P, Ca, Fe + Na, Mg, K, Pb
Villa del Foro	SP 56a	Leech-L	MRT	L	S	MET	Mg, Al, Si, P, S, Cl, Ca, Cu, Sn, Pb
Villa del Foro	SP 27	Leech-C	MRT	C	S	HMC	HMC 25,08% Mg (4,35-52,00%) Ca + Mg, Al, Si, S, K, Ti, Fe
Villa del Foro	66132	Leech-C	MRT	C	S	SOIL	Mg, Al, Si, P, K, Ca, Fe, Cu
Villa del Foro	66132	Leech-C	MRT (TO)	C	D	HMC	HMC 18,81% Mg (11,78-31,82%) Ca, Si + Mg, Al, P, S, Cl, K, Fe, Cu, Sn, Pb

(Table 25 — continued)

Archaological site	Inv. no.	Type	Location	Decoration	Analysis	Interpr.	Elem.
Villa del Foro	66131	Leech-L	MRT	L	S	HMC	HMC 14,49% Mg (12,17-18,51%) Ca + Mg, Al, Si, P, S, Fe, Cu, Sn, Pb
Villa del Foro	51877	Leech-C	MRT	C	S	LMC	LMC 4,93% Mg (0-8,82%) Ca + Mg, Si, P, Cl, Cu, Pb
Villa del Foro	RS154	Leech-C	MRT	C	S	SOIL	Si, P, Ca, Fe, Cu, Sn
Villa del Foro	RS/SP 134	Leech-L	MRT	L	S	SOIL	Mg, Al, Si, P, K, Ca, Ti, Fe, Cu
Villa del Foro	RS 135	Leech-L	MRT	L	S	MIX	Al, Si, P, Ca, Fe, Cu, Sn
Villa del Foro	RS 160	Leech-L	MRT	L	S	MIX	Mg, Al, Si, Ca, Fe, Cu, Sn, Pb
Villa del Foro	RS/SP 72	Leech-L	MRT	L	S	-	-
Villa del Foro	RS 819	Leech-L	MRT	L	S	MET	Mg, Al, Si, P, Ca, Fe, Cu, Sn, Pb
Villa del Foro	RS 822	Other	MRT	L	S	MET	Al, Si, P, Ca, Cu, As, Sn, Pb
Villa del Foro	SP 140 b	Leech-L	MRT	L	S	MET	Al, Si, P, Cl, Ca, Fe, Cu, As, Sn, Pb
Villa del Foro	SP159	Leech-L	MRT	L	S	SOIL	Mg, Al, Si, P, K, Ca, Fe, Cu, Sn, Pb
Villa del Foro	SP 16	Leech-L	MRT	L	S	MIX	Mg, Al, Si, P, K, Fe, Cu, Pb
Villa del Foro	SP16	Leech-C	MRT	C	S	MET	Mg, Al, Si, P, Cl, K, Ca, Fe, Cu, Pb
Villa del Foro	SP 217	Leech-L	MRT	C	S	SOIL	Mg, Al, Si, P, K, Ca, Ti, Fe, Cu
Villa del Foro	SP 224	Leech-L	MRT	C	S	MIX	Mg, Al, Si, P, K, Fe, Cu, Sn, Pb
Villa del Foro	SP28b	Leech-C	MRT	C	S	MET	Mg, Al, Si, P, S, Ca, Fe, Cu, Sn, Pb
Villa del Foro	51878	Leech-C	MRT	C	S	CALC	Mg, Al, Si, P, S, Cl, Ca, Cu
Villa del Foro	SP 834 a	Leech-C	MRT	C	S	HMC	HMC 10,60% Mg (10,26-10,94%) Ca + Mg, Al, Si, Ca
Villa del Foro	SP93	Leech-L	MRT	C	S	MIX	Mg, Al, Si, P, Ca, Ti, Fe, Cu, Sn, Pb
Villa del Foro	SP 97	Leech-L	MRT	L	S	SOIL	Mg, Al, Si, P, K, Ca, Ti, Fe
Villa del Foro	SP98	Leech-L	MRT	L	S	MIX	Mg, Al, Si, P, K, Ca, Fe, Cu, As, Sn, Pb
Villa del Foro, San Damiano	SP 23b	Other	MRT	C	S	SOIL	Mg, Al, Si, P, K, Ca, Fe, Cu, Zn, Pb

(Table 25 — continued)

	0	1	2	3	4	assignment
3655 cm^{-1}	/	s	w	/	/	CaO
3624 cm^{-1}	h	h	m	h	m	$Ca(OH)_2$
1755 cm^{-1}	/	vw	vw	vw	vw	
1441 cm^{-1}	/	w	w	w	w	$CaCO_3$
1088 cm^{-1}	w	mh	h	m	h	$CaCO_3$
999 cm^{-1}	vw	vw	vw	vw	vw	
715 cm^{-1}	s	w	w	w	w	$CaCO_3$
448 cm^{-1}	/	/	vw	vw	/	
363 cm^{-1}	m	w	vw	w	vw	$Ca(OH)_2$
282 cm^{-1}	w	m	m	m	m	$CaCO_3$
209 cm^{-1}	/	w	w	w	w	
157 cm^{-1}	vw	m	m	m	m	$CaCO_3$

Table 26. μ-Raman analysis: peaks position and intensity (h=hight, mh=medium-hight, m=medium, w=weight, vw=very weight, s=shoulder) in burnt corals and their assignments.

	0	1	2	3	4	assignment
3700 cm^{-1}	vw	vw	mw	w	w	
3648 cm^{-1}	vh	vh	h	m	m	$Ca(OH)_2$
3615 cm^{-1}	/	/	/	/	vw	
3522 cm^{-1}	s	s	s	/	/	
3500-3100 cm^{-1}	b	b	b	b	b	
2975 cm^{-1}	/	/	vw	vw	w	
2923 cm^{-1}	/	/	/	vw	/	
2872 cm^{-1}	/	/	vw	vw	w	
2588 cm^{-1}	/	/	/	/	s	
2514 cm^{-1}	vw	vw	vw	w	w	$CaCO_3$
1796 cm^{-1}	w	w	vw	w	mw	$CaCO_3$
1757 cm^{-1}	/	/	/	/	vw	
1659 cm^{-1}	/	vw	vw	/	/	
1648 cm^{-1}	s	/	/	s	s	$Ca(OH)_2$?
1444 cm^{-1}	s?	?	?	?	?	$Ca(OH)_2$
1416 cm^{-1}	mh	mh	h	h	h	$CaCO_3$
1130-1145 cm^{-1}	/	/	/	m	m	
1118 cm^{-1}	mw	mw	w	mw	/	
1083 cm^{-1}	/	/	w	mw	m	
876 cm^{-1}	m	m	mh	mh	h	$CaCO_3$ + $Ca(OH)_2$
856 cm^{-1}	/	/	/	m	m	
745 cm^{-1}	/	/	/	s	mw	
714 cm^{-1}	s	s	vw	mw	m	$CaCO_3$
671 cm^{-1}	s	s	/	vw	s	$CaCO_3$
621-610 cm^{-1}	/	/	m		m	

Table 27. μ-FT.IR analysis: peaks position and intensity (vw=very-hight, h=hight, mh=medium-hight, m=medium, mw=medium-weight, w=weight, vw=very weight, s=shoulder, b=broad) in burnt corals and their assignments.

	pre-combustion		post-combustion	
	Mg%	Ca%	Mg%	Ca%
0	11,97	88,03	9,32	90,68
1	9,38	90,62	9,01	90,99
2	11,71	88,29	9,12	90,88
3	14,41	85,59	8,06	91,94
4	12,76	87,24	10,19	89,81

Table 28. Pre- and post-firing comparison of the ratio of magnesium to calcium in moles (average values).

	Na	Mg	Al	Si	S	Ca	O
sample 0	0,80	5,67	0,38	0,09	0,70	41,73	50,64
sample 1	0,00	4,57	0,00	0,00	0,65	44,15	50,65
sample 2	0,00	5,69	0,00	0,00	0,70	42,91	50,70
sample 3	0,76	6,94	0,00	0,00	0,66	41,19	50,47
sample 4	0,92	6,11	0,00	0,00	0,73	41,76	50,50

Table 29. Results (atomic%) of semi-quantitative analysis on coral samples before firing.

	Na	Mg	Al	Si	S	K	Ca	Ti	Fe	Sr	O
sample 0	0,75	4,27	0,62	0,30	1,44	0,02	40,87	0,03	0,02	0,12	51,57
sample 1	0,52	4,33	0,45	0,00	0,53	0,00	43,63	0,00	0,00	0,02	50,52
sample 2	0,27	4,33	0,79	0,00	0,62	0,00	43,24	0,00	0,00	0,00	50,75
sample 3	1,38	3,77	0,26	0,04	1,55	0,00	41,43	0,00	0,00	0,00	51,58
sample 4	0,68	4,85	0,49	0,00	0,64	0,00	42,74	0,00	0,00	0,01	50,59

Table 30. Results (atomic%) of semi-quantitative analysis on coral samples after firing.

Archaeological site	Macro-area	Inv. no.	Tipology	Chronology	Location	Year of excavation	Burnt	Restored	Decoration	Analysis	Interpretation
Bagnolo S. Vito - Forcello	E	145782	bucket pendant 1A	early 5th c. BCE	M-MN		NO	?	O	D	high magnesian calcite
Bagnolo S. Vito - Forcello	E	RR 745	bucket pendant 1B	6th c. BCE	M-MN		NO	?	O	D	No dec.
Bagnolo S. Vito - Forcello	E	98797	coral branch		M-MN		NO	NO	G	D	*Corallium rubrum*
Bagnolo S. Vito - Forcello	E	98798	coral branch		M-MN		NO	NO	G	D	*Corallium rubrum*
Bagnolo S. Vito - Forcello	E	98799	coral branch		M-MN		NO	NO	G	D	*Corallium rubrum*
Bagnolo S. Vito - Forcello	E	99210	LH-Fußzierfibel	500-440 BCE	M-MN		NO	YES	T	D	No dec.
Bagnolo S. Vito - Forcello	E	RR 1272	LH-Fußzierfibel	495-475 BCE	M-MN		NO	NO	T	D	bone?
Bagnolo S. Vito - Forcello	E	99209	LH-Fußzierfibel		M-MN		NO	YES	T	D	calcite
Bagnolo S. Vito - Forcello	E	1060	coral branch	515-495 BCE	M-MN		YES	NO	G	D	medium magnesian calcite
Bagnolo S. Vito - Forcello	E	145959	LH-Fußzierfibel	500-440 BCE	M-MN		NO	?	T	D	No dec.?
Bagnolo S. Vito - Forcello	E	99211	LH-ornitomorphic	5th c. BCE	M-MN		NO	YES	C	D	*Corallium rubrum*
Bellinzago Novarese, loc. Valle Briga	G	197	Leech fibula with circular insets	525-480 BCE	N-MC	1950-1980	NO	SI	C	D	medium magnesian calcite
Bellinzago Novarese, loc. Valle Briga	G	198	Leech fibula with circular insets	525-480 BCE	N-MC	1950-1980	NO	SI	C	D	medium magnesian calcite
bellunese	P	bellunese	Leech fibula with transverse grooves		B-MC		NO	NO	T	S	medium magnesian calcite
Borgonovo V.T.	W	20.S258-2.118	Leech fibula with circular insets	525-480 BCE	P-MAVT	2000-2024	NO	NO	C	D	*Corallium rubrum*
Borgonovo V.T.	W	20.S258-2.119	Leech fibula with circular insets	525-440 BCE	P-MAVT	2000-2024	NO	NO	C	D	low magnesian calcite
Borgonovo V.T.	W	20.S258-2.171	Leech fibula with circular insets	525-480 BCE	P-MAVT	2000-2024	YES?	NO	C	D	high magnesian calcite
Borgonovo V.T.	W	20.S258-2.172	Leech fibula with circular insets	480-440 BCE	P-MAVT	2000-2024	YES?	NO	C	D	*Corallium rubrum*?
Brembate sotto	G	65	Leech fibula with transverse grooves	-	B-MA	<1900	NO	?	T	D	No dec.
Brembate sotto	G	67	Composite bow fibula, bead	-	B-MA	<1900	NO	Si	G	D	altered *Corallium rubrum*
Brembate sotto	G	3016	coral branch, pendant	6th-4th c. BCE	B-MA	<1900	NO	SI	G	D	low magnesian calcite
Brembate sotto	G	3051	Composite bow fibula, coral	480-440 BCE	B-MA	<1900	NO	?	G	D	low magnesian calcite
Brembate sotto	G	3052	Composite bow fibula, coral	480-440 BCE	B-MA	<1900	NO	?	G	D	low magnesian calcite
Brignano Frascata	L	C-FR-NE/1	Leech fibula with circular insets	525-440 BCE	MRT	1950-1980	NO	NO	C	S	*Corallium rubrum*
Brignano Frascata	L	C-FR-NE/2	Leech fibula with circular insets	525-480 BCE	MRT	1950-1980	NO	NO	C	S	*Corallium rubrum*
Brignano Frascata	L	C-FR-NE/3	Leech fibula with circular insets	525-440 BCE	MRT	1950-1980	NO	NO	C	S	*Corallium rubrum*
Brignano Frascata	L	C-FR-S/2	Late alpine fibula	480-425 BCE	MRT	1950-1980	NO	NO	C	S	No dec.
Castelletto Ticino	G	CT1144, CT20343C03E	Leech fibula with circular insets	560-525 BCE	CT-GSAC	2000-2024	NO	YES	C	D	low magnesian calcite
Castelletto Ticino	G	D2073	Leech fibula with circular insets	560-525 BCE	C-MC	<1900	YES	NO	C	D	calcite
Castelletto Ticino	G	D2077	Leech fibula with circular insets	560-525 BCE	C-MC	<1900	NO	NO	C	D	calcite
Castelletto Ticino	G	D2104	Leech fibula with circular insets	560-525 BCE	C-MC	<1900	NO	YES	C	D	medium magnesian calcite

Table 31. List of the 264 archaeological finds analysed and their interpretations (excluded bronze alteration products: see section 7.2.6): alphabetically ordered according to the name of the archaeological site; 'macro-area' column: 'G' = Golasecca, 'P' = Venetic, 'L' = Ligurian, 'E' = Etruria Padana, 'W' = Western Po Valley, 'U' = Unknown; 'Chronology' is updated on the basis of the typological subdivision used in this study (see section 4.2); 'location' column: : see section 4.5; 'Analysis' column: 'I' = in situ, 'D' = direct, 'S' = sampled; 'Decoration' column: 'C' = circular, 'L' = linear, 'T' = transversal grooves, 'G' = general, 'O' = occhio di dado.

Archaeological site	Macro-area	Inv. no.	Tipology	Chronology	Location	Year of excavation	Burnt	Restored	Decoration	Analysis	Interpretation
Castelletto Ticino	G	D2773	Leech fibula with circular insets	560-525 BCE	C-MC	<1900	NO	YES	C	D	No dec.
Castelletto Ticino	G	23.M380-9.5, SN1092	Leech fibula with circular insets	525-480 BCE	MRT	<1900	YES	YES	C	D	calcite?
Castelletto Ticino	G	2140	Leech fibula with circular insets	560-525 BCE	MRT	<1900	NO	YES	C	D	No dec.
Castelletto Ticino	G	2153	Leech fibula with circular insets	525-480 BCE	MRT	<1900	YES	YES	C	S	low magnesian calcite
Castelletto Ticino	G	91374, CT824	Longone pendant	750-675 BCE	CT-GSAC	2000-2024	NO	YES	G	D	calcite
Castelletto Ticino	G	CT1141, 18.236	beads	525-480 BCE	CT-GSAC	2000-2024	?	?	G	D	bone
Castelletto Ticino	G	D1750	Longone pendant	late 8th-7th c. BCE	C-MC	<1900	NO	NO	G	D	high magnesian calcite
Castelletto Ticino	G	1063	grooming tool - tweezer	-	N-MC	<1900	NO	?	C	D	altered *Corallium rubrum* + bone
Castelletto Ticino, Bosco del Monte	G	CT29	Leech fibula with circular insets	525-480 BCE	CT-GSAC	1900-1950	YES	YES	C	D	low magnesian calcite
Castelletto Ticino, Motto d'Egro	G	CT164, 20.S.279-3.788	Longone pendant	-	CT-GSAC	1980-2000	NO	NO	G	D	low magnesian calcite
Castelletto Ticino, Motto Falco	G	CT179	Longone pendant	-	CT-GSAC	1980-2000	NO	YES	G	D	medium magnesian calcite
Castelletto Ticino, v. Aronco	G	CT868a, CT14031X	Pendant	-	CT-GSAC		YES	YES	G	D	glass
Castelletto Ticino, v. Aronco	G	CT868b, CT14031X	beads	-	CT-GSAC		YES	YES	G	D	glass
Castelletto Ticino, v. Aronco	G	CTCT868c, 14031X	Pendant	-	CT-GSAC		YES	YES	G	D	glass
Castelletto Ticino, v. Valsesia	G	CT72820.S.279.3.780	Leech fibula with circular insets	525-480 BCE	CT-GSAC	2000-2024	?	?	C	D	high magnesian calcite
Castelletto Ticino, Via Sivo	G	23.M380-9.3	Leech fibula with transverse grooves	6th c. BCE	MRT	1980-2000	NO	NO	T	D	No dec.
Castelletto Ticino-Vigevano?	G	944	Leech fibula with circular insets	525-480 BCE	N-MC		YES?	NO	C	D	low magnesian calcite
Castelletto Ticino-Vigevano?	G	946	Leech fibula with circular insets	525-480 BCE	N-MC		YES	NO	C	D	low magnesian calcite
Castelletto Ticino-Vigevano?	G	947	Leech fibula with circular insets	525-480 BCE	N-MC		NO	NO	C	D	medium magnesian calcite
Castelletto Ticino-Vigevano?	G	949	Leech fibula with circular insets	525-480 BCE	N-MC		YES	NO	C	D	medium magnesian calcite
Castello di Annone	L	23.M380-9.4	Leech fibula with circular insets	525-440 BCE	MRT	1980-2000	NO	NO	C	D	high magnesian calcite
Caverzano-località Limade	P	287304	Leech fibula with circular insets	525-480 BCE	B-MC	1980-2000	YES	YES	C	S	low magnesian calcite
Caverzano-località Masiera	P	217	Leech fibula with circular insets	525-480 BCE	B-MC	<1900	NO	YES	C	S	*Corallium rubrum*
Caverzano-località Masiera	P	211	Leech fibula with circular insets	525-480 BCE	B-MC	<1900	YES	YES	C	S	Low magnesian calcite
Chies D'Alpago, località Prà	P	3344	Leech fibula with circular insets	525-480 BCE	B-MC	1900-1950	NO	YES	C	S	*Corallium rubrum*?
Chiomonte, La Maddalena		74795	folded-foot fibula	400-350 BCE	MRT	1980-2000	NO	YES	G	D	kaolin + illite?
Chiomonte, La Maddalena		74794	folded-foot fibula	400-350 BCE	MRT	1980-2000	NO	YES	G	D	kaolin + illite?
Coll. Assi		23-M380-9.8	Dolphin-shaped fibula	4th c. BCE	MRT		NO	YES	C	D	altered *Corallium rubrum*
Coll. Assi		23-M380-9.9	Dolphin-shaped fibula	4th c. BCE	MRT		NO	YES	C	D	No dec.
Coll. Assi		23-M380-9.10	Dolphin-shaped fibula	4th c. BCE	MRT		NO	YES	C	D	*Spondylus gaederopus*
Como, Ca' Morta, Cava Butti	G	1397	Composite bow fibula, coral	480-440 BCE	C-MC	1950-1980	NO	NO	G	D	low magnesian calcite

(Table 31 — continued)

Archaeological site	Macro-area	Inv. no.	Tipology	Chronology	Location	Year of excavation	Burnt	Restored	Decoration	Analysis	Interpretation
Como, Ca' Morta, Cava dalla Zuanna	G	2206	Leech fibula with circular insets	525-480 BCE	C-MC	1950-1980	NO	YES	C	D	low magnesian calcite
Como, Ca' Morta, Cava dalla Zuanna	G	2208	Leech fibula with circular insets	525-480 BCE	C-MC	1950-1980	NO	YES	C	D	No dec.
Como, Ca' Morta, Rebbio	G	114083	Leech fibula with circular insets	525-480 BCE	C-MC	1950-1980	NO	YES	C	D	low magnesian calcite
Como, Ca' Morta, Rebbio	G	114084	Leech fibula with circular insets	525-480 BCE	C-MC	1950-1980	YES	YES	C	D	calcite
Como, Ca' Morta, Rebbio	G	139651	Leech fibula with circular insets	525-480 BCE	C-MC	1950-1980	NO	NO	C	D	low magnesian calcite
Como, Ca' Morta, Rebbio	G	139652	Leech fibula with circular insets	525-480 BCE	C-MC	1950-1980	NO	NO	C	D	No dec.
Como, Ca' Morta, Rebbio	G	1993	Composite bow fibula, coral	675-600 BCE	C-MC	1950-1980	?	NO	G	D	bone
Como, Ca' Morta, Rebbio	G	124133	Bone	6th-5th c. BCE	C-MC		YES	NO	G	D	bone
Como, Ca' Morta, Rebbio, Cava Ballerini	G	879	Leech fibula with circular insets	525-480 BCE	C-MC	1900-1950	NO	NO	C	D	low magnesian calcite
Como, Ca' Morta, Rebbio, Cava Bianchi	G	124142	Longone pendant	750-675 BCE	C-MC		NO	NO	G	D	low magnesian calcite
Como, Ca' Morta, Rebbio, Cava Manzoni	G	864	Leech fibula		C-MC	1900-1950	NO	NO	O	D	No dec.
Como, Ca' Morta, Rebbio, Cava Manzoni	G	865	Leech fibula		C-MC	1900-1950	NO	NO	O	D	No dec.
Como, Ca' Morta, Rebbio, loc. Ronchetti	G	1230	Composite bow fibula, coral		C-MC	1950-1980	NO	YES	G	D	low magnesian calcite
Como, Ca' Morta, Rondineto	G	E5868	Leech fibula with circular insets	525-480 BCE	C-MC		NO	YES	C	D	high magnesian calcite
Como, Ca' Morta, Rondineto	G	E5873	Leech fibula with circular insets	525-440 BCE	C-MC		NO	YES	C	D	No dec.
Como, Ca' Morta, Rondineto	G	E5865	Leech fibula with circular insets	525-480 BCE	C-MC		NO	YES	C	D	No dec.
Como, Ca' Morta, terreno IACP	G	33593	Longone pendant	7th c. BCE	C-MC	1950-1980	NO	YES	G	D	gypsum
Como, Ca' Morta, terreno IACP	G	33594	Longone pendant	7th c. BCE	C-MC	1950-1980	NO	YES	G	D	calcite
Como, Ca' Morta	G	E13273	Composite bow fibula, coral	7th-5th c. BCE	C-MC	<1900	?	NO	G	D	low magnesian calcite
Como, dintorni	G	E5552	Leech fibula with circular insets	480-440 BCE	C-MC		NO	NO	C	D	No dec.
Como, dintorni	G	E5553	Leech fibula with circular insets	480-440 BCE	C-MC		NO	NO	C	D	No dec.
Como, dintorni	G	E5667	Leech fibula with circular insets	525-480 BCE	C-MC		NO	yes?	C	D	No dec.
Como, Prestino, via Isonzo	G	57210	Leech fibula with circular insets	480-440 BCE	C-MC	1980-2000	yes?	YES	C	D	*Corallium rubrum*
Como, Prestino, via Isonzo	G	57216	Leech fibula with circular insets	525-480 BCE	C-MC	1980-2000	yes?	YES	C	D	*Corallium rubrum*
Como, Prestino, via Isonzo	G	57220	Leech fibula with circular insets	525-480 BCE	C-MC	1980-2000	yes?	YES	C	D	*Corallium rubrum*
Como, Prestino, via Isonzo	G	57244	Leech fibula with circular insets	480-440 BCE	C-MC	1980-2000	yes?	YES	C	D	*Corallium rubrum*
Como, Prestino, via Isonzo	G	57250	Leech fibula with circular insets	480-440 BCE	C-MC	1980-2000	yes?	YES	C	D	*Corallium rubrum*
Como, Prestino, via Isonzo	G	57262	Leech fibula with circular insets	480-440 BCE	C-MC	1980-2000	yes?	YES	C	D	*Corallium rubrum*
Como, Rebbio, Villa Giovio	G	E13225	Leech fibula with circular insets	525-440 BCE	C-MC	1900-1950	?	NO	C	D	*Corallium rubrum* ?
Como, Respaù, Monte Olimpino	G	E5957	Composite bow fibula, coral	475-410 BCE	C-MC	<1900	NO	YES	G	D	high magnesian calcite
Como, Respaù, Monte Olimpino	G	E5958	Composite bow fibula, coral	475-410 BCE	C-MC	<1900	NO	YES	G	D	high magnesian calcite
Golasecca	G	D2049	Leech fibula with circular insets	525-480 BCE	C-MC	<1900	NO	NO	C	D	medium magnesian calcite
Golasecca	G	D2059	Leech fibula with circular insets	525-480 BCE	C-MC	<1900	NO	YES	C	D	calcite

(Table 31 — continued)

Archaeological site	Macro-area	Inv. no.	Tipology	Chronology	Location	Year of excavation	Burnt	Restored	Decoration	Analysis	Interpretation
Golasecca	G	D2064	Leech fibula with circular insets	525-480 BCE	C-MC	<1900	YES	YES	C	D	calcite
Golasecca	G	D2065	Leech fibula with circular insets	525-480 BCE	C-MC	<1900	YES	NO	C	D	medium magnesian calcite + gypsum
Golasecca	G	A0.9.4858	Leech fibula with circular insets	525-480 BCE	M-MCA		NO	NO	C	I	-
Golasecca	G	A0.9.4908	Leech fibula with circular insets	525-480 BCE	M-MCA		YES	NO	C	I	-
Golasecca	G	A0.9.4842	Leech fibula with circular insets	525-480 BCE	M-MCA		NO	YES?	C	I	calcite
Golasecca	G	D1660	grooming tool - tweezer	late 6th-5th c. BCE	C-MC	<1900	YES	NO	C	D	low magnesian calcite
Golasecca	G	D1667	Bone	-	C-MC	<1900	YES	NO	G	D	bone
Golasecca	G	D1668	Longone pendant	-	C-MC	<1900	NO	YES	G	D	low magnesian calcite
Golasecca	G	D1669	Longone pendant	-	C-MC	<1900	YES	yes?	G	D	low magnesian calcite
Golasecca	G	MV103	Longone pendant	8th-7th c. BCE	V-MC		NO	YES	G	S	low magnesian calcite
Golasecca	G	A0.9.28600	Longone pendant	late 8th-7th c. BCE	M-MCA		NO	NO	G	I	$CaCO_3$
Golasecca	G	A0.9.28598	Longone pendant	late 8th-7th c. BCE	M-MCA		NO	NO	G	I	$CaCO_3$
Golasecca	G	A0.9.28599	Bone	late 8th-7th c. BCE	M-MCA		NO	NO	G	I	$CaCO_3$
Golasecca	G	A0.9.28592	Longone pendant	late 8th-7th c. BCE	M-MCA		NO	NO	G	I	calcite
Golasecca	G	A0.9.28602	Longone pendant	late 8th-7th c. BCE	M-MCA		NO	NO	G	I	$CaCO_3$
Golasecca	G	MV4062	Leech fibula with circular insets	525-480 BCE	V-MC		YES	NO	C	S	calcite
Golasecca, loc. Galliasco	G	22.S288-1.205	Leech fibula with circular insets	525-480 BCE	SABAP VA	1950-1980	NO	NO	C	S	low magnesian calcite
Golasecca, loc. Lazzaretto	G	A0.9.17519	bucket pendant 1A		M-MCA	<1900	NO	NO	O	I	$CaCO_3$
Golasecca, loc. Monsorino	G	63413	Leech fibula with circular insets	525-480 BCE	V-MC	1980-2000	NO	YES	C	S	altered *Corallium rubrum*
Golasecca?	G	A0.9.5961	Leech fibula with circular insets	525-480 BCE	M-MCA		NO	YES	C	I	-
Golasecca?	G	A0.9.28164	Leech fibula with circular insets	525-480 BCE	M-MCA		?	NO	C	I	-
Golasecca?	G	A0.9.35542	Leech fibula with circular insets	525-480 BCE	M-MCA	1900-1950	NO	NO	C	I	$CaCO_3$
Gropello Cairoli	W	19/112	Leech fibula with circular insets	480-440 BCE	MANL	1950-1980	NO		C	D	*Corallium rubrum*
Gropello Cairoli	W	19/108	Leech fibula		MANL	1950-1980	NO		L	D	No dec.
Gropello Cairoli	W	19/109	Leech fibula		MANL	1950-1980	NO		L	D	No dec.
Gropello Cairoli	W	19/110	Leech fibula		MANL	1950-1980	NO		L	D	No dec.
Gropello Cairoli	W	19/111	Leech fibula		MANL	1950-1980	NO		L	D	No dec.
Gropello Cairoli	W	19/114	Leech fibula		MANL	1950-1980	NO		L	D	No dec.
Gropello Cairoli	W	19/115	Leech fibula		MANL	1950-1980	NO		L	D	No dec.

(Table 31 — continued)

Archaeological site	Macro-area	Inv. no.	Tipology	Chronology	Location	Year of excavation	Burnt	Restored	Decoration	Analysis	Interpretation
Gropello Cairoli	W	19/117	grooming tool		MANL	1950-1980	YES	YES	C	D	low magnesian calcite
Gropello Cairoli	W	21/178	Leech fibula		MANL	1950-1980	NO		L	D	No dec.
Gropello Cairoli	W	21/179	Serpentine fibula		MANL	1950-1980	NO	NO	L	D	No dec.
Gropello Cairoli	W	21/180	Leech fibula		MANL	1950-1980	NO	NO	L	D	No dec.
Gropello Cairoli	W	21/181	Leech fibula		MANL	1950-1980	NO	NO	L	D	No dec.
Malgesso	G	MV4025	Leech fibula with circular insets	525-480 BCE	V-MC		NO	YES	C	S	No dec.
Mantova - p.zza Santa Barbara	E	169519	Leech fibula with circular insets	525-480 BCE	M-MN	2000-2024	NO	YES	C	D	*Corallium rubrum*
Mel	P	9244	Leech fibula with circular insets	525-480 BCE	MAM	1950-1980	YES	YES	C	S	medium magnesian calcite
Mel	P	9290	Leech fibula with circular insets	525-480 BCE	MAM	1950-1980	NO	YES	C	S	low magnesian calcite
Mel	P	9289	Leech fibula with circular insets	525-480 BCE	MAM		NO	YES	C	S	low magnesian calcite
Mel	P	9271	Leech fibula with circular insets	525-480 BCE	MAM		NO	?	C	S	No dec.
Montebelluna, loc. Posmon,	P	304784	Leech fibula with circular insets	525-480 BCE	M-MSNA	2000-2024	YES	YES	C	S	low magnesian calcite
Montebelluna, loc. Posmon	P	304780	Leech fibula with circular insets	525-480 BCE	M-MSNA	2000-2024	YES	YES	C	S	No dec.
Montebelluna, Casa Tesser	P	147145	Leech fibula with circular insets	525-480 BCE	M-MSNA	1950-1980	NO	YES	C	S	No dec.
Montebelluna, Casa Tesser	P	7489	Leech fibula with circular insets	525-480 BCE	M-MSNA	1950-1980	NO	YES	C	S	No dec.
Motto Lagone	G	T1	Leech fibula with circular insets	525-480 BCE	A-MAA	1980-2000	NO	YES	C	D	*Corallium rubrum*
Motto Lagone	G	T2	bead	early 5th c. BCE	A-MAA	1980-2000	?	?	G	D	glass
Padova, vicolo Ognissanti	P	60735	Leech fibula with circular insets	525-480 BCE	P-MC		YES	YES	C	S	low magnesian calcite
Padova, vicolo Ognissanti	P	Term. staffa	Leech fibula with circular insets	525-480 BCE	P-MC		NO	YES	C	S	high magnesian calcite
Padova, vicolo San Massimo	P	65299	bucket pendant 1A	6th c. BCE	P-MC	1900-1950	NO	YES	O	S	low magnesian calcite
Padova, vicolo San Massimo	P	65300	bucket pendant 1A	6th c. BCE	P-MC	1900-1950	NO	YES	O	S	low magnesian calcite
Parre, loc. Castello	G	9	Leech fibula	475 BCE	B-MA	<1900	NO	YES	L	D	No dec.
Parre, loc. Castello	G	40	Foliate-arch fibula	475 BCE	B-MA	<1900	NO	YES	L	D	White Indian Ink
Parre, loc. Castello	G	41	Foliate-arch fibula	475 BCE	B-MA	<1900	NO	YES	L	D	White Indian Ink
Parre, loc. Castello	G	45	Leech fibula	475 BCE	B-MA	<1900	NO	YES	L	D	White Indian Ink
Parre, loc. Castello	G	46	Low-arch fibula	475 BCE	B-MA	<1900	NO	YES	L	D	White Indian Ink
Parre, loc. Castello	G	48	Navicella fibula	475 BCE	B-MA	<1900	NO	YES	L	D	White Indian Ink
Parre, loc. Castello	G	49	Navicella fibula	475 BCE	B-MA	<1900	NO	YES	L	D	White Indian Ink
Parre, loc. Castello	G	119	Navicella fibula	475 BCE	B-MA	<1900	NO	SI	L	D	White Indian Ink
Parre, loc. Castello	G	128	flat-arched fibula	475 BCE	B-MA	<1900	NO	SI	O	D	gypsum
Parre, loc. Castello	G	3002	Arch fibula	475 BCE	B-MA	<1900	NO	SI	L	D	White Indian Ink
Parre, loc. Castello	G	3564	Leech fibula	475 BCE	B-MA	<1900	NO	?	L	D	No dec.
Parre, loc. Castello	G	3565	Leech fibula	475 BCE	B-MA	<1900	NO	?	L	D	No dec.

(Table 31 — continued)

Archaeological site	Macro-area	Inv. no.	Tipology	Chronology	Location	Year of excavation	Burnt	Restored	Decoration	Analysis	Interpretation
Parre, loc. Castello	G	3569	Leech fibula	475 BCE	B-MA	<1900	NO	?	L	D	high magnesian calcite
Pianello V.T.	W	200191	Leech fibula with circular insets	525-480 BCE	P-MAVT	1980-2000	NO	YES?	C	D	high magnesian calcite
Pianello V.T.	W	201255	Leech fibula with circular insets	525-440 BCE	P-MAVT	1980-2000	YES	YES?	C	D	no dec.
Pianello V.T.	W	18711	bucket pendant 3D	5th-4th c. BCE	P-MAVT	1980-2000	NO	YES	O	D	no dec.
Pianello V.T.	W	18878	Triangolar pendant	5th-4th c. BCE	P-MAVT	1980-2000	NO	NO	O	D	no dec.
Pieve d'Alpago, Pian della Gnela	P	312348	Leech fibula with circular insets	525-480 BCE	P-SABAP	2000-2024	YES	YES	C	S	altered *Corallium rubrum*
Pieve d'Alpago, Pian della Gnela	P	312349	Leech fibula with circular insets	525-480 BCE	P-SABAP	2000-2024	YES	YES	C	S	No dec.
Pieve d'Alpago, Pian della Gnela	P	312360	Leech fibula with circular insets	525-480 BCE	P-SABAP	2000-2024	YES	?	C	S	low magnesian calcite
Pieve d'Alpago, Pian della Gnela	P	355517	Leech fibula with circular insets	525-480 BCE	P-SABAP	2000-2024	NO	YES	C	S	*Corallium rubrum*
Pieve d'Alpago, Pian della Gnela	P	355516	Leech fibula with circular insets	525-480 BCE	P-SABAP	2000-2024	NO	YES	C	S	altered *Corallium rubrum*
Pieve d'Alpago, Pian della Gnela	P	355515	Leech fibula with circular insets	525-480 BCE	P-SABAP	2000-2024	NO	YES	C	S	low magnesian calcite
Pieve d'Alpago, Pian della Gnela	P	312375	Bead		P-SABAP	2000-2024	YES	YES	G	S	medium magnesian calcite
Pieve d'Alpago, Pian della Gnela	P	355677	Beads		P-SABAP	2000-2024	?	NO	G	S	*Corallium rubrum* ?
Pieve d'Alpago, Pian della Gnela	P	355542	Beads		P-SABAP	2000-2024	?	NO	G	S	altered *Corallium rubrum*
Pieve d'Alpago, Pian della Gnela	P	355538	Beads		P-SABAP	2000-2024	YES?	NO	G	S	altered *Corallium rubrum*
Pieve d'Alpago, Pian della Gnela	P	355534	Beads		P-SABAP	2000-2024	NO	NO	G	S	altered *Corallium rubrum*
Pieve d'Alpago, Pian della Gnela	P	355678	Bead		P-SABAP	2000-2024	NO	NO	G	S	altered *Corallium rubrum*
Pieve d'Alpago, Pian della Gnela	P	355679	Bead		P-SABAP	2000-2024	NO	NO	G	S	altered *Corallium rubrum*
Piovego	P	108,3	Leech fibula with circular insets	525-480 BCE	P-UNIPD	1950-1980	NO	NO	C	S	medium magnesian calcite
Piovego	P	181844, 97.5	Leech fibula with circular insets	525-480 BCE	P-UNIPD	1950-1980	YES	YES	C	S	low magnesian calcite
Piovego	P	181843, 97.6	Leech fibula with circular insets	525-480 BCE	P-UNIPD	1950-1980	YES	YES	C	S	No dec.
Piovego	P	89,6	Leech fibula with circular insets	525-480 BCE	P-UNIPD	1950-1980	YES	NO	C	S	low magnesian calcite
Piovego	P	224255, 79.7	Leech fibula with circular insets	525-480 BCE	P-UNIPD	1950-1980	NO	NO	C	S	medium magnesian calcite
Piovego	P	22435862	Leech fibula with circular insets	525-480 BCE	P-UNIPD	1950-1980	YES	YES	C	S	No dec.
Piovego	P	22420153	Leech fibula with circular insets	525-480 BCE	P-UNIPD	1950-1980	YES	YES	C	S	high magnesian calcite
Piovego	P	5,73	Leech fibula with circular insets	525-480 BCE	P-UNIPD	1950-1980	NO	NO	C	S	*Corallium rubrum*
Piovego	P	153032, 22.7	Leech fibula with circular insets	525-480 BCE	P-UNIPD	1950-1980	NO	NO?	C	S	medium magnesian calcite
Piovego	P	149721, 29.5	Leech fibula with circular insets	525-480 BCE	P-UNIPD	1950-1980	NO	SI?	C	S	low magnesian calcite
Piovego	P	34914, 47.13	Leech fibula with circular insets	525-480 BCE	P-UNIPD	1950-1980	YES	YES	C	S	low magnesian calcite
Piovego	P	5,99	coral branch	6th-5th c. BCE	P-UNIPD	1950-1980	NO	NO	G	S	altered *Corallium rubrum*
Piovego	P	110,8	bucket pendant 1A	6th-5th c. BCE	P-UNIPD	1950-1980	YES	YES	O	S	low magnesian calcite
Piovego	P	108,7	Pendant	6th-5th c. BCE	P-UNIPD	1950-1980	NO	NO	G	S	medium magnesian calcite
Piovego	P	108,5	bucket pendant 1A	6th-5th c. BCE	P-UNIPD	1950-1980	NO	NO	O	S	low magnesian calcite

(Table 31 — continued)

Archaeological site	Macro-area	Inv. no.	Tipology	Chronology	Location	Year of excavation	Burnt	Restored	Decoration	Analysis	Interpretation
Piovego	P	95,11	LH-ornitomorphic	6th-5th c. BCE	P-UNIPD	1950-1980	YES?	NO	C	S	medium magnesian calcite
Piovego	P	149682, 25.23	Pendant	6th-5th c. BCE	P-UNIPD	1950-1980	NO	NO	G	S	altered *Corallium rubrum*
Piovego	P	95,1	grooming tool - tweezer	6th-5th c. BCE	P-UNIPD	1950-1980	NO	NO	L	S	aragonite
Piovego	P	95,1	grooming tool - scalpitorium	6th-5th c. BCE	P-UNIPD	1950-1980	NO	NO	C	S	low magnesian calcite
Piovego	P	86,3	bucket pendant 1A	6th-5th c. BCE	P-UNIPD	1950-1980	YES	YES	O	S	medium magnesian calcite
Piovego	P	110,13	Bead	6th-5th c. BCE	P-UNIPD	1950-1980	NO	NO	G	S	calcite
Pombia, loc. Monticello	G	72276-72277	Leech fibula with circular insets	525-480 BCE	MRT	1980-2000	NO	YES	C	D	calcite? + gypsum?
Pombia, loc. Monticello	G	83925	Leech fibula with circular insets	525-480 BCE	O-MCF	1980-2000	YES	YES	C	D	low magnesian calcite
Pombia, loc. Monticello	G	83937	Leech fibula with circular insets	525-480 BCE	O-MCF	1980-2000	YES	YES	C	D	low magnesian calcite
Pombia, loc. Monticello	G	83946	Leech fibula with circular insets	480-440 BCE	O-MCF	1980-2000	NO	YES	C	D	No dec.
Pombia, loc. Quara	G	83966	Leech fibula with circular insets	525-480 BCE	O-MCF	1980-2000	YES	YES	C	D	calcite
Ponte nelle Alpi-Casan	P	3366	Dragon-shaped fibula	late 5th c. BCE	B-MC	1900-1950	NO	NO	C	S	*Corallium rubrum*
Ponte nelle Alpi-Cugnan	P	3355	Leech fibula with circular insets	525-480 BCE	B-MC	1900-1950	NO	NO	C	S	low magnesian calcite
Pontecurone, loc. Cascina Torre	L	23.M380-9.6	Leech fibula with circular insets	525-480 BCE	MRT	2000-2024	NO	NO	C	D	medium magnesian calcite
Pontecurone, loc. Cascina Torre	L	RR24	grooming tool - tweezer	600-475 BCE	MRT	2000-2024	?	NO	L	S	No dec.
Rottofreno	W	259507	Leech fibula with circular insets	525-480 BCE	P-MAVT	2000-2024	NO	YES?	C	D	No dec.
Safforze	P	6602	Leech fibula with circular insets	525-480 BCE	B-MC	1900-1950	NO	NO	C	S	altered *Corallium rubrum*
Safforze	P	6600	Leech fibula with circular insets	525-480 BCE	B-MC	1900-1950	NO	NO	C	S	medium magnesian calcite
San Bernardino di Briona	G	868	Leech fibula with circular insets	525-480 BCE	N-MC	1900-1950	NO	NO	C	D	No dec.
San Bernardino di Briona	G	870	Leech fibula with circular insets	525-480 BCE	N-MC	1900-1950	NO	SI	C	D	low magnesian calcite
San Bernardino di Briona	G	NCT0100026405	Leech fibula with circular insets	525-480 BCE	MRT	1900-1950	NO	NO	C	D	medium magnesian calcite
San Bernardino di Briona	G	NCT0100026418	Leech fibula with circular insets	525-480 BCE	MRT	1900-1950	NO	NO	C	D	altered *Corallium rubrum* + gypsum + bone
San Bernardino di Briona	G	NCT0100026417	Leech fibula with circular insets	525-480 BCE	MRT	1900-1950	NO	NO	C	D	gypsum + bone
San Bernardino di Briona	G	NCT0100026415	Leech fibula with circular insets	525-480 BCE	MRT	1900-1950	NO	NO	C	D	No dec.
San Bernardino di Briona	G	23.M380-9.1	Leech fibula with circular insets	525-480 BCE	MRT	1900-1950	NO	NO	C	D	*Corallium rubrum*? + bone
San Bernardino di Briona	G	23.M380-9.2	Leech fibula with circular insets	525-480 BCE	MRT	1900-1950	NO	NO	C	D	altered *Corallium rubrum* + gypsum
San Bernardino di Briona	G	23.M380-9.7	bucket pendant 1A		MRT		NO	NO	O	D	medium magnesian calcite
Sesto Calende, asilo	G	12437	Leech fibula with circular insets	525-480 BCE	V-MC	1900-1950	NO	YES	C	S	calcite + bone + wax
Sesto Calende, asilo	G	12436	Leech fibula with circular insets	525-480 BCE	V-MC	1900-1950	NO	YES	C	S	calcite
Sesto Calende, Mulini Bellaria	G	23751	Leech fibula with circular insets	480-440 BCE	SC-MC	1950-1980	NO	YES	C	S	bone? + gypsum?
Sesto Calende, Mulini Bellaria	G	23752	Leech fibula with circular insets	480-440 BCE	SC-MC	1950-1980	NO	YES	C	S	altered *Corallium rubrum* + bone

(Table 31 — continued)

Archaeological site	Macro-area	Inv. no.	Tipology	Chronology	Location	Year of excavation	Burnt	Restored	Decoration	Analysis	Interpretation
Sesto Calende, via Moncenisio	G	172343	Longone pendant	7th c. BCE	SC-MC	1980-2000	NO	YES	G	S	low magnesian calcite
Sesto Calende, via Moncenisio	G	172344	coral branch	7th c. BCE	SC-MC	1980-2000	NO	YES	G	S	medium magnesian calcite
Sesto Calende, via Montrucco	G	4783	Longone pendant	7th c. BCE	SC-MC	1900-1950	NO	YES	G	S	low magnesian calcite
Unknown	U	A0.9.28550	Leech fibula with circular insets	525-480 BCE	M-MCA		NO	NO	C	I	-
Unknown	U	A0.9.35028	Leech fibula with circular insets	525-480 BCE	M-MCA		NO	NO	C	I	$CaCO_3$
Unknown	U	A0.9.35039	Leech fibula with circular insets	525-480 BCE	M-MCA		?	?	C	I	-
Unknown	U	A0.9.4916	Leech fibula with circular insets	525-480 BCE	M-MCA		YES	?	C	I	$CaCO_3$
Unknown	U	A0.9.28250	Leech fibula with circular insets	525-480 BCE	M-MCA		YES?	NO?	C	I	$CaCO_3$
Unknown	U	A0.9.28047	Leech fibula with circular insets	525-480 BCE	M-MCA		NO	YES?	C	I	calcite
Unknown	U	Bellini	Leech fibula with circular insets	525-480 BCE	SC-MC		NO	YES	C	S	low magnesian calcite
Unknown	G	M589/3	Leech fibula with circular insets	525-480 BCE	Bra	1950-1980	YES	YES	C	S	low magnesian calcite
Unknown	U	D2109	Pin with bead		C-MC	<1900	NO	NO	G	D	bone
Unknown	U	MV5924	amber	-	V-MC		NO	NO	G	S	No dec.
Unknown	U	MV5916	bead	-	V-MC		NO	NO	G	S	bone - deer's antler
Val Varaita, Sampeyre-Mandam	U	E17738	Navicella fibula	480-425 BCE	C-MC	<1900	NO	YES	O	D	No dec.
Villa del Foro	L	1000/E1	Leech fibula with circular insets	525-480 BCE	MRT		?	NO	C	S	medium magnesian calcite
Villa del Foro	L	SP 27	Leech fibula with circular insets	525-480 BCE	MRT	1980-2000	?	NO	C	S	*Corallium rubrum*
Villa del Foro	L	66132	Leech fibula with circular insets	525-480 BCE	MRT (TO)	1980-2000	NO	NO	C	D	high magnesian calcite
Villa del Foro	L	51877	Leech fibula with circular insets	525-480 BCE	MRT	1980-2000	YES	SI	C	S	low magnesian calcite
Villa del Foro	L	RS154	Leech fibula with circular insets	525-480 BCE	MRT	1980-2000	?	NO	C	S	No dec.
Villa del Foro	L	SP16	Leech fibula with circular insets	525-480 BCE	MRT	1980-2000	NO	NO	C	S	No dec.
Villa del Foro	L	SP28b	Leech fibula with circular insets	525-480 BCE	MRT	1980-2000	NO	NO	C	S	No dec.
Villa del Foro	L	51878	Leech fibula with circular insets	525-480 BCE	MRT	1980-2000	?	NO	C	S	calcite
Villa del Foro	L	SP 834 a	Leech fibula with circular insets	525-480 BCE	MRT	1980-2000	NO	NO	C	S	*Corallium rubrum*
Villa del Foro	L	SP 55	Leech fibula		MRT	1980-2000	?	NO	L	S	No dec.
Villa del Foro	L	SP 56a	Leech fibula	600-480 BCE	MRT	1980-2000	?	NO	L	S	No dec.
Villa del Foro	L	66131	Leech fibula	600-480 BCE	MRT	1980-2000	NO	NO	L	S	*Corallium rubrum*
Villa del Foro	L	RS/SP 134	Leech fibula	600-480 BCE	MRT	1980-2000	NO	NO	L	S	No dec.
Villa del Foro	L	RS 135	Leech fibula	600-480 BCE	MRT	1980-2000	NO	NO	L	S	No dec.
Villa del Foro	L	RS 160	Leech fibula	600-480 BCE	MRT	1980-2000	NO	NO	L	S	No dec.
Villa del Foro	L	RS/SP 72	Leech fibula		MRT	1980-2000	NO	NO	L	S	No dec.
Villa del Foro	L	RS 819	Leech fibula	6th-5th c. BCE	MRT	1980-2000	NO	NO	L	S	No dec.

(Table 31 — continued)

Villa del Foro	L	RS 822	Serpentine fibula	525-480 BCE	MRT	1980-2000	NO	NO	L	S	No dec.
Villa del Foro	L	SP 140 b	Leech fibula	600-480 BCE	MRT	1980-2000	NO	NO	L	S	No dec.
Villa del Foro	L	SP159	Fibula		MRT	1980-2000	NO	NO	L	S	No dec.
Villa del Foro	L	SP 16	Leech fibula		MRT	1980-2000	?	NO	L	S	No dec.
Villa del Foro	L	SP 217	Leech fibula	6th-5th c. BCE	MRT	2000-2024	?	NO	L	S	No dec.
Villa del Foro	L	SP 224	Leech fibula	6th-5th c. BCE	MRT	1980-2000	?	NO	L	S	No dec.
Villa del Foro	L	St66120; SP691	Navicella fibula	late 7th-6th c. BCE	MRT	1980-2000	NO	NO	L	S	No dec.
Villa del Foro	L	SP93	Fibula	525-480 BCE	MRT	1980-2000	?	NO	L	S	No dec.
Villa del Foro	L	SP 97	Leech fibula	600-480 BCE	MRT	1980-2000	NO	NO	L	S	No dec.
Villa del Foro	L	SP98	Leech fibula	600-480 BCE	MRT	1980-2000	NO	NO	L	S	No dec.
Villa del Foro, San Damiano	L	SP 23b	laminette	Roman	MRT	1980-2000	NO	NO	O	S	No dec.

(Table 31 — continued)

Archaeological site	**N. inv. stat.**	**Tipology**	**Museum**	**Results**
Bagnolo S. Vito - Forcello	99209	LH-Fußzierfibel	M-MN	malachite, cuprite?
Bellinzago Novarese, loc. Valle Briga	198	Leech fibula-circular	N-MC	apatite? brochantite?
Borgonovo V.T.	20.S258-2.118	Leech fibula-circular-foot	P-MAVT	Paraloid
Brembate sotto	67	Composite bow fibula	B-MA	malachite, apatite?
Castelletto Ticino	D2104	Leech fibula-circular	C-MC	malachite
Castelletto Ticino	23.M380-9.5	Leech fibula-circular	MRT	malachite
Castelletto Ticino	1063	grooming tool	N-MC	cassiterite
Castelletto Ticino, Bosco del Monte	CT29 B4D	Leech fibula-circular	CT-GSAC	malachite
Castelletto Ticino, Motto Falco	CT179	Longone pendant	CT-GSAC	malachite + cuprite
Castelletto Ticino-Vigevano?	944	Leech fibula-circular	N-MC	cassiterite
Castelletto Ticino-Vigevano?	947	Leech fibula-circular	N-MC	malachite
Castelletto Ticino-Vigevano?	949	Leech fibula-circular	N-MC	malachite
Como, Ca' Morta, Rebbio, loc. Ronchetti	1230	Composite bow fibula	C-MC	cuprite
Como, dintorni	E5552	Leech fibula-circular	C-MC	malachite
Como, dintorni	E5553	Leech fibula-circular	C-MC	malachite
Como, Prestino, via Isonzo	57216	Leech fibula-circular	C-MC	Paraloid
Como, Rebbio, Villa Giovio	E13225	Leech fibula-circular-foot	C-MC	cerussite
Golasecca	D2059	Leech fibula-circular	C-MC	cerussite
Parre, loc. Castello	40	Foliate-arch fibula	B-MA	beeswax
Parre, loc. Castello	46	Low-arch fibula	B-MA	malachite
Parre, loc. Castello	119	Navicella fibula	B-MA	malachite + non ident.

Table 32. μ-Raman analysis results on metal parts (the findings for which the analyses did not yield any results are not reported): alphabetically ordered according to the name of the archaeological site; 'location' column: see section 4.5.

Parre, loc. Castello	3564	Leech fibula-full-linear	B-MA	malachite
Parre, loc. Castello	3565	Leech fibula-full-linear	B-MA	malachite
Parre, loc. Castello	3569	Leech fibula-linear	B-MA	malachite
Pianello V.T.	18878	Triangolar pendant	P-MAVT	malachite
Pianello V.T.	201255	Leech fibula-circular-foot	P-MAVT	malachite
Pombia, loc. Monticello	72276-72277	Leech fibula-circular	MRT	malachite + beeswax
Pombia, loc. Monticello	83925	Leech fibula-circular	O-MCF	malachite
Pombia, loc. Monticello	83937	Leech fibula-circular-foot	O-MCF	malachite
Pombia, loc. Monticello	83946	Leech fibula-circular	O-MCF	malachite + apatite?

(Table 32 — continued)

Archaeological site	Inv. no.	Type	Location	Analysis type	unattributed d (Å)	malachite	pseudomalachite	azurite	cuprite	atacamite	partacamite	Mcguinnessite	tenorite	cerussite	pyromorphite	caracolite	teallite	cassiterite	burtite	tennantite	Mckinstryite	Silver	copper	bronze
BagnoloS.Vito-Forcello	1060	Raw	M-MN	D																				
BagnoloS.Vito-Forcello	98798	Raw	M-MN	D																				
BagnoloS.Vito-Forcello	99209	LH	M-MN	D						w							h							
BagnoloS.Vito-Forcello	99210	LH	M-MN	D																				?
BagnoloS.Vito-Forcello	99211	LH	M-MN	D	5,51																			
BagnoloS.Vito-Forcello	145782	Bucket-P	M-MN	D	5,51									w										
BagnoloS.Vito-Forcello	145959	LH	M-MN	D	5,47									w		?								
BagnoloS.Vito-Forcello	98797	Raw	M-MN	D	5,46																			
BagnoloS.Vito-Forcello	98799	Raw	M-MN	D																				
BagnoloS.Vito-Forcello	RR 1272	LH	M-MN	D	2,98																			?
BagnoloS.Vito-Forcello	RR 745	Bucket-P	M-MN	D																			?	
Brembate sotto	65	Leech-T	B-MA	D	5,57													w						m
Brembate sotto	67	Comp	B-MA	D																				
Brembate sotto	3016	Pend	B-MA	D																				
Brembate sotto	3051	Comp	B-MA	D	2.90, 3.58																			
Brembate sotto	3052	Comp	B-MA	D																				
Brignano Frascata	C-FR-NE/1	Leech-C	MRT	S																				
Brignano Frascata	C-FR-NE/2	Leech-C	MRT	S																				
Brignano Frascata	C-FR-NE/3	Leech-C	MRT	S		m																		

Table 33. XRD results (only bronze alteration products; see section 7.2.3) for the 141 analysed artefacts (direct and μ-sampling approach): alphabetically ordered according to the name of the archaeological site; ‘type’ column: bucket-P = bucket pendants; comp = composite bow fibula; groom = grooming tools; leech-C = leech fibula with circular decoration; pend = pendant and Longone al Segrino pendants; raw = raw coral branches; ‘location’ column: see section 4.5; ‘Decoration’ column = ‘G’ = General, ‘C’ = circular, ‘L’ = linear, ‘T’ =transversal grooves, ‘O’ = ‘occhio di dado’; ‘Analysis’ column: ‘I’ = in situ, ‘D’ = direct, ‘S’ = sampled; reflex intensity: ‘h’ = high; ‘m’ =medium; ‘w’ = weak; ‘?’ = doubt.

Archaeological site	Inv. no.	Type	Location	Analysis type	unattributed d (Å)	malachite	pseudomalachite	azurite	cuprite	atacamite	partacamite	Mcguinnessite	tenorite	cerussite	pyromorphite	caracolite	teallite	cassiterite	burtite	tennantite	Mckinstryite	Silver	copper	bronze
Brignano Frascata	C-FR-S/2	Leech-L	MRT	S		w												w						
Castelletto Ticino	D1750	Pend	C-MC	D																				
Castelletto Ticino	D2073	Leech-C	C-MC	D	2.6, 5.55															w				
Castelletto Ticino	D2077	Leech-C	C-MC	D													w							
Castelletto Ticino	D2104	Leech-C	C-MC	D	5,46																			
Castelletto Ticino	D2773	Leech-C	C-MC	D		h																		
Castelletto Ticino	2140	Leech-C	MRT	S		m																		
Castelletto Ticino	2153	Leech-C	MRT	S																				
Castello di Annone	23.M380-9.4	Leech-C	MRT	D																				
Chiomonte	74795	LaTène	MRT	D	3.379, 6.02								?											
Chiomonte	74794	LaTène	MRT	D																				
Como, Ca’ Morta	1397	Comp	C-MC	D																				
Como, Ca’ Morta	2206	Leech-C	C-MC	D	5,51	h																		
Como, Ca’ Morta	1993	Comp	C-MC	D																				
Como, Ca’ Morta	124133	Other	C-MC	D																				
Como, Ca’ Morta	139651	Leech-C	C-MC	D		h																		
Como, Ca’ Morta	139652	Leech-C	C-MC	D		m																		
Como, Ca’ Morta	879	Leech-C	C-MC	D	5,53																			
Como, Ca’ Morta	124142	Pend	C-MC	D																				
Como, Ca’ Morta	865	Other	C-MC	D																				
Como, Ca’ Morta	1230	Comp	C-MC	D	2.00, 5.55																			
Como, Ca’ Morta	E5868	Leech-C	C-MC	D																				
Como, Ca’ Morta	E5873	Leech-C	C-MC	D	1.45, 1.48, 1.50, 1.54, 1.56, 1.59, 1.64, 1.87																			
Como, Ca’ Morta	33593	Pend	C-MC	D																				
Como, Ca’ Morta	33594	Pend	C-MC	D																				
Como, Ca’ Morta	E13273	Comp	C-MC	D	3.51, 4.27, 5.10, 6.04												?							
Como, dintorni	E5552	Leech-C	C-MC	D	5.47, 11.50																			
Como, dintorni	E5553	Leech-C	C-MC	D	5,49	w								m										
Como, dintorni	E5667	Leech-C	C-MC	D	4.15, 5.54																			
Como, via Isonzo	57210	Leech-C	C-MC	D	3,2										m									
Como, via Isonzo	57216	Leech-C	C-MC	D																				

(Table 33 — continued)

Archaeological site	Inv. no.	Type	Location	Analysis type	unattributed d (Å)	malachite	pseudomalachite	azurite	cuprite	atacamite	partacamite	Mcguinnessite	tenorite	cerussite	pyromorphite	caracolite	teallite	cassiterite	burtite	tennantite	Mckinstryite	Silver	copper	bronze
Como, via Isonzo	57220	Leech-C	C-MC	D	5,51																			
Como, via Isonzo	57244	Leech-C	C-MC	D	5,46	m		m						w										
Como, via Isonzo	57250	Leech-C	C-MC	D	5,62			m	w															
Como, via Isonzo	57262	Leech-C	C-MC	D	5,51	w		m	w					w	w									
Como, Villa Giovio	E13225	Leech-C	C-MC	D																				
Como, Respaù	E5957	Comp	C-MC	D	5,55												w				?	?		
Como, Respaù	E5958	Comp	C-MC	D													w							
Golasecca	D1660	Groom	C-MC	D	5,55	m												m						
Golasecca	D1668	Pend	C-MC	D																				
Golasecca	D1669	Pend	C-MC	D	5,47																			
Golasecca	D2049	Leech-C	C-MC	D	5,48	m							m				w	m		m				
Golasecca	D2059	Leech-C	C-MC	D	1.54, 2.47, 2.53, 3.69, 5.02, 11.5	w			h		m	?												
Golasecca	D2064	Leech-C	C-MC	D	3.37, 4.33, 5.57								w											
Golasecca	D2065	Leech-C	C-MC	D	5.56, 9.68																			
Golasecca	MV103	Pend	V-MC	S																				
Golasecca	MV4062	Leech-C	V-MC	S													?							
Golasecca, Galliasco	22.S288-1.205	Leech-C	SABAP	S																				
Golasecca, Monsorino	63413	Leech-C	V-MC	S																				
Gropello Cairoli	19/108	Leech-L	MANL	D	2.97, 5.59																			
Gropello Cairoli	19/109	Leech-L	MANL	D	5,61																			
Gropello Cairoli	19/110	Leech-L	MANL	D	5,51															?				
Gropello Cairoli	19/111	Leech-L	MANL	D	5,53		?																	
Gropello Cairoli	19/112	Leech-C	MANL	D	5,44																			
Gropello Cairoli	19/114	Leech-L	MANL	D	2,95													h						
Gropello Cairoli	19/115	Leech-L	MANL	D	1.76, 2.30, 4.66																			
Gropello Cairoli	19/117	Groom	MANL	D	1.67, 1.75, 2.49																			
Gropello Cairoli	21/178	Leech-L	MANL	D																				
Gropello Cairoli	21/179	Leech-L	MANL	D	2.10, 4.20													?						
Gropello Cairoli	21/180	Leech-L	MANL	D																				
Gropello Cairoli	21/181	Leech-L	MANL	D														m						
Malgesso	MV4025	Leech-C	V-MC	S	2.61, 2.89, 3.69																			
Mantova	169519	Leech-C	M-MN	D												?								

(Table 33 — continued)

Archaeological site	Inv. no.	Type	Location	Analysis type	unattributed d (Å)	malachite	pseudomalachite	azurite	cuprite	atacamite	partacamite	Mcguinnessite	tenorite	cerussite	pyromorphite	caracolite	teallite	cassiterite	burtite	tennantite	Mckinstryite	Silver	copper	bronze
Parre, loc. Castello	9	Leech-L	B-MA	D	3.03, 3.31, 4.12, 5.47																			h
Parre, loc. Castello	40	other	B-MA	D	5,49	m			m															
Parre, loc. Castello	41	Other	B-MA	D	5,49	m													?					m
Parre, loc. Castello	45	Other	B-MA	D																				h
Parre, loc. Castello	46	Other	B-MA	D	4,09				h															
Parre, loc. Castello	48	Navic	B-MA	D	2.47, 4.13																			w
Parre, loc. Castello	49	Navic	B-MA	D	4,09	m		m																h
Parre, loc. Castello	119	Navic	B-MA	D	5,47	w			h															
Parre, loc. Castello	128	Other	B-MA	D	5.45, 9.25																			h
Parre, loc. Castello	3002	Other	B-MA	D	5,47	h			h															h
Parre, loc. Castello	3564	Leech-L	B-MA	D	5,45	m			m															
Parre, loc. Castello	3565	Leech-L	B-MA	D	2.83, 5.47								m				?							
Parre, loc. Castello	3569	Leech-L	B-MA	D		m			m															
Pombia	72276-7	Leech-C	MRT	D	1.76, 2.36, 2.63								m											
Pontecurone	RR24	Groom	MRT	S		w																		
S. Bernardino Briona	1524	Leech-C	MRT	D	2.37, 2.61,3.72, 4.76																			
S. Bernardino Briona	1567	Leech-C	MRT	D																				
S. Bernardino Briona	1514	Leech-C	MRT	D	3.67, 5.03, 5.98																			
S. Bernardino Briona	23.M380-9.1	Leech-C	MRT	D	2,96																			
Sesto Calende, asilo	12437	Leech-C	V-MC	S																				
Sesto Calende, asilo	12436	Leech-C	V-MC	S																				
Sesto Calende, Bellaria	23751	Leech-C	SC-MC	S	4.31, 6.81												?							
Sesto Calende, Bellaria	23752	Leech-C	SC-MC	S																				
Sesto Calende	172343	Pend	SC-MC	S																				
Sesto Calende	172344	Raw	SC-MC	S	6.41, 10.99																			
Sesto Calende	4783	Pend	SC-MC	S																				
Unknown	M589/3	Leech-C	Bra	S																				
Unknown	D2109	Other	C-MC	D	5,56																			
Unknown	bellini	Leech-C	SC-MC	S																				
Unknown	MV5924	Other	V-MC	S																				
Unknown	MV5916	Bead	V-MC	S																				
Val Varaita	E17738	Navic	C-MC	D																				
Villa del Foro	1000/E1	Leech-C	MRT	S																				

(Table 33 — continued)

Archaeological site	Inv. no.	Type	Location	Analysis type	unattributed d (Å)	malachite	pseudomalachite	azurite	cuprite	atacamite	partacamite	Mcguinnessite	tenorite	cerussite	pyromorphite	caracolite	teallite	cassiterite	burtite	tennantite	Mckinstryite	Silver	copper	bronze
Villa del Foro	SP 55	Leech-L	MRT	S																				
Villa del Foro	SP 56a	Leech-L	MRT	S									w					w						
Villa del Foro	SP 27	Leech-C	MRT	S																				
Villa del Foro	66132	Leech-C	MRT	S																				
Villa del Foro	66132	Leech-C	MRT	D	1.42, 1.86, 2.57, 3.29, 4.55												?							
Villa del Foro	66131	Leech-L	MRT	S																				
Villa del Foro	51877	Leech-C	MRT	S																				
Villa del Foro	RS154	Leech-C	MRT	S		w												w						
Villa del Foro	RS/SP 134	Leech-L	MRT	S	1.98, 3.53																			
Villa del Foro	RS 135	Leech-L	MRT	S																				
Villa del Foro	RS 160	Leech-L	MRT	S																				
Villa del Foro	RS/SP 72	Leech-L	MRT	S																				
Villa del Foro	RS 819	Leech-L	MRT	S																				
Villa del Foro	RS 822	Other	MRT	S														w						
Villa del Foro	SP 140 b	Leech-L	MRT	S														?						
Villa del Foro	SP159	Leech-L	MRT	S																				
Villa del Foro	SP 16	Leech-L	MRT	S														w						
Villa del Foro	SP16	Leech-C	MRT	S		w																		
Villa del Foro	SP 217	Leech-L	MRT	S									w											
Villa del Foro	SP 224	Leech-L	MRT	S									w					m						
Villa del Foro	SP28b	Leech-C	MRT	S									h					w						
Villa del Foro	St66120	Navic	MRT	S																				
Villa del Foro	51878	Leech-C	MRT	S									m											
Villa del Foro	SP 834 a	Leech-C	MRT	S		m																		
Villa del Foro	SP93	Leech-L	MRT	S														w						
Villa del Foro	SP 97	Leech-L	MRT	S	2,16																			
Villa del Foro	SP98	Leech-L	MRT	S	1,46																			
Villa del Foro	SP 23b	Other	MRT	S	1,72				m															

(Table 33 — continued)

Type	No.	Sn wt%			Pb wt%			Trace elem.
		Min.	Max.	Average	Min.	Max.	Average	
Longone pendants	8	0,00	3,00	0,78	0,00	0,00	0,00	
Composite fibulae	4	0,00	4,00	0,98	0,00	0,00	0,00	
Arch fibulae	5	5,00	29,00	14,00	0,00	0,64	0,13	Ni
La Tène fibulae	2	25,00	45,00	35,00	0,00	0,00	0,00	As
Leech fibulae pin	4	0,00	12,00	5,00	0,00	0,00	0,00	

Table 34. Sn and Pb wt % in artefacts requiring post-casting working.

Type	No.	Sn wt%			Pb wt%			Trace elem.
		Min.	Max.	Average	Min.	Max.	Average	
Bucket pendant	3	16,00	27,00	22,00	8,00	40,00	19,00	Ni, As, Ag
Grooming tool	3	0,00	23,00	11,00	0,00	12,00	4,00	
Leech-core-C	57	0,00	40,00	14,00	0,00	60,00	14,00	Zn, As, Ag, Sb
Leech-core-L	10	11,00	42,00	26,00	0,00	29,00	11,00	Zn, As
Leech-full-C	5	5,00	18,00	13,00	0,00	19,00	4,00	Ag
Leech-full-L	5	<1	19,00	11,00	0,00	28,00	9,00	Zn, Ag
LH-fibulae	7	4,00	24,00	18,00	5,00	21,00	14,00	As
Navicella fibulae	3	3,00	18,00	9,50	<1	<1	<1	

Table 35. Sn and Pb wt % in cast-finished artefacts [‘Leech-core’ = leech fibulae with terracotta core; ‘leech full’ = leech fibula with full arch; ‘C’ = circular decoration; ‘L’ = linear decoration].

		Etruria Padana	Golasecca	Liguria Interna	Western Po valley
Ni	Min.	0	0	0	0
	Max.	0,13	4,37	0	0
	Average	0,02	0,15	0	0
Zn	Min.	0	0	0	0
	Max.	0,21	3,16	0	0,41
	Average	0,03	0,04	0	0,05
As	Min.	0	0	0,21	0
	Max.	1,96	6,23	0,34	1,73
	Average	0,36	0,31	0,3	0,32
Ag	Min.	0	0	0	0
	Max.	0,46	17,11	0	0,59
	Average	0,06	0,33	0	0,1
Sb	Min.	0	0	0	0
	Max.	0	4,34	0	0
	Average	0	0,05	0	0

Table 36. Ni, Zn, As, Ag, Sb wt% in relation to main geographical-cultural areas.

Site	Inv. no.	Type	Burnt	Cu	Sn	Pb	Ni	Zn	As	Ag	Sb	Na	Mg	Al	Si	P	S	Cl	K	Ca	Ti	Cr	Mn	Fe	O
BagnoloS.Vito-Forcello	145782	bucket pendant 1A	NO	13,14	15,72	40,23	0,00	0,00	0,37	0,00	0,00	0,00	0,18	1,03	2,15	3,20	0,00	1,07	0,00	2,77	0,50	0,00	0,00	0,00	19,64
BagnoloS.Vito-Forcello	RR 745	bucket pendant 1B	NO	19,83	23,79	8,07	0,13	0,00	1,96	0,46	0,00	0,00	0,39	1,62	4,32	4,74	0,00	0,53	0,00	5,10	1,24	0,00	0,00	0,00	27,85
BagnoloS.Vito-Forcello	99210	LH-Fußzierfibel	NO	17,60	18,87	12,39	0,00	0,00	0,18	0,00	0,00	0,00	0,85	1,64	5,78	5,86	0,89	0,09	0,00	4,17	1,55	0,00	0,00	0,00	30,13
BagnoloS.Vito-Forcello	RR1272	LH-Fußzierfibel	NO	12,86	19,11	9,50	0,00	0,00	0,00	0,00	0,00	0,00	0,59	1,22	2,49	7,60	0,00	0,20	0,13	8,08	9,10	0,00	0,00	0,00	29,11
BagnoloS.Vito-Forcello	99209	LH-Fußzierfibel	NO	15,45	21,62	19,67	0,00	0,00	0,33	0,00	0,00	0,00	0,46	2,36	5,20	2,87	0,00	0,38	0,00	2,45	3,78	0,00	0,00	0,00	25,44
BagnoloS.Vito-Forcello	145959	LH-Fußzierfibel	NO	26,49	3,82	4,85	0,00	0,00	0,00	0,00	0,00	0,00	1,21	2,50	13,33	3,12	0,29	0,38	0,14	7,02	2,58	0,00	0,00	0,00	34,30
BagnoloS.Vito-Forcello	99211	LH -ornitomorphic	NO	14,17	17,18	11,25	0,00	0,00	0,00	0,00	0,00	0,00	1,15	3,48	8,73	3,83	0,43	0,42	0,00	4,81	3,28	0,00	0,00	0,00	31,31
Bellinzago Novarese	197	Leech fibula-circular	NO	14,24	36,45	14,80	0,00	0,00	0,06	0,00	0,00	0,09	0,58	0,72	1,55	3,20	0,60	0,87	0,00	0,95	0,00	0,00	0,00	0,14	25,75
Bellinzago Novarese	198	Leech fibula-circular	NO	19,32	26,98	17,33	0,00	0,00	1,04	0,00	0,00	0,00	0,25	0,68	2,49	3,61	0,07	0,95	0,00	2,39	0,05	0,00	0,00	1,29	23,55
Borgonovo V.T.	20.S258-2.118	Leech fibula-circular-foot	NO	20,38	25,02	16,45	0,00	0,00	1,73	0,59	0,00	0,00	0,00	1,23	5,33	2,23	0,00	0,00	0,00	1,46	0,00	0,00	0,00	0,95	24,64
Borgonovo V.T.	20.S258-2.119	Leech fibula-circular-foot	NO	16,40	13,66	27,82	0,00	0,00	0,14	0,00	0,00	0,00	0,26	1,78	6,19	3,31	0,00	0,51	0,42	2,28	0,02	0,14	0,00	2,28	24,79
Borgonovo V.T.	20.S258-2.171	Leech fibula-circular-foot	YES?	22,46	21,55	18,93	0,00	0,00	0,20	0,27	0,00	0,00	0,25	1,88	5,74	1,29	0,00	0,26	1,94	0,00	0,00	0,00	0,00	1,13	24,14
Borgonovo V.T.	20.S258-2.172	Leech fibula-circular-foot	YES?	19,37	19,05	16,75	0,00	0,00	0,00	0,00	0,00	0,00	0,54	2,40	7,93	1,60	0,00	0,47	0,10	2,47	0,00	0,00	0,00	2,65	26,67
Brembate sotto	65	Leech fibula-transverse	NO	29,82	24,42	17,70	0,00	0,00	0,00	0,00	0,00	0,00	0,82	0,67	2,46	0,38	0,50	0,89	0,00	0,61	0,00	0,00	0,00	0,66	21,07
Brembate sotto	67	Composite bow fibula	NO	64,42	0,00	0,00	0,00	0,00	0,00	0,00	0,00	0,00	0,38	0,47	2,98	0,45	2,61	0,16	0,06	2,45	0,00	0,00	0,00	0,20	25,82
Castelletto Ticino	D1750	Longone pendant	NO	51,87	0,00	0,00	0,00	0,00	0,00	0,00	0,00	0,00	0,00	2,27	11,89	0,00	0,95	0,00	0,00	2,13	0,00	0,00	0,00	0,00	30,89
Castelletto Ticino	D2073	Leech fibula-circular	YES	30,29	0,81	22,36	0,00	0,00	0,00	0,00	0,00	0,00	0,09	0,82	8,53	5,52	0,00	0,30	0,00	2,41	0,00	0,00	0,07	0,49	28,32
Castelletto Ticino	D2077	Leech fibula-full-circular	NO	38,07	5,11	19,31	0,00	0,00	0,00	0,00	0,00	0,00	0,38	1,48	2,08	5,01	0,90	0,64	0,21	1,60	0,00	0,00	0,00	0,26	24,96
Castelletto Ticino	D2077	Leech-pin	NO	61,35	0,00	0,00	0,00	0,00	0,00	0,00	0,00	0,00	0,00	0,00	2,49	1,50	0,00	1,37	1,30	8,23	0,00	0,00	0,00	0,00	23,77
Site	**Inv. no.**	**Type**	**Burnt**	**Cu**	**Sn**	**Pb**	**Ni**	**Zn**	**As**	**Ag**	**Sb**	**Na**	**Mg**	**Al**	**Si**	**P**	**S**	**Cl**	**K**	**Ca**	**Ti**	**Cr**	**Mn**	**Fe**	**O**
Castelletto Ticino	D2104	Leech fibula-circular	NO	38,93	5,24	3,56	0,00	0,00	0,00	0,00	0,00	0,00	0,15	0,93	8,43	2,17	5,10	0,59	0,08	1,50	0,20	0,00	0,00	0,00	33,13
Castelletto Ticino	D2773	Leech fibula-circular	NO	42,87	16,07	0,00	0,00	0,00	0,39	0,59	0,00	0,00	0,84	0,11	2,54	0,00	6,42	0,72	0,82	0,00	0,00	0,00	0,00	0,00	28,62
Castelletto Ticino	23.M380-9.5	Leech fibula-circular	YES	49,05	7,35	14,68	0,00	0,00	0,00	0,00	0,00	0,00	0,35	1,14	2,70	0,37	0,37	0,00	0,00	1,69	0,00	0,00	0,00	0,64	21,67
Castelletto Ticino	2140	Leech fibula-circular	NO	32,31	21,96	6,62	0,00	0,00	0,00	0,00	0,00	0,00	1,55	1,41	4,24	2,03	0,00	0,51	0,00	2,07	0,00	0,00	0,00	1,71	25,61
Castelletto Ticino	91374, CT824	Longone pendant	NO	70,44	0,00	0,00	0,00	0,00	0,00	0,00	0,00	0,00	0,00	0,00	2,37	2,04	0,00	1,12	0,00	0,70	0,00	0,00	0,00	0,00	23,34
Castelletto Ticino	CT1144	Leech fibula-circular	NO	39,80	20,08	0,00	0,00	0,00	0,11	0,49	0,00	0,00	0,21	1,47	6,14	1,46	0,99	0,04	0,00	1,11	0,00	0,00	0,00	0,26	27,83
Castelletto Ticino	CT1144	Leech-pin	NO	40,85	0,53	0,00	0,00	0,00	0,00	0,00	0,00	0,00	0,00	5,37	13,55	1,41	1,15	0,15	0,00	2,03	0,00	0,00	0,00	0,00	34,98
Castelletto Ticino	1063	grooming tool	NO	23,62	23,30	3,67	0,00	0,00	0,00	0,00	0,00	0,39	0,56	3,01	1,65	6,17	2,24	0,46	0,34	3,04	0,00	0,00	0,00	1,08	30,48
Castelletto Ticino	CT29	Leech fibula-circular	YES	24,54	23,28	0,00	0,00	0,00	0,00	0,00	0,00	0,00	0,00	8,04	10,41	0,37	0,00	0,00	0,00	1,01	0,00	0,00	0,00	0,00	32,35
Castelletto Ticino	CT164	Longone pendant	NO	42,65	0,39	0,00	0,00	0,00	0,00	0,00	0,00	0,00	0,30	1,11	14,12	1,70	0,00	0,00	0,00	6,53	0,00	0,00	0,00	0,24	32,98
Castelletto Ticino	CT179	Longone pendant	NO	71,43	0,00	0,00	0,00	0,00	0,00	0,00	0,00	0,00	0,00	1,36	2,49	0,91	0,00	0,00	0,00	0,44	0,00	0,00	0,00	0,00	23,38
Castelletto Ticino	CT728	Leech fibula-circular	?	39,68	0,00	9,13	0,00	0,00	0,00	0,00	0,00	0,00	0,45	1,96	7,09	6,79	0,55	0,41	0,22	1,61	0,00	0,00	0,06	0,60	28,81
Castelletto Ticino	23.M380-9.3	Leech fibula-transverse	NO	11,95	19,94	20,74	0,00	0,00	0,18	0,00	0,00	0,00	0,24	9,26	1,06	7,04	0,00	0,00	0,00	0,00	0,00	0,00	0,00	0,69	28,92
Castelletto Ticino-Vigevano?	944	Leech fibula-circular	YES?	24,12	24,89	13,44	0,00	0,00	0,08	0,00	0,00	0,00	0,64	3,77	3,76	3,32	1,41	0,08	0,57	2,67	0,00	0,00	0,00	1,26	19,99
Castelletto Ticino-Vigevano?	946	Leech fibula-circular	YES	28,82	0,58	0,00	0,00	0,00	0,00	0,00	0,00	0,00	0,86	3,78	12,77	1,70	4,05	0,26	0,36	7,29	0,00	0,00	0,00	1,85	37,68
Castelletto Ticino-Vigevano?	947	Leech fibula-circular	NO	29,09	0,00	26,26	0,00	0,00	0,00	0,00	0,00	0,00	1,28	2,00	6,45	1,17	1,81	0,11	0,14	4,81	0,00	0,00	0,00	1,09	25,79
Castelletto Ticino-Vigevano?	949	Leech fibula-circular	YES	39,48	4,16	0,00	0,00	0,00	0,00	0,00	0,00	0,00	0,90	2,24	10,23	0,53	1,75	0,00	0,20	6,94	0,00	0,00	0,00	1,68	31,90
Castello di Annone	23.M380-9.4	Leech fibula-circular-foot	NO	8,43	14,15	26,80	0,00	0,00	0,34	0,00	0,00	0,00	0,50	2,72	6,45	5,18	0,00	0,96	0,42	4,04	0,00	0,00	0,00	2,66	27,36

Table 37. SEM-EDS analysis results on metal parts, expressed as wt%: alphabetically ordered according to the name of the archaeological site.

Site	Inv. no.	Type	Burnt	Cu	Sn	Pb	Ni	Zn	As	Ag	Sb	Na	Mg	Al	Si	P	S	Cl	K	Ca	Ti	Cr	Mn	Fe	O
Chiomonte, La Maddalena	74795	folded-foot fibula	NO	25,84	25,12	0,00	0,00	0,00	0,00	0,00	0,00	0,00	0,00	2,26	6,92	2,59	1,28	0,20	0,00	2,57	0,00	0,00	0,00	2,94	30,29
Chiomonte, La Maddalena	74794	folded-foot fibula	NO	22,81	44,86	0,00	0,00	0,00	0,26	0,00	0,00	0,00	0,00	0,73	2,43	2,24	0,00	0,00	0,00	0,00	0,00	0,00	0,00	1,90	24,77
Como, Ca' Morta	2206	Leech fibula-full-circular	NO	13,45	14,44	0,59	0,00	0,00	0,00	5,65	0,00	0,00	0,24	1,99	5,09	0,76	9,62	0,30	0,00	10,68	0,07	0,00	0,00	1,51	35,60
Como, Ca' Morta	2208	Leech fibula-full-circular	NO	15,65	15,43	0,00	0,00	0,00	0,00	17,11	0,00	0,00	0,64	2,47	5,12	0,73	7,66	0,89	0,00	1,46	0,00	0,00	0,00	1,57	31,26
Como, Ca' Morta	1993	Composite bow fibula	?	35,62	3,79	0,00	0,00	0,00	0,00	0,00	0,00	0,00	1,27	5,00	9,42	3,12	0,95	0,29	0,00	4,99	0,00	0,00	0,00	1,59	33,96
Como, Ca' Morta	114084	Leech fibula-full-circular	YES	42,58	18,25	0,92	0,00	0,00	0,00	0,00	0,00	0,00	0,49	0,57	4,98	0,79	0,18	0,00	0,00	5,53	0,00	0,00	0,00	0,00	25,71
Como, Ca' Morta	139651	Leech fibula-circular	NO	40,89	22,30	2,43	0,00	0,00	0,20	0,00	0,00	0,00	0,33	2,24	4,98	0,46	0,00	0,00	0,13	0,00	0,00	0,00	0,00	0,76	25,28
Como, Ca' Morta	139652	Leech fibula-circular	NO	54,64	0,00	0,00	0,00	0,00	0,00	0,00	0,00	0,00	1,17	4,19	7,80	0,53	0,00	0,00	0,14	0,67	0,00	0,00	0,00	1,63	28,73
Como, Ca' Morta	879	Leech fibula-circular	NO	28,37	19,35	2,25	0,00	0,00	0,16	0,00	0,00	0,00	0,82	2,23	7,96	1,54	1,93	0,14	0,01	2,74	0,02	0,00	0,00	1,80	30,67
Como, Ca' Morta	879	Leech-pin	NO	42,06	12,25	0,00	0,00	0,00	0,00	0,00	0,00	0,00	1,14	2,04	5,97	0,67	2,80	0,43	0,27	1,70	0,00	0,04	0,00	1,22	29,42
Como, Ca' Morta	124142	Longone pendant	NO	63,39	0,00	0,00	0,00	0,00	0,00	0,00	0,00	0,00	0,69	2,57	4,42	0,78	0,00	0,00	0,31	1,40	0,00	0,00	0,00	0,82	25,61
Como, Ca' Morta	864	Leech fibula-occhio di dado	NO	23,46	38,31	0,00	0,00	0,00	0,00	0,00	0,00	0,00	0,28	3,24	4,67	0,90	0,82	0,00	0,00	0,00	0,00	0,00	0,00	1,05	27,30
Como, Ca' Morta	865	Leech fibula-occhio di dado	NO	24,74	40,22	3,51	0,00	0,00	0,60	0,00	0,00	0,00	0,12	1,80	3,01	0,79	0,17	0,00	0,00	0,29	0,00	0,08	0,00	0,48	24,20
Como, Ca' Morta	1230	Composite bow fibula	NO	47,56	1,12	0,00	0,00	0,00	0,00	0,00	0,00	0,00	0,61	0,83	12,72	0,88	1,58	0,03	0,00	1,90	0,00	0,00	0,00	0,43	32,31
Como, Ca' Morta	E5868	Leech fibula-circular	NO	21,61	13,34	14,59	0,00	0,00	0,24	0,00	0,00	0,00	0,65	2,83	2,99	6,84	0,17	0,69	0,29	2,38	0,00	0,00	0,00	5,21	28,17
Como, Ca' Morta	E5873	Leech fibula-circular-foot	NO	4,95	0,00	59,69	0,00	0,00	0,00	0,00	0,00	0,00	0,00	1,71	1,71	6,88	0,00	2,36	0,00	1,86	0,00	0,00	0,00	1,47	19,37
Como, Ca' Morta	E5865	Leech fibula-circular	NO	49,57	7,07	1,39	0,00	0,00	0,13	0,00	0,00	0,54	0,22	0,87	6,14	0,88	0,48	0,60	0,28	4,21	0,33	0,00	0,00	0,66	26,64
Como, Ca' Morta	33593	Longone pendant	NO	50,10	3,38	0,00	0,00	0,00	0,00	0,00	0,00	0,00	0,00	0,00	0,00	0,00	12,77	1,11	0,00	0,00	0,00	0,00	0,00	0,00	32,64
Como, Ca' Morta	33594	Longone pendant	NO	42,94	2,50	0,00	1,36	0,00	0,00	0,00	0,00	0,00	0,17	0,75	2,53	6,04	4,14	1,08	0,07	5,17	0,00	0,00	0,00	1,28	31,97
Como, dintorni	E5552	Leech fibula-circular	NO	34,87	13,18	10,78	0,00	0,00	6,23	1,13	0,00	0,00	0,00	0,95	2,79	0,67	2,22	0,44	0,00	0,00	0,00	0,00	0,00	2,58	24,18
Como, dintorni	E5553	Leech fibula-circular	NO	32,53	1,99	20,20	0,00	0,00	0,00	0,00	0,00	0,00	0,53	2,47	11,25	0,19	0,57	0,00	0,00	1,36	0,00	0,00	0,00	1,25	27,66
Como, dintorni	E5667	Leech fibula-circular	NO	35,25	11,23	7,01	0,00	0,00	0,61	0,00	0,00	0,00	0,90	3,25	7,65	0,00	1,27	0,00	0,73	1,65	0,00	0,00	0,00	2,26	28,20
Como, via Isonzo	57210	Leech fibula-circular	yes?	14,20	18,23	26,30	0,00	0,00	1,12	0,00	0,00	0,00	0,33	3,36	3,76	4,37	0,00	0,60	0,16	0,47	0,05	0,00	0,00	2,14	24,89
Como, via Isonzo	57216	Leech fibula-circular	yes?	38,22	7,40	6,66	0,28	0,00	1,81	0,00	4,34	0,00	0,32	3,92	2,79	5,10	0,00	0,32	0,00	0,51	0,00	0,00	0,00	0,81	27,53
Como, via Isonzo	57220	Leech fibula-circular	yes?	26,71	29,17	12,88	0,00	0,00	1,34	0,00	0,00	0,00	0,00	1,36	1,59	3,17	0,00	0,21	0,00	0,00	0,00	0,00	0,00	0,36	23,23
Como, via Isonzo	57244	Leech fibula-circular	yes?	19,50	0,00	0,38	0,00	0,00	0,00	0,00	0,00	1,14	2,35	6,56	4,78	0,71	2,82	0,55	0,60	1,63	0,00	0,00	0,00	0,77	58,20
Como, via Isonzo	57250	Leech fibula-circular	yes?	48,11	4,46	6,91	0,00	0,00	0,00	0,00	0,00	0,00	0,70	0,27	3,46	0,49	1,83	0,32	0,00	1,70	0,00	0,00	0,00	7,19	24,60
Como, via Isonzo	57262	Leech fibula-circular	yes?	14,18	4,99	48,43	0,00	0,00	0,00	0,00	0,00	0,00	0,66	0,79	4,75	1,39	0,80	1,10	0,00	3,07	0,00	0,00	0,00	0,31	19,51
Como, via Isonzo	E13225	Leech fibula-circular-foot	?	43,96	13,43	8,88	0,00	0,00	0,77	0,00	0,00	0,00	0,00	0,41	3,29	0,00	2,64	0,00	0,00	2,12	0,00	0,00	0,00	0,00	24,52
Como, M.Olimpino	E5957	Composite bow fibula	NO	46,55	0,00	0,00	0,00	0,00	0,00	0,00	0,00	0,00	0,78	1,72	12,59	1,22	2,14	0,28	0,00	0,60	0,00	0,00	0,00	0,83	33,33
Como, M.Olimpino	E5958	Composite bow fibula	NO	17,62	0,00	48,67	0,00	0,00	0,00	0,00	0,00	0,00	0,60	2,56	5,40	0,78	0,00	0,88	1,39	2,38	0,00	0,00	0,00	0,36	19,36
Golasecca	D1660	grooming tool	YES	43,66	0,00	0,00	0,00	0,00	0,00	0,00	0,00	0,00	1,28	3,65	7,82	3,58	0,87	0,52	1,45	4,04	0,00	0,00	0,00	1,02	32,12
Golasecca	D1668	Longone pendant	NO	44,96	0,00	0,00	0,00	0,00	0,00	0,00	0,00	0,00	0,72	0,93	13,40	0,00	3,14	0,47	1,51	1,40	0,00	0,00	0,00	0,00	33,46
Golasecca	D2049	Leech fibula-circular	NO	41,43	7,98	3,13	0,00	0,00	0,00	0,00	0,00	0,00	0,24	2,11	5,15	2,89	0,65	0,07	0,18	6,05	0,00	0,00	0,13	1,60	28,38
Golasecca	D2059	Leech fibula-circular	NO	63,99	0,00	5,79	0,00	0,00	0,00	0,00	0,00	0,00	0,00	0,59	1,60	0,60	0,49	0,00	0,00	0,47	0,00	0,00	0,00	4,57	21,91
Golasecca	D2064	Leech fibula-circular	YES	41,89	0,00	0,00	0,00	0,00	0,00	0,00	0,00	0,00	1,28	1,17	9,13	3,71	1,07	0,00	0,00	8,96	0,00	0,00	0,00	0,00	32,79
Gropello Cairoli	19/108	Leech fibula-linear	NO	14,34	18,61	14,39	0,00	0,00	0,00	0,00	0,00	0,00	0,00	3,41	5,47	6,92	0,00	0,00	0,00	1,57	0,00	0,00	0,00	5,25	30,06
Gropello Cairoli	19/110	Leech fibula-linear	NO	11,19	10,27	28,59	0,00	0,00	0,00	0,00	0,00	0,00	0,62	4,17	6,34	5,54	0,00	0,93	0,00	1,84	0,00	0,00	0,00	2,77	27,79

(Table 37 — continued)

Site	Inv. no.	Type	Burnt	Cu	Sn	Pb	Ni	Zn	As	Ag	Sb	Na	Mg	Al	Si	P	S	Cl	K	Ca	Ti	Cr	Mn	Fe	O
Gropello Cairoli	19/111	Leech fibula-full-linear	NO	11,45	14,26	15,27	0,00	0,00	0,00	0,00	0,00	0,00	0,45	3,48	8,78	6,06	0,00	0,00	0,65	1,87	0,00	0,00	0,00	6,00	31,72
Gropello Cairoli	19/112	Leech fibula-circular	NO	13,40	7,27	25,10	0,00	0,00	0,00	0,00	0,00	0,00	0,64	6,08	7,52	5,04	0,00	0,43	0,73	2,12	0,00	0,00	0,00	1,93	29,73
Gropello Cairoli	19/114	Leech fibula-linear	NO	21,55	24,90	25,74	0,00	0,00	0,37	0,00	0,00	0,00	0,17	1,07	1,48	2,94	0,00	1,00	0,00	0,00	0,00	0,00	0,00	0,00	20,78
Gropello Cairoli	19/115	Leech fibula-linear	NO	20,27	29,43	4,87	0,00	0,00	0,00	0,00	0,00	0,00	0,20	1,74	3,55	6,14	0,00	0,00	0,00	0,48	0,00	0,00	0,00	4,74	28,60
Gropello Cairoli	19/117	grooming tool	YES	25,13	8,84	11,67	0,00	0,00	0,00	0,00	0,00	0,00	0,00	1,77	11,01	3,74	0,00	0,00	0,00	1,69	0,00	0,00	0,00	5,42	30,77
Gropello Cairoli	21/178	Leech fibula-linear	NO	12,27	42,28	0,00	0,00	0,00	0,00	0,00	0,00	0,00	0,46	3,67	6,56	2,47	0,24	0,00	0,00	0,00	0,00	0,00	0,00	2,33	29,74
Gropello Cairoli	21/180	Leech fibula-linear	NO	12,04	13,04	9,80	0,00	0,00	0,00	0,00	0,00	0,00	1,19	5,52	7,30	6,99	0,35	0,00	0,00	2,68	0,00	0,00	0,00	7,13	33,96
Gropello Cairoli	21/181	Leech fibula-linear	NO	9,23	29,10	15,16	0,00	0,00	0,00	0,00	0,00	0,00	0,00	3,34	4,09	5,82	0,00	0,00	0,00	0,81	0,00	0,00	0,00	4,41	28,06
Mantova	169519	Leech fibula-circular	NO	5,35	10,13	26,04	0,00	0,21	0,00	0,00	0,00	0,00	0,55	0,73	1,61	9,57	0,00	0,60	0,04	8,96	8,77	0,00	0,00	0,00	27,44
Motto Lagone	T1	Leech fibula-circular	NO	19,75	25,13	21,09	0,00	0,00	1,00	0,09	0,00	0,00	0,23	1,12	1,49	3,27	0,03	1,22	0,03	2,30	0,00	0,00	0,00	1,17	22,07
Parre, loc. Castello	9	Leech fibula-full	NO	40,92	19,11	0,00	0,72	0,00	0,00	0,39	0,00	0,00	0,45	1,44	3,47	0,49	3,23	0,91	0,26	1,11	0,00	0,00	0,00	0,26	27,25
Parre, loc. Castello	40	Foliate-arch fibula	NO	42,45	29,26	0,64	0,00	0,00	0,00	0,00	0,00	0,00	0,65	0,35	1,63	0,22	0,44	0,75	0,00	0,00	0,89	0,00	0,00	0,00	22,74
Parre, loc. Castello	41	Foliate-arch fibula	NO	48,57	4,97	0,00	0,39	0,00	0,00	0,00	0,00	0,00	1,26	2,74	5,45	0,63	0,16	0,83	0,46	1,43	4,20	0,00	0,00	0,96	27,95
Parre, loc. Castello	45	Leech fibula-full	NO	46,61	9,07	0,00	1,33	0,00	0,00	0,00	0,00	0,00	0,82	2,24	4,82	0,15	2,12	1,30	0,86	1,42	1,06	0,00	0,00	0,60	27,57
Parre, loc. Castello	46	Low-arch fibula	NO	61,61	7,18	0,00	0,27	0,00	0,00	0,00	0,00	0,00	0,30	0,20	0,96	0,32	0,55	7,53	0,25	0,24	0,15	0,00	0,00	0,00	20,46
Parre, loc. Castello	48	Navicella fibula	NO	37,37	18,24	0,86	0,26	0,00	1,39	3,09	0,00	0,00	1,11	1,29	4,37	0,37	1,18	2,82	1,37	0,00	0,41	0,00	0,00	0,63	25,25
Parre, loc. Castello	49	Navicella fibula	NO	72,40	3,04	0,52	0,60	0,00	0,19	0,00	0,00	0,00	0,11	0,41	0,86	0,38	0,00	0,00	0,28	0,00	0,27	0,00	0,00	0,00	20,96
Parre, loc. Castello	119	Navicella fibula	NO	48,79	7,21	0,50	1,67	0,00	0,00	0,00	0,00	0,00	0,90	1,91	5,03	0,58	1,38	0,91	0,91	1,66	0,70	0,00	0,00	0,77	27,09
Parre, loc. Castello	128	flat-arched fibula	NO	43,77	11,83	0,00	0,11	0,00	0,00	0,00	0,00	0,00	2,24	2,21	5,06	1,61	0,88	1,55	0,69	1,20	0,00	0,00	0,00	1,09	27,77
Parre, loc. Castello	3002	Arch fibula	NO	45,42	17,95	0,00	2,40	0,00	0,00	0,00	0,00	0,00	0,31	1,68	3,65	0,15	0,66	1,27	0,33	0,61	0,31	0,00	0,00	0,60	24,66
Parre, loc. Castello	3564	Leech fibula-full-linear	NO	47,54	0,94	0,00	4,37	3,16	0,00	0,00	0,00	0,00	1,04	2,37	5,24	0,67	1,06	0,98	1,95	2,08	0,27	0,00	0,00	1,19	27,15
Parre, loc. Castello	3565	Leech fibula-full-linear	NO	41,42	11,37	28,14	0,52	0,00	0,00	0,00	0,00	0,00	1,51	2,39	5,58	0,79	1,49	1,55	1,14	2,53	0,29	0,00	0,00	1,32	0,00
Parre, loc. Castello	3569	Leech fibula-linear	NO	33,06	11,62	5,54	0,25	0,92	4,49	0,00	0,00	0,00	2,06	2,21	6,01	0,89	1,08	1,04	1,19	4,60	0,12	0,00	0,00	1,05	23,88
Pianello V.T.	18711	bucket pendant 3D	NO	7,72	0,00	2,85	0,00	0,00	0,00	0,00	0,00	0,00	0,00	5,66	25,84	0,00	0,00	1,03	0,79	13,80	0,00	0,00	0,00	0,00	42,31
Pianello V.T.	18878	Triangolar pendant	NO	12,96	25,17	19,48	0,00	0,00	0,05	0,00	0,00	0,00	0,40	2,41	6,68	2,46	0,00	0,08	0,11	2,65	0,00	0,00	0,00	1,32	26,23
Pianello V.T.	200191	Leech fibula-circular-foot	NO	18,21	16,27	33,16	0,00	0,00	0,14	0,00	0,00	0,00	0,30	0,44	2,53	1,54	0,00	0,12	0,06	4,05	0,00	0,00	0,00	0,37	22,80
Pianello V.T.	201255	Leech fibula-circular-foot	YES	17,53	21,01	32,98	0,00	0,00	0,53	0,00	0,00	0,31	0,00	0,19	1,51	1,72	0,22	1,06	0,45	2,40	0,00	0,00	0,00	1,32	18,76
Pombia	72276-7	Leech fibula-circular	NO	36,86	0,00	4,33	0,00	0,00	0,00	0,00	0,00	0,00	1,51	5,63	13,47	0,86	0,00	0,00	0,86	1,42	0,00	0,00	0,00	1,76	33,31
Pombia	72276-7	Leech-pin	NO	69,39	6,43	0,00	0,00	0,00	0,00	0,00	0,00	0,00	0,00	0,34	1,78	0,00	0,00	0,53	0,00	0,00	0,00	0,00	0,00	0,00	21,54
Pombia	83925	Leech fibula-circular	YES	46,50	0,00	1,61	0,00	0,00	0,00	0,00	0,00	0,17	0,71	4,81	10,03	0,77	0,21	0,00	0,84	1,58	0,10	0,00	0,00	1,88	30,78
Pombia	83937	Leech fibula-circular-foot	YES	24,32	26,01	11,06	0,00	0,00	1,20	0,00	0,00	0,00	0,00	5,20	2,12	1,30	0,00	0,00	0,00	4,07	0,00	0,00	0,00	0,00	24,72
Pombia	83946	Leech fibula-circular	NO	22,44	26,56	11,44	0,00	0,00	1,78	0,00	0,00	0,00	0,00	4,39	2,90	2,96	0,00	0,00	0,00	0,00	0,00	0,00	0,00	1,75	25,79
Pombia	83966	Leech fibula-circular	YES	49,25	0,00	15,34	0,00	0,00	0,00	0,00	0,00	0,00	1,89	0,43	3,93	0,89	0,28	0,00	0,27	4,60	0,00	0,00	0,00	0,00	23,13
Pontecurone	23.M380-9.6	Leech fibula-circular-foot	NO	17,14	25,27	12,13	0,00	0,00	0,34	0,00	0,00	0,00	0,42	1,70	8,60	1,23	0,00	0,17	0,60	1,71	0,00	0,00	0,00	3,53	27,17
Rottofreno	259507	Leech fibula-circular	NO	14,94	11,21	9,06	0,00	0,41	0,06	0,00	0,00	0,00	0,98	4,01	15,06	1,81	0,00	0,36	0,81	4,23	0,02	0,00	0,00	3,02	34,03
San Bernardino di Briona	868	Leech fibula-circular	NO	10,41	40,96	5,09	0,00	0,00	0,00	2,54	0,00	0,00	0,15	5,12	4,58	1,42	0,13	0,00	0,00	0,00	0,00	0,00	0,00	2,67	26,92
San Bernardino di Briona	870	Leech fibula-full-circular	NO	42,84	12,60	0,00	0,00	0,00	0,00	0,00	0,00	0,00	0,69	1,37	5,06	0,64	3,47	0,66	0,17	2,78	0,00	0,00	0,00	0,75	29,00
San Bernardino di Briona	NCT0100026405	Leech fibula-circular	NO	34,67	10,63	0,00	0,00	0,00	0,00	0,00	0,00	0,00	0,89	3,04	5,27	4,28	3,06	0,19	0,13	3,80	0,00	0,00	0,00	1,16	32,88
San Bernardino di Briona	NCT0100026418	Leech fibula-circular	NO	15,57	19,91	28,18	0,00	0,00	0,92	0,00	0,00	0,00	0,16	2,23	2,05	4,98	0,00	0,57	0,00	0,67	0,00	0,00	0,00	1,47	23,30

(Table 37 — continued)

Site	Inv. no.	Type	Burnt	Cu	Sn	Pb	Ni	Zn	As	Ag	Sb	Na	Mg	Al	Si	P	S	Cl	K	Ca	Ti	Cr	Mn	Fe	O
San Bernardino di Briona	NCT0100026417	Leech fibula-circular	NO	18,64	3,32	0,00	0,00	0,00	0,00	0,00	0,00	0,00	1,34	5,66	9,96	2,49	6,60	0,21	1,06	6,85	0,13	0,00	0,00	3,69	40,04
San Bernardino di Briona	NCT0100026415	Leech fibula-circular	NO	16,37	33,08	17,97	0,00	0,00	0,67	0,00	0,00	0,00	0,00	1,90	1,69	3,69	0,00	0,34	0,00	0,00	0,00	0,00	0,00	0,97	23,31
San Bernardino di Briona	23.M380-9.1	Leech fibula-circular-foot	NO	8,70	31,36	25,14	0,00	0,00	2,10	0,33	0,00	0,00	0,00	1,78	1,27	2,67	0,25	4,24	0,00	0,22	0,00	0,00	0,00	0,57	21,37
San Bernardino di Briona	23.M380-9.2	Leech fibula-circular-foot	NO	9,29	11,09	44,91	0,00	0,00	0,41	0,00	0,00	0,00	0,14	2,40	1,96	4,99	0,00	1,22	0,00	2,46	0,00	0,00	0,00	0,24	20,88
San Bernardino di Briona	23.M380-9.7	bucket pendant 1A	NO	34,02	26,81	7,83	0,00	0,00	0,00	0,00	0,00	0,00	0,00	0,73	0,89	3,55	0,00	0,00	0,00	2,51	0,00	0,00	0,00	0,00	23,65
Val Varaita	E17738	Navicella fibula-big	NO	17,24	44,17	6,74	0,00	0,00	0,21	0,00	0,00	0,00	0,18	0,59	1,19	3,81	1,67	0,00	0,00	0,00	0,00	0,00	0,00	0,00	24,22

(Table 37 — continued)

Inv.	Archaeological site	Core	Full-arch	Foot	foot-side support pin	spring-side support pin	ventral side support pin	Pin insertion	alternate linear dec.	Recomposed fractures	µ-fracture	Gaps	Corrosion	Addictions
E5552	Como	x									x	x		x
St. 57244	Como	x						x			x	x		x
St. 57262	Como	x				x					x			
E5553	Como	x												
E5865	Como	x				x					x	x		
St. 865	Como	x									x	x		
St. 57250	Como	x								x	x	x		
St. 879	Como	x				x	x		x		x			
St. 139651	Como	x				x	x				x	x		
St. 139652	Como	x					x		x		x			
E5667	Como	x				x	x				x	x		
E13225	Como			x										
St. 864	Como	x									x	x		
St. 57210	Como	x									x			
St. 57220	Como	x									x			
St. 2208	Como		x										x	
St. 114083	Como		x											
E5868	Como	x				x								
E5873	Como			x										
St. 2206	Como		x							x				
St. 114084	Como		x							x	x			
D2059	Golasecca	x				x	x			x	x	x		
D2049	Golasecca	x				x	x		x		x			
D2064	Golasecca	x					x							

Table 38. Table summarising the different details visible in radiography for the specimens examined.

Inv.	Archaeological site	Core	Full-arch	Foot	foot-side support pin	spring-side support pin	ventral side support pin	Pin insertion	alternate linear dec.	Recomposed fractures	µ-fracture	Gaps	Corrosion	Addictions
D2065	Golasecca	x			hole									
D2077	Castelletto Tic.		x	x										
D2104	Castelletto Tic.	x				x	x							
D2773	Castelletto Tic.	x				x	duck		x					
D2073	Castelletto Tic.	x				x	x							
CT1144	Castelletto Tic.	x					x				x	x		
CT728	Castelletto Tic.	x		x		x	x double				x			
CT29	Castelletto Tic.	x				x	x		x		x			
944	Castelletto Tic.?	x				x	x	x			x			
947	Castelletto Tic.?	x				x	x							
946	Castelletto Tic.?	x				x	x				x			
949	Castelletto Tic.?	x				x	x							
197	Bellinzago	x				x	x					x		
198	Bellinzago	x					x			x				
868	Briona-S.Bern.	x				x	x				x	x		
870	Briona-S.Bern.		x											
T1	Motto Lagone	x		x		x	x			x	x			
St. 83966	Pombia	x			hole	hole		x			x			
St. 83925	Pombia	x				x	x							
St. 83937	Pombia			x										
St. 83946	Pombia	x		x				x		x	x		x	

(Table 38 — continued)

ν_1	no pol	pol	no pol%	pol%
1081	2	0	2,06	0,00
1082	1	0	1,03	0,00
1083	1	1	1,03	2,04
1084	1	0	1,03	0,00
1085	3	1	3,09	2,04
1086	3	2	3,09	4,08
1087	11	0	11,34	0,00
1088	20	2	20,62	4,08
1089	16	7	16,49	14,29
1090	12	1	12,37	2,04
1091	21	12	21,65	24,49
1092	3	3	3,09	6,12
1093	0	4	0,00	8,16
1094	2	15	2,06	30,61
1095	0	1	0,00	2,04
1096	0	0	0,00	0,00
1097	1	0	1,03	0,00
tot	97	49	100,00	100,00

Table 39 - µ-Raman analysis: frequency of different values for the main carbonate peak (v1) in spectra with (pol) and without (no pol) polyenes as actual values and percentage values (pol% and no pol%).

ν_1	HMC	MMC	LMC	C	Ø	HMC%	MMC%	LMC%	C%	Ø%
1081	0	0	0	0	2	0,00	0,00	0,00	0,00	9,52
1082	0	0	0	0	1	0,00	0,00	0,00	0,00	4,76
1083	1	0	0	0	1	2,94	0,00	0,00	0,00	4,76
1084	0	0	1	0	0	0,00	0,00	2,08	0,00	0,00
1085	0	1	2	0	1	0,00	2,44	4,17	0,00	4,76
1086	0	1	2	0	2	0,00	2,44	4,17	0,00	9,52
1087	2	2	5	0	2	5,88	4,88	10,42	0,00	9,52
1088	0	7	12	1	2	0,00	17,07	25,00	50,00	9,52
1089	7	3	10	0	3	20,59	7,32	20,83	0,00	14,29
1090	2	5	4	1	1	5,88	12,20	8,33	50,00	4,76
1091	10	11	9	0	3	29,41	26,83	18,75	0,00	14,29
1092	3	2	1	0	0	8,82	4,88	2,08	0,00	0,00
1093	2	0	2	0	0	5,88	0,00	4,17	0,00	0,00
1094	6	9	0	0	2	17,65	21,95	0,00	0,00	9,52
1095	1	0	0	0	0	2,94	0,00	0,00	0,00	0,00
1096	0	0	0	0	0	0,00	0,00	0,00	0,00	0,00
1097	0	0	0	0	1	0,00	0,00	0,00	0,00	4,76
tot	34	41	48	2	21	100,00	100,00	100,00	100,00	100,00

Table 40 - μ-Raman analysis: frequency of the different values for the main carbonate peak (v1) in the spectra of high/medium/low magnesium calcite (HMC/MMC/LMC), in pure calcite (C) and in the absence of calcite (Ø), as actual values and percentage values.

Archaeological site	Inv. no.	ν_1	Polyenes	SEM-EDS	mol % $MgCO_3$
Bagnolo S. Vito - Forcello	145782	1090		HMC	10,57
Bagnolo S. Vito - Forcello	98797	1094	P	HMC	12,51
Bagnolo S. Vito - Forcello	98798	1094	P	HMC	10,78
Bagnolo S. Vito - Forcello	98799	1091	P	HMC	11,21
Bagnolo S. Vito - Forcello	99209	1091			
Bagnolo S. Vito - Forcello	1060	1090		MMC	8,67
Bagnolo S. Vito - Forcello	99211	1094	P	HMC	12,77
Bellinzago Novarese, loc. Valle Briga	197	1091		MMC	5,57
Bellinzago Novarese, loc. Valle Briga	198	1091		MMC	9,44
Borgonovo V.T.	20.S258-2.118	1091	P	HMC	17,6
Borgonovo V.T.	20.S258-2.119	1091		LMC	1,84
Borgonovo V.T.	20.S258-2.171	1087		HMC	13,27
Borgonovo V.T.	20.S258-2.172	1089	P		
Brembate sotto	67	1085	P	LMC	4,25
Brembate sotto	3016	1089		LMC	2,12
Brembate sotto	3051	1089		LMC	2,98
Brembate sotto	3052	1089		LMC	4,7
Brignano Frascata	C-FR-NE/1	1091	P	HMC	1,38

Table 41 - μ-Raman analysis: list of findings for which analysis identified calcite, with or without polyenes and comparison with data from semi-quantitative SEM EDS analysis (in alphabetical order, according to the name of the archaeological site; the last two columns ('SEM-EDS' and 'mol% $MgCO_3$') refer to SEM data (see section 7.1.2.5), while the previous two ('ν_1' and 'Polyenes') refer to Raman data (in the first column ν_1 value is indicated; in the 'Polyenes' column a P indicate the detection of polyenes signals).

Archaeological site	Inv. no.	ν_1	Polyenes	SEM-EDS	mol % $MgCO_3$
Brignano Frascata	C-FR-NE/2	1093	P	HMC	11,48
Brignano Frascata	C-FR-NE/3	1091	P	HMC	11,43
Castelletto Ticino	91374	1091			
Castelletto Ticino	CT20343C03E	1091		LMC	4,73
Castelletto Ticino	D1750	1092		HMC	11,27
Castelletto Ticino	D2073	1086			
Castelletto Ticino	D2104	1090		MMC	8,5
Castelletto Ticino	23.M380-9.5, SN1092	1088			
Castelletto Ticino	2153	1093	P	LMC	4,86
Castelletto Ticino	1063	1088	P	MMC	8,15
Castelletto Ticino, Bosco del Monte	CT29	1090		LMC	0,79
Castelletto Ticino, Motto d'Egro, v. Beati	20.S.279-3.788, CT164	1091		LMC	2,46
Castelletto Ticino, Motto Falco	CT179	1089		MMC	6,75
Castelletto Ticino, v. Valsesia	20.S.279.3.780, CT728	1091		HMC	11,19
Castelletto Ticino-Vigevano?	944	1088		LMC	2,25
Castelletto Ticino-Vigevano?	946	1088		LMC	1,92
Castelletto Ticino-Vigevano?	947	1091		MMC	9,13
Castelletto Ticino-Vigevano?	949	1091		MMC	6,62
Castello di Annone	23.M380-9.4	1087		HMC	11,58
Caverzano-località Limade	287304	1088		LMC	1,04
Caverzano-località Masiera	217	1094	P	MMC	9,66
Caverzano-località Masiera	211	1090		LMC	2,25
Chies D'Alpago, località Prà	3344	1094	P		
Coll. Assi	23-M380-9.8	1091	P	MMC	9,91
Coll. Assi	23-M380-9.10	1086	P	LMC	4,26
Como, Ca' Morta, Cava Butti	1397	1088		LMC	3,69
Como, Ca' Morta, Cava dalla Zuanna	2206	1089		LMC	3,99
Como, Ca' Morta, Rebbio	114083	1088		LMC	1,53
Como, Ca' Morta, Rebbio	114084	1087			
Como, Ca' Morta, Rebbio	139651	1089		LMC	4,54
Como, Ca' Morta, Rebbio	139652	1087			
Como, Ca' Morta, Rebbio, Cava Ballerini	879	1088		LMC	3,68
Como, Ca' Morta, Rebbio, Cava Bianchi	124142	1089		LMC	4,9
Como, Ca' Morta, Rebbio, loc. Ronchetti	1230	1090		MMC	5,55
Como, Ca' Morta, Rondineto	E5896	1089		HMC	16,1
Como, Ca' Morta, terreno IACP	33594	1089			
Como, Ca' Morta	E13273	1089		LMC	3,22
Como, Prestino, via Isonzo	57210	1089	P	HMC	13,64
Como, Prestino, via Isonzo	57216	1089	P	HMC	12,7
Como, Prestino, via Isonzo	57220	1083	P	HMC	17,84
Como, Prestino, via Isonzo	57244	1086	P		
Como, Prestino, via Isonzo	57250	1089	P	HMC	11
Como, Prestino, via Isonzo	57262	1089	P	HMC	18,81
Como, Rebbio, Villa Giovio	E13225	1089	P		

(Table 41 — continued)

Archaeological site	Inv. no.	ν_1	Polyenes	SEM-EDS	mol % $MgCO_3$
Como, Respaù, Monte Olimpino	E5957	1089		HMC	14,09
Como, Respaù, Monte Olimpino	E5958	1090		HMC	19,57
Golasecca	D1660	1089		LMC	4,96
Golasecca	D1668	1089		LMC	4,25
Golasecca	D1669	1087		LMC	2,39
Golasecca	D2049	1086		MMC	5,33
Golasecca	D2064	1090			
Golasecca	D2065	1089		MMC	6,89
Golasecca	MV103	1086		LMC	4,99
Golasecca	MV4062	1083			
Golasecca, loc. Galliasco	22.S288-1.205	1087		LMC	4,5
Golasecca, loc. Monsorino	63413	1089	P	MMC	9,5
Gropello Cairoli	19/112	1092	P	HMC	16,32
Gropello Cairoli	19/117	1087		LMC	4,88
Malgesso	MV4025	1081			
Mantova - p.zza Santa Barbara	169519	1094	P	HMC	11,52
Mel	9244	1087		MMC	5,07
Mel	9290	1090		LMC	4,74
Mel	9289	1091		LMC	4,29
Montebelluna, loc. Posmon, v. Cima Mandria	304784	1092		LMC	4,09
Motto Lagone	T1	1091	P	HMC	11,65
Padova, vicolo Ognissanti	60735	1084		LMC	1,59
Padova, vicolo Ognissanti	term staffa	1091		HMC	10,54
Padova, vicolo San Massimo	65299	1085		LMC	3,69
Parre, loc. Castello	3569	1089		HMC	16,2
?	M589/3	1090		LMC	3,73
Pianello V.T. (PC)	200191	1091		HMC	14,17
Pieve d'Alpago, Pian della Gnela	312348	1094	P	MMC	9,51
Pieve d'Alpago, Pian della Gnela	312360	1087		LMC	4,39
Pieve d'Alpago, Pian della Gnela	312375	1091		MMC	10,32
Pieve d'Alpago, Pian della Gnela	355677	1094	P		
Pieve d'Alpago, Pian della Gnela	355542	1094	P	MMC	9,65
Pieve d'Alpago, Pian della Gnela	355538	1094	P	MMC	8,24
Pieve d'Alpago, Pian della Gnela	355534	1094	P	MMC	7,73
Pieve d'Alpago, Pian della Gnela	355517	1094	P	HMC	1067
Pieve d'Alpago, Pian della Gnela	355516	1091	P	MMC	9,64
Pieve d'Alpago, Pian della Gnela	355678	1094	P	MMC	6,53
Pieve d'Alpago, Pian della Gnela	355679	1094	P	MMC	9,33
Piovego	5,99	1091	P	MMC	6,98
Piovego	110,8	1091		LMC	2,76
Piovego	108,7	1094		MMC	9,32
Piovego	108,5	1091		LMC	3,09
Piovego	108,3	1088		MMC	6,47
Piovego	181844	1088		LMC	2,52

(Table 41 — continued)

Archaeological site	Inv. no.	ν_1	Polyenes	SEM-EDS	mol % $MgCO_3$
Piovego	95,11	1087		MMC	6,61
Piovego	149682	1094	P	MMC	7,67
Piovego	95,1	1088		C	aragonite
Piovego	95,1	1087		LMC	4,21
Piovego	89,6	1088		LMC	1,37
Piovego	86,3	1088		MMC	7,96
Piovego	224255	1091		MMC	5,6
Piovego	224201	1094		HMC	11,03
Piovego	5,73	1091	P	HMC	11,54
Piovego	153032	1088		MMC	6,32
Piovego	149721	1091		LMC	4,61
Piovego	34914	1091		LMC	1,03
Piovego	110,13	1097			
Pombia, loc. Monticello	72276-72277	1085			
Pombia, loc. Monticello	83925	1088		LMC	2,2
Pombia, loc. Monticello	83937	1089		LMC	1047
Pombia, loc. Quara	83966	1090		C	
Ponte nelle Alpi, Casan	3366	1091	P	HMC	11,66
Ponte nelle Alpi, Cugnan	3355	1088		LMC	3,46
Pontecurone, loc. Cascina Torre	23.M380-9.6	1085		MMC	7,48
Safforze	6602	1090	P	MMC	9,64
Safforze	6600	1090		MMC	5,72
San Bernardino di Briona	870	1091		LMC	4,98
San Bernardino di Briona	1524	1091		MMC	8,86
San Bernardino di Briona	1567	1092	P	MMC	8
San Bernardino di Briona	23.M380-9.1	1091	P		
San Bernardino di Briona	23.M380-9.2	1091	P	MMC	8,38
San Bernardino di Briona	23.M380-9.7	1088		MMC	8,21
Sesto Calende, asilo	12437	1082			
Sesto Calende, asilo	12436	1081			
Sesto Calende, Mulini Bellaria	23752	1088	P	MMC	8,11
Sesto Calende, via Moncenisio	172343	1088		LMC	4,32
Sesto Calende, via Moncenisio	172344	1088		MMC	5,6
Sesto Calende, via Montrucco	4783	1088		LMC	3,61
Villa del Foro	1000/E1	1092		MMC	7,84
Villa del Foro	SP 27	1093	P	HMC	2508
Villa del Foro	66131	1095	P	HMC	14,49
Villa del Foro	51877	1093	P	LMC	4,93
Villa del Foro	51878	1088			
Villa del Foro		1092	P	HMC	10,6

(Table 41 — continued)

Archaeological site	Inv. no.	Type	Location	Dec.	Analysis	calcite	Mg-calcite	d(104)	SEM-EDS	mol% $MgCO_3$
Bagnolo S. Vito - Forcello	1060	Raw	M-MN	G	D	h		3,02	MMC	8,67
Bagnolo S. Vito - Forcello	98798	Raw	M-MN	G	D		h	2,98	HMC	10,78
Bagnolo S. Vito - Forcello	99209	LH	M-MN	T	D	w		2,85		
Bagnolo S. Vito - Forcello	99211	LH	M-MN	C	D		m	2,99	HMC	12,77
Bagnolo S. Vito - Forcello	145782	Bucket-P	M-MN	C	D	m		3,02	HMC	10,57
Bagnolo S. Vito - Forcello	98797	Raw	M-MN	G	D		h	3,01	HMC	12,51
Bagnolo S. Vito - Forcello	98799	Raw	M-MN	G	D		h	3	HMC	11,21
Brembate sotto	67	Comp	B-MA	G	D	h		3,02	LMC	4,25
Brembate sotto	3016	Pend	B-MA	G	D	h		3,03	LMC	2,12
Brembate sotto	3051	Comp	B-MA	G	D	h		3,02	LMC	2,98
Brembate sotto	3052	Comp	B-MA	G	D	h		3,02	LMC	4,7
Brignano Frascata	C-FR-NE/1	Leech-C	MR-MAT	C	S		h		HMC	10,3
Brignano Frascata	C-FR-NE/2	Leech-C	MR-MAT	C	S		h	3	HMC	11,48
Brignano Frascata	C-FR-NE/3	Leech-C	MR-MAT	C	S		h	3	HMC	11,43
Castelletto Ticino	D1750	Pend	C-MC	G	D		h	2,99	HMC	11,27
Castelletto Ticino	D2073	Leech-C	C-MC	C	D	m		3,05		
Castelletto Ticino	D2077	Leech-C	C-MC	C	D		h	3		
Castelletto Ticino	D2104	Leech-C	C-MC	C	D	h		3,06	MMC	8,5
Castelletto Ticino	2153	Leech-C	MR-MAT	C	S	h		3,04	LMC	4,86
Castello di Annone	23.M380-9.4	Leech-C	MR-MAT	C	D	m		3,02	HMC	11,58
Como, Ca' Morta, Cava Butti	1397	Comp	C-MC	G	D	h		3,03	LMC	3,69
Como, Ca' Morta, Cava dalla Zuanna	2206	Leech-C	C-MC	C	D	h		3,03	LMC	3,99
Como, Ca' Morta, Rebbio	139651	Leech-C	C-MC	C	D	h		3,02	LMC	4,54
Como, Ca' Morta, Rebbio, Cava Ballerini	879	Leech-C	C-MC	C	D	m		3,03	LMC	3,68
Como, Ca' Morta, Rebbio, Cava Bianchi	124142	Pend	C-MC	G	D	h		3,03	LMC	4,9
Como, Ca' Morta, Rebbio, loc. Ronchetti	1230	Comp	C-MC	G	D	h		3,04	MMC	5,55
Como, Ca' Morta, Rondineto	E5868	Leech-C	C-MC	C	D		h	2,99	HMC	16,1
Como, Ca' Morta, terreno IACP	33594	Pend	C-MC	G	D	h		3,01		
Como, Ca' Morta	E13273	Comp	C-MC	G	D	h		3,03	LMC	3,22
Como, Prestino, via Isonzo	57210	Leech-C	C-MC	C	D		m	2,98	HMC	13,64
Como, Prestino, via Isonzo	57216	Leech-C	C-MC	C	D		h	3	HMC	12,7

Table 42 - µ-XRD analysis: list of findings for which calcite or Mg-calcite was identified with XRD and comparison with data from semi-quantitative SEM EDS analysis (alphabetically ordered according to the name of the archaeological site; 'type' column: bucket-P = bucket pendants; comp = composite bow fibula; groom = grooming tools; leech-C = leech fibula with circular decoration; pend = pendant and Longone al Segrino pendants; raw = raw coral branches; 'location' column: see section 4.5; 'Dec.' column: 'G' = general, 'T' = transversal grooves, 'C' = circular, 'L' = linear; 'Analysis' column: 'I' = in situ, 'D' = direct, 'S' = sampled); the last two columns ('SEM-EDS' and 'mol% $MgCO_3$') refer to SEM data (see section 7.1.2.5), while the previous three ('calcite', 'Mg-calcite' and '$d_{(104)}$') refer to XRD data (reflex intensity: 'h' = high; 'm' =medium; 'w' = weak; '?' = doubt).

Archaeological site	Inv. no.	Type	Location	Dec.	Analysis	calcite	Mg-calcite	d(104)	SEM-EDS	mol% $MgCO_3$
Como, Prestino, via Isonzo	57220	Leech-C	C-MC	C	D		m	3	HMC	17,84
Como, Prestino, via Isonzo	57250	Leech-C	C-MC	C	D		m	3	HMC	11
Como, Prestino, via Isonzo	57262	Leech-C	C-MC	C	D		h	3	HMC	18,81
Como, Respaù, Monte Olimpino	E5957	Comp	C-MC	G	D		h	3,02	HMC	14,06
Como, Respaù, Monte Olimpino	E5958	Comp	C-MC	G	D		h	3,01	HMC	19,57
Golasecca	D1660	Groom	C-MC	C	D	h		3,03	LMC	4,96
Golasecca	D1668	Pend	C-MC	G	D	h		3,02	LMC	4,25
Golasecca	D1669	Pend	C-MC	G	D	h		3,04	LMC	2,39
Golasecca	D2049	Leech-C	C-MC	C	D	h		3,03	MMC	5,33
Golasecca	D2064	Leech-C	C-MC	C	D	m		3,05		
Golasecca	MV103	Pend	V-MC	G	S		h	3,01	LMC	4,99
Golasecca, loc. Galliasco	22.S288-1.205	Leech-C	SABAP VA	C	S		h	3	LMC	4,5
Golasecca, loc. Monsorino	63413	Leech-C	V-MC	C	S		h	3	MMC	9,5
Mantova - p.zza Santa Barbara	169519	Leech-C	M-MN	C	D		h	3	HMC	11,52
Parre, Castello	3569	Leech-L	B-MA	L	D	w		3,03	HMC	16,2
San Bernardino di Briona	1524	Leech-C	MR-MAT	C	D	m		3,04	MMC	8,86
San Bernardino di Briona	1567	Leech-C	MR-MAT	C	D		?	2,98	MMC	8
Sesto Calende, asilo	12437	Leech-C	V-MC	C	S	h		3,03		
Sesto Calende, asilo	12436	Leech-C	V-MC	C	S	?		3,04		
Sesto Calende, Mulini Bellaria	23752	Leech-C	SC-MC	C	S		h	3	MMC	8,11
Sesto Calende, via Moncenisio	172343	Pend	SC-MC	G	S		h	3,02	LMC	4,32
Sesto Calende, via Moncenisio	172344	Raw	SC-MC	G	S	h		3,04	MMC	5,6
Sesto Calende, via Montrucco	4783	Pend	SC-MC	G	S		h	3,03	LMC	3,61
Unknown	M589/3	Leech-C	Bra	C	S	h		3,02	LMC	3,73
Villa del Foro	1000/E1	Leech-C	MR-MAT	C	S	h		3,02	MMC	7,84
Villa del Foro	SP 27	Leech-C	MR-MAT	C	S		h		HMC	25,08
Villa del Foro	66132	Leech-C	MR-MAT	C	S	w		3,34		
Villa del Foro	66131	Leech-L	MR-MAT	L	S		h	2,99	HMC	14,49
Villa del Foro	51877	Leech-C	MR-MAT	C	S		h	3	LMC	4,93
Villa del Foro	RS 819	Leech-L	MR-MAT	L	S	w		3,33		
Villa del Foro	SP16	Leech-C	MR-MAT	C	S		?	3,34		
Villa del Foro	51878	Leech-C	MR-MAT	C	S		h	3,01		
Villa del Foro	SP 834 a	Leech-C	MR-MAT	C	S		m	3	HMC	10,6

(Table 42 — continued)

This volume investigates Iron Age ornaments from northern Italy decorated with white inlays traditionally identified as coral, with particular focus on leech fibulae. Combining typological study, archaeometric analysis and experimental archaeology, it identifies the materials used and reconstructs the techniques behind their manufacture. The results reveal the presence of Mediterranean red coral (*Corallium rubrum*) alongside other materials, offering new insights into craft production, technological knowledge and long-distance interactions in Iron Age Europe.

ISBN 979-12-5510-403-2 (Print)
ISBN 979-12-5510-404-9 (PDF)
ISBN 979-12-5510-405-6 (EPUB)
DOI 10.54103/cisalpinestudies.261